THEME 1

Wind Resource, Wind Farms and Wakes



WESC 2021
25 – 28 MAY
HANNOVER, GERMANY



Table of Contents

Theme Chairs 1
Mini-Symposium: Advances in Lattice Boltzmann Methods in Wind Energy 2
Mini-Symposium: Array-array interactions and downstream wake effects 10
Mini-Symposium: Array-array interactions and downstream wake effects (I) 11
Mini-Symposium: Array-array interactions and downstream wake effects (II) 23
Mini-Symposium: Data-driven Modeling and Optimization of Wind Farms 36
Mini-Symposium: Data-driven Modeling and Optimization of Wind Farms (I) 37
Mini-Symposium: Data-driven Modeling and Optimization of Wind Farms (II) 45
Mini-Symposium: Entrainment and Blockage Effects on Large Offshore Wind Farms 53
Mini-Symposium: Entrainment and Blockage Effects on Large Offshore Wind Farms (I) 54
Mini-Symposium: Entrainment and Blockage Effects on Large Offshore Wind Farms (II) 62
Mini-Symposium: IEA Task 31 "Wakebench" Wind Farm Flow Model Validation 76
Mini-Symposium: IEA Task 31 "Wakebench" Wind Farm Flow Model Validation (I) 77
Mini-Symposium: IEA Task 31 "Wakebench" Wind Farm Flow Model Validation (II) 86
Mini-Symposium: Interactions of large-scale offshore wind farms with the marine atmospheric boundary layer of the German Bight 95
Mini-Symposium: Lidars and floating wind energy – Collaboration of Innovative Training Networks LIKE and FLOAWER 106
Mini-Symposium: Lidars and floating wind energy – Collaboration of Innovative Training Networks LIKE and FLOAWER (I) 107
Mini-Symposium: Lidars and floating wind energy – Collaboration of Innovative Training Networks LIKE and FLOAWER (II) 120
Mini-Symposium: Lidars and numerical models – how they correspond and interact 132
Mini-Symposium: Lidars and numerical models – how they correspond and interact (I) 133
Mini-Symposium: Lidars and numerical models – how they correspond and interact (II) 145
Mini-Symposium: The pragmatic choice of wind models for Wind Resource Assessment 154
Mini-Symposium: Wind Farm Control 165
Mini-Symposium: Wind Farm Control (I) 166
Mini-Symposium: Wind Farm Control (II) 177
Mini-Symposium: Wind Farm Control (III) 187
Mini-Symposium: Wind Power Forecasting 199
Mini-Symposium: Wind Power Forecasting (I) 200
Mini-Symposium: Wind Power Forecasting (II) 210
Regular Session: Wind Resource Assessment (I) 222
Regular Session: Wind Resource Assessment (II) 234
Regular Session: Wind Resource Assessment (III) 247
Regular Session: Wind Resource Assessment (IV) 262
Regular Session: Wind Resource Assessment (V) 273
Regular Session: Large Scale Wind Farm Wake Modeling 284
Regular Session: Wind Farm Modeling and Analytical Approaches 296
Regular Session: High-Fidelity Wake Modeling 309
Regular Session: Wake Models and Data 321
Regular Session: Mesoscale Modeling and Forecasting (I) 333
Regular Session: Mesoscale Modeling and Forecasting (II) 346
Regular Session: Minute-Scale Forecasting and Power Fluctuations 361
Regular Session: Wind Farm Design and Optimization 372
Regular Session: Meteorology and Microscale Modelling (I) 388
Regular Session: Meteorology and Microscale Modelling (II) 401



Regular Session: Wakes and Farms.....411

Theme Chairs



Prof. Rebecca J. Barthelmie
Cornell University



Dr. Julia Gottschall
Fraunhofer IWES



Dr. Detlev Heinemann
Forwind, University of Oldenburg



Prof. Johan Meyers
KU Leuven

Mini-Symposium: Advances in Lattice Boltzmann Methods in Wind Energy





Stefan Ivanell
Uppsala University

Henrik Asmuth
Uppsala University

The lattice Boltzmann method (LBM) has become a promising alternative to classical computational fluid dynamics approaches. This is largely due to its excellent computational performance. Recent efforts show that the method can facilitate a wider applicability of high-fidelity fluid dynamics simulations, particularly large-eddy simulations, in the field of wind energy. The combination of the LBM and wind-energy specific models such as actuator line and disk techniques or numerical models used in the context of atmospheric boundary layers leads to various specific research questions. This mini-symposium will be concerned with recent advances and challenges of the LBM for wind turbine and farm aerodynamics, as well as atmospheric flows in general. Furthermore, future perspectives of the method and the potential for both academic and industrial applications shall be discussed. Bringing together the small but growing research community of the LBM in wind energy, the session shall serve as a forum for focused discussions among active researcher in the field. Furthermore, it shall provide an overview of the current state and future possibilities of the method to researchers outside or new to the LBM.

GPGPU-accelerated Urban Scale Wind Simulations based on Lattice-Boltzmann methods

Manfred Krafczyk[1,2,*], Martin Geier[1,2], Martin Schönherr[1,2], Konstantin Kutscher[1,2], and Anna Wellmann[1,2]
[1]Technical University of Braunschweig (IRMB)
[2]Computational Modeling in Civil Engineering (IRMB)
[*]Presenting author

Keywords: wind simulation | GPGPU | Lattice Boltzmann Method

Modeling and Simulation of wind on multiple spatio-temporal scales is not only essential for wind energy studies, but also for wind comfort and micro climate studies including air quality assessment in urban areas. This work explores the feasibility of real-time large-eddy simulations of turbulent multicomponent flow over urban canopies at the neighbourhood scale. Miscellaneous investigations have been conducted to decrease air pollution as e.g. induced by particulate matter (PM) in urban regions. PM (aka fine dust) is a critical pollutant inducing various health threats. Minimizations of the exposure to particulate matter are presently discussed by political stakeholders. The effectiveness of suggested measures e.g. closing particular streets is unclear and related measurement campaigns are expensive. Thus, numerical simulations appear to be a useful approach to evaluate the potential success of specific measures especially during the planning phase. This work focused on simulating pollution emitted by motorized vehicles as they are among the primary emitters of PM. The core component of this work is a physics-based simulation of the pollutant's transient distribution in an urban district. We achieved acceptable quantitative agreement with measurements both for the mean velocity profiles as well as for the turbulent fluctuations.

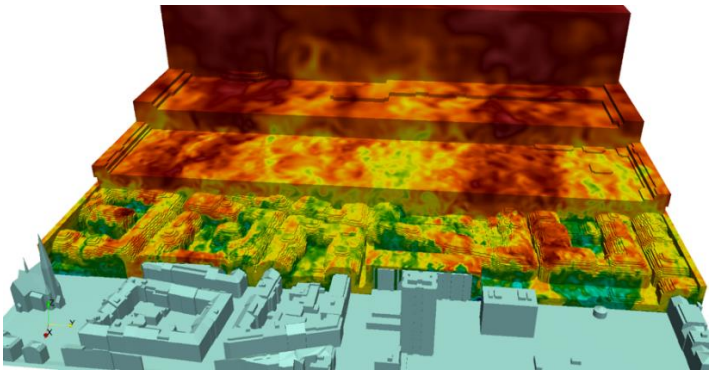


Figure 1: LES wind simulation of a Basel district using the LBM

For a realistic spatio-temporal definition of the PM emitters, an extended version of the Nagel-Schreckenberg traffic model was included. In order to obtain close to real-time computational performance, both the traffic and the CFD simulation was parallelized and ported to a General-Purpose Graphic Processing Unit (GPGPU). The implemented testcase was a 500 m by 500 m section of a densely built inner city area from Basel, Switzerland. Several hours of real time e.g. during the morning rush hour were simulated. The pollution distribution at several instances in time were compared and analyzed for multiple wind configurations. Our approach could serve as a rational basis to study the implications of pollution reduction measures related to localized traffic regulation in urban spaces. Finally, we will also present initial results of an embedded rotating grid approach for the LBM method to conduct implicit LES simulations of rotor configurations.

Investigation of the influence of the inlet boundary conditions on the turbulent flow over a smooth 3-D hill

Alain Schubiger*, and Sarah Barber
Eastern Switzerland University of Applied Sciences
*Presenting author

Keywords: Lattice Boltzmann Method | Large Eddy Simulation | high-resolution numerical modelling | Synthetic turbulence | Computational Fluid Dynamics

The growing global demand for renewable energy, especially wind energy, is leading to the need to build wind farms in increasingly complex terrains. The wind speed distribution in such terrain is very complex and the flow is characterised by variations in wind speed and wind direction, flow separation and changes in turbulence intensity.
Under such conditions, linear models provide inaccurate results for the wake region and models that are more sophisticated are required in order to reduce the uncertainty of Wind Resource Assessments (WRA) (e.g. Gong and Ibbetson, 1989; J.M.L.M. Palma et al., 2008).
In these cases, Reynolds-Averaged Navier-Stokes (RANS) Computational Fluid Dynamics (CFD) solvers such as WindSim, Meteodyn and more general Navier-Stokes solvers such as ANSYS Fluent are usually used (e.g. Ferreira et al., 1995; Maurizi et al., 1998; Kim et al., 2000, Castro et al., 2003).
Research has shown that even RANS simulation do not model the complex flows accurately enough in some situations and that Large Eddy Simulations (LES) are necessary to correctly reproduce and understand local changes in the flow field (e.g. Bechmann et al., 2011; Diebold et al., 2013; Ma and Liu, 2017; DeLeon et al., 2018).
The increase in available computing resources in recent years has enabled more and more LES applications, at least in the research environment, although LES is still far more computationally intensive than linear or RANS models.
Another promising and alternative approach to the Navier-Stokes methods is the Lattice Boltzmann Method (LBM), a numerical fluid dynamics technique based on the Boltzmann transport equation. It is used to study complex phenomena such as turbulence because it describes motion at the mesoscopic level, as opposed to the macroscopic level of conventional CFD approaches that solve the Navier-Stokes equations. It has also shown to provide significant performance gains compared to classical Navier-Stokes-based CFD (e.g. Asmuth et al., 2019, Schönherr et al., 2011).
Palabos (Parallel Lattice Boltzmann Solver) is a framework for general-purpose CFD. The open-source software library serves as a modelling platform for LBM schemes and covers a wide range of LB models and applications.
An initial study investigating the applicability of Palabos to complex terrain sites was carried out previously (Schubiger et al., 2020). In this study, it was shown that Palabos is applicable to model wind flow over complex terrain accurately at relatively low costs. However, it was concluded that further studies are required.
In this present study, Large Eddy Simulations are applied to study the turbulent flow fields over a 3-D hill using Palabos. The geometry considered follows the wind tunnel experiments conducted by Ishihara et al. (1999). There, turbulent flow over a three-dimensional circular hill was investigated using split-fiber probes.
In this work, a comparison between inlet boundary conditions for LES is performed. Three different inlet boundary conditions (fixed velocity profile with and without roughness elements and synthetic turbulence inlet) have been implemented in Palabos.
The influence on flow variables, such as vortex shedding and reattachment points and turbulence has been analysed.

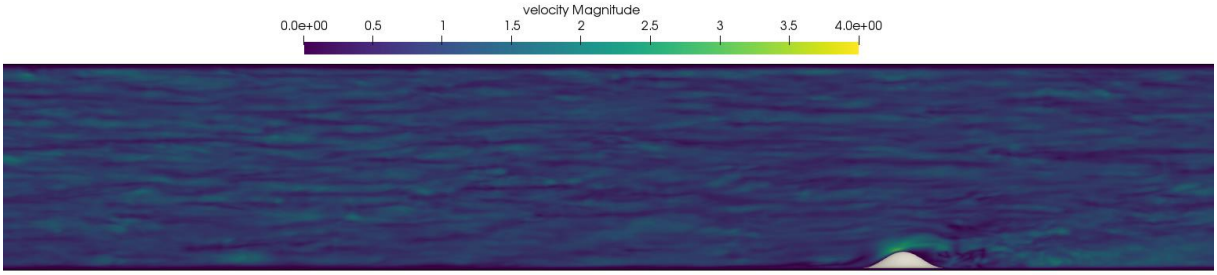


Figure 1: Instantaneous velocity field on the vertical slice at y=0

Early results show a satisfying agreement with experiments. Figure 1 shows an instantaneous velocity field at the centre surface of the simulated wind tunnel.

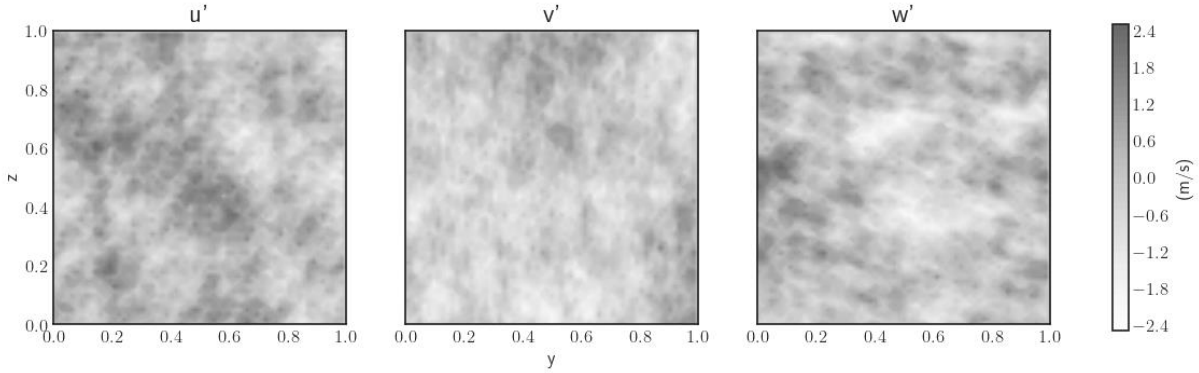


Figure 2: Snthetic fluctuations on the inlet boundary condition

Figure 2 shows the velocity fluctuations generated at the inlet boundary condition following the technique developed by Davidson (2008).

References:

Gong, W., Ibbetson, A. A wind tunnel study of turbulent flow over model hills. Boundary-Layer Meteorol 49, 113–148 (1989). https://doi.org/10.1007/BF00116408

Palma, J. M. L. M., et al. "Linear and nonlinear models in wind resource assessment and wind turbine micro-siting in complex terrain." Journal of Wind Engineering and Industrial Aerodynamics 96.12 (2008): 2308-2326.

Ferreira, A., Lopes, A., Viegas, D., and Sousa, A.: Experimental and numerical simulation of flow around two-dimensional hills, Journal of wind engineering and industrial aerodynamics, 54, 173–181, 1995.

Maurizi, A., Palma, J., and Castro, F.: Numerical simulation of the atmospheric flow in a mountainous region of the North of Portugal, 350 Journal of wind engineering and industrial aerodynamics, 74, 219–228, 1998.

Kim, H. G., Patel, V., and Lee, C. M.: Numerical simulation of wind flow over hilly terrain, Journal of wind engineering and industrial aerodynamics, 87, 45–60, 2000.

Castro, F. A., Palma, J., and Lopes, A. S.: Simulation of the Askervein Flow. Part 1: Reynolds Averaged Navier–Stokes Equations (k epsilon Turbulence Model), Boundary-Layer Meteorology, 107, 501–530, 2003.

Bechmann, A., Sørensen, N. N., Berg, J., Mann, J., and Réthoré, P.-E.: The Bolund experiment, part II: blind comparison of microscale flow models, Boundary-Layer Meteorology, 141, 245, 2011.

DeLeon, R., Sandusky, M., and Senocak, I.: Simulations of turbulent flow over complex terrain using an immersed-boundary method, Boundary-Layer Meteorology, 167, 399–420, 2018.

Ma, Y. and Liu, H.: Large-eddy simulations of atmospheric flows over complex terrain using the immersed-boundary method in the Weather Research and Forecasting Model, Boundary-Layer Meteorology, 165, 421–445, 2017.

Diebold, M., Higgins, C., Fang, J., Bechmann, A., and Parlange, M. B.: Flow over hills: a large-eddy simulation of the Bolund case, Boundary-layer meteorology, 148, 177–194, 2013.

Schönherr, Martin, et al. "Multi-thread implementations of the lattice Boltzmann method on non-uniform grids for CPUs and GPUs." Computers & Mathematics with Applications 61.12 (2011): 3730-3743.

Asmuth, Henrik, et al. "The Actuator Line Model in Lattice Boltzmann Frameworks: Numerical Sensitivity and Computational Performance." Journal of Physics: Conference Series. Vol. 1256. No. 1. IOP Publishing, 2019.

Lattice Boltzmann Large-eddy Simulation of Neutral Atmospheric Boundary Layers

Henrik Asmuth[1], Christian F. Janßen[2], Hugo Olivares Espinosa[1], and Stefan Ivanell[1]
[1]Uppsala University
[2]Technical University of Hamburg

Keywords: Lattice Boltzmann Method | Wall model | Atmospheric boundary layer

Simulations of atmospheric boundary layer (ABL) flows are essential for the majority of wind farm studies using large-eddy simulation (LES). To date, applications of the Lattice Boltzmann Method (LBM) to ABL flows remain limited, despite a growing popularity of the method in the field of wind energy. Among others, the latter can be attributed to the persistent challenge of robust LBM-specific wall modelling approaches.
In this talk we present a novel LBM wall model that builds upon classical bounce-back schemes. In this way it differs from most previous LBM wall models using so called wet-node approaches (see, e.g., Malaspinas and Sagaut, 2014), hence, reconstructing the distribution functions at wall boundary nodes from interpolated/prescribed macroscopic quantities. The novel wall model prescribes the wall stress obtained from Monin-Obukhov similarity theory by means of a direct manipulation of the momentum of the reflected distribution functions within the bounce-back scheme.
The presented model is tested in simulations of neutral atmospheric boundary layers in an openchannel-flow configuration. In the bulk the cumulant LBM is employed as well as a standard Smagorinsky sub-grid scale model with wall damping.
In an initial test series the sensitivity of the wall model is investigated with respect to the sampling location and temporal filtering of the input velocity of the wall model. A sampling off the first wallparallel layer of nodes is found to reduce the log-layer mismatch, in line with other studies (Owen et al., 2020). Also the temporal filtering improves the match with the theoretical log-low, yet, is found less sensitive than the sampling location.
Following the initial study, a subset of simulations with the properly tuned wall model is further analyzed in terms of second and higher-order velocity moments, spectra and two-point correlations.
Exemplary results are depicted in Figure 1. Given the utilized subgrid scale (SGS) model, the presented set-up is found to produce satisfactory results in terms of most analyzed statistics. A mismatch of the velocity at the first off-wall point remains as a striking persistent issue. The latter appears to be related to the over-dissipative behavior of the utilized SGS model leading to an excessive damping of near-wall turbulence. Further investigations will show the mitigation potential of other SGS models or near-wall corrections.

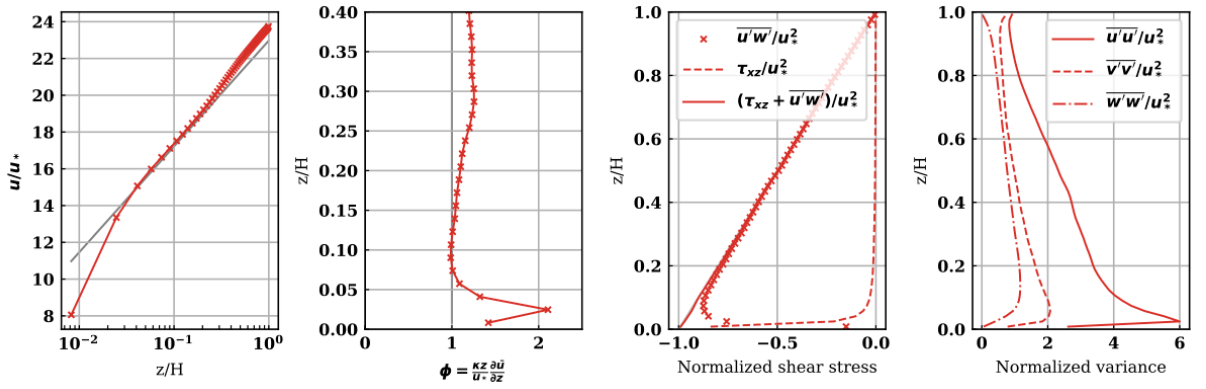


Figure 1: Horizontally and temporally averaged statistics of a neutral atmospheric boundary layer flow: Left, mean streamwise velocity u. Second from left, mean vertical gradient of u. Second from right, resolved and modelled shear stress. Right, velocity variances.

In summary, the proposed stress boundary condition is shown to be a suitable approach for wall modelling in the LBM. The discussed test series highlight the potential of the LBM for simulations of atmospheric

boundary layers. In this way it marks a crucial step towards simulations of wind farms using the LBM. Future work will be concerned with a further improvement of the presented wall model, the testing of other SGS models and eventually the application to wind farm simulations in a precurser set-up.

References:
Malaspinas, O. and Sagaut, P. (2014). Wall model for large-eddy simulation based on the lattice Boltzmann method. J. Comput. Phys., 275 (15), 25-40
Owen, H. et al. (2020). Wall-modeled large-eddy simulation in a finite element framework. Int J Num Meth in Fluids, 92(1), 20-37

A Holistic CPU/GPU Approach for the Actuator Line Model in Lattice Boltzmann Simulations

Helen Schottenhamml[1,*], Ani Anciaux-Sedrakian[2], Frédéric Blondel[2], and Ulrich Rüde[1,3]
[1]Friedrich-Alexander University Erlangen
[2]IFP Energies Nouvelles
[3]CERFACS
*Presenting author

Keywords: Lattice Boltzmann Method | actuator line model | code generation | high performance computing | heterogeneous systems with accelerators

As part of the ongoing energy revolution - the transition from fossil to renewable energy sources - wind energy plays an increasing role in the production of clean energy. The accurate simulation and prediction of wind farms flow itself is a persisting challenge due to the complex interactions between turbines and turbulent wakes. Doing so in an efficient manner is even more demanding. We approach this challenge by coupling the Lattice-Boltzmann method for the fluid with an Actuator Line model (Churchfield et al., 2017) for the turbines. The basis for the implementation is the multiphysics software framework waLBerla (Bauer et al., 2021).
The Actuator Line model reduces the computational demands by representing the blades by their forces acting on the fluid instead of explicitly resolving them. Doing so, the mesh resolution in the turbines' vicinity can be kept coarser compared to blade-resolved methods.
Besides, the Lattice-Boltzmann method is inherently well-suited for large scale applications on highperformance computing systems due to its local time evolution scheme. In particular, these methods highly benefit from the acceleration using Graphical Processing Units (GPU).
However, we do not want to restrict the end user to computing systems with graphic cards. Instead, the goal is to preserve also the CPU-only capabilities. For the Lattice-Boltzmann kernels, this is achieved by using the Python-based code generation framework lbmpy (Bauer, Köstler and Rüde, 2021). The same high-level description of the kernels can be used to generate highly-optimised code for both CPU and GPU applications. To achieve sufficient stability, even for the high Reynolds numbers for wind turbine flows, we use the cumulant Lattice-Boltzmann method for all our applications.
Even though the Actuator Line model does not benefit equally from the GPU acceleration, its GPU compliant implementation is inevitable to avoid massive communication overhead. Hence, the presented work deals with a holistic CPU/GPU software design for the wind turbines. Notably, this holistic approach derives from a mutual code base for CPU and GPU that disposes of the necessity of implementing and maintaining two different versions of physical models for CPU and GPU. Not only does this prevent code divergence of physical models, but it also directly eases the implementation effort for new models. The result is a less error-prone code base that is also performance portable. In future work, this will facilitate the setup of hybrid CPU/GPU simulations that further exploit the parallelism capabilities of the underlying hardware.
After detailing the software design itself, we will address the validation of the simulation in terms of physical properties and accuracy. Furthermore, we comment on the performance and the speed-up properties of our approach. Here, particular attention lies in the acceleration of the simulation using a GPU card. Figure 1 shows the normalised time-to-solution for different hardware setups. 30.000 timesteps were executed for a domain consisting of approximately 20 million cells with one single wind turbine.

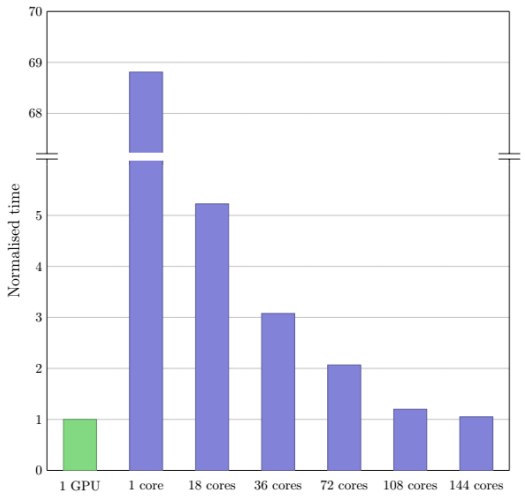


Figure 1: Preliminary performance results of the wind turbine application for CPU and GPU simulations using the holistic implementation.

Using the same implementation, the simulation on one GPU (NVIDIA P100) substantially and expectedly outperforms the simulation on one CPU core (Intel Skylake G-6140) without any accuracy loss. Only after using eight full nodes, i.e. 144 CPU cores, we achieve almost the same time-tosolution for both CPU and GPU systems.

References:

Churchfield, M., Schreck, S., Martinez, L., Meneveau, C. and Spalart, P., 2017. An Advanced Actuator Line Method for Wind Energy Applications and Beyond. 35th Wind Energy Symposium,.

Bauer, M., Eibl, S., Godenschwager, C., Kohl, N., Kuron, M., Rettinger, C., Schornbaum, F., Schwarzmeier, C., Thönnes, D., Köstler, H. and Rüde, U., 2021. waLBerla: A block-structured high-performance framework for multiphysics simulations. Computers & Mathematics with Applications, 81, pp.478-501.

Bauer, M., Köstler, H. and Rüde, U., 2021. lbmpy: Automatic code generation for efficient parallel lattice Boltzmann methods. Journal of Computational Science, 49, p.101269.

Mini-Symposium: Array-array interactions and downstream wake effects







Rebecca J. Barthelmie
Cornell University

Sara C. Pryor
Cornell University

Charlotte B. Hasager
DTU Wind Energy

Abstracts are solicited for a mini-symposium on array-array interactions and downstream wake effects of large wind farms either on- or off-shore. Much of the new wind energy installed capacity is being deployed in large arrays located areas with existing wind farms. There is increasing interest in finding techniques to model and understand the impacts of one or more wind farms either on existing installations and/or on the local meteorology. The methodology for the research can be remote or in situ measurements, numerical modeling or use of wind farm production data applied onshore or offshore. The aim is to quantify the impact of large wind farms on either neighbouring wind farms or on the meteorology of the local environment to allow the most effective use of relatively confined areas and to provide estimates of the effects on pre-existing wind farms.

Mini-Symposium: Array-array interactions and downstream wake effects (I)

Farm wakes as seen from mesoscale and high-resolution wake models

Jana Fischereit*, Kurt Schaldemose Hansen, Xiaoli Guo Larsén, Paul van der Laan, Pierre-Elouan Réthoré, and Juan Pablo Murcia Leon
DTU Wind Energy
*Presenting author

Keywords: Explicit Wake Parametrisation (EWP) | PyWake | EllipSys3d

The expansion of offshore wind energy increases the need for considering the variable meteorological background climate over larger areas as well as for taking farm wakes from neighbouring wind farms into account. Mesoscale meteorological models equipped with a wind farm parameterisation (WFP) have been identified as a useful tool for that (Fischereit et al., 2020; Veers et al., 2019).
At the same time, individual turbines cannot be resolved with a typical resolution of mesoscale models for this topic of about 1 to 3 km. High-resolution wake models, i.e. both simple engineeringtype wake models as well as CFD-RANS models, are designed for this purpose. However, their simplified assumptions of horizontally uniform inflow are not always met over larger areas.
Therefore, high resolution wake models might be less suitable for modelling farm-to-farm wakes and long-distance wakes.
With this in mind, the aim of this study is two-fold. Firstly, to evaluate for intra-farm wakes the performance of a WFP in a mesoscale model with a typical horizontal resolution against mast measurements, SCADA data from Rødsand II and high resolution wake models. Secondarily, to compare farm-to-farm and long distance wakes of a WFP and high resolution wake models.
For this study, we employ the Weather Research and Forecasting (WRF) mesoscale model (Skamarock et al., 2008) with the Explicit Wake Parameterisation (EWP, Volker et al., 2015). As highresolution CFD-RANS model, we use PyWakeEllipSys (https://topfarm.pages.windenergy.dtu.dk/cuttingedge/pywake/pywake_ellipsys), which is based on the EllipSys3D CFD flow solver (Michelsen 1992, Sørensen 1994), and different simple engineeringtype wake models included in the pyWake suite (Pedersen et al. 2019). The models are applied to the Fehmarn Belt area with the wind farms Nysted and Rødsand II. The nested WRF domain with the two wind farms is shown in Figure 1. We simulate two one-month long periods with WRF with high availability of measurement data and SCADA; one before commissioning of Rødsand II and one after commissioning of Rødsand II, respectively. After the evaluation of the performance of WRF and WRFEWP in the two periods against mast measurements, flow cases are defined for the high-resolution wake models for the post-commissioning period.

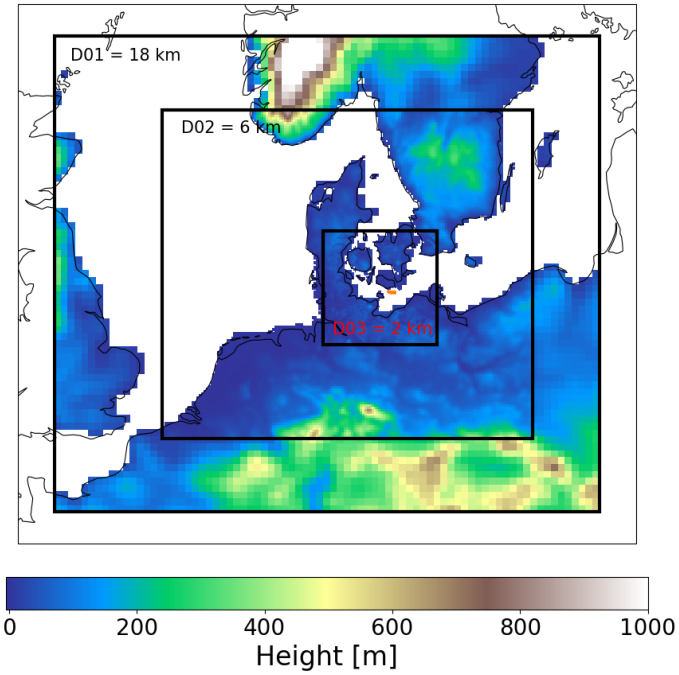


Figure 1: Nested WRF domain including wind turbines of interest (orange)

The evaluation of the WRF simulation before commissioning shows that WRF is able to simulate the background meteorological conditions in the Fehmarn belt area. After commissioning, WRF-EWP performs better than a simulation with WRF without WFP. The average wake effect during this period is about 1 m/s. Since SCADA data are only available for Rødsand II, one flow case with eastern wind and wind speeds of 10±1 m/s has been chosen for the high-resolution wake models. Initial results for the comparison for intra-farm wakes of WRF-EWP and SCADA data indicates that WRF-EWP captures the wind speed reduction inside the farm along the flow (Figure 2) but overestimates reductions perpendicular to the flow.

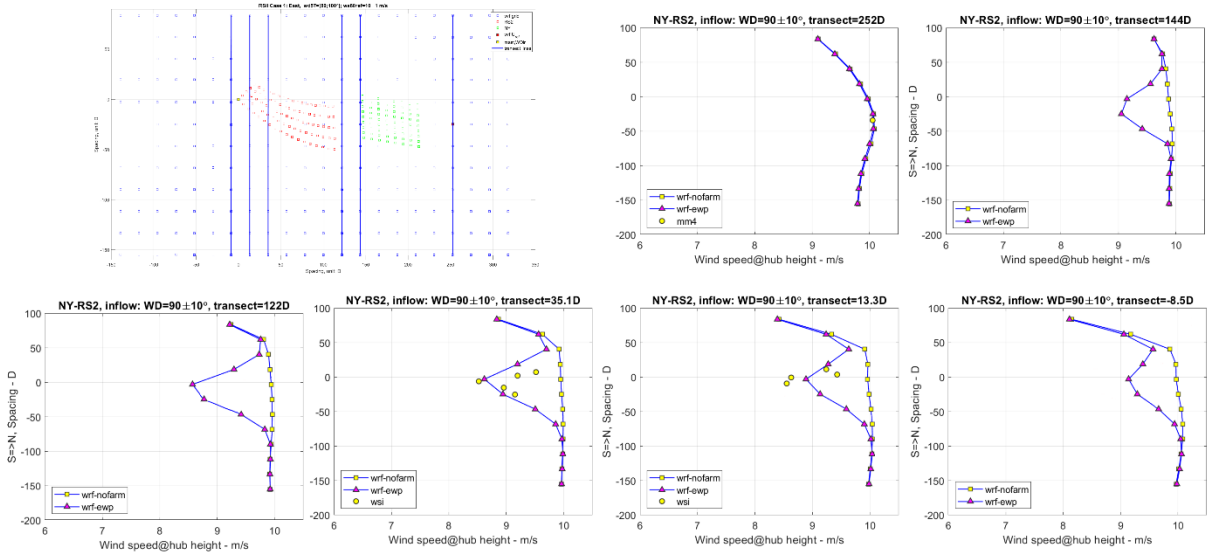


Figure 2: Wind speed at hub height at different transects through the wind farms

In the presentation, we will show results for this and other flow cases comparing WRF-EWP with different high-resolution wake models for intra-farm, farm-to-farm and long distance wakes and discuss possible improvements for the models.

References:



Fischereit, J., Brown, R., Larsén, X. G., Badger, J., and Hawkes, G., 2020, Review of mesoscale wind farm parameterisations and their applications, Boundary-Layer Meteorology, submitted

Veers, P., Dykes, K., Lantz, E., Barth, S., Bottasso, C. L., Carlson, O., Clifton, A., Green, J., Green, P., Holttinen, H., Laird, D., Lehtomäki,V., Lundquist, J. K., Manwell, J., Marquis, M., Meneveau, C., Moriarty, P., Munduate, X., Muskulus, M., Naughton, J., Pao, L., Paquette,J., et al., 2019, Grand challenges in the science of wind energy, Science, 366, https://doi.org/10.1126/science.aau2027

Skamarock, W. C., Klemp, J. B., Dudhia, J., Gill, D. O., Barker, D., Duda, M. G., Huang, X.-Y., Wang, W., and Powers, J. G.,2008, A Description of the Advanced Research WRF Version 3, Tech. rep., https://doi.org/10.5065/D68S4MVH, https://opensky.ucar.edu/islandora/object/technotes:500

Volker, P. J. H., Badger, J., Hahmann, A. N., and Ott, S., 2015, The Explicit Wake Parametrisation V1.0: a wind farm parametrisation in the mesoscale model WRF, Geoscientific Model Development, 8, 3715–3731, https://doi.org/10.5194/gmd-8-3715-2015

Pedersen, M. M., van der Laan, P., Friis-Møller, M., Rinker, J., and Réthoré., P.E., 2019, DTUWindEnergy/PyWake: PyWake (Version v1.0.10). Zenodo. http://doi.org/10.5281/zenodo.2562662

Michelsen, J. A., Basis3d - a platform for development of multiblock PDE solvers. Technical Report AFM 92-05, Technical University of Denmark, Lyngby, Denmark, 1992.

Sørensen, N. N., General purpose flow solver applied to flow over hills. PhD thesis, Risø National Laboratory, Roskilde, Denmark, 1994.

Large scale offshore wind farm effects measured with scanning lidar

Jörge Schneemann[1,*], Frauke Theuer[1], Andreas Rott[1], Gabriele Centurelli[1], Martin Dörenkämper[2], Gerald Steinfeld[1], and Martin Kühn[1]
[1]ForWind - University of Oldenburg
[2]Fraunhofer IWES
*Presenting author

Keywords: cluster wake | wind farm wake | wind farm global blockage | scanning Doppler lidar | lidar uncertainty assessment

The intensive deployment of offshore wind farms in areas like the North Sea raises the need for a refined wind resource assessment. Wind farms interact by cluster wake effects that can travel more than 50 km downstream in stable atmospheric stratification and influence the power of neighbouring wind farms [1,2]. A second important aspect in resource assessment and power prediction is the so called global blockage effect which originates in the influence of the wind farm itself on the flow. Due to the accumulated thrust of the wind farm the wind approaching the farm can be affected by a deceleration. Thus, the available power in the wind farm is reduced [3,4].
Wind farm cluster wakes have a large spatial extent and the global blockage effect has a small amplitude with a similar magnitude as the surrounding turbulence. Therefore, those offshore wind farm flow effects are comparably hard to analyse in field experiments. There is only few experimental studies dealing with offshore wind farm effects aside a growing number of numerical contributions. Cluster wakes were studied using SAR [5], research aircrafts [1], Doppler radar [6], and SCADA data [7]. While SAR and research aircrafts are able to only perform measurements within a short time frame they are able to cover wide areas. Doppler radar enables fast measurements over comparably wide areas but is currently hard to deploy in offshore wind farms due to logistical and financial constraints. SCADA data is generally available but only delivers a limited picture of the flow. The global blockage effect has just been studied in onshore field campaigns using meteorological masts so far [3]. Scanning long range Doppler lidar enables for long term wind monitoring with high accuracy and several kilometres of range.
The objective of our talk is to present our recent experimental findings on wind farm effects in the 400 MW / 80 turbines offshore wind farm Global Tech I (GTI) in the North Sea. We used a scanning long range lidar to measure the inflow of the wind farm for more than one year and estimated atmospheric stability using local meteorological measurements and reanalysis data.
We found influences of wind farm cluster wakes of wind farms situated 24 km and 55 km upstream on the power of GTI in stable and weakly unstable conditions using Lidar, SAR and SCADA data (Figure 1, [2]). Furthermore, we present first comparisons of these lidar measurements and simulations by the mesoscale model WRF and an engineering model.

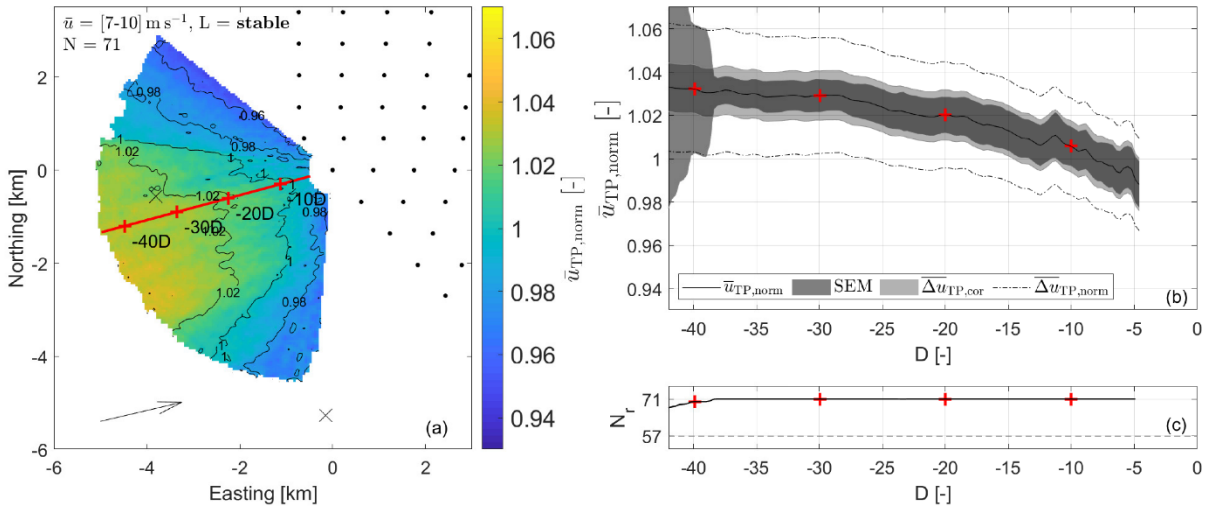


Figure 1: a) Normalized averaged lidar scans in stable atmospheric stratification upstream GTI. b) Wind speed along the virtual cut in the wind field in a) with three different uncertainty characterizations. c) Number of available lidar scans per measurement range in b).

In a second analysis we focussed on the global blockage effect. Here we analysed the inflow of GTI on a wind speed deficit towards the farm by means of averaged lidar data on which we performed an extensive uncertainty assessment. We found a wind speed deficit of 4 % with an uncertainty range from 2 % to 6 % in stable stratification and the wind farm operating in the upper partial load range (Figure 2, [8]).

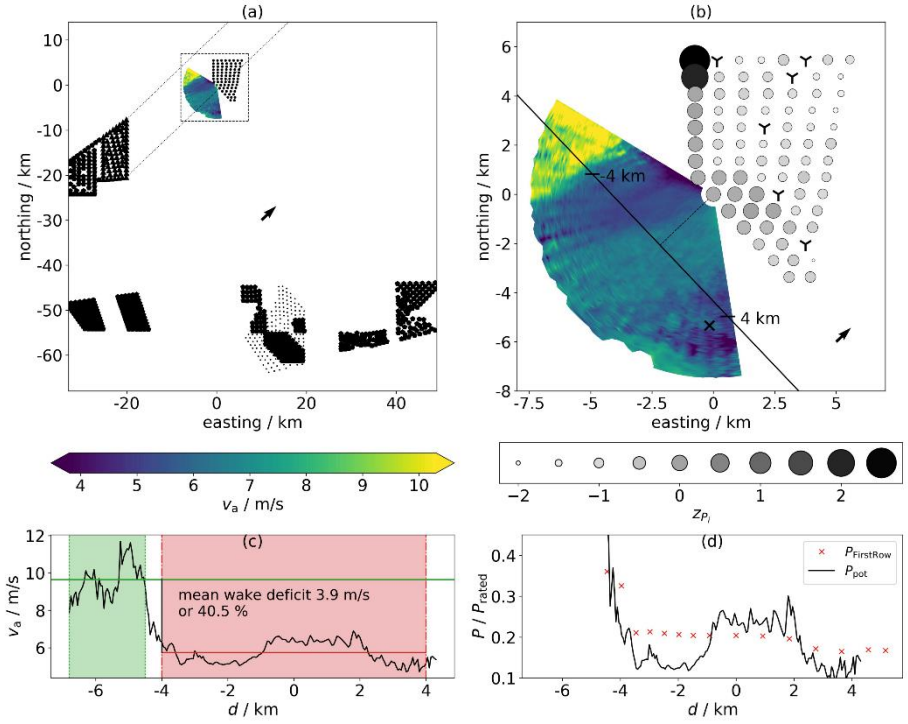


Figure 2: a) Wind farm GTI with surrounding wind farms and clusters and an upstream lidar scan. b) Zoom in on the wind farm GTI with upstream lidar scan and the z-score of the turbines power in grayscale. c) Wind speed on a virtual wake cut depicted in b). d) Available power on hub height along the wake cut together with the power from the upstream turbines.

In conclusion, we summarize that long range lidar is a valuable tool to study wind farm effects and to provide verification data for numerical wind farm flow models. The parametrization and verification of long reaching cluster wake effects and the global wind farm blockage effect is crucial for an efficient use of the limited offshore space for wind energy deployment.

References:

[1] Platis, A., Siedersleben, S. K., Bange, J., Lampert, A., Bärfuss, K.,Hankers, R., Cañadillas, B., Foreman, R., Schulz-Stellenfleth, J.,Djath, B., Neumann, T., and Emeis, S.: First in situ evidence of wakes in the far field behind offshore wind farms, Scient. Rep., 8, 2163, https://doi.org/10.1038/s41598-018-20389-y, 2018.
[2] Schneemann, J., Rott, A., Dörenkämper, M., Steinfeld, G., and Kühn, M.: Cluster wakes impact on a far-distant offshore wind farm's power, Wind Energy Science, 5, 29–49, https://doi.org/10.5194/wes-5-29-2020, 2020.
[3] Bleeg, J., Purcell, M., Ruisi, R., and Traiger, E.: Wind Farm Blockage and the Consequences of Neglecting Its Impact on Energy Production, Energies, 11, 1609, https://doi.org/10.3390/en11061609, 2018.
[4] Porté-Agel, F., Bastankhah, M., and Shamsoddin, S.: Wind-Turbine and Wind-Farm Flows: A Review, Boundary-Layer Meteorology, 174, 1–59, https://doi.org/10.1007/s10546-019-00473-0, 2019.
[5] Hasager, C., Vincent, P., Badger, J., Badger, M., Bella, A. D., Peña, A., Husson, R., and Volker, P.: Using Satellite SAR to Characterize the Wind Flow around Offshore Wind Farms, Energies, 8, 5413–5439, https://doi.org/10.3390/en8065413, 2015.
[6] Nygaard, N. G. and Newcombe, A. C.: Wake behind an offshore wind farm observed with dual-Doppler radars, J. Phys.: Conf. Ser., 1037, 072008, https://doi.org/10.1088/1742-6596/1037/7/072008, 2018.
[7] Nygaard, N. G., Steen, S. T., Poulsen, L., and Pedersen, J. G.: Modelling cluster wakes and wind farm blockage, J. Phys.: Conf. Ser., 1618, 062072, https://doi.org/10.1088/1742-6596/1618/6/062072, 2020
[8] Schneemann, J., Theuer, F., Rott, A., Dörenkämper, M., and Kühn, M.: Offshore wind farm global blockage measured with scanning lidar, Wind Energ. Sci. Discuss. [preprint], https://doi.org/10.5194/wes-2020-124, in review, 2020a.

Efficiencies of offshore wind farms in northern Europe: assessment of the performance of actual wind farms understood in the context of findings from modelling and idealized studies

Alexander Newcombe[1,*], Jake Badger[2], and Marc Imberger[2]
[1]Danish Energy Agency
[2]Technical University of Denmark
[*]Presenting author

Keywords: Offshore wind | Wind farm efficiency | Wind farm wakes | Capacity factor

Since Vindeby Offshore Wind Farm was installed in the south east of Denmark in 1991, increasingly more offshore wind farms are being installed each year in Northern Europe and around the world.
The efficiency of 62 wind farms in Northern Europe with a cumulative capacity of over 15.5 GW are assessed in this paper. The method uses a novel way of estimating the nominal energy production based on capacity factor data from the Global Wind Atlas. The efficiency is defined by the realized energy production as a fraction of the nominal energy production if there were no losses due to wakes and blockage effects. Realized energy production is obtained for each wind farm on a monthly basis from Wood Mackenzie. Losses due to wind farm cluster wakes and blockage are important to understand and model correctly, as highlighted by Nygaard et al (2020), in order to avoid overestimates of wind farm performance in the project development phase.
The efficiency calculated is dependent on several aspects, such as the power curve of the turbines used, capacity density of the wind farm, area of the wind farm, as well as wakes from neighboring wind farms, and other losses. The results presented in this paper show a loosely inversely proportional relationship between the capacity density of the wind farm and the efficiency, and wind farm size (Figure 1). This relationship is also assessed with regards to distance to neighboring wind farms. The paper also presents a statistical analysis of the wind farms to make some predictive assessment of wind farm efficiencies according to their basic properties such as area and density.

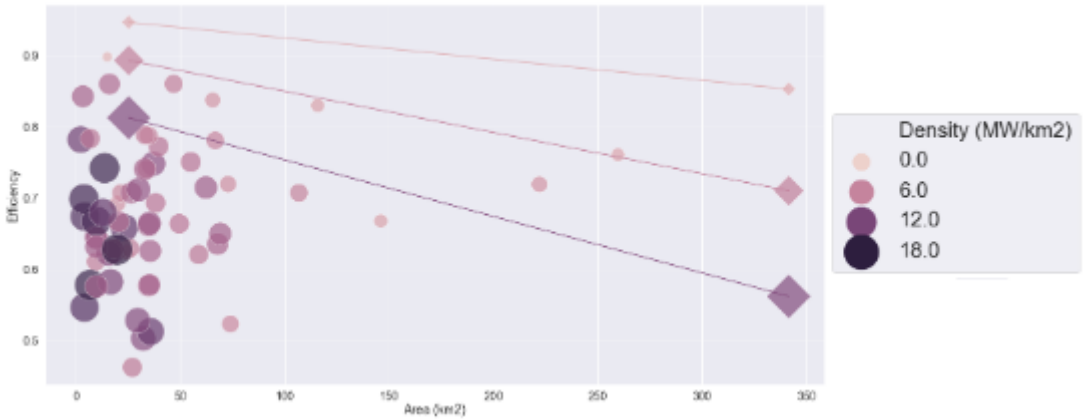


Figure 1: Circles represent empirical data (wind farms) while diamonds represent theoretical data from Volker et al (2017). Both colour and size of the markers represent capacity density [MW/km2]

The results also show that the realized efficiencies are lower than that of more idealized modelling studies (Volker et al, 2017), most likely due to wakes and blockage from neighboring wind farms (as well as from losses due to availability, electrical efficiencies and curtailments). For this reason the distance between wind farms is also assessed, to test the impact that this has on the efficiency.
Suggested ways to account for these additional reductions in wind farm efficiency are proposed. The additional efficiency reduction aspects are also tested on the published efficiency data from "Making the most

of Offshore Wind Agora Report" (2020). These data are from WRF simulations using the EWP scheme and give performance data for 20 large to very large wind farms in future scenarios for the German Bight.
The paper concludes with some policy implications, such as the need for enhanced coordination in the planning and development of offshore wind. This coordination needs to be across neighboring projects, and neighboring countries, to ensure planning and development of offshore wind in built-up areas such as northern Europe is done in a fair an efficient manner.

References:
Nygaard, N.G., Steen, S.T., Poulsen, L. and Pedersen, J.G., 2020, September. Modelling cluster wakes and wind farm blockage. In Journal of Physics: Conference Series (Vol. 1618, No. 6, p. 062072). IOP Publishing.
Volker, P.J., Hahmann, A.N., Badger, J. and Jørgensen, H.E., 2017. Prospects for generating electricity by large onshore and offshore wind farms. Environmental Research Letters, 12(3), p.034022.
Making the Most of Offshore Wind: Re-Evaluating the Potential of Offshore Wind in the German North Sea, 2020: Technical University of Denmark and Max-Planck Institute: Making the Most of Offshore Wind: Re-Evaluating the Potential of Offshore Wind in the German North Sea. Study commissioned by Agora Energiewende and Agora Verkehrswende. https://www.agora-energiewende.de/en/publications/making-the-most-of-offshore-wind/ Wood Mackenzie, 2020, Offshore Wind Power Production.

Wind farm wake effects at the Alpha Ventus offshore wind farm

Vasilis Pettas[1,*], Matthias Kretschmer[1], Andrew Clifton[1,2], and Po Wen Cheng[1]
[1]University of Stuttgart
[2]Stuttgart Wind Energy (SWE)
*Presenting author

Keywords: wind farm wakes | wakes | farm interactions | cluster wakes

As wind energy grows to a significant contributor in the electricity production mix, the number of wind farms with large turbines, especially offshore, increases as well. This leads to wind farms being built closer to each other in order to increase the spatial power density. The close proximity of these farm arrays has been shown to create wake effects which have impacts on the power production and the loading of the downstream farms (Nygaard and Hansen, 2016; Ahsbahs et al., 2020). The research community as well as industry have shown a lot of interest in the recent years to understand, quantify and model these phenomena as they have both financial and technical impacts (Lundquist et al., 2019).
In this work we present measurement data from the Alpha Ventus wind farm site (Alpha Ventus homepage). Alpha Ventus (AV) is the first German offshore wind farm operating at the North Sea since 2010. A large amount of data has been gathered since, with the RAVE research consortium managing research activities there. Alpha Ventus consists of 12 5MW turbines. Moreover, just in front of the farm there is a large, fully equipped meteorological mast, FINO1, gathering data since the preconstruction period. Since 2015 more wind farms have been constructed and commissioned in the close proximity to AV (in distances from 1.5 to 10 km) with similar size turbines but much larger in terms of total capacity. An overview of the site is given in fig1.

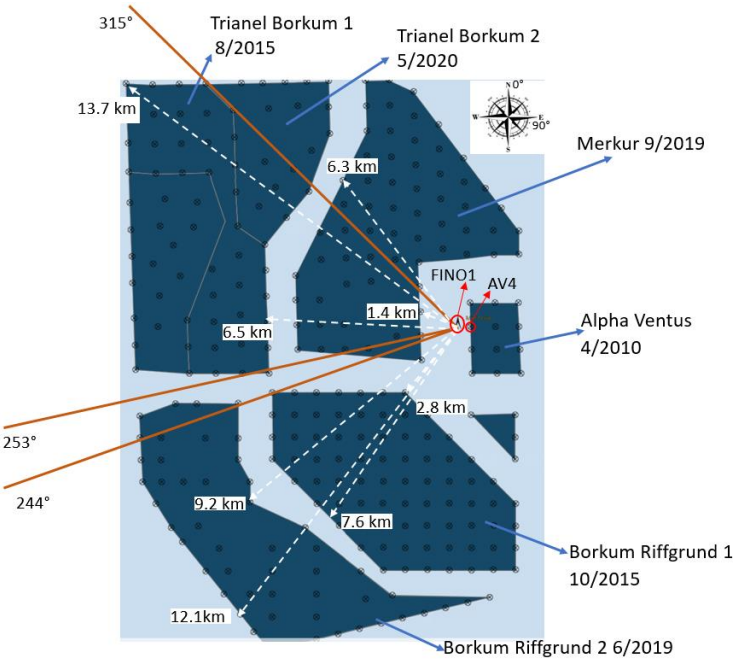


Figure 1: Schematic representation of Alpha Ventus and the neighboring wind farms along with the relative distances to FINO1, the relevant directions to FINO1 and the date they started operating

This setup gives us the unique opportunity to investigate the effects, over the years, on the local wind conditions and the turbine response as the surrounding changed from free stream conditions to operating wind farms. In this work we will present measurement data from FINO1 and the AV turbine in the direct vicinity for the period 2011-2019. The goal is to quantify the effects of the wakes of the new farms that started operating in different points in time and different distances from AV as well as to provide a comprehensive overview of the metocean conditions at the site over the years.

The results that will be shown are divided in two topics. First, effects on the environmental conditions (relevant to wind turbine operation) as they are measured by FINO1. For this, we analyse on a yearly basis: the wind speed magnitude per direction and cumulatively, the direction probability, the turbulence intensity per direction and mean wind speed (as seen in fig. 2), the wind shear per direction, the sea wave measures of peak period and significant height as well as the temperature and pressure. Second, we investigate how these changes impact the measured tower structural loads per wind speed and per direction.

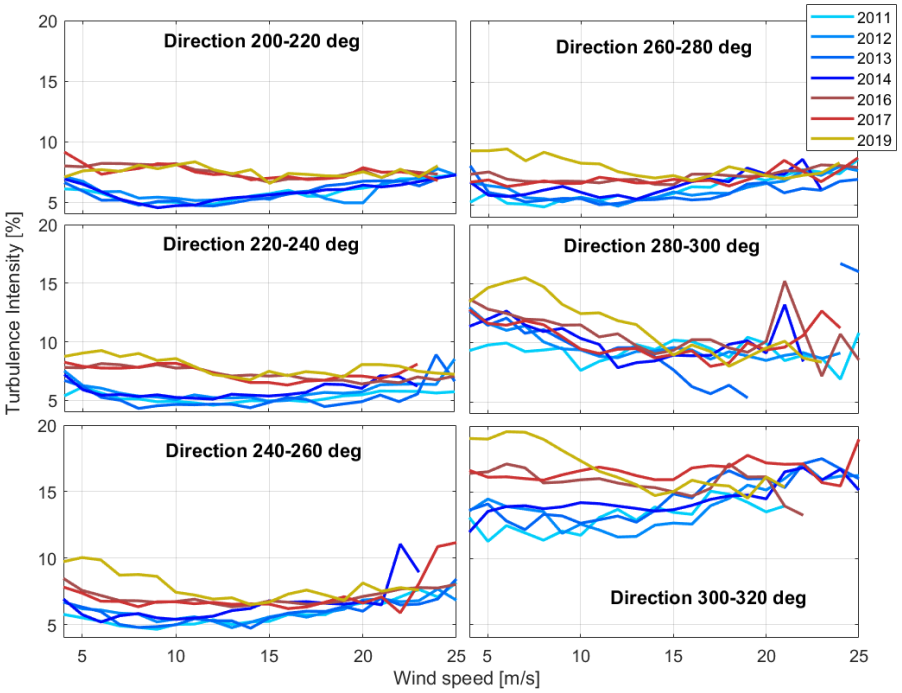


Figure 2: Turbulence intensity measured at FINO1 at hub height (90m) for different directional sectors and years. Shades of blue indicate years where AV is the only operating farm. Wind speeds are binned in 1m/s intervals and the TI values shown are the mean of each bin

The work presented here is based on a paper to be submitted to the Wind Energy Science journal within the following months.

References:

Alpha Ventus homepage (no date). Available at: https://www.alpha-ventus.de/english (Accessed: 1 December 2020).

Lundquist, J. K. et al. (2019) 'Costs and consequences of wind turbine wake effects arising from uncoordinated wind energy development', Nature Energy. Springer US, 4(1), pp. 26–34. doi: 10.1038/s41560-018-0281-2.

Ahsbahs, T. et al. (2020) 'Wind Farm Wakes from SAR and Doppler Radar', Remote Sensing, 12(3), p. 462. doi: 10.3390/rs12030462.

Nygaard, N. G. and Hansen, S. D. (2016) 'Wake effects between two neighbouring wind farms', Journal of Physics: Conference Series, 753(3), p. 032020. doi: 10.1088/1742-6596/753/3/032020.

Offshore wakes in the US East coast lease areas

R.J. Barthelmie, T.J. Shepherd, and S.C. Pryor
Cornell University

Keywords: Offshore | Wakes | WRF | Arrays

The eastern US states (CT, DE, ME, MD, MA, NH, NJ, NY, NC, PA, RI and VI) have technical offshore wind energy potential of over 2000 GW. The current total U.S. offshore wind pipeline is over 26 GW and much of the development is focused on 16 active lease areas off the eastern seaboard of these states that cover over 7000 km^2. The implication is that a very large number of wind turbines will be constructed in arrays with relatively moderate spacing between individual wind turbine and individual arrays.
To assess the magnitudes of likely wind turbine wake losses for the east coast lease areas a suite of WRF simulations have been performed for the nested domains shown in Figure 1. The outer domain comprises 110x110 16.67 km grid cells nested down to the middle domain of 210x210 5.56 km and the inner domain of 300x300 1.8 km grid cells. There are 57 layers in the vertical. The framework employed in the analyses to optimally quantify wake impacts on wind speeds while reducing computational redundancy is to simulate a number of wake scenarios that can be assembled into a wake climatology. The 11 five-day periods selected represent over 75% of wind speeds and directions as determined from 40 years of ERA5 data. Given that information regarding selected turbines and layouts is not yet available we use the IEA 15 MW reference turbine with hub-height of 150 m and rotor diameter of 240 m. The turbine spacing is 1.8 km in all simulations, as this has been agreed on for the seven northern most lease areas. This gives approximately 2000 turbine locations for the simulations.

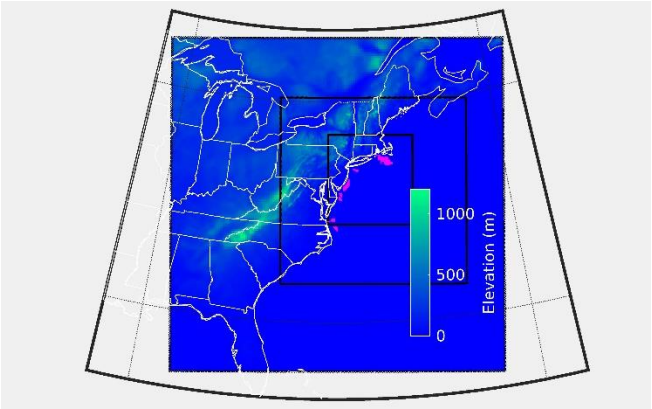


Figure 1: The three nested WRF domains (indicated by the black boxes) and the 16 offshore lease areas indicated in magnolia. Some of the lease areas are in blocks – e.g. there are 7 lease areas in the block to the south of Massachusetts.

The three-dimensional flow output from each 10-minute period in each five-day simulation is used to characterize the wake extent and intensity. The velocity deficit in the wake is computed for each grid cell as the normalized difference in the wind speed from the WRF simulations with the Fitch parameterization turned on (WT) and with the Fitch parameterization turned off (noWT). The mean wake intensity for a five day period in October 1979 under northwesterly winds with freestream wind speeds between 4 and 10 ms^{-1} is shown in Figure 2. Figure 2a shows the QKE (2*turbulent kinetic energy) with the offshore lease areas having QKE which is about 50% higher than the surrounding offshore areas. Elevated QKE is not advected over large distances. Conversely, as shown in Figure 2b the velocity deficit in the wake extends over much larger distances. The mean (time averaged) normalized velocity deficit within the lease areas are about 10% and the downwind wake extends for well over 50 km beyond the edge of the lease areas where the wind turbines are located.

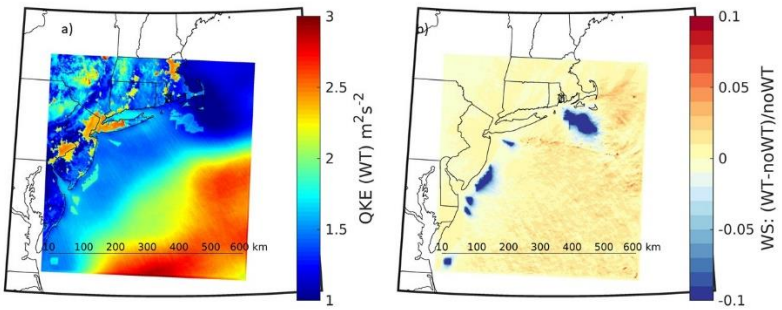


*Figure 2: WRF simulations for a five day period in October 1979. Figure 2a shows the mean QKE (=2*turbulent kinetic energy) from the WT simulations and Figure 2b the mean normalized velocity deficit.*

We will present results for both the individual wake simulations and for the assimilated wake climatology.

Mini-Symposium: Array-array interactions and downstream wake effects (II)

20% of US electricity from onshore wind: Impacts on wakes, system efficiency and regional Climate

S.C. Pryor*, R.J. Barthelmie, and T.J. Shepherd
Cornell University
*Presenting author

Keywords: Wakes | Repowering | Near-surface climate | System efficiency

U.S. wind generated electricity grew by from 182 TWh in 2014, to 191 TWh in 2015, 227 TWh in 2016, 254 TWh in 2017, 275 TWh in 2018 and 295 TWh in 2019 (data from https://www.eia.gov/energyexplained/electricity/electricity-in-the-us-generation-capacity-andsales.php).
Continued expansion of U.S. installed generation capacity is likely to be achieved via a combination of: (a) Repowering i.e. replacing aging turbines or components with newer turbines that typically have larger rated capacity and physical dimensions. Expansion of deployment locations (b) onshore and/or (c) offshore. Repowering generally requires less capital cost than development of new projects, and investment in repowering could grow to $25 billion (in 2012 US$) by 2030 (Lant et al. 2013). Thus, it is fruitful to consider the implications of larger-scale repowering on system efficiency and downstream climate effects.
Here we undertake an analysis using the Weather Research and Forecasting model with the Fitch wind farm parameterization. In our analyses, the installed capacity of the wind turbine (WT) fleet at existing deployment locations in the eastern USA is doubled or quadrupled from an initial installed capacity (IC, as of 2014) of 31 GW via repowering. There are four simulations for each year; a simulation without wind turbines, with the 2014 fleet (1WT), for the doubling of IC (2WT) and for the quadrupling of IC (4WT). The initial simulation for 2014 uses the actual wind turbine locations (Figure 1) and specifications (hub-height, rotor, rated power, power and thrust curves) for each individual wind turbine.

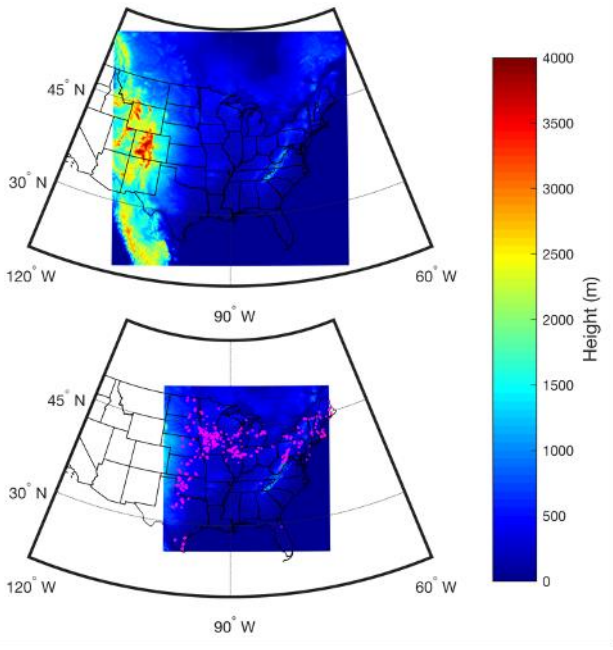


Figure 1: Terrain elevation in outer domain (above, 12 km grid resolution) and the inner domain (below 4 km grid resolution). WRF grid cells with one or more wind turbines present as of the end of 2014 are shown in magenta

In the doubling scenario, all WT that have a rated capacity < 2.1 MW are replaced with a 3 MW and those with a rated capacity > 2.1 MW are replaced with a 5.2 MW turbines. The quadrupling scenario replaces 3 MW machines with 8.2 MW turbines and holds constant the 5.2 MW wind turbines from the doubling scenario. Because wind climates and thus likely wind turbine wakes effects exhibit substantial year-to-year variability the simulations are performed for two twelve month periods; 2008 and 2015/2016 (Pryor et al. 2020). Simulation output is analyzed in order to address two research questions: First, do any areas of the eastern USA appear to reach saturation of the harnessable wind resource? Second, do either power losses due to wakes and/or near-surface local climate perturbations due to wakes substantially increase under the 2WT or 4WT scenarios?

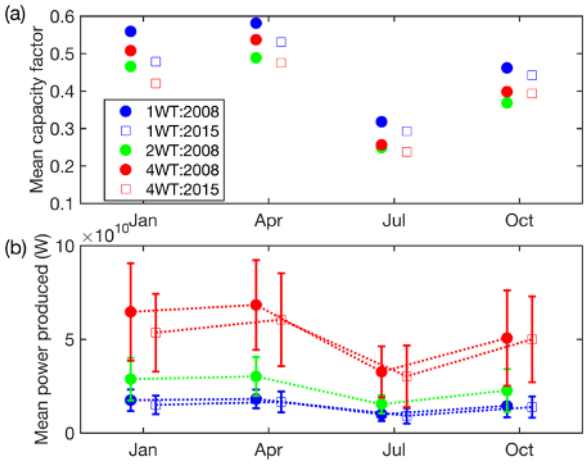


Figure 2: Mean monthly WT (a) capacity factors and (b) power production based on 10-minute power output as simulated for January, April, July and October of 2008 and 2015/2016 for the 3 WT deployment scenarios. Vertical bars in (b) denote 1 standard deviation around the mean value computed using the 10-minute power output time series.

Our results show that under the scenario of quadrupled installed capacity there is a small decrease in system-wide efficiency exhibited by annual mean capacity factor (CF) (Figure 2). For example, the gross CF for January 2008 is 56 and 48% for January 2016 for the 1WT scenario. This difference of 8% is larger than the difference between gross CF for the 1WT and 4WT scenarios in either January 2008 or 2016 (5 and 6%, respectively). Thus, although some individual grid cells in the 4WT repowering scenario are likely to be close to the limit at which maximum kinetic energy extraction occurs, power production from the entire system remains at relatively high efficiency levels. The simulated impact on near-surface climate properties at both the regional and local scales does not scale with increasing wind turbine installed capacity because the larger machines are displaced further from the surface and operate more efficiently. Thus, repowering actually results in smaller impacts on nearsurface climate close to major wind turbine arrays.

References:

Lantz, E., Leventhal, M., & Baring-Gould, I. (2013). Wind power project repowering: financial feasibility, decision drivers, and supply chain effects (No. NREL/TP-6A20-60535). National Renewable Energy Lab.(NREL), Golden, CO (United States).

Pryor S.C., Barthelmie R.J. and Shepherd T.J. (2020): 20% of US electricity from wind will have limited impacts on system efficiency and regional climate. Nature: Scientific Reports 10 541 doi:10.1038/s41598-019-57371-1

Simulating wind plant wakes in WRF: role of added turbulence kinetic energy

Julie K. Lundquist[1,3], Nicola Bodini[3], and Patrick Moriarty[3]
[1]University of Colorado at Boulder
[2]Renewable and Sustainable Energy Institute
[3]National Renewable Energy Laboratory

Keywords: wake | mesoscale | wind farm parameterization | turbulence

Wind farms affect their local environments. They remove momentum from the flow, introducing wakes. Wake signatures emerge in satellite observations of offshore wind farms (Christiansen and Hasager, 2006). Power production in downwind wind farms is affected (Nygaard, 2014; Nygaard and Hansen, 2016). Airborne measurements document the formation and propagation of wakes (Platis et al., 2018; Siedersleben et al., 2018, 2020). Remote sensing measurements, such as radar (Hirth and Schroeder, 2013; Nygaard and Newcombe, 2018) and lidar also document the wind speed deficit induced by wakes.

To predict and manage wakes in regions with multiple wind farms, parameterizations of wind farm effects in numerical weather prediction models can be helpful. The Weather Research and Forecasting (WRF) model includes a wind farm parameterization, originally defined by Fitch et al. (2012) with subsequent modifications introduced (Jiménez et al., 2015; Archer et al., 2020). The wind farm parameterization imposes a drag effect as well as additional turbulence kinetic energy (TKE) production; Xia et al. (2019) identify the competing roles of drag and TKE in the downwind impacts of wind farms.

Here we test the impact of the most recent option (Archer et al., 2020), which allows modification of the amount of TKE added by wind farms. The original parameterization calculated the turbine-added TKE as the fraction of kinetic energy removed from the atmosphere multiplied by the difference between the power coefficient and the thrust coefficient. Originally, 100% of this difference was devoted to the generation of TKE by the turbines; Archer et al. (2020) recommend only 25%. Our simulation setup follows the recommendations of Tomaszewski and Lundquist (2020), including 3-km horizontal resolution and nominally 10 m vertical resolution near the surface and throughout the wind turbine rotor region. We focus on a region in central North America with nearly 1000 turbines deployed (Figure 1): this region will be the focus of an extensive wind farm observational campaign, the US Dept. of Energy's AWAKEN field study. We use WRF model version 4.2.1 and the Wind Farm Parameterization, and consider a ten day case study in June 2018, marked by frequent low-level jets and southerly wind flow such that the wakes propagate to the north, to a site monitored by a lidar.

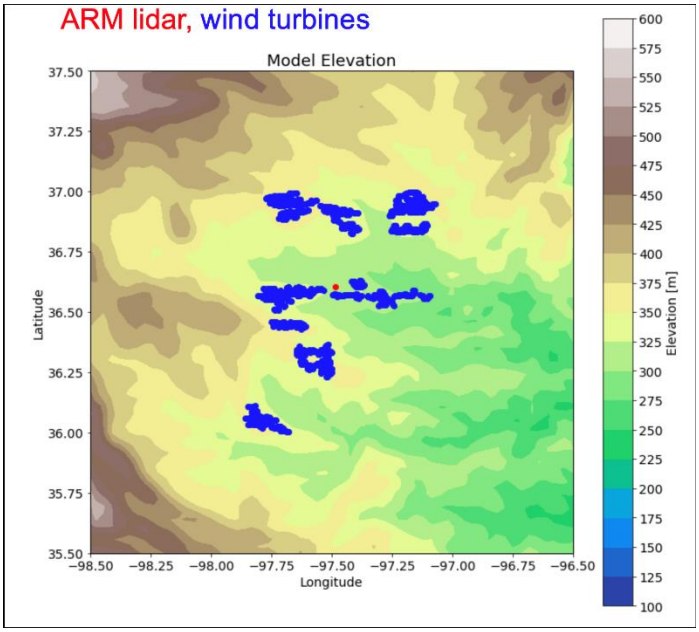


Figure 1: Map of the region with turbines in blue and the DOE ARM lidar at the ARM Central Facility in red. Contours are elevation above sea level.

Changing the turbine-added TKE introduces subtle differences in the simulations (Figure 2) at a location 3.5 km downwind of a cluster of wind turbines. (This location is of interest due to the presence of a lidar providing wind profiles.) Notably, the wake-induced acceleration under the wind turbine rotor disk disappears in the 25% TKE simulations. The magnitude of the wake in unstable conditions is unchanged at hub height and below, but the magnitude of the wake aloft is eroded in the simulation with less TKE. In stable conditions, the magnitude of the wake wind speed deficit is larger at hub height and below, but the wake wind speed deficit is smaller above hub height.

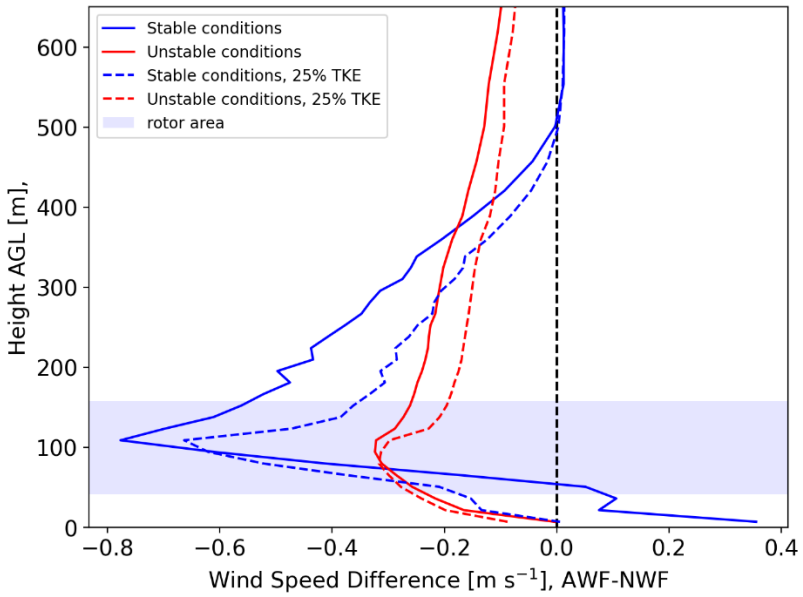


Figure 2: Median wind speed difference between simulations with and without the wind farms in stable (blue) and unstable (red conditions) at the location of the DOE ARM lidar for stable and unstable conditions. Solid lines are simulations with 100% TKE added; dashed lines are 25% TKE. The blue shaded area shows the vertical limits of the turbine rotor disks.

References:

Archer, C. L. et al. (2020) 'Two Corrections for Turbulent Kinetic Energy Generated by Wind Farms in the WRF Model', Monthly Weather Review, 148(12), pp. 4823–4835. doi: 10.1175/MWR-D-20-0097.1.

Christiansen, M. B. and Hasager, C. B. (2006) 'Using airborne and satellite SAR for wake mapping offshore', Wind Energy, 9(5), pp. 437–455. doi: 10.1002/we.196.

Fitch, A. C. et al. (2012) 'Local and Mesoscale Impacts of Wind Farms as Parameterized in a Mesoscale NWP Model', Monthly Weather Review, 140(9), pp. 3017–3038. doi: 10.1175/MWR-D-11-00352.1.
Hirth, B. D. and Schroeder, J. L. (2013) 'Documenting Wind Speed and Power Deficits behind a Utility-Scale Wind Turbine', Journal of Applied Meteorology and Climatology, 52(1), pp. 39–46. doi: 10.1175/JAMC-D-12-0145.1.
Jiménez, P. A. et al. (2015) 'Mesoscale modeling of offshore wind turbine wakes at the wind farm resolving scale: a composite-based analysis with the Weather Research and Forecasting model over Horns Rev: Mesoscale modeling at the wind farm resolving scale', Wind Energy, 18(3), pp. 559–566. doi: 10.1002/we.1708.
Nygaard, N. G. (2014) 'Wakes in very large wind farms and the effect of neighbouring wind farms', Journal of Physics: Conference Series, 524(1), p. 012162. doi: 10.1088/1742-6596/524/1/012162.
Nygaard, N. G. and Hansen, S. D. (2016) 'Wake effects between two neighbouring wind farms', Journal of Physics: Conference Series, 753(3), p. 032020. doi: 10.1088/1742-6596/753/3/032020.
Nygaard, N. G. and Newcombe, A. C. (2018) 'Wake behind an offshore wind farm observed with dual-Doppler radars', Journal of Physics: Conference Series, 1037, p. 072008. doi: 10.1088/1742-6596/1037/7/072008.
Platis, A. et al. (2018) 'First in situ evidence of wakes in the far field behind offshore wind farms', Scientific Reports, 8(1), p. 2163. doi: 10.1038/s41598-018-20389-y.
Siedersleben, S. K. et al. (2018) 'Micrometeorological impacts of offshore wind farms as seen in observations and simulations', Environmental Research Letters, 13(12), p. 124012. doi: 10.1088/1748-9326/aaea0b.
Tomaszewski, J. M. and Lundquist, J. K. (2020) 'Simulated wind farm wake sensitivity to configuration choices in the Weather Research and Forecasting model version 3.8.1', Geoscientific Model Development, 13(6), pp. 2645–2662. doi: https://doi.org/10.5194/gmd-13-2645-2020.
Xia, G. et al. (2019) 'Simulating impacts of real-world wind farms on land surface temperature using the WRF model: physical mechanisms', Climate Dynamics, 53, pp. 1723–1739. doi: 10.1007/s00382-019-04725-0.

Sensitivity of wind turbine wake effects and array-array interactions to wind farm parameterization and model resolution

Tristan Shepherd*, R.J. Barthelmie, and S.C. Pryor
Cornell University
*Presenting author

Keywords: Wind farm wakes | System efficiency | Fitch parameterization | Explicit wake parameterization | Weather Research and Forecasting Model

The Weather Research and Forecasting (WRF) model is a type of regional model suitable for studies of wind climates, energy production, and examining potential array-array interactions and climate effects from large wind turbine deployments. A wind farm parameterization represents the effects of wind turbines on the atmosphere. There is currently one such scheme publicly available for use in WRF (Fitch [Fitch et al. 2012]), and the Explicit Wake Parameterization (EWP, [Volker et al. 2015]) that is used in this study, but not yet widely available.

In the beginning of the presentation, we present results from three WRF simulations centered over the state of Iowa, which currently has the highest density of wind turbine installed capacity of any state in the United States. We assess sensitivity of climate and power losses to the selected wind farm parameterization scheme and, in doing so to achieve the second objective of quantifying the effects of array-array interactions resulting from the different representations in each scheme. The third objective is to quantify the sensitivity of any array-array interactions to model horizontal and vertical resolution. Thus, one simulation has 4 km inner-domain resolution with 41 vertical levels, another has 2 km resolution with 41 levels, and the third has 4 km resolution with 57 vertical levels.

Real wind turbine locations and wind turbine power and thrust curves are used. Each simulation runs for 9 consecutive calendar months such that three full seasonal cycles are simulated.

Results from the 4 km, 41 levels simulation show that on average, use of EWP results in smaller wake effects within wind farm arrays than the Fitch scheme. Faster wake recovery in EWP is also observed compared to the Fitch scheme (Figure 1) (Shepherd et al. 2020). This results in smaller near-surface climate impacts when the EWP parameterization is used. Capacity factors are 2 – 3 % higher in EWP than in Fitch. When model horizontal resolution is increased from 4 km to 2 km, the spatial extent of the wind farm wakes is generally reduced. This is also true for increasing the number of model vertical levels. Another relevant finding from increased vertical resolution is that increased wind speeds around wind turbine hub height result from higher vertical fidelity in the model grid, which leads to higher wind turbine power production (Pryor et al. 2020).

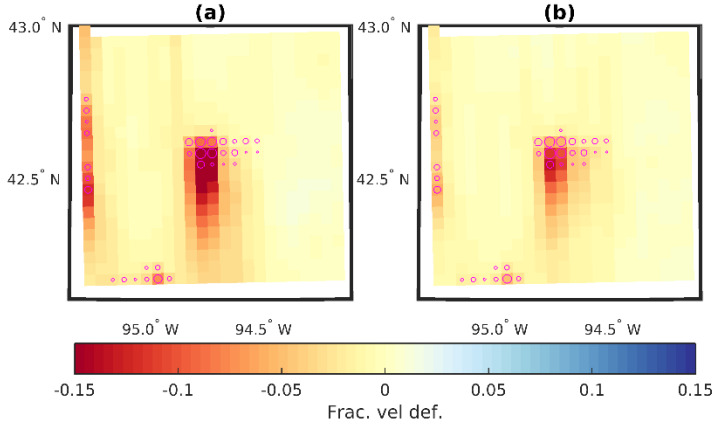


Figure 1: Mean normalized (fractional) velocity deficit at the Pomeroy wind farm cluster (located in Iowa) for (a) Fitch and (b) EWP from the third model layer (~100 m AGL). The magenta circles indicate installed capacity in each 4-km grid cell.

A coding error was recently discovered in the original formulation of the Fitch parameterization that meant wind turbine induced TKE was not being advected. A new release was made to correct that error and that also greatly reduces the added TKE (Archer et al. 2020). Thus, a fourth and fifth simulation were performed over the same domain for a two-week period in July in which the original Fitch parameterization and then a version with the new formulation are implemented to determine the impact of the revised formulation. The results indicate, lower QKE (twice TKE in the MYNN scheme) in grid cells with wind turbines, but otherwise a complex patchwork of differences in terms of power, wind speed and QKE (Figure 2). Further, the total domain wide power post-bug-fix is 96.5% of pre-bug-fix implying the new version of Fitch may be generating results that are more different from EWP.

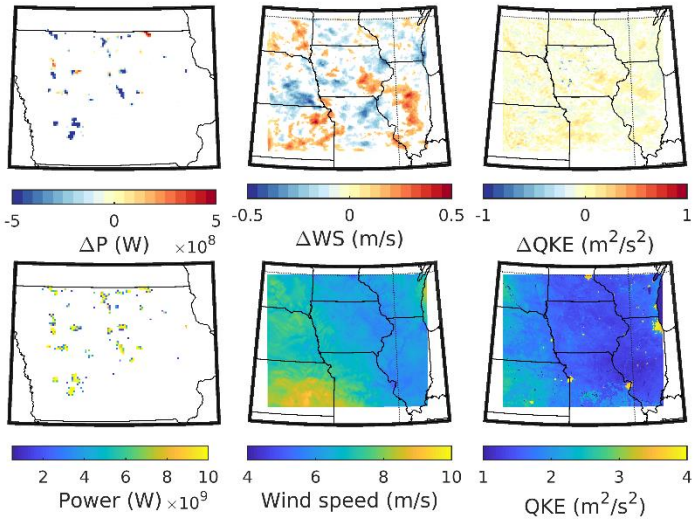


Figure 2: Comparison of pre-and-post Fitch bug-fix output for 2 simulated weeks in July. The top panel shows the difference in each variable (post-bug-fix minus pre-bug-fix) for power (P), wind speed (WS), and twice TKE from MYNN (QKE). Differences are only plotted if significant at the 95% confidence interval. The bottom panel shows the absolute values for sum of power, mean wind speed, and mean QKE.

Research funded by USDoE (DE-SC0016438 and DE-SC0016605). Computing from NSF (ACI-1541215, TG-ATM170024) and DoE (DE-AC02-05CH11231).

References:

Archer C. L., Wu S., Ma Y., and Jiménez P. A. (2020): Two corrections for turbulent kinetic energy generated by wind farms in the WRF model. Monthly Weather Review, 148(12), 4823-4835.

Fitch A. C., Olson J.B., Lundquist J.K., Dudhia J., Gupta A.K., Michalakes J., and Barstad I., (2012): Local and mesoscale impacts of wind farms as parameterized in a mesoscale NWP model. Monthly Weather Review, 140, 3017–3038.

Pryor S.C., Shepherd T.J., Volker P., Hahmann A.N. and Barthelmie R.J. (2020): 'Wind theft' from onshore wind turbine arrays: Sensitivity to wind farm parameterization and resolution. Journal of Applied Meteorology and Climatology 59, 153-174.

Shepherd T.J., Barthelmie R.J. and Pryor S.C. (2020): Sensitivity of wind turbine array downstream effects to the parameterization used in WRF. Journal of Applied Meteorology and Climatology 59, 333-361.

Volker P. J. H., Badger, J., Hahmann, A.N, and Ott S. (2015): The Explicit Wake Parametrization V1.0: A wind farm parametrization in the mesoscale model WRF. Geoscientific Model Development, 8, 3715–3731.

Integration of a 3D Planetary Boundary Layer Scheme and the Fitch Wind Farm Parameterization

Alex Rybchuk[1,*], Timothy W. Juliano[2], Julie K. Lundquist[1,3], Pedro A. Jimenez[2], Branko Kosovic[2], and Mike Optis[3]
[1]University of Colorado Boulder
[2]National Center for Atmospheric Research
[3]National Renewable Energy Laboratory
[*]Presenting author

Keywords: Wind farm parameterization | Turbulent kinetic energy | Planetary boundary layer scheme

While it is known that wind farms impact local meteorology, there is debate on how to best parameterize these effects within numerical weather prediction (NWP) models. The debate on NWP wake models focuses two central topics: the magnitude of wind speed deficits as well as the magnitude of turbulent kinetic energy (TKE) production. The Fitch et al. (2012) parameterization, incorporated in the public distribution of the Weather Research and Forecasting (WRF) model, prescribes a wind speed deficit based on the wind turbine thrust coefficient. It also defines TKE production based on the energy left over from the wind speed reduction and electricity generation.

Other parameterizations, such as the Explicit Wake Parameterization (EWP, Volker et al. 2015), do not explicitly generate TKE but assume that sufficient TKE develops from shear associated with the wind speed deficit. LES-based and observation-based studies have suggested that the Fitch parameterization produces too much TKE (Abkar and Porté-Agel 2015, Vanderwende et al. 2016, Siedersleben et al. 2020). Recent work by Archer et al. (2020) introduced the option to reduce TKE production through the introduction of an empirical coefficient into the Fitch scheme as implemented in WRF.

In tandem with this discussion on wind farm parameterizations, researchers have noted that NWPbased pre-construction wind resource assessments (i.e. those without wind farms present) tend to show significant sensitivity to the choice in planetary boundary layer (PBL) parameterization. For example, Optis et al. (2020) recently conducted a sensitivity study in offshore California, finding that annual-averaged hub-height winds are sensitive to PBL scheme in this region: the Mellor–Yamada–Nakanishi–Niino (MYNN) scheme showed winds nearly 1 m/s stronger than the Yonsei State University (YSU) scheme.

To date, the Fitch parametrization has only been coupled with the MYNN PBL scheme. In order to study the sensitivity of this wind farm parameterization to PBL scheme, we integrated the Fitch wind farm parameterization with a novel three-dimensional (3D) PBL scheme (Kosović et al. 2020). This scheme has been designed to better simulate winds in horizontally inhomogeneous conditions characteristic of flows in complex terrain and offshore flows with heterogenous surface conditions such as sea-surface temperature. In addition to the fully 3D PBL scheme, we also integrate the Fitch parameterization with a 1D analogue of this scheme. This scheme parallels the 1D behavior of the MYNN scheme, while also employing different approaches to calculate key quantities such as the characteristic length scale and closure constants.

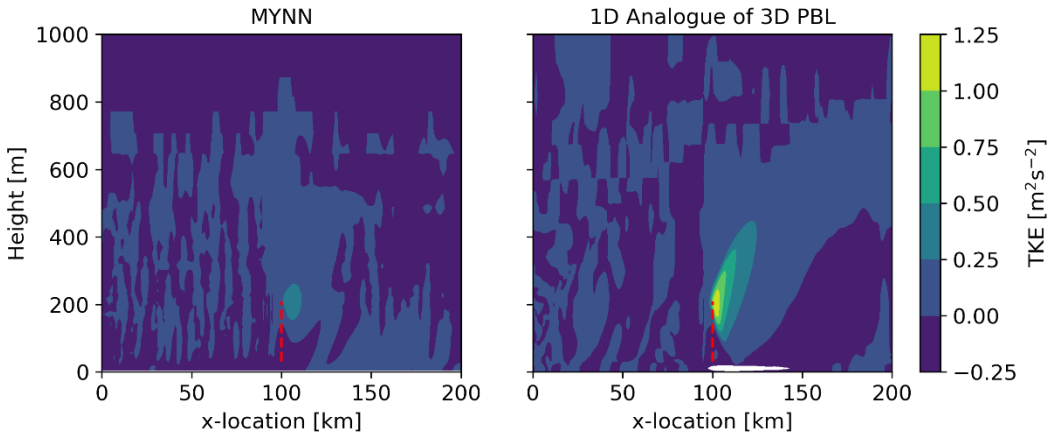


Figure 1: TKE production in the MYNN PBL scheme (left) and 1D analogue of the 3D PBL scheme (right) when TKE production is turned off within the Fitch parameterization. The location of the wind turbine disk is marked by the red dashed line

Wakes produced in simulations with the 3D PBL scheme and 1D analogue differ from those produced in MYNN simulations. Using the case study of Fitch et al. (2012), we conduct several simulations of a farm of wind turbines under neutral stratification with different PBL schemes. For one set of comparisons, the TKE production coefficient is set to zero, eliminating explicit TKE production inside of the Fitch parameterization. As a result, the MYNN scheme only weakly produces TKE at the site of the wind farm (Figure 1 left). However, the 1D analogue to the 3D PBL simulation generates at least twice as much TKE in these conditions (Figure 1 right). Consistent with the pre-construction sensitivity analysis of Yang et al. (2017), this behavior shows that TKE production within the Fitch wind farm parameterization is sensitive to the particular turbulence closure approach.

References:

Abkar, M. and Porté-Agel, F. (2015) 'A new wind-farm parameterization for large-scale atmospheric models', Journal of Renewable and Sustainable Energy, 7(1), p. 013121. doi: 10.1063/1.4907600.

Archer, C. L. et al. (2020) 'Two corrections for turbulent kinetic energy generated by wind farms in the WRF model', Monthly Weather Review, pp. 1–38. doi: 10.1175/MWR-D-20-0097.1.

Fitch, A. C. et al. (2012) 'Local and Mesoscale Impacts of Wind Farms as Parameterized in a Mesoscale NWP Model', Monthly Weather Review, 140(9), pp. 3017–3038. doi: 10.1175/MWR-D-11-00352.1.

Kosović, B. et al. (2020) 'Three-Dimensional Planetary Boundary Layer Parameterization for High-Resolution Mesoscale Simulations', Journal of Physics: Conference Series, 1452, p. 012080. doi: 10.1088/1742-6596/1452/1/012080.

Optis, M. (ORCID:0000000156176134) et al. (2020) 2020 Offshore Wind Resource Assessment for the California Pacific Outer Continental Shelf. NREL/TP-5000-77642. National Renewable Energy Lab. (NREL), Golden, CO (United States). doi: 10.2172/1677466.

Siedersleben, S. K. (ORCID:0000000284671471) et al. (2020) 'Turbulent kinetic energy over large offshore wind farms observed and simulated by the mesoscale model WRF (3.8.1)', Geoscientific Model Development (Online), 13(1). doi: https://doi.org/10.5194/gmd-13-249-2020.

Vanderwende, B. J. et al. (2016) 'Simulating effects of a wind-turbine array using LES and RANS', Journal of Advances in Modeling Earth Systems, 8(3), pp. 1376–1390. doi: https://doi.org/10.1002/2016MS000652.

Volker, P. J. H. et al. (2015) 'The Explicit Wake Parametrisation V1.0: a wind farm parametrisation in the mesoscale model WRF', Geoscientific Model Development Discussions, 8(4), pp. 3481–3522. doi: 10.5194/gmdd-8-3481-2015.

Yang, B. et al. (2017) 'Sensitivity of Turbine-Height Wind Speeds to Parameters in Planetary Boundary-Layer and Surface-Layer Schemes in the Weather Research and Forecasting Model', Boundary-Layer Meteorology, 162(1), pp. 117–142. doi: 10.1007/s10546-016-0185-2.

Long-term impacts of wind farms on local meteorology

Nicola Bodini[1,*], Julie K. Lundquist[2,3], and Patrick Moriarty[1]
[1]National Renewable Energy Laboratory
[2]University of Colorado at Boulder
[3]Renewable and Sustainable Energy Institute
[*]Presenting author

Keywords: wakes | AWAKEN | SGP | long-term meteorology

Long-term weather and climate observatories may be affected by their changing environments, such as the growth of urban areas or changing vegetation. Wind plants can also impact the local atmospheric conditions through their wakes, characterized by reduced wind speed and increased turbulence. However, the effects of the wakes on local meteorological measurements are generally difficult to discern because the magnitude and orientation of the wind plant wake changes with wind speed, wind direction, and atmospheric stability. The United States Department of Energy Atmospheric Radiation Measurement Central Facility (ARM CF) near Lamont, Oklahoma, is located in a region optimal for wind energy development (see Figure 1). In our analysis, we explore if and how the wind plants which have been built in the region in the last decade have affected the local meteorological conditions at the site.

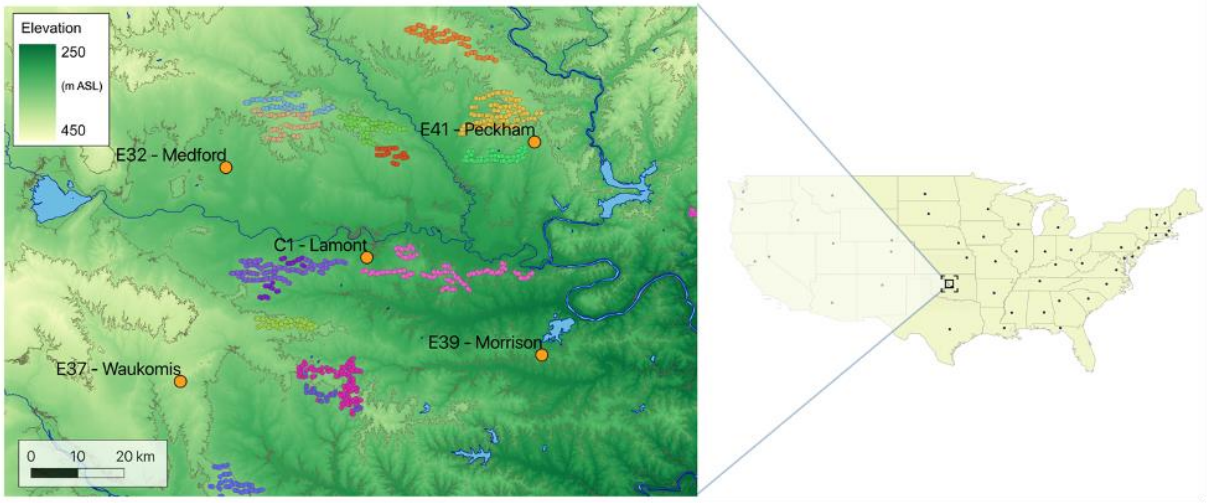


Figure 1: Map of the region and the three measurement sites whose observations are considered in the analysis. The clusters of dots show wind plants in the region.

First, we run and compare mesoscale numerical weather prediction simulations with and without inclusion of the wind plants. To do so, we use the Weather Research and Forecasting model version 4.2.1 and the Wind Farm Parameterization, and consider a ten day case study. Clear effects due to the wind farms in the area emerge. In the simulation which includes the wind farms, we see a reduced mean wind speed aloft, with deficits at about 3.5 km downwind of one of the modeled wind farms of 0.8 m s-1 in stable conditions and 0.3 m s-1 in unstable conditions (Figure 2, left panel). At the surface, we see no difference in unstable conditions, and a 0.4 m s-1 increase in mean wind speed in stable conditions. These "wake impacts" extend downwind, with the wind speed deficits being still detectable ~30 km downwind of the wind farms. Also, turbulence kinetic energy increases at the surface in the near vicinity of the wind farms, mostly during nocturnal stable conditions (+1-3 m2 s-2).

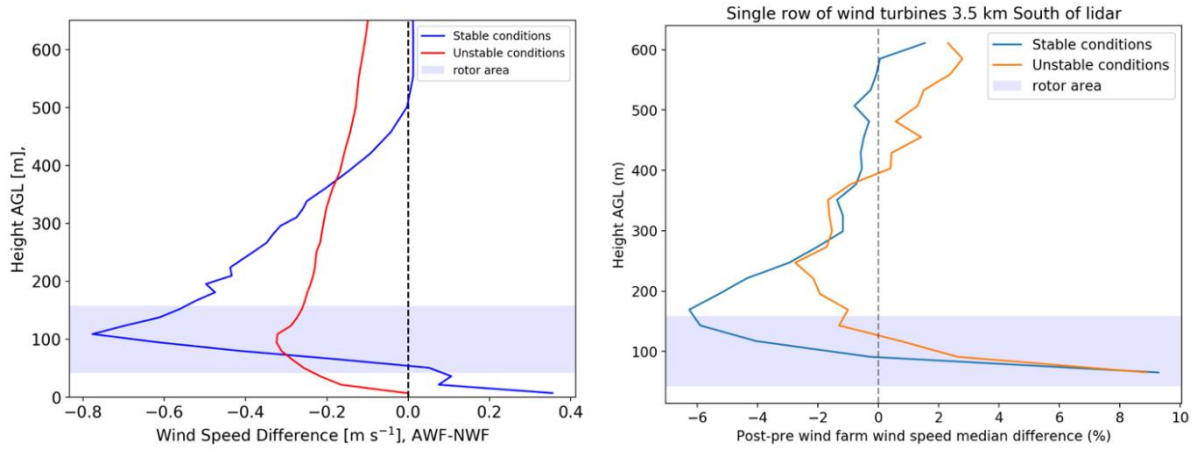


Figure 2: Median wind speed difference between periods with and without wind farms calculated from the mesoscale simulations (left) and lidar observations (right) at Lamont, for stable and unstable conditions. The blue shaded area shows the vertical limits of the turbine rotor disks.

Next, we contrast the results from the simulations with what found in the long-term (more than 8 years) observations at the site, by comparing measurements before and after the wind farms in the region were built. We find that the variability found from the observations is consistent with what seen from the mesoscale simulations. Observations from the lidar at ARM CF, about 3.5 km downwind of one of the wind farms in the region, reveal how wind speed aloft decreased of, on average, 6% in stable conditions, and 2% in unstable conditions, after the wind farms were built in the area (Figure 2, right panel). On the other hand, near-surface measurements confirm the acceleration in wind speed for stable conditions also seen in the mesoscale simulations. Turbulence kinetic energy is enhanced within the wind plant wake in stable conditions, with near-surface observations seeing an increase of over 30% at ARM CF. No significant changes are observed in unstable conditions, when the wind plant wakes erode over shorter distances.

The Jensen wind farm parameterization for the WRF model

Cristina Archer*, and Yulong Ma
University of Delaware
*Presenting author

Keywords: Jensen | wake | wind farm | wind turbine | WRF

Wind turbine wakes significantly decrease the power production of a wind farm. The turbine wakes cannot be resolved directly in mesoscale numerical models because they are sub-grid features. To explicitly account for these sub-grid turbine wakes, here we propose a new wind farm parameterization that is based on the Jensen wake loss model, a well-known analytical wake model that predicts the expansion and wind speed of an ideal wake (Katic et al. 1986). In addition, we introduce an innovative approach to treat the internal variability in wind speed and direction within a wind farm and the wind direction uncertainty.
The internal variability in wind speed and direction can only be addressed when the wind turbines in a farm are partitioned across multiple grid cell (multi-cell case). To treat the wind direction variability, we average the wind direction at the grid cell of the turbine of interest and the wind direction at the grid cell of each upstream wind turbine. To treat the wind speed variability, we introduce a new wake superposition method that is based on the sum of the squared wind speeds caused by each upstream turbine, rather than the traditional approaches that are based on the wind speed deficits (Lissaman 1979, Katic et al. 1986, Voutsinas et al. 1990, Niayifar and Porté-Agel 2016, Archer et al. 2018, Porté- Agel et al. 2020).
To treat the wind direction uncertainty, following Gaumond et al. (2014) and Göçmen et al. (2016), a Gaussian wind direction averaging method is used. At each time step, we call the Jensen parameterization seven times, for the seven angles around the flow direction ±2.5°, ±1.5°, ±0.5°, and 0°, then apply a Gaussian-weighted averaging with a standard deviation of 2°. The simulation results, whether for single- or multi-cell cases, are therefore effectively averaged over a window of wind directions that is ±2.5° around the intended wind direction, mimicking typical anemometer accuracies.

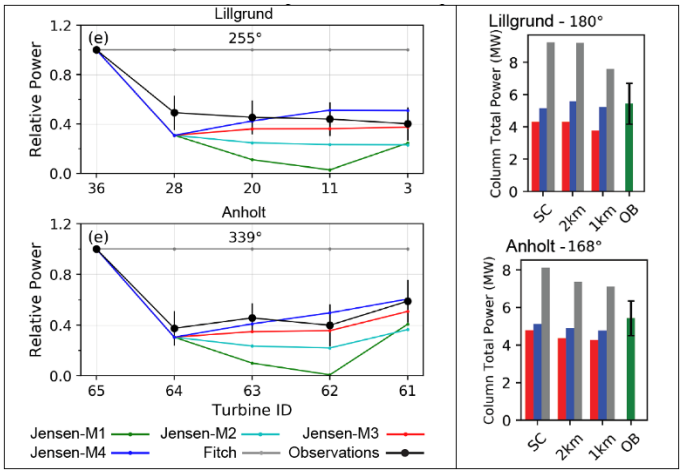


Figure 1: Relative power (left) and selected column total power (MWright) at Lillgrund (255° and 180° wind directions) and Anholt (339° and 168°) as simulated with the Jensen parameterization with wake superposition methods M1-M4, with the Fitch parameterization, and from observations. Sensitivity of power output to grid resolution from coarse (SC = single cell contains the entire wind farm) to fine (2 and 1 km) is strong in Fitch, negligible in Jensen.

The Jensen parameterization is implemented and inserted in the Weather Research and Forecasting (WRF) model. The proposed approach and parameterization are tested against observation data at two offshore wind farms: Lillgrund (small in size and tightly spaced) and Anholt (large and widely spaced). We found that relative power along columns of turbines (Figure 1, left) and power production (Figure 1, right) are predicted more accurately with the Jensen than with the conventional wind farm parameterization available in WRF by Fitch et al. (2012), which tends to overestimate both, especially for wind directions that are aligned with the turbine

columns. Turbulent kinetic energy (TKE) is overestimated with the Fitch scheme at Lillgrund (Figure 2, top), but the two parameterizations predict very similar TKE distributions at Anholt (Figure 2, bottom).

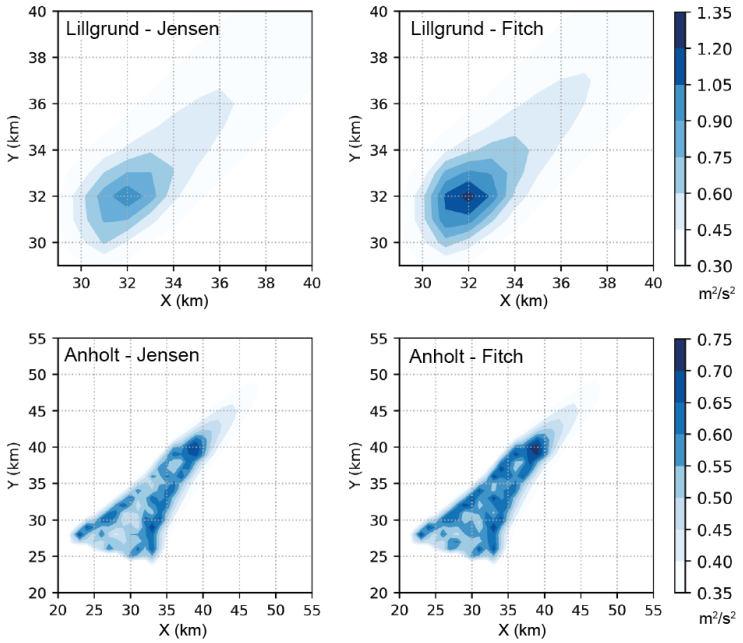


Figure 2: Turbulent Kinetic Energy (TKE, m2/s2) added by the wind turbines as simulated by the WRF model with the Jensen (left) and the Fitch (right) wind farm paramerizations at Lillgrund (top) and Anholt (bottom). Note the different color scale at the two wind farms.

The sensitivity to grid resolution is strong in the Fitch scheme, which is undesirable, whereas it is small to negligible in Jensen's. The bias in power production is generally low and negative with Jensen, while it is large and positive when the Fitch parameterization is used, especially at coarse resolution (i.e., such that the entire wind farm is contained in a single grid cell). In conclusion, the Jensen wind farm parameterization performs well with the WRF model.

References:

Archer, C. L., A. Vasel-Be-Hagh, C. Yan, S. Wu, Y. Pan, J. Brodie, and A. Maguire, 2018: Review and evaluation of wake loss models for wind energy applications. Applied Energy, 226, doi:63810.1016/j.apenergy.2018.05.085

Gaumond, M., P. E. Réthoré, S. Ott, A. Peña, A. Bechmann, and K. S. Hansen, 2014: Evaluation of the wind direction uncertainty and its impact on wake modeling at the Horns Rev offshore wind farm. Wind Energy, 17(8), 1169–1178, doi:10.1002/we.1625

Göçmen, T., P. Van der Laan, P. E. Réthoré, A. P. Diaz, G. C. Larsen, and S. Ott, 2016: Wind turbine wake models developed at the Technical University of Denmark: A review. Renewable and Sustainable Energy Reviews, 60, 752–769, doi:10.1016/j.rser.2016.01.113

Katic, I., J. Højstrup, and N. O. Jensen, 1986: A simple model for cluster efficiency. European Wind Energy Association Conference and Exhibition, 407–410.

Lissaman, P. B. S., 1979: Energy effectiveness of arbitrary arrays of wind turbines. Journal of Energy, 3(6), 323–328, doi:10.2514/3.62441

Porté-Agel, F., M. Bastankhah, and S. Shamsoddin, 2020: Wind-turbine and wind-farm flows: A review. Boundary-Layer Meteorology, 174(1), 1–59, doi:10.1007/s10546-019-00473-0

Voutsinas, S., K. Rados, and A. Zervos, 1990: On the analysis of wake effects in wind parks. Wind Engineering, 14(4), 204–219

Mini-Symposium: Data-driven Modeling and Optimization of Wind Farms





Mahdi Abkar
Aarhus University

Jens Norkaer Sørensen
DTU Wind Energy

Availability of large datasets has led to a paradigm shift in many fields of science and engineering, and fueled an increasing use of data-driven methods. In the wind energy community, there has been a growing interest in machine learning (ML) algorithms for modeling and optimization of wind farms. The complex and multiscale nature of fluid flows in wind farms, however, poses new challenges to the available ML algorithms, which are not commonly developed for problems with such a wide range of spatiotemporal scales. On the other hand, generation of big data, which is a normality in typical applications of ML, is still a costly task – both experimentally and numerically – in wind farms. Furthermore, issues such as 'informing an ML algorithm about the known physics of problems' and 'extracting physical knowledge out of data' call for special attention if ML is to be deployed to its full potential in this field. The proposed mini symposium intends to provide a forum for exchange of ideas and experience in this growing field of research. The main goal is to address the above-mentioned challenges and move towards use of data-driven methods as robust and reliable tools for wind farm modeling and optimization.

Mini-Symposium: Data-driven Modeling and Optimization of Wind Farms (I)

Predicting Linearised Wind Resource Grids using Convolutional Neural Networks in Style Transfer and Encoder-Decoder Based Architectures

Helen Sheehan[1,*], Elizabeth Traiger[2], Daniel Poole[1], and Lars Landberg[2]
[1]University of Bristol
[2]DNV GL
[*]Presenting author

Keywords: Wind Resource | WAsP | Machine Learning | Convolutional Neural Network | Neural Style Transfer

Wind flow models are key tools in describing how a wind resource varies across a wind farm project area. Commercially popular existing models are all physics-based; these include linear models such as WAsP, and more complex Computational Fluid Dynamics (CFD) models. Linear models have the advantage of fast calculation times, but at the cost of simplifying the flow physics, leading to inaccurate predictions over complex terrain. While CFD methods give more accurate results, they are more computationally expensive. Machine learning-based surrogate models have emerged as potential alternatives to CFD, promising faster results without compromising the accuracy. However, the mathematical complexity of CFD methods models means that such surrogate models are difficult to design. This work focuses on emulating linear models as the first step in this challenge.

We present two approaches using machine learning to emulate WAsP models. These surrogate models use the traditional inputs of roughness and orography grids for a particular area of terrain and predict the changes in the wind speed ("speedup") over this area; the end result is grids of the speedups due to the terrain. Our approaches take inspiration from the fields of image processing and computer vision, which use Convolutional Neural Networks (CNNs) to process information on grids and handle spatially dependent data.

The first model is a neural style transfer network utilizing Deep CNNs and computer vision techniques as in (Gatys , Ecker, & Bethge, 2015). In neural style transfer, a content image and a style reference image are combined with the resulting output image retaining the substance of the content image, but stylized as in the style reference image. This is done by optimizing the output image to match the content statistics of the content image and the style statistics of the style reference image using a CNN. The terrain grids are used as content representations and WAsP speedup as style representations, both in raster format. The resulting model based on Fast Style Transfer captures the WAsP speedups.

The second model also uses CNNs, with an architecture based on research such as (Lee & You, 2019), who have created CFD surrogate models with a CNN-based structure, with similarities to encoderdecoder models. This model has a more traditional approach where hyperparameters such as activation functions, numbers of layers and optimisers are tuned to find the optimal architecture, with an example of the results shown in Figure 1.

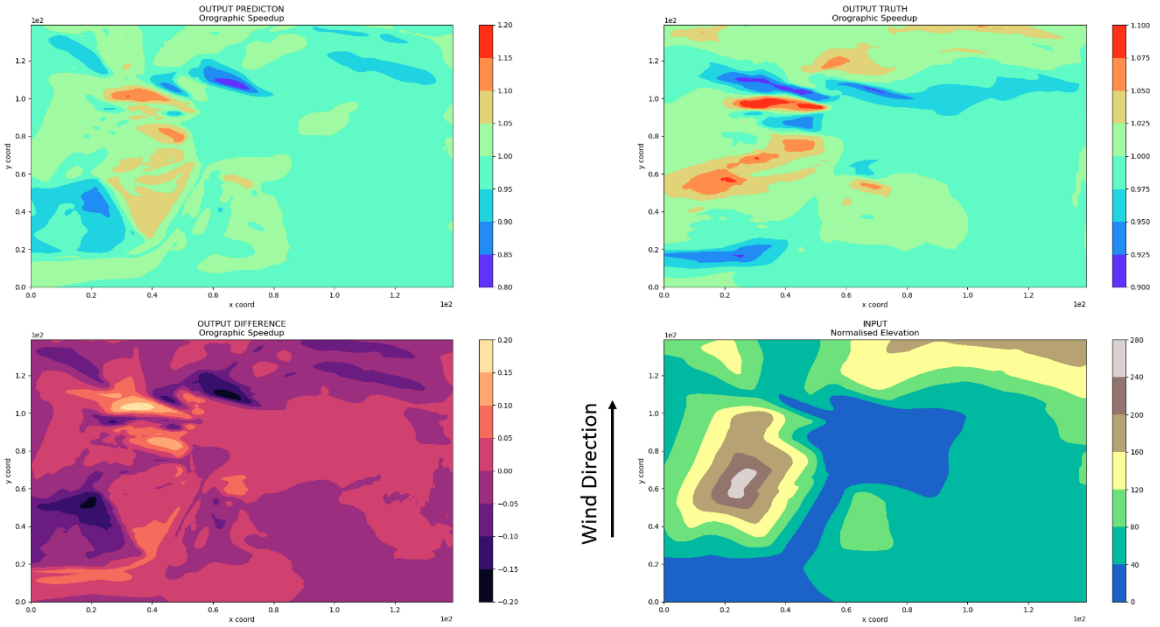


Figure 1: Orographic speedup predictions at 100m above ground level based on elevation grid data, from an example of the CNN configurations tested. This is the Waspdale example site, with wind direction from the south. Clockwise from top left: predicted speedups from the CNN-based model; speedups calculated in WAsP; elevation data (in m) used to calculate inputs to the CNN model; difference between the predicted and the WAsP speedup values.

We have investigated the sensitivity of both our approaches to variations in the terrain data, such as grid size, transformations, and complex terrain features. Both modelling approaches use feedforward networks with back-propagation. We have compared the results from the models to those achieved with a simpler model architecture which consists purely of interconnected perceptrons rather than convolutional layers. Using WAsP results as a baseline, we validated our models and provide a discussion on the strengths and weaknesses of both our approaches. We also consider issues such as the interpretability of our "black box" models, in comparison to work such as (Raissi, Perdikaris, & Karniadakis, 2019) which incorporate a user-defined physical basis into their neural networks. From this, we recommend areas for improvement, and ways in which the knowledge and experience from creating these models could be used in creating CFD surrogate models.

References:
Gatys , L. A., Ecker, A. S., & Bethge, M. (2015)."A Neural Algorithm of Artistic Style." Available at: https://arxiv.org/abs/1508.06576
Lee, S. and You, D. (2019) "Data-driven prediction of unsteady flow over a circular cylinder using deep learning," Journal of Fluid Mechanics. Cambridge University Press, 879, pp. 217–254. doi: 10.1017/jfm.2019.700.
Raissi, M., Perdikaris, P., & Karniadakis, G. E. (2019) "Physics-informed neural networks: A deep learning framework for solving forward and inverse problems involving nonlinear partial differential equations," Journal of Computational Physics, 378, pp. 686-707. doi:doi.org/10.1016/j.jcp.2018.10.045.

Data-driven RANS closure for wind turbine wakes under neutral conditions

Julia Steiner*, Richard Dwight, and Axelle Viré
Delft University of Technology
*Presenting author

Keywords: Turbulence | Data-driven modelling | RANS | Wind turbine

The state of the art in wind-farm flow-physics modeling is Large Eddy Simulation (LES) which makes accurate predictions of most relevant physics, but requires extensive computational resources. The next-fidelity model types are Reynolds-Averaged Navier-Stokes (RANS) which are two orders of magnitude cheaper, but resolve only mean quantities and model the effect of turbulence. They often fail to accurately predict key effects, such as the wake recovery rate.
Custom RANS closures designed for wind-farm wakes exist, but so far do not generalize well: there is substantial room for improvement. Further, the authors think it might be useful to have a methodology to develop a turbulence model specifically tailored to a specific location or actuator geometry.
In this article we present a systematic data-driven approach to deriving new RANS models in the wind-energy setting. Time-averaged LES data is used as ground-truth. We have a methodology to derive two optimal corrective fields: (i) a tensorial anisotropy correction field imposed directly in the Reynolds stress calculation and (ii) a scalar correction imposed in the transport equatios for the turbulent kinetic energy and the dissipation. The scalar correction field accounts for both form errors in the transport equation and errors in the turbulent kinetic energy production. These fields, when injected into the RANS equations (with a baseline k-epsilon model) reproduce the LES meanquantities.
We also combine these optimal correction terms with a logistic classifier which can disable the corrections in areas where they are not needed.
Next we build a custom RANS closure from these corrective fields and for the classifier, using a deterministic symbolic regression method to infer algebraic corrections as a function of the (resolved) mean-flow. These expressions are based on an extended integrity basis for nonlinear eddyviscosity models. Additionally, we also introduce physical features such as non-dimensionalized actuator forcing and turbulence intensity.
Further description of the methodology and previous results can be found in the attached references [1,2,3].
We demonstrate the work under neutral atmospheric conditions for multi-turbine constellations at wind-tunnel scale. There are also plans to extend the work to real-scale simulations.
The resulting RANS closures show substantial improvement over the baseline model. The results for the velocity and the turbulent kinetic energy are shown in the figure for models obtained with and without the use of a classifier.

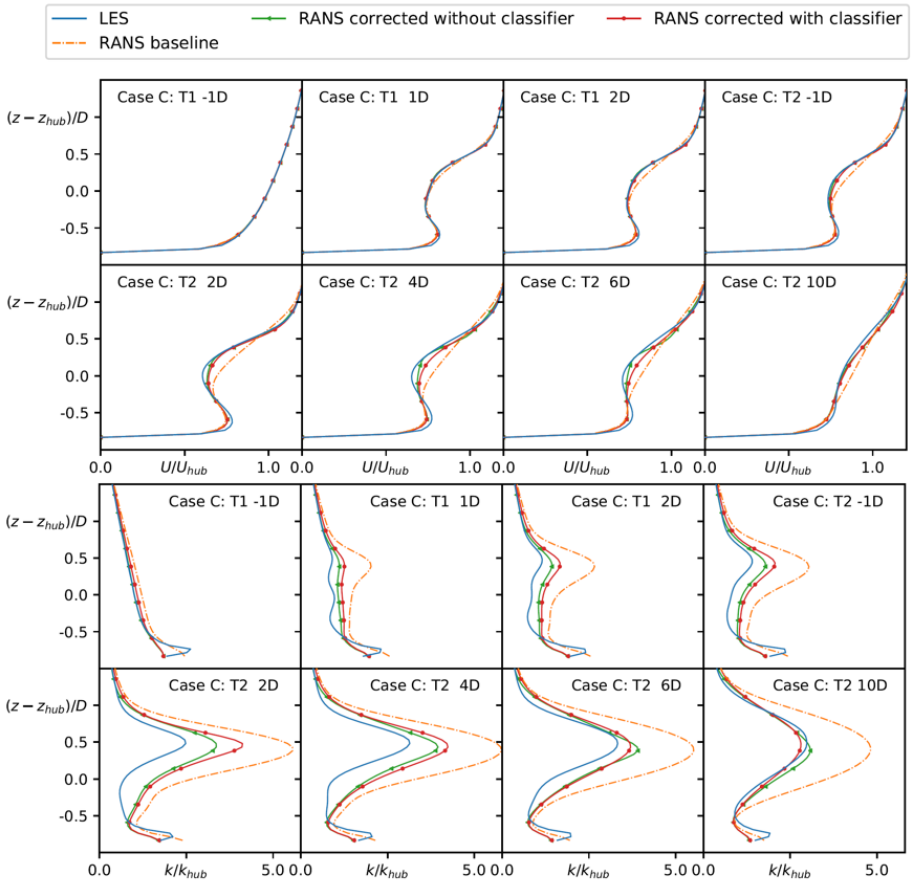


Figure 1: Comparison between LES, RANS baseline and corrected RANS models with and without the classifier via vertical slices of the velocity and turbulent kinetic energy field up and downstream of the rotor plane of two turbines in a row. The upstream turbine is yawed.

Further, the inclusion of a classifier leads to simpler yet also a bit less numerically stable models as compared to previous work where no classifier is used. Two limiter functions are introduced to fix the numerical issues. These limiters are active only very locally and for some model combinations or test cases they are not used at all. The authors think that the robustness of the models could be further improved through limiting the use of gradient-based features. But even with the limiters, the results so far have been encouraging.

References:
[1] M. Schmelzer, R. Dwight, and P. Cinnella, "Discovery of algebraic reynolds-stress models using sparse symbolic regression", Flow Turbulence and Combustion, 10 2019.
[2] J. Steiner, R. Dwight, and A. Viré, "Data-driven turbulence modeling for wind turbine wakes under neutral conditions", Journal of Physics: Conference Series, vol. 1618, p. 062051, Sep 2020.
[3] J. Steiner, R. P. Dwight, and A. Viré, "Data-driven RANS closures for wind turbine wakes under neutral conditions", arXiv:2009.10816, January 2021.

Identification of heterogeneous wind farm flow features from SCADA Data

Robert Braunbehrens*, Andreas Vad, and Carlo L. Bottasso
Technical University of Munich
*Presenting author

Keywords: SCADA | heterogeneous flow | SVD | wake model

Wind farm control and operation applications require an accurate prediction of wake effects. While low-cost engineering wake models have been greatly improved over the years, the background flow is often assumed to be homogeneous, which is hardly true. This talk proposes methods to detect long- and short-term heterogeneities in the ambient and intra-plant flow from turbine production data.
Long-term heterogeneities are spatially and ambient-condition dependent, and are caused by orographic features, obstacles and surface roughness. Even offshore, the influence of land can cause persistent gradients in the array inflow [1]. A further source for flow heterogeneity can be the wind farm itself, as caused by its interaction with the atmospheric boundary layer, leading to blockage and deep array effects. As first proposed in ref. [2], a baseline engineering flow model [3] can be adapted to a specific site by introducing parametric correction terms, which are learnt from standard operational SCADA data. In the present work, a heterogeneous flow field, characterized by both speed and direction, is parameterized in terms of shape functions and associated unknown nodal values. Optionally, the intrinsic parameters of the wake model can be identified together with the heterogeneous flow nodal quantities, resulting in a site-specific coupled simultaneous correction and tuning of the model. This possibly ill-conditioned optimization problem is solved by mapping the
unknown parameters into an orthogonal space via the singular value decomposition (SVD), solving the identification by maximum likelihood in the reduced space, and then mapping back the solution to the physical space.
Figure 1 shows the identified flow field for a commercial onshore wind farm [2]. The locations of the heterogeneous flow nodes are marked with "x" in the figure. Results indicate that the wind direction was adapted in the southern part of the farm, on account of local complex features of the terrain. To confirm the origin of these data-driven long-term flow corrections, a CFD RANS model of the terrain and its surroundings was developed in OpenFOAM. Preliminary numerical results appear to be in agreement with the data-driven corrections, supporting the claim that the identified model indeed captures actual physical effects present at the site.

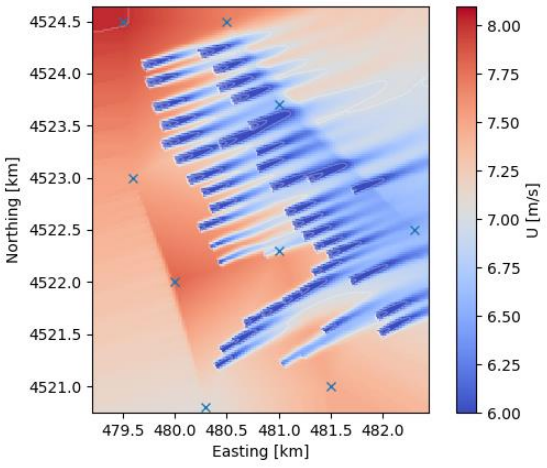


Figure 1: Heterogeneous long-term flow field for an onshore wind farm, identified from SCADA data for a 10° wide direction bin.

A second case under investigation is the Anholt offshore wind farm. Here, the flow identification algorithm was able to pick up a north-south inflow speed gradient, which is induced by the shoreline.

Additionally, results indicate a decreasing background velocity towards the trailing edge of the farm, indicative of deep-array effects. These results are being compared to a deep-array model, to confirm the nature of the observed flow heterogeneity.
The same methodology can be applied on faster time scales to identify short-term flow heterogeneities, i.e. dynamic changes in the flow caused, for example, by the propagation of a wind gust across a farm. In fact, as array sizes increase, changes in wind speed and direction cannot be assumed to affect all turbines instantaneously. Rather, ambient conditions propagate through the array. In this context, the proposed approach represents an observer that, based on operational data used in combination with a dynamic wake model, estimates the instantaneous ambient conditions in support of wind farm control applications. The presentation will illustrate this method for the Anholt farm (ca. 20x10 km) using 10 min SCADA data.

References:
[1] Peña, Alfredo, et al. "On wake modeling, wind-farm gradients, and AEP predictions at the Anholt wind farm." Wind Energy Science 3.1 (2018): 191-202.
[2] Schreiber, Johannes, et al. "Improving wind farm flow models by learning from operational data." Wind Energy Science 5.2 (2020): 647-673
[3] NREL ,FLORIS Version 2.2.4, 2020, GitHub ,https://github.com/NREL/floris

Toward wind farm modelling via physics-informed machine learning

Jeppe Dybkjær Ditlev[1,*], Kenneth Rugholm Kramer[1], Nicolai Gayle Nygaard[2], Lucas Marion[2], and Mahdi Abkar[1]
[1]Aarhus University
[2]Ørsted
*Presenting author

Keywords: Wind farm power production | Engineering wake models | Data-driven modelling | Physics-informed machine learning

In the wind energy industry, operational optimization of existing wind farms and layout optimization of new wind farms, depend on accurate power production modelling. Physics-based (engineering) wake models are mainly used for this purpose. These models have shown satisfactory performance throughout the years for these purposes; however they are based on simplistic physical assumptions, which therefore, are not able to accurately emulate the complex flows inside a wind farm. Models created using data-driven methods, can show improvements in capturing some of the complex turbulence physics inside a wind farm. However, these models have a low level of transferability to other wind farms. In this study, we combine the benefits from generic physics-based methods, with the advantages from data-driven methods. To achieve this, a physics-informed machine learning framework is introduced to integrate physics in an artificial neural network. Using an analytical wake model based on a Gaussian distribution, linear superposition method, and a variable growth rate, a wind farm efficiency is calculated and added as an additional input feature to the artificial neural network. Figure 1 schematically illustrates the proposed concept. The proposed model will be first trained on the large amount of observational data of offshore wind farms. The model will be tested in predicting the power production of the same wind farms using the observational data at a different time interval which were not used in the training process. By considering known physics about atmospheric turbulence and wind-farm aerodynamics in the training process, we aim to generalize the model and make it applicable to other wind farms not seen by the model. In particular, the data-driven model will be first trained and validated on particular wind farms, and it will be then used in predicting the power output of other wind farms.

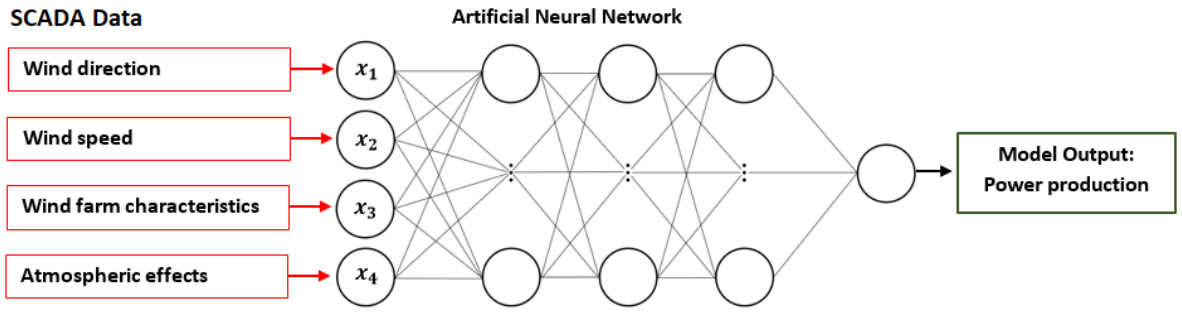


Figure 1: The proposed concept: the artificial neural network is trained based on the SCADA data and then serves as a model for wind-farm power production.

In this study, the pipeline for preprocessing of the SCADA data is explored. This process is required in order to estimate the incoming wind conditions and wind farm performance. A selection of developed variations of the physics-informed machine learning approaches has been trained and tested on Westermost Rough and Anholt offshore wind farms. The results suggest that physicsinformed machine learning increases the prediction accuracy of the purely data-driven methods.
Additionally, a generic formulation, where each individual wind turbine is modelled separately, has proven to give the best model transferability to an unknown wind farm. This method makes it possible to incorporate individual production settings for each wind turbine. The framework also allows incorporation of additional

input features influencing the wind farm efficiency, such as atmospheric stability or geophysical effects, which will add more knowledge and complexity to the model. The proposed framework and modelling methods would greatly benefit from access to larger variety of wind farm data.

Mini-Symposium: Data-driven Modeling and Optimization of Wind Farms (II)

Lowering long-term energy estimate uncertainty through better wind plant power curves

Nicola Bodini, Mike Optis, Jordan Perr-Sauer, Eric Simley, and M. Jason Fields
National Renewable Energy Laboratory

Keywords: machine learning | AEP assessment | power curves | operational analysis

Wind power plant financial transactions, both in the preconstruction and operational stages, require accurate assessment of the wind plant annual energy production (AEP) through a regression relationship between produced power and atmospheric variables, to determine a relationship that can be called a wind plant power curve. Currently, a univariate linear regression at monthly resolution is the industry standard for this relationship. However, this simple approach has several limitations, as it is unable to accurately capture the impact of variables other than wind speed on the wind plant power production, and it is also unable to model the temporal variability at sub-monthly resolution of the atmospheric properties and transfer it into the long-term wind power plant performance assessment. Here, we assess the benefits in augmenting this conventional approach by testing the value of regressions performed with multiple input variables, at a finer time resolution, and using machine-learning-based nonlinear algorithms. In fact, reducing the uncertainty connected to the long-term AEP estimates would translate in major savings for wind plant financial transactions.

In doing so, we aim to support a technical report to recommend best practices for the use of machine-learning regression models for wind power plant energy assessment purposes which is soon going to be released by the AWEA Technical Report-1 working group.

For our work, we adopt the National Renewable Energy Laboratory's open-source software package OpenOA to assess wind plant power curves. We perform our analysis for 10 wind plants in North America, all located in relatively simple terrain, from the Wind Plant Performance Prediction (WP3) Benchmark initiative, a joint industry project aimed at sharing data and performing preconstruction and operational performance reconciliation at scale.

When a univariate generalized additive model at daily resolution is used, regression uncertainty (quantified through a Monte Carlo approach) is reduced for all 10 wind farms, in absolute terms, by up to 1.0% (corresponding to a -60% relative change) compared to a univariate linear regression at monthly resolution, and a more accurate assessment of the mean long-term wind plant production is achieved. Additional input variables can also improve the regression: when temperature is added as an input to the conventional monthly linear regression, the operational analysis uncertainty connected to regression is reduced, in absolute terms, by up to 0.5% for wind power plants which experience strong seasonal variability. On the other hand, adding input variables to the machinelearning model at daily resolution does not further reduce regression uncertainty, but it still reduces the regression root-mean-square error (with up to a -15% relative difference). In fact, for example, the inclusion of wind direction as a regression input allows the wind plant power curve to adapt itself to the internal layout of the wind plant, to better represent the impact of wind turbine wakes on the overall wind plant power production (Figure 1).

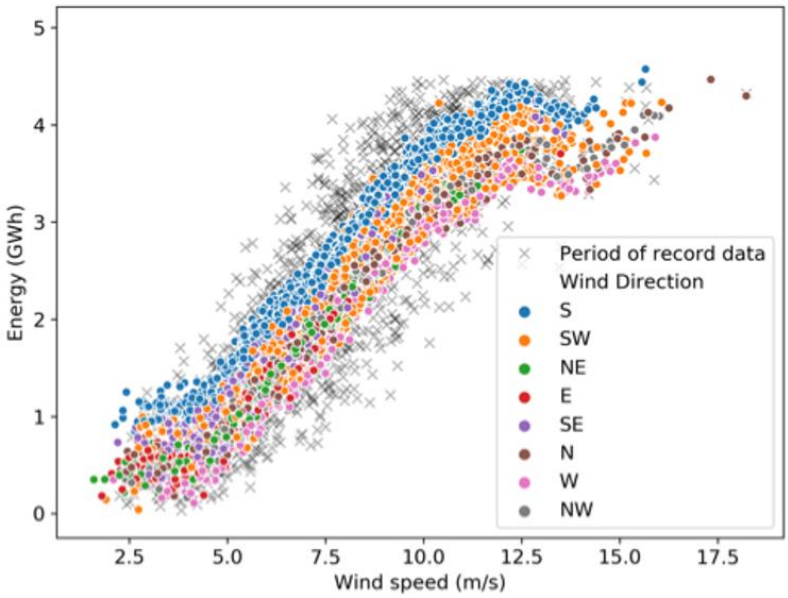


Figure 1: Wind plant power curve obtained from a GAM regression at a daily resolution using wind speed, temperature, and (sine and cosine of) wind direction as inputs. Southerly flow produces more energy than the other wind directions: this differentiation is consistent with the layout of the wind power plant, wherein the wind turbines experience significantly lower wake losses for southerly flow.

Based on these results, we conclude that a multivariate nonlinear regression at a fine time resolution should be recommended for assessing wind plant power curves.

Implications of ambient shear and thermal stratification on wind turbine nearwake dynamics

Amy Hodgkin[1,*], Sylvain Laizet[1], Georgios Deskos[2], and Nikolaos Bempedelis[1]
[1]Imperial College London
[2]National Renewable Energy Laboratory
[*]Presenting author

Keywords: wake | tip-vortex stability | large eddy simulation | actuator line method | POD

Growing capacity of wind energy calls for larger turbines (rotor diameter in the order of 200 m and hub height as high as 150 m) which operate higher up in the atmospheric boundary layer. This means that modern wind turbines may experience uneven inflow conditions across the rotor, with shear and thermal stratification present. Such conditions will ultimately alter the shape and length of their wakes and in turn impact the loading and power generation of downstream turbines that may experience wake turbulence. In order to optimise wind farm layout, as well as find optimal control solutions that maximise power output, the evolution and the properties of the wake in different atmospheric conditions must be well-understood. This study aims to further understand the effect of shear and thermal stratification on the wake properties and tip-vortex breakdown mechanisms using high-fidelity simulations and data-driven techniques such as the proper orthogonal decomposition (POD).

A suite of high-resolution simulations are carried out with the high-fidelity LES wind farm simulator, WInc3D (Deskos et al. 2020), which uses high-order compact finite-difference schemes on a uniform Cartesian mesh to solve the incompressible Navier-Stokes equations (WInc3D is part of XCompact3D, an ecosystem of high-order finite-difference solvers). The wind turbine rotor is modelled using the actuator line method (ALM). The flow can be perturbed harmonically around the blade tips in order to trigger instabilities in the flow and enable transition to turbulence. The combined effect of shear and thermal stratification on the wake is investigated in the near-wake region of 0 - 3.5R downstream of the turbine. In particular, the POD technique is used to extract coherent structures in the wake. The method of snapshots is used to find key modes and temporal coefficients; key modes and their contribution to the total energy are used for flow reconstruction and to better understand the mean features of the wake. The transition period is of particular importance to understand stability of the wake. Modelled wake properties will be compared with estimated wake properties using the stable wake length model proposed by Sarmast et al. (2014) to assess accuracy of models when applied to sheared and thermally stratified flows.

Initial simulations with shear have confirmed the correct numerical setup, with excellent comparison with the work of Kleusberg et al. (2019). Plots of the vorticity field at varying shear and perturbation frequency can be seen in figure 1.

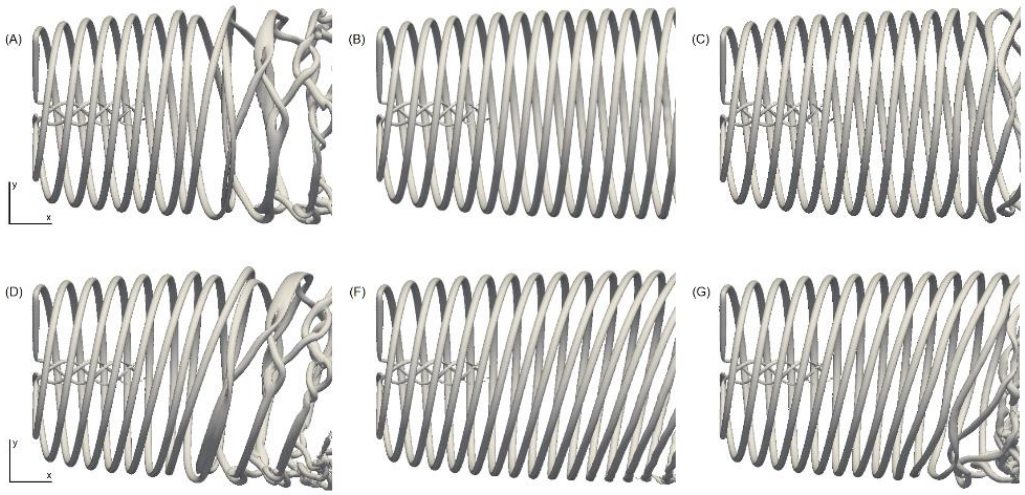


Figure 1: Vorticity field 0 - 3.5 R downstream of turbine. (A-C): no shear, (D-F): shear, (A,D): out-of-phase perturbation, (B,E): in-phase perturbation, (C,F): partial phase perturbation

The perturbation frequency affects the length at which transition to turbulence occurs and sheared effects can be seen along the bottom row. Figure 2 shows the growth rate of cases B and E (as labelled in figure 1) compared with data provided in Kleusberg et al. (2019), further confirming the correct numerical setup. As expected, when no shear is present the growth rate is equal around the turbine. Shear has the effect of increasing growth rate along the lower half and decreasing along the upper half.

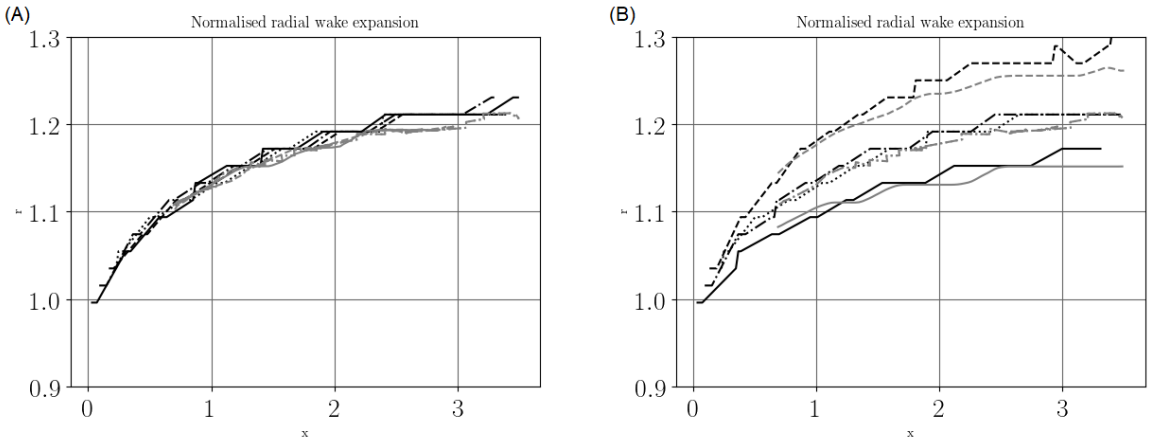


Figure 2: Growth rate for no shear (A) and shear (B) for in-phase perturbation, compared to data from Kleusberg et al. (2019) figure 8. (Black: our results, Grey: Kleusberg et al. (2019). Solid: 0°, Dash: 180°, Dash-dot: 90°, Dot: 270°)

These first results will be further discussed during the presentation along with results from thermally stratified flows.

References:

Deskos, G., Laizet, S. & Palacios, R. (2020), 'Winc3d: A novel framework for turbulence-resolving simulations of wind farm wake interactions', Wind Energy 23(3), 779–794.

Kleusberg, E., Benard, S. & Henningson, D. S. (2019), 'Tip-vortex breakdown of wind turbines subject to shear', Wind Energy 22(12), 1789–1799.

Sarmast, S., Dadfar, R., Mikkelsen, R. F., Schlatter, P., Ivanell, S., Sørensen, J. N. & Henningson, D. S. (2014), 'Mutual inductance instability of the tip vortices behind a wind turbine', Journal of Fluid Mechanics 755, 705–731.

Machine Learning Modeling of Wind Turbine Wakes: Clustering of LiDAR measurements and random-forest predictions

Giacomo Valerio Iungo[1], Stefano Letizia[1], Romit Maulik[2], Vishwas Rao[2], and Ashwin Renganathan[2]
[1]UT Dallas
[2]Argonne National Laboratory

Keywords: wind turbine | wake model | LiDAR | machine learning | clustering

Over the last decades, wind energy researchers have been seeking accurate and efficient models to predict wind power capture associated with operations of wind turbines, and generation of their wakes. A major class of models to predict wind turbine wakes falls within the branch of the CFD models, which are formulated from the Navier-Stokes equations to describe the fluid motion, while the turbulence effects on the momentum budget are modeled with different closure models entailing different levels of complexity and accuracy. These CFD models are computationally expensive and not suitable to run hundreds of simulations needed for the design and characterization of a wind farm. This motivates the use of more simplistic models, denoted as
engineering wake models, which predict the wake velocity field through analytical or empirical approaches enabling low computational cost, yet with accuracy strongly related to the tuning of the model parameters. Recently, the availability of SCADA, meteorological, and LiDAR data has motivated the optimal tuning of the model parameters using as a reference these experimental datasets (see e.g. Zhan et al., 2020a).
In this work, a machine learning model of wind turbine wakes is developed to achieve accuracy in predictions of the velocity field and power capture similar to that achievable through CFD modes, yet with computational cost as low as for engineering wake models (Maulik et al., 2021). More than 6 000 PPI scans of isolated wind turbine wakes performed with a scanning Doppler wind LiDAR are used for this study. The experimental dataset also includes meteorological data collected from a mettower located in the proximity of the wind farm and SCADA data of the wind turbines (Zhan et al., 2020b).
The variability of the wake velocity field is firstly characterized and quantified through the k-means clustering algorithm (Steinhaus 1956, MacQueen 1967, Lloyd 1982). Rather than providing as input the raw velocity fields as probed by the LiDAR, the velocity data are first projected on a lowerdimensional embedding obtained through proper orthogonal decomposition (POD). A truncated POD basis consisting of only five POD modes, which enables the reconstruction of 44% of the initial covariance matrix of the LiDAR data, is selected to reduce the dataset dimensionality and, thus, the computational costs associated with the cluster analysis (Figure 1).

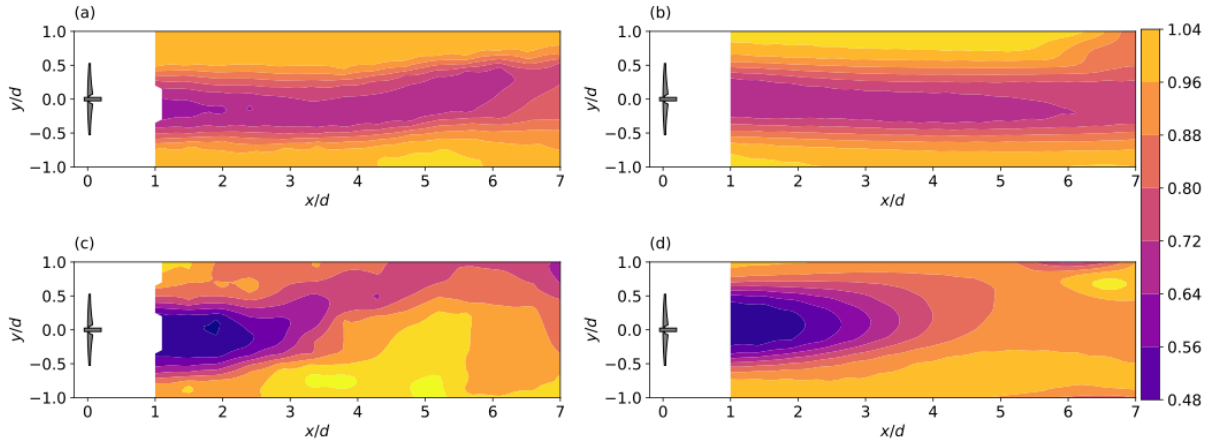


Figure 1: Reconstruction of the LiDAR wake measurements using only five POD modes. The top row shows LIDAR data for U_hub^*=1.08, =5.3%, =1, =0.005 with the true (a) and POD-reconstructed (b) velocity fields. The bottom row shows LiDAR data for U_hub^*=0.72, =15.4%, =0.51, =-0.003 with the true (c) and POD-reconstructed (d) velocity fields.

The inputs for the k-means algorithm are the Fourier coefficients of the selected POD modes. It is noteworthy that no information from the meteorological and SCADA data is provided for the cluster analysis, rather only information about the wake velocity field measured through the LiDAR is provided. A total of nine clusters have been generated to reproduce the variability of the wind turbine wakes for different incoming wind speed and atmospheric stability conditions. Subsequently, predictions of wind turbine wakes are performed with a random forest algorithm. A subset of the turbine and meteorological parameters, such as hub-height wind speed, turbulence intensity, and Bulk Richardson number, is provided as input, then the random forest algorithm selects the most probable lidar cluster associated with the provided inputs. Finally, the developed wake model has been assessed against the SCADA data of the wind farm, showing a good level of accuracy, especially if considering that the computational costs of the developed machine learning wake model are comparable to those of classical engineering wake models.

References:

Lloyd, S.:Least squares quantization in PCM, IEEE Trans. Inf. Theory, 28 (2), 129–137, 1982.

MacQueen, J.: Some methods for classification and analysis of multivariate observations. In Proceedings of the Fifth Berkeley Symposium on Mathematical Statistics And Probability, vol. 1, pp. 281–297, 1967. University of California Press.

Maulik, R., Rao, V., Renganathan, A., Letizia, S., Iungo, G.V.: Cluster analysis of wind turbine wakes measured through a scanning Doppler wind LiDAR, AIAA Scitech 2021 Forum, 1181, 2021.

Steinhaus, H.: Sur la division des corps matériels en parties. Bull. Acad. Polon. Sci., 4 (12), 801–804, 1956.

Zhan, L., Letizia, S., Iungo, G.V.: Optimal tuning of engineering wake models through lidar measurements, Wind Energy Science, 5 (4), 1601-1622, 2020a.

Zhan, L., Letizia, S., Iungo, G.V.: LiDAR measurements for an onshore wind farm: Wake variability for different incoming wind speeds and atmospheric stability regimes, Wind Energy, 23 (3), 501-527, 2020b.

Data Science for Wind Energy: An R package for facilitating wind farm operations

Abhinav Prakash*, and Yu Ding
Texas A&M University
*Presenting author

Keywords: Nonparametric regression | Software package | Wind power curve

Wind turbines churn out massive amounts of data. Analyzing these high volumes of data requires a robust and easy-to-use software environment, equipped with cutting-edge methodologies. Data Science for Wind Energy (DSWE) is an open-source package developed for R programming language.
The purpose of the package is to bring many data-driven methods used in wind energy applications under a unified framework and carry out the methods discussed in the recently published book of Data Science for Wind Energy, so that the methods can be readily accessed by practitioners as well as researchers working on wind energy applications.
The package houses many state-of-the-art data-driven techniques to model and compare wind power curves. Power curve maps the wind speed and other environmental conditions to the power produced by a turbine. A nominal power curve with one-dimensional input is shown in Figure 1.

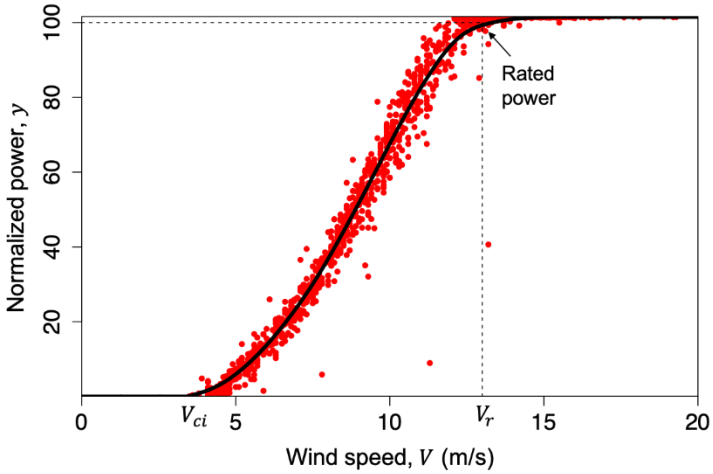


Figure 1: A nominal power curve with one-dimensional input of wind speed.

The package is available through CRAN—the official package repository of R. The functions in the package can be classified into two broad categories: 1) based on the methods researched and developed in-house by the authors; and 2) based on a variety of existing machine learning methods, such as k-nearest neighbors (kNN), support vector machines (SVM), splines (SSANOVA) and Bayesian trees (BART).
The in-house methods are specifically designed for handling machine learning problems that arise in wind power curve modeling. The available in-house methods are additive multiplicative kernel (AMK) and tempGP to model various aspects of the power curve using multi-dimensional inputs, funGP to perform a statistical comparison of power curves, and covariate matching to select probabilistically comparable environmental data subsets.
This presentation will provide an overview on the functionalities and usage of the package. To bring the state-of-the-art development to the WESC, the speaker would like to highlight a few data science related challenges in power curve modeling as well as the solutions presented by the functions included in the DSWE package.
One such important problem is the temporal overfitting problem, which has gone unnoticed and can significantly reduce the accuracy of the power curves. Temporal overfitting occurs when a regression model performs well while predicting response at test points that are from the same time domain as that of the training data; however, the model performance reduces significantly when the test data are from a different

time horizon. This problem occurs due to the temporal autocorrelation in the wind turbine data. One of the methods in the package—tempGP—has been specifically developed to handle the problem of temporal overfitting. We have found significant improvements in power curve accuracy by using the developed method. Another noteworthy work in the package is related to statistical comparison of power curves—funGP—which can be used quantify the difference between the power curves of two datasets. The package also has another statistical method to match the distributions of the environmental conditions (covariate matching) for different power curve datasets, so that the power curves are compared under similar environment conditions. We believe that this presentation would spread awareness about the cutting-edge methods on power curve modeling and performance comparison. These power curve-based methods can be used for advising both the operational strategies for a whole wind farm and that for specific turbines.

Mini-Symposium: Entrainment and Blockage Effects on Large Offshore Wind Farms





Tuhfe Göçmen
DTU Wind Energy

Jake Badger
DTU Wind Energy

By its very nature, a wind turbine extracts energy from the wind, which for a single wind turbine is replenished from the wind field on the sides and above due to the ambient turbulence. However, offshore, the turbulence is lower, and wind farms are typically larger than onshore, therefore the wind can only be replenished from above in a process called entrainment. This session will include the studies on the entrainment process to discuss whether there is a limit to the possible installation density of very large offshore wind farm clusters. Investigating the flow around large offshore wind farm clusters, the session will also include wind farm scale blockage research which investigates the reduction of the energy production due to the obstacle effect generated by dense upstream turbine rows. The session is supported by the preliminary research outcomes of Train2Wind ITN, which is a PhD and researcher training school analysing entrainment in offshore wind farms using advanced high-resolution computer modelling and wind tunnel models together with measurements of the wind field above, in and downstream of large wind farms, using lidars, radars, satellites and Unmanned Aerial Systems.

Mini-Symposium: Entrainment and Blockage Effects on Large Offshore Wind Farms (I)

Turbulent entrainment in large wind plants

Nikolaos Bempedelis[1,*], Georgios Deskos[2], and Sylvain Laizet[1]
[1]Imperial College London
[2]National Renewable Energy Laboratory
[*]Presenting author

Keywords: Turbulence | Entrainment | Large wind farms

As the support and calls for increased levels of wind energy production globally grow, the size and number of large wind plants in operation or under development keep increasing. The operation of a wind turbine in isolation is fundamentally different from when the same turbine operates as part of a wind farm, due to wake effects that are present in the latter case. These interactions have a critical effect on the flow and lead to significant power losses and additional fatigue loads on the turbines.
In large wind turbine arrays, where the turbines operate within a fully developed boundary layer (i.e. when the length of the farm extends more than ten times the height of the atmospheric boundary layer), energy enters the system vertically, via entrainment, rather than horizontally. As a result, entrainment is a critical factor for the performance of very large wind farms. Indeed, there have been efforts to identify ways of enhancing the relevant transport processes (e.g. by modifying the largescale structures of the flow (Hamilton et al., 2012), or introducing kites within the array (Ploumakis & Bierbooms (2018)).
In the present work, we use the numerical framework WInc3D/XCompact3D to perform high-fidelity simulations of the flow in large-scale wind farms of different layouts (spacing and arrangement), in an attempt to gain insight into the mechanisms of energy entrainment and its relationship with power density (power output per plant area). The wind turbines are modelled using the actuator disk method (ADM), under both neutral and non-neutral atmospheric conditions. XCompact3D makes use of high-order compact finite difference schemes to solve the flow governing equations (the incompressible Navier-Stokes equations, together with an additional equation for the temperature, where appropriate) on uniform Cartesian grids, a third-order Runge-Kutta method for time advancement, and a direct spectral solver for the Poisson equation. The framework has been validated and used in the study of a large number of relevant problems (see for example Deskos,
Laizet & Piggott (2019) and Deskos, Laizet & Palacios (2020)).
Results from our simulations are compared to past numerical studies of kinetic energy entrainment in large wind farms (e.g. VerHulst & Meneveau 2014) and analytical models that make use of parametrizations from studies of turbulent or geophysical flows to derive relationships between power output and entrainment (Luzzatto-Fegiz & Caulfield 2018). The applicability of the entrainment hypothesis and the adopted parametrizations is also investigated, where the relevant coefficients are computed via the energy-consistent methodology of van Reeuwijk & Craske (2015).

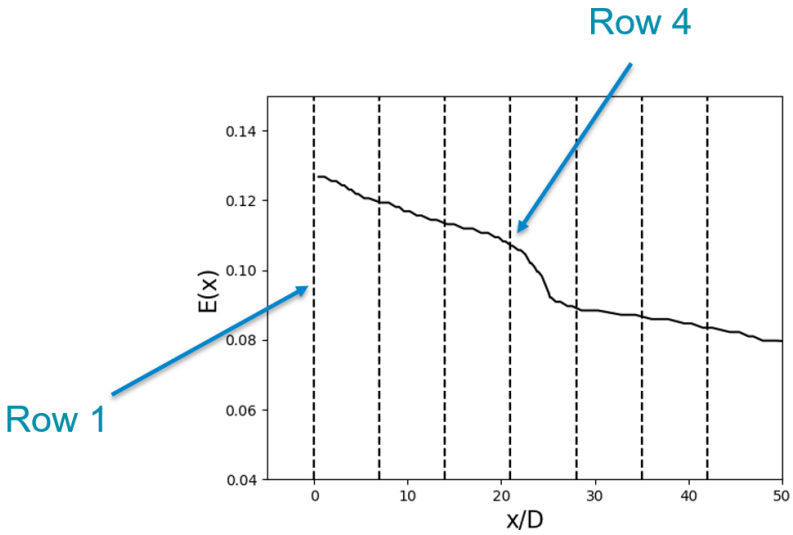


Figure 1: Entrainment coefficient as a function of streamwise distance. Simulations of the Horns Rev I offshore wind farm. Reproduced from Deskos & Laizet (2018).

Initial results show that entrainment is not uniform along a wind farm, and reduces together with power (Figure 1). As the fully developed limit is approached, entrainment tends to a constant, which has a dependence on the configuration of the wind farm.

References:

Deskos, G. and Laizet, S., 2018. Energy–consistent estimations of entrainment for fully-developed wind farms. Bulletin of the American Physical Society.

Deskos, G., Laizet, S. and Palacios, R., 2020. WInc3D: A novel framework for turbulence-resolving simulations of wind farm wake interactions. Wind Energy, 23(3), pp.779-794.

Deskos, G., Laizet, S. and Piggott, M.D., 2019. Turbulence-resolving simulations of wind turbine wakes. Renewable Energy, 134, pp.989-1002.

Hamilton, N., Suk Kang, H., Meneveau, C. and Bayoán Cal, R., 2012. Statistical analysis of kinetic energy entrainment in a model wind turbine array boundary layer. Journal of Renewable and Sustainable Energy, 4(6), 063105.

Luzzatto-Fegiz, P. and Caulfield, C.P., 2018. Entrainment model for fully-developed wind farms: Effects of atmospheric stability and an ideal limit for wind farm performance. Physical Review Fluids, 3(9), 093802.

Ploumakis, E. and Bierbooms, W., 2018. Enhanced Kinetic Energy Entrainment in Wind Farm Wakes: Large Eddy Simulation Study of a Wind Turbine Array with Kites. In Airborne Wind Energy (pp. 165-185). Springer.

van Reeuwijk, M. and Craske, J., 2015. Energy-consistent entrainment relations for jets and plumes. Journal of Fluid Mechanics, 782, pp.333-355.

VerHulst, C. and Meneveau, C., 2014. Large eddy simulation study of the kinetic energy entrainment by energetic turbulent flow structures in large wind farms. Physics of Fluids, 26(2), 025113.

The induction zone of a wind farm in stably stratified flow

Miguel Sanchez Gomez[1,*], and Julie K. Lundquist[1,2]
[1]University of Colorado Boulder
[2]National Renewable Energy Laboratory
[*]Presenting author

Keywords: wind farm blockage | wind farm induction zone | stable boundary layer

Wind turbines decelerate the wind upstream as a result of a perturbation in the flow caused by their rotor. This region of slower velocities is called the induction zone, and it can extend up to 2D upstream for a single turbine. Similarly, the presence of an array of wind turbines reduces the inflow wind speed (blockage effect) altering the wind farm energy production. Several studies have shown the existence of an induction zone upstream of large wind turbine clusters using incompressible Large-Eddy Simulations (LES), Reynolds-Averaged Navier-Stokes (RANS) simulations, lidar observations and wind tunnel experiments. LES of a neutral atmospheric boundary layer suggest the spatial extent of the induction region and magnitude of the velocity deficit increase with stronger free-atmosphere stratification (Wu and Porté-Agel, 2017). Further, this study also revealed free atmosphere stratification can trigger gravity waves and enhance the wind farm's blockage effect.

Results from RANS simulations (Bleeg et al., 2018) concluded that neglecting the induction zone effect can result in substantial long-term energy prediction bias, undermining the wind resource assessment for a wind farm. The induction zone has also been observed experimentally. Wind tunnel experiments by Segalini and Dahlberg (2020) showed the center turbines experience a larger velocity deficit than the turbines at the edges of a wind farm. They also found the velocity deficit is largely produced by the first three turbine rows of a wind plant. Also, an observational study on a large offshore wind farm reported wind speed decelerations upstream during stable conditions when the turbines were operating at a high thrust coefficient (Schneemann et al., 2020).

Here, we demonstrate the contrast between the magnitude of upwind blockage as a function of atmospheric stability. Using idealized WRF-LES simulations of a wind farm in flat terrain, we simulate three cases of stably stratified atmospheric boundary layers in a range of wind speed conditions to explore these effects. We drive the stable boundary layer using three distinct cooling rates and locate the height of the temperature inversion above the wind turbine rotor layer. Turbulence in the nested LES domain is triggered using the cell perturbation method proposed by Muñoz-Esparza et al. (2015).

The turbines are represented using a generalized actuator disk (GAD) which has been previously validated in comparison to scanning lidar measurements of wind turbine wakes (Aitken et al., 2014; Mirocha et al., 2014). As suggested by Allaerts and Meyers (2019), we maintain a 3/2 ratio for the across and along flow size of the wind farm to amplify the blockage effect.

Our idealized simulations validate the existence of an induction zone for a large wind farm in stably stratified flow. We find 2.5% and 1% wind speed reductions up to 5D and 22D upstream of the wind farm, respectively, for a stable layer forced by a -1.2 K h-1 cooling rate (Figure 1).

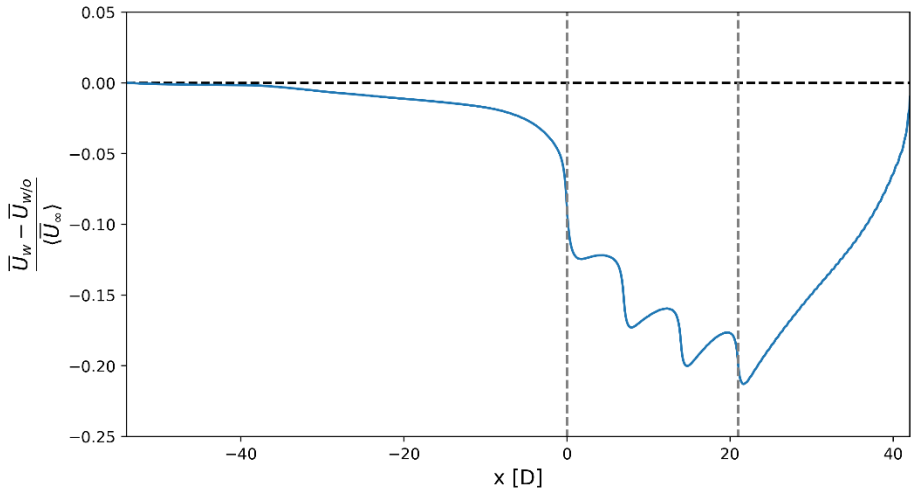


Figure 1: Hub-height wind speed deficit averaged in time and space over the north-south extent of the wind farm for the -1.2 K h-1 cooling rate. The dashed grey line marks the first and last wind turbine row. The dashed black line indicates no wind speed deficit.

When compared to the induction zone of a single turbine found by Medici et al. (2011), the cumulative blockage effect of the wind turbines is larger than the linear superposition of their individual effects. These results may be used to improve energy prediction and reduce bias in operating wind farms.

References:

Aitken, M.L., Kosović, B., Mirocha, J.D., Lundquist, J.K., 2014. Large eddy simulation of wind turbine wake dynamics in the stable boundary layer using the Weather Research and Forecasting Model. Journal of Renewable and Sustainable Energy 6, 033137. https://doi.org/10.1063/1.4885111

Allaerts, D., Meyers, J., 2019. Sensitivity and feedback of wind-farm-induced gravity waves. J. Fluid Mech. 862, 990–1028. https://doi.org/10.1017/jfm.2018.969

Bleeg, J., Purcell, M., Ruisi, R., Traiger, E., 2018. Wind Farm Blockage and the Consequences of Neglecting Its Impact on Energy Production. Energies 11, 1609. https://doi.org/10.3390/en11061609

Medici, D., Ivanell, S., Dahlberg, J.-Å., Alfredsson, P.H., 2011. The upstream flow of a wind turbine: blockage effect. Wind Energ. 14, 691–697. https://doi.org/10.1002/we.451

Mirocha, J.D., Kosovic, B., Aitken, M.L., Lundquist, J.K., 2014. Implementation of a generalized actuator disk wind turbine model into the weather research and forecasting model for large-eddy simulation applications. Journal of Renewable and Sustainable Energy 6, 013104. https://doi.org/10.1063/1.4861061

Muñoz-Esparza, D., Kosović, B., van Beeck, J., Mirocha, J., 2015. A stochastic perturbation method to generate inflow turbulence in large-eddy simulation models: Application to neutrally stratified atmospheric boundary layers. Physics of Fluids 27, 035102. https://doi.org/10.1063/1.4913572

Segalini, A., Dahlberg, J., 2020. Blockage effects in wind farms. Wind Energy 23, 120–128. https://doi.org/10.1002/we.2413

Wu, K., Porté-Agel, F., 2017. Flow Adjustment Inside and Around Large Finite-Size Wind Farms. Energies 10, 2164. https://doi.org/10.3390/en10122164

Schneemann, J., Theuer, F., Rott, A., Dörenkämper, M., Kühn, M., 2020. Offshore wind farm global blockage measured with scanning lidar (preprint). Wind and turbulence. https://doi.org/10.5194/wes-2020-124

Wind farm cumulative induction zone effect modelling with CFD

Aidan Keane*, Iain Nisbet, Gabriele Calvo, George Pickering, Jake Tulloch, Graham More, and Neil Koronka
Wood Renewables
*Presenting author

Keywords: Wind farm | cumulative induction zone effect | blockage effect | wind turbine | computational fluid dynamics

In Keane et al (2021) the cumulative induction zone effect (CIZE) arising from multiple wind turbine generator operation and interaction within a wind farm is quantified within the framework of computational fluid dynamics (CFD). Wind farm blockage and cumulative induction zone effects have also been considered by other research groups, for example, Bleeg et al (2018) and Segalini and Dahlberg (2019).
In Keane et al (2021) a CFD model was benchmarked against wind turbine induction zone wind velocity data measured by a Galion Lidar data at an offshore wind farm. Good agreement was observed between the Galion Lidar data and CFD model results for all wind speed bins considered.
The CIZE on the wind velocity was calculated by comparing the induction zone wind velocities for each wind turbine with and without the induction zones of the other wind turbines.

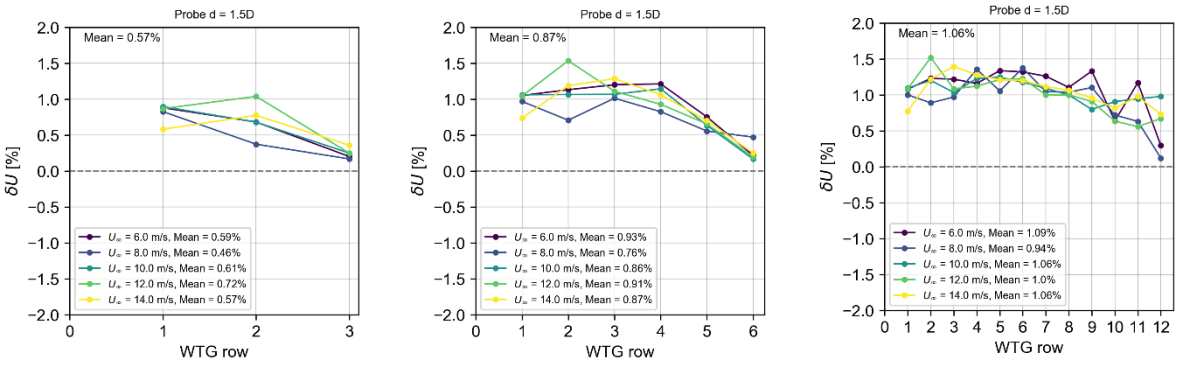


Figure 1: The downwind CIZE wind velocity reduction for the WTGs in the central column of wind farm arrays with 9 columns: C ×R = 9×3, 9×6, 9×12, plotted as a function of the wind turbine row number, for each inflow wind velocity.

A parametric study was performed, with a view to understanding and quantifying the CIZE for typical wind farm arrangements. Figure 1 shows the CIZE effect on wind velocity in the downwind directions for a selection of wind farm array configurations, for each inflow wind speed and Figure 2 shows the mean CIZE value dependence upon the density of wind turbines within an array.

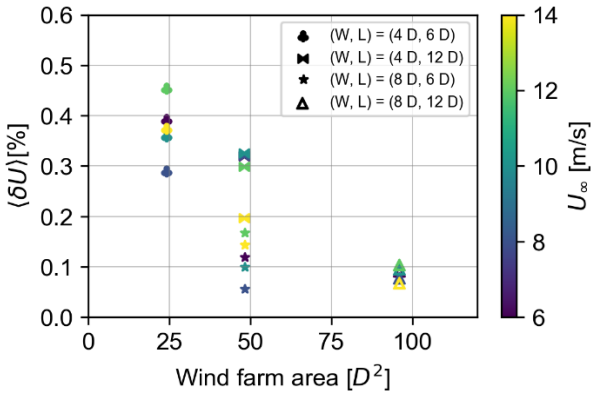


Figure 2: The mean CIZE wind velocity reduction value for the wind farm configuration D = 116 m, h = 0.8 D, columns × rows = 4 × 3, for each value of inflow wind velocity for various combinations of width and length (W, L).

Based upon the wind farm array configurations investigated, the outcomes indicate that for a centrally located column within a fixed wind farm array configuration, the CIZE wind velocity reduction appears to exhibit a relatively flat profile downwind, until the tail of the array, i.e., approximately the final four rows, where there is a relative drop-off in CIZE wind velocity reduction.

For a wind farm with a fixed number of wind turbine columns and rows, the general trend is that the CIZE wind velocity reduction decreases with increasing array width W or length L.

For a wind farm with a fixed number of rows and columns, the general trend is that the CIZE wind velocity reduction increases with increasing wind turbine rotor diameter D. The trend is less clear for the dependence upon wind turbine hub height h, but for higher wind velocities the CIZE wind velocity reduction decreases with increasing h. While most wind turbines within a wind farm experience a wind velocity reduction due to CIZE, some wind turbine can exhibit an increase in wind velocity due to CIZE. However, the occurrence of such incidences is rare and where this does occur, the overall mean values for the entire wind farm are found to be positive.

A range of wind farm array configurations have been investigated and the results can be used to advise adjustments relevant to wind farm energy production assessments. Based upon the wind farm array configurations investigated, the outcomes indicate that the cumulative induction zone effect results in a reduction in the induction zone wind velocity of approximately 0.3 to 1.6% depending on the wind farm configuration, the inflow wind velocity and the atmospheric stability conditions, and that the corresponding reduction in energy yield is approximately 0.4 to 1.2%, depending on the wind speed distribution.

References:

Keane, A., Nisbet, I., Calvo, G., Pickering, G., Tulloch, J., More, G., Koronka, N. (2021) 'Wind farm energy yield estimate reduction due to the cumulative induction zone effect', submitted January 2021.

Bleeg, J., Purcell, M., Ruisi, R. and Traiger, E. (2018) 'Wind Farm Blockage and the Consequences of Neglecting Its Impact on Energy Production' Energies 11, 1609.

Segalini, A. and Dahlberg, J-A. (2019) 'Blockage effects in wind farms' Wind Energy DOI: 10.1002/we.2413

Measuring Wind Farm Scale Blockage – First results from a 12-month scanning lidar campaign at a German offshore wind farm

Jens Riechert[1,*], Matthias Steger[1], Christiane Montavon[1], James Bleeg[1], and Carolin Schmitt[2]
[1]DNV GL
[2]EnBW
*Presenting author

Keywords: Wind farm scale blockage | Long-range scanning lidar systems | Measurement campaign | Offshore

Wind Farm Scale Blockage (blockage) is becoming a more and more commonly known phenomenon. However, the way blockage is considered in Energy Production Assessments (EPA) still depends on the in-house procedures of the companies who are doing the EPA. In order to further harmonize the way blockage is considered, a meaningful and reliable evidence base is needed. During the past years, different industry leaders published several studies related to blockage which have helped to increase the knowledge and understanding of the effect. As most of these studies are based on flow modelling [1][2][3], which can have relatively high uncertainties, more blockage-related field observations [4] are needed to improve our understanding of these effects.

In this abstract we discuss the first results from a 12-month scanning lidar campaign (Dec. 2019 – now), conducted at a German offshore wind farm. Because of its small magnitude (compared to wake effects), measuring blockage is challenging and requires great demands on the measurement equipment, especially in terms of accuracy and long-term reliability.

After conducting an intensive design study, it was decided to use two long-range scanning lidar systems (Leosphere Windcube 400S) operated in Dual Doppler (DD) mode. The operation in DD mode has great advantages compared to measurements from single lidars, allowing a direct reconstruction of the wind field quantities without assumptions of a homogenous horizontal wind flow.

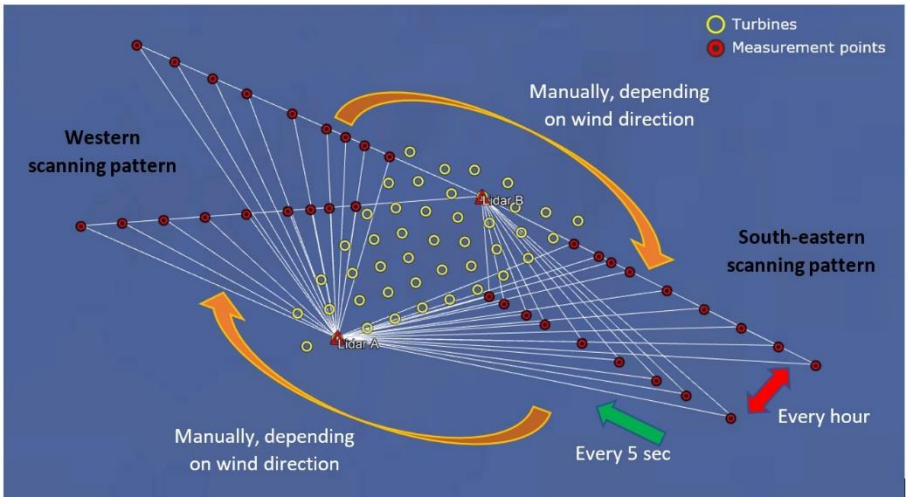


Figure 1: Measurement setup for an exemplary wind farm layout incl. measurement points, wind turbines, scanning lidar position and information about scanning schedule.

The lidar systems are installed on the transition piece of two turbines (Fig. 1). The systems are configured to measure horizontal wind speed and wind direction along two measurement lines in the western and two lines in the south-eastern part of the wind farm. Each line consists of nine measurement points, capturing distances from 0.5 km to 7 km upstream of the wind farm. In order to investigate the wind farm blockage in a most suitable way, a three-stepped scanning schedule has been introduced, moving the laser beams between measurement points within one measurement line (every 5 sec), cycle between two measurement lines (every hour) and switching between measurement areas (western/south-eastern area) depending upon the wind direction (manually).

The data measured along the measurement lines was used to discern the average spatial variation of wind speed upstream of the wind farm. In order to assess associated sensitivities, the data has been classified into different atmospheric (stable, neutral, unstable) and operational conditions (wind direction, availability of the wind farm, etc.).

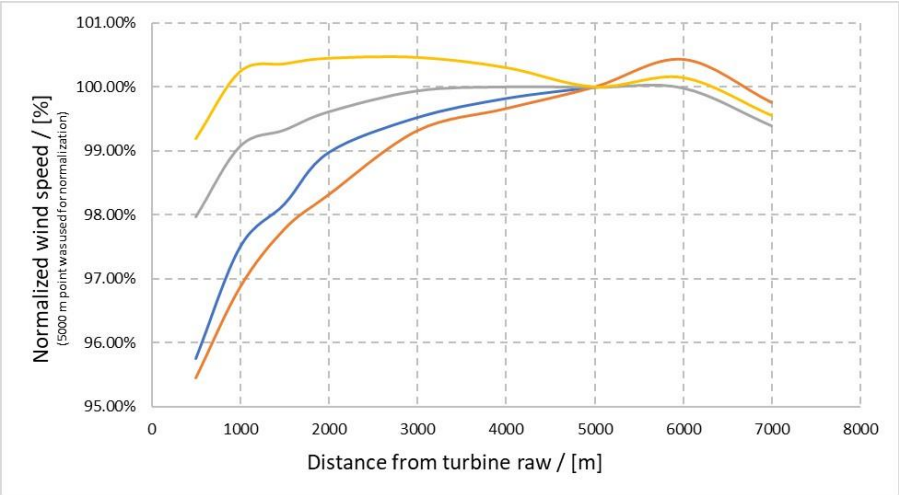


Figure 2: Example of normalized wind speed for all four measurement lines (line numbers anonymized), using a ±30° sector around the scanning lines and without stability classification.

A summary of the first results of the measurement campaign is given below:

- Fig. 2 gives an example of the normalized wind speeds along the four measurement lines.
- The results give a clear evidence that wind-farm-scale blockage exists.
- The strongest wind speed reduction is observed in the proximity of the wind farm, extending to upstream distances of approximately 3 to 5 km.
- The normalized wind speeds show strong variations between the measurement lines. Comparisons with CFD modelling [5] indicate that these variations are coupled to local site effects (e.g. coastal transition) which affect different lines in different measure.
- The magnitude of the blockage is sensitive to both atmospheric and operational condition.
- Great efforts have been put into the reduction of measurement uncertainties, especially focusing on the laser beam pointing accuracy and operational behavior of the turbine.

References:

[1] Bleeg, J.; Purcell, M.; Ruisi, R.; Traiger, E. "Wind farm blockage and the consequences of neglecting its impact on energy production." Energies 2018,11, 1609. Available at http://www.mdpi.com/1996-1073/11/6/1609, 11/2018

[2] N. G. Nygaard et al 2020 J. Phys.: Conf. Ser. 1618 062072, https://iopscience.iop.org/article/10.1088/1742-6596/1618/6/062072/pdf

[3] Branlard et al, 2020, J. Phys.: Conf. Ser. 1618 062036, https://iopscience.iop.org/article/10.1088/1742-6596/1618/6/062036/pdf

[4] Schneemann, J.; Rott, A.; Dörenkämper, M.; Theuer, F.; Kühn, M.; "Offshore wind farm global blockage measured with scanning lidar", Wind Energy Science, Available at https://wes.copernicus.org/preprints/wes-2020-124/, 11/2020

[5] Montavon et al, WESC 2021, submitted.

Mini-Symposium: Entrainment and Blockage Effects on Large Offshore Wind Farms (II)

An analytical solution for wind deficit decay behind a wind energy converter and wind energy parks using momentum conservation validated by airborne data

Moritz Mauz[1,*], Bram van Kesteren[1], Andreas Platis[1], Stefan Emeis[2], and Jens Bange[1]
[1]University of Tübingen
[2]Karlsruhe institute of Technology
[*]Presenting author

Keywords: wind energy wake deficit | analytical model | UAS data | airborne wind park data | model comparison

The wind deficit behind a wind energy converter (WEC) results from a complex interaction of forces. Kinetic energy is removed from the atmosphere, but coherent turbulent structures prevent a swift compensation of momentum within the wake behind the WEC. A detailed description of the wake is beneficial in meso-scale weather forecast (e.g. WRF models) and numerical simulations of wind wake deficits. Especially in the near to intermediate wake (0.5 - 5 rotor diameters), the dominating processes characterising the wake formation change along the wake. The conservation equation of momentum is used as a starting point to map the most important processes assuming the WEC operates at maximum efficiency in a neutral stratified boundary layer. The wake is divided into three different regions to accommodate the changing impact of atmospheric turbulence and the shear created by the WEC onto the wake. A differential equation that depicts the variable momentum transport into the wind deficit along the wake is derived and solved analytically. Additionally, a numerical solution (Euler method) of the simplified momentum conservation equation is shown to provide a quality control and error estimate to the analytical model. The analytical solution is compared to conventional WEC wake models and in-situ wake measurements behind an Enercon E- 112 converter, located in the Jade Wind Park near the North Sea coast in Germany, captured by the MASC-3 UAS (unmanned aircraft system) of the University of Tübingen. The obtained UAS data cover the distance from 0.5 – 5 at hub height behind the nacelle. The analytical and numerical model are found to be in good agreement with the data of the three measurement flights behind the WEC (Fig. 1).

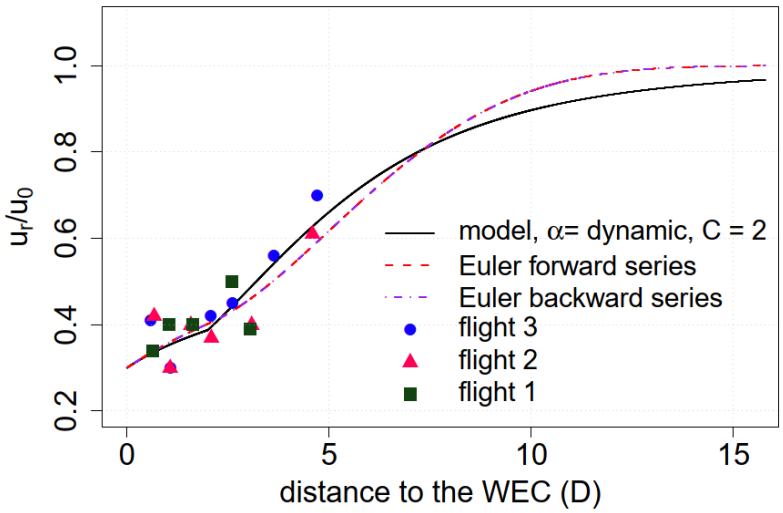


Figure 1: Normalised reduced wind speed measurements of three flights at hub height behind an Enercon E-112 WEC. The proposed new model is shown in a black solid line. The numerical Euler method in red and purple.

The presented model can also be tuned for wind park wakes. Where improvements in the wind park wake deficit prediction and wake lengths are gained.
Wind park wake behaviour and forecasting is gaining in importance quite recently. It is especially relevant in the German Bight where space for wind park clusters is limited, and wind park wake lengths of up to 60 km have been measured, e.g. behind the Amrumbank West wind park. In the presentation the analytical E10 (Emeis, 2010) wind park wake model is compared to the M20 analytical model. Both models are compared in this study to measured in-situ airborne data, captured during the WIPAFF (wind park far field) project. Two specific flights are shown with the respective model result of each analytical model. In addition a two-dimensional solution of the M20 model is presented that enables a realistic two-dimensional wake shape forecasting (Fig. 2).

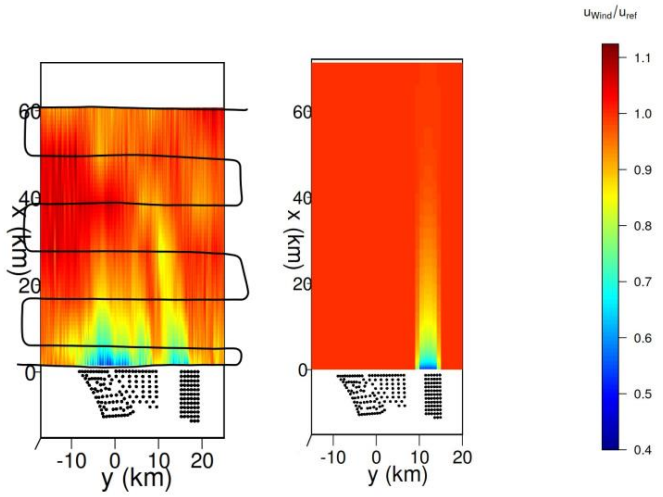


Figure 2: (Left) Visualised residual wind speed measurements behind the wind parks Nordsee Ost, Meerwind Süd-Ost and Amrumbank West (LTR) indicated by the black dots. The black solid line is the flight path of the research aircraft Do 128-6 (D-IBUF) of the TU Braunschweig. (Right) Modelled residual wind speeds behind the wind park AW using the M20 model.

The M20 model is derived from the Reynold's averaged Navier-Stokes equation for the momentum conservation. It describes the wind speed recovery in the wake of wind park (or a single converter) from an atmospheric point of view, by introducing turbulent momentum from the atmosphere aloft the wind park wake, and in the two-dimensional case, from the sides as well. Due to the facilitation of a dynamic wind deficit decay rate in the M20 model, a gain in accuracy in contrast to the E10 model is achieved.

References:
Emeis, S.: A simple analytical wind park model considering atmospheric stability, Wind Energy, 13, 459–469, https://doi.org/10.1002/we.367, https://onlinelibrary.wiley.com/doi/abs/10.1002/we.367, 2010.

Train2Wind, or how large is an infinite wind farm?

Gregor Giebel[1], Tuhfe Gocmen[1], Jakob Mann[2], Anna Maria Sempreviva[1], Haakon Lund[3], Joachim Reuder[4], Jens Bange[5], and Fernando Porté-Agel[6]
[1]DTU Wind Energy
[2]Technical University of Denmark
[3]University of Copenhagen
[4]University of Bergen
[5]University of Tübingen
[6]École Polytechnique Fédérale de Lausanne

Keywords: Entrainment | Wind resource | Wind farm cluster | Unmanned Aerial System | Marie Sklodowska Curie Action

TRAIN2WIND is a PhD TRAINing school analysing enTRAINment in offshore WIND farms with computer models and experiments. By its very nature, a wind turbine extracts energy from the wind, which is replenished from the wind field on the sides and above due to the ambient turbulence.

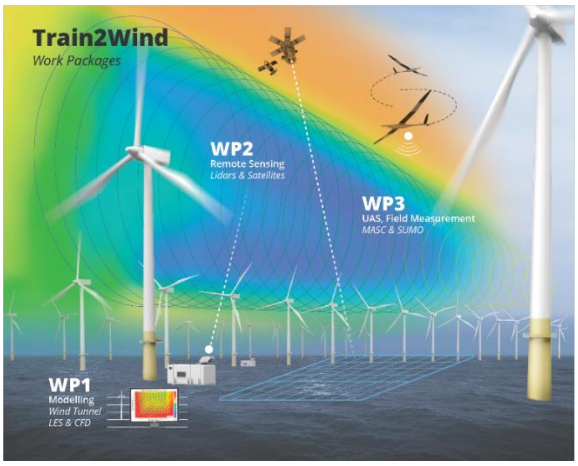


Figure 1: The setup of the Train2Wind project and envisaged experiment.

However, offshore the turbulence is lower, and wind farms are typically larger than onshore, therefore the wind can only be replenished from above in a process called entrainment. Train2Wind will investigate the entrainment process using advanced high-resolution computer modelling and wind tunnel models together with measurements of the wind field above, in and downstream of large wind farms, using lidars, radars, satellites and Unmanned Aerial Systems.
Besides the natural science package, one humanities PhD student at the University of Copenhagen will investigate the collaboration between the researchers from a social science and collaboration tools perspective.
The main work is done during the education of 18 fellows, where 13 embark on a PhD, while the other ones are employed for one year. The students will work with high-fidelity numerical simulations, lidars, unmanned aerial systems, wind tunnels and satellite data in order to understand entrainment of new momentum in very large wind farms. This changes the atmospheric boundary layer over a very extended wind farm, which becomes a wind turbine array boundary layer. The resulting change in wind resource is the main object of interest. The main planned activity is an experimental campaign at a major cluster of wind farms, probably in the North Sea. Another activity revolves around vertical axis turbines and their significantly different wake pattern, a potential mitigation measure.
So far we recruited the fellows and started with the simulations and the development of the hardware. We intend to employ a vertical take-off and landing model plane with a wing span of about 2m, which would allow to start and land from a helicopter pad offshore, and after the vertical start enjoy the advantage of a

winged plane and its much larger range and endurance. Another instrument is a hexacopter mounted with a sonic anemometer, which allows to sample in a single point much akin a conventional met mast, but at any given point in or above a large wind farm. Lidar usage and development is part of the project as well, with a floating lidar in Bergen University and long-range lidars at DTU.
There are three numerical codes used in Train2Wind: Ellipsys3D, a Large Eddy Simulation (LES) highfidelity code from DTU, WIRE-LES, another LES code from EPFL, and the Weather Research and Forecasting model run at DTU.
The outcome of the project is more knowledge of the entrainment process, and a guidance on how close to position clusters of wind farms in order not to exhaust the wind resource. The talk will give an overview of the project, highlighting the challenges.

References:
https://www.Train2Wind.eu/

Wake flows in an experimentally-modeled offshore wind farm

Guiyue Duan*, and Fernando Porté-Agel
Wind Engineering and Renewable Energy Laboratory (WiRE), École Polytechnique Fédérale de Lausanne (EPFL)
*Presenting author

Keywords: wind farm wakes | wind-tunnel experiments | atmospheric boundary layer | vertical entrainment | particle image velocimetry

The Gaussian analytical wake model [1] can predict the power performance and mean characteristics of the wake flow of a single wind turbine well, which further favors acceptable power predictions of wind farms [2]. In pursuit of higher accuracy of the predictions, we need a better understanding of the two-way interactions between the atmospheric boundary layer (ABL) flow and the wind turbine wake flows, which affect the kinetic energy available to wind turbines in wind farms and also the wake recovery. In a large wind farm, the available energy is significantly deprived by upstream wind turbines, and the lateral mixing which favors wake recovery is also constrained. Therefore, the vertical entrainment from the above boundary layer becomes the most effective way to replenish wakes and enable energy extraction [3], especially in large offshore wind farms which tend to grow in size in response to the escalating demand for wind energy.

The current study focuses on the wake flows inside and behind large offshore wind farms through wind-tunnel experiments. To understand the role of the entrainment process in the energy extraction and the turbine wake recovery, particle image velocimetry (PIV) is used to characterize the flow field of a large scaled-down wind farm in a turbulent boundary layer. The proper orthogonal decomposition (POD) technique is employed to investigate the contribution of different turbulence scales on the flow dynamics. Previous studies based on PIV experiments [4] and large-eddy simulations [5] suggest the first few POD modes could effectively capture the most energetic flow structures which dominate the large-scale turbulent motions in the vertical entrainment process. The typical length scales of these turbulent motions are then expected to be obtained by POD analysis.

Furthermore, the properties of the vertical entrainment process in both time and frequency domains are analyzed based on the data obtained from a hot-wire anemometer.

Based on the measurements and analysis techniques mentioned above, we firstly expect a better understanding of the mechanisms of flow entrainment and relate it to the power performance of the wind farm under controlled conditions, including surface roughness and atmospheric stability, which can be both adjusted in the experimental facility. The power performance will then be examined under selected active yaw control and down-regulation control over wind turbines to seek potential strategies that enhance entrainment and thus increase the power output. These measurements will provide a sound database for the development of a new analytical model that incorporates the vertical entrainment from the ABL and the wake evolution of the wind farm. We expect the new model to have acceptable predictability on the power performance of the wind farm.

The analytical model development takes inspiration from the Gaussian analytical wake model [1] for individual wind turbines, and wind farm models, including the 'top-down' model coupled with an internal boundary layer [6] and a recently-proposed entrainment model [7] as illustrated in Figure 1.

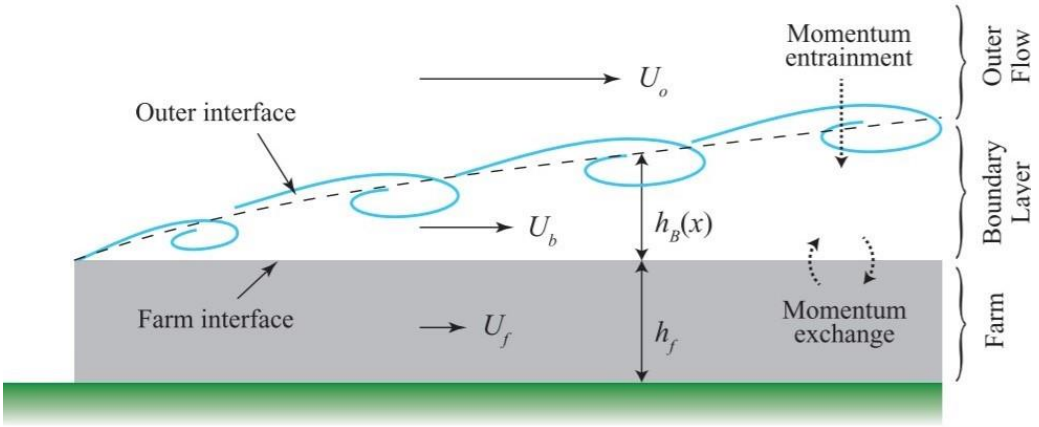


Figure 1: A sketch of the entrainment model for a wind farm. The grey box represents the wind farm regarded as a canopy. The turbulent boundary layer is originated from the leading edge of the farm. U represents the flow velocity and h stands for the height, with the subscripts, 'f', 'b/B' and 'o' indicating the wind farm, the boundary layer and the outer flow respectively [7]

Although both wind farm models capture the interactions between the wind farm and the ABL well, the 'top-down' model lacks considerations of the positioning of turbines, while the entrainment model ignores the flow inside the wind farm by considering it as a canopy. The new model will not only take the effects of the ABL stability and the wind farm layouts into account, but also predict the wake evolution through the wind farm.

References:

[1] Bastankhah, M. and Porté-Agel, F., 2014. A new analytical model for wind-turbine wakes. Renewable Energy, 70, pp.116-123.
[2] Niayifar, A. and Porté-Agel, F., 2016. Analytical modeling of wind farms: A new approach for power prediction. Energies, 9(9), p.741.
[3] Hamilton, N., Suk Kang, H., Meneveau, C. and Bayoán Cal, R., 2012. Statistical analysis of kinetic energy entrainment in a model wind turbine array boundary layer. Journal of renewable and sustainable energy, 4(6), p.063105.
[4] Newman, A.J., Drew, D.A. and Castillo, L., 2014. Pseudo spectral analysis of the energy entrainment in a scaled down wind farm. Renewable energy, 70, pp.129-141.
[5] VerHulst, C. and Meneveau, C., 2014. Large eddy simulation study of the kinetic energy entrainment by energetic turbulent flow structures in large wind farms. Physics of Fluids, 26(2), p.025113.
[6] Meneveau, C., 2012. The top-down model of wind farm boundary layers and its applications. Journal of Turbulence, (13), p.N7.
[7] Luzzatto-Fegiz, P. and Colm-cille, P.C., 2018. Entrainment model for fully-developed wind farms: Effects of atmospheric stability and an ideal limit for wind farm performance. Physical Review Fluids, 3(9), p.093802.

Atmospheric Boundary Layer Interactions with Large Wind Farms: A Large Eddy Simulation Study

Marwa Souaiby*, and Fernando Porté-Agel
École Polytechnique Fédérale de Lausanne
*Presenting author

Keywords: ABL | LES | Wind Farm Wake | Flow Regions | Large Wind Farm

Optimizing the design, control, operation, and grid integration of wind farms face the burden of predicting their performance. This challenging task is due to the complexity of the two-way multiscale interactions between the wind farms and the turbulent atmospheric boundary layer (ABL).
Consequently, the ABL structure undergoes significant alterations, which in turn affect the performance of the wind farm compared to that of theoretical stand-alone wind turbines operating in the same undisturbed boundary layer conditions.
The ABL-wind farm interaction leads in the case of flat homogeneous terrains to the formation of different flow regions, as shown in the figure (Wu and Porté-Agel, 2017; Porté-Agel, Bastankhah and Shamsoddin, 2020): wind-farm induction region, development region, fully developed region where the flow becomes fully adapted to the wind farm, and wind-farm wake region. In order to improve our understanding and prediction of these wind farm flows, it is crucial to assess the extent and flow characteristics within each of these distinct regions. Studies relying on satellite measurements (Christiansen and Hasager, 2005) and numerical simulations (Wu and Porté-Agel, 2017) have shown that wind farm wakes have a significant effect on the surface layer wind speed at relatively large downwind distances. A velocity deficit of 2% is found as far as 5 to 20 km downwind of the wind farms, depending on the ambient turbulence level, thermal stability and wind farm size. Hence, investigating and predicting the farm wake flows is essential to reduce the interactions between
neighboring wind farms when they are installed in that range of proximity.
This research will use large-eddy simulation (LES) to further assess the superposition of multiple wind turbine wakes inside wind farms and their two-way interaction with the ABL flow resulting in important changes in both the structure of the ABL and the power generation efficiency of the wind farms. Tuning-free Lagrangian scale-dependent dynamic models will be used to model the subgridscale (SGS) turbulent fluxes, whereas the turbine induced forces will be parametrized with rotational actuator disk models.

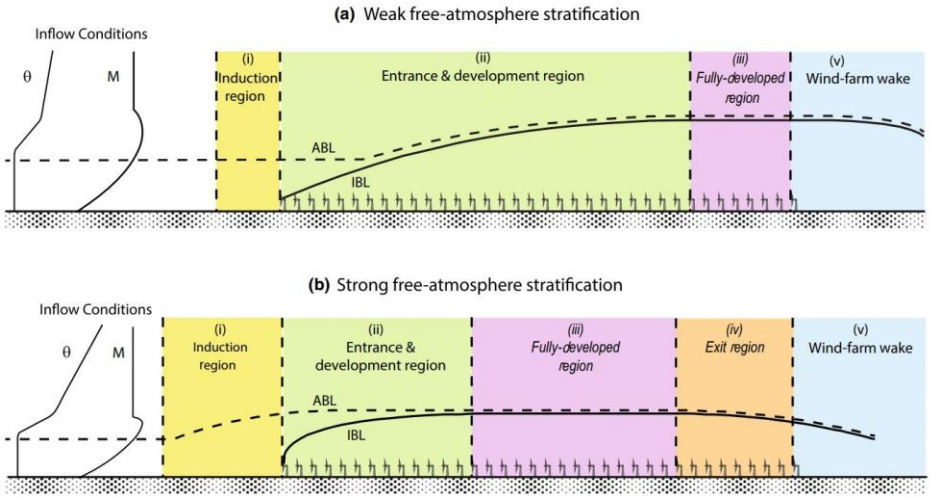


Figure 1: Schematic of different flow regions caused by the interaction of a large wind farm with a CN-ABL under weak free-atmosphere stratification (a) and strong free-atmosphere stratification (b). The dashed and continuous lines represent the top of the ABL and the farm-induced IBL, respectively. Inflow conditions are represented by vertical profiles of the mean ϑ and mean wind speed M. In italics: regions presence dictated by wind farm size and free atmospheric stratification. (Porté-Agel et al. 2020)

In this context, starting from available LES simulations of real and idealized wind farms, the LES domain and wind farm size will be expanded to investigate where the flow above the wind farm and down the surface reaches equilibrium. This setup will also be used to further examine farm-to-farm interactions with their inherent effects on the performance of neighboring wind farms. The ABL and wind farm turbulent flow interaction in the above-mentioned flow regions can be also extensively studied for different wind farm and incoming flow characteristics such as size, layout, density, the wind direction, and atmospheric stability. These numerical LES results will eventually be used for the validation and improvement of analytical wake models as well as wind-farm parameterizations for large-scale atmospheric models.

References:

Christiansen, M. B. and Hasager, C. B. (2005) 'Wake effects of large offshore wind farms identified from satellite SAR', Remote Sensing of Environment, 98(2–3), pp. 251–268. doi: 10.1016/j.rse.2005.07.009.

Porté-Agel, F., Bastankhah, M. and Shamsoddin, S. (2020) Wind-Turbine and Wind-Farm Flows: A Review, Boundary-Layer Meteorology. Springer Netherlands. doi: 10.1007/s10546-019-00473-0.

Wu, K. L. and Porté-Agel, F. (2017) 'Flow adjustment inside and around large finite-size wind farms', Energies, 10(12), pp. 4–9. doi: 10.3390/en10122164.

How can we assure that offshore wind farms will be efficient in 2050?

Oscar Garcia*, Jake Badger, and Andrea N. Hahmann
Technical University of Denmark
*Presenting author

Keywords: Mesoscale modelling | Wind farm parametrisation | WRF

New large wind farms projects are being built and planned to accomplish the energy demands in the world. As wind farms are getting larger, it is essential to ensure the efficiency of them. For instance, a large wind farm cluster in the Dutch sea is planned to be opened in 2025 with an approximate area of 400 km2 and an expected capacity of 4 GW (NEA, 2020). This corresponds to 10 MW/km2, which might lead to low-efficiency performance depending on the turbines' specific power and spacing.
According to Volker et al. (2017), for a wind farm of this size, the efficiency would fall to less than 75 % for narrow turbine spacing. Thus, to establish the possible efficiency of wind farms, factors like the location, layout design, installed capacity density and understanding the impact that wind farms themselves have on wind resources are growing in importance (Volker et al., 2017; Hou et al., 2019; Agora report, 2020). Planning and building more efficient wind farms would contribute to the mission of net-zero greenhouse emissions in 2050. To this end, the European Commission has raised offshore wind capacity targets to 300 GW by mid-century (EC, 2020). Figure 1 represents a possible scenario for offshore wind farms locations in the North Sea.

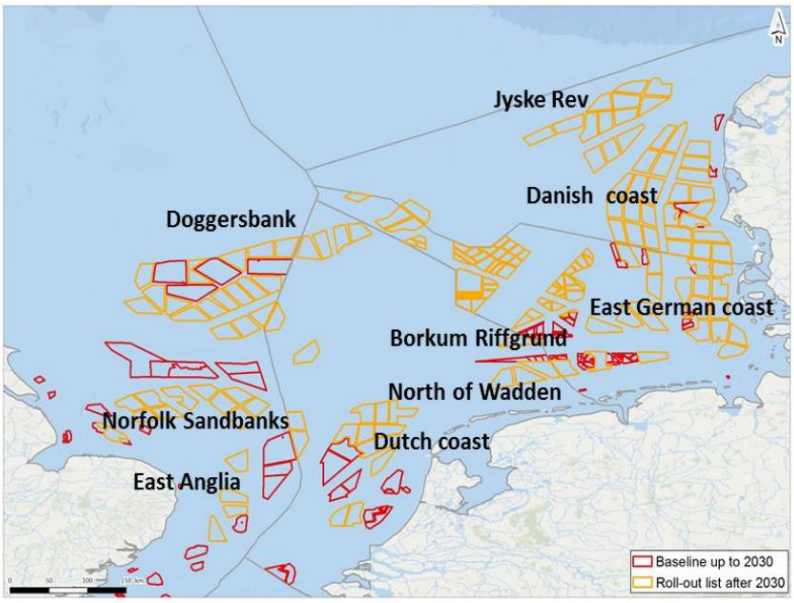


Figure 1: Possible scenario for new offshore wind farms (orange polygons) locations in the North Sea for discussion with stakeholders figure from NSWPHC, 2019).

Using high-resolution microscale models to make wind resource assessment in a large area such as the North Sea will be computationally costly. A more viable solution is using atmospheric mesoscale models. These models have been used for more than two decades for wind resource assessment (Olsen et al., 2017). However, mesoscale models used in this way and wind atlas mapping methods historically have not been accounting for the flow reduction associated with wind turbines and wind farms. Thus, a parametrisation is needed to account for this effect. Different parametrisations have been developed to address this problem. The two primary parametrisation schemes implemented in the Weather Research and Forecast (WRF; Skamarock et al., 2008) mesoscale model are the Wind Farm (Fitch et al., 2012) and Explicit Wake Parametrisation (EWP; Volker et al., 2015). While these parametrisations demonstrate progress in representing the wind turbines compared to those that apply an increased roughness, they still need to be improved.

This presentation will outline the processes for improving the EWP implemented in WRF. The hypothesis is that the parametrisation accuracy could be improved with the thrust force information from computational fluid dynamics (CFD) models. Two main aspects will be discussed; the parametrisation of the thrust forces within the model's grid-cell and added sources of Turbulent Kinetic Energy (TKE). In the first one, precalculating thrust forces using CFD models will be outlined along with a wake model's possible coupling in WRF. For the TKE aspect, the idea of "latent" TKE will be explained as an alternative approach to include the turbulence source from the turbines. Also, simulations of WRF will investigate the role of atmospheric stability and the entrainment process on the behaviour of the wind deficit and recovery.
Possible validation strategies will be presented to evaluate the results against wind measurements and power production datasets from industrial partners. The impact of the new parametrisation could lead to novel application studies: investigating the role of installed capacity density, layout and different turbine types; and the impact of future clusters of large wind farms on the environment.

References:
European Union: European Commission (2020) 'Communication from the Commission to the European Parliament, the Council, The European Economic and Social Committee and the Committee of the Regions – An EU Strategy to harness the potential of offshore renewable energy for a climate neutral future'. Brussels.
Fitch, A. C. et al. (2012) 'Local and Mesoscale Impacts of Wind Farms as Parameterized in a Mesoscale NWP Model', Monthly Weather Review, 140(9), pp. 3017–3038. doi: 10.1175/MWR-D-11-00352.1.
Hou, P. et al. (2019) 'A review of offshore wind farm layout optimization and electrical system design methods', Journal of Modern Power Systems and Clean Energy, 7(5), pp. 975–986. doi: 10.1007/s40565-019-0550-5.
Netherlands Enterprise Agency (2020) IJmuiden VER - General information. Available at: https://offshorewind.rvo.nl/generalIJmuiden (Accessed: 21 January 2021)
North Sea Wind Power Hub Consortium (2019) Cost Evaluation of North Sea Offshore Wind Post 2030. Available at: https://northseawindpowerhub.eu/cost-evaluation-of-north-sea-offshore-wind-post-2030-towards-spatial-planning/.
Olsen, B. T. et al. (2017) 'An intercomparison of mesoscale models at simple sites for wind energy applications', Wind Energy Science, 2(1), pp. 211–228. doi: 10.5194/wes-2-211-2017.
Skamarock, W. C. et al. (2008) A Description of the Advanced Research WRF Version 3, NCAR Technical note. doi: 10.5065/D68S4MVH.
Technical University of Denmark and Max-Planck-Institute (2020) 'Making the Most of Offshore Wind: Re-Evaluating the Potential of Offshore Wind in the German North Sea. Study commissioned by Agora Energiewende and Agora Verkehrswende.', in Energiewende, A., Agora Verkehrswende, T. U. of, and Denmark, M.-P.-I. for B. (eds) Making the Most of Offshore Wind: Re-Evaluating the Potential of Offshore Wind in the German North Sea, pp. 1–84.
Volker, P. J. H. et al. (2015) 'The explicit wake parametrisation V1.0: A wind farm parametrisation in the mesoscale model WRF', Geoscientific Model Development, 8(11), pp. 3715–3731. doi: 10.5194/gmd-8-3715-2015.
Volker, P. J. H. H. et al. (2017) 'Prospects for generating electricity by large onshore and offshore wind farms', Environmental Research Letters, 12(3). doi: 10.1088/1748-9326/aa5d86.

Analysis of wind wakes for a cluster of offshore wind farms from construction to operation date using satellite observations

Abdalmenem Owda*, Merete Badger, and Ioanna Karagali
Technical University of Denmark
*Presenting author

Keywords: Wind wake | Satellite | Synthetic Aperture Radar

Wind power becomes a reliable energy resource in almost every member of the European Union (EU). Wind Europe statistics (Windeurope.org, 2021) show an increased number of wind farms (113) and cumulative capacity (23.2 GW) in European waters by mid-2019. Moreover, new offshore wind investments doubled in 2020 compared with 2019. Consequently, the offshore wind farms become concentrated in clusters and this adds new challenges.
This study exploits the abundance of Synthetic Aperture Rader (SAR) data from the European Space Agency (ESA) in order to analyze wind wakes for the three Danish offshore wind farms Horns Rev 1, 2 and 3 (Fig. 1). The wind farms consist of 80, 91, and 49 turbines, respectively. Analysis of satellite observations for different periods before and after the wind farm construction enables us to compare the wind conditions with/without neighboring wind farms.

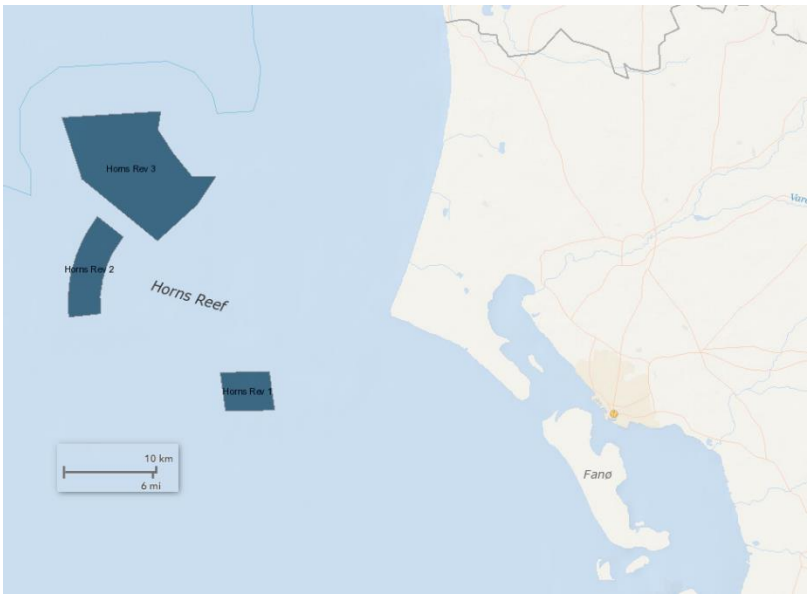


Figure 1: The Danish offshore wind farms Horns Rev 1, 2 and 3 (4coffshore.com, 2021).

Wind retrievals from SAR Sentinel 1A/B and Envisat scenes enable wind mapping at less than 1 km resolution. The main advantage of SAR observations lies in the spatial information, which allows us to study variations in the coastal winds without any a prior knowledge (Dagestad et al. 2013).
Our analysis begins with a screening for available SAR wind maps at https://satwinds.windenergy.dtu.dk/. No SAR scenes are available before the construction of Horn Rev 1. About 2600 scenes, from either Sentinel-1A/B or Envisat, exist for the period 2002-20 and a selection of these are investigated here.

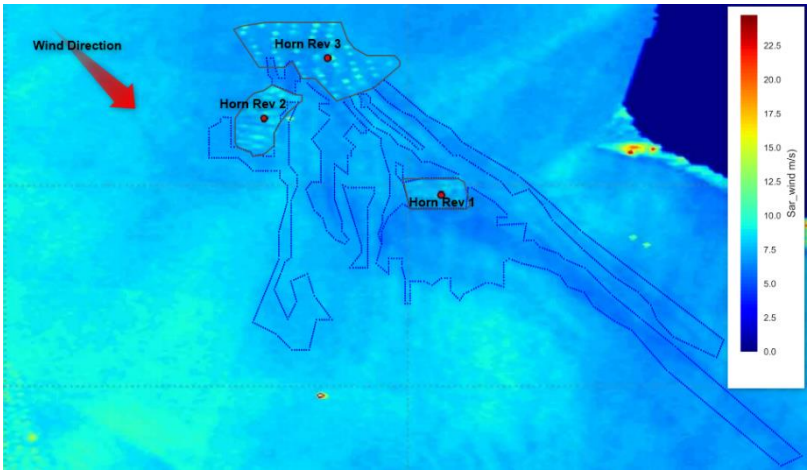


Figure 2: SAR wind map from a Sentinel-1A scene acquired at 2019-06-26T05:48:45

Some SAR scenes show significant and important information about wind wakes and several other wind phenomena. Fig. 2 shows an example SAR wind map from 2019-06-26 at 05:48 UTC when all three wind farms at Horns Rev are in operation. Wind wakes are seen as streaks extending from each wind farm and many km in the downstream direction (southeast). The wind wakes downstream from Horns Rev 3 affect Horns Rev 2 and 1 and extend several kilometers towards the land. In this example, Horns Rev 1 is subject to wind wakes from two other offshore wind farms. Remarkably, in only one scene, we could detect many interesting and potential research points e.g. the relationship between wind wakes and the distribution of wind turbines inside the wind farms. The wind wake from Horns Rev 3 looks different compared with the wake patterns from Horns Rev 2 and 1. The plotted dashed lines indicate the potential areas of downstream wind velocity deficits.

Consequently, we are going to sort SAR wind maps based on the wind flow direction and analyze wind speeds along different transects around the wind farm cluster (reference). We will then be able to quantify the wind wakes and wind deficits percentages for different periods. Because of the shallow water depth close to the land and especially near Horns Rev 1; the bathymetry effects will be considered before the transect analysis to avoid its contamination of the SAR wind retrievals. We can take the absolute wind speed, the atmospheric stability, and the turbulence intensity into consideration when we characterize wind wakes. Key results and interpretations of these analyses will be presented at the conference.

References:

Windeurope.org, (2021). Wind Europe's Official Website. [online] Available at www.windeurope.org/dataand.analysis/product/offshore-wind-energy-2020-mid-year-statstics/ [Accessed 13 Jan. 2021].

Dagestad, K.-F., Horstmann, J., Mouche, A., Perrie, W., Shen, H., Zhang, B., ... Vachon, P. (2013). Wind retrieval from synthetic aperture radar - an overview. Seasar 2012. Proceedings, 230–251.

4coffshore.com, (2021). 4COffshore's Official Website. [online]. Available at 4coffshore.com/offshorewind/ [Accessed 13 Jan. 2021].

Scientific Collaboration in Wind Energy PhD Training Networks

Grischa Fraumann*
University of Copenhagen
*Presenting author

Keywords: PhD training networks | scientific collaboration | early-stage researchers | senior researchers

Collaboration is paramount in research to solve grand challenges, and in particular within international research networks (Haman and Hertzum, 2019). The study analyses expectations and experiences regarding scientific collaboration in PhD training networks in the research area of wind energy by relying on a unique study sample. The PhD project is part of the Train2Wind (TRAINing school analysing enTRAINment in offshore WIND farms) Innovative Training Network (ITN) (Geibel et al., 2019) (see Figure 1), a project which is conducted at six higher education institutions and four industry project partners in Denmark, Germany, Norway, Sweden, Switzerland, and the US (https://www.train2wind.eu/).

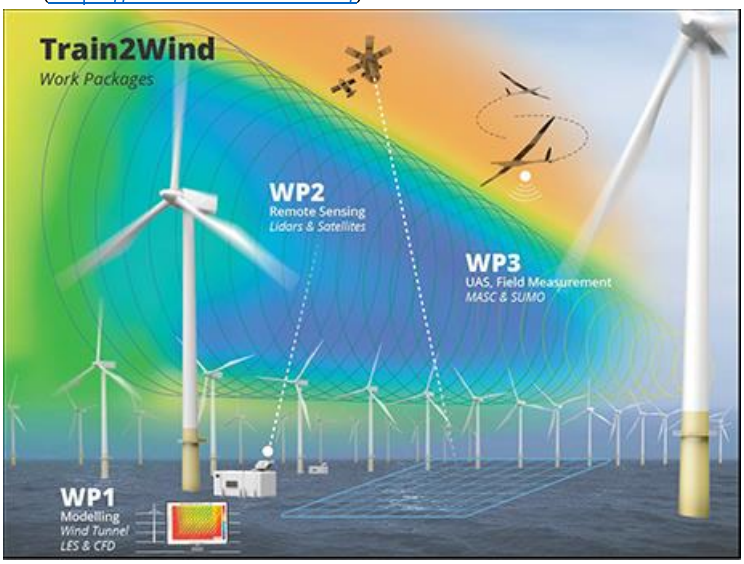


Figure 1: Overview of the Train2Wind ITN (source: Geibel et al., 2019)

The research is based on a social science perspective to study scientific collaboration (Bukvova, 2010, Sonnenwald, 2007), and will investigate what positive and
negative values participants of ITNs (i.e. PhD fellows, supervisors, and business representatives) attach to scientific collaboration. To be more precise, the collaboration readiness of the participating researchers of several ITNs will be studied. Collaboration readiness (Bietz et al., 2012) is defined as the ability by study participants to engage in collaborations, mainly based on previous experiences.
Collaboration readiness can be studied in various settings, but previous experiences, in this case, would relate to research and publishing collaborations, among others. The main research question examines what positive or negative values researchers attach to scientific collaboration in Innovative Training Networks in the research area of wind energy. Another focus is set on knowledge and research data sharing within ITNs during research processes (Bukvova, 2009), which is important for most research areas, and in particular for wind energy. The sample consists of early-stage researchers, senior researchers, and business representatives, who are members of Train2Wind, potentially other ITNs in the same research area, and wind energy researchers outside of ITNs. The data collection includes several rounds of quantitative online surveys, qualitative interviews, and participatory observations during offshore field experiments and project workshops. Offshore field
experiments are planned as part of the Train2Wind ITN. Preliminary survey results on expectations of scientific collaboration would be presented at the conference. Besides, the project will include a bibliometric analysis

of publications from completed ITNs, and the first results would be presented at the conference. The goal is to find out what kind of outcomes were produced in previous ITNs, that is what kind of research outputs can be traced back to authors of these consortiums. Correspondingly, publicly available data about the completed ITN projects will be retrieved from the European Commission's Horizon 2020 CORDIS database (https://cordis.europa.eu/en). In a second step, this data will be matched with publications in bibliographic databases, such as Web of Science (WoS), Scopus, or Dimensions. In conclusion, the study would contribute to the debate on scientific collaboration by studying researchers in a specific research area.

References:

BIETZ, M. J., ABRAMS, S., COOPER, D., STEVENS, K. R., PUGA, F., PATEL, D., OLSON, G. M. & OLSON, J. S. 2012. Improving the Odds Through the Collaboration Success Wizard. Transl Behav Med, 2, 480-486.

BUKVOVA, H. 2009. Research as a Process: A Comparison between Different Research Approaches. Working Papers on Information Systems.

BUKVOVA, H. 2010. Studying Research Collaboration: A Literature Review. Working Papers on Information Systems.

GEIBEL, G., GÖÇMEN, T., MANN, J., SEMPREVIVA, A. M., LUND, H., REUDER, J., BANGE, J. & PORTE-AGEL, F. 2019. Train2Wind, or How Large is an Infinite Wind Farm? . WindEurope Offshore 2019: Our energy, our future, Copenhagen.

HAMAN, M. & HERTZUM, M. 2019. Collaboration in a distributed research program. Journal of Documentation, 75, 334-348.

SONNENWALD, D. H. 2007. Scientific collaboration. Annual Review of Information Science and Technology, 41, 643-681.

Mini-Symposium: IEA Task 31 "Wakebench" Wind Farm Flow Model Validation





Javier Sanz Rodrigo
CENER

Patrick Moriarty
NREL

At WESC-2021 the Wakebench community will celebrate the completion of its third phase. At this stage we will be ready to present recent highlights of the Task which has made it possible to establish an international framework for wind farm flow model validation. The mini-symposium will be a good opportunity to present recent advances in the modeling of wind conditions and wake effects from mesoscale to microscale as well as experiments that can be effectively used for calibration and validation of these flow models. Most recent experiments include extensive use of remote sensing data, in particular using scanning lidar systems, which require innovative data processing techniques to reconstruct flow features that can be used for model validation. The analysis of operational wind farm data has also seen important advances leading to better quality datasets to test wind farm engineering models in the prediction of turbine and wind farm performance. Uncertainty quantification remains a challenge for most modelers due to the lack of a formal process. Hopefully Wakebench can provide guidance to solving some of these challenges.

Mini-Symposium: IEA Task 31 "Wakebench" Wind Farm Flow Model Validation (I)

Large-eddy simulation of atmospheric boundary layer problems with Alya

Herbert Owen*, Matias Avila, and Oriol Lehmkuhl*
Barcelona Supercomputing Center
*Presenting author

Keywords: Large Eddy Simulation | Swift Gabls | Alya Code

Wind energy has been and will continue to be a key contributor to the fight against CO2 emissions that cause climate change. To favor the widespread deployment of wind energy better understanding of the wind farm's flow is necessary to reduce losses, which are currently 20% for flat terrain and much higher for complex terrain. High fidelity Large Eddy Simulations, which are becoming every day more feasible and affordable thanks to the ever-growing computational resources, are recognized as an essential tool to understand the flow better and enhance wind farms and wind turbines' design. Alya is a high-performance computational mechanics code designed for massively parallel supercomputers at the Barcelona Supercomputing Center. Large Eddy Simulation of incompressible flow is currently its most important field of application. Alya has been used for wind resource assessment for more than eight years now. The wind energy involvement started with a collaboration with the wind energy company Iberdrola using RANS turbulence models. Taking advantage of LES's in-house expertise for other applications, we have been shifting towards LES usage for ABL flows. Within the Energy oriented Center of Excellence (EoCoE) European project, we have been developing Alya towards Exascale for wind energy problems. Although the main focus of EoCoE is HPC development, efforts in wind development and validation are needed to make Alya a tool that can be used by the wind energy community, which is the main objective of EoCoE. Alya uses a finite element spatial discretization on unstructured grids. The momentum equation is solved explicitly using a Runge Kutta scheme. A non-incremental fractional step scheme is used to allow for equal order interpolation of velocity and pressure. A low dissipation numerical method is obtained using an Energy, momentum, and angular momentum conserving (EMAC) form for the convective term and avoiding any additional stabilization terms [Lehmkuhl et al] . In this work, we validate Alya for two flat ABL problems: Gabls and Swift. The Gabls case deals with stable flow. Uniform size meshes with up to 2563 elements are used. For the Swift case, neutral and convective problems are analyzed. Two recent papers [Kaul et al, Mirocha et al] where the Swift problem has been solved with four state of the art codes (HiGrad, WRF-LES, SOWFA, and NALU) are used to obtain quantitative information on Alya's performance. The results with Alya agree satisfactorily with those obtained with previously cited codes for the Swift case. Alya's results are closer to those obtained with SOWFA and NALU, which are the codes that have a closer numerical scheme to Alya.

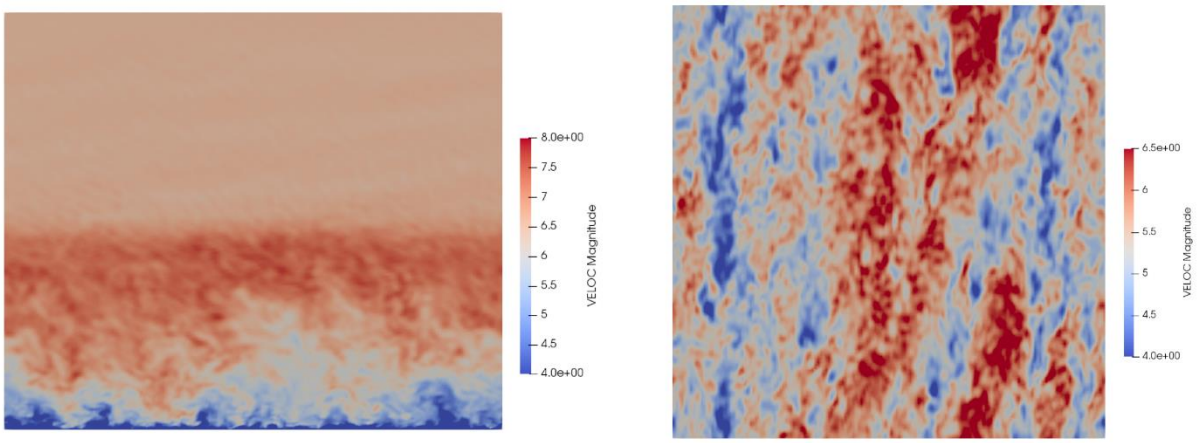


Figure 1: Instantaneous wind speeds [m s-1] for the Swift case under neutral conditions at 100 m above the surface and in a cross-stream plane midway through the domain

Figure 1 shows the instantaneous wind speeds [m s-1] for the Swift case under neutral conditions at 100 m above the surface and in a cross-stream plane midway through the domain, using a mesh with a uniform isotropic size of 15m.

References:

C M Kaul, S Ananthan, M J Churchfield, J D Mirocha, L K Berg and R Rai, 2020, 'Large-eddy simulations of idealized atmospheric boundary layers using Nalu-Wind', J. Phys.: Conf. Ser. 1452.

J D Mirocha, M J Churchfield, D Munoz Esparza, R K Rai, Y Feng, B Kosovic, S E Haupt, B Brown, B L Ennis, C Draxl, J Sanz Rodrigo, W J Shaw, L K Berg, P J Moriarty, R R Linn, V R Kotamarthi, R Balakrishnan, J W Cline, M C Robinson and S Ananthan, 2018, Wind Energy Science 3 589–613

O Lehmkuhl, G Houzeaux, H Owen, G Chrysokentis, and I Rodriguez. A low-dissipation finite element scheme for scale resolving simulations of turbulent flows. Journal of Computational Physics, 390:51–65, 2019.

Diurnal cycle simulation of thermally stratified flows over forested complex terrain

Matias Avila[1,*], Herbert Owen[1], Oriol Lehmkuhl[1,*], and Johan Arnqvist[2]
[1]Barcelona SuperComputing Center
[2]Uppsala University
*Presenting author

Keywords: Forested terrain | Thermally coupled flow | mesoscale to microscale coupling | complex terrain | Diurnal cycle simulation

The wind flow in complex terrain sites and covered by dense forests is largely affected not only by the individual contribution of the canopy and topographic elements, but also by their complex interaction with the transient processes of thermal stratification. The combined effects have a strong impact in the vertical wind profile and turbulence levels, which largely deviate from the solution obtained assuming roughness models of forests, commonly applied by the wind energy and wind engineering communities. Therefore, this work aims to present a novel simulation methodology that is realistic with the physical processes of the atmospheric boundary layer in the presence of forests, and allows us to introduce the thermal stratification effects into microscale numerical models.
The simulation of diurnal cycles over non-forested sites is typically performed imposing the temporal variations of the potential temperature at the ground. However, the presence of forests partially isolates the temperature at the ground from the wind above the forest, making this approach ineffective. Instead, this work presents the results of driving the models by the net radiative heat flux prescribed at the top of the canopy. This forcing is very convenient since it can be obtained from field measurements or from mesoscale simulations. Following [2], the heating or cooling within the forest is modeled through an exponential function that describes how the radiative heat flux decreases from the canopy top towards the ground, based on the Plant Area Density of the forest. The proposed coupling model through radiative heat transfer has been recently applied over flat terrain by the authors [1], obtaining results in close agreement with field observation data. This previous work validated the methodology and allowed us to set the kind of boundary conditions and forcing schemes which are optimal for forested sites.

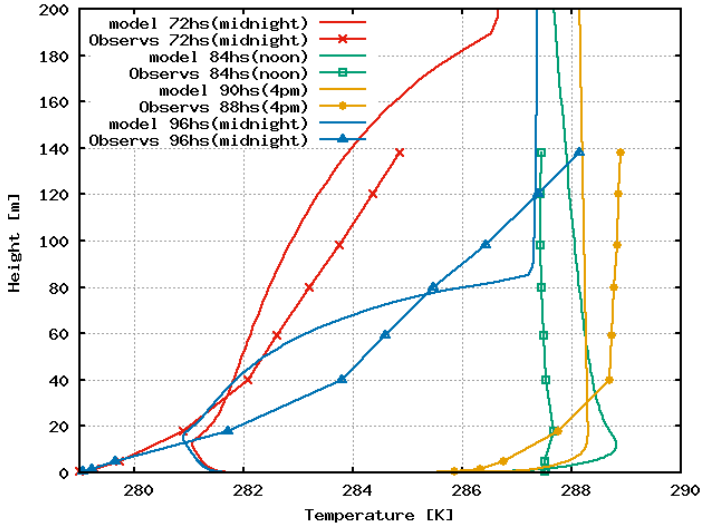


Figure 1: Observed and modelled temperarute applying the proposed model over an homogeneous and forested flat terrain

The proposed thermal coupling model is implemented in the highly parallelized finite element code Alya, which uses either RANS or LES turbulence closure models.

The methodology is presented in two tests of increasing complexity. First, the model is applied to a forest edge case in order to analyze the effects of prescribing the ground temperature in the forest clearing and below the forest. Secondly, the more complex forested site of Hornamossen, Sweden is simulated, as part of the Hornamossen Benchmark [3], where different microscale flow models are validated using transient meso-to-micro modelling. The microscale flow is driven by the large-scale pressure gradient and advection budget terms obtained from WRF as proposed in [4]. We show how the modelled wind velocity, temperature and turbulent kinetic energy compare to field observations.
Different thermal boundary conditions at ground level are validated at this inhomogeneous complex site to be valid at forest and clearings.

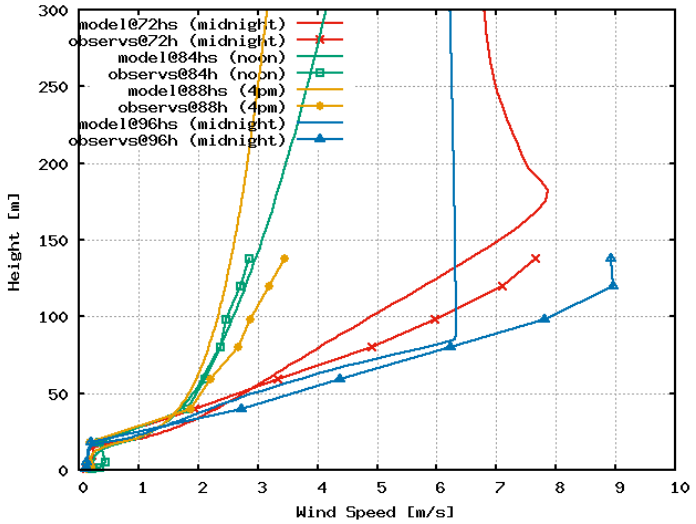


Figure 2: Observed and modelled wind speed applying the proposed model over an homogeneous and forested flat terrain

The attached figures show modelled vertical profiles of wind speed and temperature compared against field measurements at different times of the diurnal cycle. It is observed that the model is accurate predicting wind profiles over homogeneous and flat terrain. This work shows the performance of the model implemented for complex and inhomogeneous terrains.

References:

M.Avila et al. 2019. Daily cycle simulations of thermally stratified flows over forests. J. Phys.: Conf. Ser. 1256 012003

Kirk W. Brown and Winton Covey. 1966. The energy-budget evaluation of the micrometeorological transfer processes within a cornfield. Agricultural Meteorology, vol 3, 1 pp. 73-96

The Hornamossen diurnal-cycle benchmark for flow modeling in forested and moderately complex terrain (https://thewindvaneblog.com/the-hornamossen-diurnal-cycle-benchmark-for-abl-models-in-forested-and-moderatelycomplexterrain-747b60401254)

J. Sanz Rodrigo, M. Churchfield, B. Kosović. 2017. A methodology for the design and testing of atmospheric boundary layer models for wind energy applications. Wind Energ. Sci. 2: 1-20 (2017)

Evaluation of numerical site calibration results for wind turbine power performance measurement: The Alaiz case

Gang Huang[1,*] and Javier Sanz Rodrigo[2]
[1]Meteodyn
[2]Siemens Gamesa Renewable Energy
[*]Presenting author

The power performance characteristics of a wind turbine (power curve and annual energy production) are influenced by site-specific conditions such as terrain, roughness, and atmospheric stability. By carrying out a site calibration procedure, wind speed variation induced by terrain is quantified by a transfer function, namely the flow correction factor (FCF), which is then considered to support the subsequent power performance measurement.
Numerical site calibration (NSC) consists of using numerical simulation to produce the FCF between the wind speed measurement mast and the wind turbine location. To evaluate the reliability and application potential of the NSC, the project team (PT12–4) of the IEC TC 88 committee, "Wind energy generation systems," has highlighted the need for further validation through benchmarking tests.

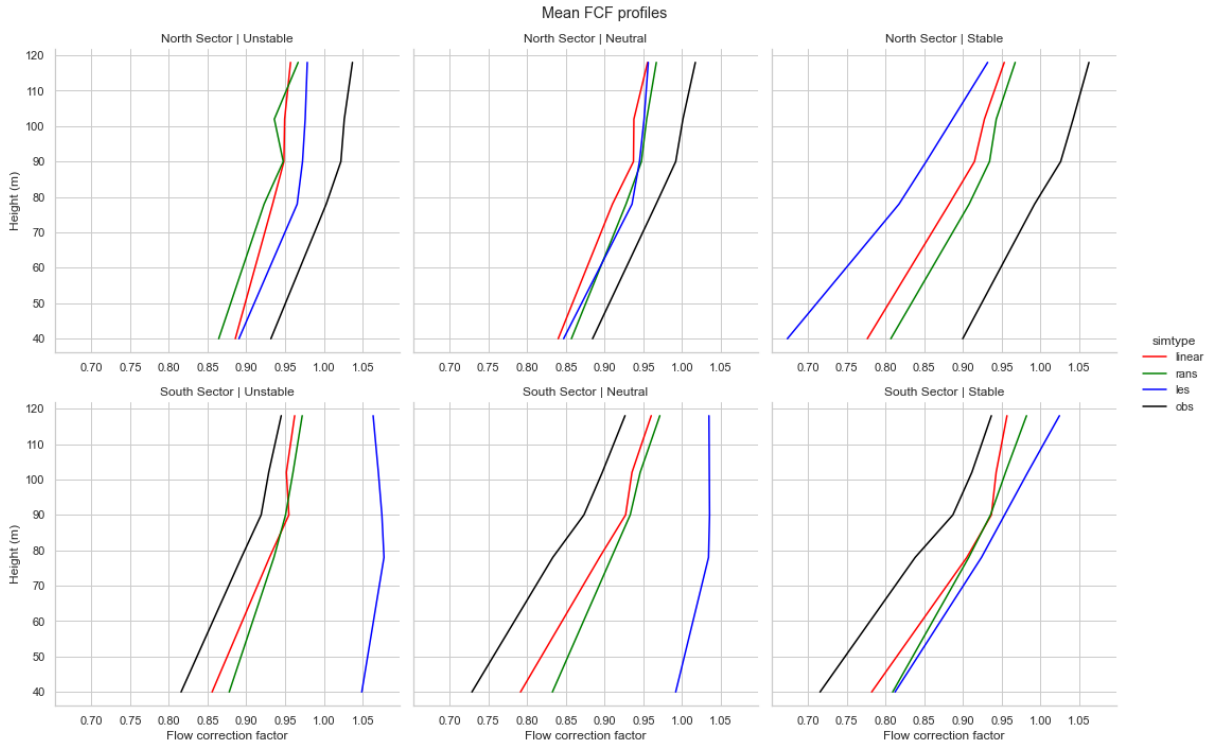


Figure 1: Mean FCF profiles

Here we report several findings gained from the preliminary results of the Alaiz NSC benchmark organized by Meteodyn under the umbrella of the IEA-Wind Task 31 "Wakebench". Several numerical tools employing different state-of-the-art flow models (linear model, RANS and LES) accomplish the NSC procedure for the Alaiz case and their performance in the prediction of FCF is evaluated and compared. As expected, a strong contrast is observed between the northerly and southerly wind profiles, under the influence of a so-called Type B terrain according to the IEC 61400-12-1 norm.
Based on the FCF values determined from the measurement data, we find a certain convergence of error values from different numerical tools to a similar trend: most models perform three times worse in the North sectors than in the South sectors. As for the question of atmospheric stability, flow patterns under the stable condition, where wind shear is higher, seem to be more difficult to capture than neutral and unstable cases.

We also remark that among users of the same numerical tool, error values can vary as high as 30% depending on user configurations such as domain size, choice of wind direction sectors and atmospheric stability parameterization. Analysis of these cases help us define best practices for conducting NSC under complex terrain that could be included in the IEC 61400–12–4 text.

Higher-Order Validation Methodology for Actuator Line LES Wake Predictions using Nacelle- Mounted LiDAR Measurements

Kenneth Brown*, Lawrence Cheung, Myra Blaylock, Alan Hsieh, Thomas Herges, and David Maniaci
Sandia National Laboratories
*Presenting author

Keywords: high-fidelity model validation | wake dynamics | nacelle-mounted LiDAR | proper orthogonal decomposition | turbulence spectra

Given the growing precedence for applying large-eddy simulation (LES) codes to wind farm design challenges, validation of these codes' wake predictions is essential. Significant work already exists validating time-averaged LES results; see the benchmarks of Moriarty et al. (2014) and Doubrawa et al. (2020), for instance. This article aims rather to advance validation methodology for higher-order quantities of interest such as related to the energetic structures and spectra that are influential for wake recovery and downstream turbine loading. Initial exploratory work on the suitability of using nacelle-mounted, downstream-facing lidar measurements for such validation of high-fidelity models was completed in Brown et al. (2020).

The present article continues the development of validation methodology from this previous work by applying the validation analyses now in the meandering frame of reference. This strategy adopts the working principle of dynamic wake meandering models that the wake acts as a passive tracer under the influence of the atmospheric boundary layer (ABL) forcing (Trujillo et al., 2011, Larsen et al., 2013). At least within the first several rows of turbines in a wind plant (Andersen et al., 2013), the meandering frame inherently offers a clearer validation of the turbine model by isolating turbineinduced phenomena within the meandering frame from the modeling of the inflow ABL conditions.

Similarly, the atmospheric unsteadiness can be compared more clearly between model and measurements by examining the spectral content of the movements of the meandering frame-ofreference itself.

Measured data for this article are acquired at three turbine diameters, D, downstream from the rotor using a rear-mounted DTU SpinnerLiDAR configuration located at the U.S. Department of Energy's Scaled Wind Farm Technology (SWiFT) facility in Texas, USA, which features three variable-speed Vestas V27 machines. The atmospheric conditions for the validation dataset, similar to the previous IEA Task 31 "Wakebench" stable case, come from 60 minutes of data from the upstream met tower in a stable nighttime boundary layer with mean hub-height wind speed of 9.28 m/s, turbulence intensity of 0.0593, and ABL power-law exponent of 0.418. These conditions are used to specify the inflow boundary conditions for the multi-physics, massively parallel LES code Nalu-Wind (Domino, 2015), which is employed with the actuator line model (Churchfield et al., 2017) to project nonvolumetric actuator forces computed in OpenFAST into the fluid volume using a uniform Gaussian projection function. A bird's-eye view of the simulation domain and five-tiered refinement region setup is provided in Figure 1.

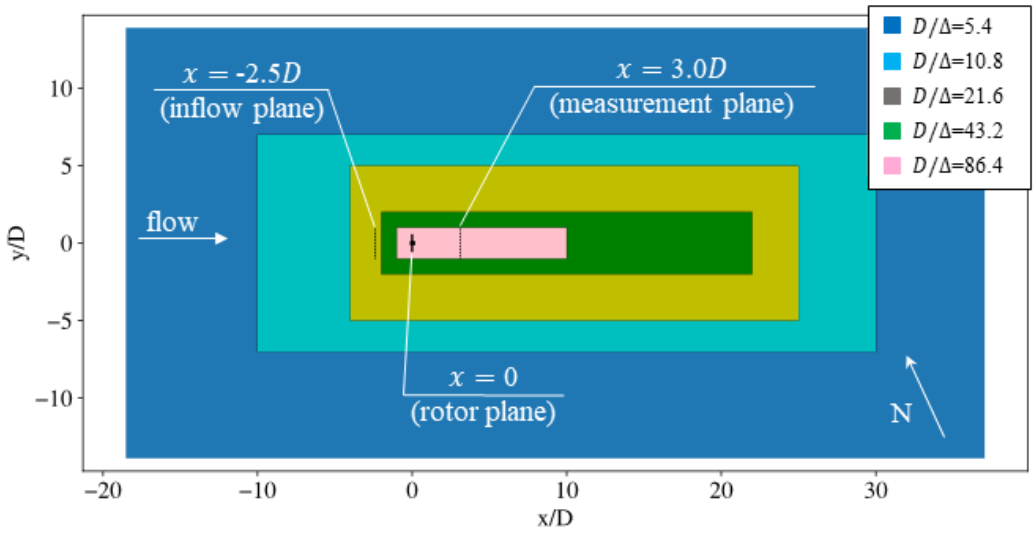


Figure 1: Bird's-eye view of the five-tiered simulation domain including the fine mesh region extending from x/D = -1 to 10. The legend indicates the ratio of the turbine diameter, D, to the element width, Δ.

Analyses will be conducted firstly on the dominant large-scale flow structures via proper orthogonal decomposition (POD). An example of the spatial modes from the POD analysis of simulated data is given in Figure 2.

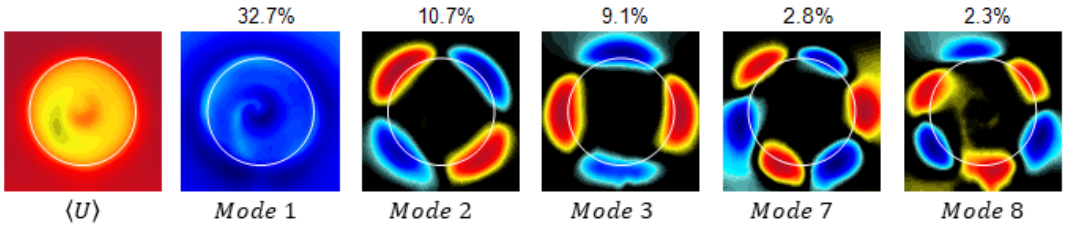


Figure 2: Simulated results including the scaled cross-stream slice of the mean flow, <U>, and several dominant POD modes at x/D = 3 calculated using 1687 snapshots. Above the mode shapes are the percent explained variation in streamwise kinetic energy per mode. Results are converged over 120 wake integral timescales. Each contour is scaled on its maximum absolute value (red = 1 and blue = -1).

The POD's optimal grouping of turbulent kinetic energy, TKE, into concentrated modes, as shown by the quadrupole structures (modes 2 – 3) and the hexapole structures (modes 7 – 8), implies the existence of dominant length scales and spatial distributions of the reoccurring shear instabilities. The final paper will additionally include analysis in the frequency domain to demonstrate methods to validate the LES modeling of the scales of turbulent motion in the meandering frame, as well as spectra of the lateral and vertical motions of the meandering frame itself. Exemplifying the validation technique with real measurement data, this article will yield both preliminary validation of Nalu-Wind and significant discussion on validation of higher-order quantities for LES.

References:

ANDERSEN, S. J., SØRENSEN, J. N. & MIKKELSEN, R. 2013. Simulation of the inherent turbulence and wake interaction inside an infinitely long row of wind turbines. Journal of Turbulence, 14, 1-24.

BROWN, K., HSIEH, A., HERGES, T. & MANIACI, D. Representation of coherent structures and turbulence spectra from a virtual SpinnerLidar for future LES wake validation. Journal of Physics: Conference Series, 2020. IOP Publishing, 062070.

CHURCHFIELD, M. J., SCHRECK, S. J., MARTINEZ, L. A., MENEVEAU, C. & SPALART, P. R. An advanced actuator line method for wind energy applications and beyond. 35th Wind Energy Symposium, 2017. 1998.

DOMINO, S. 2015. Sierra low mach module: Nalu theory manual 1.0. SAND2015-3107W, Sandia National Laboratories Unclassified Unlimited Release (UUR).

LARSEN, T. J., MADSEN, H. A., LARSEN, G. C. & HANSEN, K. S. 2013. Validation of the dynamic wake meander model for loads and power production in the Egmond aan Zee wind farm. Wind Energy, 16, 605-624.

MORIARTY, P., RODRIGO, J. S., GANCARSKI, P., CHUCHFIELD, M., NAUGHTON, J. W., HANSEN, K. S., MACHEFAUX, E., MAGUIRE, E., CASTELLANI, F. & TERZI, L. Iea-task 31 wakebench: Towards a protocol for wind farm flow model evaluation. part 2: Wind farm wake models. Journal of Physics: Conference Series, 2014. National Renewable Energy Lab.(NREL), Golden, CO (United States), 012185.

TRUJILLO, J.-J., BINGÖL, F., LARSEN, G. C., MANN, J. & KÜHN, M. 2011. Light detection and ranging measurements of wake dynamics. Part II: two-dimensional scanning. Wind Energy, 14, 61-75.

Mini-Symposium: IEA Task 31 "Wakebench" Wind Farm Flow Model Validation (II)

The American Wake Experiment (AWAKEN): Overview and Status Update

Patrick Moriarty[1,*], Nicholas Hamilton[1], Tommy Herges[2], Eliot Quon[1], and Andy Scholbrock[1]
[1]National Renewable Energy Laboratory
[2]Sandia National Laboratories
[*]Presenting author

Keywords: Wakes | Wind farm atmosphere interactions | Experimental observations

Wind farm atmospheric interaction models, including those predicting wakes, are the most significant contributor to uncertainty in the energy estimation process (Clifton et al. 2016).
Researchers and industry collaborators have made great strides towards improving these models in recent years, but additional work remains to further increase accuracy. One hurdle towards model improvement is access to detailed observations of the physical processes important for wind farm energy production and reliability at scales relevant to operating farms (see Figure 1). The American Wake Experiment (AWAKEN) is a substantial effort in the United States that will add to a growing number of relevant observational data sets needed for deeper fundamental understanding and model advancement of wind farm flows.

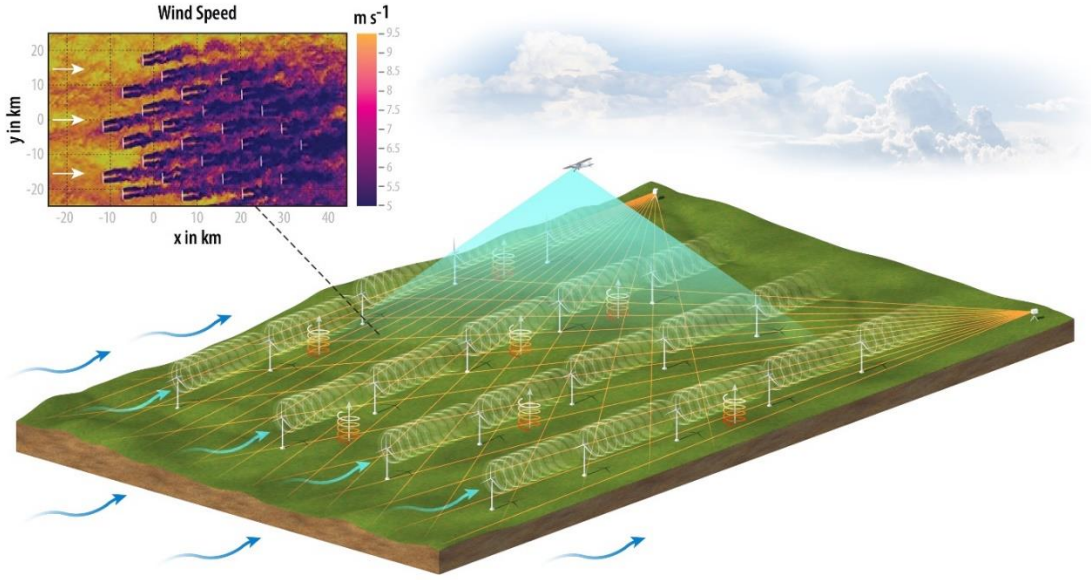


Figure 1: Top and side view of the physical processes and planned observations for the AWAKEN experiment.

AWAKEN (Moriarty et al. 2020) is an international multi-institutional field observation and model validation campaign focused on gathering the highest resolution observations of wind farm atmospheric interactions to date. Funded largely by the United States Department of Energy (US DOE), AWAKEN involves a consortium of national laboratories, academic institutions and industry who will apply their experimental and simulation expertise and make use of advanced observation technologies to better understand and model wind farm physical processes. This presentation will provide an overview of the AWAKEN project, its vision and goals, and a snapshot of the current project, which is due to commence in 2022.
AWAKEN researchers have identified a suitable test site in the central United States, which we believe will lead to a data set complementary to existing observations, many of which are offshore.
The area of focus for the field campaign is a cluster of operating wind farms in an area of Northern Oklahoma near an atmospheric measurement facility operated by the US DOE Atmospheric Radiation and Measurement

(ARM) program. Leveraging the instrumentation at the ARM facility is advantageous to researchers who will also make use of historical ARM observations available prior to wind farm construction in the area. Additional observations will be made by a variety of AWAKEN partners who will deploy state-of-the art instrumentation technologies, some of which are being specifically developed for the campaign. Close collaboration with simulation experts, using the latest modeling technology, is also critical to design the experiment and validate models across the fidelity spectrum.

The experimental design is driven by a newly developed set of testable hypotheses, some of which focus on fundamental physics, such as the impact of atmospheric stability on wake decay or the impact of wind farms on cloud formation, while others are more applied, like the scalability of wind farm control. Ultimately the AWAKEN project will produce a unique, publicly available data set, abiding by FAIR data principles (Wilkinson et al. 2016), that will be of lasting benefit to the worldwide wind energy community.

The top view (upper left) shows the simulation of a wind farm creating a wake downwind. The side view (lower right) shows individual turbine wakes, their impact on thermal fluxes and potential instruments to be deployed to observe these phenomena.

References:

Clifton, Andrew, Aaron Smith, and Michael Fields. 2016. "Wind Plant Preconstruction Energy Estimates. Current Practice and Opportunities." NREL/TP-5000-64735. National Renewable Energy Lab. (NREL), Golden, CO (United States). https://doi.org/10.2172/1248798.

Moriarty, Patrick, Nicholas Hamilton, Mithu Debnath, Tommy Herges, Brad Isom, Julie K Lundquist, David Maniaci, et al. 2020. "American WAKE ExperimeNt (AWAKEN)." NREL/TP-5000-75789. National Renewable Energy Lab. (NREL), Golden, CO (United States). https://www.nrel.gov/docs/fy20osti/75789.pdf.

Wilkinson, Mark D., Michel Dumontier, IJsbrand Jan Aalbersberg, Gabrielle Appleton, Myles Axton, Arie Baak, Niklas Blomberg, et al. 2016. "The FAIR Guiding Principles for Scientific Data Management and Stewardship." Scientific Data 3 (1): 160018. https://doi.org/10.1038/sdata.2016.18.

Farm-to-Farm interactions investigated through a WRF-RANS framework for the AWAKEN/ARISE project

Stefano Letizia[1], Mithu Debnath[2], Nicholas Hamilton[2], Eliot Quon[2], Patrick Moriarty[2], Julie K. Lundquist[2,3], and Giacomo Valerio Iungo[1]
[1]UT Dallas
[2]National Renewable Energy Laboratory
[3]University of Colorado Boulder

Keywords: farm-to-farm interactions | RANS | WRF

Recent experimental campaigns provided sound evidence of wind farm wakes extending downstream several tens of kilometers under stable atmospheric conditions (Hasager et al., 2015; Platis, et al., 2018; Djath et al.; 2018). Wind-farm wakes impact the wind resource at downwind sites, leading to a reduced wind speed, increased turbulence intensity (Nygaard, 2014), and a considerable financial loss for wind parks located in the wake of other wind farms (Lundquist et al., 2019). The velocity deficit past wind farms is affected by atmospheric stability, with more persistent wakes occurring under stable conditions (Djath, et al., 2018, Lundquist et al., 2019). Investigations on wind farm wakes are challenging due to the large spatial domain and the broad range of length scales involved, which spans from the chord length of the blade airfoils (few meters) up to mesoscales (5- 100 Km). Numerical methods for wind farm wakes are computationally demanding and often adopt a mesoscale transient model (e.g. leveraging the Weather Research and Forecasting (WRF) model) to solve the background wind field, while turbines are modeled as diffused roughness (Emeis, 2010), momentum sinks (Fitch et al. 2012; Abkar and Porté-Agel, 2015) or actuator line and/or disk models for high-fidelity simulations, such as with RANS or LES (Santoni et al., 2020). We recently developed a mid-fidelity Pseudo-2D RANS model to simulate wind farms and turbine power capture that is oneway nested with WRF simulations of the background wind field. The Pseudo-2D RANS model leverages the depth-averaged Navier Stokes approach to reduce the computational costs, including corrections for vertical fluxes. The momentum equations are solved parabolically in the streamwise direction, while continuity is enforced through an elliptic pressure solver. The background flow conditions are provided by WRF simulations, executed with and without turbine parameterization.

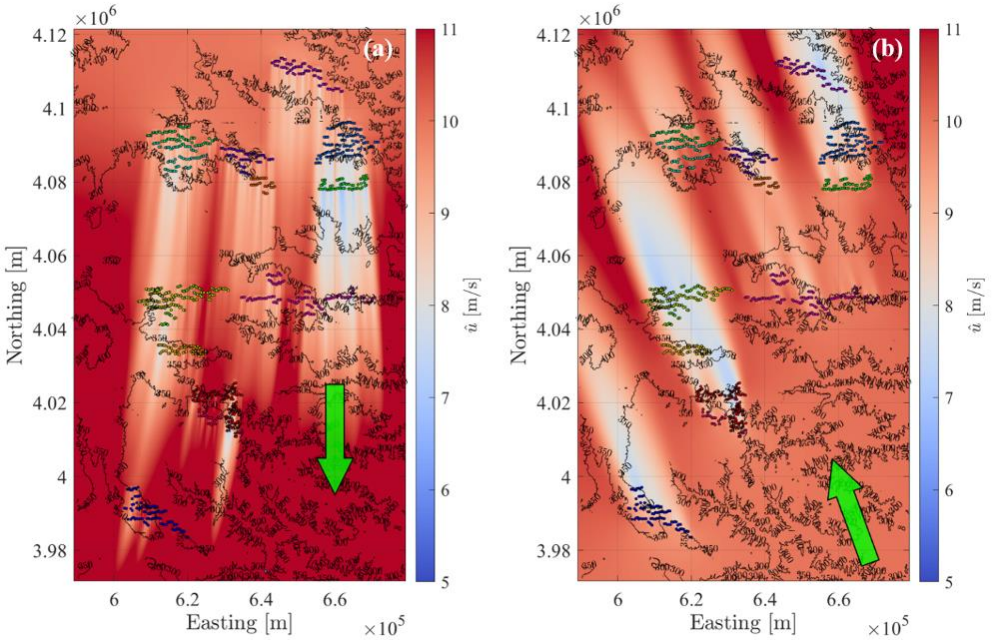


Figure 1: Mean stream wise velocity fields simulated for different wind directions

This numerical tool is applied to a cluster of 15 wind farms located in Oklahoma, US, as shown in Fig. 1. This site is a candidate for the deployment of several instruments, including scanning Doppler wind LiDARs, meteorological towers, scanning radars, and instrumented UAVs, for the AWAKEN/ARISE project (Moriarty et al., 2020). This project is a collaborative international wake observation and validation campaign focusing on the physics involved with operations of wind turbines and wind farms. The effect of the wind farms on the wind field is modeled through the thrust force over the turbine rotors, which is estimated from turbine operational data (Iungo et al., 2018). In this work, the extent and flow characteristics of wind-farm wakes are investigated for different wind and atmospheric conditions (Fig. 2), as already carried out in the past for isolated wind farms (Zhan, Letizia and Iungo, 2019).

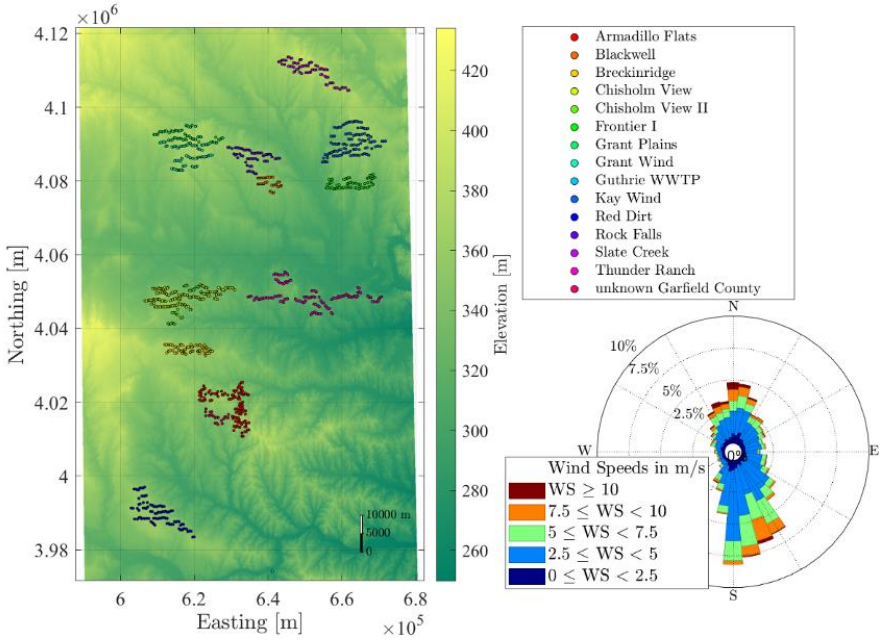


Figure 2: Map and wind rose of the site simulated through the Pseudo-2D RANS.

Ensemble-statistics of the wake flow and power capture are thoroughly analyzed and discussed for different wind and atmospheric conditions.

References:

Abkar, M., Porté-Agel, F. (2015) 'A new wind-farm parameterization for large-scale atmospheric models', J. Renew. Sustain. Energy, 7(013121).

Djath, B., Schulz-Stellenfleth, J., Cañadillas, B. (2018) 'Impact of atmospheric stability on X-band and C-band synthetic aperture radar imagery of offshore wind park wakes', J. Renew. Sustain. Energ., 10, 043301.

Emeis, S. (2010) 'A simple analytical wind park model considering atmospheric stability', Wind Energy, 13: p459-469.

Fitch, A.C., Olson, J.B. , Lundquist, J.K., Dudhia, J., Gupta, A.K., Michalakes, J., Barstad, I. (2012) 'Local and Mesoscale Impacts of Wind Farms as Parameterized in a Mesoscale NWP Model', Monthly Weather Review, 140 (9): p3017-3038.

Hasager, C.B., Vincent, P., Badger, J., Di Bella. A., Peña, A., Husson, R., Volker, P.J.H. (2015) 'Using Satellite SAR to Characterize the Wind Flow around Offshore Wind Farms', Energies, 8, p 5413-5439.

Iungo, G.V., Letizia, S., Zhan, L. (2018) 'Quantification of the axial induction exerted by utility-scale wind turbines by coupling LiDAR measurements and RANS simulations', J. Phys.: Conf. Ser., 1037, 072023.

Lundquist, J.K., DuVivier, K.K., Kaffine, D. et al. (2018) 'Costs and consequences of wind turbine wake effects arising from uncoordinated wind energy development', Nat Energy, 4, p26–34.

Moriarty, P., Hamilton, N., Debnath, M., Fao, R., Roadman, J., van Dam, J., Herges, T., Isom, B., Lundquist, J.K., Maniaci, D., et al. (2020) 'American WAKE experiment (AWAKEN). No. NREL/TP-5000-75789. National Renewable Energy Lab. (NREL), Golden, CO (United States), 2020.

Nygaard, G.N. (2014) 'Wakes in very large wind farms and the effect of neighboring wind farms', J. Phys.: Conf. Ser., 524 (012162).

Platis, A., Siedersleben, S., Bange J. et al. (2018) 'First in situ evidence of wakes in the far field behind offshore wind farms', Sci Rep, 8 (2163), p1-10.

Santoni, C., García-Cartagena, E.J., Ciri, U., Zhan, L., Iungo, G.V., Leonardi, S. (2020) 'One-way mesoscale-microscale coupling for simulating a wind farm in North Texas: Assessment against SCADA and LiDAR data', Wind Energy, 23: p691– 710.

Zhan, L., Letizia, S., Iungo, G.V. (2019) 'LiDAR measurements for an onshore wind farm: Wake variability for different incoming wind speeds and atmospheric stability regimes', Wind Energy,23 (3), p501-527.

Application of Multilevel-Multifidelity Uncertainty Quantification Towards Multi-turbine Interaction and Wake Characterization

Alan Hsieh*, David Maniaci, Gianluca Geraci, Daniel Seidl, Thomas Herges, Kenneth Brown, and James Cutler
Sandia National Laboratories
*Presenting author

Keywords: Wakes | Uncertainty Quantification | Large-Eddy Simulation

In wind energy research, uncertainty quantification (UQ) using high-fidelity computational models is necessary for predictive and accurate simulations of the complex-turbine-wake interactions in wind farms. However, the large variability present in the atmospheric conditions and operation of wind turbines give high variance to the simulated predictions coming from these high-fidelity models. With traditional UQ methods, this presents a problem as the high computational costs become prohibitive for the large number of simulations needed to reduce this variance. As a continuation of previous work [1], we consider advanced UQ methods using multilevel-multifidelity (MLMF) sampling strategies [2] that leverage cheaper low-fidelity computational models with a smaller number of high-fidelity simulations to provide effective UQ at significantly reduced computational costs compared to conventional UQ techniques such as single-level (MC) and multilevel Monte-Carlo (MLMC).
A demonstration study is completed using multi-turbine simulations of the Sandia National Laboratories' Scaled Wind Farm Technology (SWiFT) facility in neutrally stratified atmospheric boundary layer conditions. The simulated configuration will be two Vestas V27 turbines with one turbine located 5 rotor diameters downstream of the other and experimental data from SWiFT will inform the probabilistic distributions of the uncertain parameters considered in the present study. A model hierarchy was constructed using the engineering tool FAST.Farm, the Reynolds-Averaged Navier-Stokes (RANS) model WindSE, and the large eddy simulation (LES) code Nalu-Wind with varying mesh resolution levels for the latter two models as seen in Figure 1.

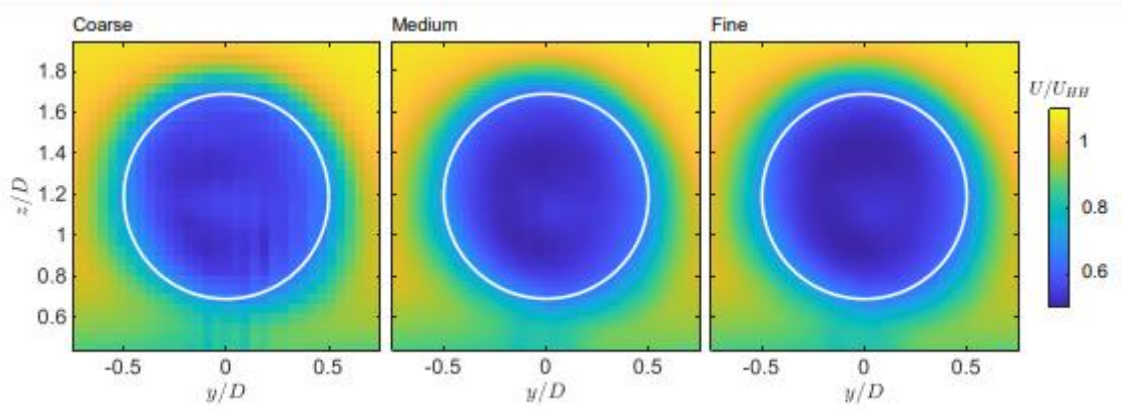


Figure 1: Wake visualizations from Nalu-Wind simulations for different mesh resolutions.

Nalu-Wind is coupled with the OpenFAST software suite to model the wind turbine loads and Nalu-Wind's actuator disk model is used to represent the turbine effects on the flow field. The Nalu-Wind simulations will use coarse, medium, and fine meshes corresponding to minimum grid spacings of 2.5m, 1.25m, and 0.625m, respectively. A twenty-sample pilot study is first conducted to ascertain the relative model outputs and correlations between the individual model levels to identify the relative efficiency of each sampling method. Secondly, a larger production-level study is done to validate the predicted trends of the pilot study. Sandia's UQ toolkit Dakota is used to provide a flexible interface between the aforementioned computational models and the UQ methods. MLMF estimators are expected to show greater efficiency compared to standard and

multilevel Monte Carlo estimators, and also provide insight on individual sub-model effectiveness for particular quantities of interest including turbine power and rotor thrust from both turbines as well as wake characteristics such as lateral wake position and integrated wake deficit at several downstream distances.

Acknowledgements
Sandia National Laboratories is a multimission laboratory managed and operated by National Technology & Engineering Solutions of Sandia, LLC, a wholly owned subsidiary of Honeywell
International Inc., for the U.S. Department of Energy's National Nuclear Security Administration under contract DE-NA0003525. The Sandia report number for this abstract is: SAND2021-0944 A.

References:
[1] Hsieh, A.S. et al. "Multilevel Uncertainty Quantification using CFD and OpenFAST Simulations of the SWiFT Facility." AIAA SciTech 2020 Forum, 2020.
[2] Geraci, G. et al. "Recent advancements in Multilevel-Multifidelity techniques for forward UQ in the DARPA Sequoia project." AIAA SciTech 2019 Forum, 2019

LiSBOA: a framework for optimal design of LiDAR scanning strategies and statistics retrieval

Stefano Letizia[1], Mithu Debnath[2], Nicholas Hamilton[2], Eliot Quon[2], Patrick Moriarty[2], Julie K. Lundquist[2,3], and Giacomo Valerio Iungo[1]
[1]UT Dallas
[2]National Renewable Energy Laboratory
[3]University of Colorado Boulder

Keywords: LiDAR | Wind farm | Wake

Remote sensing instruments, such as wind LiDARs, probe large volumes of the order of several kilometers with a sampling time of the order of few Hertz, which is adequate to investigate atmospheric turbulence. However, the limited spatio-temporal resolution poses additional challenges compared to traditional anemometry when it comes to retrieving turbulence statistics. Furthermore, multiple degrees of freedom of scanning LiDAR systems (probe volume, azimuth and elevation resolution, accumulation time, scan geometry, etc.) complicate the selection of the optimal set up for the detection of the flow features of interest.
Intending to address the above-mentioned uncertainties, we developed the LiDAR Statistical Barnes Objective Analysis, or LiSBOA (Letizia et al., 2020a and b). LiSBOA is a holistic tool for optimal LiDAR scan design and retrieval of mean and higher-order statistical moments of wind velocity from 3D datasets of line-of-sight wind speed. It requires as input the main characteristics of the flow under investigation, namely the wavelengths of interest, the characteristics variance and integral timescale, as well as the LiDAR technical specifications selected, such as probe length and accumulation time.
LiSBOA identifies the optimal LiDAR scan set up that ensures an adequate sampling of the relevant wavelengths while minimizing the statistical error. A criterion for the rejection of regions affected by insufficient resolution of the wavelengths of interest is formulated and it is based on the multidimensional version of the Shannon-Nyquist theorem (Shannon, 1974). The scan design problem is formalized as a Pareto front optimization having two objective functions, namely the data loss due to undersampling (which occurs for excessively fast scans with poor spatial resolution) and the expected statistical uncertainty on the mean.
LiSBOA uses a revisited version of the Barnes scheme (Barnes, 1964), which interpolates the scattered LiDAR data onto a Cartesian grid. An important novelty of the LiSBOA with respect to the original Barnes scheme is the reconstruction of central statistical moments from the raw data. This is a desirable feature in wind energy because it allows for retrieval of the turbulence intensity field, which is an important quantity for resource assessment and wind turbine wake analysis (see Fig. 1).

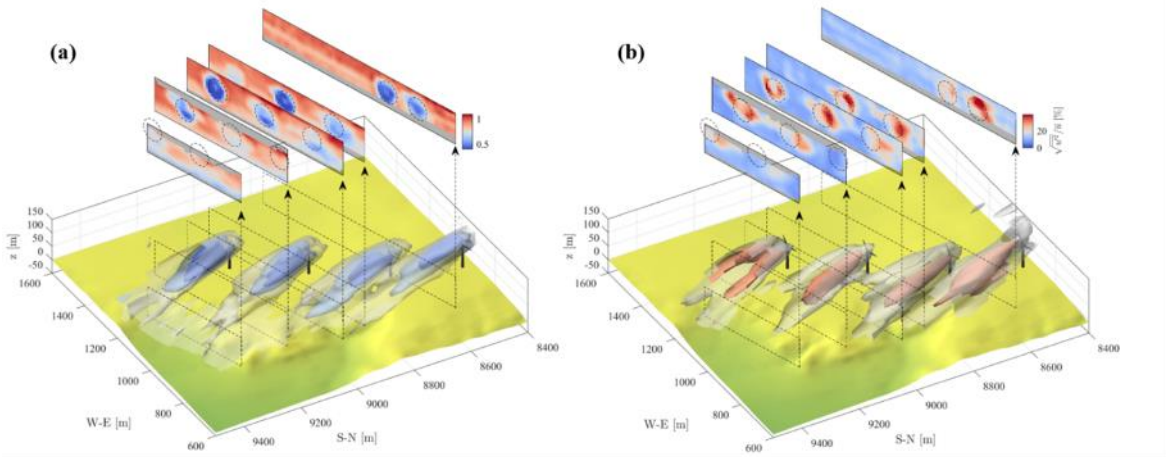


Figure 1: Wake velocity fields reconstructed from LiDAR measurements through LiSBOA: (a) mean streamwise velocity; (b) turbulence intensity.

In this work, the LiSBOA is used for the design of LiDAR scanning strategies for the AWAKEN/ARISE project (Moriarty et al., 2020), a collaborative international campaign aimed at investigating the wake interactions occurring within and across several on-shore farms. In Fig. 2, it is reported the procedure for the optimal design of LiDAR scans for NW wind directions at a candidate AWAKEN/ARISE site, which includes 15 wind farms in Oklahoma.

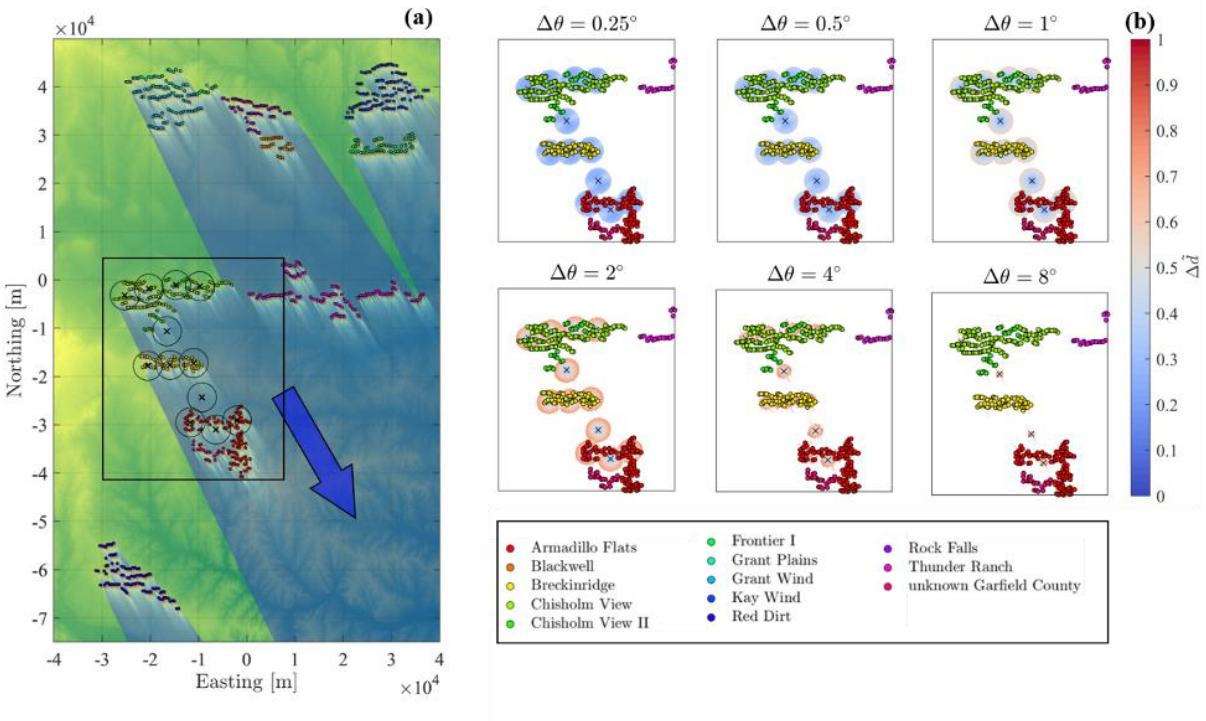


Figure 2: LiSBOA-assisted scan design for the study of multiple wake interactions occurring for NW wind at the AWAKEN/ARISE site: (a) site map showing the tentative LiDAR locations (x) and range (circles). The shaded area indicates wakes predicted through the Jensen model; (b) local data spacing maps for different azimuthal resolution of the 360° PPI scans.

In this work, we test the deployment of 12 scanning LiDARs performing 360° PPIs. Fig. 2b shows the heat map of local data spacing for different azimuth resolutions, which indicates the local spatial resolution. Local data spacing higher than 1 indicates violation of the Shannon-Nyquist constraint and guides the selection of the optimal angular resolution. Finally, we will present several LiDAR scanning strategies optimally designed for the AWAKEN/ARISE experiment.

References:

Barnes, S.L. (1964) 'A Technique for Maximizing Details in Numerical Weather Map Analysis', J. Appl. Meteorol., 3, p396–409.

Letizia, S., Iungo, G.V. (2020a) 'LiSBOA: LiDAR Statistical Barnes Objective Analysis for optimal design of LiDAR scans and retrieval of wind statistics. Part I: Theoretical framework', AMT Discussions.

Letizia, S., Iungo, G.V. (2020b) 'LiSBOA: LiDAR Statistical Barnes Objective Analysis for optimal design of LiDAR scans and retrieval of wind statistics. Part II: Applications to synthetic and real LiDAR data of wind turbine wakes', AMT Discussions.

Moriarty, P., Hamilton, N., Debnath, M., Fao, R., Roadman, J., van Dam, J., Herges, T., Isom, B., Lundquist, J.K., Maniaci, D., et al. (2020) 'American WAKE experiment (AWAKEN). No. NREL/TP-5000-75789. National Renewable Energy Lab. (NREL), Golden, CO (United States), 2020.

Shannon, C.E. (1984) 'Communication in the Presence of Noise', Proceedings of the IEEE, 72, p1192-1201.

Mini-Symposium: Interactions of large-scale offshore wind farms with the marine atmospheric boundary layer of the German Bight







Martin Dörenkämper
Fraunhofer IWES

Stefan Emeis
Karlsruhe Institute of Technology

Nicolai Nygaard
Ørsted

The German Bight is one of the areas subject to the development of offshore wind farms that has seen one of the largest expansions in recent years, with many more offshore wind farms expected to be grid-connected in the next 10-20 years. Consequently operators are facing issues of wind farm atmosphere interaction already and there is a large interest in how the future offshore wind potential will look like in industry but also wind energy science. The mini symposium shall be composed of talks that cover of all important topics of wind farm cluster atmosphere interaction such as global blockage, large-scale wake effects and their interaction with coastal effects focusing on the German Bight region. It will cover presentations focusing on numerical and analytical model results of different complexity as well as experimental data collected in the area. Besides the presentations the symposium will close with a panel discussion with the speakers and the audience.

Improving mesoscale resource assessment in coastal areas by aircraft measurements and LES-studies – recent results from the X-Wakes project

Simon Siedersleben[1], Martin Dörenkämper[2,*], Gerald Steinfeld[3], Kjell zum Berge[4], Stefan Emeis[1], Thomas Rausch[5], and Astrid Lampert[5]
[1]Karsruhe Institute of Technology
[2]Fraunhofer IWES
[3]Carl von Ossietzky Universität Oldenburg
[4]Universität Tübingen
[5]Technische Universität Braunschweig
*Presenting author

Keywords: coastal effects | German Bight | wake interaction

Mesoscale resource assessment faces three major challenges: First of all, most offshore wind farms are built within close proximity to the coast to keep the cost for installation, cables and maintenance, low. As areas are limited, the distances between offshore wind farms are often below 30 km.
However, wakes of offshore wind farms can last up to 100 km during stable conditions (Platis et al. 2020). Secondly, these long wakes are mostly associated with offshore oriented winds, resulting in an interaction of the boundary layer on land with the marine boundary layer and prevailing stably stratified conditions. Previously published studies have shown that mesoscale models lack to capture these kinds of stable stratification, resulting in turn in too low wind speeds offshore. In addition, mesoscale wind farm parametrizations need to be evaluated for the superposition of wakes. The Project X-Wakes works currently on improving simulations concerning these three issues, wake interaction, coastal effects and also global blockage. The presentation will show results from the first half of the project focusing on coastal effects.
We analyze coastal effects by presenting aircraft measurements taken in September 2020 in the vicinity of the Frisian Islands, characterized by a low-level jet (LLJ) that were subsequently simulated with the mesoscale model WRF. The airborne observations reveal the highly spatial variability of the wind field in coastal areas and the difficulties in simulating these with mesoscale models. For example, on 23 September 2020, the LLJ maximum is captured on the eastern side of the East Frisian Islands, but not in the West of the Frisian Islands by a set of mesoscale simulations (Figure 1). A comparison of the sea surface temperature (SST) measured by the aircraft with the OSTIA Data indicates that a too high SST close to the shore could have caused this deviation.

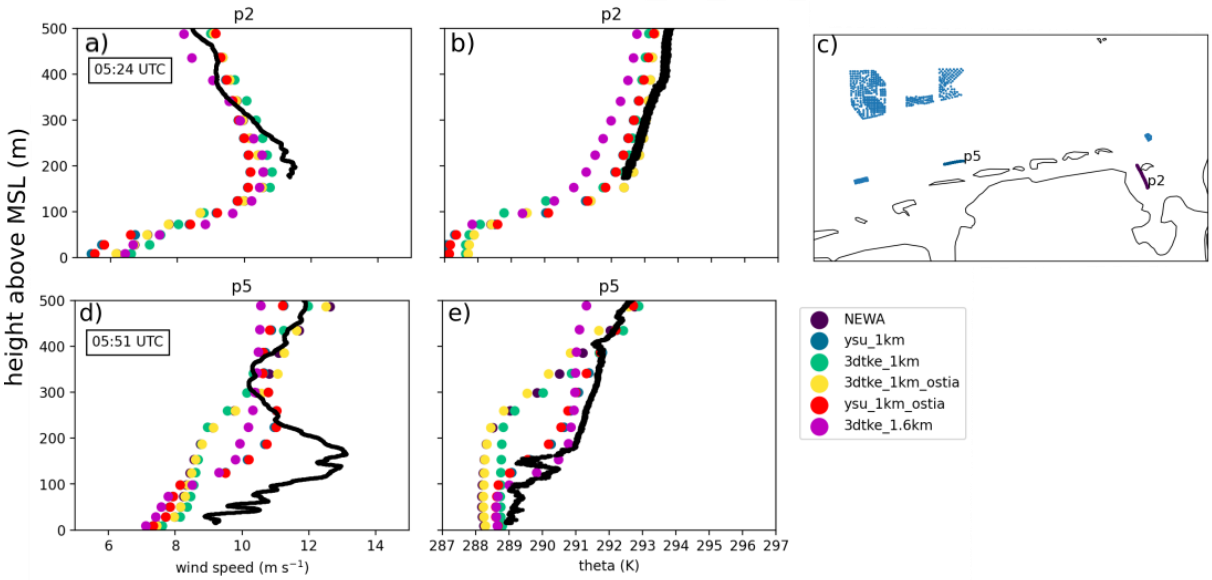


Figure 1: Vertical profiles of mesoscale WRF simulation (colored dots) and airborne observations (solid black lines) at the eastern (p2, a -b) and western side (p5, d-e) of the Frisian Island, the corresponding locations are shown in (c).

Thus, information on the SST measurements from the flight measurements will be used to enhance the results of the mesoscale simulations. Besides the influence of the SST on the coastal marine boundary layer, we investigate the impact of different land use classes on the wind speed at hub height. The German Bight is characterized by large tidal areas. Therefore, we conduct sensitivity studies to analyze the impact of these tidal areas on the wind field.

The development of the marine atmospheric boundary layer with increasing distance from the coast on the eastern side of the East Frisian Islands on 23 September 2020 is currently further investigated by the means of large-eddy simulations that apply the model PALM (Maronga et al. 2020) These simulations apply an offline nesting of the LES domain into the WRF simulations described above by making use of tools that have recently been developed by (Lin et al. 2020). It is intended to present first results from these simulations. Moreover, a general overlook of the further steps in the project will be given.

References:

Lin, D., B. Khan, M. Katurji, L. Bird, R. Faria, and L. E. Revell, 2020: WRF4PALM v1.0: A Mesoscale Dynamical Driver for the Microscale PALM Model System 6.0. Atmospheric Sciences.

Maronga, B., and Coauthors, 2020: Overview of the PALM model system 6.0. Geosci. Model Dev., 13, 1335–1372, https://doi.org/10.5194/gmd-13-1335-2020

Platis, A., Bange, J., Bärfuss, K., Cañadillas, B., Hundhausen, M., Bughsin, D., Lampert, A., Schulz-Stellenfleth, J., Siedersleben, S., Neumann, T., Emeis, S., 2020: Long-range modifications of the wind field by offshore wind parks – results of the project WIPAFF. Meteorol. Z., 29, 355–376, https://doi.org/10.1127/metz/2020/1023.

Wind-farm blockage in engineering models: A comparison with LES simulations

Beatriz Canadillas[1,*], Richard Foreman[1], Nick Robinson[1], Volker Barth[1], and Gerald Steinfeld[2]
[1]UL International
[2]Carl von Ossietzky Universität Oldenburg
*Presenting author

Keywords: Wind-farm blockage | Engineering models-Openwind | Large eddy simulation (LES) | X-Wakes

Wind-farm blockage, i.e. the reduction of incident wind speed in front of a wind farm, has recently received increasing attention from both industry and academia. Several studies have shown that yield overestimation occurs in pre-construction studies based on standard wake models that only address downstream wakes and not upstream effects. Therefore, engineering models used by the wind energy industry may need to be adjusted to account for this effect by combining the blockage effect with wake models.
We have investigated the performance of the blockage models in the Openwind [4] engineering model by comparing model output with the results of large-eddy simulations (LES) of the North Sea wind farm cluster N-4, which have been performed for varying atmospheric stability and wind direction (see Figure 1). The two cases presented here are flows from the west and south in stable conditions, where the blockage effect is expected to be most pronounced.

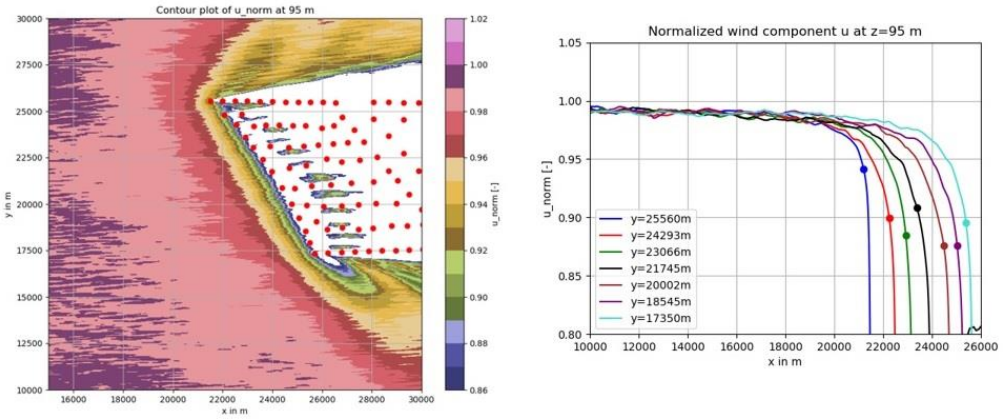


Figure 1: 2D plot of wind speed normalized by the inflow wind speed (8 m/s) close to hub height, stable ABL and wind direction=180° (left). The dots mark the position 2.5 rotor diameters upstream of wind turbines at the inflow edge of the N-4 cluster (right). Stable ABL.

The DAWM-EV (Deep Array Wake Models – Eddy Viscosity) wake model of the Openwind [4] engineering model has been coupled to three previously reported analytical blockage models: the self-similar (SS) model [1], the vortex cylinder (VC) model [2], and the potential flow (PF) model [3], which is based on a Rankine half body. In these blockage models, the upstream wind speed around the rotor axis is a function of a rotor induction factor a = a(Ct), the streamwise position (being zero at the turbine and negative upstream), and rotor diameter.
In the LES model PALM [5], the effects of the 208 wind turbines of the N-4 cluster have been considered by applying an actuator disc approach [6]. While the N4-cluster has a spatial extension of about 9.3 km in the west-east direction and 21.3 km in north–south direction, the LES domain for flow from the south has an area of about 41 × 82 km2 in order to reduce the impact of the domain boundaries on the simulated flow. The simulations have been run on up to 16,384 processor elements on the HLRN-IV HPC cluster (www.hlrn.de) to enable a spatial resolution down to 5 m. The LES results indicate that, under stable stratification, the wind speed at hub height can be reduced by 10% upstream of the N-4-cluster (figure 2).

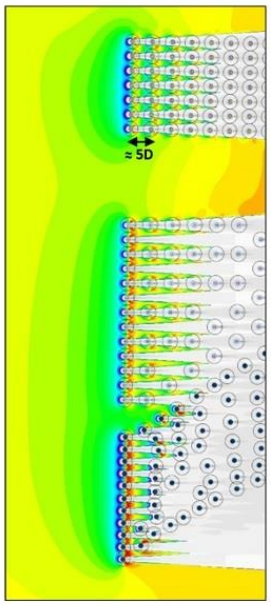


Figure 2: Openwind® simulation of Cluster N 4 (North Sea). WS=8m/s, WD=270° PF model. Neutral ABL. Rainbow scale from 7.8 m/s to 8.05 m/s. white to grey is all <7.8m/s.

The results show a promising agreement, while differences between the LES and Openwind approaches provide insights into how these models can be improved.

Acknowledgements

[1] The X-Wakes project is funded by the German ministry of Economic Affairs and Energy (BMWi) under grant number FKZ 03EE3008 (A-G) based on the basis of a decision by the German Bundestag.

[2] Computing resources were partly provided by the North-German Supercomputing Alliance (HLRN)

References:

[1] Meyer Forsting, A. R., Troldborg, N. (2015). The effect of blockage on power production for laterally aligned wind turbines. Journal of Physics: Conference Series (Online), 625, [012029]. https://doi.org/10.1088/1742-6596/625/1/012029

[2] Branlard, E., Meyer Forsting, AR. (2020). Assessing the blockage effect of wind turbines and wind farms using an analytical vortex model. Wind Energy (Online); 23: 2068– 2086. Available at: https://doi.org/10.1002/we.2546

[3] Gribben BJ., Hawkes GS. (2019) A potential flow model for wind turbine induction and wind farm blockage, Frazer-Nash Technical Paper (Online). Available at: https://www.fnc.co.uk/resources/a-potential-flow-model-for-wind-turbineinduction-and-wind-farm-blockage/

[4] Openwind user manual. Version 1.9. July 2020. Available at: https://aws-dewi.ul.com/openwind-version-1-9/

[5] Maronga, B. and 45 co-authors (2020). Overview of the PALM model system 6.0. Geosci. Model Dev., 13, 1335–1372, Available at: https://doi.org/10.5194/gmd-13-1335-2020

[6] Witha, B., Steinfeld, G., Dörenkämper, M & Heinemann, D. (2014). Large-eddy simulation of multiple wakes in offshore wind farms. Journal of Physics: Conference Series (Online), 555, [012108]. Available at: https://doi.org/10.1088/1742-6596/555/1/012108

Potential Changes in Wind Power Ramp Behaviour under a Projected Climate Change Scenario

Bedassa R. Cheneka*, Simon Watson, and Sukanta Basu
Delft University of Technology
*Presenting author

Keywords: Wind power ramps | Climate change | Offshore wind power

Offshore wind power is increasingly seen as a cost-effective source of renewable energy particularly for Northern European countries. This has led to a rapid expansion of offshore capacity and ambitious targets for future installation. The North, Irish and Baltic Seas have favourable wind resource, and the North Sea accounts for 77% of all offshore wind capacity in Europe (WindEurope, 2019). As a result of climate change, there could be potential changes in future wind power resource, including seasonal and spatial variations (Moemken et al., 2018; and Weber, Gotzens and Witthaut, 2018). However, changes in wind speed are uncertain with a significant spread of projections from different climate models (Outten and Esau, 2013). Understanding potential changes in the behaviour of wind power ramps in the future is particularly important as it influences the integration of wind power into the electricity grid. To the best of our knowledge, potential changes in the behaviour of wind power ramps under climate change have not yet been studied in Europe but a study in Eastern Japan has shown that there could be a decrease in the frequency of wind power ramps (Ohba, 2019). In this work, we have analysed the potential change in the characteristics of wind power ramps in the future for Northern European offshore wind farms, using EURO-CORDEX (Coordinated Downscaling Experiment - European Domains) CMIP5 wind speeds for the intermediate scenario, RCP4.5. These are available as three-hourly temporal and 0.11° x 0.11° spatial resolution data from six different General Circulation Models (GCMs) downscaled using the RCA4 Regional Climate Model (RCM). We convert the wind speed into wind power using a hypothetical 8 MW power curve, and we define a power ramp when the change in wind power is above 30% of rated power (Cheneka, Watson and Basu, 2020). We quantify the spatial and seasonal change in wind power ramps in the near future (2006 – 2040) and the far-future (2041 – 2075) with respect to the base period (1971 – 2005). We have made a preliminary assessment of the projected future change in wind power ramps by season for the wind farms in three areas: region A (covering Beatrice), region B (covering the Belgian cluster, Borssele I and III) and region C (covering Horns Rev 1, 2 and 3) in the North Sea (Fig.1a). (Figure 1).

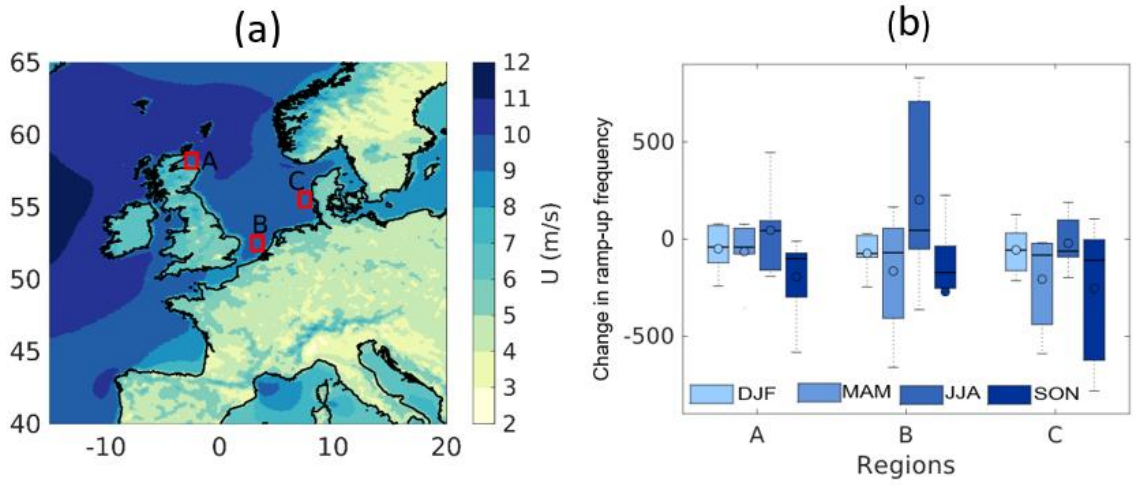


Figure 1: (a). Regions A, B and C over the North Sea. (b). Downscaled GCMs (RCA4-CNRM,RCA4-IPSL,RCA4-MPI, RCA4-ICHEC, RCA4-MOHC and RCA4-NCC) inter-quartile ranges of the seasonal change in predicted ramp-up events in the farfuture (2041 - 2075) for regions A, B and C. The circles represent the mean of the six modelled frequency change predictions.

The inter-quartile range (IQR) of wind power ramp event changes predicted by the six downscaled GCMs shows significant seasonal and spatial variation (Fig.1b). In the winter (DJF), the spread of the IQR in the far-future period is low compared with the spring (MAM), summer (JJA) and autumn (SON) seasons. In addition, the inter-seasonal variation is low over region A compared with region B and C.

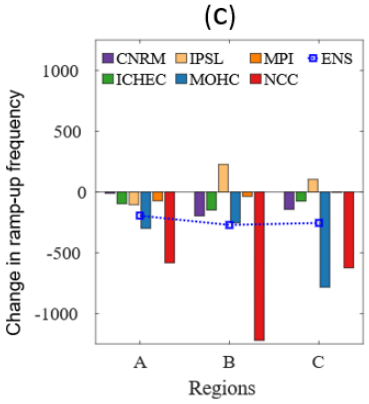


Figure 2: Ramp-up event changes predicted in the far-future for the autumn (SON) season for the six models plus the ensemble mean (ENS) marked as a blue dashed line.

Moreover, for all regions and seasons, the median change in wind power ramp events shows a negative trend except for the summer. Furthermore, we compare the results of the six models for one season, i.e. autumn (Fig. 2). All models show a decreasing trend over all regions except for RCA4-IPSL that shows a positive trend for region B and C. RCA4-NCC and RCA4-MOHC show a larger negative change in ramp events compared with the other models.

References:

Cheneka, B. R., Watson, S. J. and Basu, S. (2020) 'A simple methodology to detect and quantify wind power ramps', Wind Energy Science, 5(4), pp. 1731–1741. doi: 10.5194/wes-5-1731-2020.

Moemken, J. et al. (2018) 'Future Changes of Wind Speed and Wind Energy Potentials in EURO-CORDEX Ensemble Simulations', Journal of Geophysical Research: Atmospheres. Blackwell Publishing Ltd, 123(12), pp. 6373–6389. doi: 10.1029/2018JD028473.

Ohba, M., 2019. The impact of global warming on wind energy resources and ramp events in Japan. Atmosphere, 10(5), p.265.

Outten, S. D. and Esau, I. (2013) 'Extreme winds over Europe in the ENSEMBLES regional climate models', Atmospheric Chemistry and Physics, 13(10), pp. 5163–5172. doi: 10.5194/acp-13-5163-2013.

Weber, J., Gotzens, F. and Witthaut, D. (2018) 'Impact of strong climate change on the statistics of wind power generation in Europe', in Energy Procedia. Elsevier Ltd, pp. 22–28. doi: 10.1016/j.egypro.2018.10.004.

WindEurope(2019),'Offshore Wind in Europe windeurope.org Key trends and statistics 2019' Published in February 2020

Surface wave influences on offshore wind turbines: a coupled atmosphere-wave model investigation

Sara Porchetta[1,*], Domingo Munoz-Esparza[2], Jeroen van Beeck[1], and Nicole van Lipzig[1]
[1]KULeuven - von Karman Institute
[2]NCAR
*Presenting author

Keywords: Wind-wave interaction | COAWST | Wind farm parameterization

Offshore wind energy underwent an enormous growth within the last decades. Currently, offshore wind turbines provide 2.3% of the EU electricity demand. Last year, newly installed offshore wind turbines had a record capacity of 3.6 GW, resulting in a total offshore wind capacity of 22 GW in Europe alone (WindEurope, 2019). Due to this increase in offshore wind capacity, a good understanding of the offshore phenomena affecting wind farm power production is essential. Hence, mesoscale models are often employed, for example for offshore wind assessment studies, as well as for the investigation of wind turbine wake effects. These latter include the study of wake effects on wind speed reductions downwind of the wind farm, temperature effects and even impacts on regional-scale weather phenomena.
Recently, wind-wave interactions have been investigated by field measurements, lab experiments and numerical studies (including LES, RANS and DNS models) and these studies suggest that surface waves might have an influence on the wind, even up to hub height. There is a substantial body of literature which include wave parameters in roughness length parameterizations of mesoscale models. These roughness length parameterizations take the spatial and time variability of the offshore sea-state into account. This results in roughness length parameterization including wave age, wave steepness, sea spray etc. Additionally, wind-wave direction alignment has been found to furthermore influence the wind velocity. For example, swell waves traveling in the same direction as the wind produce an increase in wind velocity, while a decrease in wind velocity is observed for swell waves traveling in the opposed direction.

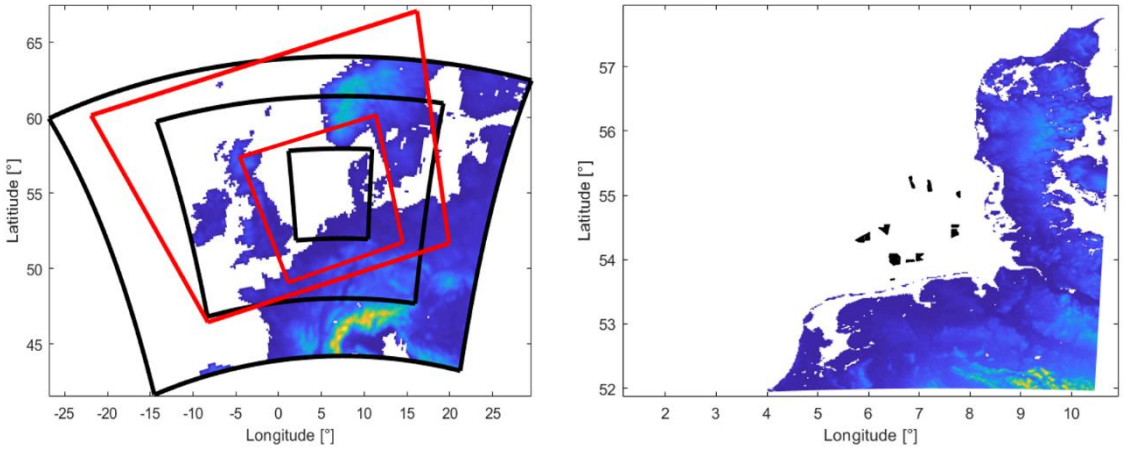


Figure 1: (left) WRF computational configuration (black) consisting of 3 nested domains and SWAN computational configuration with 2 nested domains (red). (right) Included wind farms

So far relatively little analysis of wave effects on offshore wind farms have been performed related to power production. This study therefore focuses on the effect of waves on wind farm power production by a mesoscale approach. The behavior of different wind-wave alignment directions on the power production of the wind farms has been investigated. The mesoscale model used was the Coupled Atmospheric-Ocean-Wave-Sediment Transport (COAWST) model (Warner et al., 2010) where an atmosphere only model, including the roughness length parameterization of Charnock (1955), has been compared to a coupled atmosphere-wave

model, including the roughness length parameterization of Porchetta et al. (2019) . These model integrations give insight in how the power production and wake behavior of a total of 1250 wind turbines in the North Sea are affected by surface waves. The model set-up for the atmospheric model WRF is similar to Siedersleben et al. (2020), while the wave model SWAN is set-up accordingly to Porchetta et al. (2020) . The time period simulated is from July 7 till July 15, 2010, this week represents the largest time period of consecutive opposed wind-wave directions, which allows us to study the effect of wind-wave alignment on the wind power production.

References:

Warner, J., Armstrong, B., and Zambon, J.B. (2010) Development of a Coupled Ocean-Atmosphere-Wave-Sediment Transport (COAWST) Modeling System. Ocean Modelling, 35(3), 230-244.

Charnock, H. (1955) Wind stress on a water surface. Quarterly Journal of the Royal Meteorologial Society, 81, 639-640.

Porchetta, S., Temel, O., Muñoz-Esparza, D., Reuder, J., Monbaliu, J., van Beeck, J., and van Lipzig, N. (2019) A new roughness length parameterization accounting for wind-wave (mis)alignment. Atmospheric Chemistry and Physics, 19, 6681-6700.

WindEurope: Offshore wind in Europ: available at: https://windeurope.org/data-and-analysis/product/wind-energy-ineurope-in-2019- trends-and-statistics/ (last access: 28 October 2020), 2019

Siedersleben, S.K., Pkatis, A., Lundquist, J.K., Djath, B., Lampert, A., Barfuss, K., Canadillas, B., Shulz-Stellenfleth, J., Bange, J., Neumann, T. and Emeis, S. (2020) Turbulent kinetic energy over lage offshore wind farms observed and simulated by the mesoscale model WRF (3.8.1). Geoscientific Model Development. 13, 249-268

Porchetta, S., Temel, O., Warner, J.C., Munoz-Esparza, D., Monbaliu, J., van Beeck, J. and van Lipzig, N. (2020) Evaluation of a roughness length parametrization accounting for wind-wave alignment in a coupled atmosphere-wave model. Quarterly Journal of the Royal Meteorological Society.

Influence of large-scale circulation effects on AEP calculations

Anna von Brandis[1], Lukas Vollmer[1,*], Gabriele Centurelli[2], Jonas Schmidt[1], Bughsin Djath[3], and Martin Dörenkämper[1]
[1]Fraunhofer IWES
[2]Carl von Ossietzky University of Oldenburg
[3]Helmholtz-Zentrum Geesthacht (HZG)
*Presenting author

Keywords: engineering wake models | resource assessment | array-array interaction

The assessment of the influence of upstream wakes on a offshore wind farm's annual energy production (AEP) is highly uncertain due to the unknown and changing extension plans for most offshore development areas. Simulations of multiple long-term scenarios in mesoscale models are too costly for the developer of a single wind farm. That is why engineering type models need to be able to properly model the long-distance wake development.
Recent work has demonstrated the knowledge and modelling gaps in developing a universal wind farm wake model applicable to intra- and interfarm effects. Nygaard et al. (2020) have shown that long wakes are widely underestimated by current standard wake model implementations and suggest a different treatment of the wake decay. Drastic wake deficit underestimations were concluded from airborne flight measurements in the German WIPAFF project downstream of wind farm clusters in stable atmospheric conditions (Cañadillas, 2020). These measurements show that not only magnitude but also the location of the wake might differentiate from the engineering model calculations.

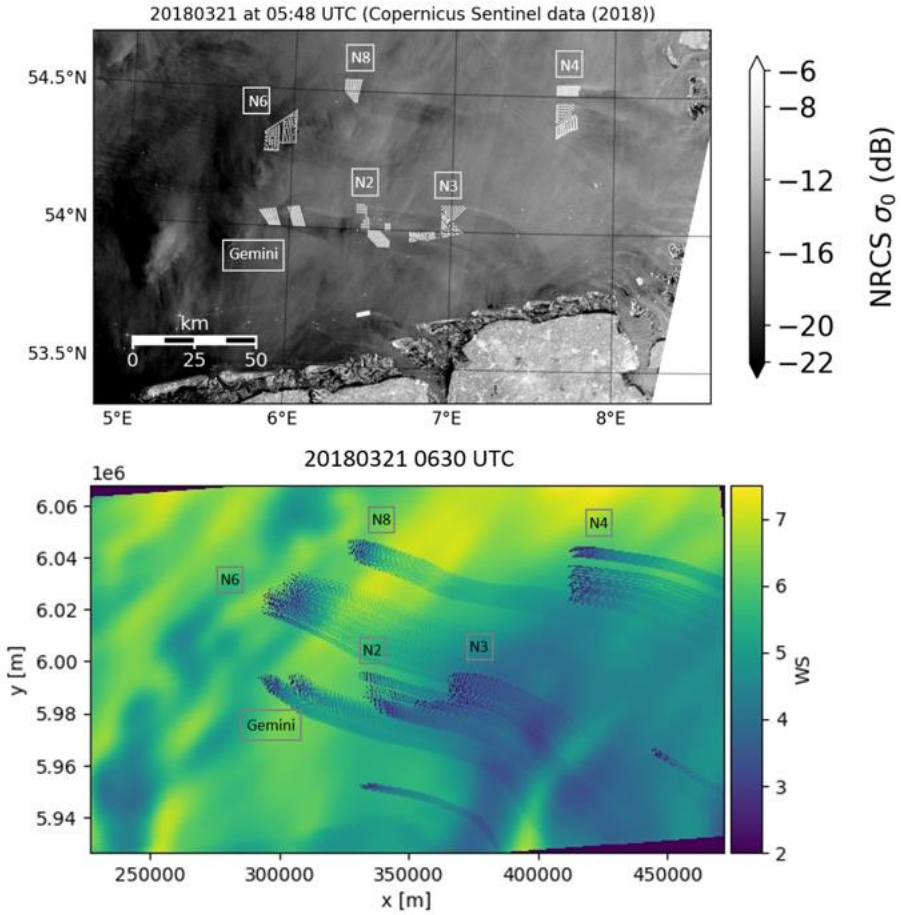


Figure 1: SAR backscatter image of the German Bight and simulation of the hub height wind speed with the combination of WRF and a wake model at the same date.

In the presented work, we looked specifically on the influence of the synoptic circulation patterns on the trajectory of wakes and the influence on the quantification of external wake losses.
As wakes generally follow the streamlines of the ambient background flow, small curvatures in the flow can already lead to large deviations in the wake influence on a wind farm located far downwind.
Using the German Bight as an example, the circulation patterns were analysed based on multi-year WRF (Skamarock, 2008) simulations.
The analysis reveals the mean pattern and the distribution of wind direction changes across the area.
For below-rated wind speeds, differences of more than 10 degree in wind direction over a distance of 100 km are occurring about 50 % of the time. That means even over shorter distances the assumption of wind direction homogeneity between two farm locations would often lead to a wrong assessment of the external wake's influence on the inflow conditions to the farm.
A quantification of the wind direction change's influence on the AEP is attempted by a scenario calculation with two large wind farms in the German Bight. To realise the representation of the circulation patterns in an engineering model, not only the wind speed field, but also the wind field streamlines are realised as ambient conditions in the Fraunhofer IWES wind farm modelling tool flappy (Farm Layout Program in Python).
The influence of the curvature of the wind field on the wake losses is compared to the baseline assumption of an homogeneous ambient wind direction. The analysis is conducted as well with tabulated mean wind conditions as in the time domain, to showcase the consequences of ignoring the non-linear effects of wake losses on the mean energy production.
The work represents one of the steps in improving the representation of large scale offshore wake and blockage losses in engineering models of the German X-Wakes project consortium.

References:

Nygaard, N., Steen, S., Poulsen, L. and Pedersen, J., 2020. Modelling cluster wakes and wind farm blockage. Journal of Physics: Conference Series, 1618, p.062072.
Cañadillas, B., Foreman, R., Barth, V., Siedersleben, S., Lampert, A., Platis, A., Djath, B., Schulz-Stellenfleth, J., Bange, J., Emeis, S. and Neumann, T., 2020. Offshore wind farm wake recovery: Airborne measurements and its representation in engineering models. Wind Energy, 23(5), pp.1249-1265.
Skamarock, W. C., Klemp, J. B., Dudhia, J., Gill, D. O., Barker, D. M., Duda, M. G., Huang, X.-Y., Wang, W., and Powers, J. G., 2008. A Description of the Advanced Research WRF Version 3, Tech. Rep. NCAR/TN-475+STR, National Center for Atmospheric Research

Mini-Symposium: Lidars and floating wind energy – Collaboration of Innovative Training Networks LIKE and FLOAWER







Jakob Mann
DTU Wind Energy

Ines Wuerth
University of Stuttgart

Oliver Bischoff
University of Stuttgart

In 2020 two new Innovative Training Networks started which will foster the training and education of 28 PhD students in the field of lidar for wind energy throughout Europe. The project LIKE (Lidar Knowledge Europe) focuses on improving the wind measurement technology and its translation into industry. FLOAWER (Floating Wind Energy Network) strives to design higher performance, economically viable floating wind turbines. In this mini-symposium we want everyone to present their newest developments of lidars for wind energy related purposes. We also encourage the Early Stage Researcher of the networks to present. The topics range from testing and refining the technology thus expanding the areas of application, to using scanning lidars, floating lidar or satellite lidar for wind resource mapping, power curve determination, wake measurement or control of single wind turbines or entire wind farms in order to increase energy production and reduce mechanical loads. All PhD projects emphasize the collaborative efforts between industry and academia and strive for a transparent use of data analysis methods.

Mini-Symposium: Lidars and floating wind energy – Collaboration of Innovative Training Networks LIKE and FLOAWER (I)

Overview of the PhD network LIKE

Jakob Mann, and Charlotte Hasager
DTU Wind Energy

Keywords: Doppler lidar | PhD network | induction | wind turbine wakes

LIdar Knowledge Europe (LIKE) fosters training and education of young researchers on emerging laser-based wind measurement technologies and their translation into industrial applications.
Unfortunately, the involved student have not been able to meet physically yet due to the corona pandemic, so you see a picture of previous PhD student gathering around a lidar on the photo.

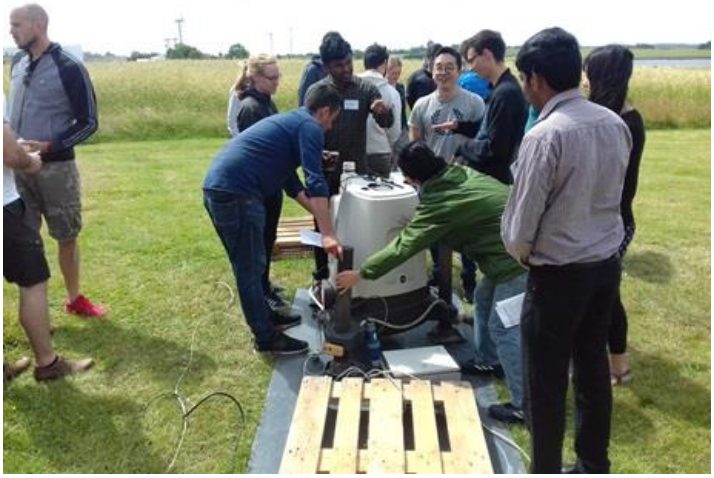


Figure 1: PhD student gathering around Doppler wind lidars before the pandemic at the DTU PhD Summer School on Remote Sensing for Wind Energy

Doppler Lidars (light detection and ranging) that measure the wind in the atmosphere remotely have reduced in price and increased in reliability over the last decade mainly done by European universities and companies serving the growing wind energy industry. This opens the possibility for new applications in many areas.
LIKE improves, tests and refines the technology thus expanding these areas of application. LIKE promotes wind energy applications such as wind resource mapping using scanning lidars and control of single wind turbines or entire wind farms in order to increase energy production and reduce mechanical loads.
LIKE maps unusual atmospheric flow patterns over airports in real-time and thus improves the safety of landing aircrafts. LIKE explores wind and turbulence under extreme conditions at the sites of future European bridges paving the road for optimal bridge design. LIKE trains 15 ESRs to an outstanding level at European academic institutions and industrial companies, thus forming strong interdisciplinary relations between industry and technical sciences. This presentation will give an overview of LIKE

Overview of the Innovative Training Network FLOAWER

Sandrine Aubrun[1], Oliver Bischoff[2], and Charlotte Bay Hasager[3]
[1]Centrale Nantes
[2]University of Stuttgart
[3]Technical University of Denmark

Keywords: Floating wind energy | PhD network | European offshore wind

This presentation will give an overview of the MSCA ITN project FLOAWER (FLOAting Wind Energy netwoRk). The FLOAting Wind Energy netwoRk (FLOAWER) is primarily designed to train researchers in the required multi-disciplinary engineering fields to better develop FOW technologies under the constraint of LCOE minimization. Indeed, while high TRLs are currently achieved due to a very conservative approach for most of the technological issues, the market will be definitely viable if the LCOE significantly decreases in the next few years: according to the Floating Wind task force of WindEurope, a reduction factor of 4 by 2030 is required. LCOE reduction requires a multidisciplinary approach, where all sub-system designs are jointly optimised.
The research programme is structured into 4 scientific work-packages:
- Wind resource assessment in deep waters
- Advanced floater analysis
- Dynamics of wind turbines
- System design to reduce LCOE

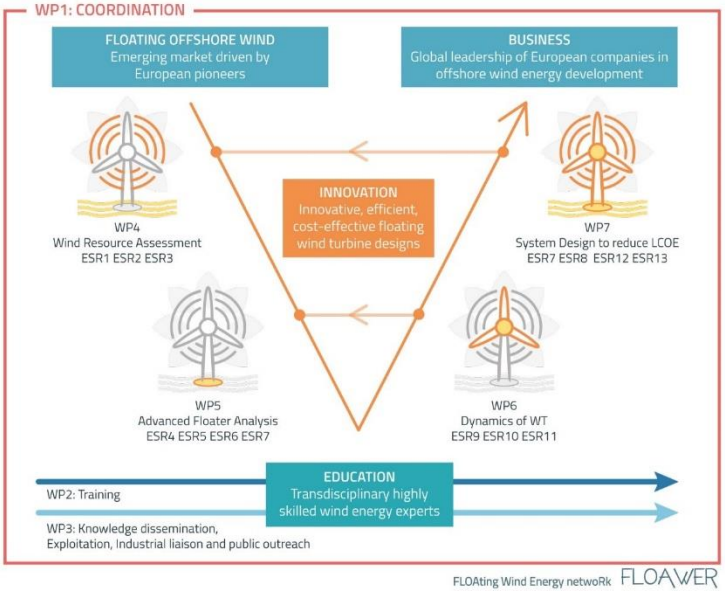


Figure 1: Flow chart of ITN-FLOAWER

FLOAWER will fulfil the following main objectives:
• Deliver leading-edge training to ESRs by addressing the state-of-the-art scientific and transversal needs of the Floating Offshore Wind (FOW) sector;
• Enable ESRs to benefit from regular mobility across the EU's most prominent industry and academic players in the FOW sector;
• Confront the ESRs to the current and upcoming engineering challenges faced by the FOW industry;
• Create a multidisciplinary environment where industries and academia share ideas and work together towards solutions accelerating the commercialisation of the FOW sector;
• Support European offshore wind energy industries to identify technological improvements by providing high performance characterization and modelling tools that can enhance their competitiveness.

Altogether, FLOAWER will train a new generation of innovation-oriented Early-Stage-Researchers (ESR), with enhanced career perspectives, who will be a key asset to tackle current and future challenges in the FOW sector and boost European competitiveness and attractiveness in this field.
Interactions with other ITN projects related to wind resource and/or wind energy (LIKE, TRAIN2WIND and STEP4WIND) are currently set-up to generate synergies between them for the benefit of the scientific advances, the offshore wind sector development and the ESR networking and personal development.

References:
FLOAWER website www.floawer-h2020.eu

Validation of Aeolus Wind Observations with in-situ Measurements and Reanalysis Dataset in Oceania

Haichen Zuo*, Charlotte Bay Hasager, and Ioanna Karagali
Technical University of Denmark
*Presenting author

Keywords: Aeolus satellite | Wind profile | Validation | Oceania

After over 15 years of design and building, the Aeolus satellite for wind observation was launched into the sun-synchronous orbit successfully by European Space Agency (ESA) in August 2018.
Equipped with an Atmospheric Laser Doppler Instrument (ALADIN), Aeolus becomes the first satellite mission to achieve wind profile measurement globally (Figure 1). The ALADIN has two separate detection channels. One is for Rayleigh scattering from air molecules, and the other is for Mie scattering from dust, ice and water droplets (Ingmann and Straume, 2016). Based on light scattering and the Doppler effect, wind profiles of global coverage can be measured from the surface to 30 km altitude with vertical range bins from 250 m to 2 km; horizontally, the resolution of each observation is 87 km that is composed of 30 measurements with a resolution of 3 km (Ingmann and Straume, 2016).

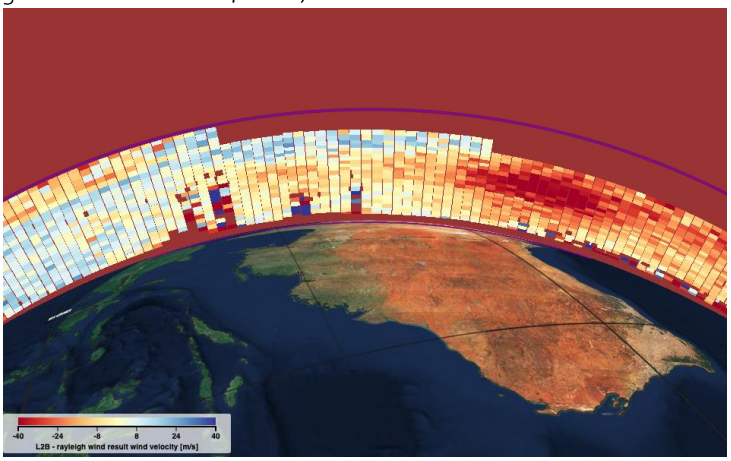


Figure 1: Aeolus L2B HLOS Rayleigh winds on 16 December 2020 over the east of the Australia. The figure was generated with the virtual research platform - VirES for Aeolus (https://aeolus.services/).

The operation of the Aeolus satellite not only makes up for the lack of uniformly distributed wind profile detection from space but can serve a variety of applications, including further exploring atmospheric dynamics, improving numerical weather predictions, better-estimating air pollutants, etc.(ESA, 2020; Rennie and Isaksen, 2020). However, the wind profiles captured by ALADIN have not been fully evaluated, especially for the Southern Hemisphere (Chou et al., 2020; Guo et al., 2020; Lux et al., 2020). Given that, this study focuses on the validation of Aeolus wind products over regions in Oceania. With the help of the EUMETNET Composite Observing System, the Level 2B product (HLOS - horizontal line-of-sight wind observations) of the Aeolus mission will be compared with in-situ measurements from wind profilers. The evaluation will also be carried out with the ERA5 reanalysis dataset generated by the European Centre for Medium-Range Weather Forecasts (ECMWF). Before conducting error analysis, all data will be collocated both in time and in space. Firstly, the
Aeolus wind profiles will be filtered based on the maximum distance to in-situ measurements less than 100 km and time difference within 60 min, and the winds from ERA5 will be extracted from the corresponding grids. All data will then be interpolated to the same heights, and the wind vectors from in-situ measurements and ERA5 reanalysis dataset will be projected onto the HLOS via the Aeolus azimuth angle. After data filtering and collocation, the error information including mean bias, random error and correlation coefficient of both

Rayleigh-clear wind and Mie-cloudy wind will be quantified. Finally, the results will be discussed by comparing with other existing studies.

The research findings of this study are expected to provide valuable information for data assimilation for numerical simulation. In particular, the potential of Aeolus wind for innovative applications, such as wind assessment for airborne wind energy as well as air route optimization, can be addressed.

References:

Chou, C.-C., Kushner, P., Mariani, Z., Rodriguez, P. and Fletcher, C. (2020) 'Validation for ESA's Aeolus Mission using the insitu instruments at Canadian Arctic and reanalysis data'. EGU General Assembly 2020, Online, 4 May. Available at: https://meetingorganizer.copernicus.org/EGU2020/EGU2020-13461.html (Accessed: 18 August 2020).

ESA (2020) Aeolus objectives, Aeolus. Available at: https://earth.esa.int/eogateway/missions/aeolus (Accessed: 5 January 2021).

Guo, J., Liu, B., Gong, W., Shi, L., Zhang, Y., Ma, Y., Zhang, J., Chen, T., Bai, K., Stoffelen, A., de Leeuw, G. and Xu, X. (2020) 'Technical Note: First comparison of wind observations from ESA's satellite mission Aeolus and ground-based Radar wind profiler network of China', Atmospheric Chemistry and Physics Discussions, pp. 1–36. doi: https://doi.org/10.5194/acp-2020-869.

Ingmann, P. and Straume, A. G. (2016) 'ADM-Aeolus Mission Requirements Document'. ESA. Available at: https://esamultimedia.esa.int/docs/EarthObservation/ADM-Aeolus_MRD.pdf (Accessed: 22 December 2020).

Lux, O., Lemmerz, C., Weiler, F., Marksteiner, U., Witschas, B., Rahm, S., Geiß, A. and Reitebuch, O. (2020) 'Intercomparison of wind observations from the European Space Agency's Aeolus satellite mission and the ALADIN Airborne Demonstrator', Atmospheric Measurement Techniques. Copernicus GmbH, 13(4), pp. 2075–2097. doi: https://doi.org/10.5194/amt-13-2075-2020.

Rennie, M. P. and Isaksen, L. (2020) 'An Assessment of the Impact of Aeolus Doppler Wind Lidar Observations for Use in Numerical Weather Prediction at ECMWF'. EGU General Assembly 2020, Online, 4–8 May 2020. Available at: https://doi.org/10.5194/egusphere-egu2020-5340 (Accessed: 9 January 2021).

Atmospheric boundary layer characterization for airborne wind energy applications

Jan Markus Diezel[1,*], Joachim Reuder[1], Jakob Mann[2], and Lode Carnel[3]
[1]University of Bergen
[2]DTU Wind Energy
[3]Kitemill AS
*Presenting author

Keywords: airborne wind energy | Lidar | atmospheric boundary layer | power curve

Airborne Wind Energy Systems (AWES) are a set of technologies that use flying tethered objects (e.g. kites) to produce power from the wind. With current test flights reaching up to a height of 500 m and the possibility to fly even higher, AWES reach heights considerably above conventional wind turbines.
It is commonly stated that winds higher up in the atmospheric boundary layer are stronger and more consistent. This statement is investigated and quantified in this research project through the use of Lidar data from several measurement locations in Norway, as well as reanalysis model data. Testing this statement is highly relevant to AWES, as the quality of the wind is a major factor determining the reliability of power production through AWES in comparison to conventional turbines.
This presentation provides an overlook over the research project and the planned analyses. The main goal of this research project is to deliver a characterization of the atmospheric boundary layer with a focus on research questions relating to AWES. For this purpose, existing measurement data will be analyzed and compared to model results. Additionally, a measurement campaign is being carried out using a Lidar wind profiler to measure the wind up to a height of 2000 m. This measurement campaign is taking place in southern Norway (Lista) for one year starting from November 2020. The unique value of this measurement campaign is that test flights of an AWES will be carried out at the same location in parallel to the Lidar measurements, which allows an estimation of the power generation of AWES as a function of the measured wind profile. Besides producing power curves, these findings can also be used to optimize the algorithms controlling the kites during operation.

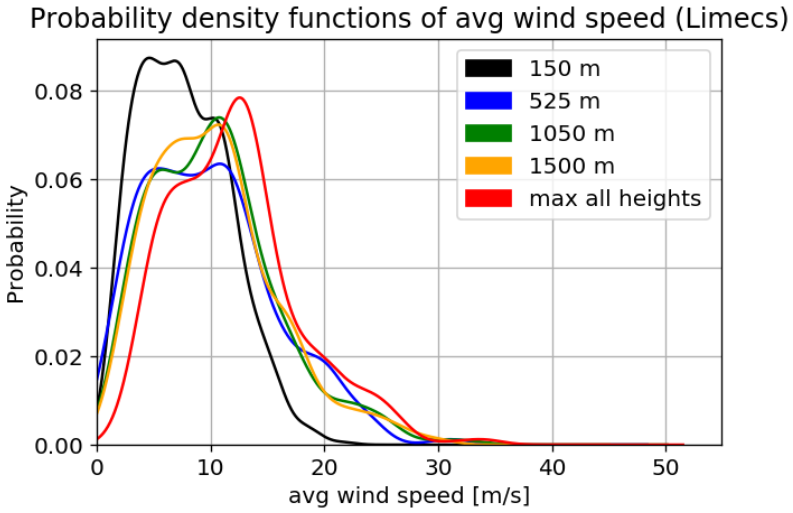


Figure 1: Estimated probability density functions from one month of 10-min averaged wind speed data measured during LIMECS (Lidar measurement campaign at Sola Airport, Norway). The red curve shows the probability density function of the maximum wind speed of each profile.

Therefore, the goal of this research project is to investigate the value of Lidar measurements for wind resource analyses and to quantify the potential of on-site Lidar measurements in improving AWES power production, e.g. compared to an operation that is only based on the results of numerical weather forecast models.

Lastly, already existing wind profile data sets from both reanalyis models and other Lidar measurement campaigns will be used to show some first analysis results. In particular, the Lidar measurement campaign at Sola Airport, Norway (LIMECS) is investigated to show the value of Lidar measurements for taking advantage of the benefits of a flexible power generation height. The measurements took place during 2013 in a period of about four months. In this analysis, only times where full profiles were measured are taken into account, so that every profile has a 100% data availability up to 1500 m. This reduces the total measurements to about a month. As the attached figure illustrates, the distribution of 10-min averaged wind speeds clearly shifts towards higher wind speeds when allowing for a variable height of AWES operation.

Exploring ferry lidar data through scatterometer winds

Daniel Hatfield*, Charlotte Hasager, and Ioanna Karagali
Technical University of Denmark
*Presenting author

Keywords: lidar | satellite | NEWA ferry lidar | ASCAT | Baltic Sea

The first ship-based lidar measurements were performed by Fraunhofer IWES where the motion correction algorithm is adapted for ship-based floating systems from Edson et al. 1998 and tested in Strobach et al. 2017 and Wolken et al. 2014. The sea-induced movement correction is dependant on floating lidar system itself - either employing motion compensation (i.e. from a stability platform) or motion detection using suitable sensors.
Satellites, as a means of wind retrieval, can provide wind observations of the ocean surface and resource distribution where these high-resolution mesoscale models perform. A scatterometer is an active radar that measures the backscatter power from transmitted pulses. This backscatter depends on the surface roughness; a complete smooth surface will result in reflection with no backscatter back to the instrument. As the roughness increases, the backscatter component increases simultaneously. The measurements of the backscatter signal from the observed area can be used to estimate the normalized radar cross section (NRCS). The NRCS is the relation between the received and transmitted power which depends on the radar settings, the atmospheric attenuation and the ocean surface characteristics. The extraction of ocean surface winds from the NRCS comes from a geophysical model function (GMF). The GMF is empirically derived and dependent on the design of the scatterometer. The wind product used in this study is the 12.5 km coastal Stress-Equivalent Wind.

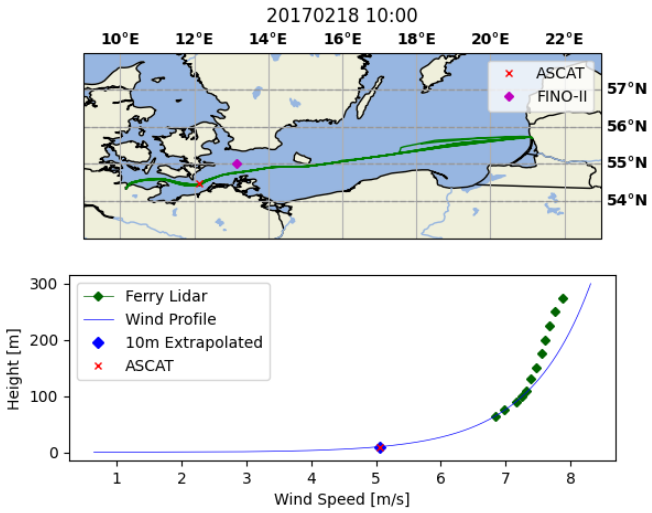


Figure 1: Extrapolation process of the lidar wind profile and corresponding ASCAT 10m wind speed.

Surface derived winds from scatterometer instruments such as the Advanced Scatterometer (ASCAT) are obtained at a height of 10m. This unfortunately is not directly applicable to wind observations needed for wind farms, as wind speed measurements at hub heights (100m+) are preferred. Vertical extrapolation from wind profiles has proven to be a great resource bringing surface winds to hub heights. The reverse can be done (i.e. "de-extrapolation" given a surface layer wind profile such as from a met mast or lidar profiler. Multiple measurements at multiple heights are taken daily where the averaged profile can be fitting and de-extrapolated down to the surface layer matching that of the derived satellite winds.
Lidar measurements are already well-tested and accepted as a standard in the offshore wind energy industry; for floating systems measurements for the motion correction of the instrument itself are needed alongside accurate, site-specific measurements of key-parameters of the wind profile. In situ measurements of wind

profiles in the deep water regime are few and site-specific, so the use of collocated scatterometer and lidar measurements can be used to verify the validity of the motion corrected data of a moving lidar system as compared to high-resolution mesoscale models.

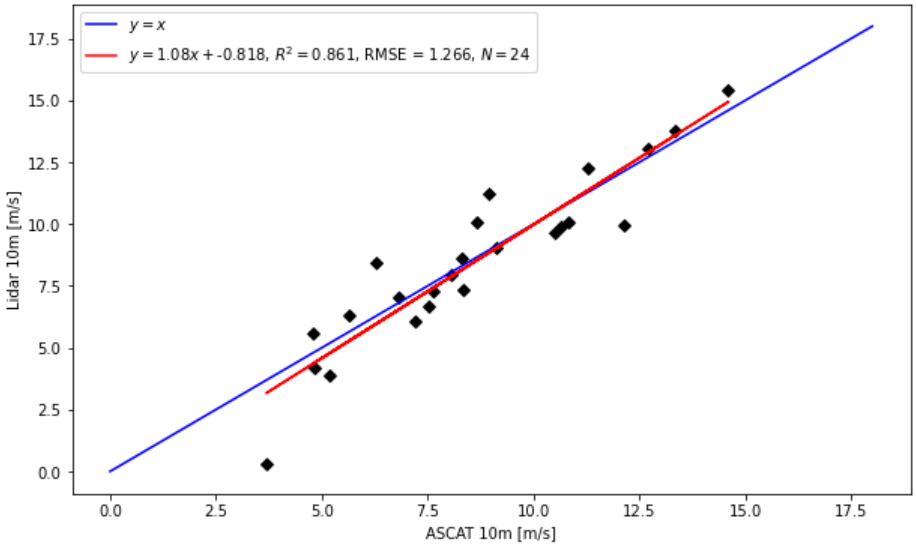


Figure 2: Scatter of ASCAT 10m wind speeds with 10m extrapolated lidar wind speeds in near-neutral conditions.

This work follows the ferry lidar campaign in the Baltic Sea of Gottschall et al. 2018. The aim is to evaluate the applicability of scatterometer winds as a means to study the motion corrected lidar wind profile measurements and data quality. Initially, the scatterometer data was compared against the FINO-II meteorological mast data to assess their performance versus traditional, fixed, measuring stations. Initial findings show that in ideal conditions, both derived wind speed and direction of the lidar/satellite have a better correlation than that of the mesoscale models, however is limited due to the availability of daily satellite measurements.

References:

J. Gottschall, E. Catalano, M. D¨orenk¨amper, and B. Witha. The NEWAFerry Lidar Experiment: Measuring mesoscalewinds in the Southern BalticSea.Remote Sensing, 10(10):1–13, 2018

G. Wolken-M¨ohlmann, J. Gottschall, and B. Lange. First verification testand wake measurement results using a ship-lidar system.Energy Procedia,53, 12 2014.

R. Zentek, S. H. E. Kohnemann, and G. Heinemann. Analysis of the per-formance of a ship-borne scanning wind lidar in the Arctic and Antarctic.Atmospheric Measurement Techniques, 11(10):5781–5795, 2018

I. Karagali, A. Pe˜na, M. Badger, and C. B. Hasager. Wind characteristicsin the north and baltic seas from the quikscat satellite.Wind Energy,17(1):123–140, 2014

M. Badger, A. Pe˜na, A. N. Hahmann, A. A. Mouche, and C. B. Hasager.Extrapolating satellite winds to turbine operating heights.Journal of Ap-plied Meteorology and Climatology, 55(4):975–991, 2016

J. B. Edson, A. A. Hinton, K. E. Prada, J. E. Hare, and C. W. Fairall.Direct Covariance Flux Estimates from Mobile Platforms at Sea*.Journalof Atmospheric and Oceanic Technology, 15(2):547–562, 04 1998.

E. J. Strobach and L. C. Sparling.The Impact of Coastal Terrain onOffshore Wind and Implications for Wind Energy. PhD thesis, Universityof Maryland, Baltimore County, 2017.

Wind resource assessment at SEM REV test site through spatially-distributed instrumentation

Ana Garcia Correa[1,*], Sandrine Aubrun[2], Boris Conan[3], and Yves Perignon[1]
[1]Ecole Centrale de Nantes
[2]Centrale Nantes
[3]LHEEA, Centrale Nantes - CNRS
*Presenting author

Keywords: floating wind energy | wind assessment | sonic anemometer

Around 80% of the offshore wind resources are located in deep waters1, more than 60 meter depth, where bottom-fixed offshore wind is not economically attractive2. In addition, average wind speeds are higher and more consistent further from shore. This means that floating offshore wind farms can produce more energy throughout the year and have high capacity factors3.
One of the challenges of wind farm development is the resource assessment phase; offshore wind farms require a solid basis for wind data before installations. Follow Sempreviva et al. recommentation, an evaluation of a regional wind resource assessment, to either involve already available data from different spots (including lighthouses and buoys) distributed over the area of interest, combined to reanalysis datasets or data from atmospheric models. That includes the Sonic anemometers, a robust instruments without moving parts that can provide high-frequency measurements (typically 10 to 100Hz) of the wind field even in harsh offshore environments. The SEM REV test site, located on the coast of France, needs to evaluate the capacity of the currently distributed instrumentation to access the local wind resource. This study, part of the FLOAWER
(Floating Wind Energy Network) MSCA ITN project, will determine the correlations between local measurements, from three different sonic anemometers at the coast and other instrumentations available. The first is localized in the Cardinaux lighthouse (h=29m), the second is localized at Teignouse lighthouse (h=35m), and the third in Kerroch tower, identified in Figure 1. Additionally, SEM REV buoy is instrumented with a sonic anemometer (h=5m) and provides data by the wind and wave interactions.

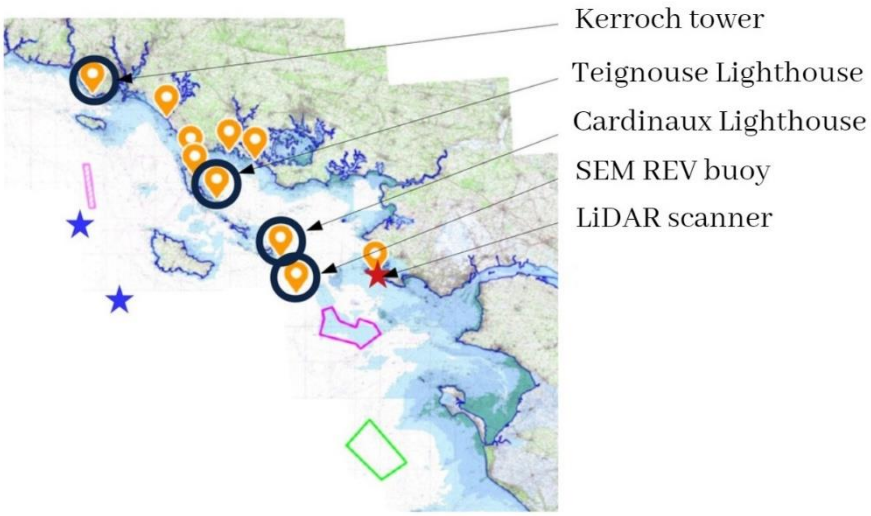


Figure 1: SEM-REV test site is located in the west coast of France. The instrumentations are identified in the figure.

Quality control routines for sonic anemometer measurements have been described by Aubinet et al.4, and Nybo et al5 and will be considered. Also, the analysis will follow the Eddy covariance flux measurements. Based on determining the correlation between changes in vertical wind velocity and deviations in a scalar quantity. The IEA Report6 for floating LiDAR (Light detection and ranging) systems recommend methods to assess wind speed and direction accuracy and defines acceptance based on Key Performance Indicators (KPIs).

Besides the sonic anemometers localized in the coast, the ERA5 modeling will be processed for the area of interest. The use of a scanning LiDAR technology is a relevant option for coastal regions7 and will be correlated in the study area. The expected results are the wind resource characterization of the SEM REV test site and the measurement of the influence of the ocean-atmosphere parameters. The goal is a contribution to reducing the levelized cost of electricity (LCOE) and the floating wind turbines can become accessible for more places.

Acknowledgements: The FLOAWER project has received funding from the European Union's Horizon 2020 research and innovation programme under the Marie Sklodowska-Curie grant agreement N° 860879.

References:

1 European Wind Energy Association (EWEA). Deep water – The next step for offshore wind energy. http://www.ewea.org/fileadmin/files/library/publications/reports/Deep_Water.pdf; July 2013, p. 15-17

2 A. Myhr, C. Bjerkseter, A. Ågotnes, T.A. Nygaard Levelised cost of energy for offshore floating wind turbines in a life cycle perspective Renew. Energy, 66 (2014), pp. 714–728

3 Sempreviva AM, Barthelmie RJ, Pryor SC. Review of methodologies for offshore wind resource assessment in European seas. Surv Geophys 2008, 29:471–497. https://doi.org/10.1007/s10712-008-9050-2.

4 Aubinet, M., Versala, T. & Papale, D. (Eds.). (2012). Eddy Covariance: A Practical Guide to Measurement and Data Analysis. Springer Science & Business Media.

5 Nybø, Astrid, Finn Gunnar Nielsen, and Joachim Reuder. "Processing of sonic anemometer measurements for offshore wind turbine applications." Journal of Physics: Conference Series. Vol. 1356. No. 1. IOP Publishing, 2019.

6 Bischoff, O., I. Würth, J. Gottschall, B. Gribben, J. Hughes, D. Stein, and H. Verhoef, 2016: Recommended Practices for Floating Lidar Systems. https://www.ieawind.org/index_page_postings/whatsNEW/IEA_Wind_Task32_StateOfArtFloatingLIDAR_Feb2016.pdf (Accessed January 12, 2021)

7 Gottschall, J., Gribben, B., Stein, D., & Würth, I. (2017). Floating lidar as an advanced offshore wind speed measurement technique: Current technology status and gap analysis in regard to full maturity. Wiley Interdisciplinary Reviews: Energy and Environment, 6(5), e250.

Normalized-wake characterization by long-range lidars

Priscila M. S. Orozco[1,*], Juan-José Trujillo[1], and Martin Kühn[2]
[1]UL International GmbH
[2]ForWind - University of Oldenburg
*Presenting author

Keywords: wake meandering | lidar measurements | wake center tracking | wake averaging

Remote sensing techniques such as lidars have proven to be the most versatile tool for measuring wind turbine wakes due to their good resolution and flexibility (Wildmann et al., 2018). Indeed, they have aided in revealing that wakes exhibit large-scale dynamics, such as wake meandering, and that the measured wake field depends on which frame of reference is used to analyze it (e.g. Trujillo et al., 2011; Beck et al., 2015). These studies on far-wake tracking have shown that there is the potential of filtering out large-scale effects to obtain a wake field unaffected by external atmospheric conditions.
This PhD project strives to evaluate this potential and its possible applications within the scope of the Lidar Knowledge Europe (LIKE) project, funded by the European Union Horizon 2020. The main objective is to prove to which extent external large-scale effects of the boundary layer can be separated from the far wake from full-field measurements. More specifically, we intend to reach a site-independent "normalized wake", analogous to the wake in an environment influenced only by small-scale turbulence. The processes and methods involved in the first phase of this PhD are summarized in the conceptual flowchart from Figure 1.

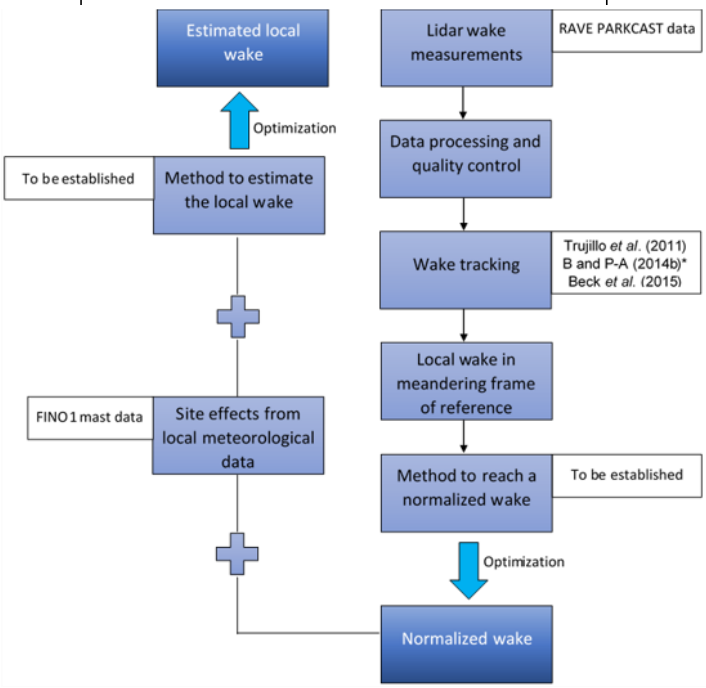


*Figure 1: Conceptual flowchart of the processes and methods involved in achieving a normalized wake and in the estimation of its local wake based on site effects (e.g. atmospheric stability). *B and P-A (2014b) stands for Bastankhah and Porté-Agel (2014b).*

Analysis techniques will be tested on singlewake lidar measurements to obtain a normalized wake under different inflow conditions. Data from the RAVE PARKCAST Project in the alpha ventus wind farm (North Sea), acquired by two long-range StreamLine-XR lidars mounted on the nacelle of turbine AV04 (one looking upwind and the other downwind), will be used at this stage. After processing the data and performing a quality control, firstly we will apply different wake tracking techniques (Trujillo et al., 2011; Bastankhah and Porté- Agel, 2014b; Beck et al., 2015) to the downwind-looking lidar measurements to estimate a local quasi-steady wake, which will be represented in a meandering frame of reference. Secondly, the aim is to spot the optimal analysis method to reach a normalized wake and perform a proof of concept of its application, i.e.,



turning it back to an estimated local wake by considering the atmospheric conditions of the measurement site. For this objective, raw and averaged meteorological data measured by the sensors from the FINO1 mast, located at approximately 400 m from the lidar measurements, will be used. Based on the findings from Beck et al. (2015), we expect that the normalized wake resulting from the lidar measurements will have more realistic wake deficits and wake length, representative of what a downstream wind turbine would actually perceive. We presume that the representation of the same wake but in a fixed frame of reference will underestimate the deficits as well as show a shorter length. Therefore, normalized-wake values will be more suitable for the validation of modeled wind speeds in wake.

References:

Bastankhah, M. and Porté-Agel, F. (2014b) 'A new analytical model for wind-turbine wakes.' Renew Energy, 70, pp. 116-123. doi: 10.1016/j.renene.2014.01.002.

Beck, H., Trujillo, J.-J. and Kühn, M. (2015). 'Analysis of wake sweeping effects based on load and long-range LiDAR measurements'. 12th German Wind Energy Conference DEWEK, Bremen, Germany, 19 May to 20 May 2015.

Trujillo, J.-J, Bingöl, F., Larsen, G.C., Mann, J. and Kühn, M. (2011). 'Light detection and ranging measurements of wake dynamics. Part II: two-dimensional scanning'. Wind Energy, 14 (1), pp. 61-75. doi: 10.1002/we.402.

Wildmann, N., Vasiljevic, N., and Gerz, T. (2018). 'Wind turbine wake measurements with automatically adjusting scanning trajectories in a multi-Doppler lidar setup'. Atmos. Meas. Tech., 11, 3801-3814. doi: 10.5194/amt-11-3801-2018.

Mini-Symposium: Lidars and floating wind energy – Collaboration of Innovative Training Networks LIKE and FLOAWER (II)

Error quantification as a function of metocean conditions and correction of wave induced turbulence intensity bias assessed with a Floating LiDAR System

Thibault Desert[1], Sandrine Aubrun[1], Graham Knapp[2], Samy Kraiem[2], MAXIME Bellorge[3], Benoit Clauzet[4], Romain Barbot[5], and Lise Mourre[5]
[1]Central Nantes
[2]CSTB Nant
[3]AKROCEAN
[4]EDF
[5]VALOREM

Keywords: Offshore | Floating | Lidar | Turbulence

In the framework of wind farm development, financing and operation, developers regularly need to reliably quantify the site turbulence intensity. This information can be used to validate wind farm layouts, to select the appropriate turbines to be installed during the development process and to optimise the wind farm operation. The current standard instrumentation to measure both velocity and turbulence intensity is via a cup or sonic anemometer mounted on a meteorological mast, with a measurement altitude as close as possible to the hub height. However, cost and technical constraints specific to offshore configurations make this solution not affordable and velocity measurement is replaced by remote sensing (LiDAR) instrumentation mounted on buoys (floating LiDAR Systems).



Figure 1: Fécamp offshore site with WINDSEA floating LiDAR system (left) and fixed platform equipped with a meteorological mast (background, right) (WINDSEA 2 @FECAMP copyright J.Vapillon – AKROCEAN)

This alternative is now accepted for wind farm developments and the quality of the obtained 10-min averaged wind speed statistics has been validated. However, this is not the case for turbulence intensity because of a large measurement error mainly due to wave induced motion.
The 24-month MATILDA project aims to quantify the error in the turbulence intensity measurement due to motion of the floating LiDAR and to propose corrections depending on the sea state. The analysis is based on the comparison of measurements performed simultaneously by a fixed LiDAR system located on Fécamp offshore platform (owner EDF Renouvelables) and by the WINDSEA floating LiDAR system during its validation campaign (owner AKROCEAN). The Fécamp platform is also equipped with a meteorological mast (owner

Eoliennes Offshore des Hautes Falaises, consortium composed of EDF Renouvelables, Enbridge and WPD Offshore).

Metoceanic conditions and algorithmic post-processing of lidar measurements have a major influence on the resulting 10min turbulent intensity estimates. Thus, the first part of the project is focusing on evaluating the magnitude of the measurement error and correlating this with the metoceanic context (boundary layer stability, sea state and wind speed) in order to fully understand the influence of each factor. The test sample is composed of 13 weeks that have been selected for the best representation of the 6 month of metoceanic conditions. Different post-processing methods are evaluated: the post-processing offered by LEOSPHERE with and without movement cancellation, and post-processing methods of our own calculated from raw data files. Then, we are implementing a correction in order to build an algorithm improving turbulence measurements by cancelling the effect of wave motion. The purpose is to build a simple and userfriendly correction based on lidar and gyroscopic 10 min measurements enhancing the precision of the turbulence estimates. We first evaluate the correction on a model simulating the lidar measurement behaviour for a full control of the inputs and the outputs before being implemented on the Fécamp database.

Methods based on raw measurement corrections like six-beams (Sathe et al., 2015) and squeezing (Kelberlau et al., 2019) are also implemented for a more sophisticated enhancement of WindCube v2 turbulence intensity estimates. They will be evaluated via an onshore campaign provided by LEOSPHERE before we apply them to the Fécamp database.

References:

Sathe, J. Mann et al. A six-beam method to measure turbulence statistics using ground-based wind lidars, Atmos. Meas. Tech., 8, 729–740, 2015

F. Kelberlau and J. Mann, Better turbulence spectra from velocity–azimuth display scanning wind lidar, Atmos. Meas. Tech., 12, 1871–1888, 2019

LIDAR Assisted Model Predictive Control of Wind Turbine

Zhaoyu Zhang*, Paolo Schito, and Alberto Zasso
Politecnico di Milano
*Presenting author

Keywords: LIDAR Measurement | Model Predictive Control | Wind Turbine Control | OpenFast | SOWFA

Traditional turbine controller usually acts slowly because of a complex electromagnetic system and huge mechanical device. It is difficult for turbines to respond to the current wind situation in a short time. In contrast to the anemometer which measures wind speed and direction on the nacelle, the development of LIDAR technology provides an opportunity to obtain wind data in advance and remotely.
In this paper, a Doppler LIDAR is manipulated to detect the optimal measurement distance and average speed of preview inflow wind in front of the rotor plane. Based on doppler theory, a Gaussian distribution weight function is applied to focus one measurement point from a big volume of the laser. Doppler Beam Swinging technique helps to reconstruct the 3D wind map from the limited information, i.e. line of sight wind speed detection of LIDAR [1]. According to multi-points results, the average wind speed and direction are calculated.
Model Predictive Control (MPC) is proposed because of its strong capability of processing the predictive information from sensors. After defining the cost function which maximizes the energy harvesting, the optimal problem is described through mathematic functions [2]. Time horizon section and feedback loop of MPC keep updating at every time step to guarantee the optimal solution in real-time. This optimal problem is computed with a MATLAB toolbox and then coupled with the turbine simulation in a DLL format.
Based on variable speed generator torque and collective pitch control, it is possible to find the optimal pitch and torque for different inflow wind speeds. There are three zones divided by wind speed at cut-in, rated and cut-off, the torque runs in an optimal strategy around the rated speed.

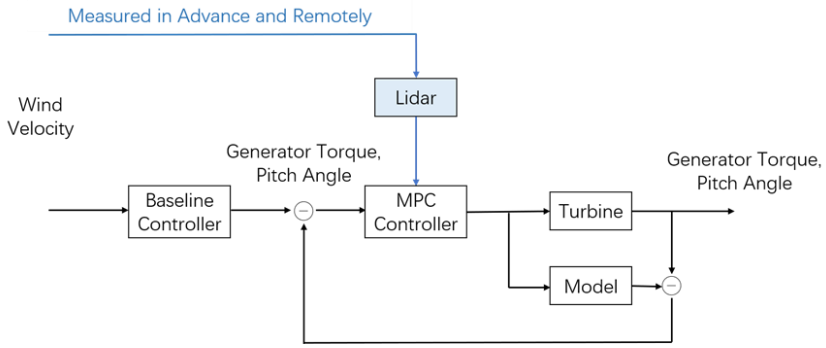


Figure 1: Structure of LIDAR Assisted MPC

Based on blade characteristics, the pitch angle and generator torque follow optimal tip speed ratio and torque restrictions respectively [3]. Lastly, we need to identify the scheduled pitch angle and torque as reference for MPC.
For the numerical simulation of the turbine, the proposed MPC is designed in the OpenFAST platform, where a 1:75 scale model of the DTU 10MW wind turbine aeroelastic model is applied [4].
OpenFAST estimates the output of the turbine, such as power generation, rotor torque and blade loads. On the other hand, high fidelity CFD of the entire wind field is accomplished in the SOWFA platform [5]. To simulate the process of LIDAR measurements, four wind sampling points from the SOWFA are compared with the wind estimation using the Doppler Beam Swinging technique.
Comparing MPC with traditional wind turbine controllers, the simulation results show that LIDAR assisted MPC has great advantages showing a power generation increase. In future research, the wake and turbulence will be involved in the LIDAR measurement to reduce their effects on the downstream turbine and maximize the power of the wind farm.

References:
[1] J.-P. Cariou, "Pulsed lidars," in Remote Sensing for Wind Energy, DTU Wind Energy-E-Report-0029(EN), June 2013, ch. 5, pp. 104–121.
[2] Schlipf, D., Schlipf, D.J. and Kühn, M. (2013), Nonlinear model predictive control of wind turbines using LIDAR. Wind Energ., 16: 1107-1129. https://doi.org/10.1002/we.1533.
[3] J. Jonkman, M. Buhl Jr., "Fast users guide,", no. NREL/EL-500-29798, National Renewable Energy Laboratory, Golden, Colo, USA, 2005.
[4] Bayati, I., Belloli, M., Bernini, L. and Zasso, A., 2017. Aerodynamic design methodology for wind tunnel tests of wind turbine rotors. Journal of Wind Engineering and Industrial Aerodynamics, 167, pp.217-227.
[5] Fleming, P., Gebraad, P., van Wingerden, J.W., Lee, S., Churchfield, M., Scholbrock, A., Michalakes, J., Johnson, K. and Moriarty, P., 2013. SOWFA super-controller: A high-fidelity tool for evaluating wind plant control approaches (No. NREL/CP-5000-57175). National Renewable Energy Lab.(NREL), Golden, CO (United States).

Evaluating the performance of ship-based lidar measurements by comparing the data from a short- and long-range lidar profiler in the Atlantic Ocean

Hugo Rubio[1,*], Julia Gottschall[1], and Jakob Mann[2]
[1]Fraunhofer IWES
[2]Technical University of Denmark
[*]Presenting author

Keywords: ship lidar | offshore wind resource | floating lidar measurements

The increasing interest in developing offshore wind farms have brought to light remote sensing devices as a more flexible and cost-efficient alternative to conventional meteorological masts for measuring relevant wind resources and site conditions. Nowadays, there are several options for the use of these devices, such as their installation on wind turbines´ platforms, in a buoy or on a ship.
This last option, so-called ship-based lidar technology, consists of a vertical Doppler lidar profiler placed on board a ship, and it allows to measure offshore winds and conditions along the ship track.
The evaluation of ship-lidar data against numerical (mesoscale) meteorological model data in previous studies has shown a good correlation between these two kinds of data sets (Gottschall, Catalano, Dörenkämper, & Witha, 2018). However, further and a more detailed investigation of the performance and particularities of these kinds of measurements is required.
As part of the EUREC4A project, a new ship-based lidar measurement campaign was conducted to measure offshore winds within a vast region in the Atlantic Ocean. In the first part of this campaign, lasting from November 2019 to January 2020, a short-range Windcube v2 (WLS7) lidar was installed on board of the research vessel (RV) Merian, travelling from Emden (Germany) to Barbados islands and measuring wind data up to 250 m height. In the second part, both the previously mentioned short-range device and a long-range Windcube (WLS70) lidar were installed on board of RV Meteor, going from Barbados to the Azores during two and a half months between January and March 2020, and recording wind data up to 2000 m height. The retrieved wind data is corrected for the effects of ship motions using a post-processing correction algorithm (Wolken-Möhlmann & Gottschall, 2014).

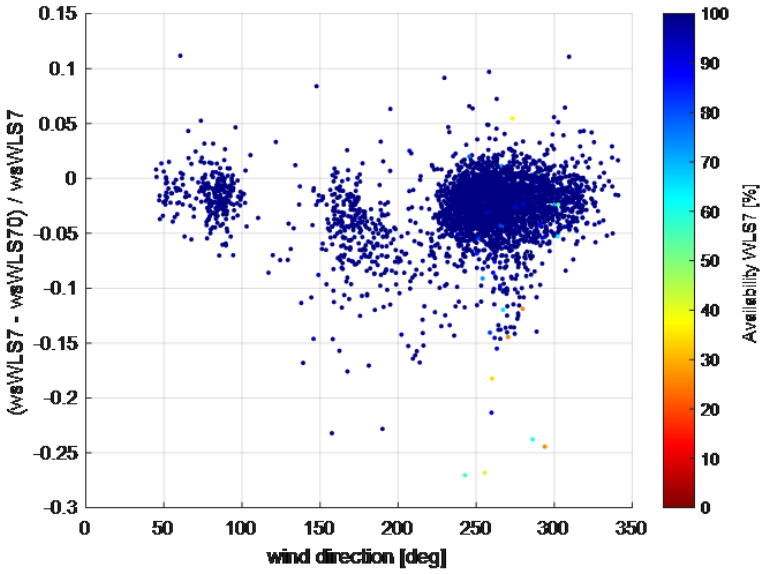


Figure 1: Normalized wind speed difference between short-range (WLS7) and long-range (WLS70) lidars depending on wind direction. The color bar represents the data availability of each 10- min averaged datum.

The main goal of the study presented here is to investigate the accuracy of the wind measurements retrieved by ship-lidar systems during the aforementioned measurement campaign. To achieve this, and due to the

absence of in-situ measured reference data, measurements from both lidars devices are compared and examined through a sensitivity analysis. For this, we evaluate the performance of these difference ship-lidar devices (with a different measurement geometry) depending on external parameters like wind direction, ship motions and velocity or data availability.

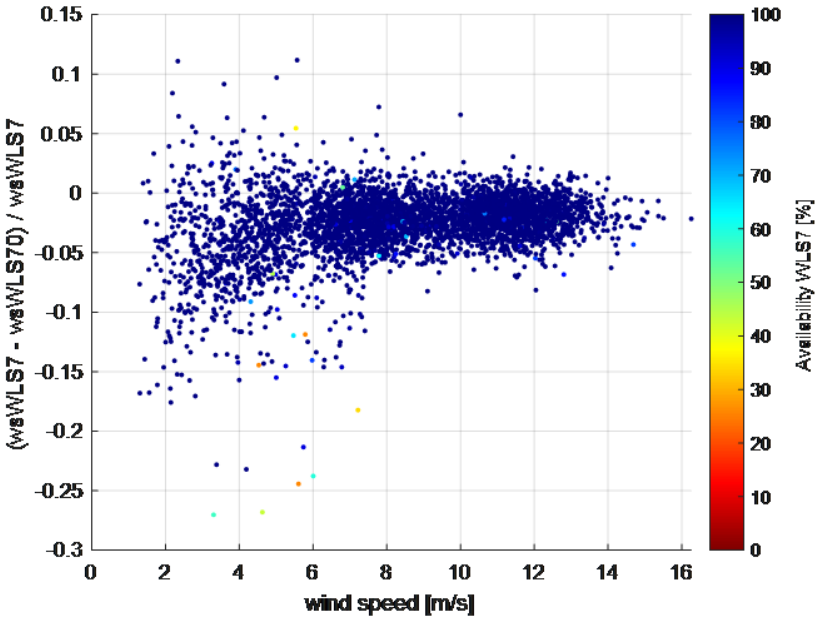


Figure 2: Normalized wind speed difference between short-range (WLS7) and long-range (WLS70) lidars depending on wind speed. The color bar represents the data availability of each 10- min averaged datum.

The original purpose of the RV Meteor measurement campaign was to combine short- and longrange lidars to assess an extended wind profile. However, the more detailed analysis and evaluation of these observations carried out in this study will help to gain a valuable experience and knowledge on ship-lidar technology particularities. On the one hand, the results of this study will highlight useful considerations for the optimal design and execution of new ship-based measuring campaigns, as well as provide a better understanding about the most suitable device and system set-up for ship-lidar applications. On the other hand, they will highlight insights about the conditions that enhance or deteriorate the accuracy of this type of measurements, and therefore, about the considerations to be made when processing and analyzing data retrieved by this technology.

References:

Gottschall, J., Catalano, E., Dörenkämper, M., & Witha, B. (2018). The NEWA Ferry Lidar Experiment: Measuring Mesoscale Winds in the Southern Baltic Sea. Remote Sensing, 10(10), 1620. https://doi.org/10.3390/rs10101620

Wolken-Möhlmann, G., & Gottschall, J. (2014). Ship-based lidar measurement in the wake of an offshore wind farm. Retrieved from https://iopscience.iop.org/article/10.1088/1742-6596/555/1/012043/pdf

Turbulence measurements using a triple-Doppler lidar technique

Lukas Pauscher[1,*], Florian Jäger[1], Andreas Körner[1,2], Tobias Klaas[1], and Kira Gramitzky[1,2]
[1]Fraunhofer IEE
[2]University of Kassel
*Presenting author

Keywords: lidar | multi-lidar | site assessment | turbulence measurements

Multi-lidars have proven to be a promising technology in measuring turbulence conditions in site assessments for wind farms. For multi-lidar measurements the beams of two or more lidars are intersected to measure in the point of interest. This way multi-lidar approaches overcome the problem of separated probe volumes for each beam - one of the weaknesses of classical profiling lidars. Remaining challenges are the probe volume averaging along the beam and the slow sampling rate if multiple points are to be scanned in the multi-lidar setup. This study evaluates triple-Doppler lidar measurements to derive variances of the horizontal wind speed (and thus turbulence intensities) from a triple-lidar configuration.
If the elevation angels for the lidar beams are small, the variance of the horizontal wind speed can be derived using two different algorithms. The classical approach calculates the velocity vector for each time step and then derives the variances of the individual components. The second approach (radial variances approach) derives the radial velocity variances for each beam and then combines them to derive the velocity variances. This study focuses on the radial variances approach and for the first time presents an experimental investigation of the technique. Moreover, simulations using the spectral tensor of Mann (1994) and based on the framework of Peña and Mann (2019) are carried out to theoretically assess the effects of probe-volume averaging.

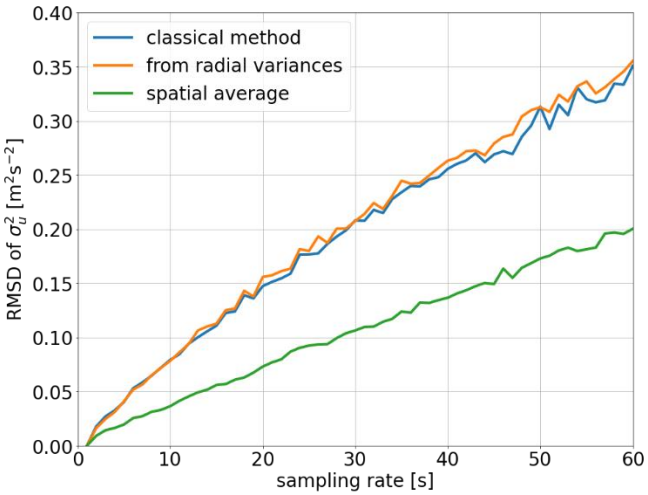


Figure 1: Root mean square deviation (RMSD) of the variances of the horizontal wind speed derived from three different methods for varying sampling rates; for a detailed explanation of the different methods see text. The RMSD is calculated using the difference between the variance at the specific sampling rate and the sampling rate at 1 s.

Slow sampling rates introduce random errors in the measurement of the radial variances. This is especially important in the context of site assessment where the representative turbulence intensity is used. Therefore, in a second step the radial variances approach is extended to use multiple range gates along the beam around the intersection point. This spatial averaging is introduced to 'stabilise' the radial variances and intended to mitigate the effects of a low sampling rate.
Comparison of the triple-lidar with measurements from a reference mast (115 m height) shows a high correlation of the measured variances of the horizontal wind speed and slightly lower values for the multi-lidar measurement. Simulation of the turbulence attenuation by probe volume averaging produces values similar to those experimentally observed. In practical applications, the choice of the turbulent length scale is

shown to introduce uncertainty here. For the experimental setup with three lidars, which are placed in favourable angles towards the measurement point, the directional dependence of the simulated probe-volume averaging is rather small.
Artificially reducing the sampling rate is used to analyse the effects of increased random errors. This also significantly affects the representative turbulence intensity. For the experiment a sampling rate of 30 s resulted in an increase of the measured representative turbulence intensity with similar magnitude as the reduction caused probe-volume averaging. The random errors in the variance of the horizontal wind vector components can be significantly reduced by deriving a spatial average of the radial variances around the intersection point before computing the variances of the horizontal wind vector components (see Figure).

References:
Mann, J 1994, 'The spatial structure of neutral atmospheric surface-layer turbulence', Journal of Fluid Mechanics, vol. 273, pp. 141-168.
Peña, A & Mann, J 2019, 'Turbulence measurements with dual-doppler scanning lidars', Remote Sensing, vol. 11, no. 20, 2444. https://doi.org/10.3390/rs11202444

Compacted measurement volume of continuous-wave Lidar with a novel optical configuration

Liqin Jin*, Jakob Mann, and Mikael Sjöholm
Technical University of Denmark
*Presenting author

Keywords: Continuous-wave Lidar | Lorentzian weighting function | compacted measurement volume

Doppler Lidars are increasingly being used in the wind energy industry to assess wind resources and measure the turbulent wind flow approaching the wind turbine rotor. For the class of Doppler Lidars called continuous-wave Lidar, which can be made cheap and robust, the problems are that the measurement volume is quite large for long measurement distances because the effective probe volume varies as the 4th power of the focus range (Peña et al. 2015). The larger and larger turbines also increase the measurement volume if specific measurement distance is interested, like 2Drotor or 3Drotor, for turbine controlling and wake modelling. Besides, large measurement volume makes the Lidars quite susceptible to moving objects far away from the intended measurement point. These drawbacks are problematic for wind turbine applications. However, it is possible to deploy optical components to solve these problems and make the measurement volume more compact.

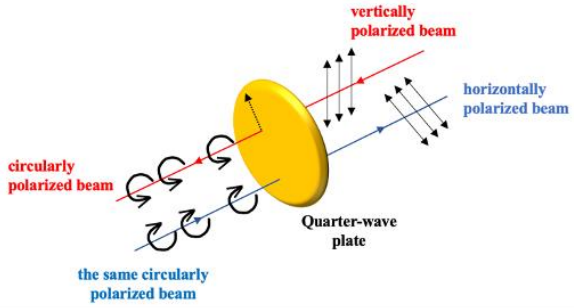


Figure 1: Illustration of the principle of the quarter-wave plate.

A Doppler Lidar measures the line-of-sight velocity parallel to the laser beam and employs the Lorentzian weighting function with the peak at the focus point to derive the weighted averaged wind speed. The sensitivity decays away from the focus point but only as d−2 where d is the distance from the focus. If the backscatter is strong even far away from the focus point, a false signal will be detected. Harris et al. (2001) suggested a bi-static solution with one emitting and one receiving telescope to solve this problem. But this bi-static system has several disadvantages, such as expensive and complicated setup, difficult to change focus and reduced signal to noise ratio. The novel idea is to retrofit the Lidar system, without any change in the other components and the analysis software, by using quarter-wave plates, to effectively suppress strong backscatter that occurs far away from the focus point and to reduce the probe length. If a vertically polarised beam goes through the same quarter-wave plate twice, it will become horizontally polarised. This resultant horizontally polarised signal will not beat with the original signal inside the Lidar system, as is shown in the first figure. Therefore, backscattered signal from out-of-focus aerosols can be greatly reduced and the effective focus will be more compact.

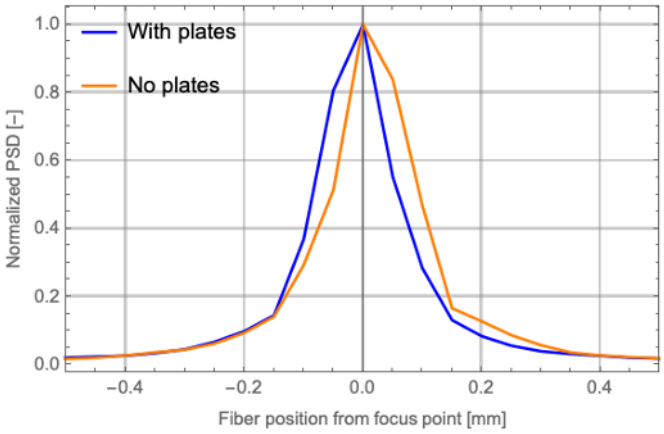


Figure 2: Lorentzian weighting function of continuous-wave Lidar with/without quarter-wave plates

Several lab experiments have been conducted to verify this concept. The results show that hard targets, like running belt and the flying wheel, can change the polarisation of the emitted beam. Even though the signal backscattered by the out-of-focus particles will go through one plate twice, the polarisation of the returned signal is not purely horizontally polarised. Thus, the quarter-wave plate can't help much in this case. However, diffuse particles (smoke) have been tested, and the results are shown in the second figure. The Lorentzian weighting function is not symmetric, and one side of the blue curve is narrowed nearby the focus point. The current measurement is quite preliminary and that the reduction in the full width at half-maxima (FWHM) length of the weighting function is almost invisible.

References:
Peña, A, Hasager, CB, Badger, M, Barthelmie, RJ, Bingöl, F, Cariou, J-P, Emeis, S, Frandsen, ST, Harris, M, Karagali, I, Larsen, SE, Mann, J, Mikkelsen, T, Pitter, M, Pryor, S, Sathe, A, Schlipf, D, Slinger, C & Wagner, R 2015, Remote Sensing for Wind Energy. DTU Wind Energy E, no. 0084(EN), DTU Wind Energy.
Harris M, Constant G, Ward C. Continuous-wave bistatic laser Doppler wind sensor. Applied Optics. 2001 Mar;40(9):1501-1506. DOI: 10.1364/ao.40.001501.

Robotic Lidar Wind Flow and Velocity Measurements

Shahbaz Pathan* , Mikael Sjöholm, and Jakob Mann
Technical University of Denmark
*Presenting author

Keywords: Robotic Lidar | Lidic | Wind Velocity | Wind Flow Measurement | Automation

Remote sensing of wind at short distances in wind tunnels using continuous-wave Doppler lidars is gaining interest as exemplified by for instance (Sjöholm et al., 2017). Here we report about the developments of a robotic-borne scanning wind lidar. The concept is tested in several lab experiments at DTU Wind Energy, Risø, Denmark under the European Union project Marie Skłodowska-Curie Actions: Lidar Knowledge Europe (Like). One new experiment is the mapping of velocity on a rotating wheel and another is measurement of flow from a wind blower. The small lidar telescope previously developed at DTU, Wind Energy, Denmark is used together with a scanning and steering mechanism in the form of a collaborative robotic arm. The lidar signals are synchronized with the movement of the robotic arm using GProgramming (LabVIEW), which makes it an embedded system, in order to get lidar signal information which is wind velocity measurement synchronized with position. The two loops running in parallel in the software are the robot coordination and the Lidar code. The computer program sends commands to the laser and the robotic arm and also processes and records the backscattered signals. The continuous-wave lidar employed uses a fiber laser with an erbium-doped fibre amplifier operating at a wavelength of 1.56 micrometer. The light is coupled through an optical circulator into a short telescope with 1-inch optics and a fixed focus, although the focusing range can manually be adjusted. The backscattered light received and a fraction of the originally generated laser light are mixed and detected by a photodetector. The beat signals in the Mega-Hertz range contain information about the wind speed and are digitized for further post-processing. The sign of the velocity is actually achieved by using an in-phase, quadrature-phase detection scheme utilizing two detection paths.

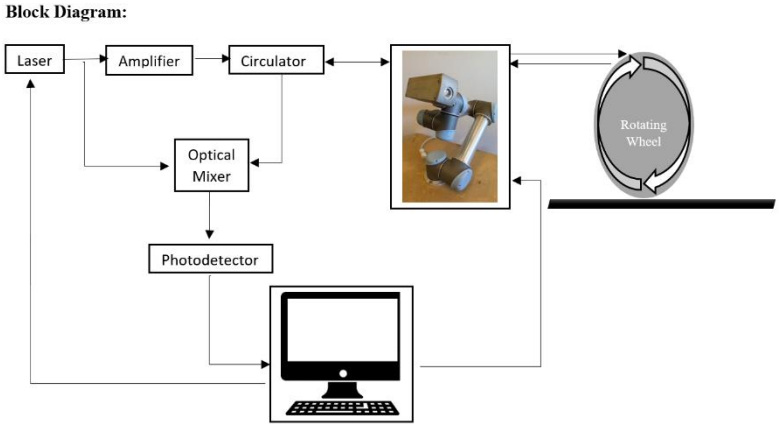


Figure 1: Block Diagram of Instrumentation Setup at DTU, Risø, Denmark

The robot used in this research is a collaborative UR5 by Universal Robots whose mechanism is based on Denavit–Hartenberg parameters. Before applying the coordinate information on the robot in real time, the robot is tested through virtual machines in order to save robot from accidental damage.
The program developed using G-Programming in LabVIEW is connected to a virtual machine by the interface configuration on the virtual machine and the internet protocol configuration for the robot on a computer program in order to test movement of the robot virtually.
The approach developed and investigated proposes a new concept of wind scanning and processing at different positions synchronized with the lidar wind signals. The results obtained through this robotic lidar concept could be helpful for new wind lidar instrumentation.



Acknowledgement: This research is part of the Innovation Training Network Marie Skłodowska-Curie Actions: Lidar Knowledge Europe (LIKE) project which is funded by European Union Horizon-2020 under the grant number 858358. The authors are very thankful to European Union.

References:

Sjöholm, M, Vignaroli, A, Angelou, N, Nielsen, MB, Mann, J, Mikkelsen, TK, Bolstad, HC, Merz, KO, Sætran, LR, Mühle, FV, Tiihonen, M & Lehtomäki, V 2017, 'Lidars for Wind Tunnels - an IRPWind Joint Experiment Project', Energy Procedia, vol. 137, pp. 339-345. https://doi.org/10.1016/j.egypro.2017.10.358

Mikael Sjöholm et al. (2017): A classical model wind turbine wake "blind test" revisited by remote sensing lidars. Wind Energy Science Conference 2017, WESC2017 - DTU Copenhagen 2017, Book of abstracts, p 207

http://www.windscanner.eu

https://www.msca-like.eu

Mini-Symposium: Lidars and numerical models – how they correspond and interact



Julia Gottschall
Fraunhofer IWES



Peter Clive
Black & Veatch

Since their emergence about 15 years ago, wind lidars have changed the wind industry, and in particular the way how we assess, map and investigate atmospheric flows that are relevant for the utilization of wind energy. While the first ground-based vertical profilers brought into the market were intended as a replacement for met masts only, the more advanced technologies (including scanning lidar systems but also devices placed on buoys, ships and not least wind turbines) offer many more opportunities. This enables a completely new approach to the investigation of real wind fields and thus the validation and possible calibration of numerical models that are used where real measurements are not possible or economically feasible. For this mini-symposium, we call for contributions covering the opportunities, advances, challenges and limitations of combining numerical flow models and wind lidar measurements. We invite presentations on specific validation campaigns, evaluations of these, or methodologies applied.

Mini-Symposium: Lidars and numerical models – how they correspond and interact (I)

What is more accurate – a wind lidar measurement or the ouput of a numerical model?

Julia Gottschall*
Fraunhofer IWES
*Presenting author

Keywords: scanning wind lidar | numerical flow model | uncertainty quantification

Both lidar measurements and numerical flow models have become indispensable in wind energy research and various applications in the wind industry. Often they are used in combination, to calibrate the other data source or for correction. This inevitably raises the question of which data source we trust more or attribute greater accuracy to. Even if this question seems simple and straightforward at first, it is not easy to answer. Of course, an assessment depends on the one hand on the flow model used and its input data, and on the other hand on the measuring device, the measuring strategy and the processing of the data – to name just a few aspects. Of essential importance are also the overall context of the respective application and the metrological assumptions for the definition of an uncertainty.
We illustrate the considerations using the example of a methodology we developed for making use of scanning lidar measurements in an onshore wind resource assessment. The measurements are used to calibrate the output data of a numerical flow model and with this not just quantify but potentially also reduce the uncertainties of the final wind resource estimate. The scanning lidar is configured to perform PPI scans and the numerical flow data are projected onto this geometry. Deviations in the recorded and derived line-of-sight wind speeds are used to identify deficiencies of the model and as starting point for an improvement and tuning. Before this calibration can be carried out, the uncertainties of the lidar measurements must be understood and quantified, which can be achieved on the basis of an uncertainty model. The findings of an evaluation performed for a moderately site in central Germany suggest that the use of the methodology offers a promising opportunity to control the uncertainty of the applied flow models, which can otherwise only be estimated very roughly.
The results of the example study indicate that the answer to our initial question is not so much given by the properties of the measurements or the models themselves, but by the methodology that is defined in advance for a specific application. Whether the correct assumptions about the accuracy of measurement and/or model data have been made for the establishment of the methodology can be assessed in terms of a quantification of the associated uncertainties, provided that this is sufficiently complete.

References:
J. Gottschall: Advancing wind resource assessment in complex terrain with scanning lidar measurements. Preprint - submitted to Energies, 2021.

Optimal tuning of engineering wake models through LiDAR measurements

Lu Zhan*, Stefano Letizia, and Giacomo Valerio Iungo
University of Technology at Dallas
*Presenting author

Keywords: wind turbine | wake model | lidar

Engineering wake models provide the invaluable advantage to predict wind turbine wakes, power capture, and, in turn, annual energy production for an entire wind farm with very low computational costs compared to higher-fidelity numerical tools. However, wake and power predictions obtained with engineering wake models can be insufficiently accurate for wind farm optimization problems due to the ad-hoc tuning of the model parameters, which are typically strongly dependent on the characteristics of the site and power plant under investigation.
For this work, LiDAR measurements collected for individual turbine wakes evolving over a flat terrain are leveraged to perform optimal tuning of the parameters of four widely used engineering wake models, namely the Jensen (Jensen 1983), Bastankhah (Bastankhah & Porté-Agel, 2014), Larsen (Larsen 1988), and Ainslie (Ainslie 1988) wake models. About 10 000 PPI LiDAR scans of isolated wind turbine wakes are processed to provide the nondimensional average velocity fields used for this study (Zhan et al., 2020a, 2020b). LiDAR measurements are clustered according to different categories of inflow condition, namely 13 bins of the hub-height wind speed and five regimes of static atmospheric stability. The LiDAR scans within each cluster are averaged through a technique based on the Barnes scheme (Barnes, 1964; Newsom et al., 2017; Letizia et al., 2020a,b). For more details on the cluster analysis and the calculation of the ensemble statistics of the lidar data see Zhan et al. (2020a), while the clustered statistics of the LiDAR data are publicly available on Zenodo (Iungo, 2020).

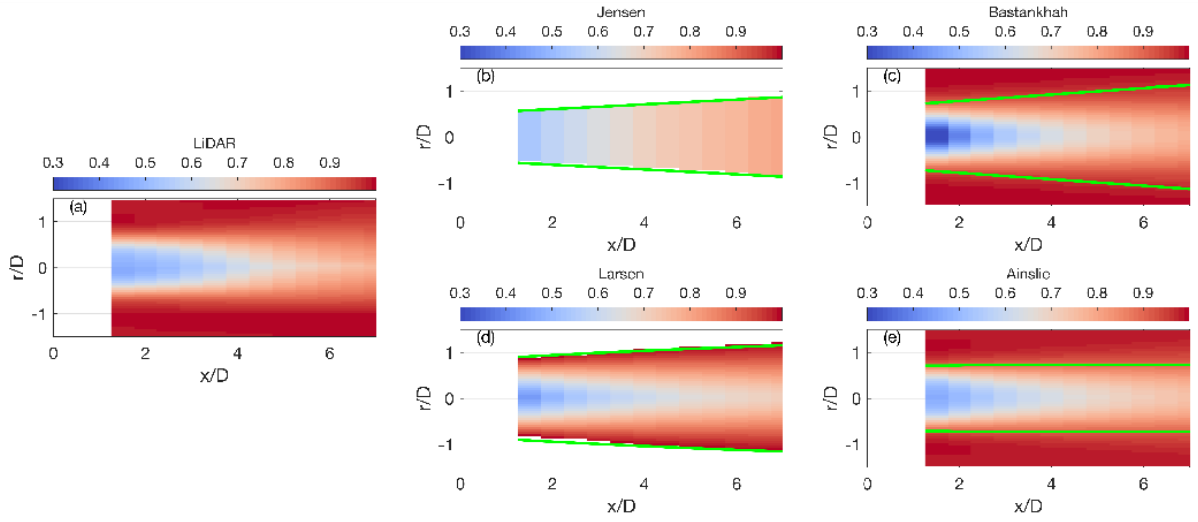


Figure 1: Normalized velocity for the cluster with U_hub^* of [0.76, 0.81] and TI of [13.5 %, 19.4 %]: (a) lidar data, (b) Jensen wake model,(c) Bastankhah wake model, (d) Larsen wake model, (d) Ainslie wake model. The green lines represent the wake edges, while for (c) they represent the spanwise position corresponding to 2σ.

The average wake velocity fields for the various clusters of the LiDAR dataset are used as a reference for the optimization of the wake-model parameters, which is performed by minimizing the mean percentage error between the wake flow predicted through the models and the mean velocity fields measured through a scanning Doppler wind LiDAR. The results of the optimal-tuning procedure show that the thrust coefficient obtained through this numerical approach is in good agreement with the values obtained by applying the mass and streamwise momentum budgets on the mean LiDAR data (Iungo et al., 2018b). Furthermore, the model parameters representing the wake turbulent expansion and recovery are roughly linearly proportional

to the incoming wind turbulence intensity at hub height. This study shows that the Jensen model has a lower yet comparable accuracy than the remaining three wake models. The Larsen wake model generally shows better accuracy than the Jensen model yet lower than for the Bastankhah and Ainslie wake models. The Bastankhah wake model has shown great accuracy in wake predictions upon the optimal tuning of the model parameters. However, we recommend using the Bastankhah wake model only for downstream locations and wind conditions for which the Pearson correlation coefficient between the actual velocity field and the Gaussian model is expected to be higher than 0.99. Finally, the Ainslie wake model has shown great accuracy, indicating that the mixing-length model for the RANS equations is a simple yet efficient turbulence closure model to capture the effects of incoming turbulence and wake-generated turbulence on wake downstream evolution and recovery (Iungo et al., 2018b).

References:

Ainslie, J.F., 1988. Calculating the flow field in the wake of wind turbines. Journal of Wind Engineering and Industrial Aerodynamics, 27(1-3), pp.213-224.

Barnes, S.L., 1964. A technique for maximizing details in numerical weather map analysis. Journal of Applied Meteorology and Climatology, 3(4), pp.396-409.

Bastankhah, M. and Porté-Agel, F., 2014. A new analytical model for wind-turbine wakes. Renewable Energy, 70, pp.116-123.

Iungo, G.V., Letizia, S. and Zhan, L., 2018a, June. Quantification of the axial induction exerted by utility-scale wind turbines by coupling LiDAR measurements and RANS simulations. In Journal of Physics: Conference Series (Vol. 1037).

Iungo, G.V., Santhanagopalan, V., Ciri, U., Viola, F., Zhan, L., Rotea, M.A. and Leonardi, S., 2018b. Parabolic RANS solver for low-computational-cost simulations of wind turbine wakes. Wind Energy, 21(3), pp.184-197.

Jensen, N.O., 1983. A note on wind generator interaction. Risø National Laboratory, Copenhagen, Denmark.

Larsen, G.C., 1988. A simple wake calculation procedure. Risø National Laboratory, Copenhagen, Denmark.

Letizia, S., Zhan, L. and Iungo, G.V., 2020a. LiSBOA: LiDAR Statistical Barnes Objective Analysis for optimal design of LiDAR scans and retrieval of wind statistics. Part I: Theoretical framework. Atmospheric Measurement Techniques Discussions, 2020. https://doi.org/10.5194/amt-2020-227, in review.

Letizia, S., Zhan, L. and Iungo, G.V., 2020b. LiSBOA: LiDAR Statistical Barnes Objective Analysis for optimal design of LiDAR scans and retrieval of wind statistics. Part II: Applications to LiDAR data of wind turbine wakes. Atmospheric Measurement Techniques Discussions, 2020. https://doi.org/10.5194/amt-2020-228, in review.

Newsom, R.K., Brewer, W.A., Wilczak, J.M., Wolfe, D.E., Oncley, S.P. and Lundquist, J.K., 2017. Validating precision estimates in horizontal wind measurements from a Doppler lidar. Atmospheric Measurement Techniques (Online), 10(NREL/JA-5000-68401).

Zhan, L., Letizia, S. and Valerio Iungo, G., 2020a. LiDAR measurements for an onshore wind farm: Wake variability for different incoming wind speeds and atmospheric stability regimes. Wind Energy, 23(3), pp.501-527.

Zhan, L., Letizia, S. and Iungo, G.V., 2020b. Optimal tuning of engineering wake models through lidar measurements. Wind Energy Science, 5(4), pp.1601-1622.

Scanning lidar and engineering models: Improved prediction of offshore wind farm wake Development

Arjun Anantharaman[1,*], Jörge Schneemann[1], Stoyan Kanev[2], Edwin Bot[2], and Martin Kühn[1]
[1]ForWind – University of Oldenburg
[2]TNO Energy Transition, Petten, The Netherlands
*Presenting author

Keywords: Long-range scanning lidar | Wake modelling | Flow measurements | Cluster wakes

With an increasing number of wind farms offshore, more and more wind farms will be in proximity to each other. This results in the operation of wind farms in the (partial) wake region, characterised by lower wind speeds and potential energy contained within. Consequently, wind farm wakes have been shown to adversely impact the power production of their neighbours even at long ranges (Platis et al., 2018; Schneemann et al., 2020). A recent study (Nygaard et al., 2020) adapted an engineering model to better represent wakes of entire wind farms and validated it with SCADA data. However, further model improvements require flow field data for validation, which can be provided through long-range scanning lidars.

The objective of the current work is to tune and validate the wind farm wake representation in an engineering model dependent on the atmospheric stability, using long-range scanning lidar data and meteorological measurements. We use the tool "FarmFlow" (Bot and Kanev, 2020) to model this wake under different atmospheric conditions using the lidar data as a benchmark. It solves the Parabolised Navier Stokes (PNS) equations in three dimensions, using the k-epsilon closure model.

The model has been tested for neutral atmospheric conditions (validated within the farm) and is currently being modified to accommodate different atmospheric stabilities and for the flow behind the wind farm.

A long-range Doppler lidar placed on the transition piece of an offshore wind turbine in a 400 MW offshore wind farm (GlobalTech I) situated in the German North Sea enables wind velocity monitoring of up to 8 km. The scans (150 seconds each) are averaged over 90 minutes, where the wind direction remains nearly constant. Sensors mounted alongside the lidar give simultaneous temperature, pressure and humidity values, which are then combined with reanalysis data from the OSTIA data set to characterize the atmospheric stability.

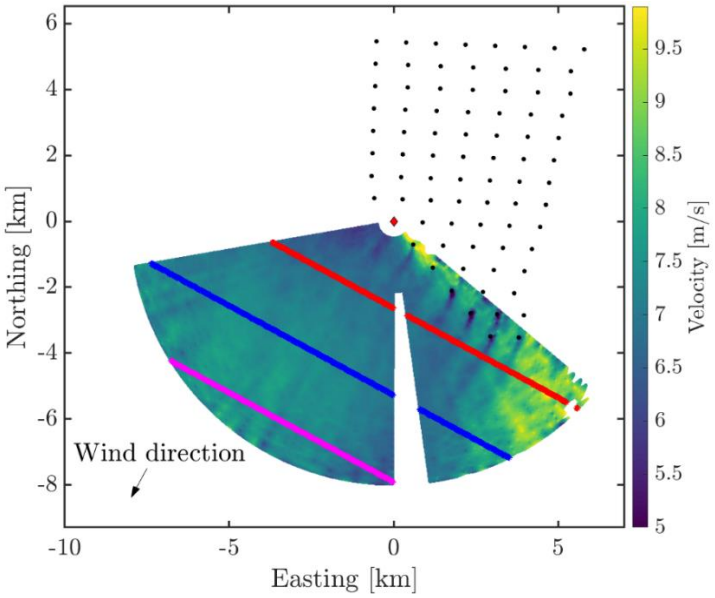


Figure 1: Lidar (red diamond, 0.8° elevation) scan, averaged over 90 min that shows the wake from the wind farm (turbines marked with black dots) for NE wind in an unstable atmosphere. The lines perpendicular to the wind direction (red, blue and pink) are 20D, 40D and 0D downstream from the lidar, respectively.

Figure 1 displays the time-averaged Plan-Position-Indicator scans (0.8° elevation), used to observe the wakes downstream of the wind farm. A sharp boundary is observed between the wind farm wake and the free-stream wind at hub height that is partially sustained downstream (~ 60 rotor diameters 'D') for weakly unstable and unstable atmospheric conditions. Differences in the wind speed within the wake region and the free stream (velocity deficit) are compared at successive downstream distances.

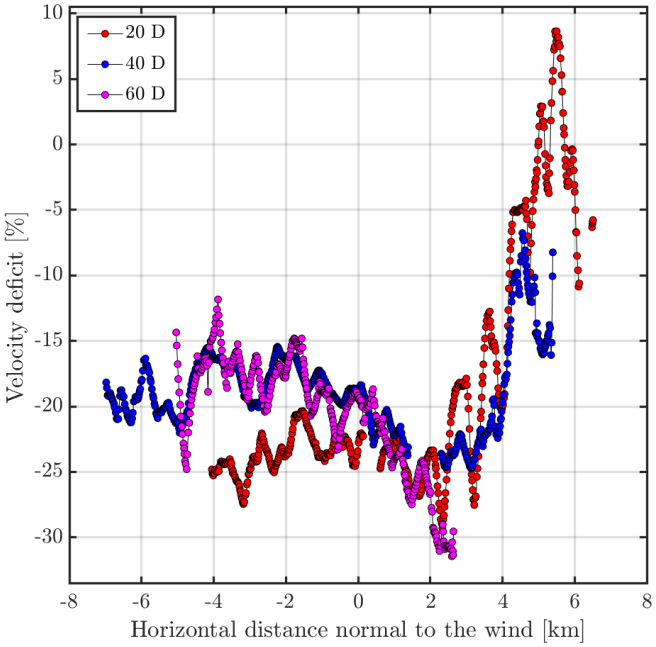


Figure 2: Velocity deficits (% difference of the velocity from the measured points to the free stream) perpendicular to the wind direction as a function of the horizontal distance. The colours of the lines correspond to those marked in Figure 1.

In Figure 2, the deficit (averaged in the wake region) reduces from 21% to 19% as we move further downstream from 20D to 60D. Initial results indicate that the wake strength decays slowly in unstable conditions, where quicker recovery to free-stream conditions is expected due to enhanced vertical mixing. The deficit from the near wind farm wake region was thus quantified using scanning lidar measurements in primarily unstable atmospheric conditions. Results from these lidar measurements (primarily the velocity deficit profile in Figure 2) will be used to validate the FarmFlow model predictions. Additionally, more models will be incorporated in this comparative study to further justify the use of lidar measurements as a benchmarking tool for wind farm wake models.

References:

Bot, E. T. G. and Kanev, S. (2020) 'Farmflow: Extensively validated and dedicated model for wind farm control'. TNO.

Nygaard, N. G. et al. (2020) 'Modelling cluster wakes and wind farm blockage', Journal of Physics: Conference Series, 1618, p. 062072. doi: 10.1088/1742-6596/1618/6/062072.

Platis, A. et al. (2018) 'First in situ evidence of wakes in the far field behind offshore wind farms', Scientific Reports. Nature Publishing Group, 8(1), pp. 1–10. doi: 10.1038/s41598-018-20389-y.

Schneemann, J. et al. (2020) 'Cluster wakes impact on a far-distant offshore wind farm's power', Wind Energy Science, 5(1), pp. 29–49. doi: 10.5194/wes-5-29-2020.

Validation of an analytical full wind turbine wake model with Galion Lidar

Aidan Keane*
Wood Renewables
*Presenting author

Keywords: wind turbine | double-Gaussian wake model | wind lidar | aerodynamics

A recently proposed wind turbine wake model is validated against the wake measurement data obtained from a Galion Lidar situated on the nacelle of a 5 MW utility scale wind turbine. The high resolution and range capabilities of the Galion Lidar provide data for the full extent of the wind turbine wake including the near wake.

The wake model is based upon conservation of momentum within the context of actuator disc theory, and the assumption of a distribution of the double-Gaussian type for the velocity deficit in the wake and can predict the wind velocity distribution for all distances downwind of a wind turbine, including the near wake. Bastankhah and Port´e-Agel (2014) developed a single-Gaussian wake model encapsulating the characteristics of the mid to far wake, and the technique was developed further by Keane (2021) to account for the double-Gaussian velocity deficit in the near wake, as is evident in the measurements of Vermeer et al (2003), Aitken et al (2014) and Abraham et al (2019).

The Galion Lidar collects line-of-sight radial wind velocities and the full scan range of the lidar is 20 rotor diameters. However, for this analysis the wake model fitting was conducted within 6 rotor diameters in order to avoid the potential impact of downwind turbines upon the wake profile. The lidar data was subject to standard filtering and, in addition, to the criterion that the wake direction was within ±1 degree in order to exclude wakes subject to yaw. Full 2-dimensional model fitting to horizontal lidar scan data is carried out for the full range of inflow wind velocities of primary interest, namely 4 to 16 m/s, whilst the four wake parameters are varied independently.

Various combinations of wake model parameter fitting were investigated and estimates of the quality of the fit have been made, in particular, the goodness-of-fit measure R squared value of the regression of the wind velocity predicted by the model with the wind velocity inferred from the measured lidar data, and the root-mean-square error (RMSE) of the fit. The differences in parameter fitting procedures were shown to be marginal, but those with greater number of free parameters show better agreement between the model and measured data overall.

The wind velocity profiles of the wake model are all broadly in line with the measured lidar data as can be seen in Figure 1. There are several factors which could contribute to the observed deviations between the wake data and the wake model, namely wake meandering and turbulence and vortex effects.

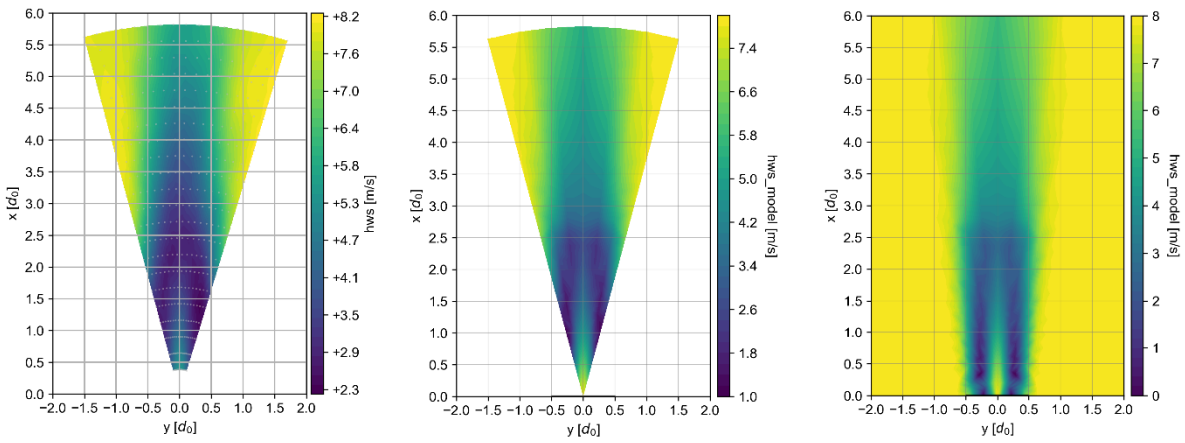


Figure 1: A visual comparison of the wind velocity derived from the measured Galion Lidar data scan arc (left), the corresponding wind velocity of the wake model (centre), and the wind velocity of the full wake model (right) for inflow wind velocity 8 m/s. The plot of the measured lidar data is a mean of 64 individual wake scans.

Figure 2 shows a visual comparison of the wind velocity derived from the measured Galion Lidar arc scan data and the corresponding wind velocity of the wake model. The analysis reveals characteristics of the wind turbine wake velocity deficit for the full wake, including the near wake to within close proximity of the wind turbine rotor.

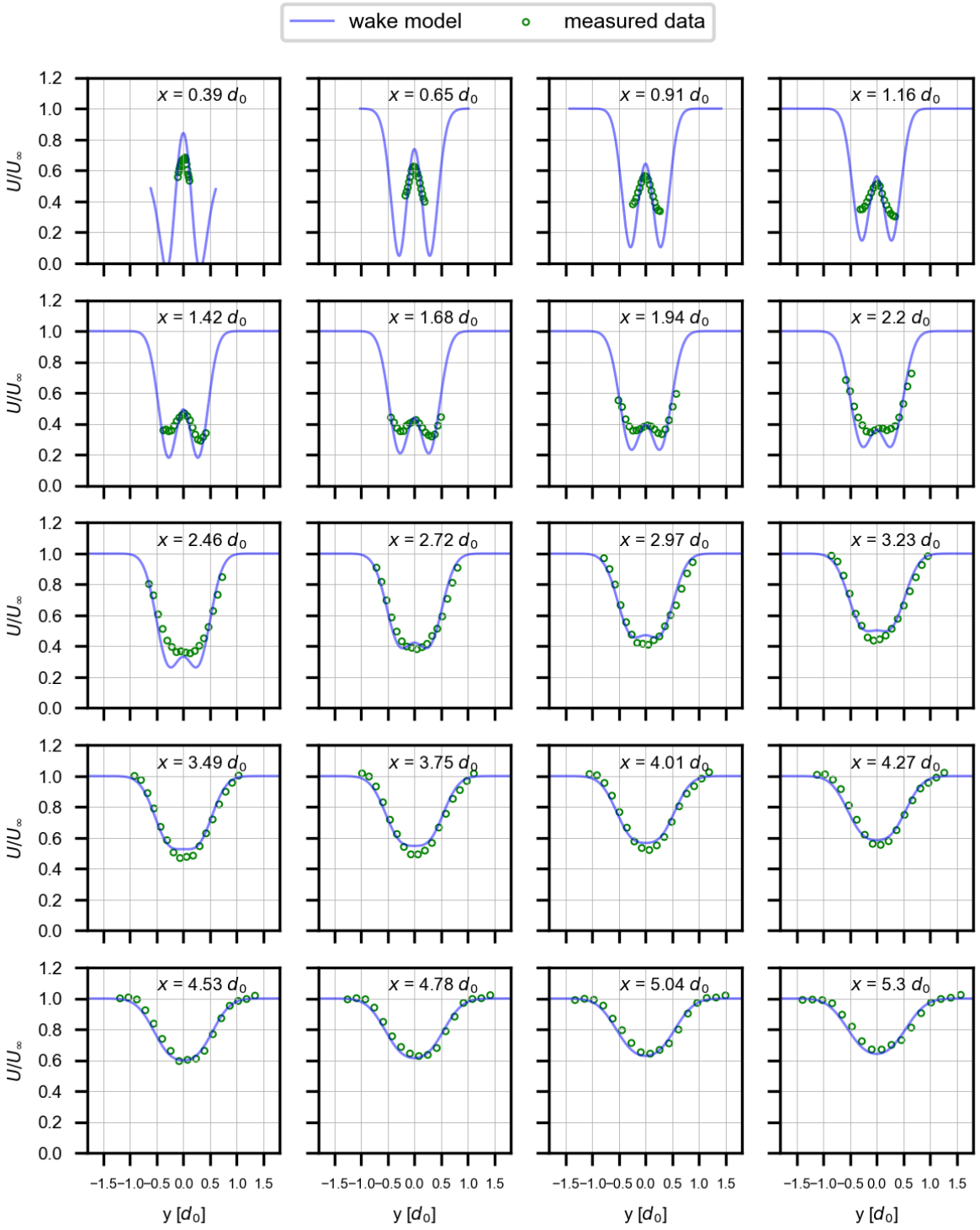


Figure 2: The 2-dimensional model fit for inflow wind velocity 8 m/s. The plots show the normalised measured and modelled wind velocities versus horizontal lidar scan arc distance for each successive lidar range gate downwind measurement distance x.

References:
Bastankhah, M. and Port´e-Agel, F., (2014) 'A new analytical model for wind-turbine Wakes', Renewable Energy 70 (2014) pp116–123
Keane, A. (2021) 'Advancement of an analytical double-Gaussian full wind turbine wake model', Renewable Energy in production
Vermeer, L., Sørensen, J. and Crespo, A., (2003) 'Wind turbine wake aerodynamics', Progress in Aerospace Sciences. 39 pp. 467–510

Aitken, M., Banta, R., Pichugina, Y. and Lundquist, J. (2014) 'Quantifying wind turbine wake characteristics from scanning remote sensor data', J. Atmos. Oceanic Technol. 31 pp. 765–787
Abraham, A., Dasari, T., Hong, J., (2019) 'Effect of turbine nacelle and tower on the near wake of a utility-scale wind turbine', Journal of Wind Engineering and Industrial Aerodynamics 193 103981

Comparison of Large Eddy Simulations against measurements from the Lillgrund offshore windfarm

Ishaan Sood*, and Johan Meyers
Katholieke Universiteit Leuven
*Presenting author

Keywords: Large Eddy Simulations | Lillgrund windfarm | LiDAR measurements

Coordinated windfarm control strategies such as wake steering and axial induction control have emerged as promising candidates for mitigating losses due to turbine-wake interactions within large farms (Munters, 2018; Yilmaz, 2018). While field-measurements are indispensable for validating windfarm control strategies, in practice they tend to be sparse, case-specific and expensive to procure. As an alternative, high fidelity numerical tools such as large eddy simulation (LES) provide a virtual environment to efficiently test control strategies and record measurements (Breton, 2017).
However, proper validation of numerical models against field-measurements is essential to ensure the reliability of their performance. To address this issue, a measurement campaign was carried out at the Lillgrund windfarm to gather data for the validation of numerical windfarm simulations tools.
Two long-range LiDAR's were used to record the flow field information in turbine inflow and wake planes respectively, which were supplemented by simultaneous power and loading measurements from individual wind turbines. Wind speed and direction measurement data at the hub height of the Lillgrund wind turbines can be seen in figure 1.

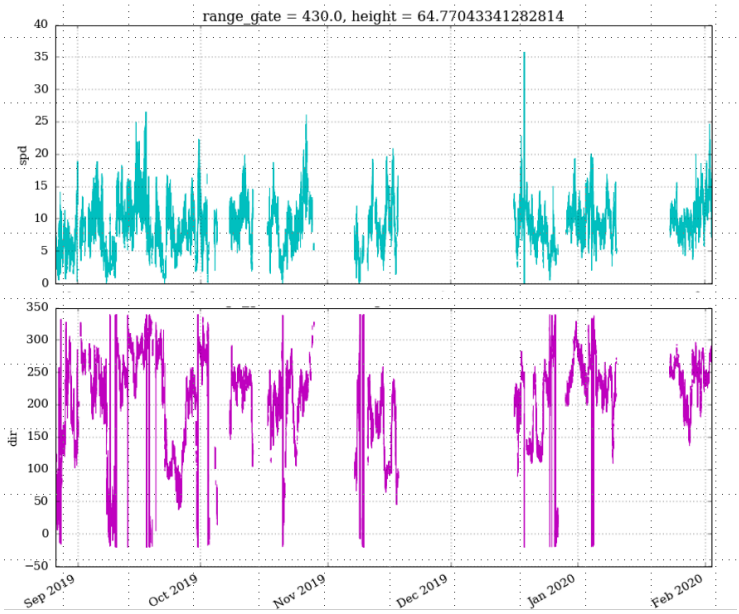


Figure 1: Wind speed and direction time series at hub height

In this work, we aim to use the Lillgrund measurement data to validate SP-Wind, an in-house pseudospectral LES code developed by the Turbulent Flow Simulation and Optimization (TFSO) group of KU Leuven, see eg., Goit, 2015. The 48 Siemens 2.3 MW turbines of the Lillgrund windfarm are represented on the simulation grid using an Aeroelastic Actuator Sector Model (AASM) (Vitsas, 2016).
One of the most expensive aspect of running Windfarm LES is the generation of turbulent inflow conditions using precursor simulations to accurately represent the conditions in the field during the measurement campaign (Munters, 2016) . To mitigate this cost, we propose a methodology of reusing a previously generated precursor inflow database, comprising of two pressure driven boundary layers (PDBL) of different surface roughness, and 3 conventionally neutral boundary layers (CNBL) of different capping inversion height and

strengths (Sood, 2020). An optimization framework is developed which applies transformations to the inflow datasets and compares it to the flow data collected from LiDAR's at the Lillgrund windfarm. Preliminary results showing the mean vertical velocity profile matches for a PDBL and a CNBL case are presented in figure 2, which show good agreement with two different time periods from the LiDAR measurements. After identifying instances where the numerical simulations best match the real flow conditions at the Lillgrund windfarm, SPWind is used to run large eddy simulations. Numerical measurements of individual wind turbine power production, loading and wake effects are compared against the data obtained from the Lillgrund measurement campaign.

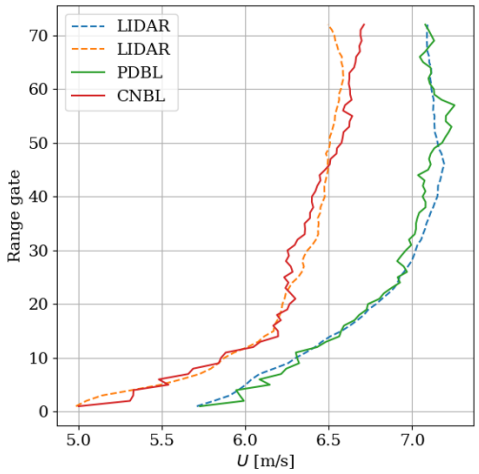


Figure 2: Mean velocity comparison at vertical inflow plane

The authors received funding from the European Union's Horizon 2020 research and innovation program under grant agreement no. 727680 (TotalControl). The computational resources and services used in this work were provided by the VSC (Flemish Supercomputer Center), funded by the Research Foundation - Flanders (FWO) and the Flemish Government – department EWI.

References:

Breton, S.P., Sumner, J., Sørensen, J.N., Hansen, K.S., Sarmast, S., Ivanell, S., 2017. A survey of modelling methods for highfidelity wind farm simulations using large eddy simulation. Philos. Trans. R. Soc. A Math. Phys. Eng. Sci. 375. https://doi.org/10.1098/rsta.2016.0097

Munters, W., Meneveau, C., Meyers, J., 2016. Turbulent Inflow Precursor Method with Time-Varying Direction for Large Eddy Simulations and Applications to Wind Farms. Boundary-Layer Meteorol. 159, 305–328. https://doi.org/10.1007/s10546-016-0127-z

Munters, W., Meyers, J., 2018. Dynamic strategies for yaw and induction control of wind farms based on large-eddy simulation and optimization. Energies 11. https://doi.org/10.3390/en11010177

Sood, I., Munters, W., Meyers, J., 2020. Effect of conventionally neutral boundary layer height on turbine performance and wake mixing in offshore windfarms. J. Phys. Conf. Ser. 1618. https://doi.org/10.1088/17426596/1618/6/062049

Vitsas, A., Meyers, J., 2016. Multiscale aeroelastic simulations of large wind farms in the atmospheric boundary layer. J. Phys. Conf. Ser. 753, 082020. https://doi.org/10.1088/1742-6596/753/8/082020

Goit, J.P., Meyers, J., 2015. Optimal control of energy extraction in wind-farm boundary layers. J. Fluid Mech. 768, 5–50. https://doi.org/10.1017/jfm.2015.70

Modelling Wind Farm Scale Blockage – First results from a 12-month scanning lidar campaign at a German offshore wind farm

Christiane Montavon[1,*], James Bleeg[1], Jens Riechert[1], Matthias Steger[1], Stefan Soderberg[1], and Carolin Schmitt[2]
[1]DNV
[2]EnBW
*Presenting author

Keywords: blockage | modelling | CFD WRF | lidar

The wind industry is increasingly accepting that wind-farm-scale blockage needs to be accounted for when carrying out an energy production assessment (EPA) for a wind farm. However, the various tools being developed to calculate blockage correction factors provide results that can differ significantly when applied to the same wind farm (Winterwind, 2020). While measurements and validation of blockage effects has already started, most of it has so far focused on near-turbine induction effects (Asimakopoulos et al, 2014, Ettrup-Brink & Nygaard, 2016, Branlard et al, 2020), or on secondary effects of blockage as it affects the pattern of production of leading turbines (Nygaard et al, 2020). Only recently have contributions been looking at the effect of blockage at the wind farm scale and on its effect on the flow field at larger upstream distances (Bleeg et al, 2018, Schneemann et al, 2020). To address the need for further validation of wind-farm-scale blockage, a measurement campaign was initiated for a German offshore wind farm, providing a unique data set for validation.
The campaign, which relies on a dual scanning lidar system, measuring along 4 lines extending to distances of up to 7km upstream of the wind farm, will be described in a separate WESC submission (Riechert et al, 2021).

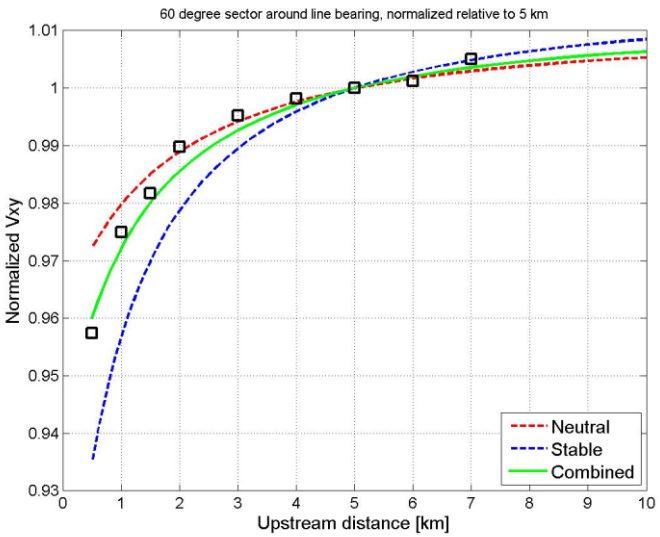


Figure 1: Normalized wind speed for one scanning line, for a 60° sector centered around the bearing of the scanning line. Points are from the dual doppler scanning lidars, lines from the CFD simulations with WRF informed boundary conditions. Note that the strong wind speed reduction shown here is specific to the selected conditions and is not representative of the average conditions at the wind farm

The current contribution presents some blockage validation for a RANS CFD model, in which the turbines are modelled via actuator disks. The model was used to simulate the flow field within and around the wind farm. An example of normalised wind speeds predicted by the CFD model for one of the measuring lines is shown in Fig 1, where it is compared to the lidar data for the same conditions.

CFD predicted pattern of production along strings of leading turbines (Fig.2), as well as for the whole array, are also compared with measured pattern of production from the SCADA data, for periods concurrent with the lidar measurements.

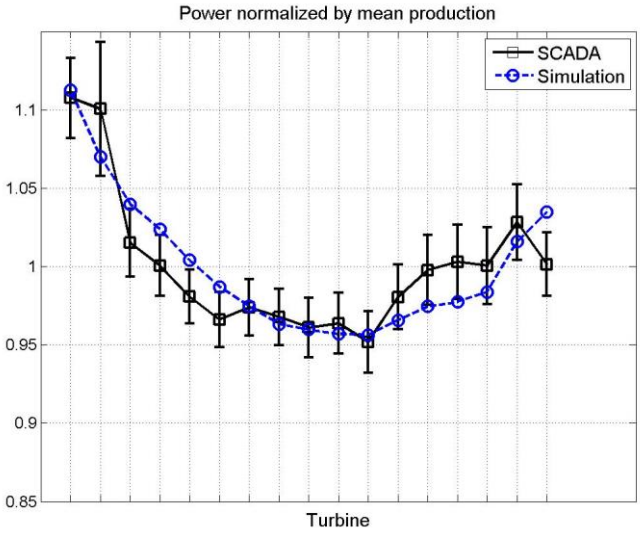


Figure 2: Example of pattern of production along string of leading turbines on the eastern side of the wind farm.

While the data from the lidar campaign shows very different normalised wind speed trends along the measurement lines for westerly and south-easterly wind directions, the CFD was able to capture the trends reasonably well, when driven with realistic boundary conditions.
The main conclusions from the project so far are that:

- Wind speed reduction upstream of the wind farm can be seen along the scanning lines to distances of up to 3 – 5 km (i.e. 25 to 40 rotor diameters) for the westerly wind directions and even further out for easterly directions, both in the lidar data and CFD results.
- Non-homogeneities in the background flow (e.g. from coastal transition) can partially mask blockage, without necessarily reducing the magnitude of its effect on power production.
- The CFD model, especially when driven with boundary conditions informed from WRF, provides realistic wind speed reductions and pattern of production. For some directions, a realistic wind speed distribution upstream of the wind farm requires the modelling of the effect of the coastal transition.
- The magnitude of blockage is sensitive to stability conditions both within and above the boundary layer. An accurate calculation of blockage correction factor will likely require a model that can account for stability effects.

References:

[1] Winterwind 2020, https://windren.se/WW2020/00_1_57_Summary_of_Workshop_on_the_Wind_Farm_Blockage_Effect_Onshore.pdf
[2] Asimakopoulos et al, 2014, Offshore Compression Zone measurement and visualisation, EWEA 2014, Barcelona.
[3] Ettrup-Brink & Nygaard, 2016, Measurements of the wind turbine induction zone, 21st meeting of the Power Curve Working Group, 13 December 2016, Glasgow.
[4] Branlard et al, 2020, J. Phys.: Conf. Ser. 1618 062036, https://iopscience.iop.org/article/10.1088/1742-6596/1618/6/062036/pdf
[5] N. G. Nygaard et al 2020 J. Phys.: Conf. Ser. 1618 062072, https://iopscience.iop.org/article/10.1088/1742-6596/1618/6/062072/pdf
[6] Bleeg, J.; Purcell, M.; Ruisi, R.; Traiger, E. "Wind farm blockage and the consequences of neglecting its impact on energy production." Energies 2018,11, 1609. Available at http://www.mdpi.com/1996-1073/11/6/1609, 11/2018
[7] Schneemann, J.; Rott, A.; Dörenkämper, M.; Theuer, F.; Kühn, M.; "Offshore wind farm global blockage measured with scanning lidar", Wind Energy Science, Available at https://wes.copernicus.org/preprints/wes-2020-124/, 11/2020
[8] Riechert et al, WESC 2021, submitted.

Mini-Symposium: Lidars and numerical models – how they correspond and interact (II)

Optimal lidar scanning pattern for wake composition under yaw misalignment

Balthazar Sengers*, Gerald Steinfeld, Marijn van Dooren, Detlev Heinemann, and Martin Kühn
ForWind - University of Oldenburg
*Presenting author

Keywords: Pulsed lidar | PPI | LES | Synthetic | Three-dimensional

Introduction

Upstream facing lidars measuring inflow conditions can be used for power curve measurements and wind turbine control, while downstream facing lidars sampling turbine wakes gather high-quality data necessary for e.g. wake model validation. Typically, a wake-tracking pulsed lidar mounted on the turbine nacelle measures a single plan position indicator (PPI) scan at hub height. Although quick, this strategy only provides data in a 2D-plane.

Attempts have been made to capture information in the vertical. Beck and Kühn (2019) proposed a scanning pattern of alternating PPI and range height indicator (RHI) scans to obtain information in both dimensions. Although promising, wake shape deformations due to wind veer or yaw misalignment cannot be captured. Brugger et al (2020) used nine PPI scans at different elevation angles, allowing to describe non-circular wake shapes in a vertical plane.

Objective

This study aims to optimize this strategy of multiple PPI scans by evaluating different scanning strategies, including number of PPI scans, their elevation angles and angular speed (following Carbajo Fuertes and Porté-Agel (2018)). This optimization is based on Large-Eddy Simulations (LES), allowing for a systematic uncertainty analysis of the proposed scanning patterns. This leads to a better understanding of the impact of a scanning strategy on the measurement quality, which is vital information when planning field campaigns.

Methods

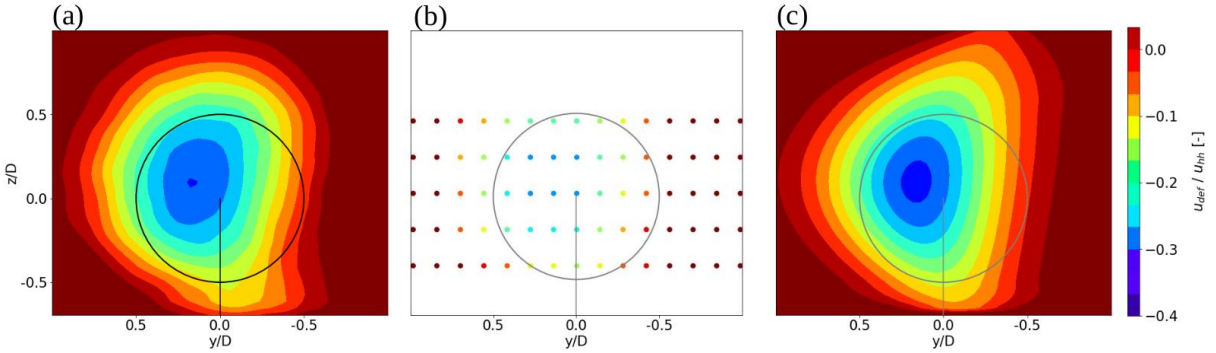


Figure 1: Example of wake composition method for a wind turbine with a yaw angle of 15 ° in a neutral boundary layer. (a) represents the LES wind field, (b) the extracted synthetic lidar data and (c) the corresponding composed wake.

The PArallelized Large-eddy simulation Model (PALM) coupled with the aeroelastic code FAST representing the NREL 5MW turbine provides the numerical wind fields. One neutral and one stable boundary layer with turbine yaw angles of -15°, 0°, 15° have been simulated. Synthetic lidar data is subsequently generated by employing the lidar solver LiXim (Trabucchi, 2019) with a specified accumulation time of 0.2 s.

Utilizing the Multiple 1D Gaussian method proposed by Sengers et al (2020), information at only a few altitudes is needed to estimate key wake characteristics like center position, deficit, curliness, tilt angle and size. Subsequently, this information can be used in the composition methodology proposed in Sengers et al

(2021) to obtain a wind field in the vertical plane. An illustrative example using five PPI scans is shown in Figure 1.

Results

The preliminary results shown here focused on optimizing the scanning pattern for the rotor area at 5 and 6 D downstream. Tests with 1, 3, 5 and 7 PPI scans with fixed elevation angle intervals and angular speeds ω of 4, 8 and 12° s-1 have been carried out. Figure 2 suggests that 5 PPI scans results in the highest accuracy. The angular speed seems to have a smaller effect, where ω = 4° s-1 appears to have a slightly higher accuracy. These results suggest that a resolution too low lacks accuracy due to data sparsity, whereas a resolution too high misses accuracy due to long scanning times. This indicates the existence of an optimum scanning strategy, in this case 5 PPI scans with ω = 8° s-1.

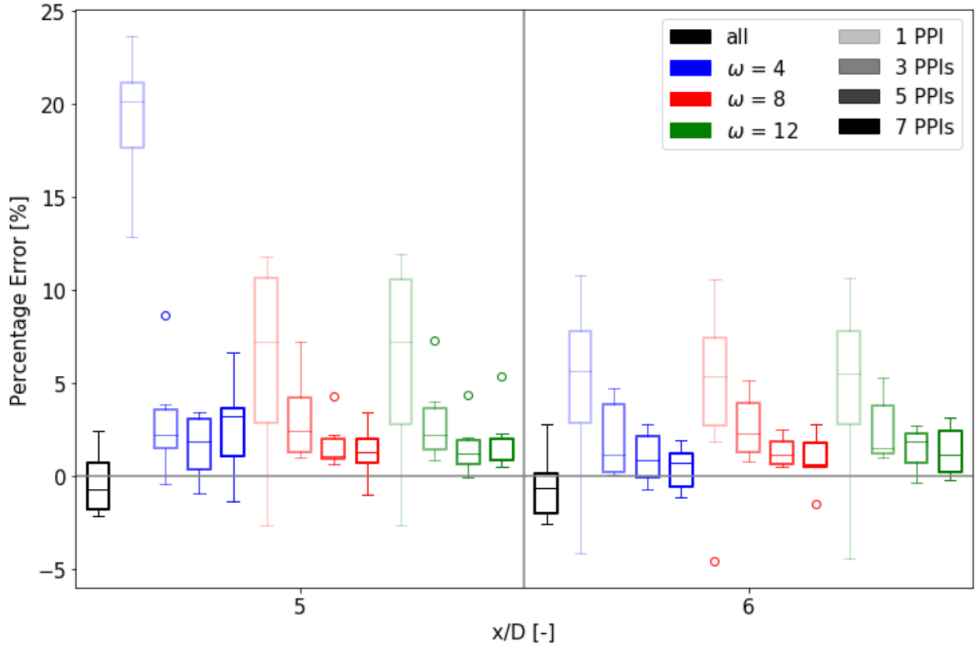


*Figure 2: Percentage Error of Available Power (PE = (Pcomp-PLES)/PLES*100% (u3eff,compu3eff, LES)/u3eff,LES*100%). Black indicates the use of all numerical data, hence the error introduced by the composition algorithm. Blue, red and green indicate synthetic lidar data with different angular speeds and the opaqueness represents the number of PPI scans.*

Outlook

In ongoing research, tests with irregular elevation angle intervals are conducted. An optimal scanning strategy based on synthetic lidar data will be applied to free-field campaign with a commercial 3.5 MW turbine carried out until April 2021. These measurements will be compared to wind fields obtained from LES coupled with the FAST model of this turbine. Preliminary results are expected to be shown at the conference.

References:

Beck, H. and Kühn, M., 2019. Reconstruction of Three-Dimensional Dynamic Wind-Turbine Wake Wind Fields with Volumetric Long-Range Wind Doppler LiDAR Measurements. Remote Sensing, 11(22), p.2665.

Brugger, P., Debnath, M., Scholbrock, A., Fleming, P., Moriarty, P., Simley, E., Jager, D., Roadman, J., Murphy, M., Zong, H. and Porté-Agel, F., 2020. Lidar measurements of yawed-wind-turbine wakes: characterization and validation of analytical models. Wind Energy Science, 5(4), pp.1253-1272.

Carbajo Fuertes, F. and Porté-Agel, F., 2018. Using a virtual Lidar approach to assess the accuracy of the volumetric reconstruction of a wind turbine wake. Remote Sensing, 10(5), p.721.

Trabucchi, D., 2019. Lidar measurements and engineering modelling of wind turbine wakes (Doctoral dissertation, University of Oldenburg).

Sengers, B.A.M., Steinfeld, G., Heinemann, D. and Kühn, M., 2020. A new method to characterize the curled wake shape under yaw misalignment. In Journal of Physics: Conference Series (Vol. 1618, No. 6, p. 062050). IOP Publishing.

Sengers, B.A.M., Zech, M., Jacobs, P., Steinfeld, G., Heinemann, D. and Kühn, M., 2021. Framework for a statistical wake steering model. Manuscript in preparation

Turbulence intensity corrections of pulse-based profiling Doppler lidars

Mithu Debnath*, and Patrick Moriarty
National Renewable Energy Laboratory
*Presenting author

Keywords: Lidar | Virtual lidar | Turbulence intensity

The design and operation of a wind energy projects requires observations of wind speed, wind direction, and turbulence intensity data in order to estimate the energy yield for the project and load on the turbines under different atmospheric conditions. Commercial remote sensing instruments have acceptable accuracy for mean wind speed and direction needed for a wind energy project development relative to the met tower observations. However, lidar has bias and lower accuracy for turbulence measurements (Sathe et al., 2013; Newman et al., 2016; Debnath, 2020) due to the large probe volume and assumptions needed to retrieve the wind speed components.

Lidar measures line-of-sight (LOS) wind speed observations along the emitted laser direction, and commercial pulse-based profiling lidars retrieve wind speed components with an assumption of horizontal homogeneity. Horizontal homogeneity assumes wind speed is constant within the conical circle used to retrieve wind speed at a given height of the atmospheric boundary layer (ABL) profile.

Lidar measures wind speed along the LOS of the conical circle at a certain time before moving to the next target location. The multiple LOS wind speeds within the conical circle create contamination in the turbulence statistics of retrieved wind speed components (Kelberlau and Mann, 2019, 2020) due to the time and space lag within the LOS wind speeds on the circle. In this paper, we evaluate methods for reducing the error inherent in lidar observations of turbulence intensity.

There are two scientific approaches used to evaluate contamination in the high-frequency measurements and correct the turbulence intensity measured by a profiling lidar. The set of observations used in this study are from a field campaign with a commercial WindCube v2 pulsebased profiling lidar and a collocated meteorological tower. The lidar measurements are evaluated against the cup anemometer measurements under different atmospheric stability conditions (Figure 1). A series of large-eddy simulations (LES) has also been used to investigate the lidar measurements under different controlled atmospheric conditions. Three different atmospheric boundary layers have been chosen based on field data presented in Doubrawa et al., 2020. In these time-varying ABL profiles, virtual lidar within the LES recreates LOS data in a similar manner as the WindCube-v2 lidar, and the sampling frequency and retrieval process are varied for each case. The roles of atmospheric

stability, time and space separation between LOS wind speeds, and the retrieval process on the turbulence intensity measured by the pulse-based profiling lidar are evaluated in this work.

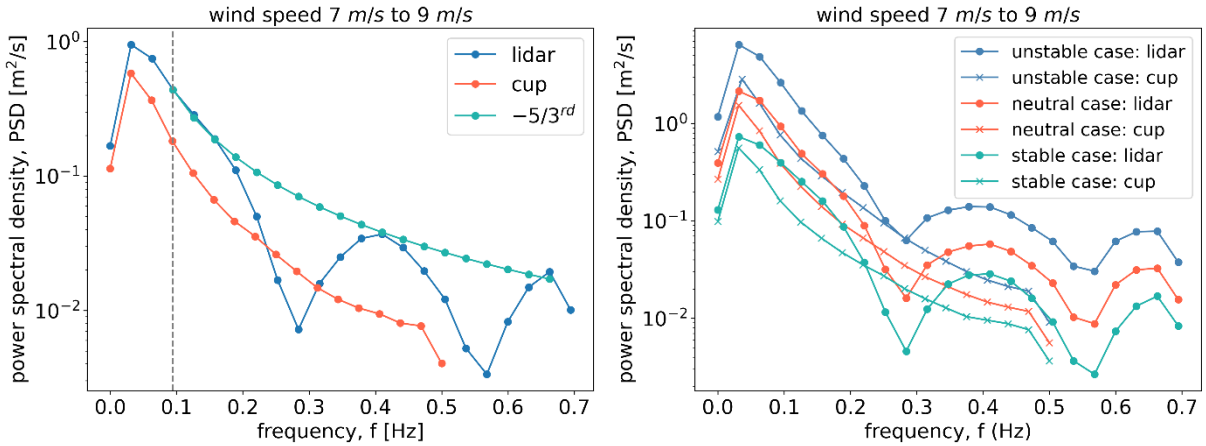


Figure 1: The power spectral density of wind speed measured by the lidar and cup anemometer with all the data (left) and under different atmopsheric conditions (right).

Results show that the lidar scanning strategy should be modified to reduce the contamination in the highfrequency measurement and obtain more reliable turbulence intensity measurement. The presented work leads a design of lidar scan geometry and retrieval process to have an improved turbulence intensity measurement by the pulse-based profiling lidars.

References:

Sathe, A. and Mann, J., 2013. A review of turbulence measurements using ground-based wind lidars, Atmos. Meas. Tech., 6, 3147–3167, https://doi.org/10.5194/amt-6-3147-2013.

Newman, J. F., Klein, P. M., Wharton, S., Sathe, A., Bonin, T. A., Chilson, P. B., and Muschinski, A., 2016. Evaluation of three lidar scanning strategies for turbulence measurements, Atmos. Meas. Tech., 9, 1993–2013, https://doi.org/10.5194/amt-9-1993-2016.

Debnath, M., 2020. Virtual remote sensing instruments, AWEA Wind Resource & Project Energy Assessment Virtual Summit.

Kelberlau, F. and Mann, J., 2019. Better turbulence spectra from velocity–azimuth display scanning wind lidar, Atmos. Meas. Tech., 12, 1871–1888, https://doi.org/10.5194/amt-12-1871-2019.

Kelberlau, F. and Mann, J., 2020. Cross-contamination effect on turbulence spectra from Doppler beam swinging wind lidar, Wind Energ. Sci., 5, 519–541, https://doi.org/10.5194/wes-5-519-2020.

Doubrawa, P, Quon, EW, Martinez-Tossas, LA, et al., 2020. Multimodel validation of single wakes in neutral and stratified atmospheric conditions. Wind Energy; 23: 2027– 2055. https://doi.org/10.1002/we.2543.

Assessment of Offshore Model Wind Speed Performance in the Northwestern Atlantic Ocean Using Lidar Buoy Data

Lindsay Sheridan*, Brian Gaudet, Gabriel Garcia Medina, and Raghu Krishnamurthy
Pacific Northwest National Laboratory
*Presenting author

Keywords: offshore wind | lidar buoy | reanalysis

As the offshore wind industry continues to gain momentum globally, reanalysis products remain essential tools for the lifecycle of a wind farm. These regional and global long-term models provide project siting recommendations and production estimates, along with insight into spatial and temporal variability in the wind resource. Reanalyses allow for analysis into the frequency and trends in extreme wind events, such as ramps, and also serve as inputs to higher-resolution localized models. With such wide-ranging impacts on the offshore wind industry, the need for validation of reanalysis products is strong, particularly at typical turbine hub heights.

Pacific Northwest National Laboratory (PNNL) operates two AXYS WindSentinelTM buoys for the United States Department of Energy (DOE) in order to collect meteorological and oceanographic data, including hub height wind speed, in areas of interest for offshore wind development. The initial lidar buoy deployments off the United States Atlantic coast offer distinct wind resource assessments for potential near shore (5 km off of Atlantic City, New Jersey) and farther offshore (42 km off of Virginia Beach, Virginia) wind farms. The lidar buoys were deployed for longer than one year (November 2015 – February 2017 at the New Jersey location and December 2014 – May 2016 at the Virginia location), allowing for analysis of the wind resource for an entire seasonal cycle.

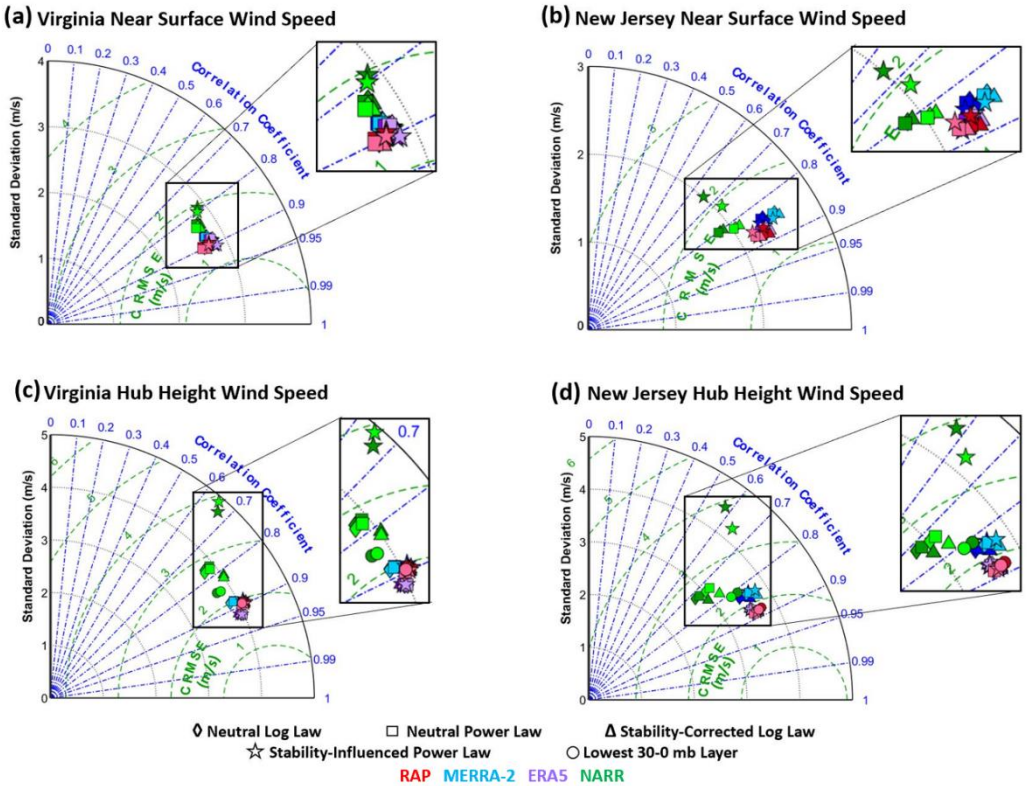


Figure 1: Near surface (4 m) and hub height (90 m) reanalysis wind speed error metrics over the (a), (c) Virginia and (b), (d) New Jersey lidar buoy deployment lifetimes.

Observations from the initial deployments of the DOE lidar buoys are employed to evaluate the performance of Modern Era Retrospective Analysis for Research and Applications-2 (MERRA-2), the North American Regional Reanalysis (NARR), the European Center for Medium-Range Weather Forecasts (ECMWF) Reanalysis 5th generation (ERA5), the Climate Forecast System Reanalysis (CFSR), and the National Oceanic and Atmospheric Administration (NOAA) assimilation system Rapid Refresh (RAP). Biases and degrees of correspondence are determined for each reanalysis product in order to provide insights on the performance and uncertainty for long-term wind resource characterization (Sheridan et al., 2020).

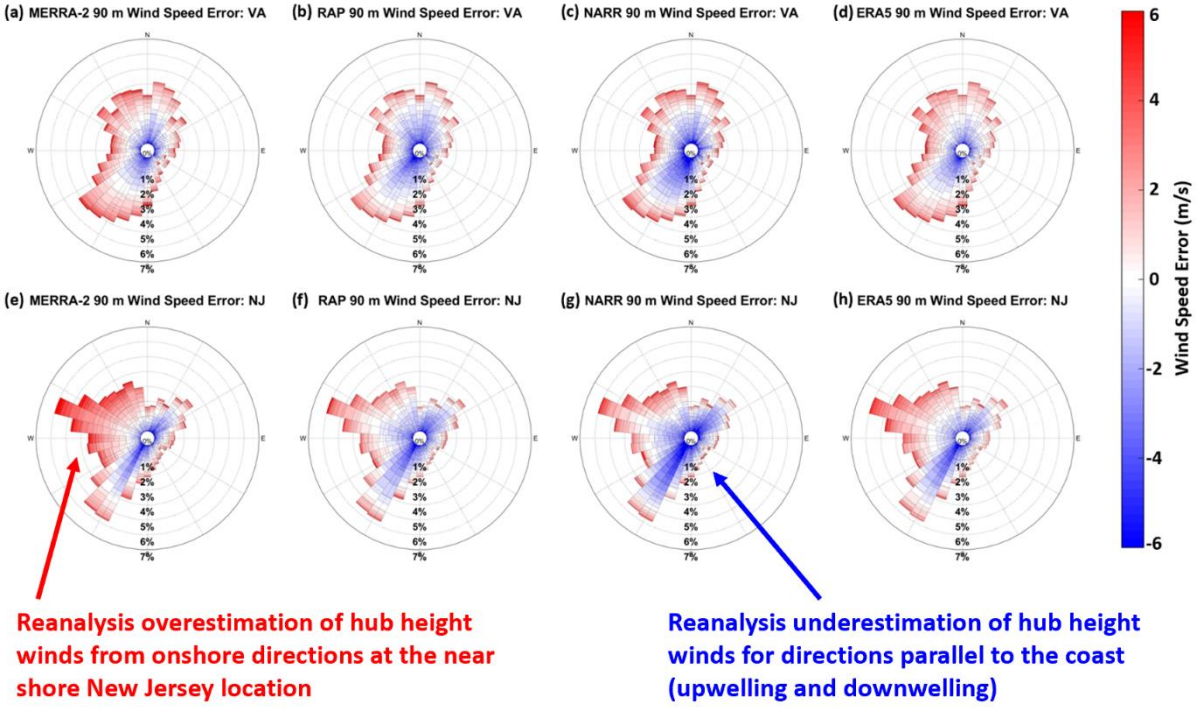


Figure 2: (a), (e) MERRA-2, (b), (f) RAP, (c), (g) NARR, and (d), (h) ERA5 hub height (90 m) wind speed error roses for the Virginia (top) and New Jersey (bottom) deployments. The 90 m lidar wind direction observations are used to bin the errors.

With the baseline metrics determined, an investigation into the sources of large deviations between the modeled and observed wind speeds during the U.S. East Coast lidar buoy deployments will be presented. Consistent sources of reanalysis model error include stably stratified flow conditions, high wind shear, flow parallel to the coastline, and tropical and winter storms. Large model errors during winter and tropical storm events, high wind speed events, and ramp events are often the result of wind speed timing and magnitude offsets.

Finally, select cases during the buoy deployments that exhibit large reanalysis error are modelled using the higher-resolution Weather Research and Forecasting (WRF) atmospheric model coupled with a wave prediction model, WaveWatch3. Typical atmospheric reanalyses do not incorporate the dynamic evolution of wave characteristics, and a coupled atmosphere/wave modeling system shows promise for improved accuracy in simulations of offshore wind profiles.

References:

Sheridan L.M., R. Krishnamurthy, A.M. Gorton, W.J. Shaw, and R.K. Newsom. (2020) "Validation of Reanalysis-Based Offshore Wind Resource Characterization Using Lidar Buoy Observations." Marine Technology Society Journal 54, no. 6:44-61. doi:10.4031/MTSJ.54.6.13

Validation of Novel Wind Speed Extrapolation Models using Offshore Floating Lidar

Mike Optis*, Nicola Bodini, Mithu Debnath, and Paula Doubrawa
National Renewable Energy Laboratory
*Presenting author

Keywords: Floating lidar | Wind speed extrapolation | Machine learning | Wind resource assessment | Offshore wind

The U.S. offshore wind areas in the mid-Atlantic lack sufficient hub height measurements of the wind resource but are rich in near-surface measurements. These data include both satellite-based and buoy-based measurements, which combined provide good spatial and temporal coverage of nearsurface winds. The ability to extrapolate these data to hub height is essential to offshore wind energy stakeholders to quantify and characterize the offshore wind resource and to validate mesoscale models.
Typical approaches to extrapolating these measurements to hub height include the conventional logarithmic profile and power law. These approaches are generally deficient for offshore extrapolation because their assumptions break down in stable atmospheric conditions and they require information not typically available from near-surface offshore stations (e.g., friction velocity for log profile, two measurement heights for power law).

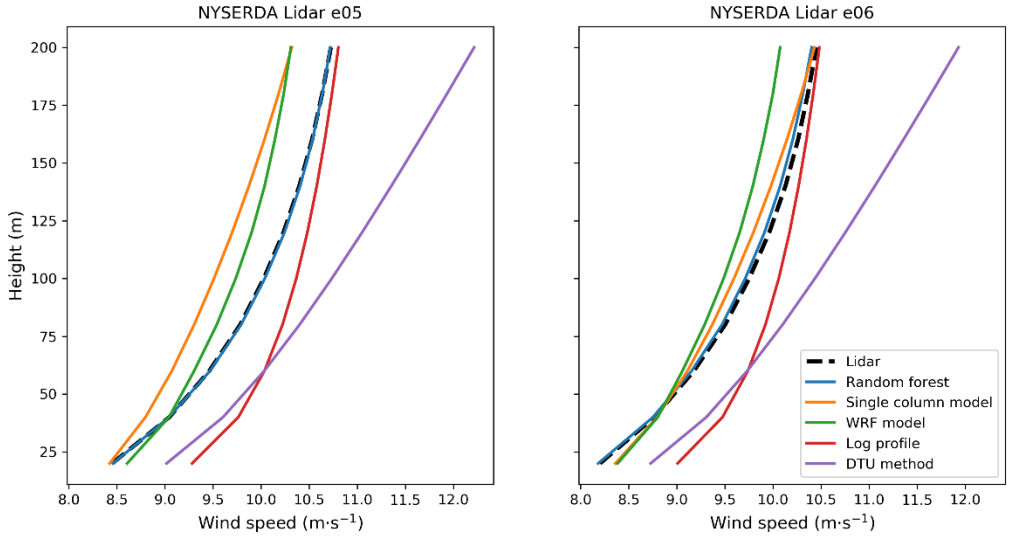


Figure 1: Mean modeled and observed wind profiles at two floating lidars (labeled E05 and E06) deployed in current New Jersey, USA wind energy call areas. The dotted line denotes the observed profile and solid colors denote the different models.

Here we present two novel approaches for extrapolating offshore wind speeds that are better suited for offshore wind speed extrapolation. The first is a gradient boosting machine learning (ML) algorithm trained to predict the wind profile from near-surface measurements; the second is a singlecolumn model which is driven at the lower boundary by near-surface observations and above by the geostrophic wind diagnosed from the ERA5 reanalysis product. We compare these novel approaches against the logarithmic profile and the WRF mesoscale model using validation data from two floating lidars recently deployed off the coast of New Jersey.
Results show that the ML model significantly outperforms all other models in simulating the mean wind profiles (Figure 1) as well as in all time series based performance metrics (Figure 2). We further find that this outperformance holds across all atmospheric stability regimes and times of day.

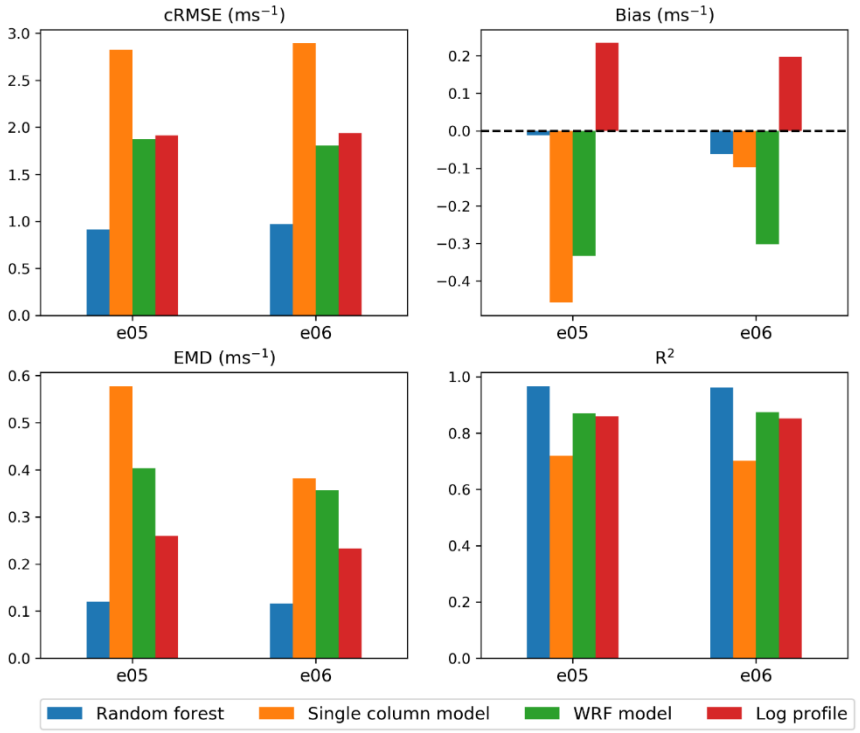


Figure 2: Performance metrics for the different vertical extrapolation models based on the rotor-equivalent wind speed for a 10-MW wind turbine. Note that EMD denotes the Earth Mover's Distance metric.

Critically, we find that the use of the air-sea temperature difference is a key input in improving model predictions, which provides some information on atmospheric stability aloft. Indeed, extreme wind shear and low-level jets are common under such conditions, and we find again that the ML model best simulates these extreme conditions.

We further show that ML model performance does not degrade when trained at one floating lidar and evaluated at the other lidar 83 kilometers away. This result has important implications for the generalization of an ML-based extrapolation approach across all offshore areas. This result has important implications for global offshore wind speed extrapolation using this ML method and satellite-based measurements of 10-meter winds and will be the focus of future studies.

By contrast, the SCM did not perform well in this study. Critically, it lacked information of the air-sea temperature difference and was therefore unable to account for atmospheric stability. Future work will focus on incorporating this air-sea temperature difference as a lower boundary condition.

Based on this work, we recommend that ML approaches supplant conventional extrapolation approaches for offshore wind speed extrapolation.

The implications of emerging data sharing protocols for the integration of lidar measurements and wind flow models

Peter Clive*
Black & Veatch (U.K.) Limited
*Presenting author

Keywords: Lidar | Digital integration | Wind models

In renewables in general, and wind energy in particular, our current approach to

- Data acquisition and analysis, and
- Integration of these processes into digital workflows places complexity at the edge.

This is because wind resource is not a conventional feed stock, but paradigms and procedures developed to handle conventional feedstocks are still adopted to deal with renewable energy assessments. As a consequence we either

- Neglect this complexity (e.g. treating the wind resource as a primitive data type rather than a complex object that integrates flow models and those measured data that provide validation and boundary conditions) or
- Incur analysis overhead in a suboptimal way, due to a lack of satisfactory protocols for digital integration of measurements and models.

Data sharing protocols are emerging that support this integration of measurement and models, such as lidar and CFD, into digital objects describing wind conditions, and allow us to interface these objects with other digital tools in the wind energy value chain. For example Open Energy describes a data provider (DP) / data service provider (DSP) arrangement that allows us to break complexity down and assimilate it in wider systems in a standardised way. For example, using the Open Energy protocol, a DSP can

- Integrate resource models and lidar data from a DP into
- A digital wind object that is passed to another DSP who
- Manages the interface with a objects representing generation assets and
- Produces forecasts for a client who
- Schedules inspections, operations, repair and maintenance, or
- Trades energy, and so on.

This presentation will discuss some of the challenges and opportunities that these emerging data sharing and integration protocols represent, and the role of lidar in supporting them.

Mini-Symposium: The pragmatic choice of wind models for Wind Resource Assessment



Sarah Barber
University of Applied Sciences Eastern Switzerland

The accuracy of the estimation of the wind resource has an enormous effect on the expected rate of return of a wind energy project. Due to the complex nature of the weather and of the wind flow over the earth's surface, it can be very challenging to measure and model the wind resource correctly. For a given project, the modeller is faced with a difficult choice of a wide range of simulation tools with varying accuracies and costs. If the choice of model is made incorrectly, either many resources are wasted in needlessly high accuracy simulations, or the rate of return is inaccurate and investors risk losing large amounts of money. In previous research, a method has been introduced for predicting the accuracy and costs of different simulation tools for a given project, without having to carry out any simulations in advance. In this mini-symposium, this new method will be tested and examined further by comparing the accuracy and costs of different simulation tools for various sites, including the Perdigao site as part of the IEA Wind Task 31 Comparison Metrics Simulation Challenge 2020.

The Pragmatic Choice of Wind Model in Complex Terrain – Decision Tool Development

Sarah Barber[1], Alain Schubiger[1], Sara Koller[2], Andreas Rumpf[3], and Hermann Knaus[3]
[1]Eastern Switzerland University of Applied Sciences
[2]Meteotest AG
[3]Hochschule Esslingen

Keywords: Complex terrain | Wind resource assessment | Comparison metrics | Accuracy | Costs

For a given Wind Resource Assessment (WRA) project, the modeller is faced with a difficult choice of simulation tools and calculation steps with varying accuracies, complexities and costs. The most costeffective choice is expected to be a compromise between performance and cost (Figure 1). In order to help modellers choose the most suitable workflow for a given project, a new method for estimating the accuracy, or skill, and cost of a given workflow was developed previously [1]. This method involves estimating scores for a range of weighted parameters relating to the skill and cost of the workflow, using a pre-defined template. The method was shown to work well for various tools at the Bolund Hill site [2], but further tests are required on different sites.

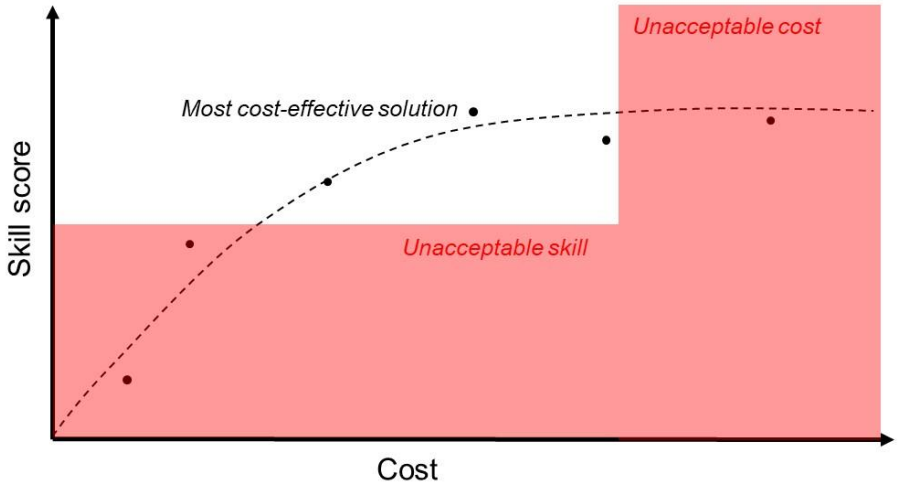


Figure 1: Expected skill score vs. cost score for an example wind energy project.

For the present work, therefore, the method is tested at two further complex terrain sites as follows: Firstly, at the complex terrain site of Stoetten in southern Germany [3], workflows are developed for carrying out WRAs using various simulation tools: ANSYS CFX and ANSYS Fluent as well as the commercial tools WindSIM and WindPro and the PALM [4]. The skill and cost scores are estimated for each workflow according to [1] and [5]. WRAs are then carried out for each workflow based on input measurement data from a met mast [3], and the Annual Energy Production (AEP) of a fictive wind turbine positioned at a second location is estimated. Measurement data from a lidar at this second location is used to assess the accuracy of both the wind speed and AEP predictions from each workflow, allowing the actual skill score of each workflow to be determined. The actual costs of each workflow are determined from the real costs after completing the calculations.
Secondly, at the complex terrain site of Perdigão in Portugal [6], a new simulation challenge was designed and run [7]. The goal of this challenge was to collect data regarding the estimated and actual skill and cost scores of a range of different simulation tools for a complex terrain site. The same method is applied as described above, but for a range of workflows submitted by external challenge participants.

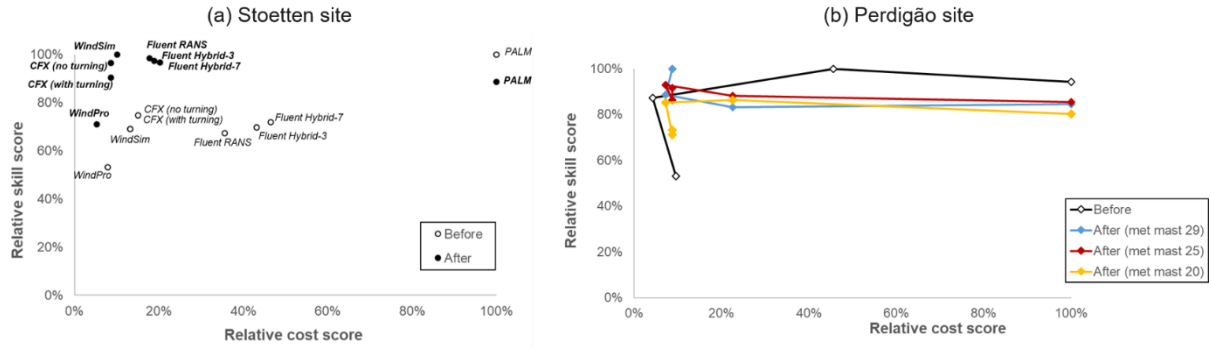


Figure 2: Predicted ("before") and actual ("after") scores for the WRA workflows applied in this work (wind speed estimation), (a) for the Stoetten site and (b) for the Perdigão site. Figure 2: Predicted ("before") and actual ("after") skill scores vs. cost scores for the WRA workflows applied in this work (wind speed estimation), (a) for the Stoetten site and (b) for the Perdigão site.

Initial results of these two projects show that there are wide range of different factors affecting the accuracy of the AEP calculation, as well as the performance of the simulation tools themselves. For each site, the estimated skill and cost scores ("before") are compared to the actual scores ("after") of the wind speed simulation for each workflow in Figure 2, in order to assess the quality of the new method (the results of the AEP calculation will be shown in the presentation). For the Stoetten site, the different workflows are marked next to each point. It can be seen that, although there are some discrepancies in the absolute values, the shape of the "before" and "after" distributions are similar, both of them indicating that either the WindSim or CFX workflows are most efficient for this site. For the Perdigão site, the individual models are not marked due to confidentiality reasons. Similarly to the Stoetten site, a similar curve shape can be seen, indicating that it is possible to estimate the most suitable workflow for this site using this method. Further analysis will be discussed in the final presentation.

References:

S. Barber, A. Schubiger and H. Nordborg (2019), A new process for the pragmatic choice of wind models in complex terrain – quantification of "skill score" and "cost", Wind Energy Science Conference,Cork, Ireland

S. Barber, A. Schubiger, S. Koller, A. Rumpf, H. Knaus and H. Nordborg (2020a), Actual Total Cost reduction of commercial CFD modelling tools for Wind Resource Assessment in complex terrain, Journal of Physics Conference Series Volume 1618

S. Barber, M. Buehler and H. Nordborg (2020b), IEA Wind Task 31: Design of a new comparison metrics simulation challenge for wind resource assessment in complex terrain Stage 1, Journal of Physics Conference Series 1102:012002

J. Berg, J. Mann, A. Bechmann, M. S. Courtney, and H. E. Jorgensen (2011), The Bolund Experiment Part i: Flow over a steep, three-dimensional hill. Boundary-Layer Meteorology, 141(2):219–243

H. J. S. Fernando et al. (2019) The Perdigao: Peering into microscale details of mountain winds. Bulletin of the American Meteorological Society, 100(5):799–819

S. Raasch and M. Schröter (2001): PALM - a large-eddy simulation model performing on massively parallel computers. Meteorol. Z. 10, 363–372

C. Schulz, M. Hofsäß, J. Anger, A. Rautenberg, T. Lutz, P. Wen Cheng, and J. Bange (2016), Comparison of different measurement techniques and a CFD simulation in complex terrain. Journal of Physics: Conference Series, 753:082017

The effect of flow turning on Annual Energy Production estimations in complex terrain

Andreas Rumpf[1], Sarah Barber[2], and Hermann Knaus[1]
[1]Hochschule Esslingen
[2]Eastern Switzerland University of Applied Sciences

Keywords: site to site relations, complex terrain | CFD, annual energy generation | Measure-Correlate-Predict

Supplementary Computational Fluid Dynamics (CFD) simulations with high spatial resolution can highlight local characteristics, but mostly give a spotlight on temporal limited aerodynamic conditions occurring at a wind farm location. Standard CFD tools used for complex terrain sites in the industry do not always consider the effects of relative flow turning between different positions within a site (WindSim [1], MeteoDyn [2], WASP CFD [3,4]). Speed-up factors are commonly determined for site to site relations. The manner, how speed-up factors are attributed, can lead to a variation of the wind assessment prediction if wind turning has a cross-sectoral impact on the investigated site. For modellers, the process of computing the AEP is a quality criteria [5-7]. Especially for projected sites, where the wind frequency concentrates only on a small proportion of the wind rose, an optimised determination of the speed-up factors is preferable.
In this work, therefore, the relative flow turning is examined and its effect on the Annual Energy Production (AEP) is examined.
Methods:
The investigated area considers an escarpment close to Stötten in the Swabian Alb in Germany. The simulation is carried out using Ansys CFX Version 17.2 and the numerical setup is based on an anelastic formulation of the Navier-Stokes equation considering the Coriolis force and land use by means of a canopy model. Digital height and land use models are used describing complex terrain in the model with high accuracy [8,9].

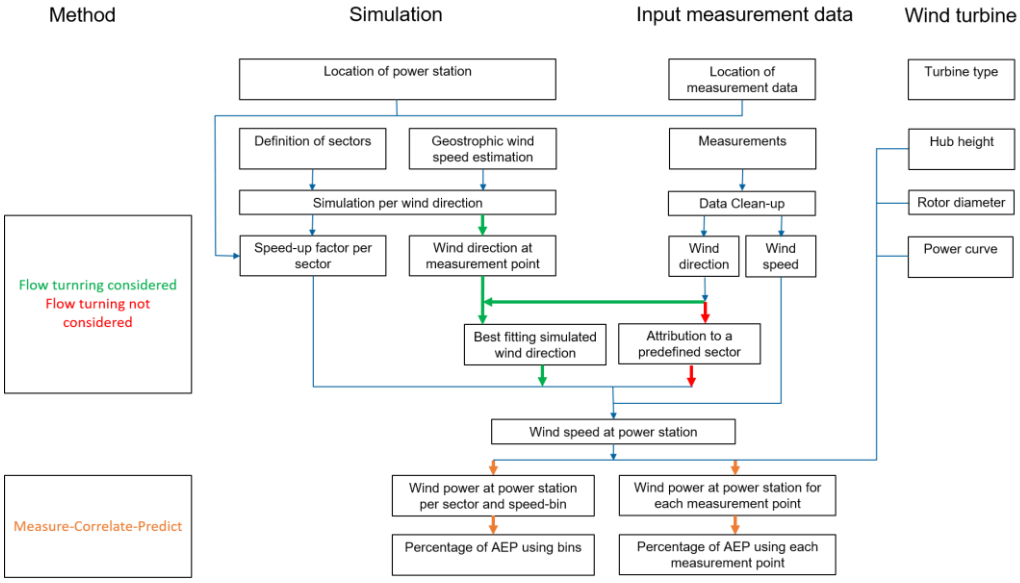


Figure 1) Schematic of the predictive Annual Energy Production with and without considering cross-sectoral wind turn and the Measure-Correlate-Predict – methods using a frequency distribution or a timeline

Figure 1 gives an overview of the employed process of the AEP estimation. Simulations at the corresponding landscape were conducted for 12 equally sized sectors at a common geostrophic wind speed. The simulations give 12 speed-up factors as a relation for the velocity at the known point of measurements [10] and the velocity at the fictive wind power station. The measured wind speed can simply be scaled with the speed-up factor of the current sector to which the measured wind speed is attributed (see red path in figure 1). An

issue herby is, that the initially defined boundary conditions can lead to different, and especially cross-sectoral wind-directions at the locations of interest.
Considering the wind turning within the simulated domain, the attribution of the speed-up factor is optimised cross-sectoral following the green path in figure 1. The next step obtaining an AEP employs Measure-Correlate-Predict-Methods were either the power curve of a fictive wind turbine is applied to the timeline of measured data, or to an discretised frequency distribution of the wind speed.

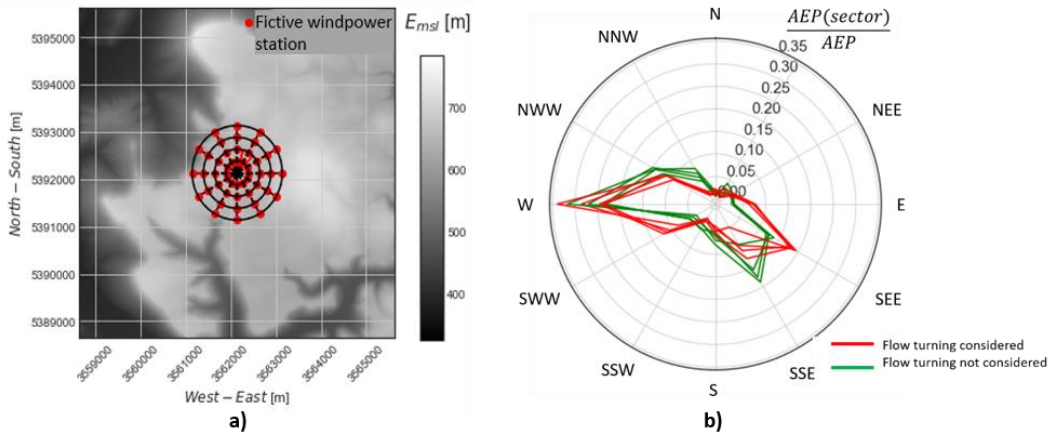


Figure 2) a) Elevation model of the investigated area close to Stötten b) Exemplarily result comparing the presented methods at a radius of 5 times the rotor hub heigh

Results:
The complexity of the investigated site can be seen by its gradients in figure 2 a). Not visualised are the considered presence of forest and local classification of land use leading to complex impact of the wind regime. In order to quantify the variation of the AEP, the described processes are employed for multiple locations around the location with available measurement data [9] at the central location of the simulated domain. Site-to-site variations of the AEP of up to 7 % are clear to see in figure 2 b) for the investigated points using a common AEP-process. Comparing results were wind turn is considered leads to shift of the predicted AEP per sector and a variation up to 10 % of the sectoral AEP.

References:
[1] Wallbank, T. (2008). WindSim validation study. CFD validation in complex terrain;
[2] Clarenc, T., Girard, N., Delaunay, D., & Chantelot, A. (2007). Wind farm production assessment in complex terrain: New validations of Meteodyn WT. In European Wind Energy Conference.
[3] Bowen, A. J., & Mortensen, N. G. (2004). WAsP prediction errors due to site orography;
[4] Mortensen, N. G., Bowen, A. J., & Antoniou, I. (2006). Improving WAsP predictions in (too) complex terrain. In 2006 European Wind Energy Conference and Exhibition. European Wind Energy Association (EWEA);
[5] S. Barber, A. Schubiger, S. Koller, A. Rumpf, H. Knaus and H. Nordborg (2020), Actual Total Cost reduction of commercial CFD modelling tools for Wind Resource Assessment in complex terrain, Journal of Physics Conference Series Volume 1618;
[6] S. Barber, M. Buehler and H. Nordborg (2020), IEA Wind Task 31: Design of a new comparison metrics simulation challenge for wind resource assessment in complex terrain Stage 1, Journal of Physics Conference Series 1102:012002;
[7] S. Barber, A. Schubiger and H. Nordborg (2019), A new process for the pragmatic choice of wind models in complex terrain – quantification of "skill score" and "cost", Wind Energy Science Conference,Cork, Ireland.
[8] Knaus, H., Rautenberg, A., & Bange, J. (2017). Model comparison of two different non-hydrostatic formulations for the Navier-Stokes equations simulating wind flow in complex terrain. Journal of Wind Engineering and Industrial Aerodynamics, 169, 290-307.
[9] Knaus, H., Hofsäß, M., Rautenberg, A., & Bange, J. (2018). Application of different turbulence models simulating wind flow in complex terrain: a case study for the WindForS Test Site. Computation, 6(3), 43.
[10] C. Schulz, M. Hofsäß, J. Anger, A. Rautenberg, T. Lutz, P. Wen Cheng, and J. Bange (2016), Comparison of different measurement techniques and a cfd simulation in complex terrain. Journal of Physics: Conference Series, 753:082017.

Wind-speed time series prediction at the Perdigão site using "E-Wind"

Sebastian Remmler*, Judith Langner, and Marcus Letzel
WRD Management Support GmbH
*Presenting author

Keywords: RANS | OpenFOAM | CFD | Time series | Wind resource assessment

Every year, ENERCON's Wind Farm Engineering department assesses hundreds of potential wind farm sites of different size and complexity. In order to simplify the tool chain and speed-up this process, we have integrated the whole process of wind resource assessment into our highly automatized solution "E-Wind" (Alletto, et al., 2018).

E-Wind features fully automated mesh generation, OpenFOAM-based RANS simulations for prescribed geostrophic wind directions, vertical calibration (i. e. comparison of the simulated vertical wind profiles to the available measurement data), automatic adaption of the computational parameters (scaling of the surface roughness and atmospheric stability) according to the calibration, prediction of the gross wind-speed time series at the turbine positions based on measured time series and simulated speed-up factors and prediction of waked wind-speed time series based on an analytic wake model as well as prediction of annual energy production of wind turbines.

The incompressible RANS simulations in OpenFOAM utilize a k-epsilon turbulence model adapted to atmospheric boundary layer flows in thermally stable or unstable conditions based on the work of Koblitz et al. (2015). Furthermore, we included Coriolis force and a forest model (Sogachev, et al., 2012). Our implementation is publicly available in OpenFOAM v2006 (OpenCFD Ltd, 2020).

Within the "Comparison metrics microscale simulation challenge for wind resource assessment" (Barber, et al., 2020), we have used E-Wind to predict wind-speed time series at the Perdigão site based on measured time series at mast 29 (on the north-eastern ridge). We simulated 24 different wind directions on a mesh with 1.8 million cells (25m horizontal resolution) using CORINE Land Cover (2012) and SRTM (1-arc second) elevation data as basis.

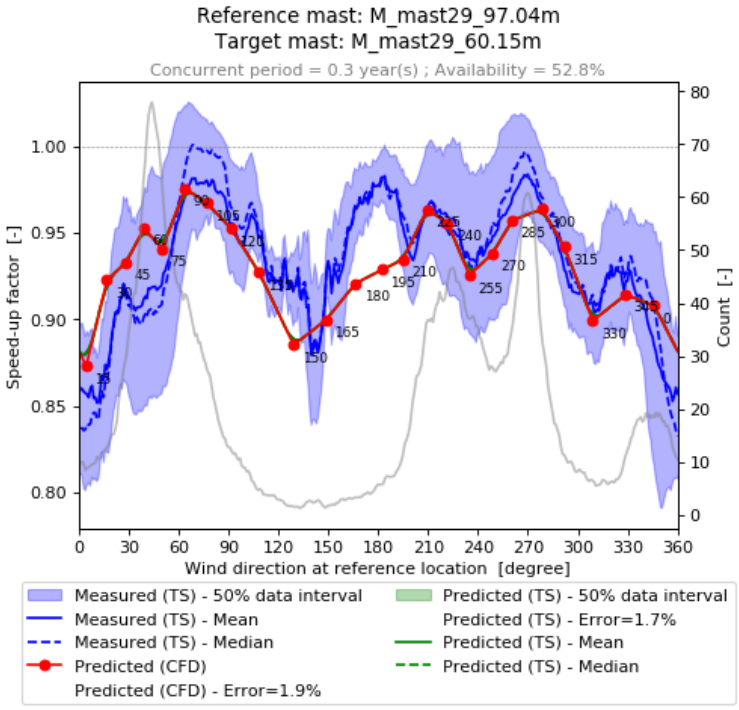


Figure 1: Measured and simulated speed-up between heights 97m and 60m at mast 29 vs. local wind direction at the mast. Additionally, the grey line indicates the measured frequency per wind direction.

After applying a stability calibration to each simulated wind direction individually, we obtain a good agreement of the average vertical shear at the reference mast; see Figure 1. The shear exponent error averaged over the whole time series is -0.01, which we consider a good agreement between measurement and simulation. For the southwestern sectors, we achieved a good calibration with neutral or weakly unstable conditions; while for the northeastern sectors, we had to apply strongly stable conditions to achieve the shown calibration result.

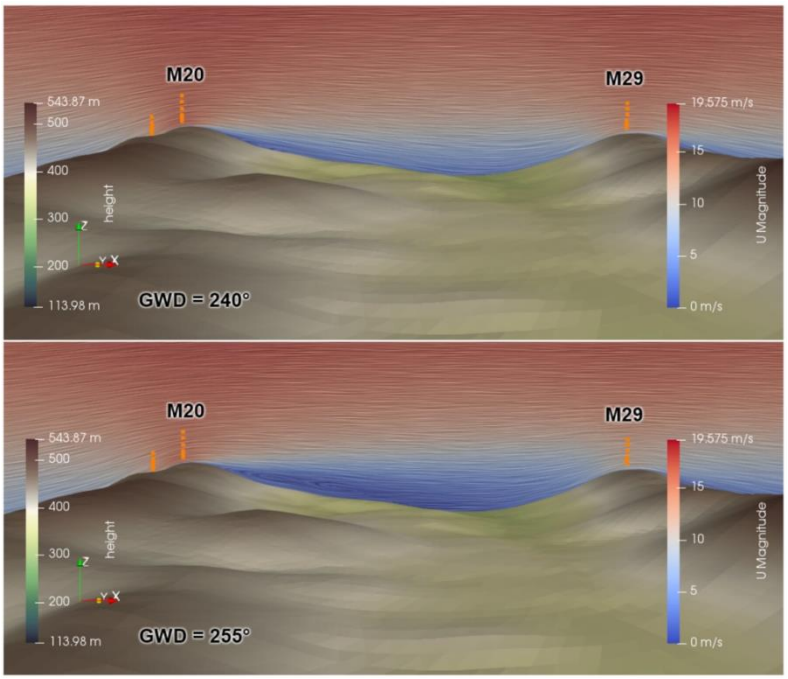


Figure 2: Visualization of simulated wind speeds in the vertical plane connecting mast 20 and mast 29 for two different geostrophic wind directions (GWD top: 240°; bottom: 255°), view from Southeast

In order to check the horizontal extrapolation accuracy, we compare the measured and simulated speed-up factors between mast 29 (reference) and 20 (located on the opposite ridge). For some geostrophic wind directions (GWD), we find very good agreement, but for others, we under-estimate the wind speed over the downwind ridge. There is evidence that this is due to an over-estimation of the recirculation behind the upwind ridge. In Figure 2, we compare the velocity fields for two simulations from the southwestern sector:
GWD = 240°: acceptable matching of simulated speed-up between masts 29 and 20 with measurements, simulated small recirculation region
GWD = 255°: strongly under-estimated wind speed at mast 29 compared to mast 20, simulated larger recirculation region
In the paper, we will discuss possible reasons and counter-measures for the observed underestimation of wind speed over the downwind ridge.

References:
Alletto, M. et al., 2018. E-Wind: Steady state CFD approach for stratified flows used for site assessment at Enercon. J. Phys. Conf. Ser., 1037(7), p. 072020.
Barber, S., Buehler, M. & Nordborg, H., 2020. IEA Wind Task 31: Design of a new comparison metrics simulation challenge for wind resource assessment in complex terrain Stage 1. J. Phys. Conf. Ser., 1618(6), p. 062013.
Koblitz, T. et al., 2015. Computational Fluid Dynamics model of stratified atmospheric boundary-layer flow. Wind Energy, 18(1), pp. 75-89.
OpenCFD Ltd, 2020. OpenFOAM® v2006: New boundary conditions. [Online] Available at: https://www.openfoam.com/releases/openfoam-v2006/boundary-conditions.php

Wind resource assessment over real complex topography: a procedure to integrate field data with high-fidelity numerical simulations

Federico Bernardoni*, Umberto Ciri, and Stefano Leonardi
University of Texas at Dallas
*Presenting author

Keywords: Wind-resource-assessment | Large-Eddy-Simulations | Stochastic-Analysis | Topography

In 2019, about 95% of the global wind power production came from onshore wind farms[1]. Depending on the complexity of the terrain, the topography might affect the performance of onshore wind turbines. Terrain topography generates turbulence and it locally changes the wind resources affecting both the power production and load fluctuations on wind turbines.
During wind resources assessment for new sites, data are usually available only in a few locations where met-towers are located. However, the local interaction of the terrain topography and the atmospheric boundary layer may make the measurements not representative of the operational conditions at the turbine locations.
In this study, we considered the complex terrain of the Vale do Cobrao, located in central Portugal.
This site consists of two parallel ridges (figure 1) with prevalent winds coming from the direction perpendicular to the ridges. A wind turbine is located on the top of the Southern ridge. In 2017 the Perdigao field campaign[2] collected wind data at several locations inside the valley and on the ridges. For the present study data were available from March 9th to June 17th 2017 at one mettower on the top of the Northern ridge. Data at all the other met-tower locations will be available for validation in [3] and results discussed at the conference.

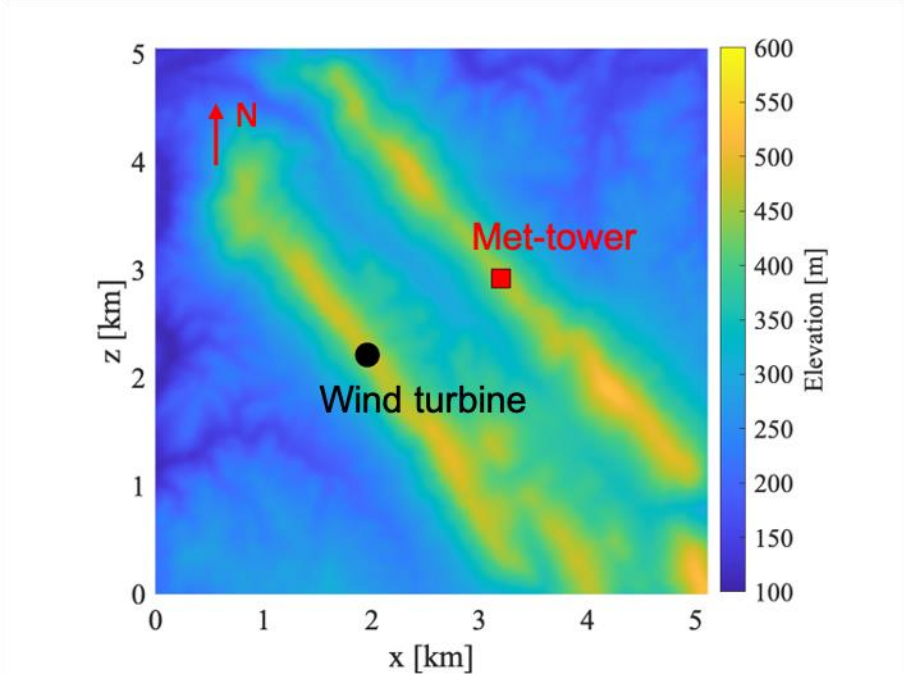


Figure 1: Topography map of the Perdigao site, PT.

Large Eddy Simulations of the flow over the site topography have been carried out with different wind conditions. Using polynomial chaos expansion, we built a surrogate model able to estimate the wind average velocity at other met-tower locations and the turbine power production as function of the wind velocity and direction at the reference met-tower.

Using the data collected in the field campaign at the met-tower, we performed a stochastic analysis to obtain the wind vectors averaged over the observation period at every desired location in each 30° wind sector. The Annual Energy Production (AEP) was estimated as well.
We found that for the same wind speed measurements at the met-tower location, the fluctuations of the power production of the turbine are highly dependent on the wind direction (figure 2). This is due to the fact that the met-tower and the turbine are located on the two opposite ridges of the valley. For example, for winds coming from NE directions, the met-tower is located on the upstream ridge while the turbine on the downstream one. Thus, coherent turbulent structures originated from the upstream ridge directly impinge on the turbine decreasing the average power production and increasing the fluctuations. The opposite happens when wind comes from SW directions.

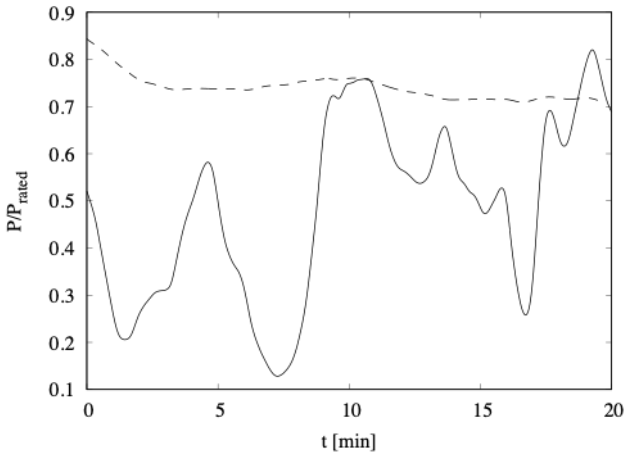


Figure 2: Power production of the turbine with different wind directions. Solid line: wind coming from North-East. Dashed line: wind coming from South-West.

Using the described approach, we obtained an error on the AEP estimation of about 7% with respect to the AEP measured in 2015. We expect to validate also our velocity estimation with the reference data after the conclusion of the comparison study[3], when all the data will be made available.
Using only limited data, that would be available in a real wind resources assessment, and integrating them with high-fidelity numerical simulations, the proposed procedure represents a valuable tool for pre-constructions wind site assessments in presence of complex terrain topography.

References:
[1] "Global wind report" (2019). Global Wind Energy Council.
[2] Fernando, H. J. S., et al. (2019). "The Perdigao: Peering into microscale details of mountain winds." Bulletin of the American Meteorological Society 100.5, 799-819.
[3] Barber, S., Buehler, M., & Nordborg, H. (2020). "IEA Wind Task 31: Design of a new comparison metrics simulation challenge for wind resource assessment in complex terrain Stage 1." Journal of Physics: Conference Series, Vol. 1618, No. 6, p. 062013. IOP Publishing.

Influence of thermal stability and forest canopy in non-neutral atmospheric boundary modelling over complex terrain

Kartik Venkatraman[1,2,*], Trond-Ola Hågbo[1,3], Sophia Buckingham[1], and Knut Erik Teigen Giljarhus[3]
[1]Von Karman Institute for Fluid Dynamics
[2]Université de Sherbrooke
[3]University of Stavanger, Norway
[*]Presenting author

Keywords: stability | canopy | RANS | OpenFOAM | recirculation

Improving numerical modeling tools for complex terrains demand accounting for various microscale phenomena such as flow recirculation and forest canopy effect. Such microscale flow features have a significant impact on local wind resource assessment and wind turbine loading. However, low-fidelity wind farm models commonly used in the industry do not account for such complex flow phenomena.
Well-informed siting of wind turbines can substantially increase the electric power produced while ensuring minimal structural fatigue. This work aims to study the influence of flow physics such as buoyancy forces, Coriolis forces, and the effect of forest canopy in the prediction accuracy of computed wind profiles under different atmospheric stability conditions.
A three-dimensional steady Reynolds-averaged Navier-Stokes (RANS) equations based model is set up using OpenFOAM to simulate the flow over a complex terrain site comprising two parallel ridges located near Perdigão, Portugal. A 5 km × 5 km terrain of the Perdigao site is constructed from elevation data centered around a 100m met-mast located on the north-east ridge. A cylindrical computational domain with a smoothing region from complex to flat terrain was applied towards the outer boundaries. It enables defining a homogeneous boundary profile and provides convergent solutions when simulating wind from multiple cardinal directions. The influence of the mesh is studied using two different strategies, a structured mesh setup generated with the tool terrainBlockMesher and an unstructured mesh setup generated with the tool snappyHexMesh.

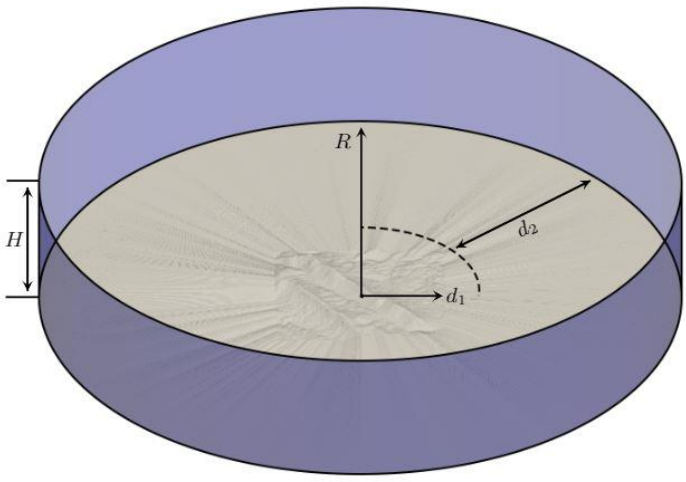


Figure 1: Cylindrical domain showing the Perdigao terrain in the centre. A smoothing region from complex to flat terrain was applied towards the outer boundaries.

Inflow conditions are provided based on a log-law type profile calibrated to match the met mast measurements at 100m. The physical processes are taken into account through source terms in the non-neutral solver buoyantBoussinesqSimpleFoam. The forest canopy is modeled as a porous medium based on a modified k-ε model that considers the drag and turbulence source terms produced by the canopy layer. Met-mast measurement data is corrected for orientation and filtered to remove non-physical values and then

classified for thermal stability based on the gradient Richardson number. Simulations are then performed for different atmospheric stability conditions by applying a modification to the estimated turbulence mixing length scale and surface heat flux.

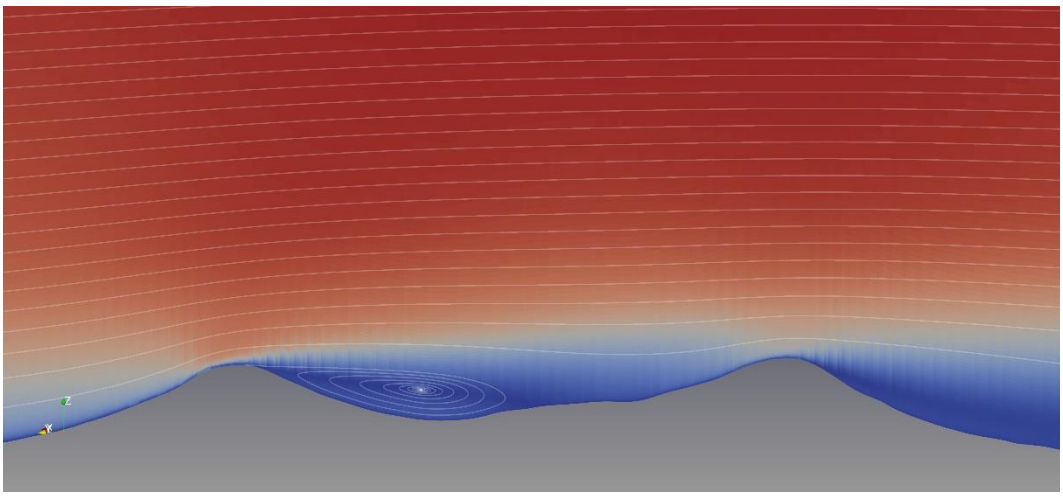


Figure 2: Contour of velocity profile taken over a plane parallel to flow direction for 45 degree, depicting the recirculation zones on the lee side of the ridges and speed up over hill top, for a case of neutral stability with forest canopy modelled as a porous medium

The primary wind directions are found to be perpendicular to the ridges. The model capability to predict the flow recirculation in the valley for different stability conditions will be analyzed and compared with lidar scans from the Perdigão 2017 field campaign taken along a transect across the ridges. Comparing simulation results for neutral conditions to field measurements provides insight into the applied method accuracy. The wind simulations proved to provide reasonable wind velocity predictions with less than 10% error compared to the measured average wind velocity at the met mast for most of the data points and wind directions. Introducing trees as porous media significantly improved the model's accuracy at lower levels without notably increasing the required computational power. The Coriolis term is found to have negligible influence over the scale considered. The suggested method is an efficient and relatively reliable way to predict wind behavior over complex terrain. The inclusion of non-neutral effects can be reasonable to model when optimizing wind turbine siting as it can improve the accuracy of the predicted wind speed at hub height and flow in recirculation zones.

Mini-Symposium: Wind Farm Control



Gregor Giebel
DTU Wind Energy



Paul Veers
NREL



Paul Fleming
NREL



Katherine Dykes
DTU Wind Energy



Johan Meyers
KU Leuven



Carlo L. Bottasso
TU Munich



Jan-Willem van Wingerden
Delft University of Technology

Wind Farm Control offers the possibility to increase power production and reduce loads by clever collaborative behaviour of the wind turbines in a farm. While a central wind farm controller was used since 2003 to allow for downregulation, the modern scientific topic distinguishes between wind farm flow control and control of the electrical part of the plant. The former has seen a lot of work over the last 15 years, first by downregulating the front row turbines to leave more wind to the turbines behind, and later by intentional yawing of the turbines and thereby, the wake in order not to hit a downstream turbine. Both techniques have potentially positive effects on the combined farm production and/or the aggregated loading of the turbines. Several other schemes for increased wake dissolution have also been proposed since. In the electrical arena, the provision of ancillary services and the reduction of losses were the main drivers, though some ancillary services (e.g. reserve power provision) also use flow control. We therefore invite talks regarding real-time wake modelling and state estimation, wind farm flow models, control algorithms, load assessment for wind farm control, wind-farm control experiments and any other topic fitting to wind farm control.

Mini-Symposium: Wind Farm Control (I)

Maturing FLORIS towards a Dynamic Wind Farm Model: The inclusion of time-dependent wake propagation, time-varying atmospheric conditions and heterogeneous inflow conditions

Marcus Becker[1,*], Bastian Ritter[2,3], Bart Doekemeijer[4], Daan van der Hoek[1], and Jan-Willem van Wingerden[1]
[1]Delft University of Technology
[2]Technical University of Darmstadt
[3]Wölfel Wind Systems GmbH
[4]National Renewable Energy Laboratory
*Presenting author

Keywords: FLORIDyn | Dynamic Wake Modelling | FLORIS | Wind Farm Control

To reduce the costs of offshore wind energy, wind turbines are built in large wind farms. It is well known that the turbines influence each other and reduce the efficiency of the farm. A wind farm wide model-based control strategy which takes the turbine interactions into account can compensate for some of these effects. It could increase the efficiency of existing and future wind farms.
The control strategy has to overcome several challenges: complex flow interactions between the turbines, large delays between state changes and effects and spatially heterogeneous wind conditions which change over time. Model Predictive Control (MPC) approaches have shown promising results in the past. A hinge point for the MPC design is the adequate surrogate wind farm model and how it copes with the time-varying wake dynamics. Such a surrogate model has to be computational cheap enough to allow real time control and accurate enough to facilitate an improved performance also under realistic conditions. The so-called Flow Redirection and Induction in Steady State (FLORIS) models for instance have proven to be an easy to use, easy to tune, computationally inexpensive and powerful wake modelling tool though lacking dynamical effects.

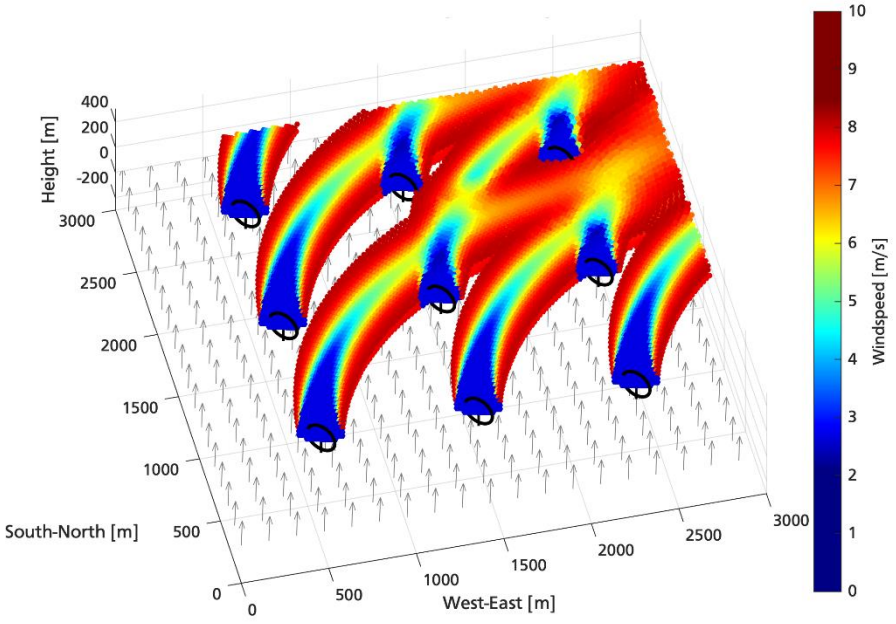
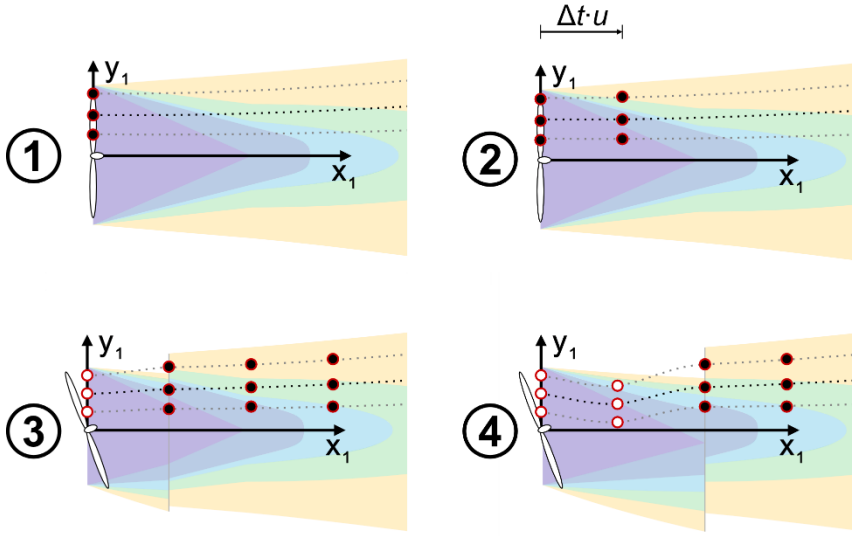


Figure 1: Nine turbine wind farm during a 60 degree wind direction change with OPs plotted at hub height

In the presented work, a dynamic version of the widely adapted Gaussian FLORIS model is developed. It is adapted to simulate multiple wind turbine wakes and take spatially heterogeneous wind conditions into account. Time-varying dynamic behavior is achieved by introducing so-called Observation Points at the rotor plane of each turbine. These propagate through the wake with the free wind speed and simulate the delayed effect of turbine state changes. The chosen approach is a modified version of the FLORIDyn model. A basic, computationally inexpensive wind field model is developed to provide spatially heterogeneous wind field conditions including wind shear. The calculation of the aerodynamic thrust CT and power CP coefficients is adapted as a function of the blade pitch and the tip-speed-ratio to be more in line with the real conditions. The new FLORIDyn model is validated in two, three and nine turbine cases and compared to the high fidelity CFD simulation SOWFA. Tested scenarios include a yaw sweep, stepwise increase of the yaw angle, changing CT and CP coefficients and a wind direction change. In the steady state cases, FLORIDyn meets the average generated power by the turbines with relative errors between -0.82 % and 22.15 %. In a flow field comparison FLORIDyn lacks accuracy in the near wake area but has a very good agreement with SOWFA in the far wake area which is practically more relevant for the purpose of model-based wind farm control. The developed code is computationally efficient with one time step (in a two turbines setup) with overall 20.000 Observation points taking about 24ms to compute in MATLAB on a state-of-the-art notebook.



Description: Propagation of wind turbine state changes through the wake with the Observation Points

In a nutshell, the new representation of FLORIDyn provides very promising results in terms of model accuracy and computational performance. It provides a unique feature set with the ability to simulate dynamic parametric wake models in a changing, heterogeneous environment. The work presented here lays the groundwork for a dynamic wake model which can be part of a real time wind farm control strategy. The developed MATLAB code is publicly available on GitHub under the GPL-3.0 License.

References:

[1] Bastankhah, Majid, and Fernando Porté-Agel. "Experimental and Theoretical Study of Wind Turbine Wakes in Yawed Conditions." Journal of Fluid Mechanics 806 (November 10, 2016): 506–41. https://doi.org/10.1017/jfm.2016.595.

[2] Gebraad, Pieter M. O., and J. W. van Wingerden. "A Control-Oriented Dynamic Model for Wakes in Wind Plants." Journal of Physics: Conference Series 524 (June 2014): 012186. https://doi.org/10.1088/1742-6596/524/1/012186.

[3] Farrell, Alayna, Jennifer King, Caroline Draxl, Rafael Mudafort, Nicholas Hamilton, Christopher J Bay, Paul Fleming, and Eric Simley. "Design and Analysis of a Spatially Heterogeneous Wake." Wind Energy Science, 2020, 25. https://doi.org/10.5194/wes-2020-57.

The Modularized FLORIS Framework for Wind Farm Controls and Wake Modeling

Rafael Mudafort*, Christopher J. Bay, Paul Fleming, Nicholas Hamilton, Robert Hammond, Jennifer King, Luis A. Martínez-Tossas, Eric Simley, and P.J. Stanley
National Renewable Energy Laboratory
*Presenting author

Keywords: wind farm controls | wake steering | wake modeling

The FLORIS software package [1] is a controls-oriented simulation environment that computes the steady-state wake effects on the flow field of a wind plant. The software includes specific areas designated as the "FLORIS framework" that enable user-developed code. This work explains the modularity and usability of the framework in order to establish FLORIS as a platform for implementation and evaluation of wake models.
The FLORIS software is implemented in an object-oriented programming paradigm in the Python programming language. At a high-level, FLORIS is divided into front-end and back-end components.
In the front-end, users provide input data describing individual turbines, turbine positioning in a wind plant, atmospheric conditions, and the configuration parameters for a chosen wake model. A set of high-level commands are available for users to interact with the model of the physical plant as well as wake model, turbine controls, and simulation settings. In the back end, low-level components construct a representation of the wind plant and drive the simulation in a fixed solver scheme. The solver loops over each turbine to aggregate its impact on the flow field capturing the effects of upstream turbines where necessary. Though its functionality is well documented [2], the back-end portion of the software should remain opaque to most users. The "FLORIS framework" is a portion of the software that provides hooks directly into the back-end. It enables users to implement new models for select steps in the solve or swap existing models within the framework. It also ensures compatibility with the rest of the software through the established application programmer interface (API).
As of version 2.2.4, the "FLORIS framework" consists of one principal area, the wake models, which are divided into four independent model types:
- Deflection
- Velocity deficit
- Turbulence
- Combination

These models compute their respective influence on the wake and pass the result to the FLORIS solver to be included in the overall computation. Figure 1 outlines the framework and their relationship to the FLORIS software.

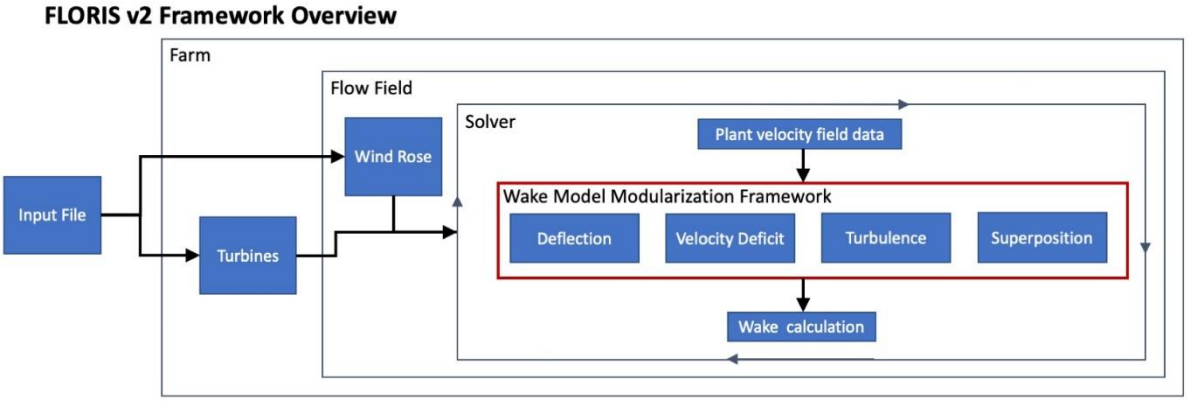


Figure 1: Outline of the FLORIS v2.2.4 software, solver sequence, and framework components. The wake model components make up the "FLORIS framework" and are configured by user inputs. They are sequentially coupled in the included solver scheme and may be swapped for a user-given model. The other components are "back end" tools included in the FLORIS software.

Within the FLORIS solver, the wake model framework components are coupled sequentially. Given a turbine and its current state (i.e., physical dimensions, control settings) as well as the flow field state (i.e., speed, direction, turbulence intensity), the wake deflection models calculate a deflection field describing the spanwise deflection of the wake centerline. The deflection is given to the velocity deficit models which compute the impact of the turbine on the velocity of the flow field. The velocity deficit is represented as a field of deviations from the free-stream velocity field for each velocity component. The wake turbulence models are an optional plug-in for modeling the turbulence intensity due to upstream wake conditions at a given turbine. Finally, the wake combination models iteratively aggregate each turbine's wake (comprised of the three first three components) describing the full farm velocity field in a single construct [3, 4].

We are actively working to expand the framework to support modularization in other aspects of the FLORIS software. Specifically, we are working to support various solver schemes such as an iterative solver to capture deep array and blockage effects and a full-farm solver for algorithmic efficiency.

Further formalization and documentation of the framework are in progress.

References:

[1] FLORIS. Version 2.2.4 (2020). Available at https://github.com/NREL/floris.

[2] NREL. (2020). FLORIS Code Reference [Online]. Available at: https://floris.readthedocs.io/en/master/source/code.html

[3] Annoni, J., Fleming, P., Scholbrock, A., Roadman, J., Dana, S., Adcock, C., Porte-Agel, F., Raach, S., Haizmann, F. and Schlipf, D., 2018. Analysis of control-oriented wake modeling tools using lidar field results. Wind Energy Science, 3(2), pp.819-831.

[4] Hamilton, N., Bay, C., Fleming, P., King, J. and Martínez-Tossas, L., 2020. Comparison of modular analytical wake models to the Lillgrund wind plant. Journal of Renewable and Sustainable Energy, 12(5), p.053311.

Results of a validation campaign on wake steering using static yaw angles

Paul Fleming[1,*], Michael Sinner[1], Tom Young[2], Marine Lannic[2], Jennifer King[1], and Eric Simley[1]
[1]National Renewable Energy Laboratory
[2]RES
*Presenting author

Keywords: wind farm control | wake steering | field campaign

Wind farm control is a form of control in which the control actions of individual turbines within a farm are coordinated to improve global farm performance. Wake steering is a method of wind farm control in which yaw offsets are applied to upstream wind turbines to decrease wake losses in downstream turbines and thereby increase overall wind farm power production. [Wagenaar, 2012].
This method of wind farm control has been a focused of area of study, and has shown promise in both computational large-eddy simulation studies [see for example, Fleming, 2014] as well as in wind tunnel studies [see for example, Bastankhah 2019, Campagnolo 2016].
There is however increasing effort placed on evaluating wake steering control at the full scale, by implementing wake steering controllers on turbines within commercial farms. To date, there have been several public reports of full-scale wake steering validation campaigns published. Some example publications include [Fleming 2017, Howland 2019, Doekemeijer 2020 and Fleming 2020]. In each of these studies, one or several turbines within a farm implement wake steering via yaw offset, and the results are compared to model predictions. These studies are critical in establishing the viability of wake steering in realistic conditions and assessing the accuracy of the engineering models used in design and analysis of wind farm control approaches.
In this presentation, we review analysis of a new field validation campaign of wake steering. The campaign implements wake steering on a single turbine of a commercial wind farm. The campaign is different than the previous studies mentioned in that the applied offsets are of fixed angle, rather than given by a schedule of offsets by wind direction. Importantly, the offsets were applied for all wind directions where there turbines downstream of the controlled turbine (not just those for which it would be optimal to do so). The offsets were toggled on and off hourly to provide balanced data sets of normal and yawed operation. The experiment allows for the comparison of wake steering field campaign results to engineering models, such as the open-source FLORIS model [FLORIS, 2020].
By using fixed offsets, the comparisons between field results and model predictions can be made focused on the physical impacts, absent control considerations such as tracking a changing offset.

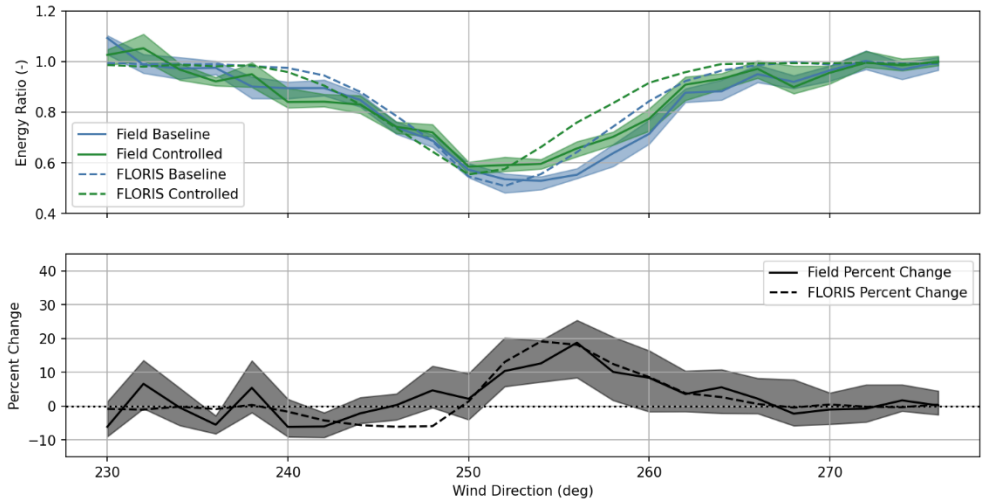


Figure 1: Comparison of energy ratio (above) and change in energy ratio (below) for a waked turbine in normal (blue) and yawed (green) operation of the upwind turbine. Solid lines represent field validation data while dashed are FLORIS predictions.

Results of the campaign show strong agreement between the FLORIS model and results of wake steering. The results are used to assess both the power losses of upstream turbines, as well as the gains realized on downstream turbines. In the figure, the energy ratios (the percentage of energy produced versus a non-waked reference turbine by wind direction) of the downstream turbine for normal and yawed conditions is compared between field data FLORIS, showing good agreement.
Finally, second-order predictions of the latest models, such as those made by the Gauss-Curl-Hybrid [King, 2020] model of wake steering, are assessed using the data.

References:

Wagenaar, J.W., Machielse, L. and Schepers, J., 2012. Controlling wind in ECN's scaled wind farm. Proc. Europe Premier Wind Energy Event, pp.685-694.
Fleming, P.A., Gebraad, P.M., Lee, S., van Wingerden, J.W., Johnson, K., Churchfield, M., Michalakes, J., Spalart, P. and Moriarty, P., 2014. Evaluating techniques for redirecting turbine wakes using SOWFA. Renewable Energy, 70, pp.211-218.
Bastankhah, M. and Porté-Agel, F., 2019. Wind farm power optimization via yaw angle control: A wind tunnel study. Journal of Renewable and Sustainable Energy, 11(2), p.023301.
Campagnolo, F., Petrović, V., Bottasso, C.L. and Croce, A., 2016, July. Wind tunnel testing of wake control strategies. In 2016 American Control Conference (ACC) (pp. 513-518). IEEE.
Fleming, P., Annoni, J., Shah, J.J., Wang, L., Ananthan, S., Zhang, Z., Hutchings, K., Wang, P., Chen, W. and Chen, L., 2017. Field test of wake steering at an offshore wind farm. Wind Energy Science Discussions, 2(NREL/JA-5000-67623).
Howland, M.F., Lele, S.K. and Dabiri, J.O., 2019. Wind farm power optimization through wake steering. Proceedings of the National Academy of Sciences, 116(29), pp.14495-14500.
Doekemeijer, B.M., Kern, S., Maturu, S., Kanev, S., Salbert, B., Schreiber, J., Campagnolo, F., Bottasso, C.L., Schuler, S., Wilts, F. and Neumann, T., 2020. Field experiment for open-loop yaw-based wake steering at a commercial onshore wind farm in italy. Wind Energy Science Discussions, pp.1-22.
Fleming, P., King, J., Simley, E., Roadman, J., Scholbrock, A., Murphy, P., Lundquist, J.K., Moriarty, P., Fleming, K., Dam, J.V. and Bay, C., 2020. Continued results from a field campaign of wake steering applied at a commercial wind farm–Part 2. Wind Energy Science, 5(3), pp.945-958.
FLORIS. Version 2.2.4 (2020). Available at https://github.com/NREL/floris.
King, J., Fleming, P., King, R., Martínez-Tossas, L.A., Bay, C.J., Mudafort, R. and Simley, E., 2020. Controls-oriented model for secondary effects of wake steering. Wind Energy Science Discussions, pp.1-22.

Results from a Wake Steering Wind Farm Control Experiment at a Commercial Wind Farm: Investigating the Wind Speed Dependence of Wake Steering Performance

Eric Simley[1], Paul Fleming[1], Nicolas Girard[2], Lucas Alloin[3], Emma Godefroy[3], and Thomas Duc[3,*]
[1]National Renewable Energy Laboratory
[2]ENGIE Digital
[3]ENGIE Green
[*]Presenting author

Keywords: wind farm control | wake steering | field tests | FLORIS | nacelle lidar

Wind farm flow control has gained significant interest in the research community as well as industry and has been increasingly studied over the past few years (Boersma et al., 2017). Strategies such as wake steering are now considered as very promising for mitigating wake effects and optimizing the annual energy production of wind farms. Indeed, several full-scale field tests have been realized on subsets of wind farms and tend to confirm that gains in combined power production can be achieved in practice (Fleming et al. (2017), Fleming et al. (2019), Howland, Lele and Dabiri (2019), Fleming et al. (2020), Doekemeijer et al. (2020)).
In this presentation results from an additional field test, realized in the scope of the French national project SMARTEOLE, are presented and discussed. A subset of two turbines in a wind farm is used to investigate the benefit of wake steering, by controlling the upstream turbine SMV6 and analyzing its effect on the downstream turbine SMV5 (see Figure 1). The wake steering controller is toggled on and off every hour to analyze the benefit of wake steering in similar wind conditions as the baseline controller. A nacelle-mounted lidar and a GNSS compass are installed on the controlled turbine to monitor the turbine misalignment and its nacelle position, respectively, over the full duration of the field campaign (from mid-February to end of May 2020).
First, the achieved yaw offsets measured by the turbine's nacelle wind vane and the nacelle lidar are compared, and discrepancies of a few degrees are found. These discrepancies are explained by the inability of the turbine to accurately measure the relative wind direction for the complete wind speed range.

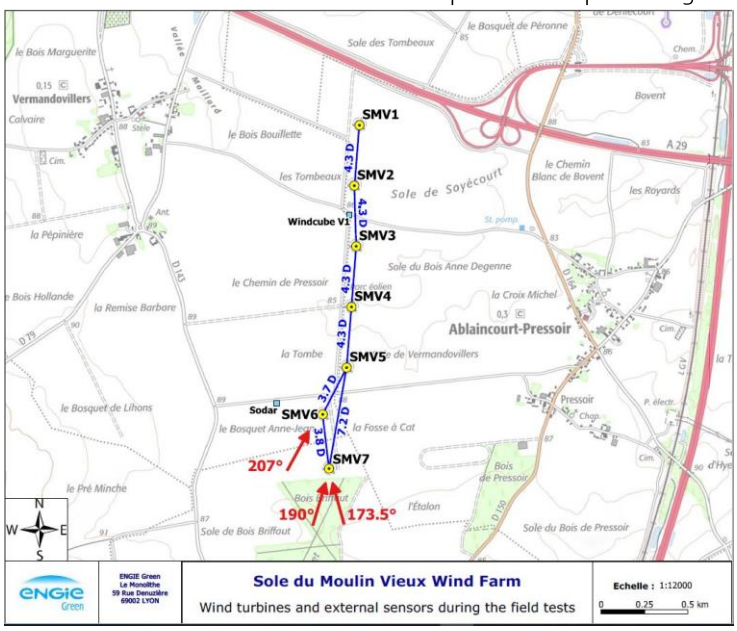


Figure 1: Layout of the wind farm and experimental setup for the wake steering field tests. The two turbines considered are SMV6 (upstream) and SMV5 (downstream). A WindCube Nacelle lidar and a GNSS compass were installed on top of SMV6. Inter-distances between wind turbines and azimuths related to both SMV6 and SMV5 are shown.

Next, the loss of production of the upstream wind turbine from yaw misalignment is studied as a function of wind speed using the nacelle lidar. This is done by analyzing the power exponent applied to the cosine of the yaw misalignment for several wind speed bins. The obtained results are in line with expectations: higher exponents (~2.5) are found for wind speeds in region 2 of the power curve (meaning higher power losses), while the exponent is found to decrease significantly as wind speed increases towards the rated wind speed. Finally, the experimental data are used to estimate the energy gain for the combined upstream and downstream turbines {SMV5 + SMV6}. As can be seen Figure 2, positive gains are found for the wake steering sector. These gains are relatively well predicted by the FLORIS engineering wake model considering the same incoming wind flow conditions.

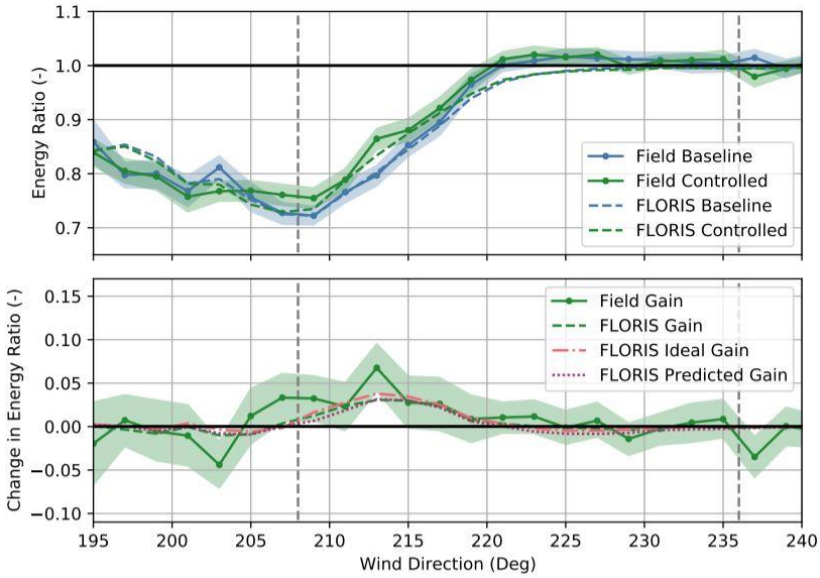


Figure 2: Energy ratios for baseline and controlled operation and change in energy ratio for Turbines SMV5 and SMV6 combined. Energy ratios are derived from field observations as well as FLORIS calculations using 1) observed yaw offsets, 2)ideal, intended yaw offsets, and 3) predicted yaw offsets using the wind direction uncertainty model. The gray dashed lines encompass the intended wake steering region.

The wind speed dependance of the energy gains is analyzed, suggesting that wake steering is more profitable for high wind speeds (10 – 12 m/s). Indeed, for these near-rated conditions, the loss of energy at the upstream turbine due to yaw misalignment is greatly reduced while a larger-than expected increase in downstream power production is achieved thanks to the wake deflection. On the other hand, for lower wind speed bins (4 – 6 and 6 – 8 m/s), gains are more chaotic and the benefit of the wind farm control is not as clear, likely in part because of high wind direction variability.

References:

Boersma, S., Doekemeijer, B., Gebraad, P., Fleming, P., Annoni, J., Scholbrock, A., Frederik, J. and van Wingerden, J., 2017. A tutorial on control-oriented modeling and control of wind farms. 2017 American Control Conference (ACC),.

Doekemeijer, B., Kern, S., Maturu, S., Kanev, S., Salbert, B., Schreiber, J., Campagnolo, F., Bottasso, C., Schuler, S., Wilts, F., Neumann, T., Potenza, G., Calabretta, F., Fioretti, F. and van Wingerden, J., 2020. Field experiment for open-loop yaw-based wake steering at a commercial onshore wind farm in Italy. Wind Energy Science Discussions.

Fleming, P., Annoni, J., Shah, J., Wang, L., Ananthan, S., Zhang, Z., Hutchings, K., Wang, P., Chen, W. and Chen, L., 2017. Field test of wake steering at an offshore wind farm. Wind Energy Science, 2(1), pp.229-239.

Fleming, P., King, J., Dykes, K., Simley, E., Roadman, J., Scholbrock, A., Murphy, P., Lundquist, J., Moriarty, P., Fleming, K., van Dam, J., Bay, C., Mudafort, R., Lopez, H., Skopek, J., Scott, M., Ryan, B., Guernsey, C. and Brake, D., 2019. Initial results from a field campaign of wake steering applied at a commercial wind farm – Part 1. Wind Energy Science, 4(2), pp.273-285.

Fleming, P., King, J., Simley, E., Roadman, J., Scholbrock, A., Murphy, P., Lundquist, J., Moriarty, P., Fleming, K., van Dam, J., Bay, C., Mudafort, R., Jager, D., Skopek, J., Scott, M., Ryan, B., Guernsey, C. and Brake, D., 2020. Continued results from a field campaign of wake steering applied at a commercial wind farm – Part 2. Wind Energy Science, 5(3), pp.945-958.

Howland, M., Lele, S. and Dabiri, J., 2019. Wind farm power optimization through wake steering. Proceedings of the National Academy of Sciences, 116(29), pp.14495-14500.

Wind Farm Flow Control in Flexible Electricity Markets – Initial Results of FarmConners Market Showcases

Michael Smailes[1,*], Tuhfe Göcmen[2], Irene Eguinoa[3], Kaushik Das[4], Matti J. Koivisto[4], and Konstanze Kölle[5]
[1]ORE Catapult
[2]DTU Wind Energy
[3]CENER
[4]Technical University of Denmark
[5]SINTEF
[*]Presenting author

Keywords: Wind Farm Flow Control | Electricity Market Integration | Wake Steering | Induction Control | Revenue Based Optimization

For the EU to meet its ambitious Carbon Dioxide reduction targets, the makeup of the power system will have to shift dramatically over the next decade. Wind energy will play an increasingly significant role, with the rate of penetration expected to accelerate sharply. This will continue to drive the electricity prices for wind down while increasing variability, incentivizing wind farm operators to maximize revenue in place of power generation. Wind Farm Control (WFC) in its broadest sense is defined as the coordinated operation of different wind turbines within a wind farm to serve a common goal. In this way WFC is ideally suited to facilitate this new dynamic. Wind Farm Flow Control (WFFC) is a subset of WFC and concerns the manipulation of the wakes induced by upstream wind turbines to maximize power generation or track a particular power reference while alleviating loads on wind turbines.
While the variance of the power gain and load alleviation that can be achieved via WFFC has been well reported in the literature (Kheirabadi and Nagamune, 2019, pp 45 – 73; Knudsen, Bak and Svenstrup, 2015, pp 1333-1351), the FarmConners project has identified that there is currently insufficient evidence demonstrating the economic benefit of integrating WFFC into the WFC structure. In response, the FarmConners project developed several showcases to demonstrate how load alleviation and power gain variance via WFFC on a reference wind farm correspond to added economic benefit for the wind farm operator.

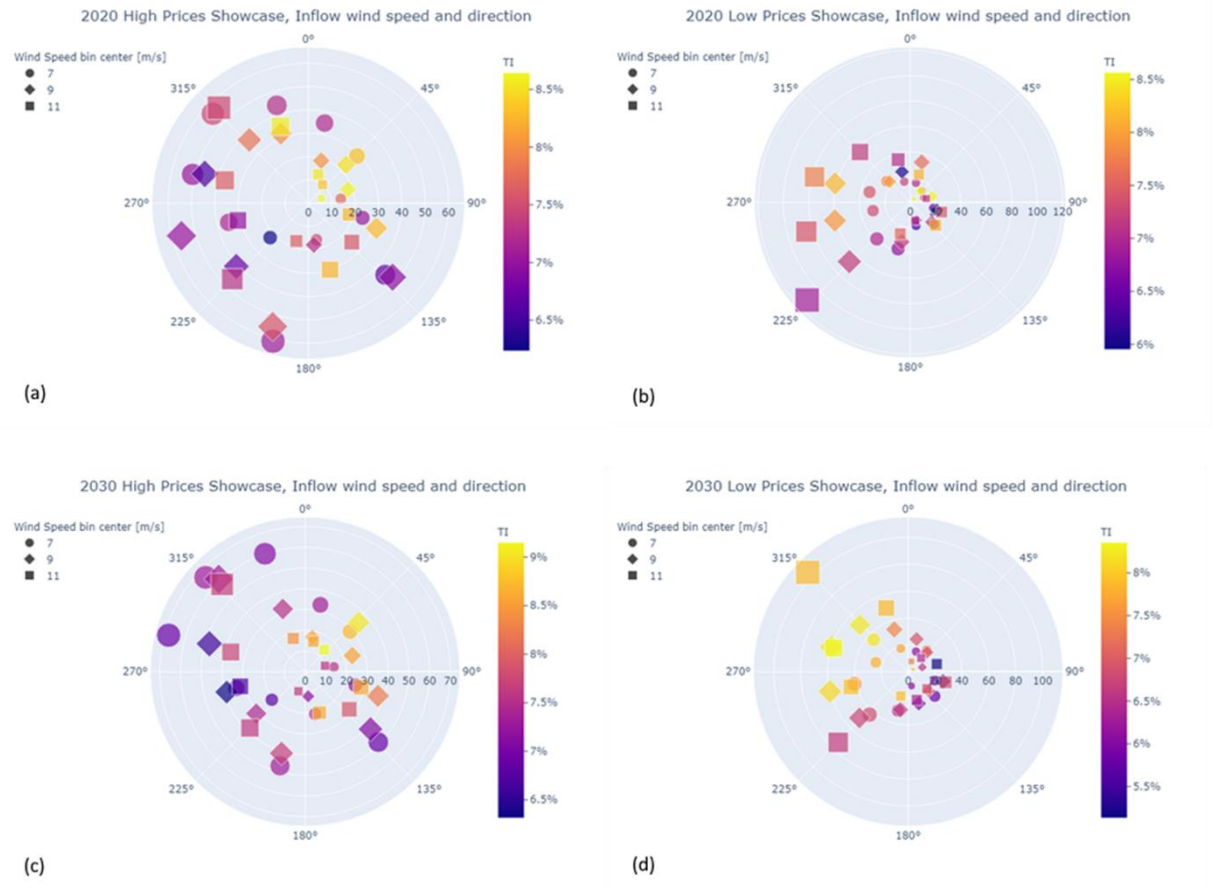


Figure 1: Overview of the meteorological data for High and Low electricity prices Market Showcases. The symbols show the wind speed bins in the region of interest for WFFC. The colour indicates the ambient turbulent intensity levels per wind direction sector. The frequency on the x-axis refers to the number of hourly samples available for particular inflow case within the indicated market showcase.

These showcases were based on the Total Control Reference Windfarm (TC-RWP) and on a time series of weather simulations and estimated electricity prices for 2020 and 2030, generated using the DTU Balancing Tool Chain. The weather simulations for the chosen location of the TC-RWP in Western Denmark are run using data from 2012. The North Sea region is included in the energy systems modelling, and hourly day-ahead prices in the relevant Danish price region (DK1) are obtained. The spot-market prices are used as fixed inputs for the TC-RWP in the showcases. The 2020 and 2030 scenarios are both based on the same weather data but are coupled with different energy systems representing the composition in 2020 and 2030 (electric loads, CO2 price, installed generation capacities, etc.). Figure 1 illustrates the weather simulations binned with respect to high and low electricity prices for 2020 and 2030 scenarios. Table 1 summarizes all the market showcases, where the weather input for TSO-driven case is to be considered as continuous hourly time series for
July and August periods of the weather simulation year 2012.

1.	**High Electricity Prices**
1.1	Highest 25% of **2020** DA prices + **Figure 1(a)** as inflow
1.2	Highest 25% of **2030** DA prices + **Figure 1(c)** as inflow
2.	**Low Electricity Prices**
2.1	Lowest 25% of **2020** DA prices + **Figure 1(b)** as inflow
2.2	Lowest 25% of **2030** DA prices + **Figure 1(d)** as inflow
3.	**TSO-driven**
3.1	Maximum **75% of the rated capacity of TC-RWP** + hourly weather time series for July and August in provided meteorological year 2012

Table 1: Summary of the FarmConners Market Showcases

The showcases were first advertised at the Wind Integration Workshop 2020 to encourage researchers to simulate their WFFC approaches using realistic market prices. The work in this presentation will show the preliminary simulation results submitted by the researchers and hence begin to determine the economic benefit that WFFC can bring to wind farm operators.

References:
Kheirabadi, A. and Nagamune, R. (2019). A quantitative review of wind farm control with the objective of wind farm power maximization. Journal of Wind Engineering and Industrial Aerodynamics, 192, pp. 45 – 73
Knudsen, T., Bak, T. and Svenstrup M. (2015). Survey of wind farm control – power and fatigue optimization. . Journal of Wind Engineering and Industrial Aerodynamics, 18, pp 1333 – 1351

Mini-Symposium: Wind Farm Control (II)

Increasing Turbine Density for Wind Plants Through Combined Layout and Yaw Optimization

Christopher J. Bay*, Andrew P. J. Stanley, John Jasa, and Jennifer King
National Renewable Energy Laboratory
*Presenting author

Keywords: wind farm optimization | wake steering | co-design | wind farm layout

Turbine layouts in wind plants are often designed to minimize wake interactions between turbines to increase energy production. Wake steering is the control strategy in which a turbine is yawed away from the incoming wind direction to induce a deflection on its wake downstream. This deflection can steer the wake away from downstream turbines resulting in an overall increase in energy production for the plant. The model of wake steering used in the optimizations is the Gauss-Curl Hybrid (GCH) model [1] implemented in the control-oriented wind farm software known as FLORIS [2]. When a turbine is yawed away from the incoming wind direction, counter-rotating vortices are produced which increase mixing in the wake and cause the wake deflection [3, 4]. The GCH model includes analytic descriptions of these physics known as secondary steering and yaw added recovery, capturing these effects in a computationally feasible model. See [1] for more details.
In this work, we present results from combined layout and yaw optimizations that give increased density of wind turbines while producing the same amount of energy. These optimizations are along a single line of turbines that could only move in the x-direction to illustrate the potential of wake steering for increasing wind turbine density.
The optimizations consisted of two initial inter-turbine spacings (7 and 9 rotor diameters, or 7D and 9D) for varying numbers of turbines from 2 to 9. The turbine model used is the NREL 5MW reference turbine [5] with a rotor diameter of 126 m. The wind was assumed to be in line with the turbines and at 8m/s. The optimization minimizes the average distance between the turbines, subject to constraints. Constraints included an initial energy production constraint such that the optimized layout/yaw solution is required to produce the same energy as the initial aligned layout.
Furthermore, a minimum spacing constraint of 3D was implemented between the turbines for practical purposes as well as the accuracy of the GCH model in the near wake. The design variables of the optimization included the turbine positions in the x direction as well as yaw settings for each turbine, giving 2*n number of variables where n is the number of turbines. The optimization algorithm used was SLSQP implemented in the python module SciPy [6] and the code used to produce these results is available on the FLORIS GitHub repository [2].

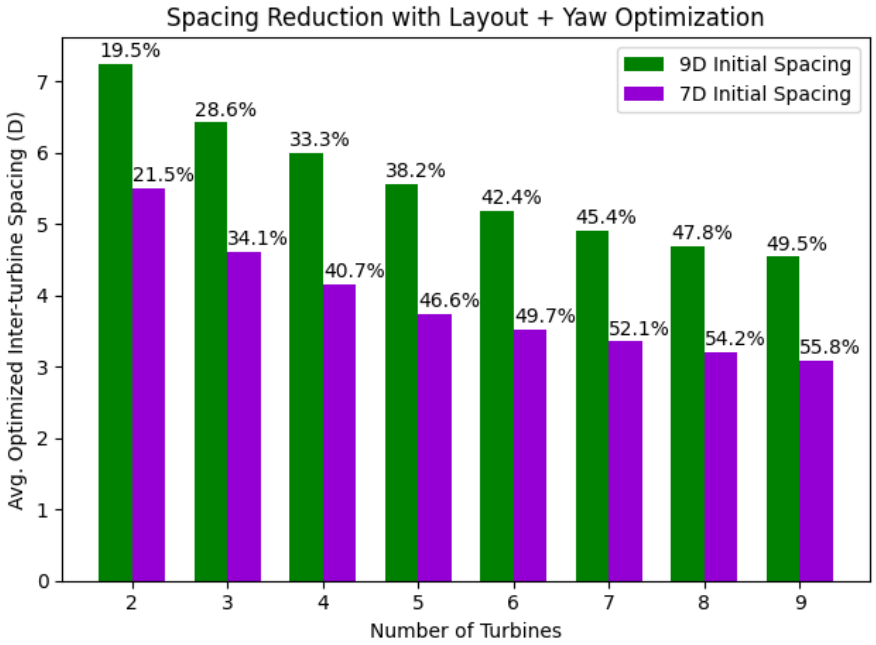


Figure 1: The 1-dimensional spacing reductions achieved by layout and yaw optimization while maintaining the energy output of the initial layout. Optimizations were run for two initial spacings (7D and 9D, each with their own initial energy output) with a varying number of turbines. The greatest relative reductions in spacing (shown in percentages) came from layouts with higher number of turbines.

Average inter-turbine spacings achieved with the optimizations are shown in Figure 1. As the number of turbines increases, denser turbine arrays are achievable while maintaining the initial energy output. This is most likely because of the increased flexibility that comes with more turbines being able to recover energy due to wake steering. Furthermore, the initial 7D layout produced denser arrays as the initial energy production of the 7D layout is less than the 9D layout.

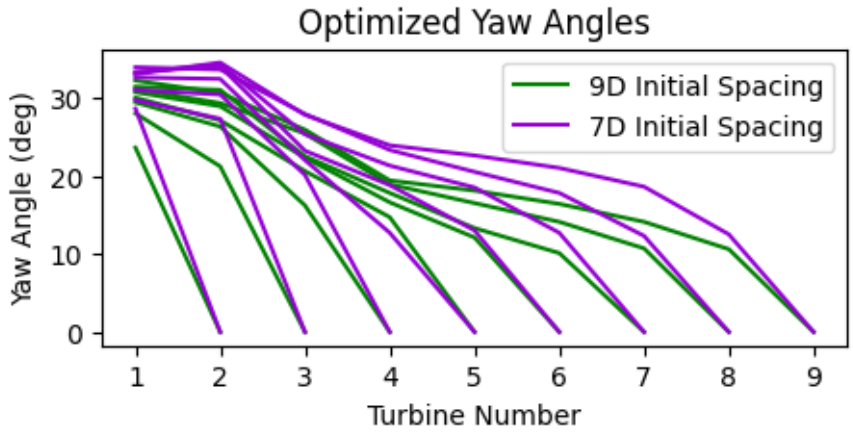


Figure 2: Optimized yaw angles for each of the combined layout and yaw optimizations. The highest yaw angles are found in the most upstream turbines, while generally decreasing thereafter until reaching zero for the last turbine. This trend matches published results from wind tunnel studies [8].

Figure 2 shows the yaw angles produced by the optimizations for each of the cases. The most upstream turbines show the most yaw, which then generally decreases with each downstream turbine, in line with wind tunnel studies [7]. Overall higher yaw angles are observed for the 7D initial spacing, which is needed due to their smaller optimized layouts. Further work is needed to determine possible densities for full wind plants, but these initial results show promise for significant increases.

References:

[1] King, J., Fleming, P., King, R., Martínez-Tossas, L.A., Bay, C.J., Mudafort, R. and Simley, E., 2020. Controls-oriented model for secondary effects of wake steering. Wind Energy Science Discussions, pp.1-22.
[2] FLORIS. Version 2.2.4 (2020). Available at https://github.com/NREL/floris.
[3] Shapiro, C.R., Gayme, D.F. and Meneveau, C., 2018. Modelling yawed wind turbine wakes: a lifting line approach. Journal of Fluid Mechanics, 841.
[4] Martínez-Tossas, L.A., Annoni, J., Fleming, P.A. and Churchfield, M.J., 2019. The aerodynamics of the curled wake: A simplified model in view of flow control. Wind Energy Science (Online), 4(NREL/JA-5000-73451).
[5] Jonkman, J., Butterfield, S., Musial, W. and Scott, G., 2009. Definition of a 5-MW reference wind turbine for offshore system development (No. NREL/TP-500-38060). National Renewable Energy Lab.(NREL), Golden, CO (United States).
[6] Virtanen, P., Gommers, R., Oliphant, T.E., Haberland, M., Reddy, T., Cournapeau, D., Burovski, E., Peterson, P., Weckesser, W., Bright, J. and van der Walt, S.J., 2020. SciPy 1.0: fundamental algorithms for scientific computing in Python. Nature methods, 17(3), pp.261-272.
[7] Bastankhah, M. and Porté-Agel, F., 2019. Wind farm power optimization via yaw angle control: A wind tunnel study. Journal of Renewable and Sustainable Energy, 11(2), p.023301.

Electrical design and control for grid code compliance and ancillary service provision

Til Kristrian Vrana*
SINTEF Energi
*Presenting author

Keywords: Grid Code Compliance | Ancillary Services | Wind Power Plant Control | Auxiliary Equipment

The design of the wind power plant control is determined by the main control objective. This has traditionally been pure energy supply to the extreme case of an ideal grid, focussing on maximum power tracking, and todays control system are generally designed around this underlaying main target. This can be seen as wind-determined wind power plant control.
Another possible objective could be the power supply of an electrical load with fluctuating power demand, without any other parallel sources of supply. This could be seen as the other extreme (as compared to the ideal grid), where maximum power tracking becomes irrelevant. This could be seen as grid-determined wind power plant control.
The reality lays somewhere between these two extreme objectives, but as the "Energiewende" is gradually being implemented, the objective slowly shift from the first to the second extreme case.
While maximum power tracking remains important, additional control features for grid code compliance have come and their extend is increasing with steadily stricter grid code requirements.
Ancillary service provision also adds control side-objectives, weakening the dominating role of maximum power tracking.
When looking far into the future (e.g. 2050) the situation will be much closer to the second extreme than what we are used to. In windy nights, wind power might easily become the only relevant source of power in the grid, and maximum trackable power can often exceed demand. Grid code requirements will be (must be) much stricter than today, and ancillary service provision will play an important role. Wind power plants will need to supply the amount of power that the grid needs at that exact moment. Will maximum power tracking based control be a good approach in such a future?

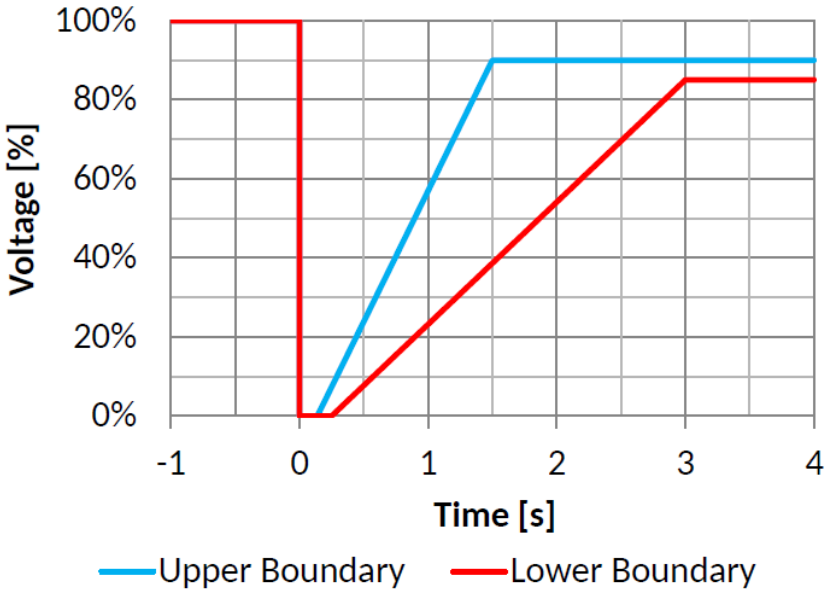


Figure 1: Example of the fault ride through requirement as provided by ENTSO-E.

Generally, there are two approaches how a wind power plant can comply to grid code requirements and provide ancillary services. It can be done through:

1. The wind turbine controllers (or wind power plant controllers)
2. Additional equipment (at turbine or power plant level)

As an example, Fault-ride-through capability can be provided through controls, but this is resulting in a rotor speed increase that has to be handled. The problem can also be solved with additional electrical equipment that can waste excess energy during the grid fault. This enables the wind turbine controller to more or less "ignore" the grid fault, as it can rely on a more reliable energy consumption even in case of a grid fault.

Provision of virtual inertia introduces grid-frequency-dependent power output fluctuations. Adding a battery as an energy storage emulating the rotating kinetic energy of the "virtual grid side generator" enables wind power plant control to avoid larger changes. However, using the kinetic energy from the rotor manipulates normal rotor speed control and therefore affects the overall turbine control.

Adding additional equipment costs money, but it can reduce control complexity and mechanical loads (fast torque fluctuations), which can imply cost savings. In the end, it is an economical optimisation decision, where the cost for extra equipment are quite easy to quantify, while the cost of added control complexity and mechanical load pulses might be much harder to quantify. In the future, with stricter requirements and more ancillary service provision, this questions on "how to provide the desired response" will come back many times, where the electrical design directly influences the control.

Bankability of Wind Farm Control

Lars Landberg*, Ervin Bossanyi, Renzo Ruisi, Nicholas Skeen, Giuseppe Ferraro, Matthew Harrison, Keir Harman, Andreas Manjock, Nikolai Hille, and Anja Neubert
DNV GL
*Presenting author

Keywords: Wind farm control | Bankability | modelling | uncertainty

Wind farm control has recently started its journey from being a purely academic discipline to a method that gets implemented in and controls operating wind farms. For this journey to be a success it is necessary to ensure that all stakeholders in the process are aligned and in agreement about the models to use, the benefits and the associated uncertainties. Of particular interest is when wind farm control can be considered bankable. A method/process/procedure is defined as bankable when there is an acceptance in an entire industry – amongst banks, investors, insurance, manufacturers, consultants, certification bodies etc – that it is robust, well-defined, with a proven track record, effects known and uncertainties understood to such a level that loans and investments can be safely employed. In this paper we will describe the stages that we propose are required to go for wind farm control from being experimental/potential to bankable. A progression is proposed where potential is the first stage, the next stage is validated, this moves into investable and finally ends with bankable. The requirements for each of these stages will be described in detail in the paper.
In order to move from one stage to the next a number of requirements needs to be fulfilled, these include reliability of models, validation of models, number of successful experiments conducted, and robustness of uncertainty estimates (see image 1). During the process of developing these stages it was realised that a further level of granularity is required: different applications might have different requirements. Therefore, each of the stages will need to be discussed taking the specific requirements of the development (pre-construction) phase, retrofitting (post-construction) phase, OEMs, and certification into account.
The outcome of the analysis will be presented in the paper, where each requirement for each stage will be detailed.

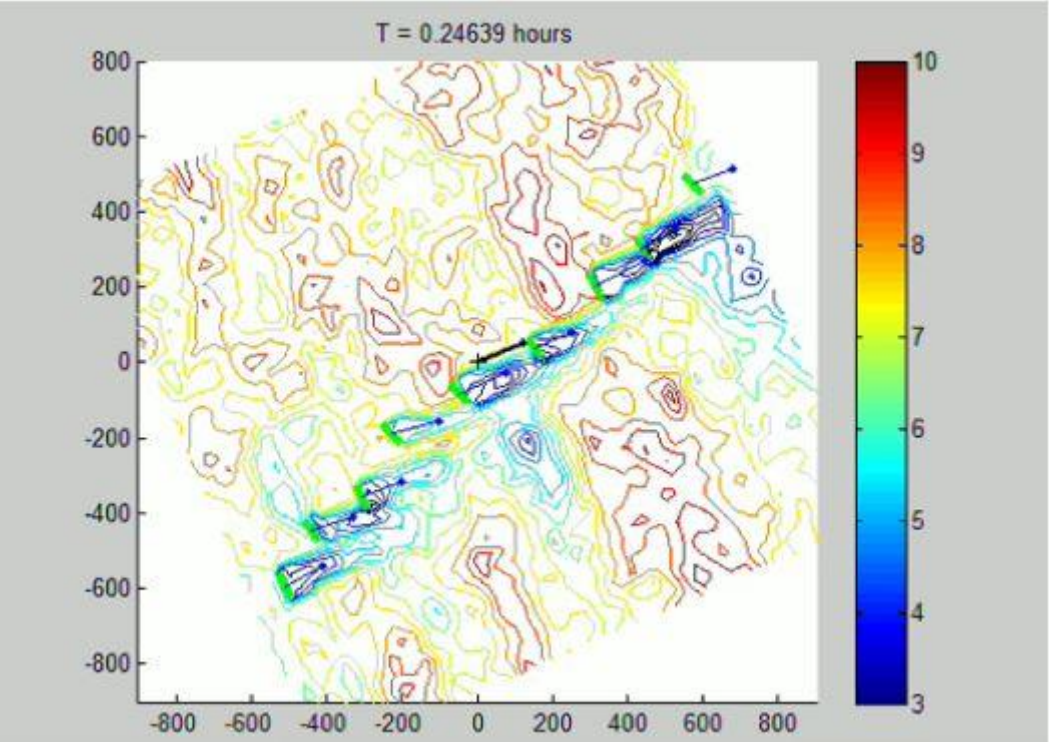


Figure 1: Modelling flow in a wind farm

Method

Through an analysis of each of the potential applications of wind farm control, combined with input from stakeholders, a list of requirements was drawn up and the level that these requirements were to be met determined. Granularity was necessary in order to make sure that different applications were treated appropriately. Proposal were drafted and discussed within a wide group of experts.

Results

The results of the analysis and discussions were that a certain level of granularity was indeed required, and in the presentation the specific requirements for each of the stages (potential, validated, investable, and bankable) and for each of the applications (pre-, post-construction and OEM) will be described.

Conclusions

It is clear that the wind energy industry is moving towards bankability of wind farm control. Our analysis has shown that we are not there yet, however, and we have detailed what is required to move wind farm control through the different stages.

Wind farm performance optimization from design phase

Elena Cantero*, Joseba Garciandia, and Irene Eguinoa
CENER
*Presenting author

Keywords: Wind farm performance | optimization | wind farm design phase | wind sector management | effective turbulence intensity

In the design and development phase of a wind farm, a site suitability assessment of each wind turbine must be carried out according to the IEC 61400-1 standard [1].
Depending on the site conditions, the distribution of the wind turbines and the distances between them, some or all of the turbines within a wind farm may be influenced by the wake effects from nearby machines. This is affected not only by the farm layout but also by the orography of the site.
The wake effects create added turbulence in the wind [2], which can affect turbines increasing their loads.
For some wind farms, it may be necessary to even shut down certain turbines for certain wind conditions. This is usually referred to as Wind Sector Management (WSM) strategy [3] [4]. And the way in which the WSM strategy is defined could result in a reduction of the energy production of the wind farm. Such strategies are already defined at the design phase of the wind farm, impacting the return of investment calculation for the farm.
The definition of this WSM strategy consists of, for each pair of turbines, deciding which one to shut down, the turbine upstream (the one creating the turbulence) or the one downstream (the one suffering the increased loads). In many cases, this is usually a manual and user-dependent process that does not guarantee obtaining the optimal result and that can be a time consuming and costly task depending on the size of the wind farm.
In order to obtain a strategy that minimizes energy losses and whose calculation is traceable and repeatable; an optimization process based on genetic algorithms has been developed for the definition of this WSM strategy.
The result is a tool, CePO (CENER Production Optimizer), which optimizes the performance of wind farm operation by an automated WSM strategy definition that maximizes wind farm production and minimizes effective turbulence intensity in each wind turbine position. In addition, the tool reduces user dedication time and ensures traceability and a systematic procedure.

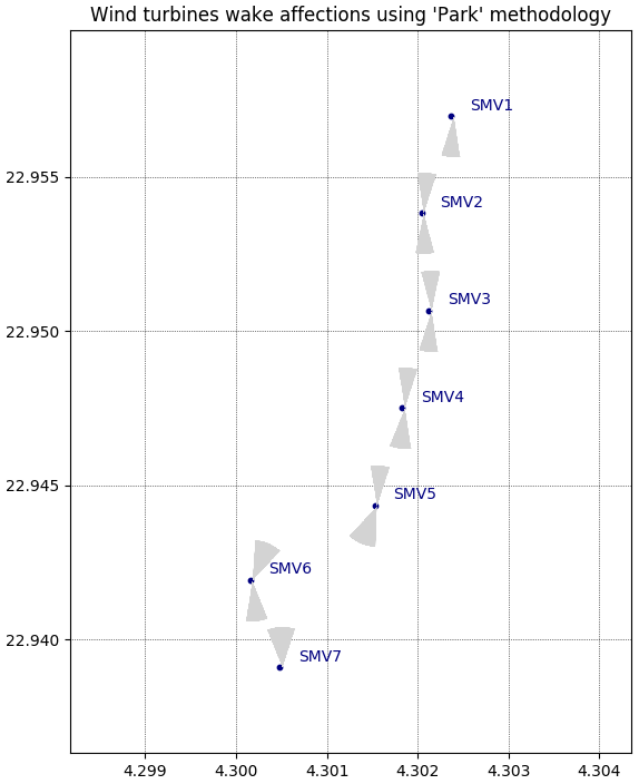


Figure 1: Layout of the SMV Wind Farm and wake affections angles in each turbine according to Park methodology.

As an example, Sole du Moulin Vieux (SMV) onshore wind farm in France , made up of 7 wind turbines [5] (see Figure 1), has been analyzed with CePO. In several of the positions the value of the effective turbulence intensity obtained exceeds the value of the subclass A turbulence intensity to which the installed wind turbine belongs. A WSM stop strategy has been manually defined to reduce these values. This strategy represents an energy loss of 3.50%. The same process has been carried out with CePO and the strategy obtained represents a loss of 2.33% (see Figure 2).

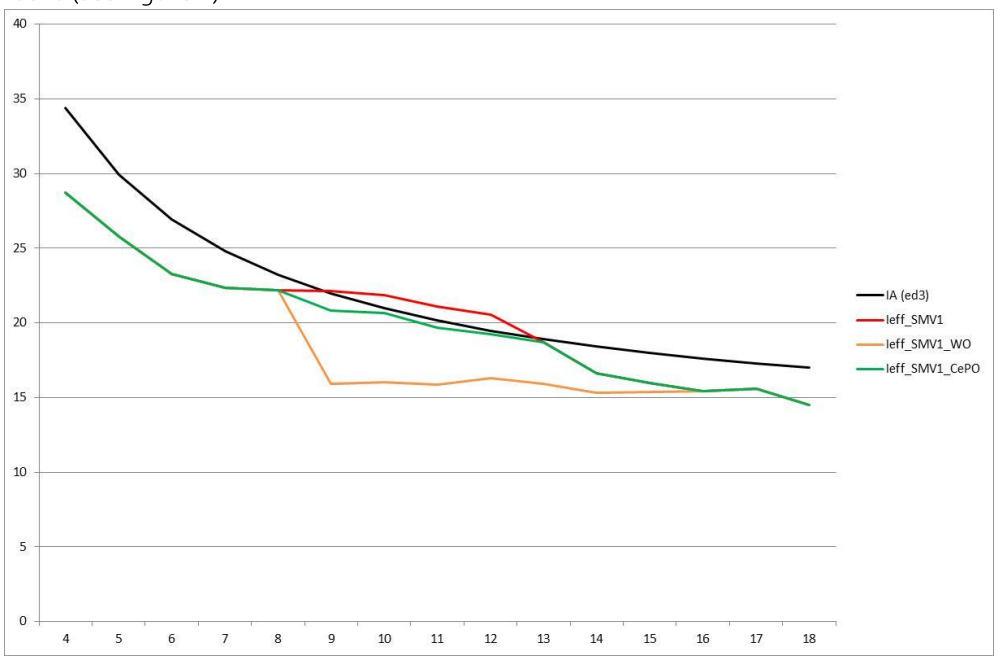


Figure 2: Effective turbulence intensity at SMV1, without WSM strategy (red line), with no optimized WSM strategy (orange line) and with CePO optimized WSM strategy (green line).

The conclusions obtained from this exercise are that CePO minimizes the losses associated with usual WSM strategies, reduces the time to obtain results and assures repeatability and optimum finding.

References:
Bossanyi, E. and Jorge, T. (2016) 'Optimisation of wind plant sector management for energy and loads', in 2016 European Control Conference (ECC), pp. 922–927. doi: 10.1109/ECC.2016.7810407.
Duc, T. et al. (2019) 'Local turbulence parameterization improves the Jensen wake model and its implementation for power optimization of an operating wind farm', Wind Energy Science, 4(2), pp. 287–302. doi: 10.5194/wes-4-287-2019.
Frandsen, S. T. (2007) Turbulence and turbulence- generated structural loading in wind turbine clusters, Risoe National Laboratory. Risoe-R; No. 1188.
Iec61400-1 (ED3) 2005-08 (2005) Wind turbines - Part 1: Design requirements. doi: 10.5594/J09750.
Nielsen, M., Jørgensen, H. E. and Frandsen, S. T. (2009) 'Wind and wake models for IEC 61400-1 site assessment', European Wind Energy Conference and Exhibition 2009, EWEC 2009, 6, pp. 3765–3770.

Mini-Symposium: Wind Farm Control (III)

Towards Dynamic Wind Turbine Wake Control for Lowered Cost of Energy

Kenneth Brown*, Nathaniel deVelder, Daniel Houck, David Maniaci, Carsten Westergaard, Joshua Paquette, and Christopher Kelley
Sandia National Laboratories
*Presenting author

Keywords: dynamic wake control | wake recovery | near-wake length | tip vortex | mutual inductance instability

One of the largest remaining opportunities to reduce the cost of wind energy comes from substantial gains in the understanding of complex wind plant aerodynamics and atmospheric phenomena, according to the U.S. Department of Energy (Zayas, 2014). As evidence, measurements over a range of modern wind plants across Europe (Nygaard, 2014) and the U.S. (El-Asha et al., 2017) show that the second row of turbines in a wind plant captures around 20% less power than the first when the turbines are aligned with the wind, and this falls to around 40% for turbines located deep within the array. Advances in wind plant layouts and wake steering techniques can improve plant performance, but the turbine spacing is still fundamentally constrained by the turbine wake. In addition to this performance aspect, the turbulence of wakes significantly degrades the fatigue life of downstream turbines (Herges et al., 2018). These problems can be traced back to the failure of the wake to fully "recover" from its depleted state after passing momentum to the turbine blades.
A fundamentally more appealing turbine control paradigm, which has begun to receive serious attention, is to leverage the turbine as a flow actuator to dynamically excite unstable modes in the wake, thereby producing accelerated wake breakdown and recovery. With a low-fidelity approach, Brown et al. (2021) has recently demonstrated a dynamic wake control (DWC) treatment showing up to 80% reduction in near-wake length as shown in Figure 1. The DWC treatment approach is to harmonically vary the turbine rotation rate and blade pitch to influence the flow behind the turbine.

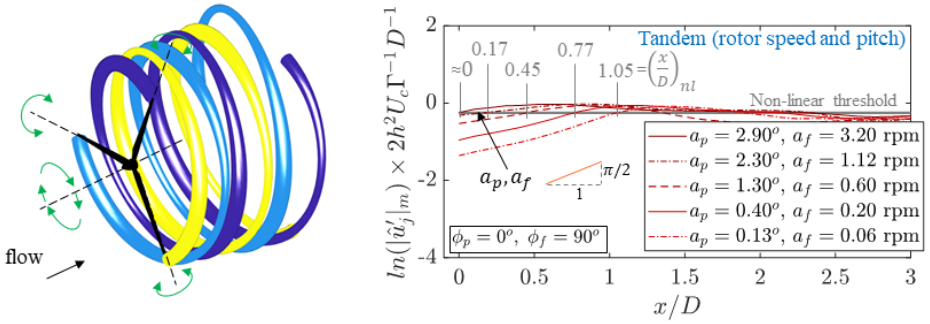


Figure 1: Free-vortex wake method results from Brown et al. (2021). Left: Example of trajectory of the outermost tip vortex filaments (displacements scaled for clarity). Right: Growth of maximum instability Fourier coefficients along the axial coordinate with tandem harmonic actuation. The effects of rotor inertia, blade aeroelasticity, drivetrain dynamics, and pitch-speed interaction are not considered.

With appropriate actuation, tip vortex structures behind the turbine are intentionally paired together to excite the mutual inductance instability and initiate the desired wake recovery.
A shortcoming of the preliminary DWC scheme, and indeed of most of those in related literature (the term dynamic induction control, or DIC, is also used in literature), is the failure to adequately address a critical remaining risk to industry buy-in: the cost/benefit of the DWC approach including turbine lifetime considerations. A question arises: how large of a net wind plant power gain can be realized without significantly decreasing turbine lifetime?

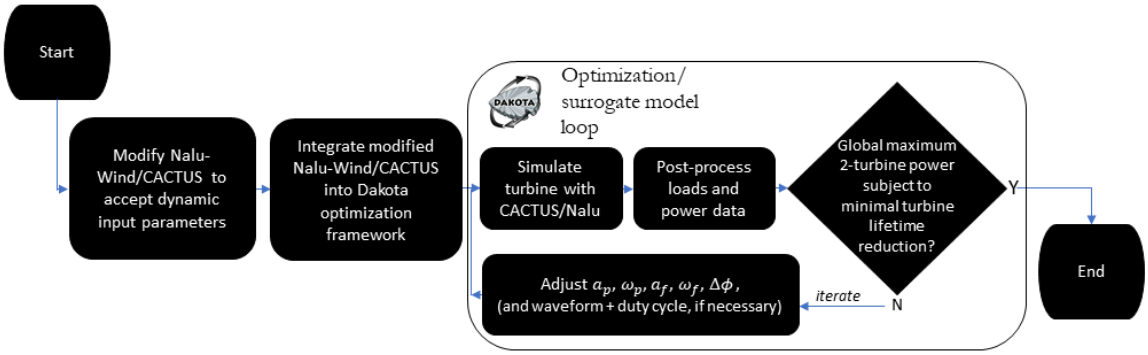


Figure 2: Schematic of the optimization workplan for the ongoing work. Parameters for adjustment include dynamic pitch amplitude and frequency, a_p and \omega_p, respectively, dynamic rotor speed amplitude and frequency, a_f and \omega_f, respectively, as well as phase offset between the two control vectors, \Delta\phi.

The current ongoing work centers on optimizing the nascent DWC scheme to maximize power of a simple two-turbine array while constraining the increase in cyclic loads on both turbines. The approach, diagramed in Figure 2, will ultimately leverage the Dakota optimization framework, which offers the potential to appropriately delegate some expensive objective function evaluations of a requisite high-fidelity model to a lower-fidelity one, thus critically enabling the expensive optimization problem. The high-fidelity model is the state-of-the-art multi-physics simulation code Nalu-Wind in actuator line formulation (Domino, 2015). This code will be complimented in the future by the mid-fidelity free vortex code CACTUS (Murray and Barone, 2013). Both codes will be adapted to take as inputs DWC actions for blade pitch and rotor speed.

This presentation details the progress to-date towards the above workplan. The ultimate outcome of the optimization will yield not only a global optimum but also sensitivities of the best performing cases to the DWC parameters, such as the actuation amplitudes, frequencies, and phases. Such knowledge, coupled with corresponding sensitivities of damage equivalent loads for each DWC scheme, will offer a window into the potential of DWC for reduced cost of energy.

References:

BROWN, K., HOUCK, D. & MANIACI, D. C. Rapidly Recovering Wind Turbine Wakes with Dynamic Pitch and Rotor Speed Control. AIAA Scitech 2021 Forum, 2021. 1182.

DOMINO, S. 2015. Sierra low mach module: Nalu theory manual 1.0. SAND2015-3107W, Sandia National Laboratories Unclassified Unlimited Release (UUR).

EL-ASHA, S., ZHAN, L. & IUNGO, G. V. 2017. Quantification of power losses due to wind turbine wake interactions through SCADA, meteorological and wind LiDAR data. Wind Energy, 20, 1823-1839.

HERGES, T., BERG, J. C., BRYANT, J., WHITE, J., PAQUETTE, J. & NAUGHTON, B. T. Detailed analysis of a waked turbine using a high-resolution scanning lidar. Journal of Physics: Conference Series, 2018.

MURRAY, J. C. & BARONE, M. 2013. CACTUS User's Manual. Sandia National Laboratories, Albuquerque, NM.

NYGAARD, N. G. Wakes in very large wind farms and the effect of neighbouring wind farms. Journal of Physics: Conference Series, 2014. IOP Publishing, 012162.

ZAYAS, J. Wind Overview. Sandia 2014 Wind Turbine Blade Workshop, 2014 Sandia National Laboratories.

Mid-fidelity simulations and comparisons of five techniques for axial induction control of a wind turbine

Dan Houck*, David Maniaci, and Chris Kelley
Sandia National Laboratories
*Presenting author

Keywords: axial induction control | derate | free vortex wake method | simulation | wakes

As wind energy progresses, attention has shifted from optimizing individual turbines to optimizing wind farms to mitigate the negative effects of upstream turbines' wakes. In addition to turbine siting, there has been very promising research into coordinating turbine controls within a wind farm to maximize its total power. Axial induction control (AIC) is one method that has been heavily researched, and it involves derating upstream turbines for the benefit of downstream turbines. By reducing the power production of upstream turbines, the effects of their wakes are mitigated and downstream turbines produce more power as a result. The net result of this is an increase in total power.

Previous research into AIC has produced mixed results and has been largely inconclusive as to its effectiveness. Some of the inconclusiveness of previous studies can be attributed to two particular criticisms: the use of low-fidelity wake models and the oversimplification of turbine controls. First, low-fidelity models approximate, or simply do not include, wake dynamics that are known to be important to the wake decay process. Second, many previous studies do not differentiate among the multiple combinations of controls that may achieve the same power production. There is an infinity of combinations of pitch and tip speed ratio (TSR) that can produce a particular derate (see Figure 1).

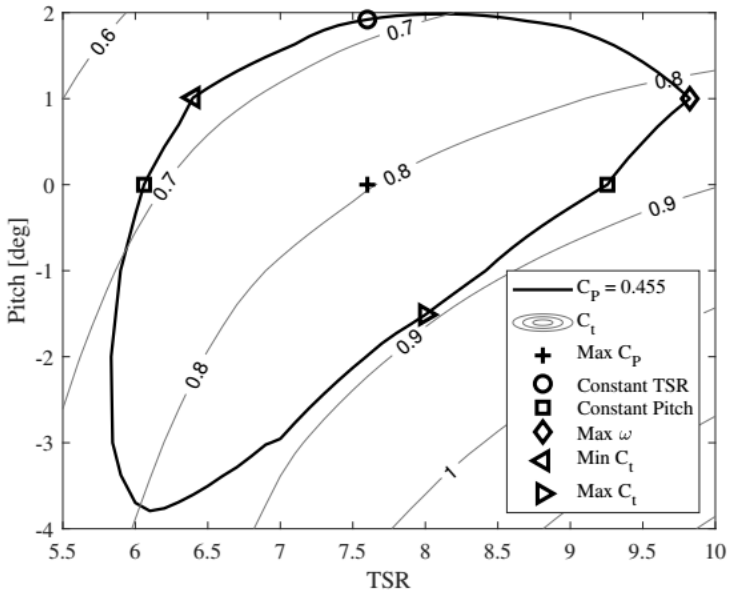


Figure 1: A contour curve of constant CP as a function of pitch and TSR showing five different possible ways of achieving it when derating from the maximum CP.

Low-fidelity models, and even some higher fidelity methods, only provide details of the target power for the derate or an alternative such as the target thrust or induction. How the derate is achieved affects the qualities of the wake that is produced, so this information is vital to understanding the success or failure of an AIC method.

This study aims to address these challenges in researching AIC by using a mid-fidelity free vortex wake method (FVWM) to simulate a turbine operating with a variety of derates. FVWMs provide higher accuracy than blade element momentum (BEM) methods or wake models at computational speeds that are much faster than LES



or direct numerical simulations (DNS) and can include the effects of a turbine's pitch and tip speed ratio, and so its induction and thrust as well. To further investigate the multiple pathways to a given target power when derating, we evaluate the differences in the wake when using five different strategies to achieve derates of 10%, 20%, and 40% of the baseline power production: constant pitch, constant tip speed ratio, maximum rotation rate, minimum thrust, and maximum thrust. When considering the simulated turbine and a virtual downstream turbine, our results indicate that minimizing the thrust of the derated turbine yields the highest combined power of the two turbines, though the placement of the downstream turbine is an important consideration in choosing a derate method as the rates of decay and spatial distributions of energy vary considerably among the methods.

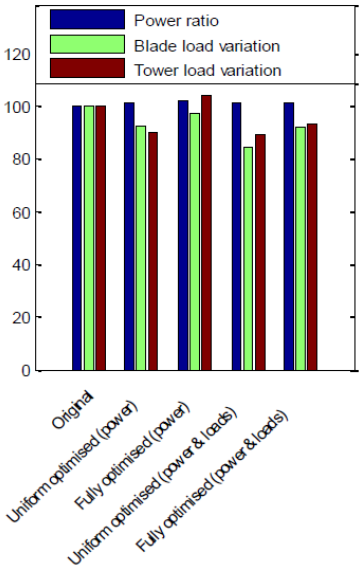
Sandia National Laboratories is a multimission laboratory managed and operated by National Technology & Engineering Solutions of Sandia, LLC, a wholly owned subsidiary of Honeywell International Inc., for the U.S. Department of Energy's National Nuclear Security Administration under contract DE-NA0003525.

Simple induction control scheme for wind farms

Ervin Bossanyi
DNV GL

Keywords: Wind farms | Induction control | Setpoint optimisation | Wake effects | Wind turbine loads

In the context of wind farm control, induction control involves reducing the power output of some turbines to weaken their wakes, allowing downstream turbines to produce more. In principle this could result in an overall gain in energy capture. Any gain is likely to be small, perhaps of the order of 1% depending on many factors such as wind farm layout and wind conditions, but this is worthwhile if it can be demonstrated to be achieved reliably. Furthermore, it is likely to be accompanied by a reduction in turbine fatigue loading, which may, for example, be utilised to extend the plant lifetime.
To date, practical realisations have used whole-farm optimisation procedures to generate tables of control setpoints for each individual turbine, which vary with wind speed and direction, and maybe turbulence or atmospheric stability. Few full-scale field test results have been reported, but van der Hoek, D et al (2019) and Bossanyi and Ruisi (2020) have given some indications of positive results.
Calculated optimal setpoints will depend critically on the accuracy of the wake model used, and if poorly defined, could even decrease rather than increase the power gain. This paper explores a simplification of the concept, which would give a lower power gain but might prove more robust.
Compared to the optimal "greedy" control setting for a single turbine, a suboptimal setting is calculated which sacrifices a small amount of power while reducing the thrust more significantly.
Applying this setting to all turbines in the wind farm could already result in an increase in overall power production, because of the reduced wake losses resulting from lower thrust. In other words, even with all turbines having identical control setting, the optimal setting in the wind farm context is different from the optimal setting for a stand-alone turbine.



	Power	Blade root load	Tower base load
Original	1.0000	1.0000	1.0000
Uniform optimised (power)	1.0144	0.9234	0.9005
Fully optimised (power)	1.0171	0.9719	1.0428
Uniform optimised (power & loads)	1.0141	0.8437	0.8893
Fully optimised (power & loads)	1.0154	0.9167	0.9339

Figure 1: Overall result of different schemes

Figure 1: Overall result of different schemes

Some example results are given for Lillgrund wind farm, which is the subject of research as part of the EU project TotalControl (www.totalcontrolproject.eu). This wind farm has an unusually tight layout, which is favourable for exploring ways to mitigate the resulting large wake losses. Figure 1 gives the results for one particular wind speed and direction of four different optimisation schemes, compared to the normal ("greedy") turbine settings, showing total power and a measure of the amount of variation between turbines of two key

damage equivalent loads. The 'uniform optimised' cases use a common setting across all turbines, while the 'fully optimised' cases calculate a different setting for each turbine. In terms of power, the uniform case already achieves 84% of the power increase of the fully optimised case, and is more beneficial for loads. Results ('power and loads') are also shown for optimisations against a weighted merit function with 90% weighting on power and 5% on each of the loading measures, showing that if desired, some of the power gain can be sacrificed to further reduce the load variations.

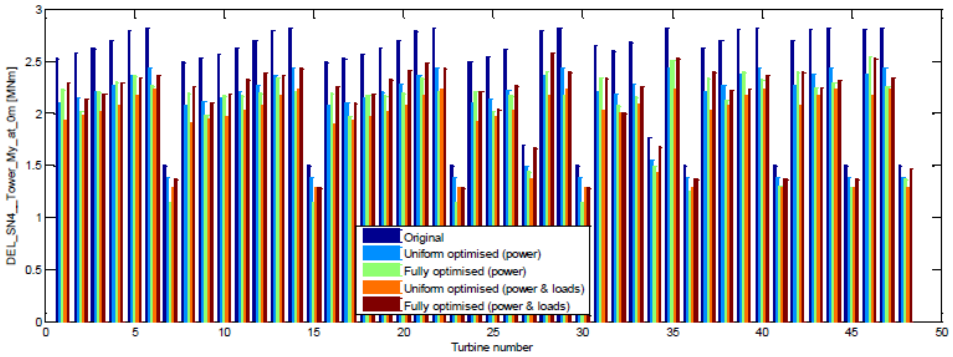


Figure 2: Damage equivalent tower base loads for each turbine with the different schemes

Figure 2: Damage equivalent tower base loads for each turbine with the different schemes

Figure 2 illustrates how the damage equivalent loads on each turbine change with the different schemes.

References:
van der Hoek, D et al (2019), Effects of axial induction control on wind farm energy production – A field test, Renewable Energy 140 994e1003.
Bossanyi, E A and Ruisi, R (2020), Axial induction controller field test at Sedini wind farm, Wind Energ. Sci. Discuss., https://doi.org/10.5194/wes-2020-88, in review.

Exploiting vortex roll-up mechanism to promote wake recovery through a periodic and asymmetric collective pitch motion

Alessandro Croce* , Stefano Cacciola, Roberto Praticò, Sebastiano Stipa, Valerio Arcari, and Mariana Montenegro Montero
Politecnico di Milano
*Presenting author

Keywords: Dynamic Induction Control | Large Eddy Simulation | Vortex roll-up | Wind Farm Control | Fast Wake Recovery

Novel technologies aimed at promoting a faster wake recovery were recently proposed as a possible way to increase the power produced by the whole farm [1]. In fact, in a wind farm, downstream turbines will benefit from an accelerated recovery of the upstream rotor wakes in terms of produced power. Among all possibilities to achieve this goal, this paper focuses on the so-called dynamic induction control (DIC), which consists in a variation of the upstream rotor thrust generated through a suitable blade pitch motion, which, in turn, produces an in-wake mixing responsible for the faster recovery.
Even though this technique proved to be promising in silico and in wind tunnel tests [2], the physical mechanism generating the increased wake velocity is still to be fully understood. Clearly, an improved comprehension of DIC working principles may be exploited for synthesizing different controls able to boost those fluid-mechanics phenomena underlying DIC.
This paper deals with a CFD simulation campaign aimed at analyzing the fluid-mechanics of DIC and exploiting such knowledge to improve its effectiveness. The analyses were carried out with the software SOWFA coupled with OpenFAST [3, 4].

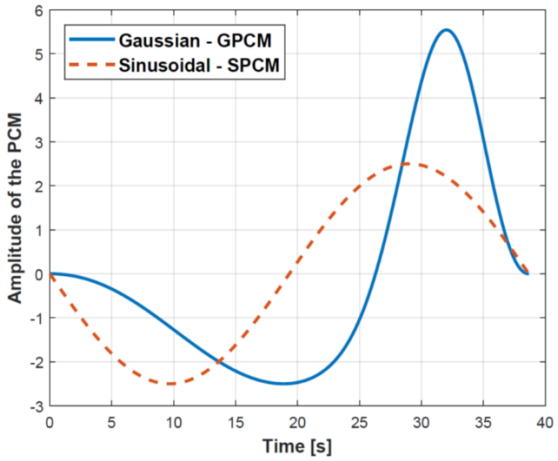


Figure 1: Pitch motion for SPCM (dashed line) and GPCM (solid line)

The simulations considered the reference 5MW wind turbine model [5] and an inflow condition with 9 m/s speed and 5% turbulence intensity. Figure 1 shows the two different zero-mean periodic pitch functions, with the same minimum value and period, used for generating DIC. The first (SPCM) is a classical sinusoidal function, while the second (GPCM) is a combination of Gaussian functions, with a significant asymmetry between the negative and positive peaks defined to boost DIC effectiveness.
At present, from the analyses already accomplished, it is possible to derive the following conclusions.
The near wake region is typically shielded from the outer flow by the vortices released at blade tips and re-energization starts in the far wake after such vortices dissipate. With dynamic induction control, the rotor releases vortices of variable magnitude creating regions of higher vorticity around which the shear layer may roll up easily, increasing the exchange of energy with the outer flow. The GPCM strategy boosts such

mechanism by anticipating the vortex roll-up, due to an increased difference between high and low vorticity cores, induced by the larger difference between pitch angle peaks.

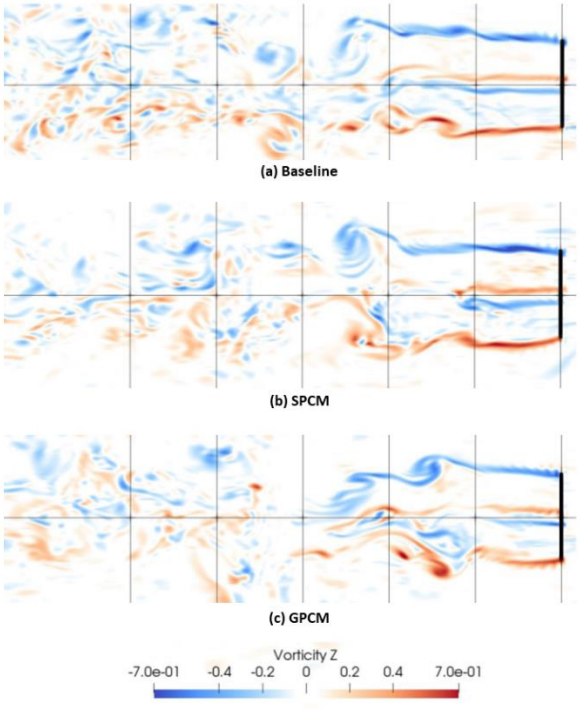


Figure 2: Vorticity plot in a horizontal plane at hub height at the instant of vortex roll-up

Figure 2 provides a demonstration for that. The plots represent the vorticity field in a horizontal plane at hub height at the instant of vortex roll-up. Rotor location and downstream distances multiple of diameter D are represented by black thick and thin lines, respectively. Clearly, in the baseline case (a), the vortex that rolls up at 2.5 D is not enough strong and dissolves at 3.5 D breaking into random vorticity. On the other side, in the SPCM case (b), a huge core of high vorticity rolls up at 2.5 D and lasts longer promoting the exchange of energy with outer flow. Finally, in the GPCM case (c), roll-up occurs before, at 1.5 D, yielding a sensible wake recovery already at 2 and 3D.
In the final presentation, the physics of the DIC will be explained in detail along with the quantification of the impact of SPCM and GPCM technique on the total power of a simple twoturbine farm.

Acknowledgement: we acknowledge the CINECA award under the ISCRA initiative, for the availability of high-performance computing resources and support.

References:
[1] Munters, W. and Meyers, J. (2018). Towards practical dynamic induction control of wind farms: analysis of optimally controlled wind-farm boundary layers and sinusoidal induction control of first-row turbines. Wind Energy Science, 3, pp. 409-425. Available at: https://doi.org/10.5194/wes-3-409-2018.
[2] Frederik, J.A. and Weber, R. and Cacciola, S. and Campagnolo, F. and Croce, A. and Bottasso, C. and van Wingerden, J.-W. (2020). Periodic dynamic induction control of wind farms: proving the potential in simulations and wind tunnel experiments. Wind Energy Science, 5(1), pp. 245-257. Available at: https://doi.org/10.5194/wes-5-245-2020.
[3] NWTC design code-SOWFA (2012). Churchfield, M. and Lee, S., National Renewable Energy Laboratory (NREL). Available at: http://wind.nrel.gov/designcodes/simulators/SOWFA.
[4] OpenFAST (2012). Jonkman, J.M. and Sprague, M., National Renewable Energy Laboratory (NREL). Available at: https://www.nrel.gov/wind/nwtc/openfast.html.
[5] Jonkman, J., Butterfield, S., Musial, W. and Scott, G. (2009). Definition of a 5-MW Reference Wind Turbine for Offshore System Development. Technical report - NREL/TP-500-38060. Available at: https://www.nrel.gov/docs/fy09osti/38060.pdf.

Adaptive time-series based wind farm optimization

Jonas Schmidt[1,*], Lukas Vollmer[1], Niklas Requate[1], and Tobias Meyer[1]
[1]Fraunhofer IWES
[*]Presenting author

Keywords: Wind farm control | Wind farm optimization | Wake steering | Wake effect

One widely used approach in wind farm control is based on separate sector-based optimizations for given inflow conditions per sector. The aim of these optimizations is to maximize power generation by reducing power of upwind turbines or by offsetting their yaw angle to reduce the wake effect on downwind turbines. Commonly, the optimization problem is solved by assuming steady-state wind conditions (wind speed, direction, turbulence intensity, etc). During actual wind farm operation, this assumption does not hold. Instead, continuous adaptation of all turbines is required.
In many approaches, the wind farm adaptation itself is based on an evaluation of inflow conditions and a selection of the best-fitting optimal solution. Therefore, the yawing dynamics are neglected inside of the optimization and only considered in a separate subsequent step (Bossanyi 2018; Doekemeijer 2020).
Failures or planned work in a wind farm imply changes in the wind farm configuration. Failures can include turbines running in local greedy control, e.g. due to a communication system fault that disconnects them from the wind farm controller. Planned work on turbines, e.g. maintenance, leads to a shutdown of individual turbines. These temporary changes must be considered.
Adaptation dynamics are mostly limited by the yawing dynamics of the wind turbines. For a sufficiently slow time step between two consecutive optimal solutions, yawing dynamics can be neglected. However, for faster adaptation cycles they must be considered. Another problem that is particularly difficult to resolve with a static sector-based optimization is the symmetry problem for wake steering, where a wake can be steered away from a downwind turbine to the same effect by either misaligning the upwind turbine with a yaw offset to the right or to the left. In sector-based optimization, these solutions are equal. However, in operation, a situation might arise where a leftsteering solution is best for one time step, but a right-steering solution is best for the following time step. Such sudden flipping changes in yaw angle should be avoided.

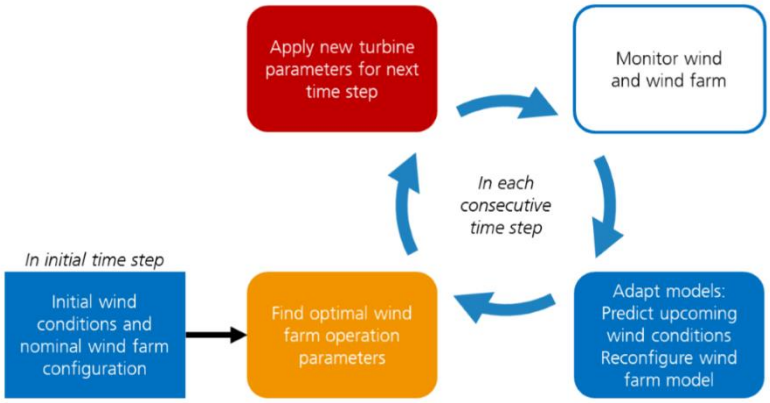


Figure 1: The proposed time-series based wind farm control algorithm.

We propose to solve these issues by periodically updating the turbine parameters in regular time steps, e.g., 10 minutes, cf. Fig. 1. Each parameter update is the result of an optimization that takes the current wind farm state into account and avoids large jumps in parameter space. This is realized by incorporating a penalty for large deviation from the current values. A crucial ingredient for our approach is the short-term prediction of the wind conditions for the next time step. In this work a very simple local weather prediction model is considered, based on the set of previously monitored conditions at each turbine.
During each step, the wind farm model is reconfigured to closely model the actual wind farm in this time instant. For turbines which are shut off or which are running in local greedy control, their behavior is included

in the model. The optimization of the next parameter step is then run based on the predicted upcoming wind conditions and the reconfigured wind farm model. For each wind prediction time step, the energy-optimal solution is computed independently. Our approach is similar to Model-Predictive Control and could be enhanced by a yaw dynamics model in the future.
This proof-of-principle type paper demonstrates the functionality and the benefit that arises from the described approach, based on widely tested in-house simulation tools.

References:
Bossanyi, Ervin (2018). Combining induction control and wake steering for wind farm energy and fatigue loads optimisation. Journal of Physics: Conference Series 1037, 32011. https://doi.org/10.1088/1742-6596/1037/3/032011.
Doekemeijer, B. M. (2020). Closing the loop in model-based wind farm control. Delft University of Technology. https://doi.org/10.4233/UUID:35022242-B3BA-48D9-B3F6-C6AB20B8CC19.

Curled wake shape evolution downstream of yawed wind turbines: a theoretical study

Majid Bastankhah[1,*], Carl Shapiro[2], Sina Shamsoddin[3], Dennice Gayme[2], and Charles Meneveau[2]
[1]Durham University
[2]Johns Hopkins University
[3]Swiss Finance & Property Group
*Presenting author

Keywords: wake steering | yaw angle control | analytical wake model

Wake mitigation strategies often aim to increase the available kinetic energy in latter turbine rows at the expense of limiting the efficiency of wind turbines in front rows. According to several recent studies (e.g. Campagnolo et al. 2016, Bastankhah and Porte-Agel 2019, Fleming et al. 2019), wake steering is arguably one of the most promising approaches to achieve this type of wake mitigation. In this method, yaw angle control is used to redirect wakes away from downwind turbines. Although turbines that intentionally operate in yawed conditions no longer produce their maximum nominal power, the total wind farm efficiency can be improved due to a larger power generation of downwind turbines.

To realise the full potential of wake steering, it is imperative to improve our ability to predict wake flows under yawed conditions. One of the main differences between the wakes of yawed turbines and their unyawed counterparts is the formation of a curled wake (i.e., wake with a kidney-shape cross-section) in their downwind region. The curled wake cross-section is attributed to the existence of a counter-rotating vortex pair (CVP) in the wake of a yawed rotor (Howland et al. 2016). Although recent numerical and theoretical advances have vastly improved our ability to model yawed turbine wakes, existing analytical wake models (e.g., Bastankhah and Porte-Agel 2016, Shapiro et al. 2018) cannot still capture the curled shape of yawed turbine wakes. Apart from low computational costs, analytical models often have simple and explicit representations that can be used in wind farm control studies without the need of any prior fluid mechanics or numerical computing knowledge.

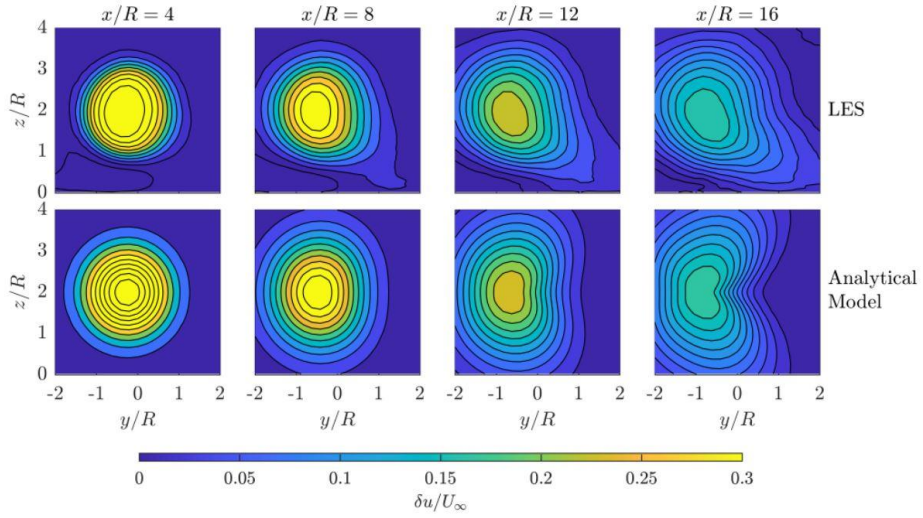


Figure 1. Contour plots of normalized velocity deficit in the curling wake behind a yawed wind turbine in turbulent inflow with a yaw angle of 20 degrees, where R is the rotor radius.

The current study aims at developing a new analytical model that can efficiently and realistically predict the shape of the wake downstream of yawed turbines. To achieve this goal, we first develop a new time-dependent mathematical relationship to determine the evolution of the vortex sheet, shedding from the circumference of a yawed rotor. The vortex-sheet based model solution is based on a power series expansion valid at short times assuming initially small deviations from a circular wake shape. The approach is then combined with a

standard analytical wake model to predict the curled shape of the wake and the distribution of velocity deficit downwind of a yawed turbine. Model predictions are compared with large-eddy simulation (LES) data for wakes of turbines with various yaw angles and inflow conditions. For example, figure 1 shows contours of velocity deficits, normalised by the incoming velocity at the hub height, at different streamwise positions for a turbine with a yaw angle of 20 degrees. As shown in the figure, the developed model is able to acceptably predict the major trends in the shape evolution of the curled wake downwind of a yawed turbine.

References:

Bastankhah, M. and Porté-Agel, F., 2016. Experimental and theoretical study of wind turbine wakes in yawed conditions. Journal of Fluid Mechanics, 806, p.506.

Bastankhah, M. and Porté-Agel, F., 2019. Wind farm power optimization via yaw angle control: A wind tunnel study. Journal of Renewable and Sustainable Energy, 11(2), p.023301.

Campagnolo, F., Petrovic, V., Schreiber, J., Nanos, E.M., Croce, A. and Bottasso, C.L., 2016, September. Wind tunnel testing of a closed-loop wake deflection controller for wind farm power maximization. In Journal of Physics: Conference Series (Vol. 753, No. 3, p. 032006).

Fleming, P., King, J., Dykes, K., Simley, E., Roadman, J., Scholbrock, A., Murphy, P., Lundquist, J.K., Moriarty, P., Fleming, K. and van Dam, J., 2019. Initial results from a field campaign of wake steering applied at a commercial wind farm–Part 1. Wind Energy Science (Online), 4(NREL/JA-5000-73991).

Howland, M.F., Bossuyt, J., Martínez-Tossas, L.A., Meyers, J. and Meneveau, C., 2016. Wake structure in actuator disk models of wind turbines in yaw under uniform inflow conditions. Journal of Renewable and Sustainable Energy, 8(4), p.043301.

Shapiro, C.R., Gayme, D.F. and Meneveau, C., 2018. Modelling yawed wind turbine wakes: a lifting line approach. Journal of Fluid Mechanics, 841.

Mini-Symposium: Wind Power Forecasting



Gregor Giebel
DTU Wind Energy



Corinna Möhrlen
WEPROG



John Zack
UL Renewables



Ricardo Jorge Bessa
INESC TEC

Wind power forecasts are used in the power system since over 25 years. Throughout the years, both the scope of the forecasts changed from simple deterministic forecasts of the wind power generation, to probabilistic forecasts covering and including the uncertainty of power generation, ramps, shut-down risks, icing and other extreme event issues. The forecast use also changed from being input to central power system scheduling, to serve as information to decision-making for wind power traders, system operators, wind farm operators and developers and others in the power industry. Recent advances include direct decision-aid based on probabilistic wind power forecast relevant input data. We invite talks across the whole spectrum of wind power forecasting: Numerical Weather Prediction advances including Ensemble Forecasting, new and innovative power prediction methods, methods to optimally integrate forecasts in decision-making processes, and best practice in using the forecasts at end-users. We encourage use cases with focus on probabilistic methods and extreme events, but contributions in grid stability, wind farm control, trading, O&M, scheduling, optimization with storage and PV, dynamic line rating and others are also welcome. Applications at different time-scales ranging from minutes up to seasonal time scales are of interest.

Mini-Symposium: Wind Power Forecasting (I)

IEA Wind Task 36 – Forecast and Usage Improvements

Gregor Giebel[1,*], Will Shaw[2], Helmut Frank[3], Caroline Draxl[4], John Zack[5], Pierre Pinson[6], Corinna Möhrlen[7], George Kariniotakis[8], and Ricardo Bessa[9]
[1]DTU Wind Energy
[2]Pacific North-West National Laboratory
[3]Deutscher Wetterdienst
[4]National Renewable Energy Laboratory
[5]UL Renewables
[6]DTU Management
[7]WEPROG
[8]MINES ParisTech
[9]INESC TEC
[*]Presenting author

Keywords: Forecasting | Wind modelling | IEA Wind | Weather prediction | Power prediction

The International Energy Agency (IEA) Wind Task 36 on Wind Power Forecasting organises international collaboration, among national weather centres with an interest and/or large projects on wind forecast improvements (NOAA, DWD, ...), forecast vendors and forecast users to facilitate scientific exchange to be prepared for future challenges. Collaboration is open to IEA Wind member states; 12 countries are already actively collaborating.
The talk discusses the general setup of the Task, and the latest developments. Among those are decision making under uncertainty. To this aim, a series of forecasting experiments are being developed and one initial experiment was tested by a wide audience. The forecasting experiments took the form of a game, during which the participants could experience the benefit of probabilistic information on their decisions to trade.
Other results include an information portal for meteorological data, and the IEA Recommended Practice for Forecast Solution Selection which is divided into 3 parts: (1) "Forecast Solution Selection Process", (2) "Designing and Executing Forecasting Benchmarks and Trials", and (3) "Evaluation of Forecasts and Forecast Solutions". The Recommended Practice guideline encourages forecast users to establish a framework of metrics that help identify, whether the user's forecast performance criteria effectively incentivize the forecast provider to optimize towards the forecast target variable that has the most value for the user's application(s). For this year, we intend to update the guideline in the light of the experiences throughout the industry in its initial application, and after collecting this experience at 3 Open Space workshops.

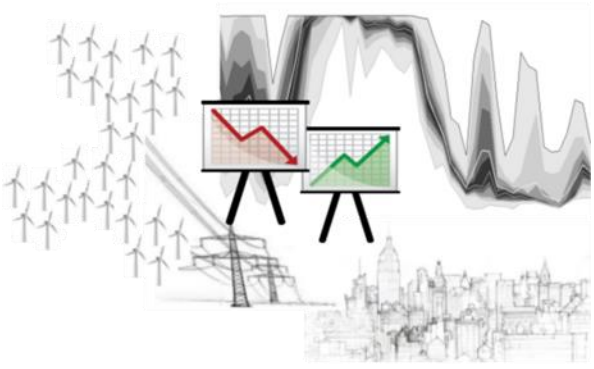


Figure 1: The visual identity of IEA Wind Task 36 Forecasting.



The Task is divided in three work packages: Work Package (WP) 1 is a collaboration on the improvement of the scientific basis for the wind predictions themselves. This includes numerical weather prediction (NWP) model physics, but also widely distributed information on accessible datasets. This WP also currently organises a benchmark for NWP models, based on the Wind Forecast Improvement Project 2 (WFIP2) datasets. WP2 deals with the power conversion from the wind speed forecasts and the associated vendor issues. Amongst other things, WP2 published the IEA Recommended Practice on how to select an optimal wind power forecast solution for a specific application. The focus of WP3 is on the engagement of end users to disseminate the best practice in the use of wind power predictions, especially probabilistic forecasts and also what kind of measurements are required in real-time environments.
A major activity of the Task is the organisation of workshops and special sessions at conferences, like this one. Previous workshops on e.g. forecasting on the minute scale including lidars, a workshop on the value of forecasts, or special sessions on the Wind Energy Science Conference, the Wind Integration Workshop, the ESIG Meteorology and Market Design for Grid Services workshops are still visible online from the IEAWindForecasting YouTube channel.

References:
www.IEAWindForecasting.dk

Research directions and results in the Smart4RES project for improving renewable energy forecasting

Georges Kariniotakis[1,*], Simon Camal[1], Akylas Statigakos[1], Pierre Pinson[2], Gregor Giebel[2], Liyang Han[2], Ricardo Bessa[3], Raphael Legrand[4], Quentin Libois[3], Marie Cassas[4], Matthias Lange[5], Stefan Wilbert[6], Bijan Nouri[6], Alexandre Neto[7], Remco Verzijlbergh[8], Gerrit Deen[8], Ganesh Sauba[9], George Sideratos[10], and Christos Vitellas[11]

[1]MINES ParisTech, PSL University
[2]Technical University of Denmark
[3]INESC TEC
[4]Meteo France
[5]Energy & Meteo Systems
[6]German Aerospace Center (DLR)
[7]EDP CNET
[8]WHIFFLE
[9]DNV GL
[10]NTUA
[11]DEDDIE
*Presenting author

Keywords: Renewable forecasting | Data science | Weather predictions | Grid integration

In this presentation we will show the research directions and innovative solutions developed in the European Horizon 2020 project Smart4RES (http://www.smart4res.eu) for better modelling and forecasting of weather variables necessary to optimise the integration of renewable energy (RES) production (i.e. wind, solar, run-of-the-river hydro) into power systems and electricity markets.

Smart4RES started in November 2019 and gathers experts from several disciplines, from meteorology and renewable generation to market- and grid-integration. It aims to contribute to reach very high RES penetrations in power grids of 2030 and beyond, through thematic objectives including:

- Improvement of weather forecasting with focus on variables that are important for RES applications,
- Improvement of RES power forecasting and better estimation of uncertainties,
- Streamlined extraction of optimal value through new forecasting products, data market places, and novel business models,
- New data-driven optimization and decision-aid tools for market and grid management applications.
- Validation of new models in living labs and assessment of forecasting value vs costly remedies to hedge uncertainties (i.e. storage).

Smart4RES focuses both on improving forecasting models of weather (e.g. physical models, data assimilation, Large Eddy Simulation, enabling weather forecasts seamless) and RES production (e.g. seamless models, highly resolved predictions), and on addressing applications in power grids.

Developments in the project have been formalized in Use Cases that cover a large range of time frames, technologies and geographical scales. For example, use-cases on power grids refer to the provision of ancillary services to the upper-level grid (e.g., balancing power) and the local grid (e.g., voltage control and congestion management), where the accurate forecasts of variable generation are key for accurate decision-making. A grid state forecasting will quantify dynamically the flexibility potential of RES in distribution grids. Collaborative forecasting investigates the improvement associated to local data sharing between distributed RES plants. This data sharing paves the way to a data market where agents exchange measurements, predictions or other types of valuable data.

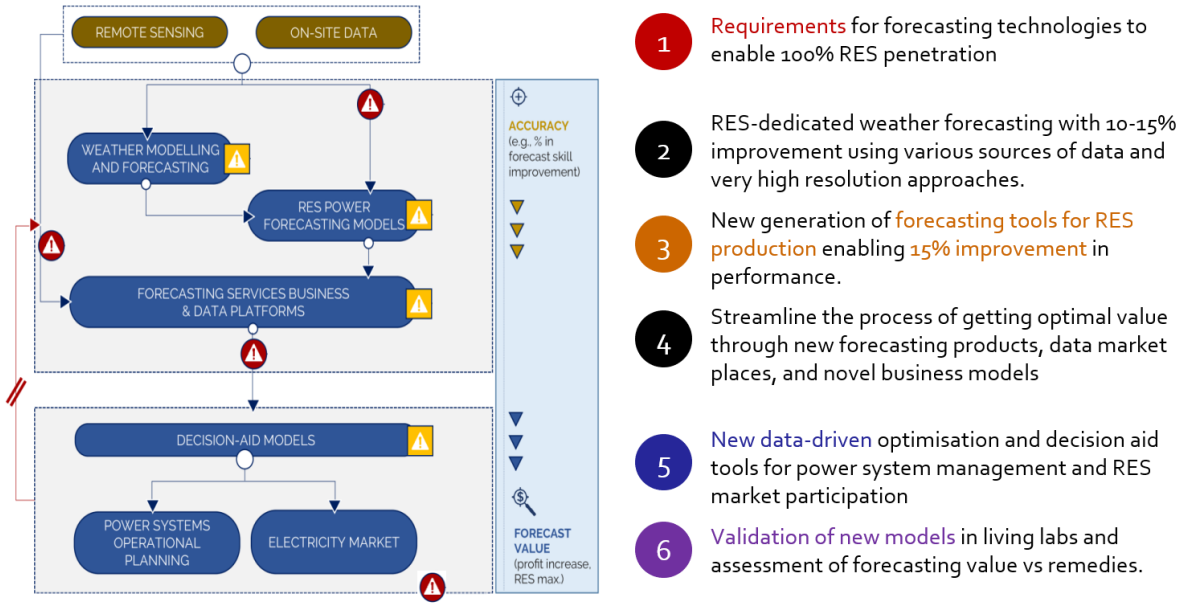


Figure 1: Overview of Smart4RES research priorities for improving the whole model and value chain of RES forecasting

Lastly, data-driven approaches will streamline decision-making by simplifying the model chain of bidding RES production, storage dispatch or predictive management electricity grids. They will also provide interpretable hindsight to decision-makers by integrating the decisions of experts (human-in-the-loop) and will be tested in realistic laboratory conditions (software-in-the-loop).

In this presentation we focus on the work done for improving modelling and forecasting of weather variables with accent to wind energy; i.e. through innovative measuring set-ups; through the development of seamless numerical weather prediction (NWP) approaches to be able to couple outputs of NWP models with different resolutions; through ultra-high resolution NWPs based on Large Eddy Simulation. We present results using data from real world test cases considered in the project. Finally, we assess how the new forecasting products may bring value to the applications.

Improving operational wind power forecasts by downscaling wind forecasting in complex terrains using WRF

Brice Olivier, and Quentin Loridant
meteo*swift

Keywords: WRF | Complex terrain | Downscaling | Wind power forecasting

Wind energy is a fast growing source of renewable energy that could produce 60% of all electricity in the European Union before 2050 (European Green Deal, 2020). However, wind power generation is known for its production instability due to the stochastic nature of the wind as well as the chaotic characteristics of the weather. Wind energy integration into power grids relies on wind power forecasts, which need to be as accurate as possible. Sometimes, onshore wind turbines are located on complex terrains due to spatial restrictions, leading to more wind condition uncertainty and creation of local phenomena (Draxl et al, 2021). Such areas sometimes lack a local Numerical Weather Prediction (NWP) model or are inaptly managed by the local NWPs. In the past decade, the Weather Research and Forecasting Model (WRF) has been used to tackle this issue and improve wind forecasts (Jimenez et al, 2010; Jimenez and Dudhia, 2013). There have been attempts to study the impact of WRF on wind power forecasts, as noted in Zhao et al (2012), Castellani et al (2016) and Che et al (2016). However, these studies were conducted on a single wind farm, at times with the dual aim of modeling wake effects in WRF and studying the impact on the neighbouring environment (Prosper et al, 2019). Additionally, WRF has been perceived as a benefit only available in selected meteorological research centers, leaving a gap between these studies and industrial constraints. For this work, a super-calculator was simulated using cloud computing. This system gives the opportunity to run WRF in real-time by launching computing resources on request. A dedicated study of wind power forecasts (WPF) is proposed, with day-ahead forecasting operational constraints, in an ensemble Machine learning framework (Ren, Suganthan and Srikanth, 2015).

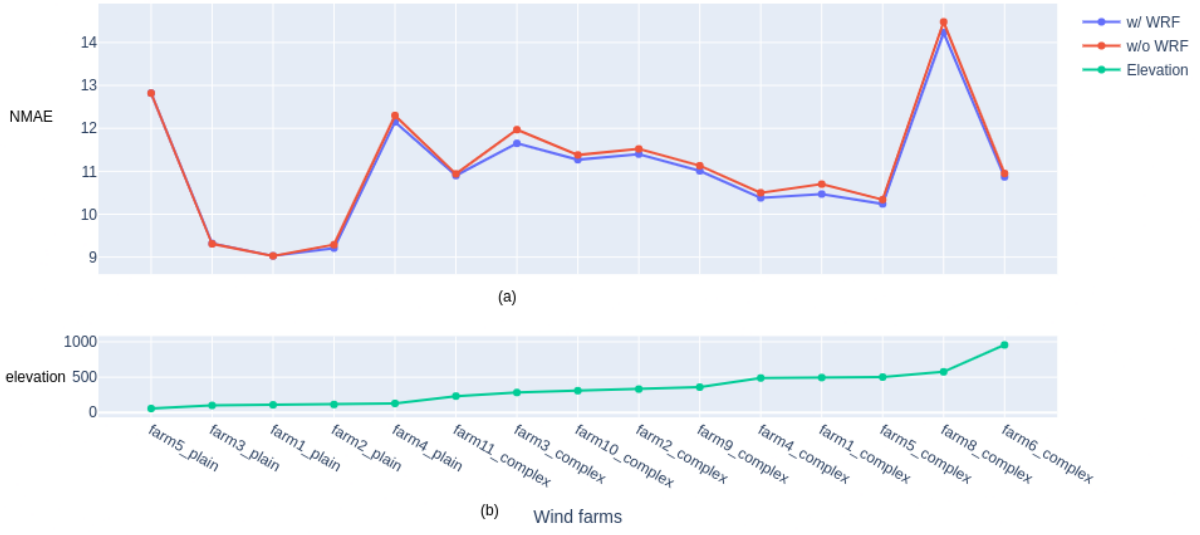


Figure 1: (a) represents the normalized mean absolute error (NMAE) of forecasts using WRF (blue) and forecasts not using WRF (red) for each farm. (b) shows farms ranked by elevation (green) and categorized into two types of topography: plains and complex terrains. The figure shows an improvement of forecasts in terms of NMAE for farms located on complex terrains.

This framework uses global NWPs combined with several WRF domains: a parent domain and two nested domains with horizontal resolutions of 9km, 3km and 1km, respectively. Moreover, a weather model and a feature selection procedure are used to measure the real world impact of WRF on WPF. Results are computed with a thorough evaluation process, using a pool of 15 wind farms located on two European sites, comprising complex terrains and plains. Wind power is forecasted on an initial training batch of 1 year, along with a time

series cross-validation (Hyndman and Athanasopoulos, 2018) on an average of 2.25-year wind power and weather data history. Results show that when used as a standalone weather model, low resolution WRF performs worse than other NWPs, giving a +1.27% of WPF normalized mean absolute error (NMAE) on average. Although when incorporated in the proposed machine learning framework, WRF data improves the WPF by -0.20% of NMAE on average on complex terrains and -0.04% of NMAE on average on plains. Under Diebold-Mariano test (Messner et al, 2020), 9 out of 10 complex terrain farms had p value < 0.05 and 1 out of 5 plain farms had p value < 0.05. The automated weather selection feature also suggests that a sufficient downscaling should be performed for optimal results, as the highest resolution was kept for every single complex terrain wind farm.

References:

Draxl, C., Worsnop, R. P., Xia, G., Pichugina, Y., Chand, D., Lundquist, J. K., ... & Berg, L. K. (2021). Mountain waves can impact wind power generation. Wind Energy Science, 6(1), 45-60.

Jiménez, P. A., González-Rouco, J. F., García-Bustamante, E., Navarro, J., Montávez, J. P., De Arellano, J. V. G., ... & Muñoz-Roldan, A. (2010). Surface wind regionalization over complex terrain: Evaluation and analysis of a high-resolution WRF simulation. Journal of Applied Meteorology and Climatology, 49(2), 268-287.

Jiménez, P. A., & Dudhia, J. (2013). On the ability of the WRF model to reproduce the surface wind direction over complex terrain. Journal of Applied Meteorology and Climatology, 52(7), 1610-1617.

Zhao, P., Wang, J., Xia, J., Dai, Y., Sheng, Y., & Yue, J. (2012). Performance evaluation and accuracy enhancement of a day ahead wind power forecasting system in China. Renewable Energy, 43, 234-241.

Castellani, F., Astolfi, D., Mana, M., Burlando, M., Meißner, C., & Piccioni, E. (2016, September). Wind power forecasting techniques in complex terrain: ANN vs. ANN-CFD hybrid approach. In Journal of Physics: Conference Series (Vol. 753, No. 8, p. 082002).

Che, Y., Peng, X., Delle Monache, L., Kawaguchi, T., & Xiao, F. (2016). A wind power forecasting system based on the weather research and forecasting model and Kalman filtering over a wind-farm in Japan. Journal of Renewable and Sustainable Energy, 8(1), 013302.

Prósper, M. A., Otero-Casal, C., Fernández, F. C., & Miguez-Macho, G. (2019). Wind power forecasting for a real onshore wind farm on complex terrain using WRF high resolution simulations. Renewable Energy, 135, 674-686.

Ren, Y., Suganthan, P. N., & Srikanth, N. (2015). Ensemble methods for wind and solar power forecasting—A state-of-the-art review. Renewable and Sustainable Energy Reviews, 50, 82-91.

Hyndman, R. J., & Athanasopoulos, G. (2018). Forecasting: principles and practice. OTexts.

Messner, J. W., Pinson, P., Browell, J., Bjerregård, M. B., & Schicker, I. (2020). Evaluation of wind power forecasts—An up to-date view. Wind Energy, 23(6), 1461-1481.

A streaming dynamic mode decomposition approach to wind farm forecasting

Jaime Liew[1,*], Tuhfe Göcmen[2], Wai Hou Lio[1], and Gunner Chr. Larsen[1]
[1]Technical University of Denmark
[2]DTU Wind Energy
*Presenting author

Keywords: dynamic mode decomposition | power forecasting | streaming data | wind farm control

Forecasting in wind energy is a crucial task to perform effective wind farm control or to participate in the energy market. Performing effective forecasts is notoriously difficult in a wind farm due to the complexity and non-stationarity of the system. While many forecasting methods exist, many fail to capture both short and long term variations in the wind farm system. We demonstrate a data-driven system identification approach to forecasting based on the dynamic mode decomposition (DMD) methodology. While DMD is becoming increasingly popular in wind energy literature (Cassamo 2020; Annoni 2018), its implementation is often not suited for real-time applications. The presented algorithm is modified to work with streaming data by adjusting the DMD modes continuously as new data is made available. The method is capable of characterizing non-linear, time-varying, multidimensional time-series data in a computationally efficient manner. The method is applied to high-frequency power output data from the Lillgrund wind farm, showing that the method is an effective and robust tool for capturing short term dynamics while adapting to long term changes such as wind speed and direction changes.

The forecasting method makes use of two computationally efficient updating schemes to adjust the DMD model. The first scheme is a streaming singular value decomposition (SVD)(Hemati 2014), which performs a model reduction on the data. The algorithm adjusts the SVD basis as needed by either adding or removing basis vectors. These adjustments tend to occur when the statistical nature of the time series data change, for example, when a turbine shuts down, or the wind speed and direction change. The second updating scheme is a streaming linear regression model, which uses an exponentially decaying weighting (Zhang 2019). The combination of the two schemes forms the streaming DMD model.

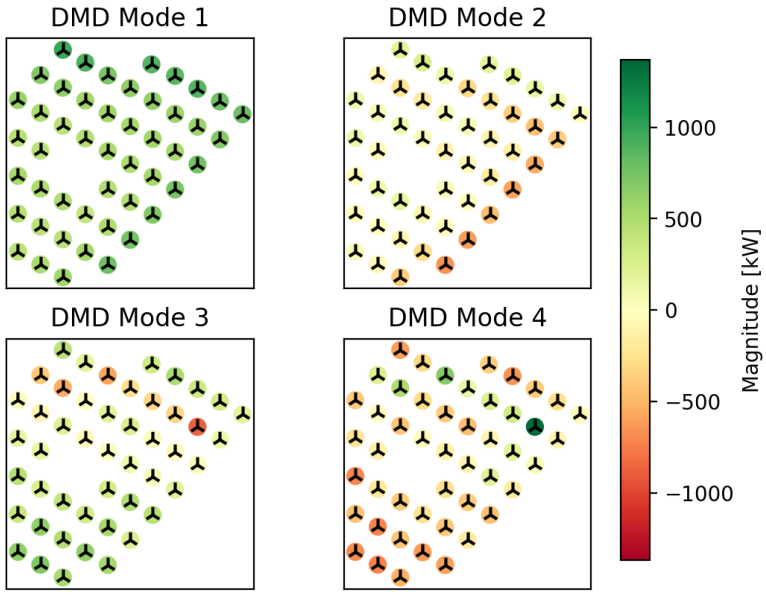


Figure 1: The first 4 out of 30 DMD modes describing the wind farm state at a particular point in time. The state of the wind farm can be approximated as a linear combination of all DMD modes. Mode one shows easterly wake effects, and modes 2, 3, and 4 show correlated turbine clusters.

The algorithm is applied to a 24-hour time series data set comprising of the power output of each of the 48 turbines in Lillgrund sampled at 2Hz. The algorithm can forecast the power output of each turbine several minutes into the future. Figure 1 shows the root mean square error of forecasts of each turbine 3 minutes into the future, showing that streaming DMD outperforms both persistence forecasting (by 21.9% on average), and non-streaming DMD forecasting (by 10.9% on average).

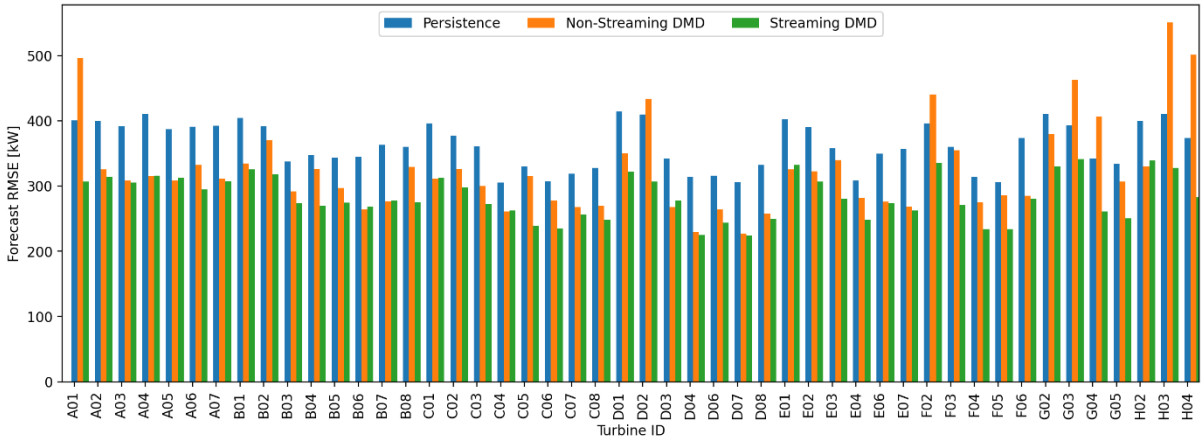


Figure 2: Root mean square error of power forecasts for individual turbines. Forecasts are performed 180 seconds into the future. Streaming DMD (green) is shown to outperform persistence forecasting (blue) by 20.9% and non-streaming DMD (orange) by 10.9% on average. (24 hour data set at 2Hz, Lillgrund wind farm, below rated conditions).

Additional insight can be found in the DMD modes, which can reveal spatial patterns in the wind farm. This can be seen in Figure 2, showing the first 4 of 30 DMD modes at a particular point in time.
Easterly wake effects can be seen in mode 1, as well as correlated turbine clusters in modes 2 to 4.
The algorithm performs well below rated power and remains stable during wind speed and direction changes, and changes in turbine operating points. The presented streaming algorithm has applications in wind farm control, as it can model and predict short term time-varying dynamic interactions between wind turbines in a data-driven, and computationally inexpensive manner.

References:

Cassamo, N. and van Wingerden, J.W., 2020. On the potential of reduced order models for wind farm control: a Koopman dynamic mode decomposition approach. Energies, 13(24), p.6513.

Annoni, J., Taylor, T., Bay, C., Johnson, K., Pao, L., Fleming, P. and Dykes, K., 2018, June. Sparse-Sensor Placement for Wind Farm Control. In Journal of Physics. Conference Series (Vol. 1037, No. NREL/JA-5000-71428). National Renewable Energy Lab.(NREL), Golden, CO (United States).

Hemati, M.S., Williams, M.O. and Rowley, C.W., 2014. Dynamic mode decomposition for large and streaming datasets. Physics of Fluids, 26(11), p.111701.

Zhang, H., Rowley, C.W., Deem, E.A. and Cattafesta, L.N., 2019. Online dynamic mode decomposition for time-varying systems. SIAM Journal on Applied Dynamical Systems, 18(3), pp.1586-1609.

Short-term trading of wind energy production using data-driven prescriptive optimization

Akylas Stratigakos*, Simon Camal, Timothee Blondel, and George Kariniotakis
MINES ParisTech, PSL University
*Presenting author

Keywords: wind power forecasting | electricity markets | data-driven optimization | trading

The participation of Wind Power Plants (WPPs) in competitive electricity markets requires several forecasting and decision-making tools. WPP operators submit offers in market auctions, which are closed ahead of delivery (e.g. the day before), therefore the uncertainty of wind production should be accurately taken into consideration in the offering strategy. The standard approach to tackle this conditional stochastic optimization problem is to first deploy a forecasting model to predict uncertain parameters like wind production and market prices and, subsequently, use those predictions as inputs in a stochastic optimization problem. This constitutes a modelling chain, which generally requires substantial tuning effort in order to obtain optimal trading decisions. Furthermore, the relationship between offering decisions and explanatory data (e.g. weather conditions at the WPP site) is indirect, making it difficult to analyze the impact of those conditions on the trading revenue.

In this work, we present an alternative approach based on data-driven deterministic optimization, which integrates forecasting and optimization tools with the goal of using predictive algorithms to directly prescribe optimal decisions. Specifically, we consider the problem of a WPP offering energy in a day-ahead (DA) market, subject to imbalance costs. In this case, the optimal offering strategy relies on the estimation of the conditional distribution of wind production [1] given explanatory data.

Following recent advances in data-driven optimization [2], we propose using weights obtained by predictive local learning algorithms and approximating the conditional stochastic optimization problem with a weighted version of the sample average approximation (SAA) method. This approach effectively links explanatory data to decisions, which are termed Predictive Prescriptions.

A high level description of the two approaches is presented in Figure 1 below. A use case of a virtual power plant (VPP) participating in a DA market under a dual price balancing mechanism is presented.

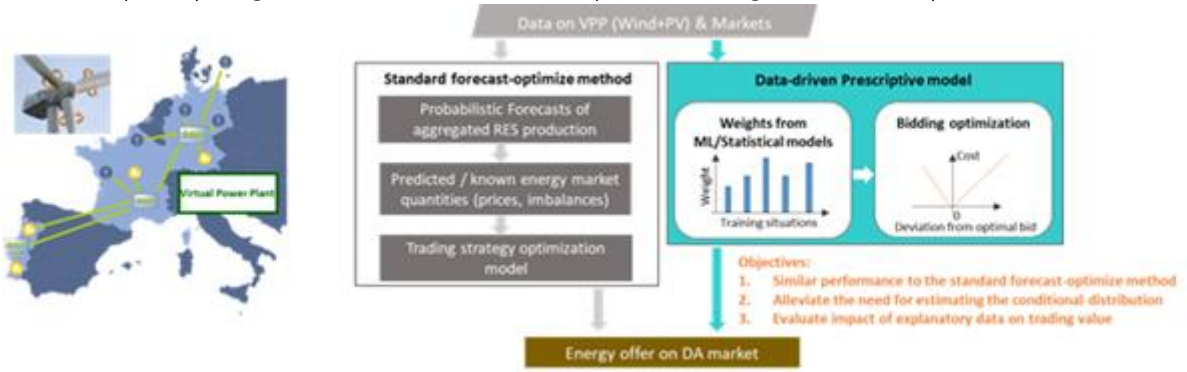


Figure 1: High level description of the proposed approaches

We consider the more general case of a VPP composed of wind and PV power plants (though with a higher share of wind). First, we implement feature selection via forward selection, and the Max Relevance-Min Redundancy approach [3] to obtain a better understanding of the features correlations and assess their impact on forecast accuracy. Second, we form and evaluate predictive prescriptions using different local learning algorithms, such as k-Nearest Neighbors, kernel regression, and variants of decision trees. We conduct numerical experiments to study the sensitivity of prescriptions to dimension reduction and the size of the training sample. Finally, we measure the impact of explanatory variables on the forecast value, i.e., trading revenue, by estimating a metric of prescriptiveness. Results with real data indicate that the proposed approach

achieves similar performance in terms of trading revenue with the standard approach, without the need of explicitly modeling the full distributional uncertainty. Furthermore, it allows to directly measure the impact of explanatory variables in forecast value.

References:
Pinson, P., Chevallier, C. and Kariniotakis, G.N., 2007. Trading wind generation from short-term probabilistic forecasts of wind power. IEEE Transactions on Power Systems, 22(3), pp.1148-1156.
Bertsimas, D. and Kallus, N., 2020. From predictive to prescriptive analytics. Management Science, 66(3), pp.1025-1044.
Peng, H., Long, F. and Ding, C., 2005. Feature selection based on mutual information criteria of max-dependency, maxrelevance, and min-redundancy. IEEE Transactions on pattern analysis and machine intelligence, 27(8), pp.1226-1238.

Mini-Symposium: Wind Power Forecasting (II)

Forecast combination and adaptation for improved ramp forecasts

Rosemary Tawn*, and Jethro Browell
University of Strathclyde
*Presenting author

Keywords: Wind power forecasting | Forecast combination | Probabilistic forecasts | ramp events

It is commonly accepted that a model combining forecasts from several distinct models tends to outperform single model forecasts (Hall 2007) (see image). However, there is no established approach to combine multiple different probabilistic forecast distributions, and it has also been suggested that combined forecasts may serve to smooth out useful information such as power fluctuations and ramps (Abuella 2019). Wind power ramp events are some of the most important for decision-makers: severe ramps may require actions such as curtailment of turbines to limit a fast ramp up, or utilisation of energy storage or even load curtailment to balance a severe downward ramp (Ferreira 2011). Meanwhile, forecast skill is often lower around power ramps due to timing and amplitude errors, reducing ability to manage the power system optimally. An example of a timing error is shown in the attached image. Previous research (Gallego-Castillo 2015 and Cui 2019) has developed specialised ramp forecasts that predict the probability of ramp events, but this is often separate from a power forecast.

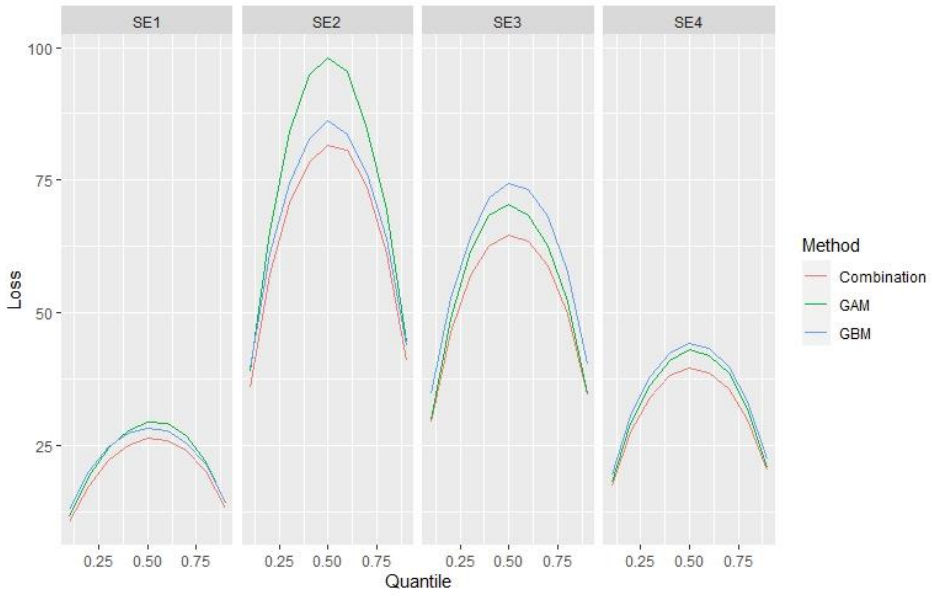


Figure 1: Pinball loss for wind power quantile forecasts for four regions of Sweden. Combination forecasts give improvement across all quantiles for all areas, over existing state of the art forecasts. Forecasts plotted are from Browell (2020).

This work proposes a forecast combination approach to produce probabilistic wind power forecasts with improved performance around times of ramps. By using probabilistic forecasts of key ramp characteristics such as ramp rate, duration and magnitude as well as a set of probabilistic power forecasts as inputs to a forecast combination and adjustment stage, it is anticipated that forecast skill around ramp events is improved. Day-ahead forecasts based on the outputs of physical weather models are able to predict the presence of a ramp ahead of its arrival at a site but may include magnitude or timing errors. In contrast, very short-term (up to 6 hours ahead) models based on site power measurements are sensitive to recent changes in observed conditions but do not have 'awareness' of incoming weather fronts until they arrive. In this work,

a set of distinct very short term models is supplemented with a day-ahead model to gain the benefits of diverse forecast inputs.

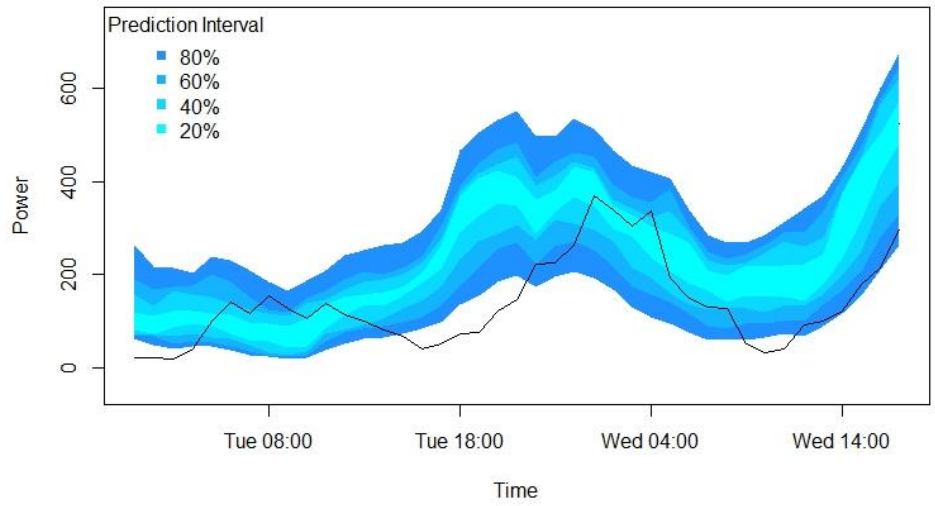


Figure 2: Example of a timing error of forecast: the general trajectory of the forecast is correct, but offset from the observed power by several hours. Again, power data and forecasts are from the EEM wind power forecasting competition (Browell 2020).

To improve forecast skill around ramp events, the forecast combination stage includes a penalty for errors in ramp rate alongside the usual penalty for forecast power errors in the loss function. A similar approach has been applied for adjusting combined solar forecasts (Abuella 2019), but this work would extend this in the following ways:

- Using probabilistic, rather than deterministic, forecasts as inputs to the combination and ramp adjustment stage, with feature selection to determine the most informative quantiles
- Working in a quantile regression framework to produce calibrated quantile forecasts, explicitly specifying the loss function with a parameter to control the relative penalty placed on errors in ramp rates
- In addition to ramp rate, including forecasts of other ramp features such as timing, duration and magnitude as inputs to the forecast combination and ramp adjustment stage, similar to the conditional probabilistic ramp forecasts in Cui (2019).
- Comprehensive evaluation of both general model skill and performance around ramp events, distinguishing also between upwards and downwards ramps as these events lead to different general actions within the power system.
- Benchmarking against other forecast combination approaches where forecasts are not adapted for ramp events, and comparison against a single-stage model that uses all forecast input data simultaneously, rather than separate models built with different inputs.

References:

1. Hall, S. G. and Mitchell, J. (2007) 'Combining density forecasts', International Journal of Forecasting, 23 pp1-13.
2. Abuella, M. and Chowdhury, B. (2019) 'Forecasting of solar ramp events: A post-processing approach', Renewable Energy 133 pp1380-1392.
3. Ferreira, C., Gama, J., Matias, L., Botterud, A., Wang, J., and INESC Porto. (2011) A survey on wind power ramp forecasting [online]. United States, doi:10.2172/1008309.
4. Gallego-Castillo, C., Cuerva-Tejero, A. and Lopez-Garcia, O. (2015) 'A review on the recent history of wind power ramp forecasting', Renewable and Sustainable Energy Reviews 52 pp1148-1157.
5. Cui, M., Krishnan, V., Hodge, B-M. and Zhang, J. (2019) 'A copula-based conditional probabilistic forecast model for wind power ramps', IEEE Transactions on Smart Grid 10(4) pp3870-3882.
6. Browell, J., Gilbert, C., Tawn, R. and May, L. (2020) 'Quantile Combination for the EEM20 Wind Power Forecasting Competition', 2020 17th International Conference on the European Energy Market (EEM), Stockholm, Sweden, pp. 1-6.

Machine learning and Analog Ensemble techniques for temporal extrapolation of long-term wind resource uncertainty

Nicola Bodini[1,*], Mike Optis[1], Weiming Hu[2], and Guido Cervone[2]
[1]National Renewable Energy Laboratory
[2]Penn State University
[*]Presenting author

Keywords: machine learning | uncertainty quantification | offshore wind energy | ensemble forecasting

To accurately plan and manage wind farms, not only the time-varying wind resource at the site of interest needs to be assessed, but also the uncertainty connected to this estimate. Numerical weather prediction models at the mesoscale represent a valuable way to characterize the wind resource offshore, given the challenges connected with measuring hub height wind speed offshore.
The uncertainty associated to modeled wind speed is often estimated by running multiple ensemble members, obtained by perturbing initial conditions, external forcings, or numerical schemes.
However, creating such a numerical ensemble of long-term wind resource data over a large region represents a challenge given the substantial computational capacity it requires. Here, we propose novel approaches to leverage artificial intelligence-based techniques to overcome the limits of the conventional methods for numerical wind speed uncertainty quantification.
We quantify parametric uncertainty in hub height wind speed in a region covering the proposed offshore wind energy lease areas in California. We run the Weather Research and Forecasting (WRF) model version 4.1.2 with 16 ensemble members for a single year, while a single WRF run is performed for the remaining 19 years of the period of interest (Optis et al. 2020). We then apply and compare two different artificial intelligence-based approaches to temporally extrapolate to the full 20-year period the WRF parametric uncertainty in hub-height wind speed quantified from the shortterm ensemble variability. As a baseline, we use the Analog Ensemble technique (Delle Monache et al. 2013) to generate parametric uncertainty estimates over the 20-year period. We contrast this approach against a novel approach in which a gradient boosting machine learning model is trained on the single year of WRF ensembles to extrapolate wind speed parametric uncertainty to the remaining 19 years of single model run. We find that both approaches provide accurate predictions of wind speed parametric uncertainty. Notably, the parametric uncertainty predicted by both methods increases towards the coast (Figure 1). For the proposed wind energy lease areas in the region, hourly uncertainty in hub height wind speed is predicted to be around 15% of the mean wind speed value at the sites.

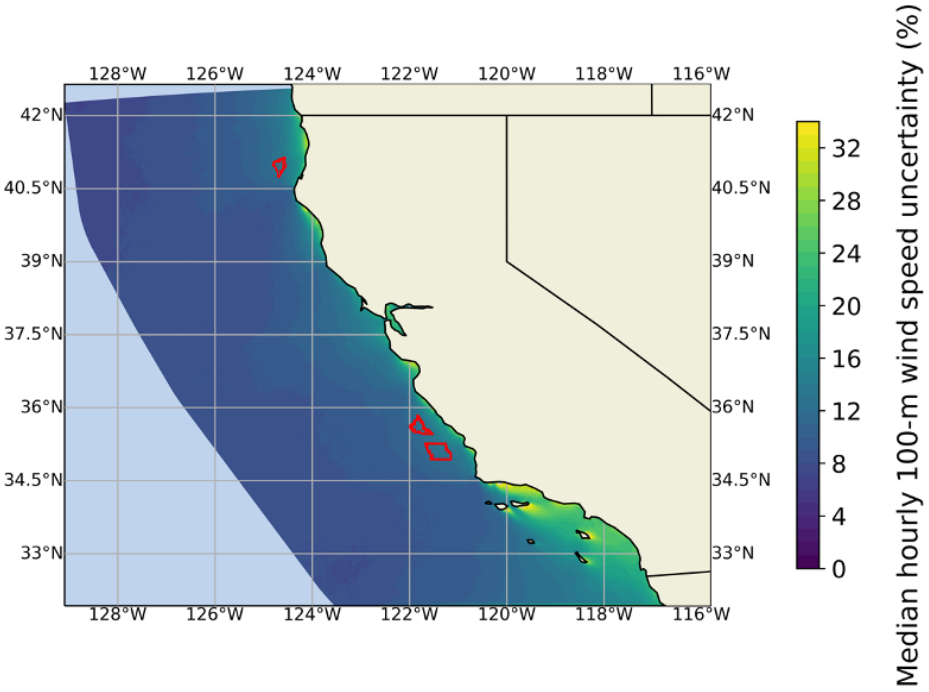


Figure 1: Long-term median parametric uncertainty in hourly 100-m wind speed calculated for offshore California, where offshore wind energy development is being planned (lease areas highlighted in red). Results from the proposed machine learning approach.

Our proposed approaches provide significant benefits as they allow for a long-term quantification of wind speed parametric uncertainty without the need of running numerical ensembles over the long period of interest. However, in order to quantify not only the wind speed parametric uncertainty, but the full wind speed uncertainty (i.e., including the bias between modeled and observed wind resource), we then expand both our proposed AI-based approaches to temporally extrapolate the full wind resource uncertainty. We will show preliminary results over the North Atlantic region, where several offshore wind plants are being planned, and where two floating lidars with publicly available data have been deployed for over one year. We will quantify the error between the WRF-predicted and observed hub height wind speed over the one year of overlap between the two data sources, and then extrapolate that uncertainty to the full 20-year period needed for wind energy resource assessment purposes.

References:

Delle Monache, L., Eckel, F.A., Rife, D.L., Nagarajan, B. and Searight, K., 2013. Probabilistic weather prediction with an analog ensemble. Monthly Weather Review, 141(10), pp.3498-3516.

Optis, Mike, Alex Rybchuk, Nicola Bodini, Michael Rossol, and Walter Musial. 2020. 2020 Offshore Wind Resource Assessment for the California Pacific Outer Continental Shelf. Golden, CO: National Renewable Energy Laboratory. NREL/TP-5000-77642. https://www.nrel.gov/docs/fy21osti/77642.pdf.

Probabilistic Day-Ahead Forecasting using an Analog Ensemble Approach for Wind Farm Grid Services

Andrew Kumler[1,2,*], Julie K. Lundquist[2,1], and Jennifer King[1]
[1]National Renewable Energy Laboratory
[2]University of Colorado - Boulder
[*]Presenting author

Keywords: Probabilistic forecasting | Numerical weather prediction | Wind power forecasting

Wind resource assessment and wind power forecasting are used in research and industry to anticipate future power output at scales ranging from individual wind turbines to entire wind farms.
Probabilistic day-ahead wind forecasting is useful for anticipating how a wind farm could potentially participate in the day-ahead market by providing upper and lower bounds for expected power generation, thus informing grid operators of its uncertainty. Understanding this uncertainty is part of a larger project focused on building a platform that combines efforts in weather forecasting, aerodynamic and economic modeling to create maximum value of a wind plant to better provide services to the grid. This effort is also known as the Atmosphere to Electrons to Grid (A2E2G) project.
One method for producing a probabilistic forecast is through the analog ensemble approach (Delle Monache et al., 2011). This method leverages historical forecasts and their corresponding observations as a training data set from which future forecasts can be made. For some future forecast, the most similar historical forecasts (analogs) are identified on a regular time basis such as once per a 3-hour window. The most similar analogs, based on a metric such as root mean square error (RMSE), are recorded and their corresponding verifying observations are used as an ensemble member for this future forecast. Prior work in this area demonstrates improvements over raw Numerical Weather Prediction (NWP) forecasts and shows skill similar to techniques such as logistic regression and machine learning (Delle Monache et al., 2013; Alessandrini et al., 2015).
Here, we take the High-Resolution Rapid Refresh model (HRRR) day-ahead forecast (0-36 hours) to create a probabilistic day-ahead forecast using an analog ensemble approach. The HRRR has an hourly temporal resolution, with a spatial resolution of 3 km. The 12 UTC HRRR model run is downloaded every day for one year from August 2019 - July 2020, with the first 11 months serving as a bank of analogs from which the forecasting algorithm can create a probabilistic forecast. Once downloaded, the original HRRR forecast is temporally interpolated to 5-minutes, aligning with both the temporal resolution of the observations as well as the timescale relevant for day-ahead power forecasts. The forecast is validated at the M2 tower at the Flatirons Campus of the National Renewable Energy Laboratory (NREL) at a typical wind turbine height of 80 m. Variables such as wind speed, wind direction, and turbulence intensity are incorporated into the probabilistic forecast model and weighted according to their relative importance to the forecast.

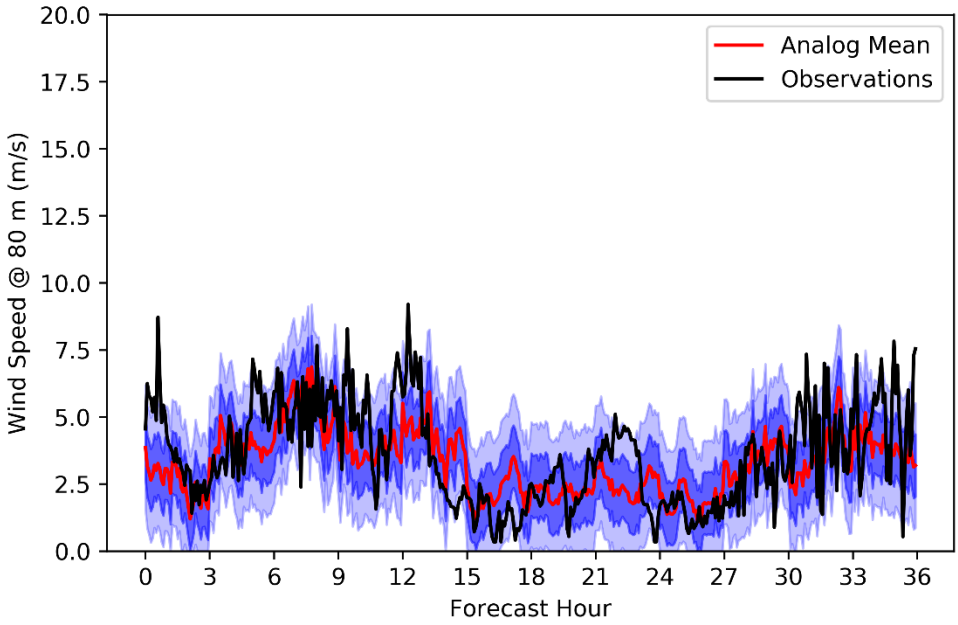


Figure 1: An example probabilistic day-ahead forecast for July 30th, 2020. The dark purple shading represents one standard deviation from the mean, while the light purple shading represents two standard deviations.

Based on metrics such as mean bias error (MBE), mean absolute error (MAE), and root mean square error, the analog ensemble forecast outperforms the raw HRRR forecast during the testing period of July 2020. Figure 1 illustrates an example day-ahead forecast compared against the verifying observations. The general variability and ramps are captured throughout the day, with potential to further improve the analog ensemble model through machine learning techniques.

References:
Alessandrini, S. et al. (2015) 'A novel application of an analog ensemble for short-term wind power forecasting', Renewable Energy, 76, pp. 768–781. doi: 10.1016/j.renene.2014.11.061.
Delle Monache, L. et al. (2011) 'Kalman Filter and Analog Schemes to Postprocess Numerical Weather Predictions', Monthly Weather Review, 139(11), pp. 3554–3570. doi: 10.1175/2011MWR3653.1.
Delle Monache, L. et al. (2013) 'Probabilistic Weather Prediction with an Analog Ensemble', Monthly Weather Review, 141(10), pp. 3498–3516. doi: 10.1175/MWR-D-12-00281.1.

Integration of wind energy uncertainty in predictive grid management: can we make it simple?

Ricardo Bessa*, Luis Teixeira, and Hodjat Mariji
INESC TEC - Institute for Systems and Computer Engineering, Technology and Science
*Presenting author

Keywords: Forecast uncertainty | Decision-aid | Flexibility

It is widely recognized by both academia and industry that renewable energy sources (RES) uncertainty forecasting can provide more information, enable risk quantification in power system operation and lead to economic savings and reliability improvement. The literature about stochastic approaches that integrate RES forecast uncertainty in various use cases, e.g. congestion management, unit commitment, economic dispatch, reserves setting, optimal power flow, is very extensive (Bessa, 2014). However, the consensus today is that there is a mismatch between the proposed methods and their adoption by the industry. The main reason is that stochastic methodologies, e.g. stochastic optimal power flow (OPF) (Soares, 2018), in comparison to expert knowledge, require higher computational times and are difficult to interpret by end-users.
The work described in this paper is in the context of the operation of electrical grids under forecast uncertainty from RES and load. The main goal is to manage the technical constraints of the electrical grid (i.e., congestion management and voltage control) in the operational planning time horizon (next day). The methodology illustrated in Figure 1 is divided in two main phases: (1) modelling of electrical grid sensitivities and forecast uncertainties; (2) decision-aid phase with the decision-maker balances flexibility risk and costs to make a final decision about flexibility activation. Flexibility is here defined as active and reactive power modulation in the grid nodes (e.g., available via a specific market mechanism), which can be from distributed generation, demand response, storage (operated by a third-party), etc., aggregated or not by market players.

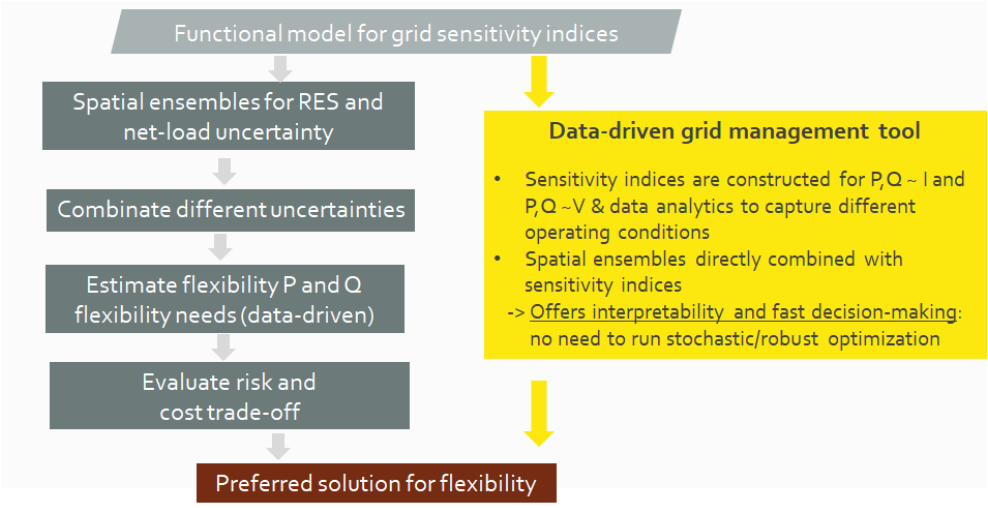


Figure 1: Predictive grid management methodology

A case-study with an 24-bus electrical grid is used to show the impact of forecast uncertainty in grid technical problems and how the use of sensitivity indices (linearization of the power flow equations) can help the decision-maker (human operator) to better understand the impact of uncertainty and derive fast remedial actions. In fact, the main goal of this work is to use a frugal approach where the decision-maker can easily identify the branches/bus more exposed to forecast uncertainty and find the top 3 flexible resources to pre-book in case of technical problems in real-time.
The main innovation is the approach adopted to integrate forecast uncertainty in active/reactive flexibility management in electrical grids. The typical representation of uncertainty by ensembles (Bessa, 2017) is explored, but instead of integrating the ensembles in stochastic optimization, a Monte Carlo approach is used

to combine different uncertainties (i.e., sensitivity indices estimation, forecast uncertainty) and construct a distribution of required flexibility to solve technical problems.

Another potential result is a methodology that forecasts the amount of flexibility requirements per node to handle technical constraints originated by forecast errors and high RES integration.

The research leading to this work is being carried out as a part of the Smart4RES project (European Union's Horizon 2020, No. 864337). The sole responsibility of this publication lies with the author. The European Union is not responsible for any use that may be made of the information contained therein.

References:

Bessa, R., Moreira, C., Silva, B., Matos, M. (2014). Handling renewable energy variability and uncertainty in power systems operation. Wiley Interdisciplinary Reviews: Energy and Environment, 3(2), pp. 156-178.

Soares, T., Bessa, R. J., Pinson, P., Morais, H. (2018). Active distribution grid management based on robust AC optimal power flow. IEEE Transactions on Smart Grid, 9(6), pp. 6229-6241.

Bessa, R. J., Möhrlen, C., Fundel, V., Siefert, M., Browell, J., Haglund El Gaidi, S., Hodge, B, Cali, U., Kariniotakis, G. (2017). Towards improved understanding of the applicability of uncertainty forecasts in the electric power industry. Energies, 10(9), pp. 1402.

Overcoming psychological Barriers of using Probabilistic Power Forecasting with Games and Experiments

Corinna Möhrlen[1,*], Nadine Fleischhut[2], Ricardo Bessa[3], and Gregor Giebel[4]
[1]WEPROG
[2]Max Planck Institute for Human Development
[3]INESC TEC - Institute for Systems and Computer Engineering, Technology and Science
[4]DTU Wind Energy
[*]Presenting author

Keywords: decision making with weather uncertainty | ensemble forecasting | adaptive rationality | risk and uncertainty communication

The challenges of climate change require unprecedented investments in renewable energy sources(RES) and a fundamental transformation of existing infrastructures such as the power grid.
With increasing penetration levels of RES and more and more extreme weather conditions due to climate change, the uncertainty of weather and power production forecasts can no longer be ignored for grid operation. However, current approaches are mostly based on deterministic weather forecasts, which provide no means to explicitly represent the varying uncertainty of forecasts. That is, these methods have reached their limit, because they neither model nor convey forecast uncertainties. Instead, new methods for power production forecasts and strategies to implement robust forecasts into decision processes are called for that explicitly model uncertainty and allow to communicate forecast uncertainty to end-users such as market participants and system operators [Bessa2019].
Integrating uncertainty into the decision process is important,because RES can be used at much lower costs than traditional energy sources due to the high flexibility, even though this is only onesided for down-regulation and with limited capacity for balancing power at the grid level. And, probabilistic uncertainty forecasts have been shown to improve decisions in other weather related domains (e.g. [Joslyn2013]). In order to support the power industry in the adaptation of uncertainty forecasts into their business practices, IEA Wind Task 36 has started an initiative in collaboration with the Max Planck Institute of Human Development to investigate existing psychological barriers in the industry to adopt probabilistic forecasts and to support human decision processes.

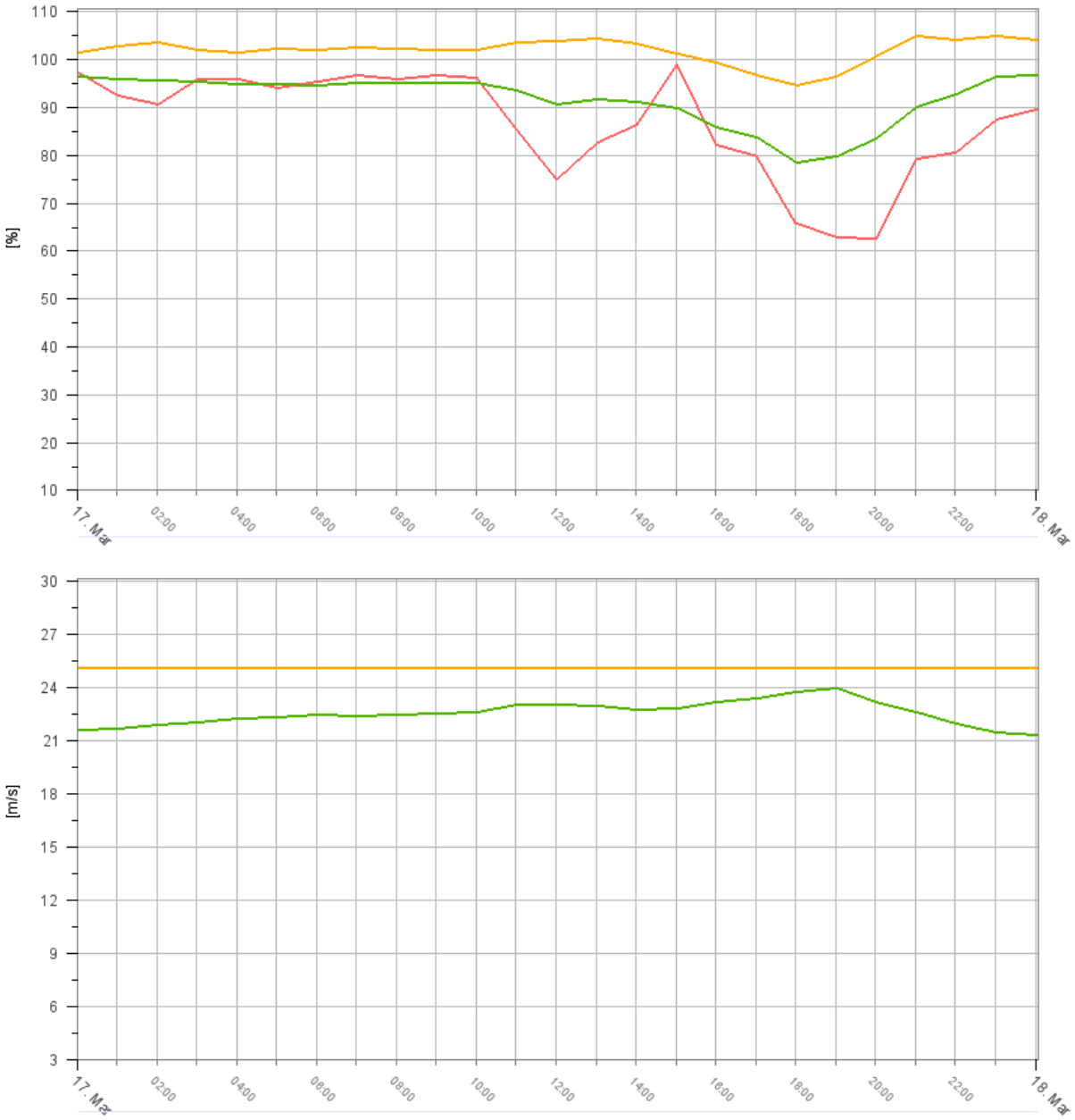


Figure 1: Deterministic forecast example. Upper graph shows 3 day-ahead wind power, lower graph shows wind speed, where the yellow line marks the threshold (25 m/s) around which a high-speed shutdown can occur.

Our main goal is to empirically investigate the psychological barriers to the adoption of probabilistic forecasts and enable stakeholders to understand and explore their benefit and usefulness. To this end, we will run a series of experiments that simulate typical decision applications, e.g. of traders or system operators, and that will be able to benefit from probabilistic forecasts, and ensemble forecasts in particular. We will be describing the first two experiments that focused on a typical trading scenario with offshore wind power forecasts. The experiments were designed as "decision games" in order to demonstrate the potential benefit of uncertainty forecasts for a typical decision task in the power industry (see figure 1).

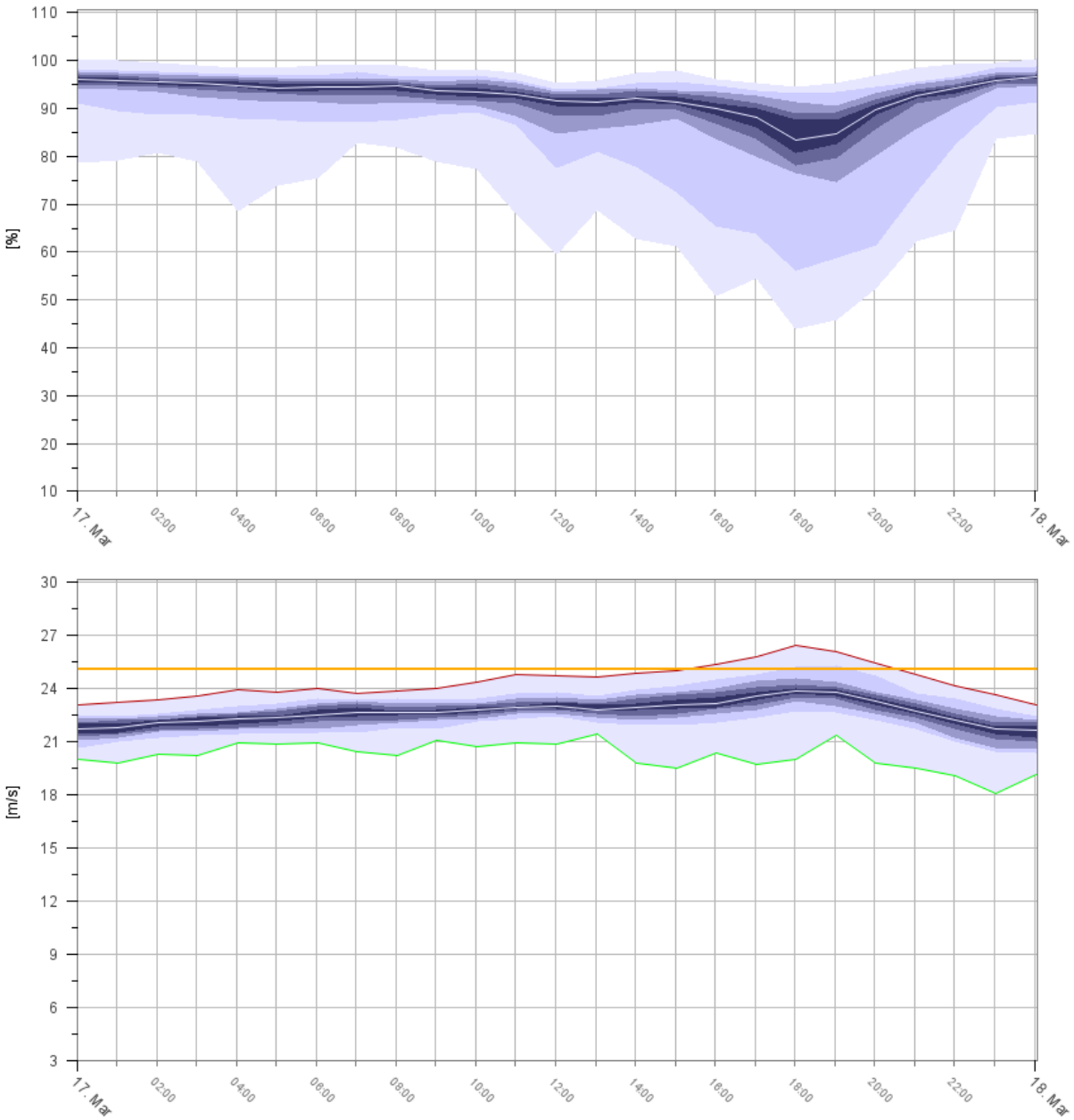


Figure 2: Probabilistic forecast example. Upper graph shows 9 percentiles (P10..P90) in colour bands from a 75 member Multi-Scheme EPS (MSEPS, e.g. [Pahlow et al. 2008]) for day-ahead wind power, lower graph shows the same for wind speed, where the yellow line marks the threshold (25 m/s) around which a high-speed shutdown can occur.

The games have been introduced in an IEA Wind Task 36 workshop in January 2020 and thereafter released. When closed for final evaluation, the experiments had been played by more than hundred participants. The experiments have revealed a number of interesting aspects regarding decision making with and without uncertainty information from probabilistic ensemble forecasts. Although we can conclude that there is a potential benefit, and most participants also confirmed in the follow-up questionnaire that they clearly preferred to have probabilistic fore-casts at hand when making decisions on extreme events, there are still many open questions. We will discuss these open questions, present the results of these experiments, the lessons learnt and investigate together with the audience the future directions for the coming decision experiments and training tools that we plan to design to assist the industry in the integration of weather uncertainty into their daily decision making.

References:
[1] R. J. Bessa, C. Möhrlen, V. Fundel, et. al., "Towards improved understanding of the applicability of uncertainty forecasts in the electric power industry, Energies, vol. 10, no. 9, p. 1402, 2017.
[2] Joslyn S, LeClerc J. Decisions With Uncertainty: The Glass Half Full. Current Directions in Psychological Science., 22(4):308-315, 2013.

Regular Session: Wind Resource Assessment (I)

New wind atlas generation for Europe and Germany based on ERA5

Martin Schneider*, and André Glücksmann
anemos GmbH
*Presenting author

Keywords: wind atlas | remodelling approach | meso-microscale coupling | site-specific | anemos

High resolved mesoscale wind simulations are a more and more common approach to assess the wind resource. An increasing number of legal restrictions for planned wind farms needs high qualitative time series of ten minutes temporal resolution. In particular, the WRF model is widely used for wind simulations providing a variety of literature within the field of wind energy as an open source model. In the last two years ERA5 became the state-of-the-art reanalysis dataset for Europe.
Several wind atlas projects such as NEWA, Global Wind Atlas 3.0 or the EMD WRF Europe+ wind atlas are now based on ERA5 reanalysis.
In a project for the German federal environment office, anemos developed a new generation of wind atlases for Germany and Europe based on the ERA5 Reanalysis data. This project also aimed to challenge one of the WRF drawbacks: the average deviation (bias) in wind speed is high in comparison to measurements, onshore often reaching an overestimation of 5 - 10%. This issue weakens the meaningfulness of modelling of the wind resource since the field of application is limited if the absolute value of the simulations is not useable. Consequently, anemos implemented a Remodelling approach that decreases the bias of the simulated wind speed (Weiter 2019).

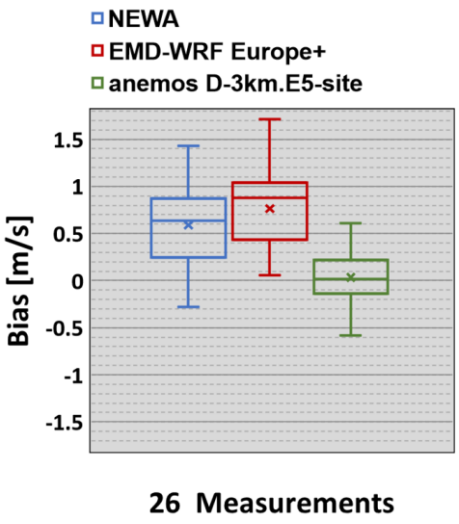


Figure 1: Box plot of the bias for 26 independent sites. Compared is the final version of the anemos wind atlas with the NEWA and EMD-WRF Europe+ wind atlas.

This Remodelling approach has already shown proven effectiveness. Numerous high-quality wind measurements in the simulation area are used to create a post-processing optimization method for WRF simulations. Now this approach has been updated. The basic concept is to use sub-grid information, which is not part of the original WRF simulation, and wind measurement data in order to derive wind direction-dependent scaling parameters that are finally applied on each wind speed time series of the data set. Since ERA5 reanalysis data shows a bias within the annual cycle, a correction of this was newly implemented in the optimization approach. Furthermore, the coupling between the mesoscale to the microscale was improved. From CFD-Model runs, a statistical height and roughness correction was developed and implemented. Finally,

this upgraded Remodelling approach results in high-quality and site-specific time series. It significantly reduces the bias (Fig. 1) in wind speed and additionally results in an increase in correlation (Fig. 2) in most cases.

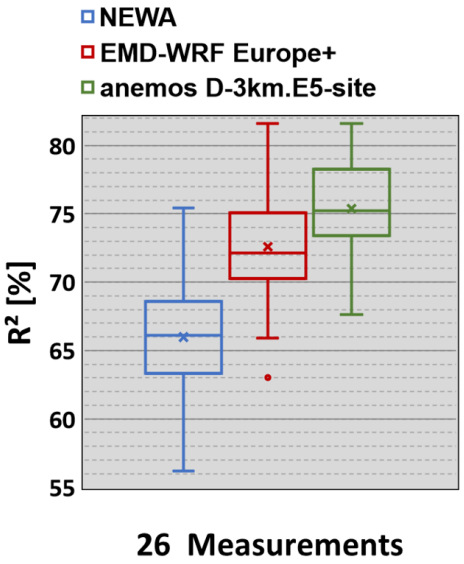


Figure 2: Box plot of the correlation coefficient for 26 independent sites. Compared is the final version of the anemos wind atlas with the NEWA and EMD-WRF Europe+ wind atlas.

The verification of the new wind atlases is of crucial importance in order to gain knowledge about their quality and limits, more precisely the uncertainty. Thus, anemos participated in 'The NEWA Ferry Lidar Benchmark: Comparing mesoscale models with lidar measurements along a ship route' (Witha 2019) with its downscaled ERA5 wind atlases and achieved one of the best results in correlation and bias. Furthermore, an external verification with 66 measurement sites shows a standard deviation of the bias of 4.5% for the mean wind speed. Advantages of the new anemos wind atlas generation are highlighted by comparing independent wind measurements with the anemos wind atlas and e.g. NEWA or EMD WRF Europe+ (see. Fig. 1 & 2).

References:

Weiter, A., M. Schneider, D. Peltret und H.-T. Mengelkamp: Electricity production by wind turbines as a means for the verification of wind simulations. Meteorol. Z., 28, 1, 69-77, doi: 10.1127/metz/2019/0924

Witha, B., A.N. Hahmann, T. Sile, M. Dörenkämper, Y. Ezber, E. Garcia-Bustamante, J. Fidel Gonzalez-Rouco, G. Leroy, J., Navarro, 2019: NEWA, Report on WRF model sensitivity studies and specifications for the mesoscale wind atlas production runs, https://zenodo.org/record/2682604#.XnH3GohKiHt

A model-chain for wind resource assessment in complex terrain via statistical-dynamical downscaling using dynamical tendencies for meso-micro coupling

Bjarke Tobias Olsen*, and Dalibor Cavar
Technical University of Denmark
*Presenting author

Keywords: Mesoscale to microscale coupling | Complex terrain | Statistical-dynamical downscaling | Downscaling

The study presents a model-chain for estimating wind resources in complex terrain by statisticaldynamical downscaling. The model-chain consists of the Weather Research and Forecasting (WRF) mesoscale model dynamically one-way coupled to the EllipSys3D microscale model via dynamical tendencies (Olsen, 2018).
The EllipSys3D microscale model, developed at DTU, is a CFD model capable of representing a simplified set of atmospheric boundary layer physics. It uses a dry-atmosphere incompressible unsteady Reynolds-Averaged Navier-Stokes model formulation and includes buoyancy forces via the Boussinesq approximation. Turbulence is modeled using the kepsilon model modified for non-neutral stability conditions (Sogachev et al., 2012). To avoid gravity waves reflecting on the top boundary of the microscale domain, causing disruption of the flow near the surface, Rayleigh damping is used in the top 1000 m of the domain.
One-way coupling between WRF and EllipSys3D is achieved by forcing the microscale model via dynamical tendencies extracted from the mesoscale model, as suggested by Bosveld et al. (2014), Sanz-Rodrigo et al. (2016, 2017), and others. The tendencies, consisting of advection and pressuregradient terms, are extracted from WRF and represent the time-varying atmospheric mesoscale conditions at the site. The tendencies are added as additional source terms in the relevant governing equations in the microscale model.

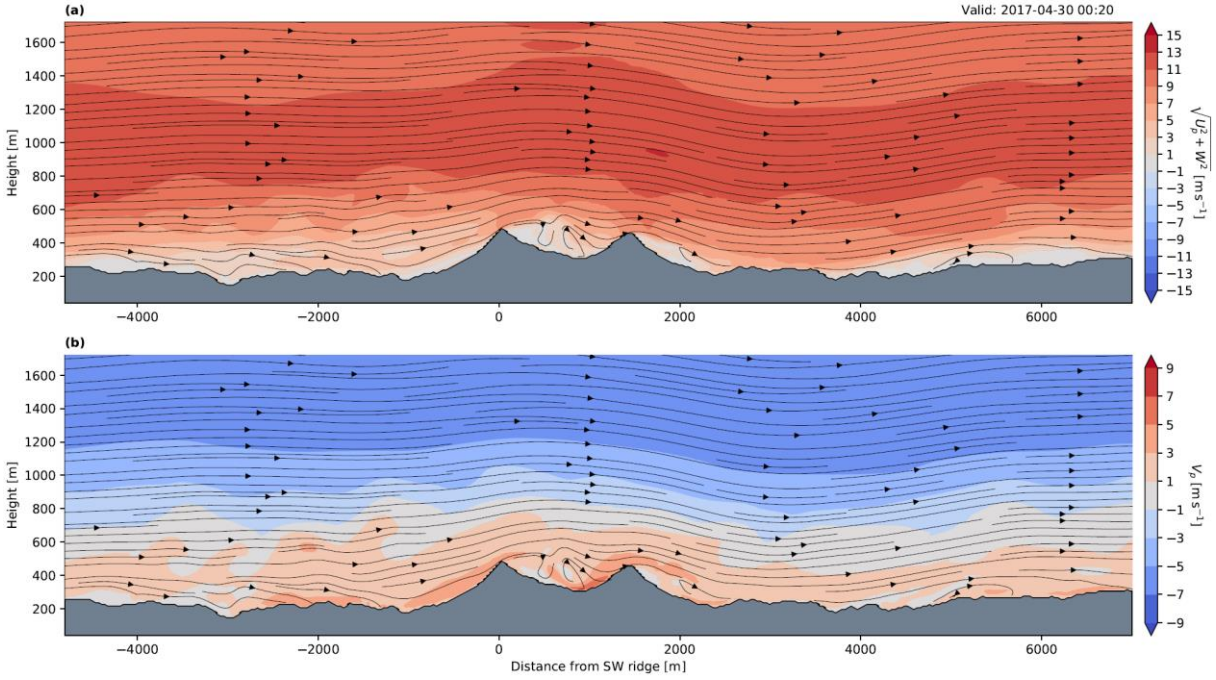


Figure 1: Snapshot of a the EllipSys3D URANS simulation along a vertical cross-section across the Perdigão doublehill. The top panel shows the plane-wise velocity (a) and in the bottom panel the cross-plane velocity is shown (b). Both panels have the plane-wise velocity streamlines overlayed in black.

To ensure scale-separation between the microscale flow and the mesoscale tendencies, the tendencies are extracted from a single WRF grid-column in a domain with a horizontal grid-spacing approximately of the same footprint as the entire microscale grid. Since the microscale grid is forced via body-forces in the full volume, periodic boundary conditions are used and the surface elevation is relaxed to a constant height in a

buffer-region along the edges of the microscale grid. The timevarying surface temperature in the WRF grid-cell is used as the lower boundary condition for temperature in the microscale model. To ensure consistency with the mesoscale model, and to remove excess heat, nudging towards the temperature in the WRF grid-column is imposed.

The mesoscale to microscale model-chain is used to estimate wind resources at a site by statisticaldynamical downscaling, wherein a limited number of representative days are chosen and downscaled with the microscale model. The representative days are selected via Monte-Carlo sampling from the WRF data, such that the average conditions of all the days match the average conditions for the full long-term period.

To evaluate the methodology, the complex double-hill site at Perdigão in Portugal is used. The site was subject to extensive measurements in 2017 in the New European Wind Atlas (NEWA) research project (Fernando et al., 2019). Half a year of measurements, taken over a one year period at the site, is taken as the target period for the downscaling and used for validation of the long-term wind statistics. Figure 1 shows a snapshot of the flow, simulated by the EllipSys3D model, along a vertical cross-section across the double-hill site.

References:

Olsen, B.T., 2018. Mesoscale to microscale coupling for determining site conditions in complex terrain (Doctoral dissertation, PhD thesis, DTU Wind Energy, https://doi.org/10.11581/00000036).

Bosveld, F.C., Baas, P., van Meijgaard, E., de Bruijn, E.I.F., Steeneveld, G.J., Holtslag, A.A.M. (2014) "The Third GABLS Intercomparison Case for Evaluation Studies of Boundary-Layer Models. Part A: Case Selection and Set-Up", Boundary-Layer Meteorology, 152(2), pp. 133–156. doi: 10.1007/s10546-014-9917-3.

Sogachev, A., Kelly, M., Leclerc, M.Y. (2012) "Consistent two-equation closure modelling for atmospheric research: buoyancy and vegetation implementations", Boundary-Layer Meteorology, 145(2), pp. 307–327. doi: 10.1007/s10546-012-9726- 5.

Sanz Rodrigo, J., Churchfield, M. and Kosovic, B. (2016) "Atmospheric boundary layer modeling based on mesoscale tendencies and data assimilation at microscale", Wind Energy Science Discussions, (August), pp. 1–38. doi:10.5194/wes-2016-26.

Sanz Rodrigo, J., Churchfield, M., Kosovic, B. (2017) "Results of the GABLS3 diurnal-cycle benchmark for wind energy applications", Journal of Physics: Conference Series, 854(1). doi:10.1088/1742-6596/854/1/012037.

Fernando, H.J.S., Mann, J., Palma, J.M.L.M., Lundquist, J.K., Barthelmie, R.J., Belo-Pereira, M., Brown, W.O.J., Chow, F.K., Gerz, T., Hocut, C.M. and Klein, P.M., 2019. The Perdigao: Peering into microscale details of mountain winds. Bulletin of the American Meteorological Society, 100(5), pp.799-819.

Integrated wind resource modelling with WRF and PyWAsP

Rogier Floors[1], Andrea N. Hahmann[1], Dalibor Cavar[1], Bjarke Tobias Olsen[1], Neil Davis[1], Alfredo Peña[1], Niels Gylling Mortensen[1], Andreas Bechmann[1], Jens Carsten Hansen[1], Chris Lennard[2], Leon Prinsloo[3], and Jake Badger[1]

[1]Technical University of Denmark
[2]University of Cape Town
[3]Council for Scientific and Industrial Research (CSIR)

Keywords: Wind resource | WRF | WAsP | Downscaling | Microscale modelling

The regional wind climate provides vital information for locating optimal areas for the siting of wind power plants and developing regional action plans to reduce fossil fuels for electricity generation.
The output from long-term simulations using a mesoscale model (with 10-2 km grid spacing) is now widely used to generate the wind climatology necessary for calculating the wind energy resources of a given geographical area. Nevertheless, for these wind climatologies to be useful, they need to be validated against measurements and serve as input to microscale models for further downscaling (Badger et al., 2014).
According to the Numerical Wind Atlas concept, we can remove the mesoscale model grid effects to obtain a generalized wind climate (GWC) and further downscale with a microscale model to any site within the same regional wind climate (Badger et al., 2014; Lennard et al., 2015). We have made considerable improvements to the generalization procedures in the NEWA project (Dörenkämper et al., 2020).
In a first approach, we use the same methodology as in the NEWA project to generalize the WRF model output. This generalization relies on the linearized microscale model LINCOM to compute orographic speedups and uses internal boundary layer theory to compute roughness speedups (Sempreviva et al., 1990). Finally, it uses the geostrophic drag law to compute the geostrophic wind climate according to the procedure outlined in Badger et al. (2014). The downscaling then transforms the generalized wind climates with a similar geostrophic drag law, and applies the microscale speedup effects derived from the analysis of high-resolution elevation and roughness maps with the microscale model to obtain the downscaled microscale wind climate using the WAsP model chain (Troen and Petersen, 1989).
The second generalization procedure solely relies on the WAsP model engine: we argue that this is a more consistent approach: the same model is used to remove the mesoscale effects and to apply the microscale effects. Also, it has the added benefit that it can apply a newly developed stability model to both the generalization and the downscaling procedures. We performed the generalization and downscaling with PyWAsP version 0.4.1 with the baroclinicity model switched off (Floors et al., 2018).
A wealth of validation data has recently become available in wind resource atlases (NEWA, WASA 3, Mexico). These data allow for an evaluation of the added value of performing mesoscale simulations with the WRF model compared to the ERA5 reanalysis data used as boundary conditions. We further perform WRF simulations downscaling using the microscale approaches described above. We evaluated all approaches at 17 meteorological masts in non-complex terrain in South Africa (Figure 1).

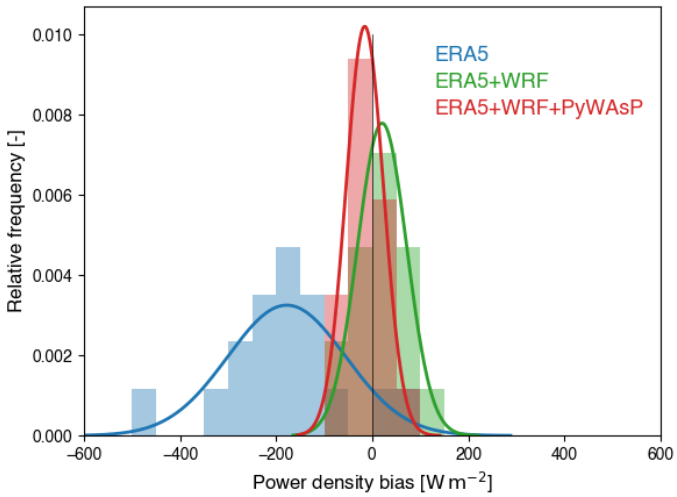


Figure 1: Bias in power density at 17 meteorological masts in South Africa using ERA5, ERA5 downscaled with WRF, and WRF downscaled with PyWAsP.

The ERA5 output severely under-predicts the mean power density at nearly all sites, whereas the WRF simulations have a mean power density bias close to zero. Adding the microscale PyWAsP downscaling further improves the results, with a reduced spread between model and observations.
In addition to these results, we also present and discuss the differences between the LINCOM and PyWAsP generalizations.

References:

Badger, J., Frank, H., Hahmann, A. N., & Giebel, G. (2014). Wind-Climate Estimation Based on Mesoscale and Microscale Modeling: Statistical-Dynamical Downscaling for Wind Energy Applications. Journal of Applied Meteorology and Climatology, 53(8), 1901–1919. https://doi.org/10.1175/JAMC-D-13-0147.1

Dörenkämper, M., and Coauthors (2020): The Making of the New European Wind Atlas - Part 2: Production and evaluation. Geosci. Model Dev., 13, 5079–5102, https://doi.org/10.5194/gmd-13-5079-2020.

Floors, R. R., Troen, I., & Kelly, M. C. (2018). Implementation of large-scale average geostrophic wind shear in WAsP 12.1. DTU Wind Energy Report E-0169, 10 pp. https://orbit.dtu.dk/en/publications/implementation-of-large-scale-averagegeostrophic-wind-shear-in-w (last access 28 January 2021).

Lennard, C., Hahmann, A. N., Badger, J., Mortensen, N. G., & Argent, B. (2015). Development of a Numerical Wind Atlas for South Africa. Energy Procedia, 76, 128–137. https://doi.org/10.1016/j.egypro.2015.07.873

Sempreviva, A. M., Larsen, S. E., Mortensen, N. G., & Troen, I. (1990). Response of neutral boundary layers to changes of roughness. Boundary-Layer Meteorology, 50(1–4), 205–225. https://doi.org/10.1007/BF00120525

Troen, I. and Petersen, E. L. (1989): European Wind Atlas. Risø National Laboratory, 656 pp. https://orbit.dtu.dk/en/publications/european-wind-atlas (last access 28 January 2021).

Calculation of a global atlas of expected wind turbine design class

Lasse Svenningsen[1,*], René M. M. Slot[1], Morten L. Thøgersen[1], Xiaoli Larsén[2], Neil Davis[2], Ásta Hannesdóttir[2], Mark Kelly[2], Bjarke Olsen[2], Rogier Floors[2], and Marc Imberger[2]
[1]EMD International A/S
[2]Technical University of Denmark
*Presenting author

Keywords: Global atlas | Siting parameters | Design class | Site suitability | Response model

The GASP project develops the first 'Global Atlas of Siting Parameters' in high spatial resolution (250m). Here we present the work in GASP to establish a global atlas of expected wind turbine design classes. This atlas will benefit authorities and the industry broadly as a first-line estimate of turbine design class for very fast initial decision making when prospecting sites in new regions.
GASP builds upon the existing wind resource map in the Global Wind Atlas and extends it with additional important site parameters. The combined set of site parameters in GASP form the required input to determine the structural loads which decide if a wind turbine design class is suitable for a prospect site.
As part of GASP we also demonstrate how the accuracy of the site parameters can be significantly improved regionally by calibrating the model with scattered wind measurements. The regional calibration employs a heteroscedastic Gaussian Process Regression (GPR) machine learning method and is demonstrated for the entire country of Sweden. Calibration results are promising using geospatial predictors derived from recent regional and global databases.

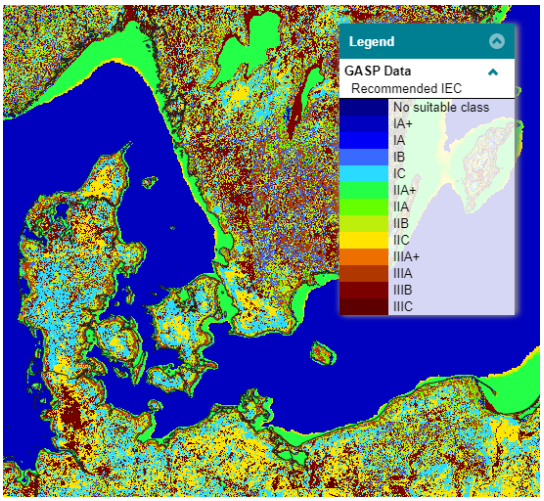


Figure 1: Preliminary illustration of expected design classes for a region around Denmark. Taken from a development version of windprospecting.com.

Wind turbine design classes are defined in the IEC61400-1 ed. 4 standard (IEC., 2019) which lists their design requirements. The standard also defines the required set of site parameters for assessment of the suitability of a given design class at a prospect site. These parameters include wind speed distribution, turbulence, wind shear, flow inclination and air density, as well as assessment of the terrain complexity and 50-year extreme wind speed.
In site suitability assessment the set of site parameters is input to load calculations for each turbine component, and the resulting loads are then compared to the design loads for the relevant design class. Design loads are obtained using the design climate defined for each design class in the standard (IEC., 2019). In GASP we predict the structural loads for 1012 different site locations using the fast and accurate response surface method 'Load Response' described in (Toft et al., 2016) and implemented on EMD's 5000+ core HPC cluster. Representative generic response models are established using three reference turbine models whose aeroelastic design is available in the public domain, as e.g. the NREL 5MW (Jonkman et al., 2009).

Most wind turbines are installed in a park layout where each wind turbine sheds wake on its neighbouring turbines, thereby increasing the level of turbulence. To realistically account for wake effects we adopt a standard grid layout with a spacing of 5 rotor diameters (RD) between turbines in the main wind direction and 3 RD orthogonal to this. This allows for calculation of an atlas of expected design class both with and without wake effects.

By April 2021 the GASP maps of resource, site parameters and expected turbine design classes will be freely available from the website windprospecting.com. The data will also be available within the standard desktop softwares windPRO and WAsP, and lastly for direct machine access via a RESTbased API service ('EMD-API') suitable for integration, big-data and machine learning applications.

References:
IEC. (2019) 'International Standard IEC 61400-1 ed. 4, "Wind Turbines - Part 1: Design Requirements".'
Jonkman, J. M. et al. (2009) Definition of a 5-MW reference wind turbine for offshore system development. NREL/TP-500- 38060. National Renewable Energy Laboratory.
Toft, H. S. et al. (2016) 'Assessment of wind turbine structural integrity using response surface methodology', Engineering Structures. Elsevier Ltd, 106, pp. 471–483. doi: 10.1016/j.engstruct.2015.10.043.

Wind resource assessment using a novel meso-microscale coupling framework based on two-level self-organized maps clustering

Pablo Duran*, and Arne R. Gravdahl
WindSim AS
*Presenting author

Keywords: Computational Fluid Dynamics | RANS | Weather Research and Forecasting model | Machine Learning | Annual Energy Production

Mesoscale meteorological models can provide an important wealth of information about the wind conditions at a location. A promising way for Computational Fluid Dynamic (CFD) models to benefit from this information is to utilize mesoscale simulation results as boundary conditions for the microscale simulations (Sanz Rodrigo et al., 2017). However, the common practice in the industry for Annual Energy Production estimations using CFD models is to assume steady-state flow. This assumption requires to somehow aggregate the mesoscale data in few cases to be then used as boundary conditions. When using CFD models, the industry typically conducts 12 to 36 simulations with different wind directions. Following that framework, a possible approach to aggregate the mesoscale data is to compute the mean field by wind direction (Durán, Meiβner and Casso, 2020).
Nevertheless, this approach falls in the danger of aggregating completely different wind conditions (e.g. atmospheric stability) which might produce mesoscale fields that are representative of neither.
.

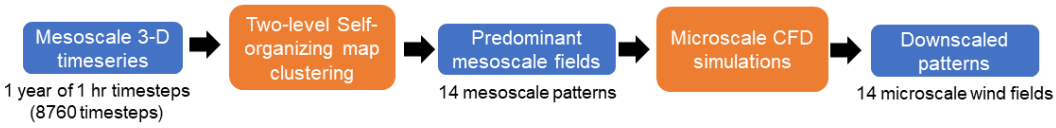


Figure 1: Proposed meso-microscale coupling framework suitable for wind resource assessment. Blue and orange boxes correspond to data and processes, respectively. Below each blue box, the data corresponding to the validation study used in this work is indicated.

As an alternative, we have developed a meso-microscale coupling framework (Figure 1) that consists in obtaining the most predominant wind conditions in a fully automated manner, utilizing a two-level self-organized maps clustering technique (Vesanto and Alhoniemi, 2000; Kohonen, 2001). This clustering technique is based on an unsupervised learning algorithm and it does not require to know the total number of clusters in advance. All training parameters are predefined based on previous studies (Durán et al., 2020) and therefore no input parameters from the user are required. For each of the detected predominant wind conditions, one 3D mesoscale field is obtained, which is then used to derive the boundary conditions of a CFD model. As a study case, we utilized meteorological mast measurements located in a rolling area in the Atacama Desert belonging to a commercial wind energy project. The site present predominant winds from a few directions and a marked diurnal and seasonal cycle, where we believe the proposed approach can be the most beneficial. One year of mesoscale data is obtained using the Weather Research and Forecasting (WRF) model covering the area of the measurements and the WindSim software is utilized for CFD simulations.
The clustering technique derived 14 mesoscale patterns of varying wind and potential temperature conditions across the site. We demonstrate capability of the automatic classification to organize the extracted patterns according to the wind conditions represented in the mesoscale like atmospheric stability, wind speed, shear, and wind direction (Figure 2). Furthermore, we show that as expected, some of these conditions are correlated, like atmospheric stability and shear. We also show that the probability distributions of these patterns depend on seasons as well as on diurnal cycles.

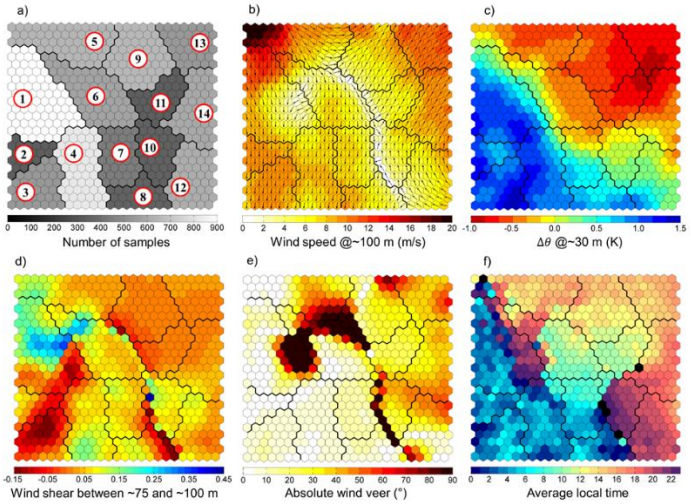


Figure 2: Ordering of several quantities in the Self-organizing map (SOM). The SOM corresponds to an abstract 2-D representation of N-D underlying mesoscale data. Nodes (represented by hexagons) close to each other have similar properties. The dark lines in the map show the partition of the SOM by which the final clustering is based on.

The 14 mesoscale patterns are downscaled with WindSim and validated against the onsite measurements. For comparison, the same validation is conducted directly with the mesoscale patterns as well as with standalone WindSim simulations. Compared to the standalone CFD simulations, the proposed meso-microscale coupling framework has a total reduction of crosschecking error of 4.0%, with a maximum of 20% reduction the pattern with neutral and low-shear conditions. Compared to the mesoscale WRF fields, the total reduction of cross-checking error was of 2.7%, with a maximum of 15% reduction in one of the stably stratified patterns

References:

Durán, P. et al. (2020) 'Automated classification of simulated wind field patterns from multiphysics ensemble forecasts', Wind Energy, p. we.2462. doi: 10.1002/we.2462.

Durán, P., Meiβner, C. and Casso, P. (2020) 'A new meso-microscale coupled modelling framework for wind resource assessment: A validation study', Renewable Energy. Submitted to Renewable Energy, 160, pp. 538–554. doi: 10.1016/j.renene.2020.06.074.

Kohonen, T. K. (2001) Self-Organizing Maps. 3rd edn. New York: Springer-Verlag.

Sanz Rodrigo, J. et al. (2017) 'Mesoscale to microscale wind farm flow modeling and evaluation', Wiley Interdisciplinary Reviews: Energy and Environment, 6(2). doi: 10.1002/wene.214.

Vesanto, J. and Alhoniemi, E. (2000) 'Clustering of the self-organizing map', IEEE Transactions on Neural Networks, 11(3), pp. 586–600. doi: 10.1109/72.846731.

Optimising the WRF model configuration for the Mexican Wind Atlas

Andrea N. Hahmann[1,*], Ramón Lira Arguello[2], Bjarke Olsen[1], Dalibor Cavar[1], Rogier Floors[1], and Alfredo Peña[1]

[1]Technical University of Denmark

[2]Instituto Nacional de Electricidad y Energías Limpias (INEEL), Mexico

*Presenting author

Keywords: wind energy resources | mesoscale modelling | model evaluation | Mexican wind atlas

Long-term simulations of the wind with Numerical Weather Prediction models (e.g. the Weather, Research and Forecasting (WRF) model) are nowadays the basis of most modern regional wind atlases (Draxl et al., 2015; Wijnant et al., 2019; Dörenkämper et al., 2020). In general, these models are not explicitly developed for wind energy applications, and the simulations need to be correctly configured to predict the regional wind climate's characteristics accurately. The recent New European Wind Atlas (NEWA; Dörenkämper et al., 2020) and Wind Atlas of South Africa (WASA; Hahmann et al., 2018) used similar strategies to find the configuration that reduced the simulation errors of the wind speed distribution against data from measurement sites. The optimisation in these two regions was based mostly on varying the WRF model physical parameterizations (e.g. surface and planetary boundary layer). The tested simulation ensemble showed small differences in long-term mean wind speed statistics (Hahmann et al., 2020).

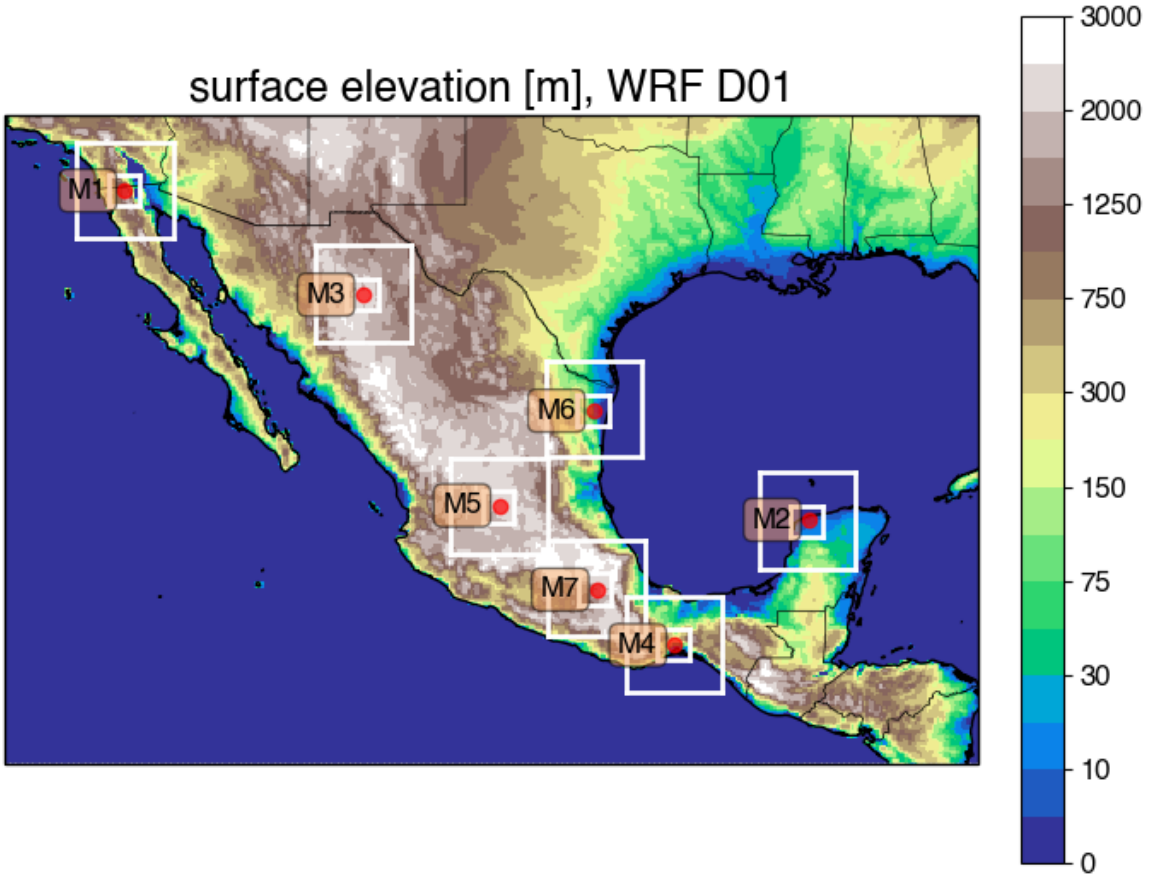


Figure 1: Terrain elevation and model domain configuration of the multi-grid simulations.

Mexico's wind climate has posed challenges that we have not experienced in other previous regional wind atlases. For example, in the region of the Istmo of Tehuantepec (Mexico's "wind basket"), simulations using WRF tend to overestimate the wind speed (and so its mean) severely. When looking at data from a high-

quality mast in the central highlands, the simulated mean wind speeds were 40-50% larger than those observed. These limitations could not be resolved by simply replacing one PBL scheme with another. Still, the domains' size, horizontal grid spacing and location, and balancing use of the forcing reanalysis (spectral nudging) played a more significant role. However, only very high-resolution (~ 1 km) at some complex terrain sites will bring the mesoscale model simulations close to the observed wind speed values. Updating the land use maps and surface roughness length tables or downscaling using the microscale model PyWAsP (Dörenkämper et al., 2020; Floors et al., 2021) had only a small palliative effect at these sites.

This presentation guides the audience by configuring a WRF simulation showcasing the essential issues encountered and how to solve them. We show that one can use nudging and varying domain size to balance the synoptic forcing's importance from the reanalysis versus the region's fine detail mesoscale features.

Finally, we showcase two long-term WRF model simulations. First, an experimental run where we surround each site by two small high-resolution nested grids (3 km x 3 km and 1 km x 1 km; see the figure). Second, the final Mexican wind atlas covering all of Mexico, with three 3 km x 3 km overlapping nested grids. We evaluate both simulations against data from seven tall masts, located in very diverse environments and wind climate conditions covering Mexico. The evaluation includes both raw WRF and downscaled wind climatologies at these masts.

References:

Hahmann, A. N., and Coauthors, 2020: The making of the New European Wind Atlas - Part 1: Model sensitivity. Geosci. Model Dev., 13, 5053–5078, https://doi.org/10.5194/gmd-13-5053-2020.

Dörenkämper, M., and Coauthors, 2020: The Making of the New European Wind Atlas - Part 2: Production and evaluation. Geosci. Model Dev., 13, 5079–5102, https://doi.org/10.5194/gmd-13-5079-2020.

Draxl, C., A. Clifton, B.-M. Hodge, and J. McCaa, 2015: The Wind Integration National Dataset (WIND) Toolkit. Appl. Energy, 151, 355–366, https://doi.org/10.1016/j.apenergy.2015.03.121.

Wijnant, I., van Ulft, B., van Stratum, B., Barkmeijer, J., Onvlee, J., de Valk, C., Knoop, S., Kok, S., Marseille, G., Baltink, H. K., and Stepek, A.: The Dutch Offshore Wind Atlas (DOWA): Description of the dataset, Tech. Rep. TR-380, Royal Nether- lands Meteorological Institute (KNMI), available at: https:// www.dutchoffshorewindatlas.nl/.

Hahmann, A., Pian, A., Lennard, C., and Mortensen, N. G, 2018: Mesoscale Modelling for the Wind Atlas of South Africa (WASA) Project – Phase II, Tech. Rep. E-0188, DTU Wind Energy, Denmark, https://orbit.dtu.dk/files/192964222/DTU_Wind_Energy_E_0188.pdf.

Floors, R., A. N. Hahmann, D. Cavar, B. Olsen, N. Davis, A. Peña, C. Lennard, N. G. Mortensen, A. Bechmann, L. Pinsloo, J. C. Hansen, J. Badger, 2021: Integrated wind resource modelling with WRF and PyWAsP. Abstract submitted to WESC 2021.

Regular Session: Wind Resource Assessment (II)

Optimization of wind measurements for resource assessment using the new LiMeS tool and the lidar availability map

Doron Callies[1,2,*], Lukas Pauscher[1], Florian Jäger[1], Tobias Klaas[1], Yannik Woll[1], Tobias Dienwiebel[1], Alexander Basse[2], Tina Beyer[3], and Benjamin Roesner[4]
[1]Fraunhofer Institute for Energy Economics and Energy System Technology (IEE)
[2]University of Kassel
[3]Ramboll
[4]University of Marburg
[*]Presenting author

Keywords: lidar | measurement strategies | lidar availability | digitalization of resource assessment | uncertainties

Modern lidars are small, lightweight and mobile. Thus, they offer a high degree of flexibility in measurements to determine the wind resource for wind energy projects. So far, however, these flexibilities have hardly been used because the systematic comparison of different measurement strategies is a major challenge. Important choices for measurement strategies include the number of measurement points in the wind farm, the measurement duration at these measurement points and the selection of the measurement technology (lidar and/or measurement mast). To evaluate the measurement strategy, it is necessary to quantify the resulting overall uncertainty and the costs of the measurement in each case.
For this purpose, a tool was developed in python which allows the evaluation of measurement strategies. It is designed to take into account the different uncertainties (horizontal extrapolation, long-term correction, lidar measurement error in complex terrain, vertical extrapolation, measurement device specific uncertainties) and to perform an optimization for different measurement scenarios (e.g. different number of lidars and/or measurement masts) or different financial budgets for the measurement.
The uncertainty of the horizontal extrapolation was calculated using an approach of (Clerc et al.2012). The function estimating the uncertainty of the vertical extrapolation as well as the uncertainty for the long-term correction were derived by the profound results within the LiMeS project. To estimate the lidar measurement error due to complex terrain a lidar error map based on CFD simulations was implemented. Short-term lidar measurements can be correlated to an annual measurement, which significantly reduces the uncertainty of the short-term measurement compared to a stand-alone short-term measurement. All other uncertainties that are not directly linked to the measurement strategy (e. g. uncertainty of power curve and losses) were are derived based on expert guess.
The optimization of the measurement strategy is performed based on these different uncertainty functions using a heuristic algorithm. Finally, to estimate the economic benefit of a measurement strategy a module was implemented, which allows the determination of the effect of an uncertainty reduction to the financing conditions of the planned wind farm project.
The LiMeS tool was used to calculate various examples of wind farm layouts in terrain of varying complexity. As an example, the results of a wind farm with a hub height of 150 m in complex terrain are shown below. The optimized measurement setup and its costs for different measurement strategies are shown in figure 1.

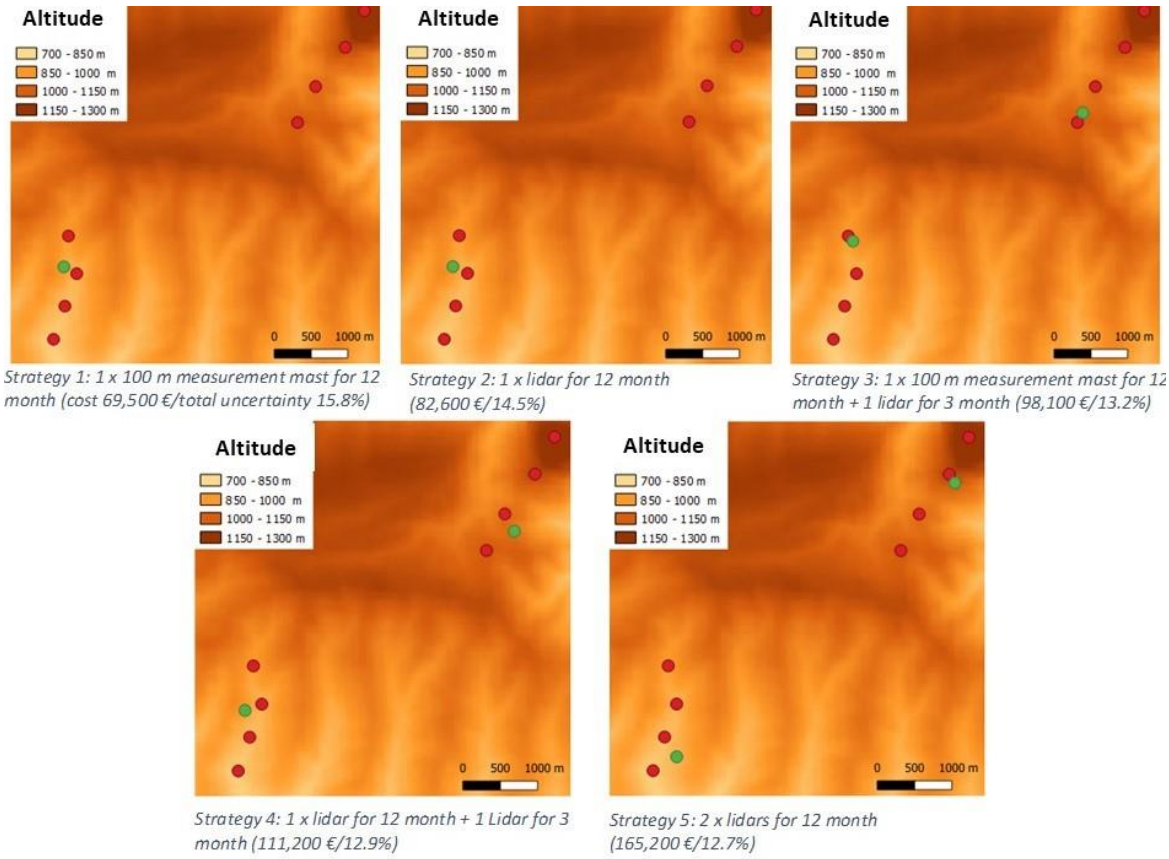


Figure 1: Results of the optimization of different measurement strategies at a complex wind farm site (red dots are wind turbines, green dots are measurement devices, the costs for measurements are estimates based on current prices in Germany and represent approximations, the calculated total uncertainty includes all typical uncertainties of a yield estimation and refers to energy yield)

There are five different strategies leading to different uncertainties and costs.
In addition to the tool, a special availability map for lidar measurements in Germany was calculated with a resolution of about 3 km by 3 km (see figure 2).

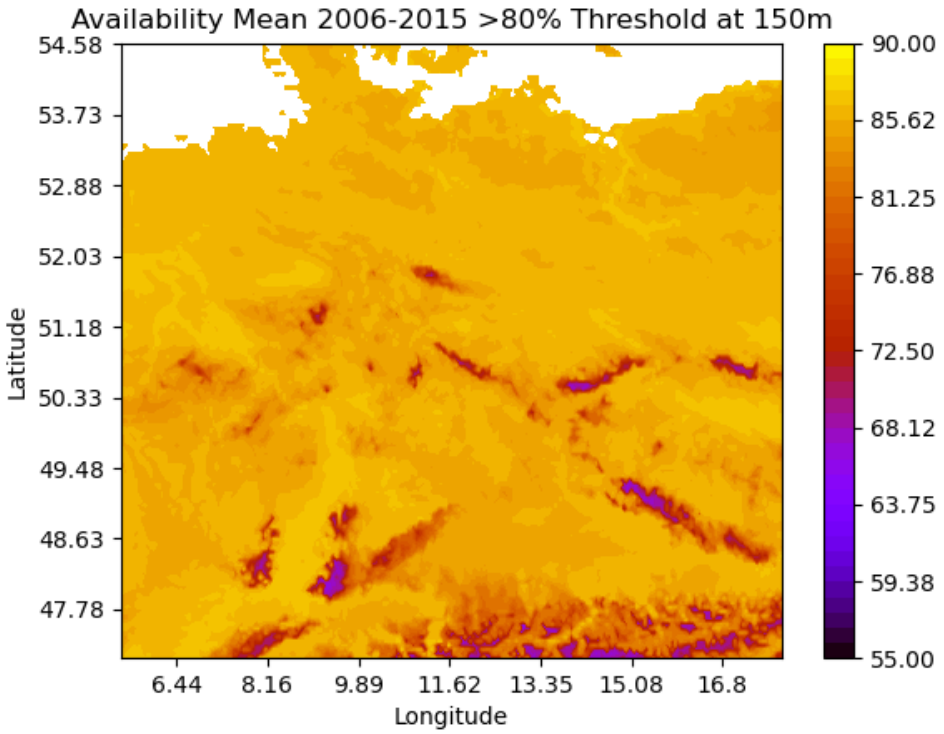


Figure 2: Lidar availability map for Germany

The map depicts the long-term annual mean as well as the long-term monthly means of the expected lidar availability. The map shows that especially in autumn and winter months in the German middle and high mountains significant availability reductions at hub height (about 150 m) can be expected. For the creation of the map, an empirical function was derived based on long-term time series of the cloud base altitude and measurement data from Windcube lidars. This lidar availability map can now be used to estimate the measurement availability of a lidar at a planned project site before the measurement campaign and to decide whether a lidar is appropriate suitable measurement device for this location and measurement period.

References:

Clerc, A.; Anderson, M; Stuart, P; Habenicht, G; (2012) 'A systematic method for quantifying wind flow modelling uncertainty in wind resource assessment', Journal of Wind Engineering and Industrial Aerodynamics, Volume 111, 2012, Pages 85-94, ISSN 0167-6105, https://doi.org/10.1016/j.jweia.2012.08.006.

Modelisation of Lidar deviation to point measurement: model, validation with onsite data and demonstration of more accurate wind field retrieval method

Matthieu Boquet[1,*], Paul Mazoyer[2], Peter Rosenbusch[1], and Andrew Black[2]
[1]Leosphere
[2]Vaisala
[*]Presenting author

Keywords: Lidar | RSD | Accuracy | Wind measurement | Uncertainty

The difference between actual and predicted wind farms power production showed that the prediction is accurate but still not precise (see WFIP-2). It shows that the wind industry still needs to improve models and measurements to further de-risk projects. With standards wind field retrieval methods, measurement uncertainty ranges from 2% to 3%.
We present a method to enhance wind speed measurement uncertainty using ground-based Lidars.
The measurement uncertainty is assessed by tracing back the measurement to national standard i.e. comparing the measurement to calibrated wind tunnel speeds. Since Lidar does not fit into a tunnel, it is compared outdoor to a cup anemometer mounted on a mast. The cup anemometer is calibrated in a tunnel, the loop can be closed: lidar is compared to tunnel wind speed. Comparing Lidar to cup anemometer comes down to comparing volume measurement to point measurement. Modern lidars still show a certain level of deviation to cup anemometer measurement due to their wind field retrieval method in high turbulence environments. This can be seen on the graph that shows deviation of lidar to cup for various TI values for one typical averaging method 'scalar averaging'.
A new wind field retrieval method called "hybrid", developed by Leosphere, is designed to better convert volume measurement into point measurement. Preliminary results have been published, we present here a the full validation of the method over more than 4 years of lidar data along with the equations that model the deviation between volume measurement and point measurement due to turbulence decorrelation. The equations capture both the deviation due to vector and scalar averaging. To our knowledge, model of scalar averaging deviation has not been published yet while model of vector averaging has already been published ([1]). Based on these equations, we are able to demonstrate that the method "hybrid" provides the best estimation of cup measurement for monostatic Lidars.

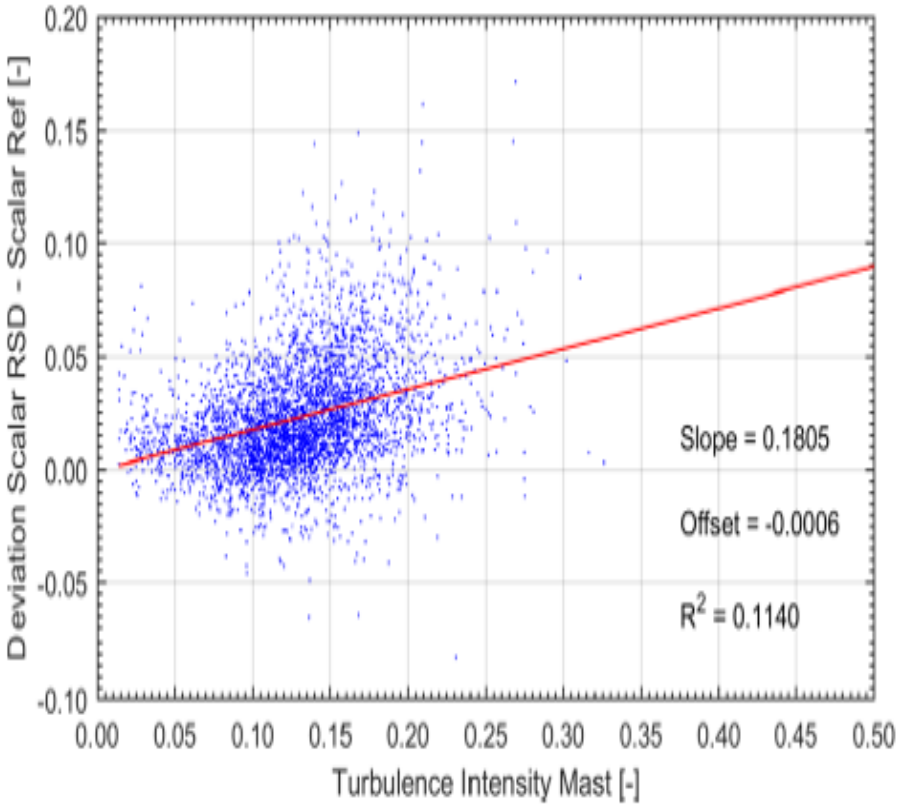


Figure 1: Lidar deviation to cup with turbulence intensity for 'scalar averaging'

At all sites, given that it is simple terrain, the Windcube shows a deviation lower than 1% compared to the mast. It also shows negligible sensitivity to the different turbulence parameters (turbulence intensity, the standard deviation of direction, vertical turbulence) at all heights. As predicted by the theory, the "hybrid" estimates the cup measurement with very little influence of the turbulence parameters. The results are rather robust showing little variation for different types of turbulence structures, and especially little variation is observed for different atmospheric stabilities.

Uncertainty remains a key proxy of one project risk assessment. The contribution to the uncertainty of measurement is not negligible. Therefore, the measurement uncertainty directly converts into losses of point of LCOE. Leosphere has developed a method that applies to the Windcube to reduce uncertainty.

Validating this method on a several datasets, the mean performances of the method can be assessed along with the uncertainty of the Windcube. Especially, it shows the Windcube accuracy is not sensitive to turbulence when using the "hybrid" method.

References:

Clive, P., (2008). 'Compensation of vector and volume averaging bias in lidar wind speed measurements', 14th International Symposium for the Advancement of Boundary Layer Remote Sensing. Risø-DTU, Denmark, 14TH 2008. Glasgow G42 7JG, UK: IOP Conf. Series: Earth and Environmental Science 1 (2008) 012036, pp.1-10.

Measurement of sub-mesoscale structures in the atmospheric boundary layer with Doppler wind lidar during the FESSTVaL campaign

Norman Wildmann[1,*], Frank Beyrich[2], Carola Detring[2], Noviana Dewani[3], Matthias Mauder[4], Eileen Päschke[2], Felix Schmitt[1,4], Julian Steinheuer[5], and Kevin Wolz[4]
[1]German Aerospace Center
[2]DWD
[3]University of Frankfurt
[4]Karlsruhe Institute of Technology
[5]University of Cologne
*Presenting author

Keywords: wind | turbulence | lidar

The FESSTVaL (Field Experiment on sub-mesoscale spatio-temporal variability in Lindenberg) campaign was initiated by the Hans-Ertel-Zentrum für Wetterforschung (HErZ) of the German Meteorological Service (Deutscher Wetterdienst, DWD). Sub-mesoscale structures in the atmospheric boundary layer (ABL) that are targeted in the campaign are for example gusts and cold pools.
Especially gusts are of high interest for wind energy science, so that the results of FESSTVaL can be of high interest for the wind energy community. An essential part of the observational plan of the campaign are wind measurements with Doppler wind lidars. Due to the Sars-CoV-2 pandemics, the campaign could not be realized as planned, but had to be significantly reduced in the number of participants and divided into smaller sub-campaigns (so called "FESST@home" experiments). From May to August 2020, the campaign FESST@MOL was organized at the Boundary Layer Field Site (Grenzschichtmessfeld, GM) Falkenberg of the Lindenberg Meteorological Observatory - Richard- Aßmann-Observatory (MOL-RAO). Here, DWD runs a comprehensive operational measurement program of micrometeorological and boundary layer measurements including the use of a variety of wind sensors and measurement systems. In-situ wind and turbulence measurements are available from a 99 m meteorological mast at the site. During FESST@MOL, the operational measurement program at MOL-RAO was extended by the operation of six Doppler lidar systems provided by DLR and KIT (Karlsruhe Institute of Technology). It was a major goal of this campaign to test and to compare different scanning configurations to derive both wind and turbulence information from Doppler lidar measurements.

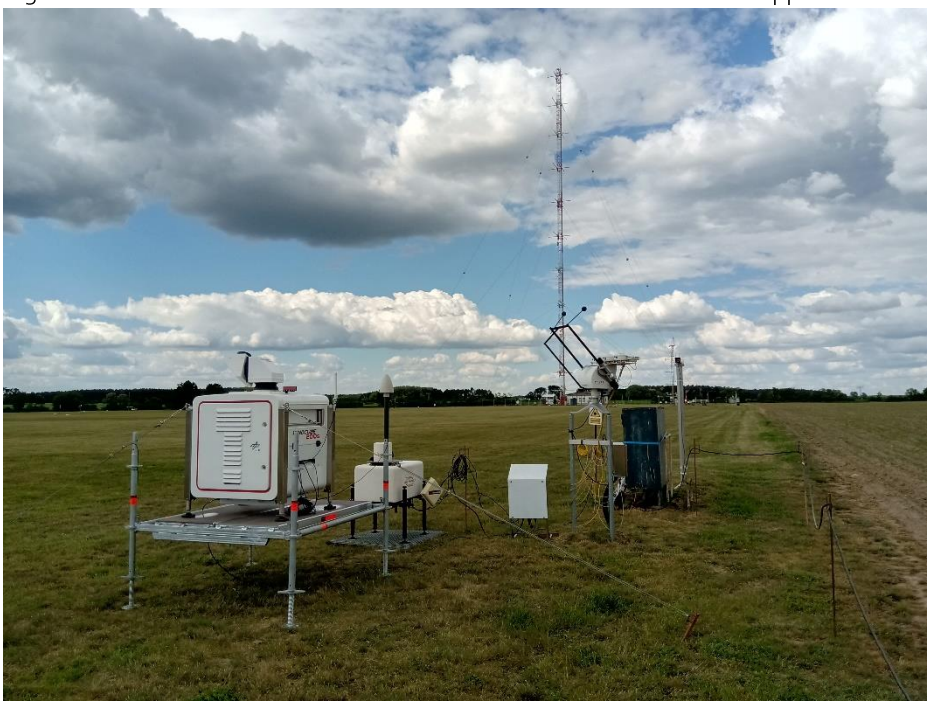


Figure 1: Leosphere Windcube 200S and Halo Photonics Streamline in front of 99 m mast at GM Falkenberg.

Five different kinds of scanning strategies with Doppler lidar were pursued during FESST@MOL to investigate turbulence and sub-mesoscale structures. Virtual tower measurements were realised with three synchronized lidars to obtain the three-dimensional wind vector profile in the lowest 750 m. Vertical stare measurements of a single lidar were done to obtain TKE dissipation rate. Slow, continuous VAD scans were performed to measure wind profiles, but also profiles of TKE and its dissipation rate, assuming spatial homogeneity of the flow. A fast continuous VAD mode was developed to particularly retrieve gusts. Low elevation angle PPI scans with two lidars and an additional RHI scan were performed to capture two-dimensional structures close to the surface. The different scanning strategies were performed with different instruments in parallel so that their results can be compared and synthesized, including the in-situ measurements at the GM Falkenberg as well. We will present an overview and preliminary results of the lidar measurements, with a special focus on the PPI and RHI scans. For these planar scans, analyses are performed in order to extract the dominant scales of turbulence in the observed areas. For large parts of the campaign, the direction of the RHI scans were adapted to the main wind direction as measured at the 99 m tower. This way, it can be observed how turbulent structures are advected, causing alternating loads on potential wind turbines in the flow. The synthesis of the data of all systems is still ongoing and the most promising scanning strategies will be repeated in 2021 for the main FESSTVaL campaign.

Synchronised WindScanner Measurements Between Two Closely Spaced Wind Turbines

Anantha Padmanabhan Kidambi Sekar*, Paul Hulsman, Marijn van Dooren, and Martin Kühn
ForWind - University of Oldenburg
*Presenting author

Keywords: windscanner lidar | remote sensing | induction zone | wake measurements

Two synchronised WindScanners were installed to measure the wind fields in the region between two commercial wind turbines located at a wind farm in Germany. Wind turbines are being increasingly clustered together in wind farms resulting in complex interactions in the region between them (Stevens, 2017). Developments in the field of lidar technology has led to scanning lidars capable of performing very high-resolution measurements of the flow structures in the atmospheric boundary layer and turbine-turbine interactions. In this work, the 2-dimensional flow behaviour in the region between two turbines is measured and characterised using synchronised short-range lidar WindScanners (Mikkelsen, 2020). The measurements were performed in a wind farm consisting of two 3.5 MW eno126 turbines, each of diameter D = 126 m and with a separation distance of 340 m corresponding to 2.7D. Due to the close proximity between the two turbines, the region between them is a mixture of the near wake region of the upstream turbine and the induction zone of the downstream region, resulting in a highly complex flow field. Characterising these interactions are
important for developing and validating models that can simulate the flow in and around wind farms.

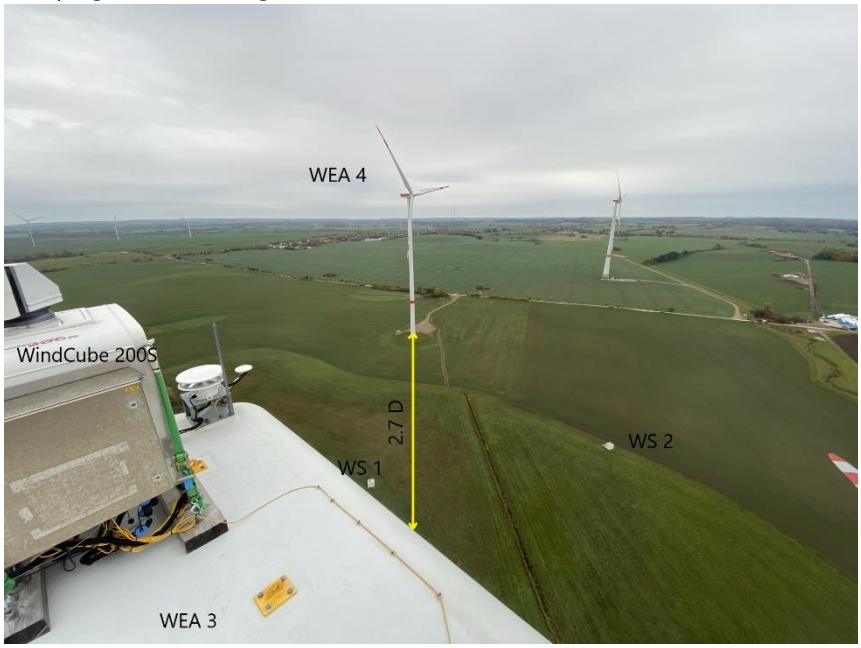


Figure 1: Measurement set-up at Kirch Mulsow, Germany seen from the nacelle of the upstream turbine (WEA3) towards the downstream turbine (WEA4). The WindScanners WS1 and WS2 are installed on containers between the two turbines.

The WindScanners developed by DTU Wind Energy are continuous-wave lidars with a scanhead capable of steering the laser beam to a desired point in space (Mikkelsen, 2008). For the ongoing measurement campaign, two WindScanners were installed in the region on a plane perpendicular the two turbines WEA3 and WEA4 as seen in Figure 1 with a separation distance of 105.4 m. With their modified 6" telescopes, the WindScanners are capable of measuring up to a maximum distance of 300 m which makes the measurement of the inflow and wake of these large turbines possible. The scanners are placed such that they can measure the 2D wind vector at different points inside the region of interest. Fast scanning trajectories are performed covering an areas of interest in the horizontal and vertical directions perpendicular to the rotor plane centered around

the rotor axis to obtain time averaged flow fields. These trajectories reveal the behaviour of the longitudinal and lateral wind speeds in the zone of interest. One such scan is shown in Figure 2, where a horizontal scan reveals the wake the from the upstream turbine impinging partially on the downstream turbine.

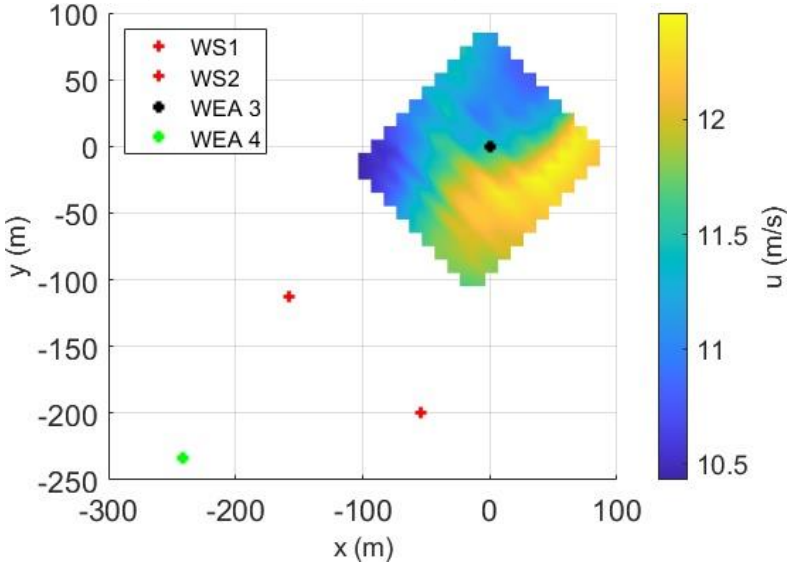


Figure 2: The 30 minute averaged longitudinal velocity component measured by the WindScanners on a horizontal plane centered around the rotor axis. The two turbines were not perfectly alligned during the measurements, and a clear partial wake at WEA4 from WEA3 is visible (Wind direction was 210°).

The WindScanners are further supported by wake measurements from a rear-facing WindCube 200S long range lidar on the nacelle of the upstream turbine WEA3, operational data of both turbines and a met mast. With this unique set-up, it is possible to characterise the interaction between two closely spaced turbines for a range of wind speeds, stratification conditions and yaw setting of the upstream turbine (wake deflection). Depending on the operational setting of either turbine, the WindScanners can also measure the effect of a single turbine in isolation, i.e., the near wake or the induction zone depending on whether the downstream or upstream turbine is switched off. The sensitivity of the results to sources of error will be discussed considering the uncertainty in 2D velocity decomposition from the line-of-sight measurements and the uncertainty associated with the volume averaging effect.

References:

Mikkelsen, T. et al., 2008. Windscanner: 3-D wind and turbulence measurements from three steerable Doppler lidars. s.l., IOP conference series: earth and environmental science (Vol. 1, No. 012018, p. 9). IOP Publishing.

Mikkelsen, T. et al., 2020. Lidar Scanning of Induction Zone Wind Fields over Sloping Terrain. s.l., Journal of Physics: Conference Series (Vol. 1452, p. 012081).

Stevens, R. et al., 2017. Flow structure and turbulence in wind farms. Annual review of fluid mechanics.

Uncertainties of multiple-point measurements with multi lidar

Florian Jäger[1,*], Lukas Pauscher[1], Doron Callies[1,2], Kira Gramitzky[2,1], and Felipe Trolldenier[1,2]
[1]Fraunhofer IEE
[2]University of Kassel
*Presenting author

Keywords: multi lidar | windscanner | measurement uncertainty

Long-range scanning lidars have a great potential for wind resource and site assessment, especially when used synchronously as a multi-lidar system. Their flexible scanning head together with a range up to several kilometres allow measuring the wind conditions in many different locations with just one measurement setup. In this way, horizontal extrapolation using CFD simulations can become redundant. Additionally, since multi lidars focus their laser beams in a single point, the error of profiling Doppler lidars in complex terrain (Pauscher et al., 2016) can be avoided and the systems have a great potential to measure turbulence intensity more accurately than lidar profilers do (Peña and Mann, 2019).
However, there is still little experience with multi-lidar measurements in practical applications, especially when they are used to measure 10-minutes statistics simultaneously at multiple measurement points. The continuous movement of the scanning head might affect the accuracy of the laser beam alignment. This can have a significant effect on the measured wind speed, especially when alignment errors of the elevation angle occur, since even small deviations in elevation can lead to differences in measurement height of several meters. Moreover, unfavourable angles between laser beams can have a big impact on the uncertainty of horizontal wind speed and direction.
Increasing the number of involved scanning lidars can reduce this risk especially for a multiple-point measurement and can lead to smaller overall uncertainties at the same time. However, the actual benefit of using more devices is still unclear. This paper explores this topic by discussing the following questions:
1. How big is the influence of the moving scanning head on the alignment stability?
2. What is the impact of the measurement setup on the uncertainty of the horizontal wind speed and direction for different wind conditions?
3. How big is the benefit of using three or more scanners for the estimation of the horizontal wind speed and direction against a dual-lidar system?

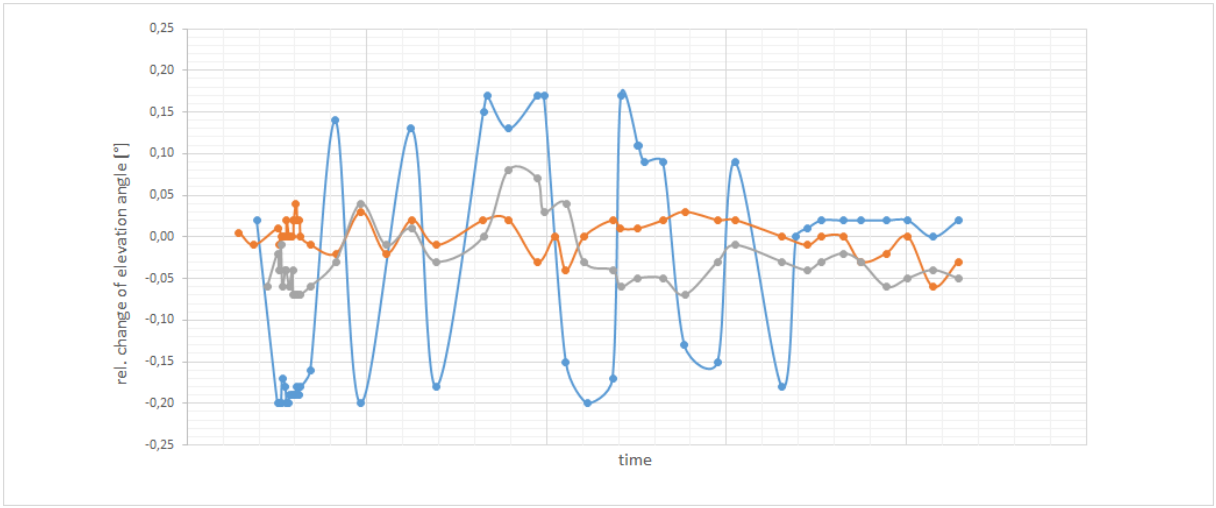


Figure 1: Development of the relative changes in elevation angle over time for three scanning lidars.

For this purpose, an analysis of the alignment stability of scanning lidars in multiple-point scanning mode during a measurement campaign was carried out and will be presented in this paper. The campaign took place in complex terrain and three scanning lidars were involved. The analysis is based on weekly CNR scans of hard

targets. It demonstrates the importance of a continuous alignment monitoring during the whole measurement campaign to observe drifts and jumps in alignment and therefore to avoid resulting errors in derived wind statistics. Figure 1 shows the development of relative changes in elevation angle during the measurement campaign.

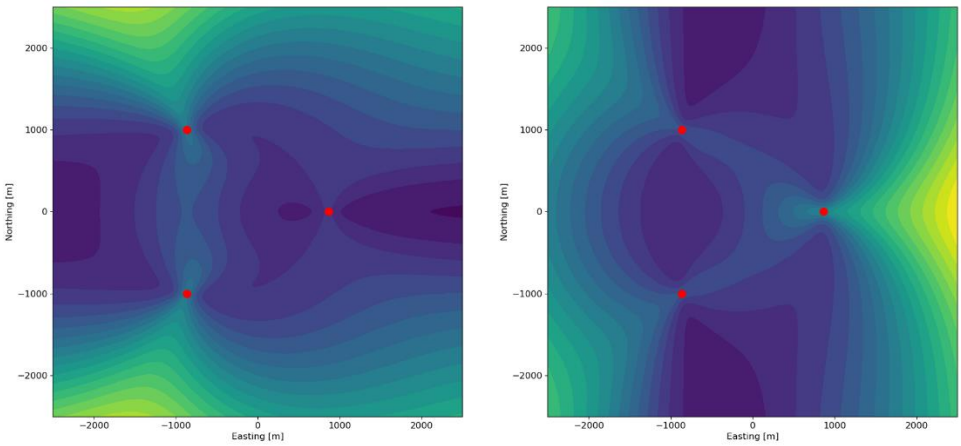


Figure 2: Two examples for modelled uncertainty of horizontal wind speed at 150 m a.g.l.: left plot results from west wind (270°) and right plot from south wind (180°). The red dots mark the position of scanning lidars. Dark areas indicate low, bright areas indicate high uncertainties due to different angles between the laser beams.

In addition, the presented work extends the existing analysis of dual-lidar measurements of Vasiljević et al. (2020) to more than two scanning lidars. It also includes the influence of the elevation angle and the wind direction on the uncertainty of horizontal wind speed and direction. An example of derived uncertainty maps of horizontal wind speed for two different wind directions is shown in figure 2. Using a practical example it is demonstrated how the measurement uncertainty can be reduced by using more than two scanning lidars.

References:

Pauscher, L., Vasiljevic, N., Callies, D., Lea, G., Mann, J., Klaas, T., Hieronimus, J., Gottschall, J., Schwesig, A., Kühn, M. and Courtney, M. (2016) 'An Inter-Comparison Study of Multi- and DBS Lidar Measurements in Complex Terrain.', Remote Sensing, vol. 8, no. 7, p. 667.
Peña, A. and Mann, J. (2019) 'Turbulence Measurements with Dual-Doppler Scanning Lidars', Remote Sensing, vol. 11, no. 20, p. 2444.
Vasiljević, N., Courtney, M. and Pedersen, A. T. (2020) 'Uncertainty model for dual-Doppler retrievals of wind speed and wind direction', Atmos. Meas. Tech. Discuss. [preprint], in review.

The MALIBU concept: Can we assess the uncertainty of a floating lidar system for a new location using existing trial data?

Gerrit Wolken-Möhlmann[1,*], Oliver Bischoff[2], and Julia Gottschall[1]
[1]Fraunhofer IWES
[2]University Stuttgart
[*]Presenting author

Keywords: Floating LiDAR System | Verification | Uncertainty | Data quality assessment

Introduction

Floating lidar system (FLS) pre-campaign verifications have two purposes: to check the FLS' data quality as well as provide the basis for assessing the data uncertainty. This requires a certain measurement period connected to a high planning complexity and costs. A methodology for assessing the uncertainty omitting a system verification and reducing the campaign preparation to a system operation trial is desirable.

Here we describe a concept, developed within the publicly funded MALIBU project, to assess the uncertainty for different locations or areas. Therefor we create a FLS type specific binned matrix with the environmental variable (EV) dimensions wind speed, wave height and peak periods. Input for this matrix are existing long-term measurement data or alternatively, FLS measurement simulation results. Combining this matrix - which represents the FLS' behaviour for given environmental variables - with the distribution of this distinct EV for a given location, we reproduce an FLS uncertainty.

Methodology

FLS measurements may be affected by environmental conditions. These conditions, described by environmental variables (EV), can be described by statistical means like e.g., the complex inflow wind field and the mean wind speed, or the sea state excited buoy motions. These EV affect the process of FLS measurements and hence the measurement uncertainty. We assume, that each combination of environmental variables refers to a distribution of obtained 10-minutes mean wind speeds for an FLS type, or, if compared to the reference wind speed, wind speed deviations Δv. By reducing the environmental variables to reference wind speed, significant wave height Hs and peak period Tp as well as defining a well-defined binning, we are generating a three-dimensional matrix. Each cell contains characteristic information about the obtained wind speeds or wind speed deviations Δv(v, Hs, Tp) for this type of FLS and the distinct environmental conditions. Within this work, the information for each cell is deduced from a long- term measurement of this FLS type next to a reference mast; as an alternative, and for the assessment of not yet realized FLS, the cell information may be generated by floating LiDAR measurement simulation, conducted in a further part of the MALIBU project.

In a next step, the environmental characteristics for a location are defined by the density function P(u, Hs, Tp) for the combination of the environmental variables. The density function may be deduced from existing measurements or from globally available model data, like ECMWF ERA5.

The combination of the density function P(u, Hs, Tp) that represents the frequency of occurring environmental conditions with the FLS-type characteristic matrix is the base for a standard uncertainty assessment for the given location. An overview over the methodology is shown in Figure 1.

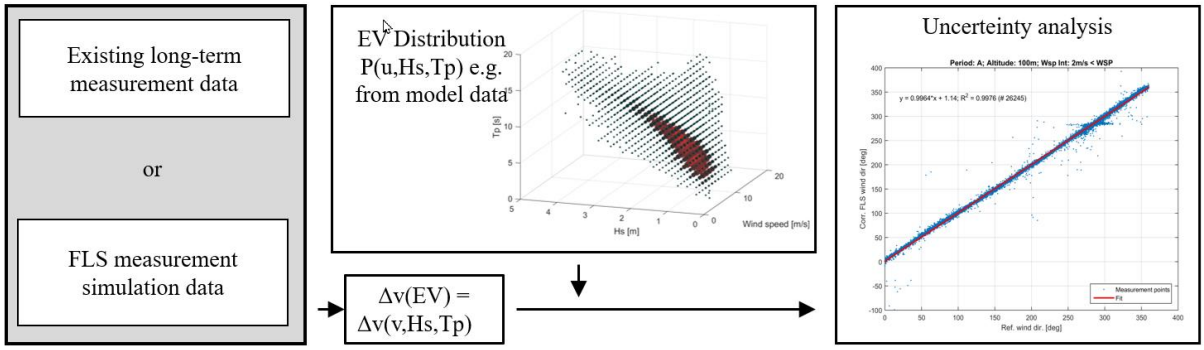


Figure 1: Sketch of the methodology.

Result

We have presented a method to assess the FLS type specific uncertainty for a given location. Input is, on the one hand, site specific information from measurement or model data, as well as FLS characteristics generated from existing long-term trials of FLS measurement simulations.

The results can be used to reduce the required time for pre-campaign trials by reducing the trial to the functionality check, or to assess the FLS characteristics for future measurement campaigns.

Regular Session: Wind Resource Assessment (III)

The analytical wind farm efficiency and wake model EFFWAKE

Stefan Emeis[1,*], Andreas Platis[2], and Martin Dörenkämper[3]
[1]Karlsruhe Institute of Technology
[2]University of Tübingen
[3]Fraunhofer IWES
[*]Presenting author

Keywords: wind farm efficiency | wind farm wake length | analytical model

About 10 years ago the analytical wind farm efficiency and wake model EFFWAKE was developed which is based on a simple budget consideration between extracted momentum from the wind by a wind farm and re-supplied momentum from higher atmospheric levels (Emeis 2010). The spreadsheet-based model is able to calculate the efficiency and the length of the trailing wake of infinitely large wind farms as a function of farm power density, roughness of the surface on which the farm is built, and atmospheric thermal stability. Driving force is the undisturbed wind speed at hub height. In its latest version (Emeis 2018) EFFWAKE also considers the turbulence generated by the operating wind turbines.
When EFFWAKE was developed it could only be checked against existing other numerical wind farm models, because large wind farms which came close to the assumptions on which EFFWAKE is based were not yet existing. Main assumption is that replenishment of extracted momentum only happens by turbulent fluxes from above but not from the sides of the farm. The impact of this assumption will be demonstrated by a comparison with an industry model in which the farm size is varied while keeping the spatial power density of the farm constant.
Meanwhile, large offshore wind farms have been erected which come closer to EFFWAKE's assumptions. The research project WIPAFF conducted in 2015 to 2019 was the first project within which in situ aircraft measurements of wakes of large offshore wind farms in the North Sea were made (a summary of the results is given in Platis et al. 2020a). This offered the unique chance to check EFFWAKE with real measured data. Given the simplicity of EFFWAKE the checks were satisfying but also pointed to weaknesses of the simple analytical approach (Platis et al. 2020b). Some highlights from this comparison will be shown.

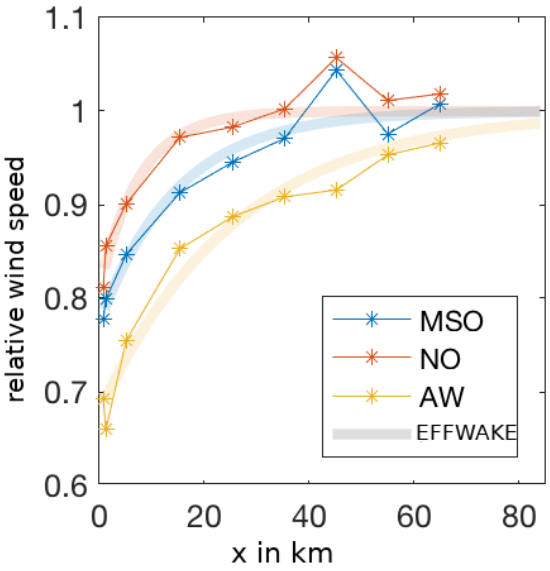


Figure 1: Relative wind speed deficit of a measurement flight of the WIPAFF project on 8th August, 2017, downstream of the wind farm cluster Amrumpark West, Nordsee Ost, Meerwind Süd/Ost (AW/NO/MSO). Solid lines and stars indicate observed relative wind speed deficit. Shaded lines represent EFFWAKE model solutions for each wake. Adapted from Platis et al. 2020b.

Finally, a recent application of EFFWAKE is shown. Based on the confidence deduced from the above mentioned checks, EFFWAKE can be used for first a priory estimations of wind farm efficiency and lengths of farm wakes for future even larger wind farms without using any noteworthy computational resources. An example for such estimations is the efficiency of planned large offshore wind farms. EFFWAKE can be used to estimate the efficiency of such farms as function of the installed power density, i.e., the number of wind turbines per unit area. One feature of EFFWAKE's simplicity is that only the power density of a farm can be specified irrespective of the actual spatial arrangement of the turbines within a wind farm. This also means that wind direction is no relevant input parameter of EFFWAKE. By series of runs of EFFWAKE the relation between the wind speed distribution (either measured or taken from a climatology) and the rated wind speed of the designated wind turbines can be included into the estimations as well. This will support the efforts to effectively use the available offshore areas for a reliable electrical power supply.

References:

Emeis, S., 2010: A simple analytical wind park model considering atmospheric stability. Wind Energy, 13, 459-469. DOI: 10.1002/we.367

Emeis, S., 2018: Wind Energy Meteorology - Atmospheric Physics for Wind Power Generation. 2nd Edition. Springer, Heidelberg etc., XXVI+255 pp. DOI: 10.1007/978-3-319-72859-9.

Platis, A., J. Bange, K. Bärfuss, B. Cañadillas, M. Hundhausen, B. Djath, A. Lampert, J. Schulz-Stellenfleth, S. Siedersleben, T. Neumann, S. Emeis, 2020a: Long-range modifications of the wind field by offshore wind parks – results of the project WIPAFF. Meteorol. Z. (Contr. Atm. Sci.), 29, 355-376. DOI: 10.1127/metz/2020/1023

Platis, A., M. Hundhausen, M. Mauz, S. Siedersleben, A. Lampert, K. Bärfuss, B. Djath, J. Schulz-Stellenfleth, B. Canadillas, T. Neumann, S. Emeis, J. Bange, 2020b: Evaluation of a simple analytical model for offshore wind farm wake recovery by in situ data and Weather Research and Forecasting simulations. Wind Energy, online first. DOI: 10.1002/we.2568

Simple model for assessment of energy production and costs of offshore wind farms

Jens Nørkær Sørensen, and Gunner Chr. Larsen
Technical University of Denmark

Keywords: Offshore wind farms | Energy production | Levelized cost of energy | Capex and Opex

Today, more than 100 offshore wind farms have been erected in Europe, contributing with an installed capacity of more than 20 GW, of which more than one third have been established within the past three years [1]. With respect to global installations of offshore wind power, 6.1 GW of capacity was installed in 2019, and more than 205 GW of new offshore wind capacity is forecast through 2030 [2]. This rapid development demands access to fast and accurate predictive tools for assessing site-dependent energy production and costs.

The aim of the present work is to develop a simple, robust and reliable numerical framework that may aid developers and decision-makers in assessing the economic aspects of developing offshore wind power at a specific site. The idea is to have a tool to make initial cost analyses without the need of detailed technical information regarding the utilized wind turbines or the actual topology of the wind farm. Hence, the model only requires information on turbine size (rotor diameter and nameplate capacity), size of wind farm (number of turbines and wind farm area), and site Weibull parameters as well as water depths and distance to the coast. The output of the tool is the average annual power production, power intensity (power per unit area), installation costs (CAPEX), operation and maintenance costs (OPEX), and Levelised Cost of Energy (LCoE).

In the developed model, we employ the atmospheric wind farm boundary layer model of Frandsen [3] to assess the wind turbine array (wake) effect in the atmospheric boundary layer, and combine it with a wind resource model based on the site Weibull distribution adjusted for wake effects. As cost model, we employ a set of simple parametrical expressions for the most essential wind farm cost elements (see Sørensen and Larsen [4]).

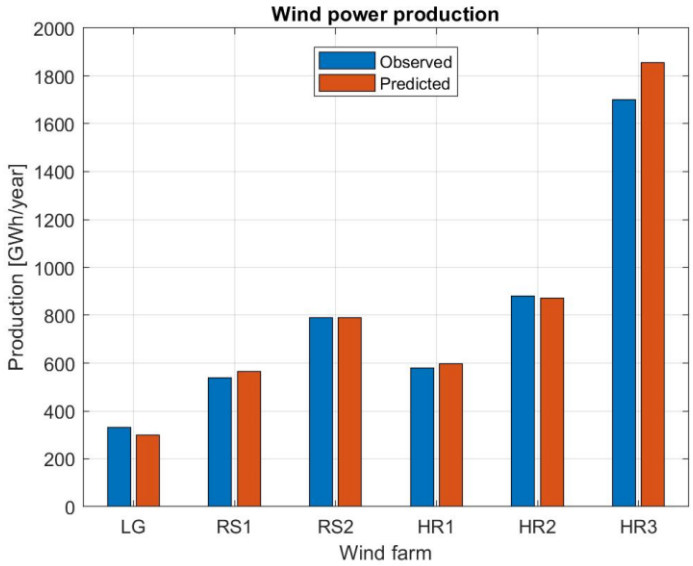


Figure 1: Comparison between computed and actual production data for different wind farms

In Fig. 1 computed wind power production (GWh/year) are compared to actual production data for different wind farms (LG: Lillgrund; RS1: Rødsand 1; RS2: Rødsand 2; HR1: Horns Rev 1; HR2: Horns Rev 2; HR3: Horns Rev 3). It is here seen that the model is capable of computing the annual energy or power production within an accuracy of about 5%. Comparing the wind power production per area unit (MW/km2) for the different wind farms, shows large differences in actual power production per area unit between the different wind

farms. The expense of having a high intensity of power yield, however, is that the LCoE increases. In spite of its high power intensity, the LCoE for the Lillgrund wind farm is about double as big as for the other wind farms. It should be mentioned, however, that it is difficult to get actual LCoE data from the developers and therefore also difficult to validate the numerical predictions of LCoE. For the newly established Kriegers Flak wind farm in the Baltic Sea, the computed LCoE is found to be 51.4 Euro/MWh. The actual cost price of energy is, according to Vattenfall [5], anticipated to be 49.6 Euro/MWh (37,2 øre/kWh), which is within a difference of 4%.

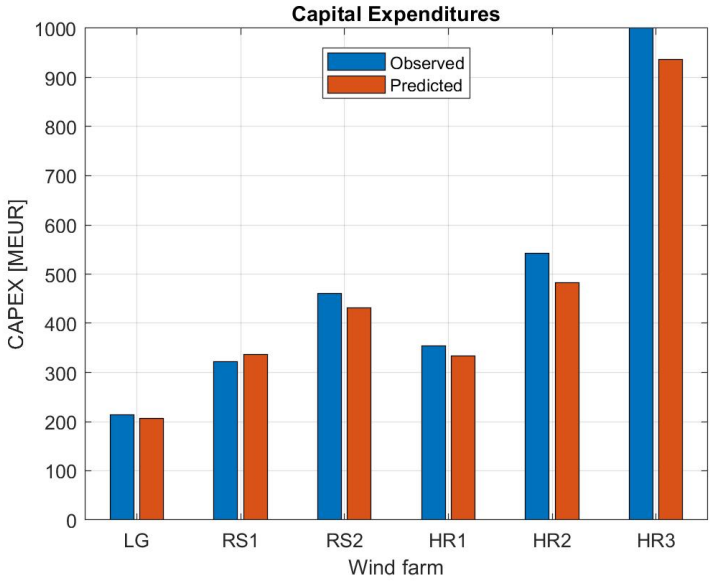


Figure 2: Comparison between computed and actual CAPEX for different wind farms

Fig. 2 compares in CAPEX (M€) in 2019 prices. As for the energy production, we here get an accuracy of 5%. Hence, in spite of its simplistic nature, the model is found to predict costs and power production of offshore wind farms with a surprisingly high accuracy.

References:
1. Wind Europe: Offshore Wind in Europe: Key trends and statistics 2018. Published in February 2019 by WindEurope.org. https://windeurope.org/wp-content/uploads/files/about-wind/statistics/WindEurope-Annual-Offshore-Statistics-2018.pdf
2. GWEC: Global Offshore Wind Report 2020. https://gwec.net/wp-content/uploads/2020/12/GWEC-Global-Offshore-Wind-Report-2020.pdf
3. Frandsen, S.T. (1992) On the Wind Speed Reduction in the Centre of Large Clusters of Wind Turbines. Journal of Wind Engineering and Industrial Aerodynamics, 39, pp. 251-265.
4. Sørensen, J.N. and Larsen, G.C. (2021) A minimalistic prediction model to determine energy production and costs of offshore wind farms. Energies, 14, 448. https://doi.org/10.3390/en14020448
5. Vattenfall homepage: https://group.vattenfall.com/dk/vores-forretning/vindprojekter-i-danmark/kriegers-flak

To what extent can the Kinetic Energy Budget of the Atmosphere approach explain the reduction in offshore generation efficiency of developments planned in the German Bight by 2050

Jonathan Minz[1,2,*], Marc Imberger[3], Axel Kleidon[1], and Jake Badger[3]
[1]Max Planck Institute of Biogeochemistry
[2]Universität Hohenheim
[3]Technical University of Denmark
[*]Presenting author

Keywords: Offshore wind energy | Resource estimation | Kinetic Energy Budget | WRF | Mesoscale wind farm modelling

Regional wind energy estimation is driven primarily by wind speed and turbine characteristics. However, a recent assessment of the offshore wind energy potentials in the German Bight by Agora Energiewiende, highlighted the need for national energy transition scenarios to account for the atmospheric response to large wind turbine deployments (> 104km2). This study used two approaches, namely, the Weather Research and Forecasting model with Explicit Wake Parameterization (WRF EWP) and the Kinetic Energy Budget of the Atmosphere (KEBA) model. It was found that if all of the anticipated 50 - 70 GW of capacity is installed in the German Bight by 2050, expected yields could go down from 4000 full load hours (FLH) to between 3300 and 3000. Whereas WRF is a comprehensive simulation of the atmosphere, KEBA is much simpler in its representation of the wind turbine deployment and its interaction with the atmosphere. It models the fluxes from the
free atmosphere into the wind park volume as being balanced by the wind park generation, wake losses, surface dissipation, and the remnant kinetic energy in the wind behind the wind park. The wind park volume, defined by the width and length of the wind park and the height of the boundary layer, determines the total kinetic energy available to the wind turbines for extraction. Thus, increasing capacity density i.e. the density of turbines, leads to greater extraction of kinetic energy from the wind. This slows down wind speeds over the wind park, thereby resulting in lower generation from the wind park along with lower capacity factors.

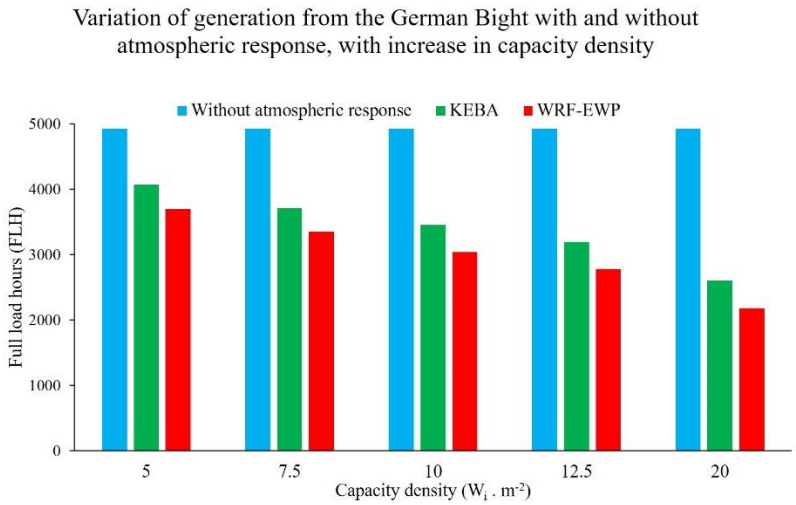


Figure 1: The figure shows that wind speed-based approach overestimates generation from the German Bight (~7000km2). Most common estimates of wind energy generation assume that ~4000 full load hours can be generated offshore. However, including the atmospheric response to large wind parks reduces generation, which reduces further as wind parks become denser.

Estimates from both these approaches were within 20% of each other. In our analysis, we use the results from this study to elicit variables which are important for parameterizing the atmospheric response to large-scale wind turbine deployments. The inclusion of these variables into regional wind energy potential

estimation is likely to improve predictions relative to the common approach. We investigate the role of atmospheric variables like wind direction, atmospheric stability, boundary layer height and surface friction on large scale generation by comparing the estimates of the two modelling approaches. We consider the WRF simulations of large-scale power generation and atmospheric circulation as the most realistic available representation, since farms of the scale that we consider in this study are not yet in operation. We also identify potential limitations of the kinetic energy budget concept which underpins the simpler KEBA model. A detailed comparison of the two methods also provides insights into why the simple KEBA model work so well. We posit that regional estimates of wind energy potential must include a fuller picture of the atmospheric processes determining generation rather than just its drivers i.e. wind speed and turbine characteristics, as is commonly the case. The KEBA model presents a simple approach for including the effects of atmospheric response to large scale wind turbine deployment. This would facilitate the development of more realistic energy transformation scenarios and decarbonisation pathways.

References:

Agora Energiewende, Agora Verkehrswende, Technical University of Denmark and Max-Planck-Institute for Biogeochemistry (2020): Making the Most of Offshore Wind: Re-Evaluating the Potential of Offshore Wind in the German North Sea.

Kleidon, A. and Miller, L. M.: The Kinetic Energy Budget of the Atmosphere (KEBA) model 1.0: a simple yet physical approach for estimating regional wind energy resource potentials that includes the kinetic energy removal effect by wind turbines, Geosci. Model Dev., 13, 4993–5005, https://doi.org/10.5194/gmd-13-4993-2020, 2020.

Volker, P. J. H., Badger, J., Hahmann, A. N., and Ott, S.: The Explicit Wake Parametrisation V1.0: a wind farm parametrisation in the mesoscale model WRF, Geosci. Model Dev., 8, 3715–3731, https://doi.org/10.5194/gmd-8-3715-2015, 2015.

The interaction of naturally occurring atmospheric gravity waves with an offshore wind farm

Sarah Ollier[1,*], and Simon Watson[2]
[1]Loughborough University
[2]Delft University of Technology
*Presenting author

Keywords: Atmospheric gravity waves | lee waves | CFD | ERA5 | SCADA

In recent years there has been increased interest in the interaction between atmospheric gravity waves (AGWs), otherwise known as lee waves, and windfarms. AGWs occur frequently offshore when winds pass over obstacles in neutral or stable surface conditions with a temperature inversion acting as a capping layer. Recent studies have investigated interactions with AGWs forced by upstream topography close to offshore windfarms (Ollier, Watson and Montavon, 2018) and onshore windfarms (Draxl et al., 2021). There is also growing research into AGWs produced by wind farms (Allaerts and Meyers, 2017, 2019; Allaerts et al., 2018).

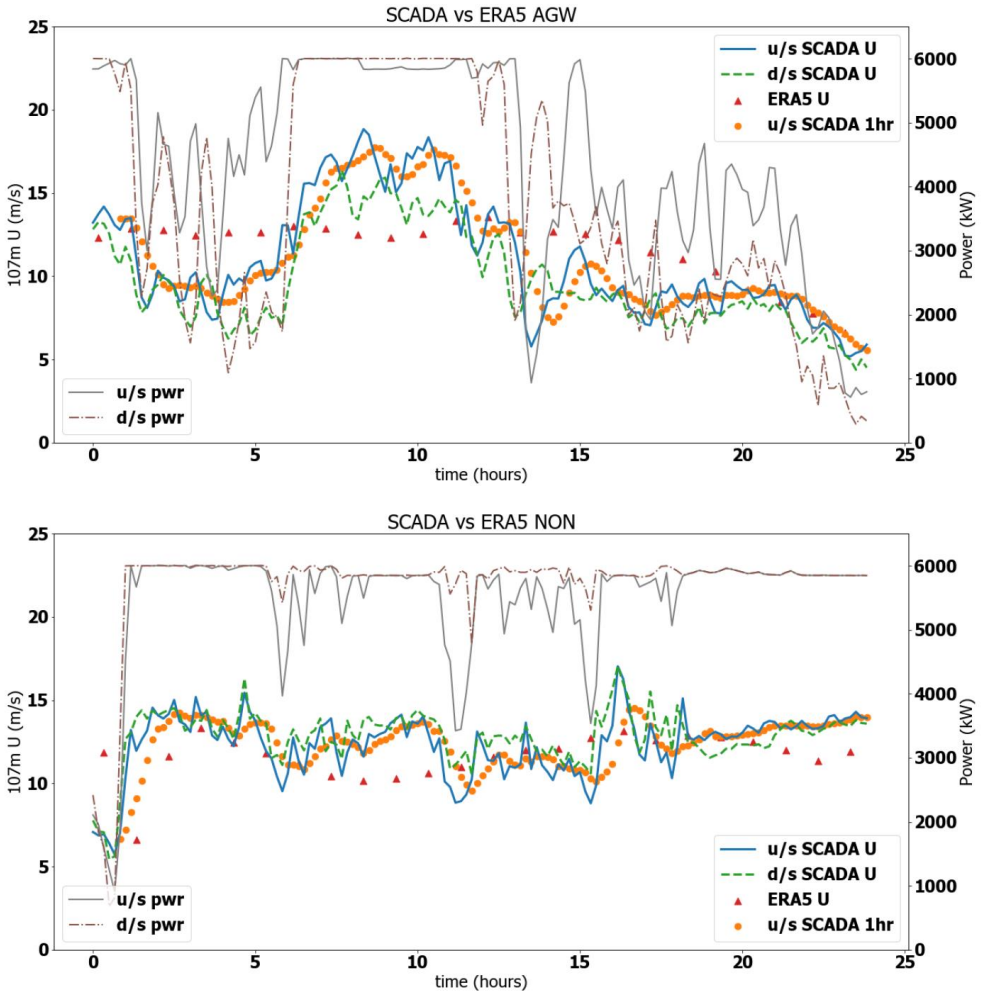


Figure 1: 24 hour timeseries around the AGW case (above), and non AGW case (below) – during non AGW case. ERA5 hub-height windspeed (red triangles) vs. SCADA hub height windspeeds for the upstream (blue solid line) and downstream (green dotted line) turbines, orange dotted line shows upstream turbine windspeeds smoothed with rolling 1 hour means. Power output from upstream (grey solid line) and downstream (brown dash-dot line) turbines.

This research investigates the impacts of AGWs forced by W-SW winds over short, near coastal hills on a UK operational windfarm in the North Sea. AGW events were frequently observed in the region of the offshore

windfarm site based on 10m wind fields inferred by Synthetic Aperture Radar (SAR) (DTU-WE, no date) measurements across a 2 year period. The impacts on hub height wind speeds experienced across the wind farm and associated power generation for these events are investigated using operational SCADA data at 10-minute resolution (fig. 1.), hourly resolution ERA5 Reanalysis data (fig. 1.) and Computational Fluid Dynamics (CFD) analysis in ANSYS Windmodeller (fig.2).

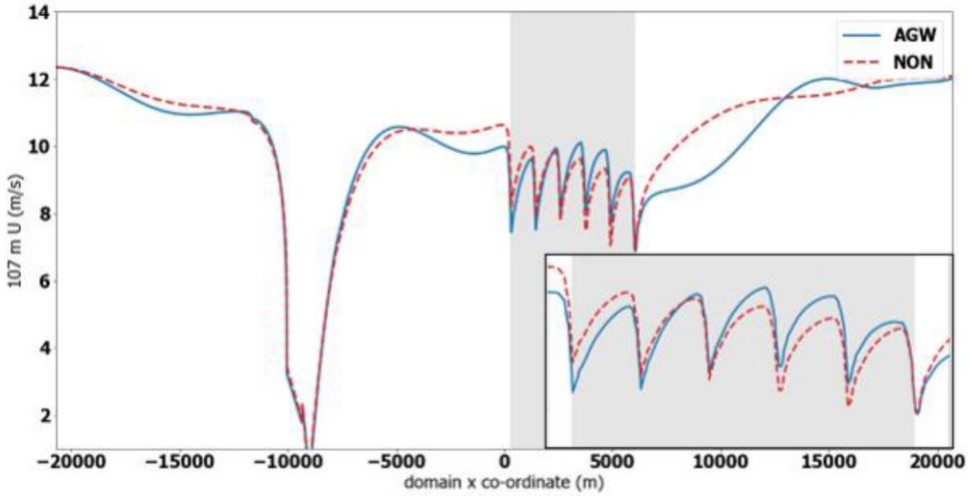


Figure 2: Hub height windspeeds from the AGW day (blue line) and a non AGW (red dashed line) through the CFD domain in line with the southern row of the windfarm. The grey shaded region shows the wind farm extent, the bottom right shows a zoomed in view of the windfarm extent. The rapid dip in windspeeds at -1000 m shows the location of the simple hill.

Figure 1 compares an AGW event and a day without AGWs, both identified in SAR, with comparable inflow conditions from ERA5. Data are shown from a turbine in the first and final row of the windfarm to demonstrate different sections of the wave, which has a wavelength approximately 25% larger than the longitudinal extent of the wind farm. In this example windspeeds experienced by the two turbines strongly diverges from the trend in ERA5 windspeeds when AGWs are present (up to 5 m/s difference). When the windspeeds are below rated, the power output of the two turbines oscillates strongly, At the opposing edges of the windfarm, power outputs are inversely correlated, suggesting if AGWs are not taken into account, estimates for windfarm output may poorly represent the variability in windspeeds experienced in different areas of the wind farm and overall power output. As expected, the agreement between the datasets is more consistent when AGWs are not present; the absolute windspeeds tend to be 0-2 m/s higher than the ERA5 data and the general
trend is very similar. There is much more agreement between upstream and downstream turbine data.
For a better understanding of the spatial interaction with the wind farm and the AGWs, the inflow conditions for the AGW day were used as boundary conditions for an ANSYS Windmodeller k-e RANS CFD model of the windfarm. A second simulation using the same wind speed and direction as the AGW day, but with the atmospheric stability conditions from a non AGW day was run for comparison. The two case studies are represented in a 41.5km x 20km x 25km domain, containing a simple hill upstream of the windfarm and Rayleigh damping aloft and at the outflow. Fig. 2 shows preliminary results of the windspeeds through the domain in line with the southern row of the windfarm during the AGW day and no AGW day. Variation in windspeeds is apparent from the wake losses in both cases. However, in the AGW case, the AGW peak is within the wind farm extent and the wind speeds increase and decrease in phase with the wave.

References:

Allaerts, D. et al. (2018) 'Annual impact of wind-farm gravity waves on the Belgian-Dutch offshore wind-farm cluster', Journal of Physics: Conference Series, 1037(7). doi: 10.1088/1742-6596/1037/7/072006.

Allaerts, D. and Meyers, J. (2017) 'Boundary-layer development and gravity waves in conventionally neutral wind farms', Journal of Fluid Mechanics. Cambridge, UK: Cambridge University Press, 814, pp. 95–130. doi: 10.1017/jfm.2017.11.

Allaerts, D. and Meyers, J. (2019) 'Sensitivity and feedback of wind-farm-induced gravity waves', Journal of Fluid Mechanics. Cambridge University Press, 862, pp. 990–1028. doi: 10.1017/jfm.2018.969.

Draxl, C. et al. (2021) 'Mountain waves can impact wind power generation', Wind Energy Science, 6(1), pp. 45–60. doi: 10.5194/wes-6-45-2021.
DTU-WE (no date) 'ENVISAT and Sentinel 1 surface wind field processing'. Danish Technical University (DTU) Department of Wind Energy. Available at: https://satwinds.windenergy.dtu.dk/.
Ollier, S. J., Watson, S. J. and Montavon, C. (2018) 'Atmospheric gravity wave impacts on an offshore wind farm', IOP Conf. Series: Journal of Physics, 1037. doi: doi :10.1088/1742-6596/1037/7/072050.

Horizontal Roll Vortices in RANS simulations of stably stratified atmospheric boundary layer

Michael Alletto, Alexander Radi, Hamza Musaddiq, Jamal Adib*, Judith Langner, and Marcus Letzel
Enercon
*Presenting author

Keywords: Atmospheric boundary layers | wind resource assessment | flow instability | RANS

Reynolds-Averaged Navier Stokes (RANS) solvers have developed into a defacto standard tool for the numerical simulation of atmospheric wind flows in complex terrain in the wind energy community.
Enercon is employing the in-house OpenFOAM based tool E-Wind [1], whose modified "k-" turbulence model for the atmospheric boundary layer has been made public with OpenFOAM`s release v2006 [2]. This model includes the effects of terrain roughness, buoyancy due to ground heating/cooling and Coriolis force.
Recently, Enercon engineers have made the observation of "Horizontal Roll Vortices" (HRV) in E-Wind flow fields, which can be described as large-scale streamwise streaks of fluctuating streamwise velocity component of up to 6m/s. In a cross-stream plane view, these flow inhomogeneities take the form of co-rotating vortices of 3-4km cross-stream wavelength, with vortex cores located at 200-700m above ground level (AGL), depending on the boundary layer height.

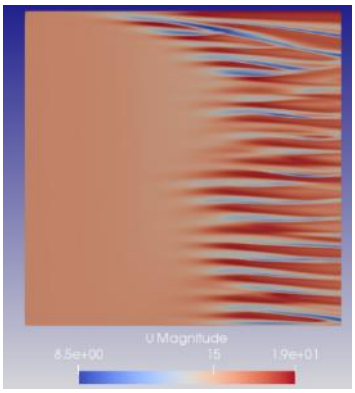


Figure 1: Horizontal cut at 200m height through the streamwise velocity field of a 80x80km² domain showing the appearance of HRVs (flow is from left to right).

Similar coherent structures are known from field measurements [3],[4], as well as from Large Eddy Simulations [5]. However, the authors do not consider such events as representative for a time-averaged state of the atmosphere as modelled by the E-Wind RANS solver, and treat them as undesired anomalies. The presentation will discuss detailed parameter studies aiming to understand under which circumstances the HRVs appear, what parameters influence their strength, and explore means on how to suppress them in RANS simulations. Extensive numerical studies on a flat plate showed that the HRVs become stronger and move closer to the ground for more stable stratification, and that they need extensive computational domains to develop (more than 40km in streamwise direction, as seen in Figure 1). Furthermore – and highly relevant for project application – ground inhomogeneities such as distributed terrain roughness, forest patches or complex terrain geometry tend to trigger the HRVs earlier, reducing this fetch to under 20km.

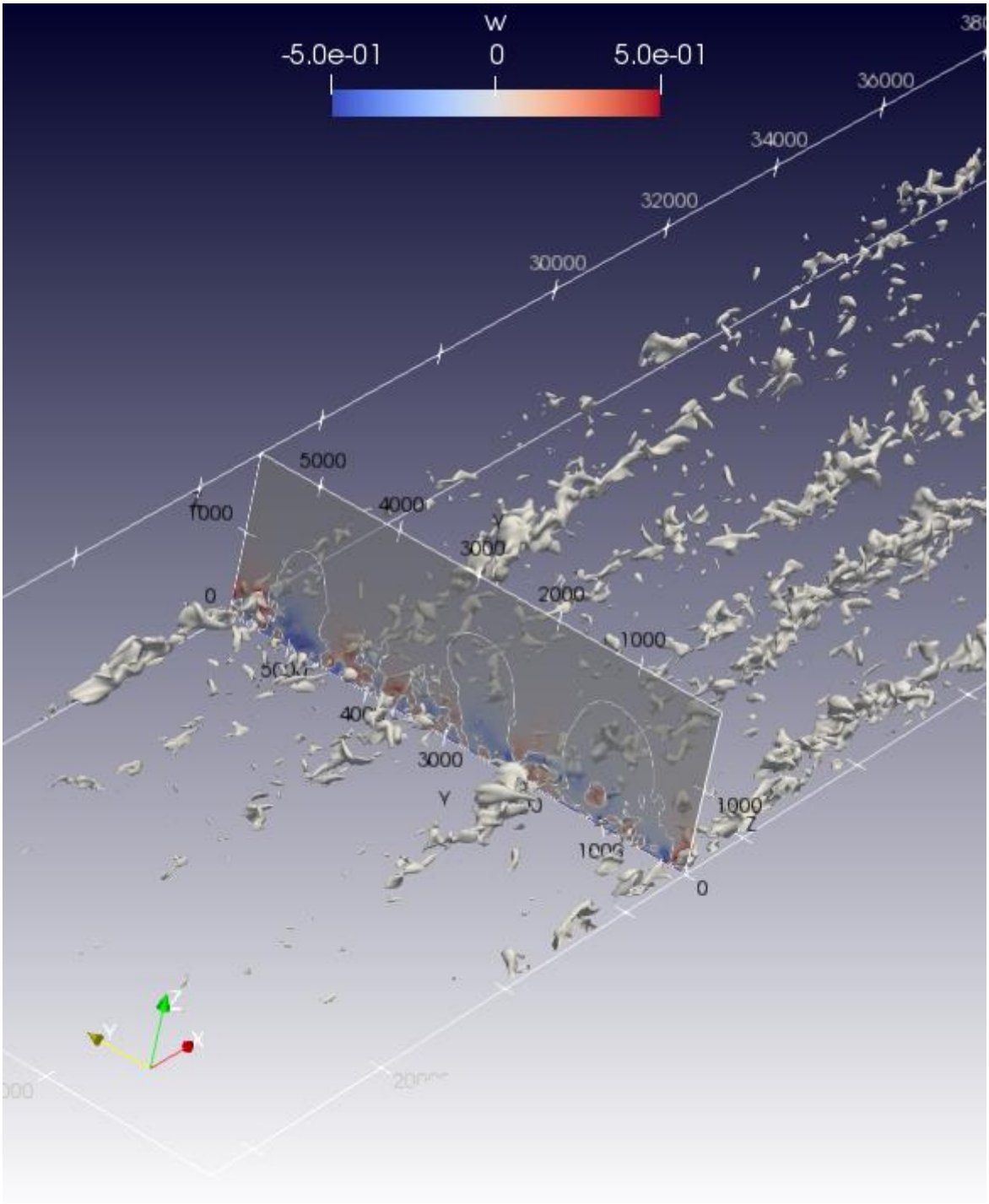


Figure 2: Coherent streamwise structures in the vertical velocity component field of a LES simulation.

The HRVs could also be reproduced under specific inflow conditions by Large Eddy Simulations . For this, the inflow into the domain was defined as a steady Ekman spiral, generated by a 1D precursor run. After approximately 20km, the initially laminar flow developed turbulent streamwise streaks with all characteristics of HRVs, before falling apart into isotropic turbulence (Figure 2). When removing the cross-stream component from the inflow profile, thus "flattening" the Ekman spiral to a pure 1D profile, the transition to isotropic turbulence occurred further upstream and did not exhibit HRVs. All performed studies indicate that the appearance of the HRVs is linked to the exact shape of the 3D wind velocity profile.

From many attempts to suppress the development of these undesired structures, two methods were identified as not fully satisfactory, but effective: A) The removal of the cross-stream component of the inflow velocity profile, effectively scarifying the Ekman spiral; B) Artificial damping of the vertical velocity component in a

narrow height band close to the vortex cores. The later solution is not applicable in complex terrain, as it results in unintended flow acceleration above high terrain features.

We aim for community feedback on similar observations with their own wind resource assessment tools, and on acceptable solutions how to avoid or suppress the HRVs in RANS simulations. We also encourage the community to reproduce the HRVs with the turbulence model recently made public in OpenFOAM v2006.

References:

[1] Alletto, Michael, Alexander Radi, Jamal Adib, Judith Langner, Carlos Peralta, Andree Altmikus, and Marcus Letzel. 2018. "E-Wind: Steady state CFD approach for stratified flows used for site assessment at Enercon." J. Phys. Conf. Ser. 1037 (7): 072020.

[2] OpenFOAM® v2006: New boundary conditions. (2020, 06 30). Retrieved from OpenFOAM: https://www.openfoam.com/releases/openfoam-v2006/boundary-conditions.php

[3] Large-scale coherent structures in the atmosphere over a flat terrain, Leonardo Alcayaga et al 2020 J. Phys.: Conf. Ser. 1618 062030

[4] Lemone, Margaret Anne. "The structure and dynamics of horizontal roll vortices in the planetary boundary layer." Journal of the Atmospheric Sciences 30.6 (1973): 1077-1091.

[5] Churchfield, Matthew J., et al. Wind energy-related atmospheric boundary layer large-eddy simulation using OpenFOAM. No. NREL/CP-500-48905. National Renewable Energy Lab.(NREL), Golden, CO (United States), 2010.

Extreme Winds and Risk Analysis in Turkey based on the Different Statistical Methods

Tolga Kara[1,*], Sena Ecem Yakut[1], Osman Tek[2], Metin Teköz[2], Merve Aksakal[1], and Ahmet Duran Sahin[1]

[1]Istanbul Technical University
[2]Turkish State Meteorological Service
*Presenting author

Keywords: Extreme Wind Speed | Risk Analysis | Annual Maximum Method | Peak over Threshold Value Method | Extreme Wind Speed Model

Extreme atmospheric phenomena have been increased due to the impact of climate variability and change. Accurate estimation and evaluation of extreme events have become a critical issue to reduce its damage to economic values. From the perspective of wind energy applications, high wind speeds affect energy production, wind turbine stability, lifetime, and hence, it is crucial to possess precise information about high wind speeds in wind farms. In this regard, the assessment of extreme wind conditions is a vital subject for every country's agenda.

The generated 10-minute average wind speed data from the New European Wind Atlas project within the period of 2016-2017 used for this study. Here, both the Annual Maximum Method (AMM) and Peak-over-Threshold Method (POTM) for the regional analysis of extreme wind speeds in Turkey were applied. Extreme wind speeds for various return periods of 2, 20, and 50-years were predicted using the AMM. As a result of the analysis made using the POTM, extreme wind speeds for various return periods of 10, 50, and 100-years were estimated.

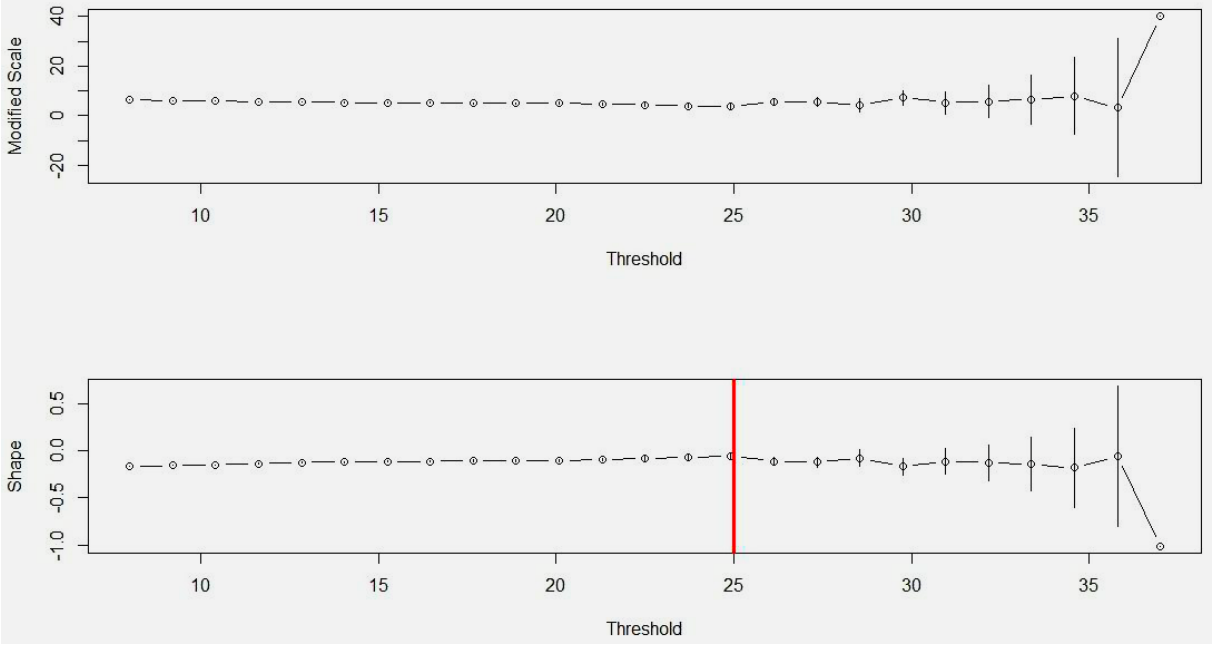


Fig 3. Threshold selection for the Mediterranean region using tcplot function

To select the threshold, the POT package which has various tools to define an appropriate desired value, including the tcplot and mrlplot functions were preferred (Ribatet, 2009). Fig. 3 shows the threshold selection for the Mediterranean region using the tcplot function in R software, and it is determined clearly that a threshold of 25 m/sec is an appropriate selection. For the foremost reasonable threshold selection, the mrlplot function could be additionally implemented. Fig. 1a displays the mean residual life plot for the Mediterranean region using the mrlplot function. We have evaluated that there is a non-linear behavior detected above 27

m/s in this figure. Hence, it is decided that we should select the threshold value as 25 m/s as determined after the results of the tcplot function. As seen in Fig. 6, the probability plot and Quantile-Quantile plot (Q-Q plot) were applied to the dataset and these methods represented well agreement with the data through the entire range. We have estimated that there will be 35 m/s as an extreme wind in 10 years, and approximately 37 m/s in 50 years and 39 m/s extreme wind in 100 years would be.

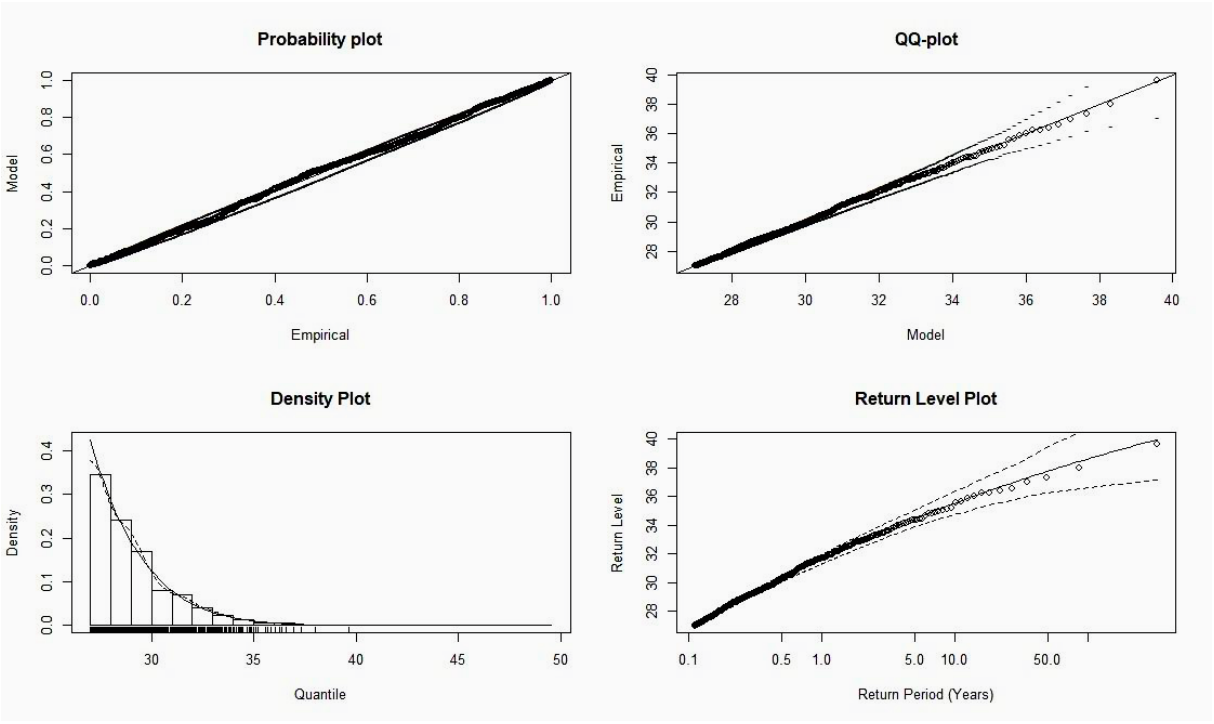


Fig 6. Statistical description plot of extreme winds in Mediterranean region

The maximum wind speeds as a reference value for every city in Turkey by applying the Steady Extreme Wind Speed Model (EWM) in IEC Standard 61400-1 were calculated. Extreme winds which will be repeated in 1-year and 50-years were calculated using these reference values. We have calculated that, in Marmara and Aegean Region, the highest extreme wind speeds with different return periods of 10, 50, and 100-years were estimated using POTM as 40 m/s and 45 m/s respectively. Consistent with the EWM results, the highest wind speed in 2016 within the return period of 50-years was expected to occur in Antalya and estimated as 49.05 m/s. Similarly, for the period of 1-year, the maximum wind speed was expected to occur in Antalya and estimated as 39.24 m/s. Comparing the results of 2016 and 2017, there have been no significant differences in estimated extreme wind speeds. As mentioned above, the highest wind speed in 2017 was expected to occur
in Antalya, which is estimated as 37.68 m/s for the return period of 1-year, and 47.1 m/s for 50-years.

References:

International Electrotechnical Commission, 2006. Wind turbines-part 1: design requirements. IEC 614001 Ed. 3.

Rohatgi, J., Araújo, A. and Primo, A.R., 2013. Extreme wind speeds and their prediction for wind turbines. Wind Engineering, 37(6), pp.595-603.

Abild, J., Andersen, E.Y. and Rosbjerg, D.D., 1992. The climate of extreme winds at the Great Belt, Denmark. Journal of Wind Engineering and Industrial Aerodynamics, 41(1-3), pp.521-532.

Ribatet, M. and Dutang, C., 2009. POT: Generalized Pareto distribution and peaks over threshold. R package versions, pp.1-1.

Dukes, M.D.G. and Palutikof, J.P., 1995. Estimation of extreme wind speeds with very long return periods. Journal of Applied Meteorology, 34(9), pp.1950-1961.

Fisher, R.A. and Tippett, L.H.C., 1928, April. Limiting forms of the frequency distribution of the largest or smallest member of a sample. In Mathematical Proceedings of the Cambridge Philosophical Society (Vol. 24, No. 2, pp. 180-190). Cambridge University Press.

Galambos, J. and Macri, N., 1999. Classical extreme value model and prediction of extreme winds. Journal of Structural Engineering, 125(7), pp.792-794.

Gumbel, E.J., 2004. Statistics of extremes. Courier Corporation.

Linde, C., 2020. Mission. [online] NEW EUROPEAN WIND ATLAS. Available at: http://www.neweuropeanwindatlas.eu [Accessed 15 March 2019].
Hansen, B.O., Larsén, X.G., Kelly, M.C., Rathmann, O.S., Berg, J., Bechmann, A., Sempreviva, A.M. and Jørgensen, H.E., 2016. Extreme Wind Calculation Applying Spectral Correction Method–Test and Validation.

Regular Session: Wind Resource Assessment (IV)

Long-term correction and conditional time series simulation by a diffusion-based transformation

Morten Nielsen*
DTU Wind Energy
*Presenting author

Keywords: long-term correction | measure-correlate-predict | time series simulation | uncertainty

The wind climate at a potential wind energy site is typically predicted by local meteorological observations. For practical reasons the observation period is limited to a few years, so there is a risk that the resulting wind climate will deviate from the long-term climate. The strategy of the measure-correlate-predict (MCP) method is first to establish a statistical model between concurrent local observations and reference data from a nearby measurement station or numerical weather simulation. This model is then used for correction of reference data from a long period, so they represent the local wind better (Carta, Velazquez and Cabrera, 2013).

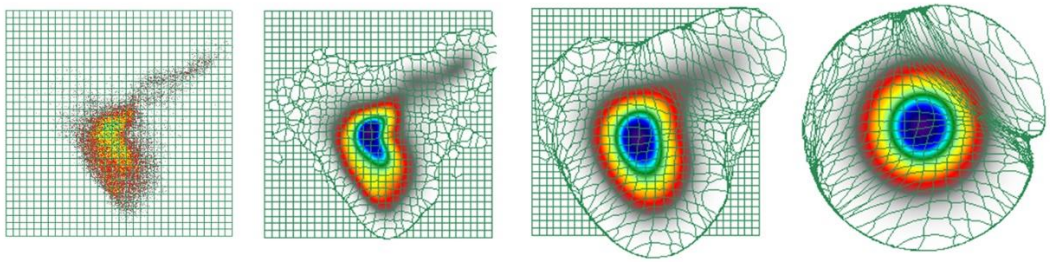


Figure 1: Development of density map and grid during the forward diffusion process.

This paper presents a new variant of the MCP method based on a transformation of the 2D probability density distribution of the wind vector into a 2D Gaussian distribution (Nielsen 2019). The transformation is non-parametric and inspired by the diffusion-based cartogram method Gastner and Newman (2004). It both corrects wind speed and direction. The algorithm considers diffusion of an empirical wind-vector distribution into a 2D Gaussian probability distribution. The diffusion process is analysed by deformation of a grid covering the distribution map. Grid deformation during the forward diffusion processes defines the transformation from wind data to auxiliary Gaussian variables, while the backwards diffusion process defines the reverse transformation from Gaussian variables to wind vectors, see Figures 1 and 2. Linear regression between the transformed local observations and reference data establish the statistical relation between the Gaussian variables. The long-term local wind climate is modelled by 1) forward transformation of a long reference time series, 2) linear correction of the corresponding Gaussian parameters, 3) reverse transformation into wind data for the site of prediction, and 4) suitable statistics for wind resource assessment.

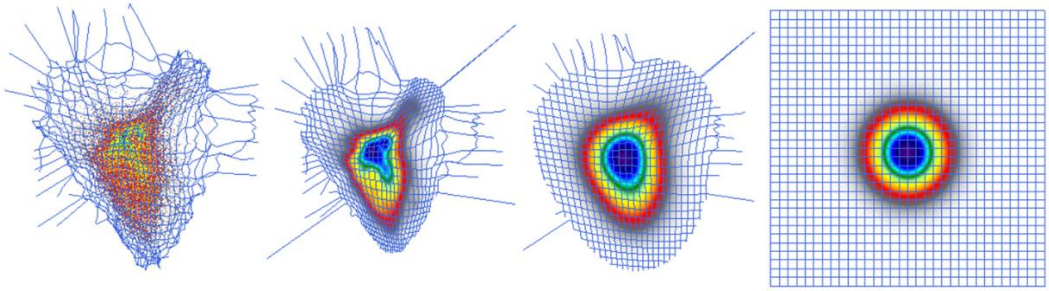


Figure 2: Development of density map and grid during the backward diffusion process.

Time series of local winds and reference data are imperfectly correlated, and this is significant for forecasting. Linear regression provides uncertainties of predicted Gaussian variables, and we translate this uncertainty into error estimates for local wind predictions by the inverse transformation. The polar transformation from wind vector components to wind speed and direction, and our non-linear transformation, predicts time-varying uncertainty with more directional uncertainty for low wind speeds.

Time series of local wind conditions with realistic auto-correlation and cross-correlation with reference data, are produced by conditional Fourier simulation of Gaussian time series, similar to Nielsen, Larsen and Hansen (2007). For this purpose, we use spectral correlations for the period of concurrent data with extrapolation to low frequencies.

The new MCP method and selection of traditional methods were tested by field observations made for the Wind Atlas for South Africa (Mortensen et al., 2014) and reference data simulated by the weather research and forecasting model WRF (Hahmann et al., 2015). Short periods of concurrent data were selected, and the accuracy of the predictions was evaluated by comparison with the entire period of local data. The new model performed well, except for short periods of current data, say less than three months. The problem is that the diffusion-based transformation becomes undefined beyond the range of concurrent data. For such conditions, we therefore apply predictions of a simpler MCP method more suitable for extrapolation or, as a last resort, the raw uncorrected data.

The MCP uncertainty of key parameters, like the mean wind speed or mean wind power density, is estimated by jackknife resampling.

References:

Carta, J. A., Velazquez, S. & Cabrera, P. (2013) A review of measure-correlate-predict ´ (MCP) methods used to estimate long-term wind characteristics at a target site, Renew. Sust. Energ. Rev., 27, 362–400.

Gastner, M. T. & Newman, M. E. J. (2004) Diffusion-based method for producing density-equalizing maps, Proc. Natl. Acad. Sci., 101, 7499–504.

Hahmann, A., Lennard, C., Badger, J., Vincent, C., Kelly, M., Volker, P., Argent, B. & Refslund, J. (2015). Mesoscale modelling for the Wind Atlas of South Africa (WASA) project, DTU Wind Energy, Denmark.

Mortensen, N., Hansen, J., Kelly, M., Prinsloo, E., Mabille, E. & Szewczuk, S. (2014) Wind Atlas for South Africa (WASA) Station and Site Description Report, DTU Wind Energy E-0071, DTU Wind Energy, Denmark.

Nielsen, M., Larsen, G. C. and Hansen, K. S. (2007) Simulation of inhomogeneous, non-stationary and non-Gaussian turbulent winds, J. Phys.: Conf. Series, 75, 012060

Nielsen, M. (2019) Long-term correction of wind observations by diffusion-based transformation, DTU Wind Energy E-0183, DTU Wind Energy, Denmark.

Optimizing MCP-based gap filling with Machine Learning approaches using Hyperparameter tuning and feature engineering

Sandra Schwegmann[1,*], Martin Dörenkämper[1], Lukas Vollmer[1], and Julia Gottschall[1]
[1]Fraunhofer IWES
[*]Presenting author

Keywords: Measure-Correlate-Predict | Machine Learning | Gap Filling | Met Mast data

At the beginning of each wind energy project, an as accurate as possible characterization of the site specific wind resources is needed for any economic considerations of the project. The estimation of wind resources for wind parks is usually based on short-term measurements (mostly one year) on site, which are then extended according to their correlation with a reference time series, mostly based on adjacent grid points from either mesoscale models like WRF or reanalysis data like ERA-5.
This connection is calculated via the so-called Measure-Correlate-Predict (MCP) approach and its accuracy strongly depends on the identification of the underlying patterns that connect the reference time series with the measurements. However, measurements often suffer from data gaps which may cover several days and even up to months. Long or often re-occurring data gaps may then result in a distortion of the wind siting statistics and thus it might be desirable to close those gaps with alternative data (Gottschall & Dörenkämper 2020).
Recently, Machine Learning (ML) approaches have turned out to be a very useful tool for data gap filling (e.g., Körner et al, 2018) and a couple of other applications in wind energy resource issues (e.g., Stetco et al, 2019; Optis et al, 2021). However, those studies focus basically only on one or two ML approaches. Furthermore, the suitable set of additional features needed to obtain high accuracies in the predicted data points is basically not shown for wind resource assessments.

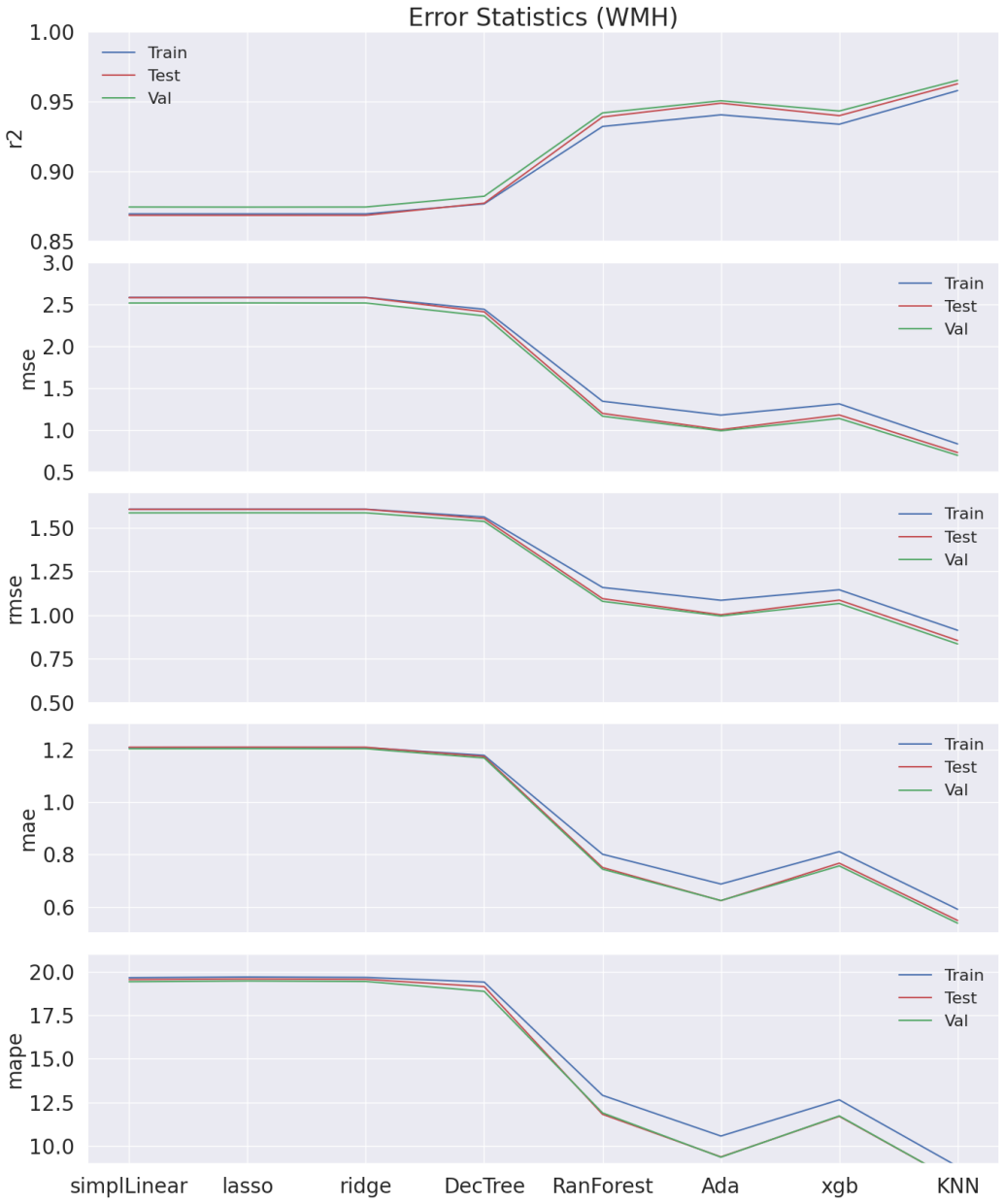


Figure 1: Error statistic for regression models using wind direction, month and hour of day as additional features. The ensemble models Random Forest (RanForest), AdaBoost and XGBoost as well as the k-Nearest Neighbors (KNN) model show a clear improvement compared to linear models and the Decision Tree Regressor (DecTree).

In this study we intend to close this gap by investigating, how uncertainties may be reduced by comparing various machine learning models suitable for regression problems to classically used linear regression approaches. For that, we trained and tested the models with the comprehensive Met Mast data set measured at Fino 2. As measure of model performance, metrics like R2, Root Mean Square Error and Mean Absolut Percentage Error are compared. However, before comparing the individual models, the models themselves

were optimized using skikit-learns GridSearchCV (Pedregosa et al., 2011) and a set of hyperparameters which were chosen individually for each model.

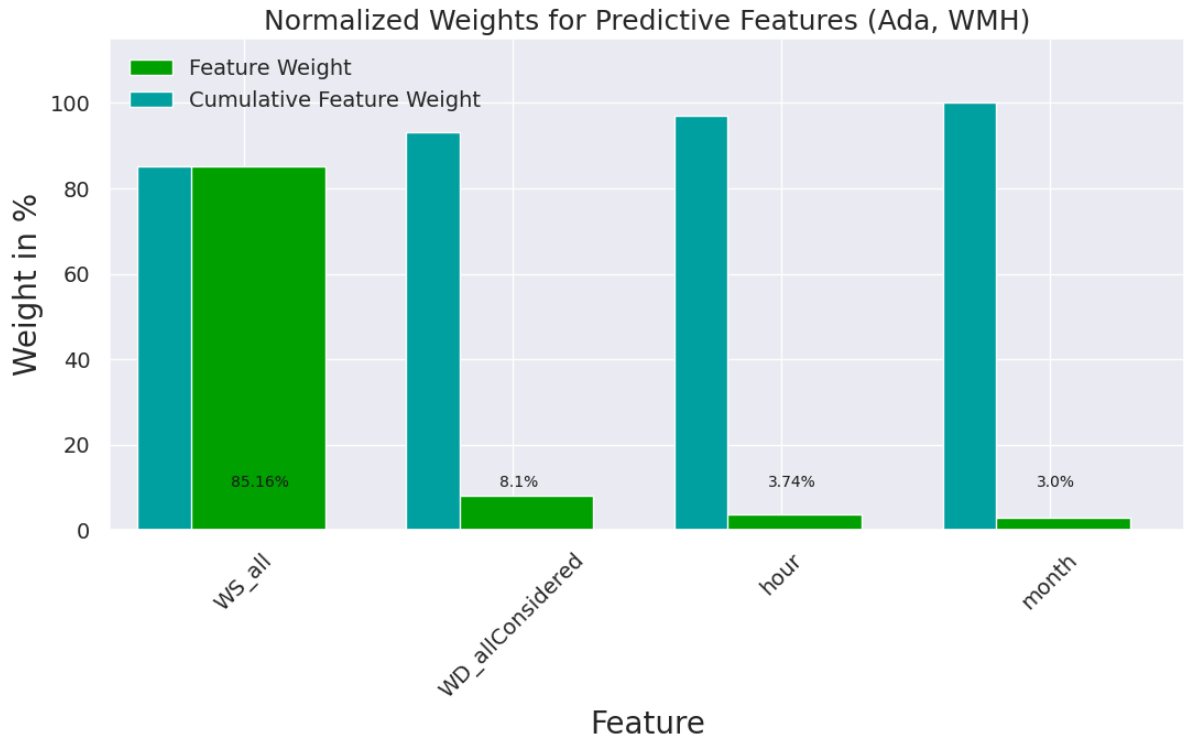


Figure 2: Importance of different features for prediction of wind speed using the AdaBoost regression model. Wind speed and wind direction show the strongest impact, but also month and hour of day have some impact.

In addition to investigating which model might be most suitable, we also studied which features are needed to improve the prediction of missing wind speed data within the time series. First results indicate that, when solely wind speed of the measurements and reference time series were correlated, ML models can rarely beat standard linear regression. In some cases, ML performs even worse than the classical approach. However, when starting to use more features, like wind speed, month (considering seasons) or hour of day (considering diurnal signals), errors in the more complex ML models decrease clearly (Figure 1). This implies that ML models including a set of additional features (see Figure 2 for an example of feature importances) have the potential to better capture the correlation between two measurement sites and hence to predict missing wind conditions with higher accuracy.

References:

Gottschall, J. & Dörenkämper, M. (2020) Understanding and mitigating the impact of data gaps on offshore wind resource estimates. Wind Energ. Sci. Discuss. [preprint], Available from: https://doi.org/10.5194/wes-2020-102, in review

Körner, P., Kronenberg, R., Genzel, S. & Bernhofer, C. (2018) Introducing Gradient Boosting as a universal gap filling tool for meteorological time series. Meteorol. Z., 27, Available from: https://doi.org/10.1127/metz/2018/0908

Optis, M., Bodini, N., Debnath, M. & Doubrawa, P. (2021) New methods to improve the vertical extrapolation of nearsurface offshore wind speeds, Wind Energ. Sci. Discuss. [preprint], Available from: https://doi.org/10.5194/wes-2021-5 , in review

Pedregosa, F., Varoquaux, G., Gramfort, A., Michel, V., Thirion, B., Grisel, O., Blondel, M., Prettenhofer, P., Weiss, R., Dubourg, V., Vanderplas, J., Passos, A., Cournapeau, D., Brucher,M., Perrot,M. & Duchesnay, E. (2011) Scikit-learn:Machine Learning in Python, Journal of Machine Learning Research, 12, 2825–2830

Stetco, A., Dinmohammadi, F., Zhao, X., Robu, V., Flynn, D., Barnes, M., Keane, J., Nenadic, G. (2019) Machine learning methods for wind turbine condition monitoring: A review. Renewable Energy, Volume 133, Available from: https://doi.org/10.1016/j.renene.2018.10.047

Automated identification of Dunkelflaute events: a convolutional neural network-based autoencoder approach

Bowen Li*, Sukanta Basu, Simon Watson, and Herman Russchenberg
Delft University of Technology
*Presenting author

Keywords: Dunkelflaute identification | Convolutional neural network | Autoencoder | K-means clustering

For the European energy system, non-dispatchable generation such as wind and solar power will be playing increasingly important roles. Unfavourable weather conditions, like simultaneous low wind and overcast conditions, will present ever greater challenges to system operators. One such phenomenon is dubbed 'Dunkelflaute' which leads to low levels of wind and solar power production and is causing serious concern to the renewable energy industry. In previous work [1,2], we have concluded that periods of Dunkelflaute are not uncommon using Belgian and Dutch power production data. Notably, a number of these Dunkelflaute events lasted for several consecutive days and necessitated the purchase of power from neighbouring countries, often at a high market price.

These findings suggest that there is a need for better identification and characterization of such Dunkelflaute events, especially those of long duration.

A better understanding of the wind and solar patterns during Dunkelflaute events can be important for event identification and forecasting. The capabilities of the contemporary mesoscale models to reliably simulate or forecast Dunkelflaute events are described in [1,2]. However, utilizing Numerical Weather Prediction (NWP) models to forecast or analyse a large number of Dunkelflaute cases in different countries is computationally impractical. Instead, with increasingly publicly available weather data, a data-driven deep learning approach can be used to classify wind and solar patterns and increase understanding of those specific patterns corresponding to Dunkelflaute periods. The classification work can significantly reduce the number of NWP runs required to model Dunkelflaute events. In this study, unlabelled data is used in the classification of weather patterns. We investigate if unsupervised learning methods can facilitate wind and solar pattern classification for further characterisation of Dunkelflaute events.

10-year wind and solar radiation data are used as input for the unsupervised learning model. In order to decrease the dimensionality and find the most important information from the variables for clustering, an autoencoder is used. An autoencoder is a type of unsupervised artificial neural network that consists of encoding and decoding parts. A number of learning structures are first compared to determine the most promising encoder-decoder accuracy. A novel asymmetric convolutional neural network (CNN) structure is shown to be the best autoencoder for capturing spatial patterns. The decoded information is then used for classification using K-means clustering. The resulting 20 clusters are analyzed and explored for weather patterns corresponding to Dunkelflaute. Notably, three clusters are characterised with low wind speed and solar radiation over the Belgian area, though they have different magnitude and spatial patterns.

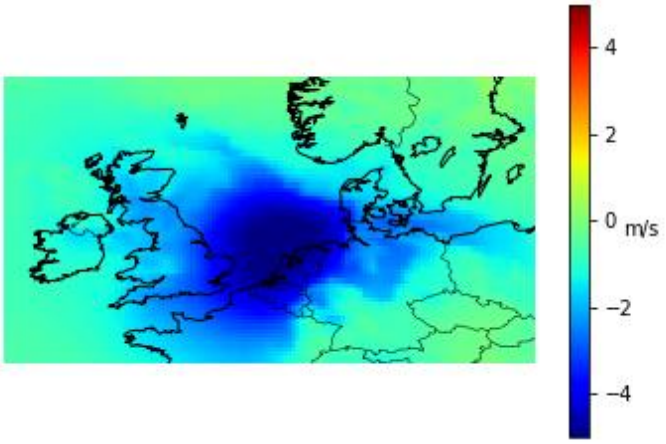


Figure 1: Map of averaged anomalies of wind speed for a specific cluster corresponding to Dunkelflaute in Belgium.

The averaged anomalies of wind speed in one of the Dunkelflaute clusters in Belgium are shown in Figure 1, which shows the averaged anomalies of all examples in the cluster with respect to the 10-year mean wind speed. Finally, the identified Dunkelflaute time periods are validated with 4-year aggregated wind and solar power production data for Belgium. A good match was seen between observed Dunkelflaute periods and those tagged as such using our clustering approach demonstrating the potential of the proposed unsupervised learning model for the identification of Dunkelflaute events.

References:

[1] Li, B., Basu, S., Watson, S.J. and Russchenberg, H.W., 2021. Mesoscale modeling of a "Dunkelflaute" event. Wind Energy, 24(1), pp.5-23.

[2] Li, B., Basu, S., Watson, S.J. and Russchenberg, H.W., 2020, September. Quantifying the Predictability of a 'Dunkelflaute'Event by Utilizing a Mesoscale Model. In Journal of Physics: Conference Series (Vol. 1618, No. 6, p. 062042). IOP Publishing.

A Use Case for a Numerical Self Consistency Test in Preparation of a Power Curve Measurement Site

Matthias Arnold[1,*], Pascal Weihing[1], Alexander Radi[2], and Timo Kühn[1]
[1]Wobben Research and Development GmbH
[2]Wobben Research and Development Management Support GmbH
*Presenting author

Keywords: Site Assessment | Numerical Self Consistency Test | Lattice Structure Wake | Power Curve Measurement

In order to plan the time schedule for the market entry of a new wind turbine type, the completion time of the power curve measurement needs to be known a priori and thus the prediction of the feasible measurement sectors is of essence.
Within this presentation, a site assessment for an exemplary site for power curve measurement will be discussed. It will be shown, how numerical simulations can be facilitated to improve the prediction of the measurement period. At the site in question, a high voltage power line passes south-west of the possible point of installation. Based on the definitions of the IEC61400-12-1 ed.2, each mast of the power line is considered as a solid obstacle, resulting in the exclusion of the affected wind sectors. However, as the main wind direction at the site is south-west, these sector restrictions would render the site unsuitable for power curve measurements, as the remaining free sectors are too small to complete the measurement in a reasonable schedule.

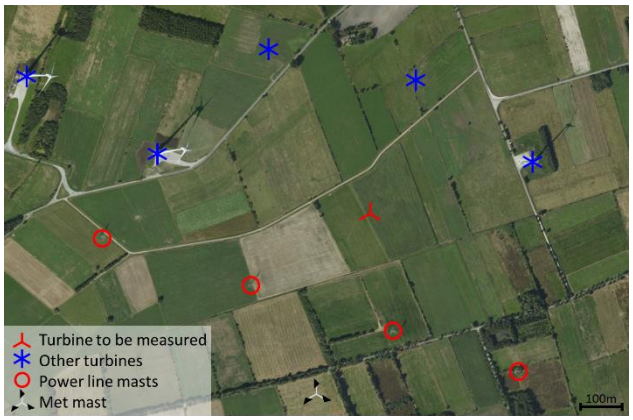


Figure 1: Aerial map of discussed site

In a second step of the presentation, this observation, that the site is rendered unfeasible by the definition of power line masts as obstacles will then be compared to a statistical analysis of Enercon's field experiences with candidate prototype sites. This statistical analysis shows that power line masts and other lattice structures are a significant issue for a considerable number of sites. However, the IEC61400-12-1 ed.2 standard does not take the solidity of a structure into account to define whether it is an obstacle or not. Yet, the low solidity of the power line mast will result in a much weaker wake compared to a solid structure. Thus, the obstacle definition of a lattice power line mast is challenged here based on numerical simulations.
By facilitating high resolution scale resolving flow simulation methods, the wake of a power mast is evaluated. These simulations with the CFD solver FLOWer are used to estimate the wake velocity profile of the lattice structure, which is then applied to a BEM model of the candidate prototype turbine. By performing this analysis for a range of wind directions, a numerical self consistency test is performed for the site.

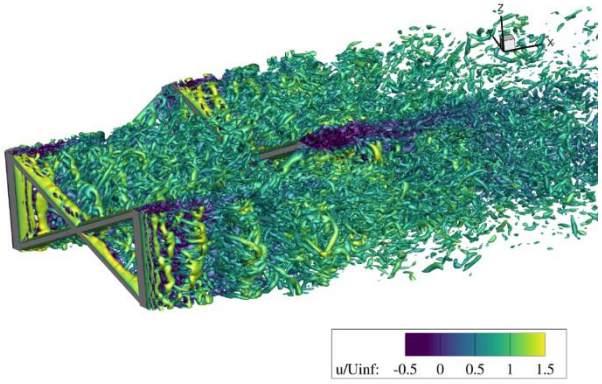


Figure 2: Simulated near-wake of a lattice segment

These simulations prove, that even when considering a worst case scenario for the wake evolution, the impact on the turbines' power generation is below the critical limits of the measurements self consistency test, as defined in the IEC standard. Thus, in contrast to the estimation of the IEC standard, the site is predicted by the simulations to be suitable for a power curve measurement with regards to the studied measurement sectors.

This application presents how numerical simulation can be facilitated, by means of a detailed obstacle analysis within a numerical self consistency test, to predict the suitability or disturbance of wind sectors during measurements. Subsequently, this approach can be used to predict, whether a power curve measurement at a site can be completed within a reasonable schedule.

Estimation of wind resources and wind energy production using the ERA5 reanalysis data

Gianni Goretti*
Technological University Dublin
*Presenting author

Keywords: ERA5 | Wind resource assessment | Wind power assessment | Wind farm design

This work presents a new tool to estimate wind energy production for any wind farm at arbitrary locations using the ERA5 reanalysis data set.
The proposed methodology is valid both for the design of new wind farms and the assessment of existing plants, where site measurements are not available, and consists of the following steps.
1. Information on the wind farm is collected, which at minimum include the location, hub height and wind turbine power curves.
2. The wind speed at the site is estimated with a Measure-Correlate-Predict approach (Manwell, McGowan and Rogers, 2010), as discussed in step 3. The ERA5 hourly data on single levels (Hersbach et al., 2018) from the Copernicus Climate Change Service (C3S) provide the reference data set. These data are available from 1979 to present on a regular lat-lon grid of 0.25 degrees. The four nearest grid points around the wind farm are identified and the vertical wind shear is characterised at each grid point using the log law approach (Wortman, 1983): wind speeds at hub height are calculated.
3. Next, wind speeds at the wind farm location are estimated using the variance method (Rogers, Rogers and Manwell, 2005). Grid points values calculated in step 2 constitute the reference data sets and the statistical parameters in the variance relationship are estimated recursively. It follows that four sets of estimates are obtained, one from each grid point.
4. The average wind speed at the wind farm location is finally calculated using bilinear interpolation on the four sets of estimates from step 3 (see Figure 1).
5. If information on the wind farm layout is available, the probability distribution of wind directions at the site is estimated recursively using a joint probabilistic approach (García-Rojo, 2004). From this estimated distribution, the prevailing wind direction at the site is determined.
6. A wind farm power curve is developed based on the manufacturer's power curve, expert judgement and information on the location, if available (e.g. wind farm layout, prevailing wind direction, terrain).
7. The hourly estimates of wind speed are converted into power through the power curve and the hourly energy production of the wind farm is calculated.

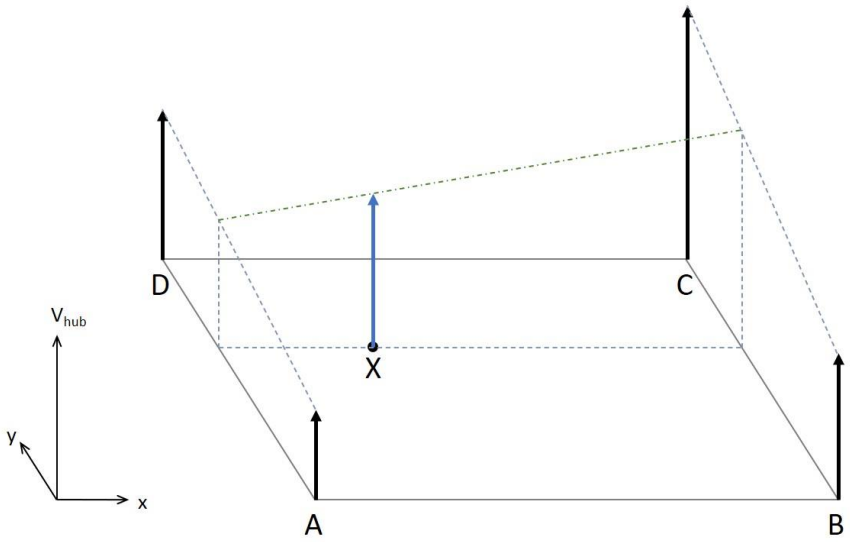


Figure 1: Bilinear interpolation of wind speed at hub height for wind farm location X. A, B, C, and D are the four nearest points on the ERA5 grid.

The proposed methodology is applied to a number of existing wind farms for which measurements of wind speed and power output are available for one year or longer. The wind farms have different sizes and are located on different terrain types. The performance of the tool is evaluated in terms of wind resource assessment and energy production estimation.

The influence of various factors on the accuracy of the predictions is assessed, including the length of the reference data sets, time of the year, distance from grid points, terrain type, wind farm size, and the quality of the power curve model.

References:

García-Rojo, R. (2004) 'Algorithm for the estimation of the long-term wind climate at a meteorological mast using a joint probabilistic approach', Wind Engineering. doi: 10.1260/0309524041211378.

Hersbach, H. et al. (2018) ERA5 hourly data on single levels from 1979 to present, Copernicus Climate Change Service (C3S) Climate Data Store (CDS). doi: 10.24381/cds.adbb2d47.

Manwell, J. F., McGowan, J. G. and Rogers, A. L. (2010) Wind Energy Explained: Theory, Design and Application, Wind Energy Explained: Theory, Design and Application. doi: 10.1002/9781119994367.

Rogers, A. L., Rogers, J. W. and Manwell, J. F. (2005) 'Comparison of the performance of four measure-correlate-predict algorithms', Journal of Wind Engineering and Industrial Aerodynamics. doi: 10.1016/j.jweia.2004.12.002.

Wortman, A. J. (1983) 'Introduction to wind turbine engineering.' Butterworth, Boston, MA.

Regular Session: Wind Resource Assessment (V)

Study of Coastal effects relevant for the offshore windfarm sector using spaceborne synthetic aperture radar data

Bughsin Djath[1,*], Johannes Schulz-Stellenfleth[1], Simon Siedersleben[2], and Beatriz Cañadillas[3]
[1]Helmholtz-Zentrum Geesthacht
[2]Karlsruhe Institute of Technology
[3]UL International GmbH
*Presenting author

Keywords: Synthetic Aperture Radar | Offshore wind energy | Atmospheric stability | Coastal effects

In the coastal zone complex atmospheric processes are caused by large differences between the land and ocean surface in particular concerning momentum and heat fluxes. The smoother sea surface leads to wind speeds, which are usually higher over the ocean than over land. In addition, there are complicated effects caused by temperature gradients in the ocean due to water depth variations.
This study focuses on the investigation of the change in the horizontal wind field, the atmospheric stability and temperature between the coast and up to 200 km offshore.
The wind resources at 10 m height are assessed from synthetic aperture radar (SAR) data acquired by the satellites Sentinel-1A and Sentinel-1B over the German Bight within the period from 2017 to 2020 with a focus on offshore wind directions. The satellite data provide information on sea surface roughness, which can be linked to near surface wind speed (Figure 1) (Djath et al., [2018]; Djath and Schulz-Stellenfleth [2019]). Information on the air-sea thermal components is provided by insitu measurements taken at the FINO 1 platform and model data from the German weather service (DWD).

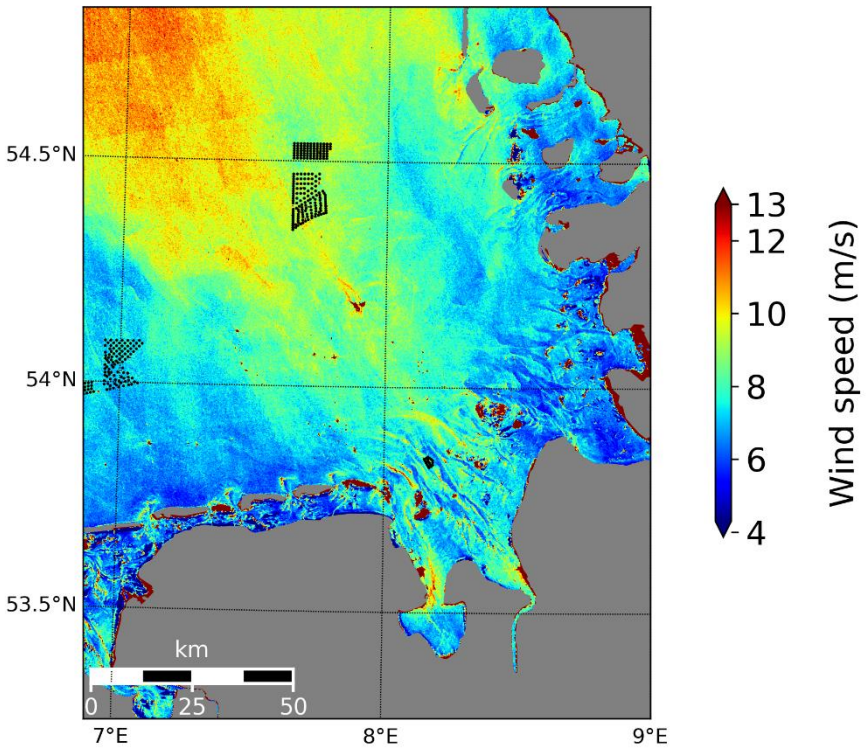


Figure 1: Derived 10-m wind speed from Sentinel 1B on 14.03.2020 at 17:16.

The SAR data show a significant increase of wind speed offshore in most cases. Increasing wind speeds between land and sea over fetch distances of 70 km and more are often detected. The increase Δu_10 (Δu_10

= u_offshore - u_coast) in horizontal wind speed between offshore and the coast exceeds 1.5 m/s in most cases. The gap Δu_10 increases for high wind speeds. Also, strong thermal stability tends to influence the horizontal wind gradient by not only reducing Δu_10, but increasing the fetch distance over more than 100 km as well.

Furthermore, SAR observations show that the heterogeneous structure of the coastline leads to strong variations of wind speeds in the along coast direction. A simple parametric model to replicate this effect is also presented. The implications for the existing and planned offshore wind parks in the German Bight are discussed.

As the stability is strongly influenced by water temperature, a climatological analysis of the SST over the German Bight was performed showing that gradients in water depth between the coast and sea clearly impact the distribution of sea surface temperature (SST) throughout the seasons, with the highest values in summer. The shallow water near the coast warms quicker in summer and cools faster in winter than the deeper water. This has consequences for the spatial distribution of stability.

Examples of SAR measurements are shown where horizontal gradients in stability obviously have a strong impact on offshore wind speed gradients.

The results will be discussed in the context of numerical modelling activities in the research and industrial community (Siedersleben et al., [2020]; Cañadillas et al., [2020]).

References:

Djath, B. and Schulz-Stellenfleth, J. (2019). Wind speed deficits downstream offshore wind parks - A new automised estimation technique based on satellite synthetic aperture radar data. Meteorologische Zeitschrift 28, 499–515. https://doi.org/10.1127/metz/2019/0992

Djath, B. and Schulz-Stellenfleth, J. and Canadillas, B. (2018). Impact of atmospheric stability on X-band and C-band Synthetic Aperture Radar imagery of offshore windpark wakes. Journal of sustainable and renewable Energy 10. https://doi.org/10.1063/1.5020437

Cañadillas, B. and Foreman, R. and Barth, V.and Siedersleben, S. and Lampert, A. and Platis, A. and Djath, B. and Schulz-Stellenfleth, J. and Bange, J. and Emeis, S. and Neumann, T. (2020). Offshore wind farm wake recovery: Airborne measurements and its representation in engineering models. Wind Energy 1–17. https://doi.org/10.1002/we.2484

Siedersleben, S.K. and Platis, A. and Lundquist, J.K. and Djath, B. and Lampert, A. and Bärfuss, K. and Canadillas, B. and Schulz-Stellenfleth, J. and Bange, J. and Neumann, T. and Emeis, S. (2020). Turbulent kinetic energy overlarge offshore windfarms observed and simulated by the mesoscale model WRF (3.8.1). Geosci. Model Dev. 13, 249–2020. https://doi.org/10.5194/gmd-13-249-2020

Generating wind ressources maps at hub height with SAR and machine learning

Louis de Montera[1,*], Henrick Berger[1], Romain Husson[1], Pascal Appelghem[2], Guerlou Laurent[1], and Mauricio Fragoso[1]
[1]CLS
[2]Atmosky
*Presenting author

Keywords: SAR | wind resource | machine learning | Sentinel-1

In this study, we generate high resolution maps of the wind power at 200m above sea level with Sentinel-1 SAR and machine learning. The algorithm inputs are the SAR wind speed at 10m, several geometrical parameters of the sensor and several parameters related to the atmospheric stability provided by a numerical model. The training phase is done using floating Lidars. The algorithm is able to produce wind power maps at hub height having an error below 5%. Compared to the numerical model alone, the new maps show a much higher level of detail and important difference. In particular, the numerical model is found to overestimate the wind power along the coast and underestimate it further offshore. This method can be beneficial to optimize wind far siting and better estimate the coastal gradient.

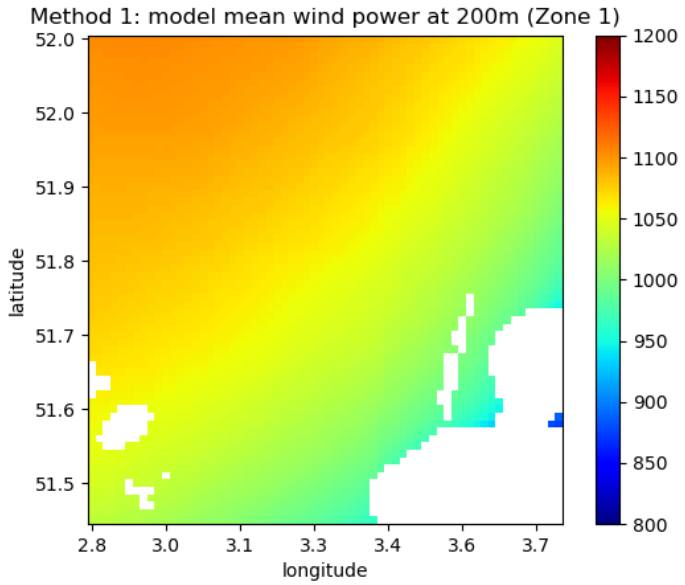


Figure 1: Wind power at 200m estimated with a high resolution numerical model

In order to extrapolate SAR surface winds at hub height, the extrapolation ratios found with the insitu Lidar data are first analyzed. It is found that the classical power law model of the wind profile is not accurate at high altitudes. Then, the performance of a numerical model is assessed. The model wind speeds are found to be inaccurate below 40m and slightly biased above this altitude (5%).

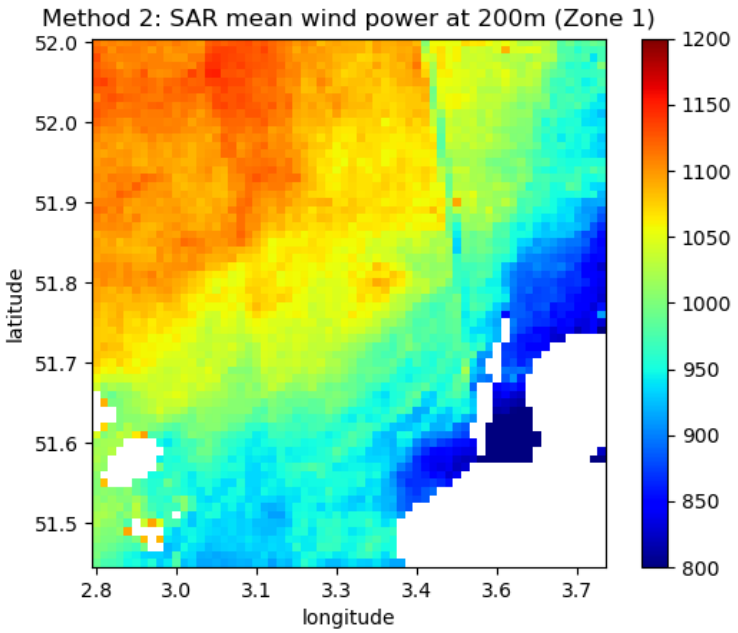


Figure 2: Wind power at 200m estimated with SAR and machine learning

However, the extrapolation ratios between 40m and higher altitudes provided by the model are very accurate (1%). Then, several approaches are used to extrapolate the SAR surface winds. The first one consists in using a power law with an exponent of 0.11 found in the literature. As expected, the extrapolation is biased and inaccurate, even if the exponent is tuned. The second approach consists in extrapolating the SAR surface winds at 40m with the power law and then scaling them at higher altitudes with the model extrapolation ratio. This approach is successful in terms of extrapolation ratio. However, it is biased in terms of mean wind speed, which can be partly compensated if the SAR surface winds are optimized with machine learning beforehand. The last approach consists in using machine learning to learn directly the Lidar wind speeds at hub height. In order to do that, three parameters provided by the numerical model are added as input to the algorithm, namely, the surface heat flux, the temperature difference between the sea and the air, and the extrapolation ratio given by the model. This approach is found to be accurate and can provide an unbiased estimate of the mean wind speed at 200m with a high precision (2 %). However, the distribution plots show that the machine learning is not able to conserve the wind speed standard deviation, therefore a correction is applied. The wind power is then calculated using the method of the moment and the Weibull distribution and found to have an error below 5% at 200m compared to the Lidars.

Using Earth Observation ocean winds for wind energy

Ioanna Karagali* , Merete Badger, and Charlotte Bay Hasager
Technical University of Denmark
*Presenting author

Keywords: Sentinel1 | ASCAT | Offshore wind | Earth Observation

Satellite-based remote sensing is one of the primary modes of Earth Observation and ocean winds are one of the first parameters to be monitored; now approaching their third decade, with continuous improvements and increase in spatial and temporal coverage. Meanwhile, increase in installed and planned offshore wind energy capacity triggers challenges for more and better observations of the remote oceanic environment. Satellite-derived ocean winds offer a unique opportunity to characterize the offshore environment prior to deciding the installation of in-situ measuring stations and performing high-resolution simulations.
Typical space-borne sensors to retrieve ocean winds are scatterometers (Vogelzang & Stoffelen 2012) and Synthetic Aperture Radars (SAR, Horstmann et al 2003); radars that measure the signal backscattered from the ocean surface due to roughness elements in equilibrium with the local wind; using empirical formulas, the wind speed and direction is retrieved. Shorter archives of scatterometer and SAR winds have been used for wind resource characterization in various parts of the global ocean (Hasager et al 2020). This study demonstrates and summarises the applicability of satellite-based ocean surface winds for a range of needs stemming from the offshore wind energy sector, focused on understanding and monitoring the offshore wind climate.

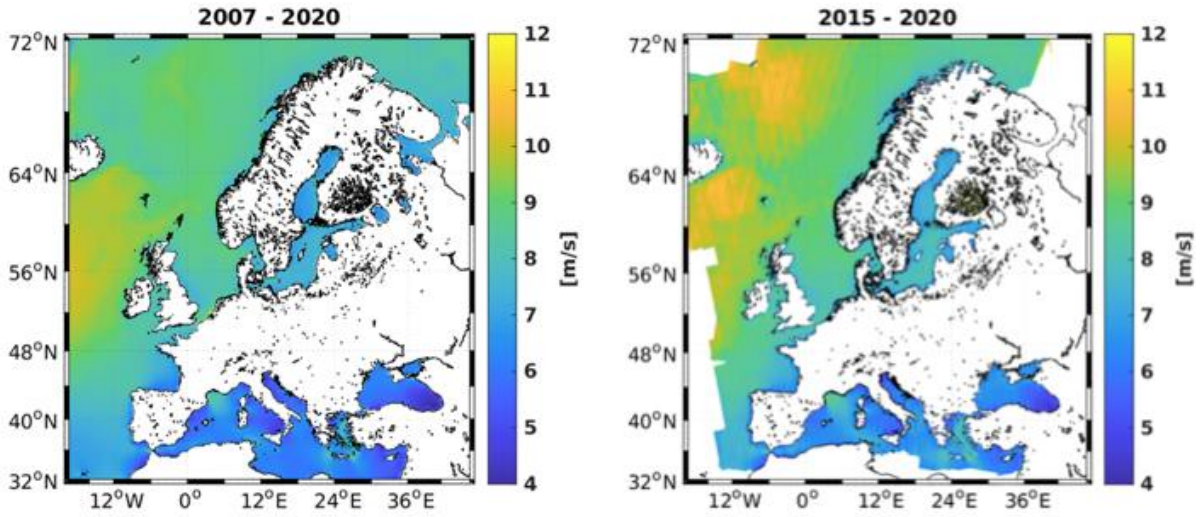


Figure 1: Mean wind speed at 10 m above the surface from different space-borne sensors.

For example, Figure 1 shows mean wind speed estimated from the ASCAT scatteometer, from 2007 to 2020, and the Sentinel 1 SAR winds from 2015 to 2020; these are operationally retrieved at DTU Wind Energy (publicly available at https://satwinds.windenergy.dtu.dk) and have been recently postprocessed to obtain gridded daily products. Effects of sampling patterns can be identified for the SAR wind due to sporadic sampling and viewing patters, although this product is of higher spatial resolution compared to ASCAT. White areas indicate regions where no data have been collected and processed to wind speeds.

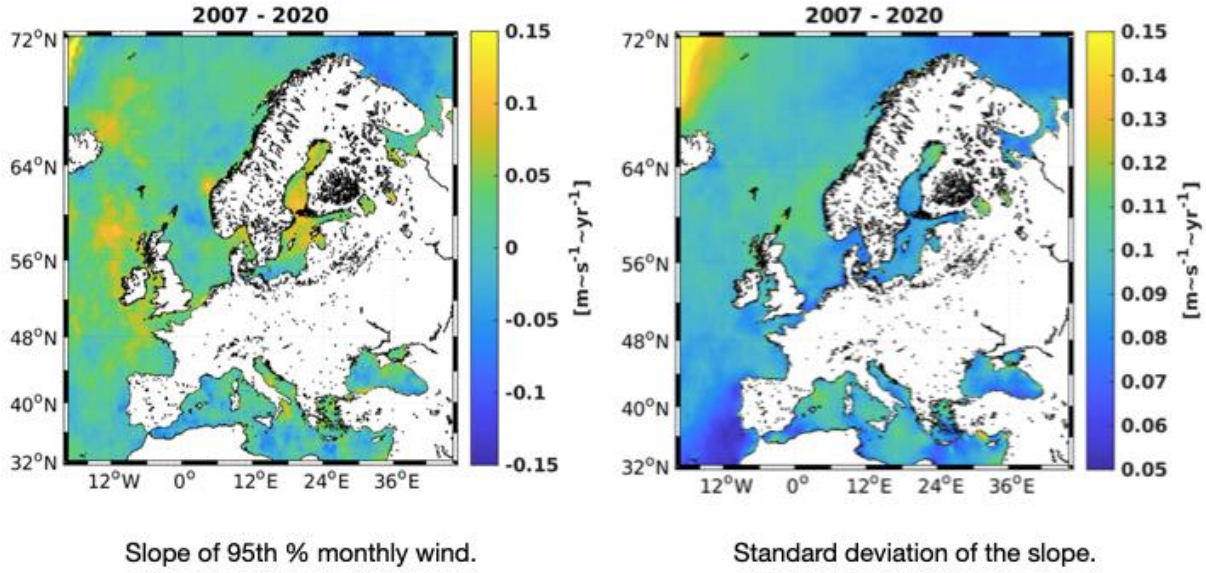


Figure 2: 95th percentile of monthly ASCAT wind speed values used for linear regression.

Figure 2 shows the trend (left) of the linear regression's slope and its standard deviation (right), applied on the 95th percentile monthly wind speeds from ASCAT between 2007 and 2020, i.e. during 14 years. A mixed spatial pattern of increasing and decreasing 95th % wind speed trends per year is identified, where the North Atlantic region along with the Northern Baltic Sea show the highest positive trends, in the order of 0.15 m s-1 year-1. The spatial variability of the linear regression slope (left) is attributed to differences in the wind speed trends over the ocean which can be associated with an increase in extreme wind speeds and associated storms in the last decade, influenced by large scale circulation patterns and changes in the sea surface temperature. Such results indicate if winds have been decreasing or increasing in a certain area over the period of data availability and provide an insight, with some confidence, of what can be expected in the future. This can be valuable as supporting information on the expected annual energy production of planned offshore wind farms.

References:

Hasager, C. B., Hahmann, A. N., Ahsbahs, T. T., Karagali, I., Sile, T., Badger, M., & Mann, J. (2020). Europe's offshore winds assessed with synthetic aperture radar, ASCAT and WRF. Wind Energy Science, 5(1), 375–390.

Horstmann, J., Schiller, H., Schulz-Stellenfleth, J., & Lehner, S. (2003). Global wind speed retrieval from SAR. IEEE Transactions on Geoscience and Remote Sensing, 41(10), 2277–2286.

Vogelzang, J., & Stoffelen, A. (2012). Scatterometer wind vector products for application in meteorology and oceanography. Journal of Sea Research, 74, 16–25.

Evaluation of a high-resolution dynamical downscaling of ERA5 with COSMO-CLM for the North Sea

Ruben Borgers[1,*], Johan Meyers[1], and Nicole van Lipzig[1]
[1]Katholieke Universiteit Leuven
[*]Presenting author

Keywords: COSMO-CLM | ERA5 | CMIP6 | Dynamical Downscaling | Wind farm parametrization

The growing importance of offshore wind energy emphasizes the need for realistic projections of the energy yield of wind farms over their lifetime. Analyses of CMIP5 projections, either directly (Devis et al., 2018) or downscaled (Reyers et al. (2016); Carvalho et al. (2017)) show that, even though nearfuture wind speed changes over Europe and the North Sea are uncertain across models, these changes should be taken into account by wind industries due to the potentially large impact on the energy yield.
However, these past studies have not included the effect of the interaction between the atmospheric flow and offshore wind farms on the energy yield. In this study, we aim to include this interaction, thereby improving the quantification of the lifetime energy production including its uncertainty for wind farms over the North Sea for the 2020-2050 period. This will be done through the dynamical downscaling of several CMIP6-model realisations to a spatial resolution of 2.8km using the COSMOCLM regional climate model which includes the wind farm parametrization by Fitch et al. (2012) that was recently implemented (Chatterjee et al., 2016; Akhtar et al., 2020, Figure 1). As more and larger offshore wind farms emerge, energy losses due to array-array and cluster interactions are also likely to increase. To investigate these array-array and cluster effects, different scenarios for future wind farm deployment will be implemented in the model and compared. The research will be outlined as follows: first, to evaluate the quality of COSMO-CLM wind data at 2.8km resolution, a 30-year reanalysis dataset (ERA5) will be downscaled and tested against observations. Next, a number of models from the CMIP6 ensemble will be selected that spans the range of uncertainty for the 2020-2050 period. The CMIP6-model realisations will then be downscaled by COSMO-CLM in combination with future wind farm deployment scenarios that will be developed based on targets for European offshore wind energy. After downscaling, the generated wind data near hub-height will be used to estimate lifetime yield of windfarms over the study region.

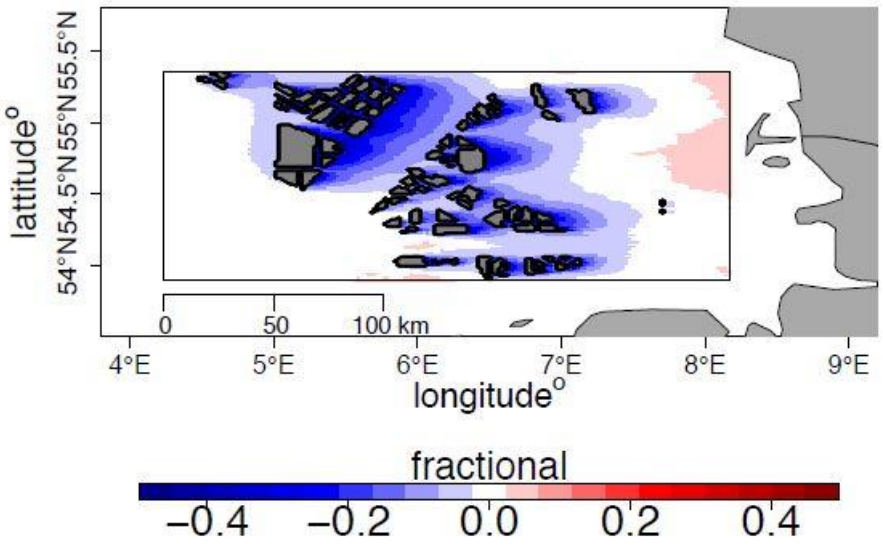


Figure 1: Fractional difference in westerly wind power at hub height between a simulation with the wind farm parametrization engaged and the same simulation without this parametrization as modelled by COSMO-CLM for the German Bight. The inner box represents the

analysis domain. White grid boxes represent non-significant differences. Grey polygons represent wind farm locations (Chatterjee, 2020).

For WESC2021, we aim to present (a subset of) the high-resolution, 30-year ERA5-driven output of COSMO-CLM, including a comparative analysis of the generated wind data with observations from the Fino1 platform, QuikSCAT wind data, buoys and measuring poles. This analysis can then be used as a measure for the quality of the simulated wind fields, which is a fundamental uncertainty in an assessment of wind energy potential. While reanalysis-driven wind fields generated by COSMO-CLM for the North Sea have already been tested against observations in the past (Geyer et al., 2015), the present study will evaluate model results at a higher, convection-permitting spatial resolution and attempt to incorporate observational data from other measurement stations.
This planned study frames within the FREEWIND project of KU Leuven (freewind-project.eu) which aims to provide advanced wind farm planning and forecasting tools in the course of the following 4 years.

References:
Akhtar, N., & Rockel, B. (2020, May). Mesoscale resolving high-resolution simulation of wind farms in COSMO-CLM 5. In EGU General Assembly Conference Abstracts (p. 7178).
Carvalho, D., Rocha, A., Gómez-Gesteira, M., & Santos, C. S. (2017). Potential impacts of climate change on European wind energy resource under the CMIP5 future climate projections. Renewable Energy, 101, 29-40.
Chatterjee, F., Allaerts, D., Blahak, U., Meyers, J., & van Lipzig, N. P. M. (2016). Evaluation of a wind-farm parametrization in a regional climate model using large eddy simulations. Quarterly Journal of the Royal Meteorological Society, 142(701), 3152-3161.
Chatterjee, F. (2020). Wind farm impacts on the regional climate of the German Bight: A regional climate model study.
Devis, A., Van Lipzig, N. P., & Demuzere, M. (2018). Should future wind speed changes be taken into account in wind farm development?. Environmental Research Letters, 13(6), 064012.
Fitch, A. C., Olson, J. B., Lundquist, J. K., Dudhia, J., Gupta, A. K., Michalakes, J., & Barstad, I. (2012). Local and mesoscale impacts of wind farms as parameterized in a mesoscale NWP model. Monthly Weather Review, 140(9), 3017-3038.
Geyer, B., Weisse, R., Bisling, P., & Winterfeldt, J. (2015). Climatology of North Sea wind energy derived from a model hindcast for 1958–2012. Journal of Wind Engineering and Industrial Aerodynamics, 147, 18-29.
Reyers, M., Moemken, J., & Pinto, J. G. (2016). Future changes of wind energy potentials over Europe in a large CMIP5 multi-model ensemble. International Journal of Climatology, 36(2), 783-796.

10-year mesoscale wind resource assessment of the small island developing state of Fiji using the Weather Research and Forecasting (WRF) model

Kunal Dayal*, John Cater, Michael Kingan, Gilles Bellon, and Rajnish Sharma
The University of Auckland
*Presenting author

Keywords: Fiji | WRF | Mesoscale | Wind resource assessment

This study presents a recent decade (2009 – 2018) mesoscale wind-resource assessment of the small island developing state (SIDS) of Fiji using the Weather Research and Forecasting (WRF) model.
Previous studies evaluating the WRF model for simulating surface winds and the diurnal cycle of wind speed for the SIDS of Fiji showed that the 1.33 km by 1.33 km grid resolution in a 20 km – 4 km – 1.33 km grid sequence is not appropriate to evaluate the surface winds for Fiji, as it was suspected that the topography was not adequately resolved [1]. Following this work, a grid sensitivity study of the WRF model for simulating the surface winds for the SIDS of Fiji was conducted and it was concluded that the 1 km by 1 km grid resolution of the 15 km – 5 km – 1 km grid sequence was appropriate [2].

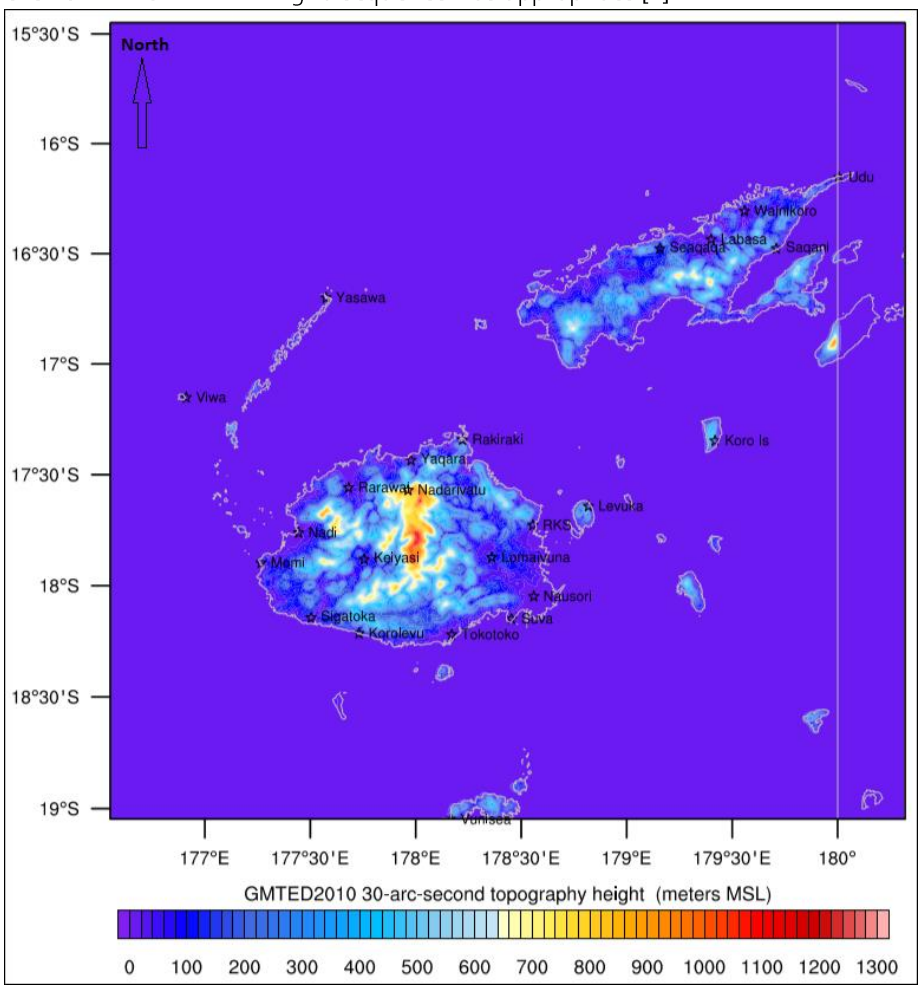


Figure 1: Topographical map of the study area (Fiji) with the locations of the AWSs.

In the present study, the 10-year model simulations were performed using the dynamical downscaling method employing the well-tested tropical suite of the physics parameterization scheme in WRF [3, 4]. The initial and boundary conditions for the SIDS of Fiji were obtained from 6-hourly NCEP-FNL (Final) Operational Global Analysis data at 1°×1° grid resolution. Other static fields were obtained and interpolated from USGS

GMTED2010, 21-class MODIS and MODIS FPAR at a resolution of 30-arc-seconds from the NCAR database. Figure 1 presents the topographic map of Fiji with the locations of the AWSs. The input data from NCEP-FNL were downscaled using three two-way nested domains of d01=1500 km×1500 km (100×100 grid cells), d02=755 km×755 km (151×151 grid cells) and d03=401 km×401 km (401×401 grid cells) at grid resolutions of 15 km×15 km, 5 km×5 km and 1 km×1 km, respectively. This analysis evaluates the wind speed and Weibull distributions, diurnal and annual wind speed patterns, resource maps of annual and seasonal wind speed, model statistical analysis and annual wind speed variability.

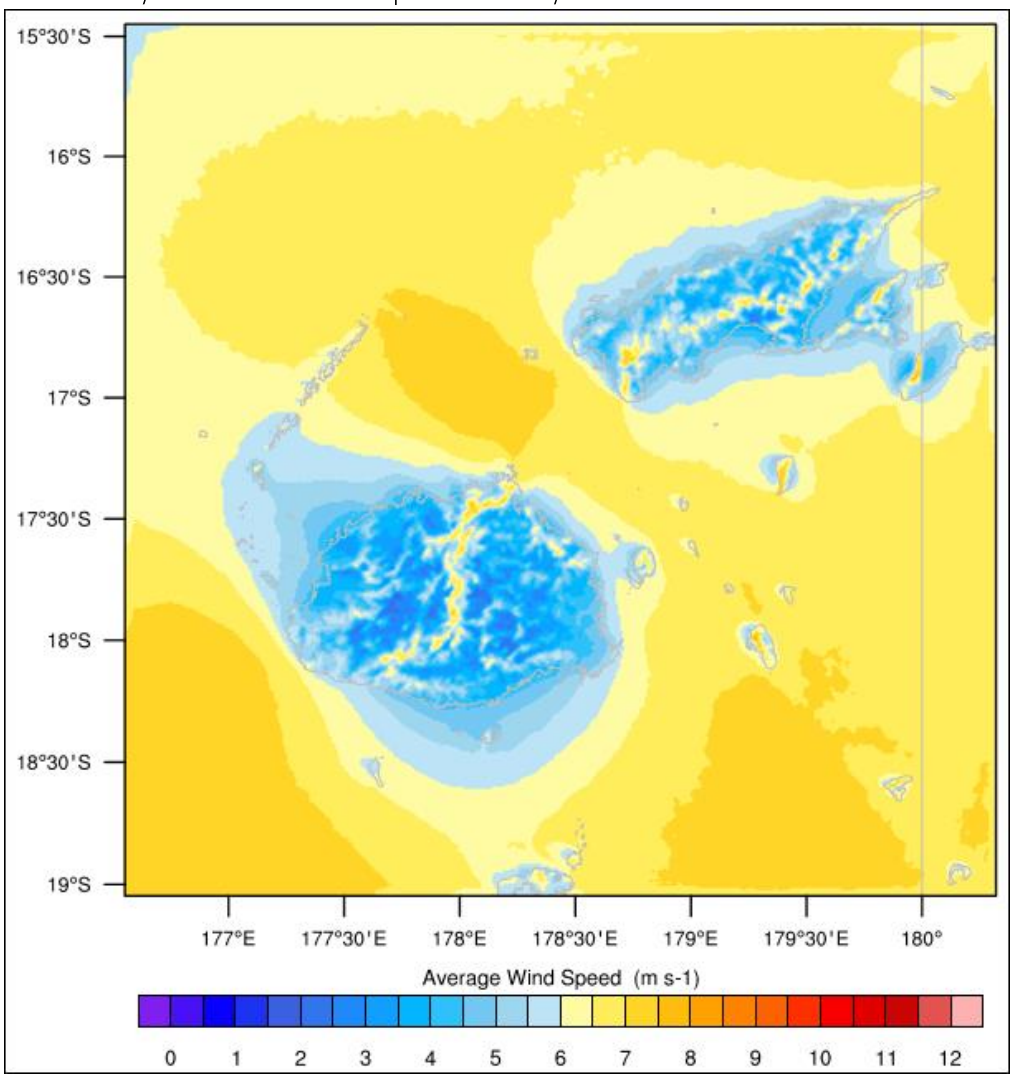


Figure 2. 10-year annual 55 m elevation mean wind speed raster map of Fiji.

The results revealed that the WRF model wind resource parameters are in good agreement with the observations. Figure 2 presents the 55 m elevation mean wind speed map of Fiji. Higher wind speeds are observed during austral winter than in austral summer. Numerous high wind-resource areas are identified in this study, which were previously unknown. The annual mean wind speed and wind power density varies from 1.5 - 8 m/s and 50 - 350 W/m2, respectively for onshore land areas @ 55 m elevation. This indicates that there is potential for utility-scale wind power generation at selected locations with wind speed and power density greater than 6.4 m/s and 300 W/m2 (NREL, Wind Power Class 3). An estimated 100 MW of wind farms can be accommodated for utility-scale wind power applications on Viti Levu and Vanua Levu. The model statistical evaluation shows an overall bias of 0.62 m/s, which is a 30.91 % overestimate in comparison with the measured wind speed, RMSE of 2.22 m/s and STDE of 2.00 m/s. The relatively low STDE is an indication that the model adequately captures the physical processes. The annual wind speed variability is low in the order of less than 1 m/s over the study period. The diurnal cycle correlation and the Weibull PDFs correlation between the measured and the simulated wind speed are 0.81 and 0.88 for 24 AWSs, respectively.

References:
Dayal, K. K., Cater, J. E., Kingan, M. J., Bellon, G. D. and Sharma, R. N. (2020). Evaluating of the WRF model for simulating the surface winds and the diurnal cycle of wind speed for the small island state of Fiji. Journal of Physics: Conference Series, 1618, 062025.
Dayal, K. K., Cater, J. E., Kingan, M. J., Bellon, G. D. and Sharma, R. N. (2020). A grid sensitivity study of the Weather Research and Forecasting (WRF) model for simulating the surface winds for the small island state of Fiji. 22nd Australasian Fluid Mechanics Conference AFMC 2020, Brisbane, QLD Australia, 7-10 December 2020.
Skamarock, W. C., Klemp, J. B., Dudhia, J., Gill, D. O., Barker, D. M., Duda, M. G., Huang, X. Y., Wand, W. and Powers, J. G. (2008). A Description of the Advanced Research WRF Version 3. NCAR Technical Note, NCAR/TN-475+STR. Wang, W. et al. (2018). WRF-ARW User Guide V3.9.

Regular Session: Large Scale Wind Farm Wake Modeling

Quantifying Uncertainty of Wake Impacts in US Offshore Wind Resource Areas

David Rosencrans[1,2,*], Julie K. Lundquist[1,3,] and Mike Optis[2]
[1]University of Colorado at Boulder
[2]National Renewable Energy Laboratory
[3]Renewable and Sustainable Energy Institute
[*]Presenting author

Keywords: wind energy | offshore wind | wind farm wakes | power

Offshore wind is a promising asset for meeting the energy demands of the United States' coastal population. Across the Atlantic Outer Continental Shelf, several US Wind Energy Lease Areas await construction in order to harvest the promising wind resource. The proposed wind farms in the mid- Atlantic offshore areas will be densely packed into clusters due to spatial and societal limitations. In European waters, densely packed wind farm clusters can create wind speed deficits, or wakes, observed by satellite, by lidar, and by aircraft. These wakes can undermine the power production of downwind farms (Nygaard 2014). In stably stratified regimes, wakes are stronger and propagate further downwind. Hence, the negative impacts of wakes vary by ambient meteorological conditions.

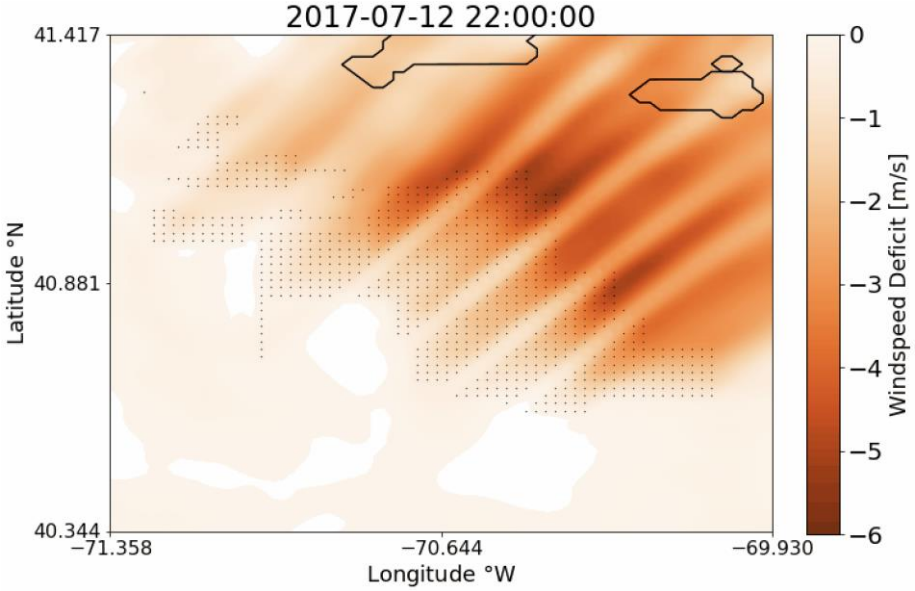


Figure 1: Wakes induced by a wind farm cluster. Black dots represent the locations of 12MW wind turbines. The colored contour depicts the reduction of wind speed due to the farms.

Stable stratification is prevalent across all US Wind Energy Lease Areas in the mid-Atlantic region, as shown by offshore lidar measurements (Bodini et al. 2019). To assess a possible worst-case scenario, we choose a stably stratified case with wind speeds near rated wind speed and wind directions aligned along the longest axis of the proposed Vineyard Wind lease area. We carry out Weather Research and Forecasting (WRF) model simulations with and without turbines (Fitch et al. 2012) to quantify the wake effect, using vertical resolution sufficient to resolve the turbine rotor region and the region beneath the 12 MW turbines (Tomaszewski & Lundquist 2020). When the entire region is built out with turbines (Figure 1), wakes reduce the power production of a single wind farm within the cluster by 10% over this two-day period. As seen in Figure 2, when wind speeds are below rated, the wake effects from the larger group of wind farms undermines the power production at Vineyard Wind. But when wind speeds exceed the rated wind speed, between 11 July 1800 and 12 July 0800, the wake effects exert no impact on the power production at Vineyard Wind.

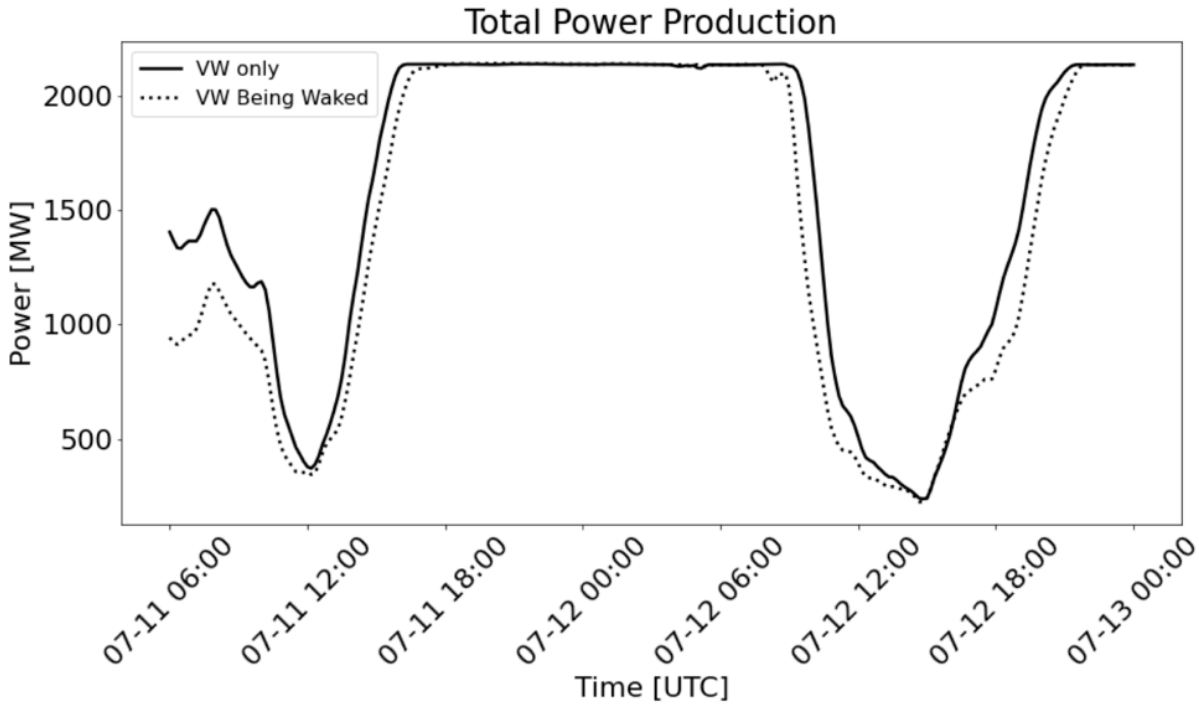


Figure 2: Power production over a two-day period. The solid line depicts the power production of the Vineyard Wind (VW) wind farm by itself. The dotted line depicts the reduced power production of VW in the presence of wakes from neighboring wind farms.

This presentation will share results from year-long simulations that are now in production. A wider temporal range of data provides the means to assess the overall wind resource in the mid-Atlantic in addition to quantification of power output to the electrical grid during peak energy demand times.

We anticipate that the yearly averaged power deficit will be less than 10% due to the inclusion of periods of unstable stratification that occur throughout the year, making offshore wind a viable option for meeting coastal energy needs. We will quantify how simulated wakes vary by atmospheric stability, wind speed, wind direction, and surface-forcing from sea-surface temperature datasets.

Finally, we also explore the impact of the turbine-added turbulent kinetic energy (TKE) in these simulations. The current WRF wind farm parameterization may introduce too much TKE (Vanderwende et al. 2016, Siedersleben et al. 2020, Archer et al. 2020). To evaluate uncertainty in the impacts of wakes on a wind farm within a cluster, we employ a range of wind farm-generated TKE options to quantify the interaction of turbine-generated TKE with meteorology to define wind farm wakes.

References:

Archer C. L., Wu S., Ma Y., Jiminez P. (2020). 'Two corrections for turbulent kinetic energy generated by wind farms in the WRF model'. Monthly weather review. 148(12).

Bodini N., Lundquist J. K., Kirincich A. (2019). 'U.S. east coast lidar measurements show offshore wind turbines will encounter very low atmospheric turbulence'. Geophysical research letters. 46(10).

Fitch A. C., Olson J. B., Lundquist J. K., Dudhia J., Gupta A. K., Michalakes J., Barstad I. (2012). 'Local and Mesoscale Impacts of Wind Farms as Parameterized in a Mesoscale NWP Model'. Monthly weather review. 140(9).

Nygaard N. (2014). 'Wakes in very large wind farms and the effect of neighboring wind farms'. Journal of physics. 524.

Siedersleben S. K., Platis A., Lundquist J. K., Djath B., Lampert A., Barfuss K., Canadillas B., Schulz-Stellenfleth J., Bange J., Neumann T., Emeis S. (2020). 'Turbulent kinetic energy over large offshore wind farms observed and simulated by the mesoscale model WRF'. Geoscientific Model Development. 13(1).

Tomaszewski J., Lundquist J. K. (2020). 'Simulated wind farm wake sensitivity to configuration choices in the Weather Research and Forecasting model version 3.8.1'. Geoscientific model development. 13(6).

Vanderwende B., Kosovic B., Lundquist J. K., Mirocha J. D. (2016). 'Simulating effects of a wind-turbine array using LES and RANS'. Journal of advances in modeling earth systems. 8(3).

How atmospheric pressure gradients and Coriolis forces control the power density of large wind farms

Enrico Antonini*, and Ken Caldeira
Carnegie Institution for Science
*Presenting author

Keywords: Turbine-atmosphere interaction | Power density | Geophysical limits | Coriolis force | Atmospheric pressure gradient

Wind energy has been one of the fastest growing renewable energy technologies, driven by demand for low or net-zero emission energy systems, increasing government support, and public receptiveness. The worldwide share of electricity generated from wind in 2019 amounted to just 5.3%, but its growth has been exponential over the past decades and some current projections see wind energy's share reaching one-quarter to one-third globally by 2050. In such scenarios, wind farms are expected to increase both in number and spatial scale.
When wind turbines are arranged in clusters, their performance is mutually affected, and their energy generation is reduced relative to what it would be if they were widely separated.
Understanding the physics regulating the performance of large-scale wind farms is one of the current challenges in wind energy science. For such large systems, the extraction of energy from the atmosphere is limited by the potential energy availability and replenishment rate to the turbines.
Observations and numerical simulations have indicated an upper bound to the power density in the order of 1 W/m2. However, for spatial scales for which the Coriolis force, pressure-gradient force, and other larger-scale atmospheric physics are important, no theoretical foundation has yet been provided.

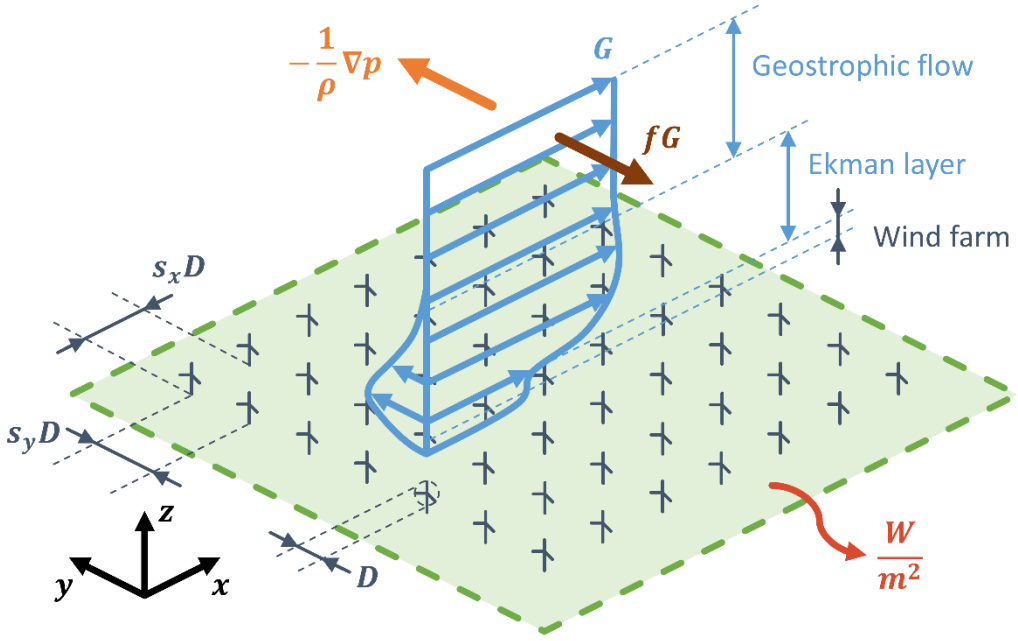


Figure 1: An illustration of the fundamental phenomena and parameters that govern the energy extraction of large-scale wind farms. The geostrophic wind, G, is the result of the balance between the pressure-gradient force, – 1/ρp, and the Coriolis force, fG, where f is the Coriolis parameter. Wind turbines of diameter D are arranged on a regular grid with horizontal spacings of dimensions sxD and syD.

Here [1], we study the role of atmospheric pressure gradients and the latitude-dependent Coriolis parameter on the power density of large-scale wind farms by means of both numerical atmospheric simulations and an analytical framework. We consider a representative, idealized scenario in which a wind farm extends infinitely (see attached figure) to understand the primary mechanisms of energy extraction. This configuration has been

used to study such large systems because it enables focusing only on the vertical transport of momentum and kinetic energy, underlying a statistical horizontal homogeneity and negligible horizontal fluxes. The atmospheric simulations are conducted with the Weather Research and Forecasting (WRF) model, where the wind turbines are parametrized as sinks of momentum and sources of turbulence kinetic energy in a doubly periodic, limited computational domain. The analytic framework combines governing equations from atmospheric fluid dynamics (particularly, the Ekman layer equations) and wind farm fluid dynamics to give a closed-form relation that ultimately can be used to estimate the power density of large-scale wind farms.
We illustrate that energy transport to regional-scale wind farms is primarily governed by horizontal pressure gradients and their interaction with the Coriolis force and turbine-induced surface drag within the latitude-dependent Ekman layer. The energy is supplied by the pressure-gradient force within the Ekman layer and transported downward to the turbines; it does not originate from the overlying free troposphere (above the planetary boundary layer) as previously suggested. We show that regions with higher horizontal pressure gradients have a higher energy availability and, consequently, higher energy generation per unit surface area. We also show that, for the same horizontal pressure gradient, the power density is higher in lower latitudes, suggesting that the replenishment rate of kinetic energy depends also on the degree to which the pressure-gradient force is opposed by the Coriolis force.

References:
[1] Antonini, E.G.A. and Caldeira, K. (2021). Atmospheric pressure gradients and Coriolis forces provide geophysical limits to power density of large wind farms. Applied Energy, 281, 116048.

Analysis of a wind farm with a hybrid (aligned-random) pattern using the Area Localized Coupled (ALC) model

Genevieve M. Starke[1,*], Charles Meneveau[1], Jennifer King[2], and Dennice Gayme[1]
[1]Johns Hopkins University
[2]National Renewable Energy Laboratory
*Presenting author

Keywords: coupled model | power prediction | top-down model | wake model

Accurate predictions of the power produced by a given wind farm are essential to increasing the percentage of electrical demand served by wind sources. These predictions are usually accomplished through low-order wake models. However, the development and validation of such models have usually focused on regularly arrayed wind turbine placements, and they are typically not directly applicable to wind farms with irregularly placed turbines. The Area Localized Coupled (ALC) model overcomes this limitation through coupling a localized large-scale (top-down) model with a wake model (bottom-up) to consider additional flow physics. The "top-down" model is on the atmospheric scale and describes the interaction of the wind farm with the atmospheric boundary layer (ABL) (Frandsen et al, 2006; Calaf, Meneveau and Meyers, 2010). Our implementation includes a developing internal boundary layer formulation (Meneveau, 2012) implemented in local regions reaching each turbine. The localization is achieved using Voronoi tessellation (Shapiro, 2019) to define areas that "belong" to each turbine. The internal boundary layer development depends on a roughness length expressed in terms of a planform thrust coefficient which represents the total momentum extraction upstream of each turbine. For the bottom-up portion of the model, we use a wake model defined in Shapiro (2019), featuring a wake velocity defect profile that initializes as a top-hat profile at the rotor and transitions to a Gaussian profile as it moves downstream, as shown in Figure 1 (left panel). It also uses a linear superposition of velocity deficits for interacting wakes. The downstream evolution of the wake is modeled using a wake expansion coefficient, taken to be the ratio between the friction and freestream velocities, multiplied by a free dimensionless parameter.

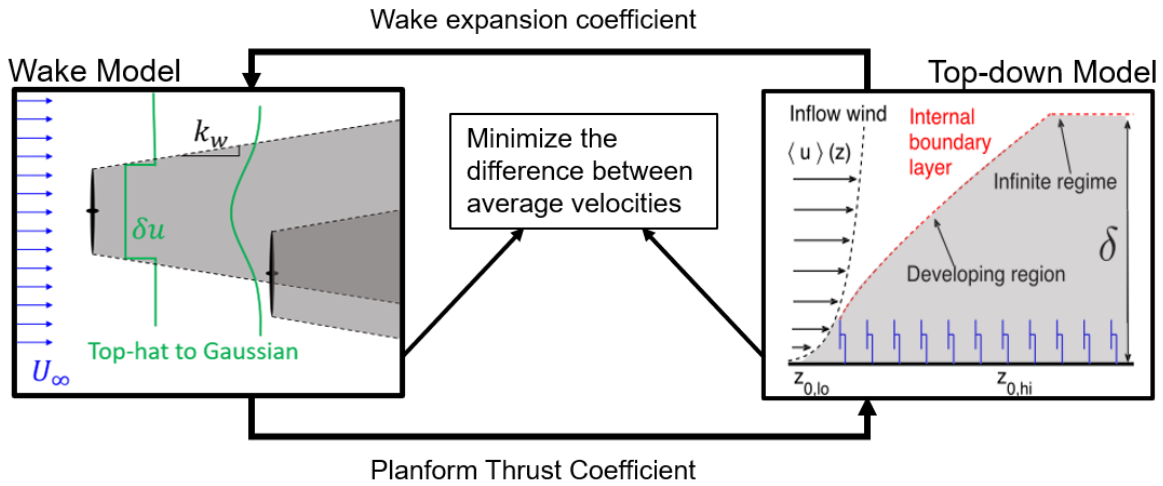


Figure 1: A schematic representation of the ALC model, where the wake model informs the top-down model through the planform thrust coefficient, and the top-down model informs the wake model through the wake expansion coefficient. The free parameter is set by minimizing the sum of the squares difference between the average hub-height velocities given by each model.

This model parameter is determined by minimizing the mean square difference between the hubheight velocity predictions from the wake and top-down portions of the ALC model. The optimization is performed by iterating between the two models, as shown in Figure 1, providing the coupling between the two constitutive parts of the ALC model. The final output is the wake model calculated using the optimized wake

expansion coefficient. The localization, computation of the planform thrust coefficient, velocity deficit evolution in the wake model and use of varying velocity inflow conditions across the farm inlet enable this model to be applied to arbitrary wind turbine configurations. The approach also provides more information about the flow than conventional wake models, such as the local friction velocity, which can be used as a local surrogate for turbulence intensity.

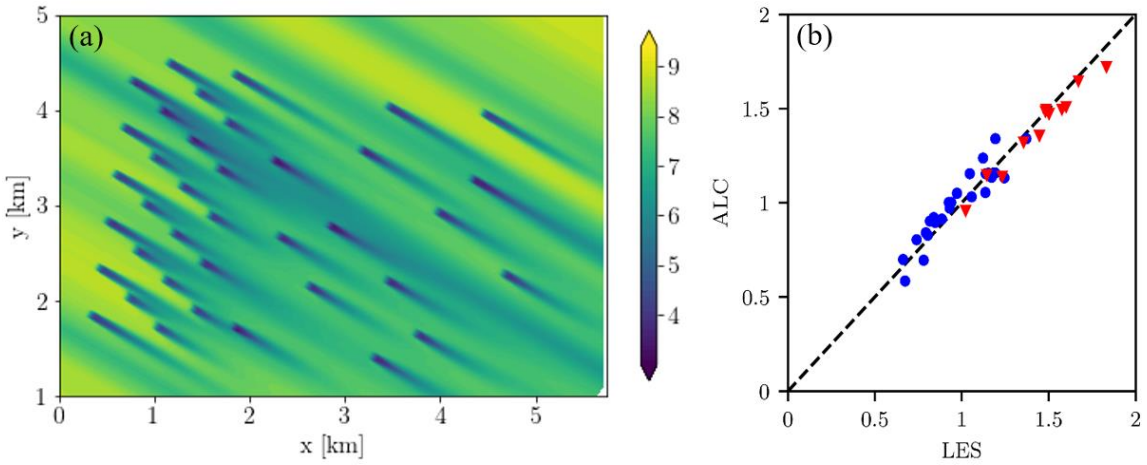


Figure 2: This figure shows (a) the results from the ALC model for the hybrid wind farm at an inflow angle of 290 degrees (where 270 degrees is left-to-right), and (b) the turbine-specific comparison of the power from the ALC model for an inflow direction of 270 degrees taken from Starke (2020).

In this study, the ALC model is applied to the Horns Rev wind farm and a hybrid aligned-random wind farm. The hybrid aligned-random wind farm is a good test case due to the range of turbine configurations including one portion of turbines in a regular array and another portion of the wind farm randomly arranged. Figure 2a provides an example result of the average velocity field produced from the ALC model at an inflow direction of 290 degrees. Figure 2b shows the individual power generated at each turbine as predicted from the ALC model compared with large eddy simulation for a representative case of 270 degrees (Starke et al., 2020). Results for additional wind directions along with detailed analysis of trends in the wake expansion coefficient and turbulence properties across the farm for different inflow directions will be discussed during the presentation.

References:

Calaf, M., Meneveau, C. and Meyers, J. (2010) "Large eddy simulation study of fully developed wind-turbine array boundary layers", Physics of Fluids, 22.

Frandsen, S., Barthelmie, R., Pryor, S., Rathmann, O., Larsen, S., Højstrup, J. and Thøgersen, M. (2006) "Analytical modelling of wind speed deficit in large offshore wind farms", Wind Energy, 9, p39-53.

Meneveau, C. (2012) "The top-down model of wind farm boundary layers and its applications", Journal of Turbulence, 13(N7).

Shapiro C.R., Starke, G.M., Gayme, D.F. and Meneveau, C. (2019) "A wake modeling paradigm for wind farm design and control", Energies, 12.

Starke, G.M, Meneveau, C., King, J.R. and Gayme, D.F., (2020) "The Area Localized Coupled model for analytical mean flow prediction in arbitrary wind farm geometries", Arxiv preprint.

Evaluation on the predictive capability of actuator disk model in simulating wakes of turbines of different designs

Guodan Dong*, Xiaolei Yang, and Zhaobin Li
Institute of Mechanics, Chinese Academy of Sciences
*Presenting author

Keywords: actuator disk model | actuator surface model | wind turbine wakes

The commitment of countries to become carbon neural in the next few decades calls for increasing research efforts to reduce the levelized cost of wind energy because of its renewability and sustainability [1]. In wind turbine and wind farm simulations, the actuator disk (AD), actuator line (AL) and actuator surface (AS) models are commonly used to parameterize the interaction between the incoming flow and turbine blades instead of solving the boundary layer around turbine blades [2].
The AD model neglects the geometry of the rotating blade and represents it as a fixed circular permeable disk. The AS model considers the turbine blades geometry and represents the turbine blades as finite number of two dimensional surfaces. These surfaces are formed by the foil chords at different radial positions [3]. In this work, we evaluate the capability of the AD model in predicting wakes of two different utility-scale wind turbines, i.e. the EOLOS 2.5 MW wind turbine at University of Minnesota and the NREL 5 MW wind turbine, by comparing the predictions from large-eddy simulations with the AD model with those from the AS model. In both AD and AS simulations, an actuator surface model for nacelle is employed. To make the comparison fair, the forces exerted on the AD are provided by the corresponding AS simulation. Two types of AD models are considered, i.e. with/without the tangential force denoted as AD-R and AD-NR, respectively.

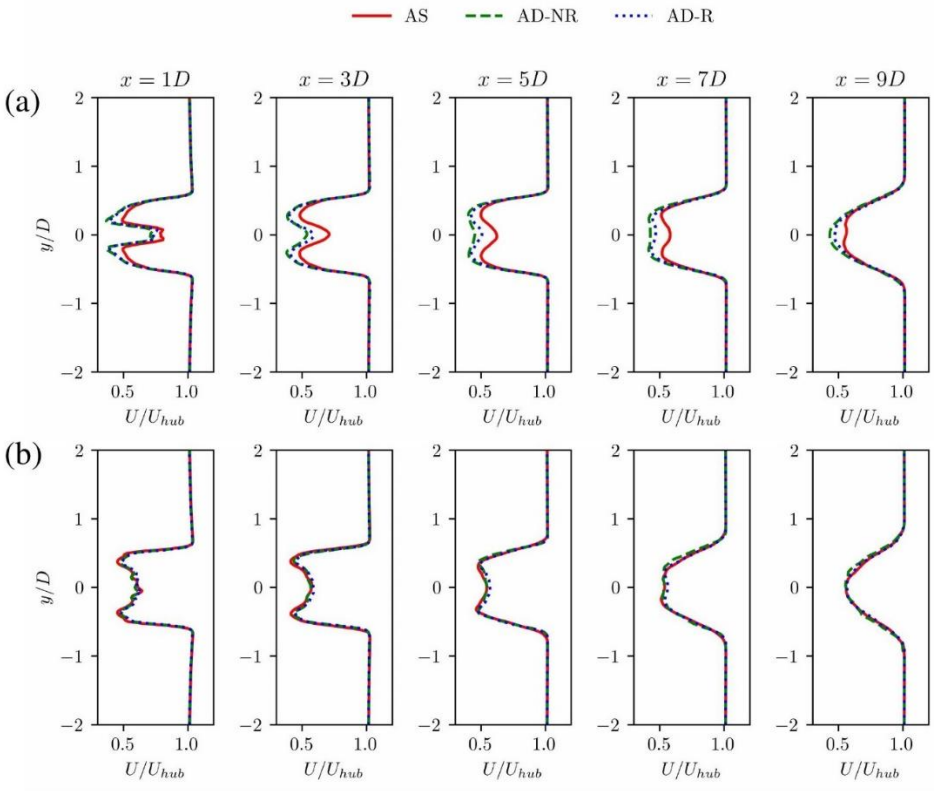


Figure 1: The time-averaged streamwise velocity (U) profiles in the horizontal x-y plane at different turbine downstream positions for (a) the EOLOS turbine and (b) the NREL turbine.

The comparisons show that the AD model has different performance in simulating different wind turbines. Specifically, AD predictions of the NREL turbine agree well with the AS predictions. For the EOLOS turbine, on

the other hand, significant differences are observed for both time-averaged velocity profiles and turbulent kinetic energy profiles. An example of the comparison is shown in Figure 1 for the time-averaged streamwise velocity (U) profiles for both EOLOS and NREL turbines. It can be seen that streamwise velocity profiles of the EOLOS turbine computed by the AD model over predict the velocity deficit when compared with the results of the AS model. Specifically, at $x < 7D$ turbine downstream positions, large discrepancies are observed near the blade tip and rotor center. At $x = 9D$ turbine downstream position, the discrepancy mainly appears near center of the rotor. For the NREL turbine, from near wake to far wake, the streamwise velocity profiles computed by the AD model are in good agreement with those predicted by the AS model. For both EOLOS and NREL turbines, taking into account the rotational effect does not significantly affect the simulations results. Systematic comparisons of the AD results with the AS results and discussions on the possible reason causing the different predictive capability for different turbine designs will be presented in the conference.

References:

Meneveau, C., 2019. Big wind power: Seven questions for turbulence research. Journal of Turbulence, 20(1), pp.2-20.
Yang, X. and Sotiropoulos, F., 2018. A new class of actuator surface models for wind turbines. Wind Energy, 21(5), pp.285- 302.
Li, Z. and Yang, X., 2020. Evaluation of Actuator Disk Model Relative to Actuator Surface Model for Predicting Utility-Scale Wind Turbine Wakes. Energies, 13(14), p.3574.

Effects of vertical shear on the wake centerline deflection behind a non-yawed wind turbine

Zhaobin LI*, Guodan Dong, and Xiaolei Yang
Institute of Mechanics, Chinese Academy of Sciences
*Presenting author

Keywords: wind turbine wake | wake deflection | vertical shear

Wind turbine's wake characterized by reduced wind velocity and increased turbulence intensity negatively impact the downwind neighbors. For this reason, accurately predicting the wake centerline position is thus important for estimating the influence of the wake on the downwind turbines. Counterintuitively, the wake centerline is reported to be skewed on one side even when the rotor axis is aligned with the wind direction. Understanding such a deflection is important for defining the wake influencing region and to implement wake steering strategies, e.g., yaw control to deflect the wake to one side to avoid the neighbor turbine. In the literature, the wake deflection behind a non-yawed turbine is attributed to a transverse velocity induced by an imaginary vortex, which is symmetric to the wake rotation with respect to the ground[1][2]. This imaginary vortex theory is based on potential theory and neglects the vertical shear of the incoming flow. However, when vertical shear exists in the inflow, the wake rotation may roll up low velocity wind in the lower layer to one side of the wake and roll down high-speed wind to the other sides, and thus lead to a skewed wake.

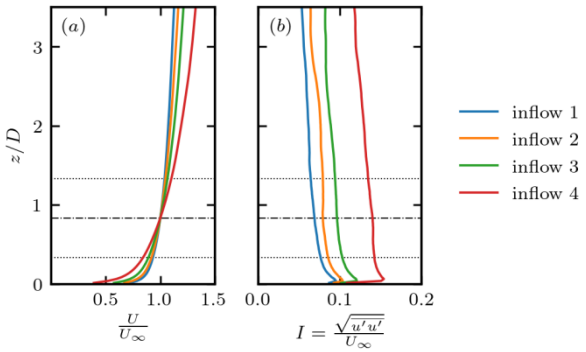


Figure 1: Vertical profile of nflow characteristics: (a) time averaged velocity, (b) turbulence intensity.

In this work, we quantify the effect of inflow vertical shear on the wake behind a non-yawed 2MW Clipper wind turbine with Large Eddy Simulations. In the simulation, the turbine' blade and the nacelle are parametrized with a well validated actuator surface method. As shown in Figure 1, four inflow conditions with increasing vertical shear are employed. All the inflows have the same normalized streamwise velocity at the turbine hub height (illustrated by a point-dashed line). The vertical shear increases from inflow 1 to inflow 4. The inflow turbulence intensity increases from approximately TI = 7% of inflow 1 to TI = 15% of inflow 4. In all the inflow conditions, the turbine operates at a fixed tip speed ratio TSR = 8.

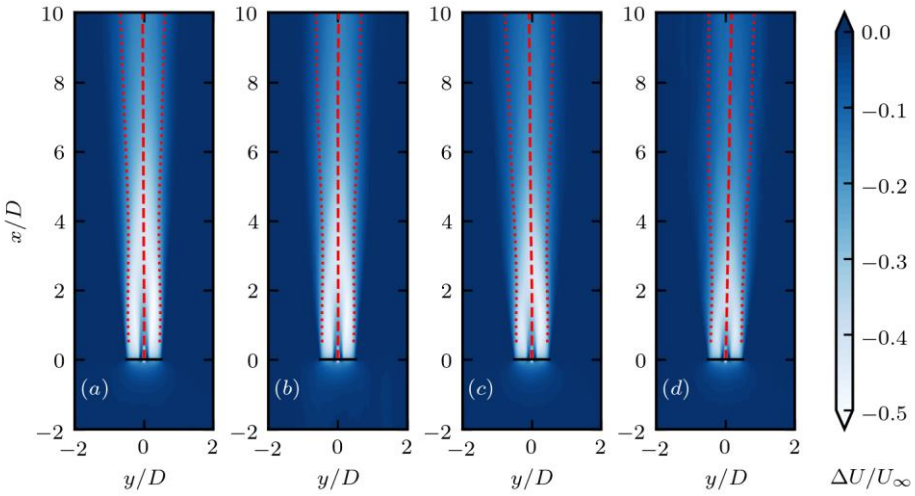


Figure 2: Velocity deficit at the hub height plane. Subplots (a)-(d) correspond to inflows 1-4. The red dashed lines illustrate the wake centerline, and the red dots show the wake width.

Figure 2 shows the time-averaged streamwise velocity at the height of the turbine's hub. Figures 2 (a)-(d) represent the results for inflow 1 to 4, respectively. The results show an interesting phenomenon, i.e., the deflection of the wake center is dependent on the inflow condition. As seen, for inflow 1, 2 and 3, the wake centerline is almost straight, and only the case with inflow 4 induces a wake apparently skewed to the right side. This difference cannot be well explained by the imaginary vortex theory, because this theory would predict the same deflection since the wake rotational velocity is the same in all these cases. Detailed analysis probing into the influence of vertical shear and rotational direction on wake deflection will be presented at the conference to provide a different understanding on this wake deflection phenomenon.

References:
[1] Fleming PA, et al., Evaluating techniques for redirecting turbine wakes using SOWFA, Renewable Energy (2014)
[2] Bastankhah, M., Porté-Agel, F., Experimental and theoretical study of wind turbine wakes in yawed conditions. Journal of Fluid Mechanics (2016)

The "Wake-Diffusion" Rotor: A Wake-Mitigation Concept

Matthew Churchfield[1], Senu Sirnivas[1], and Andreas Knauer[2]
[1]National Renewable Energy Laboratory
[2]Equinor

Keywords: wakes | wake mitigation | wind tunnel experiment | large-eddy simulation

The topic of mitigation of wind farm efficiency losses caused by wind turbine wake effects is vibrant. Much of the recent past work has focused on means to either deflect wakes laterally through intentional yaw misalignment (Fleming et al., 2014) or to decrease the wake momentum deficit through some means of controlling axial induction (Annoni et al., 2015). Additionally, the idea of exciting instability in the wake through blade pitch oscillation to accelerate wake recovery has also been explored (Frederik et al., 2020). Any of these wake mitigation methods accepts the penalty of reducing single wind turbine performance for the gain of increasing collective wind farm energy capture.

In this work, we examine a method for wake mitigation termed the "wake-diffusion" rotor concept developed by Equinor. This method aims to reduce wake losses by using a non-standard radial loading profile of the blades that introduces steeper radial gradients into the streamwise wake flow meant to enhance shear-generated turbulence, and hence, turbulent mixing in the wake. The main ideas is that this turbulent mixing will accelerate the diffusion of the wake momentum deficit with the surrounding, higher speed winds. As with other wake-mitigation methods, the non-standard blade loading profile reduces the energy capture of a single turbine, but the benefit of accelerated wake recover holds promise to boost the collective wind farm efficiency.

The "wake-diffusion" concept has been studied experimentally with a miniature wind turbine in a wind tunnel at the Norwegian University of Science and Technology. In that experiment, wake measurement of two different rotors with non-standard loading profiles, along with a baseline rotor, were performed using hot-wire anemometers and laser-doppler anemometry. In an effort to fill gaps in what could practically be measured during the wind-tunnel measurement campaign, high-fidelity fluid flow simulations of the wind-tunnel experiment were also performed using the high performance computing capabilities at the National Renewable Energy Laboratory and the Simulator for Wind Farm Applications (SOWFA) code. These large-eddy simulations employed actuator line aerodynamics to generate wakes. Contours of the instantaneous wake flow field for both the baseline and a wake-diffusion rotor are shown in Figure 1. The wind tunnel measurements are of high quality and yielded promising mean and turbulent information about increased wake mixing caused by the wake-diffusion rotor. With the large-eddy simulations, additional information, including momentum and turbulent kinetic energy budgets can be computed. It is also relatively easy to vary more parameters and study the effect on downstream turbines using large-eddy simulations.

In this presentation, we will introduce the wake-diffusion rotor concept, present results from the wind-tunnel field campaign, and show information from the large-eddy simulations. and then talk about plans for future studies in which we simulate wake interactions generated by wake-diffusion rotors.

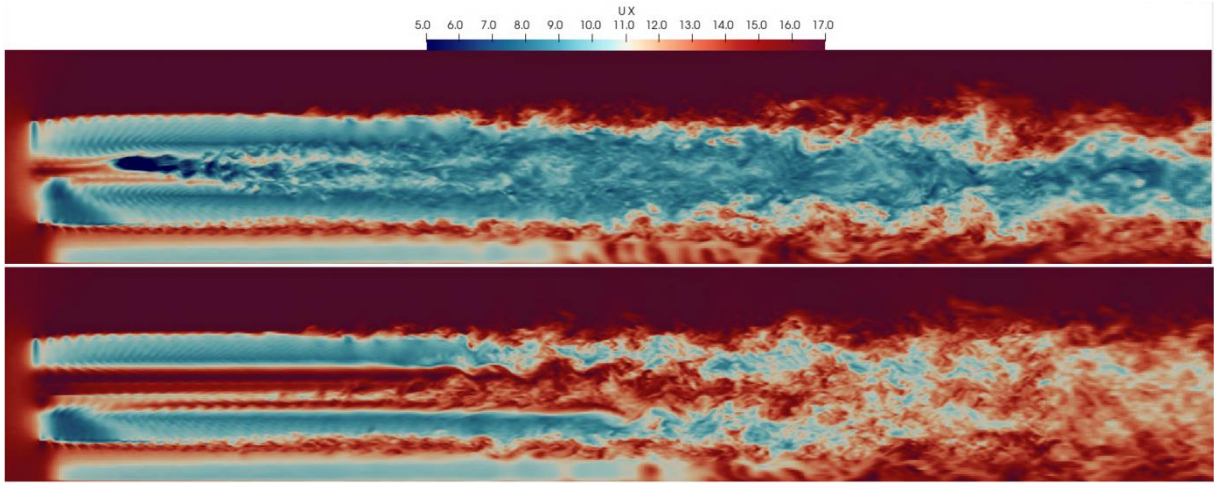


Figure 1: Contours of instantaneous velocity in a vertical cut plane aligned with the flow and passing through the rotor center for the baseline (upper) and wake-diffusion (lower) rotor large-eddy simulations.

References:
Fleming, P., Gebraad, P., Lee, S., van Wingerden, J.-W., Johnson, K., Churchfield, M., Mikalakes, J., Spalart, P., and Moriarty, P., Evaluating Techniques for Redirecting Turbine Wakes using SOWFA, Renewable Energy, 70, pp. 211-218, 2014.
Annoni, J., Gebraad, P., Scholbrock, A., Fleming, P., van Wingerden, J.-W., Analysis of Axial-Induction-Based Wind Plant Control Using an Engineering and a High-Order Wind Plant Model, Wind Energy, 19(6), pp. 1135-1150, 2015.
Frederik, J., Doekemeijer, B., Mulders, S., van Wingerden, J.-W., The Helix Approach: Using Dynamic Individual Pitch Control to Enhance Wake Mixing in Wind Farms, Wind Energy, 23(8), pp. 1739-1751, 2020.

Regular Session: Wind Farm Modeling and Analytical Approaches

Analytical solution for the cumulative wake of wind turbines in wind farms

Majid Bastankhah[1], Bridget L. Welch[1], Luis A. Martínez-Tossas[2], Jennifer King[2], and Paul Fleming[2]
[1]Durham University
[2]National Renewable Energy Laboratory

Keywords: wake superposition | wind farm flows | analytical wake model

Engineering (i.e., control-oriented) wake models are arguably still the most popular tools in the wind energy industry for the design and active control of wind farms due to their simplicity and low computational cost (Stevens and Meneveau 2017, Porte-Agel et al. 2020). The main aim of this paper is to address the puzzling question of "how should one estimate cumulative wake effects in wind farms based on engineering wake models?", given the abundance of wake superposition methods in the literature. This aim is achieved by directly solving flow governing equations for a turbine that experiences upwind turbine wakes. The developed model can therefore predict the flow distribution in a wind farm without the need for any specific superposition method. The LES data for wind farms with different number of rows are used to perform a budget analysis of the integral form of the mass and momentum equations for turbine wakes in wind farms. Results show that there are important non-negligible terms (e.g., pressure and Reynolds normal and shear stress terms) other than the momentum deficit and thrust force in this equation. However, the so-called conservation of momentum deficit (i.e., the equality of the momentum deficit term and thrust force) seems to be fairly valid in the far wake, at least for a moderately sized wind farm. A modified version of the conservation of momentum deficit is also introduced in an attempt to provide slightly better results at short downwind distances as well as in the far wake of turbines deep inside a wind farm.
Performing LES with and without the presence of turbines allows us to properly examine some model assumptions. The data for both full-wake and partial-wake conditions show that wake velocity-deficit profiles are self-similar if they are defined with respect to the wind flow at the same position but in the absence of the turbine. While a Gaussian profile can successfully represent the self-similar profile of the wake at the centre, it falls short in capturing the flow speed-up at wake edges. This results in an underprediction of efficiency for certain turbines in primary rows that experience flow speed-up between adjacent columns.
To quantify the wind farm flow distribution using this analytical model, the only necessary empirical input is the wake recovery rate. Provided that this is properly estimated for turbines within wind farms, our results show, overall, that the proposed model is able to provide acceptable predictions.

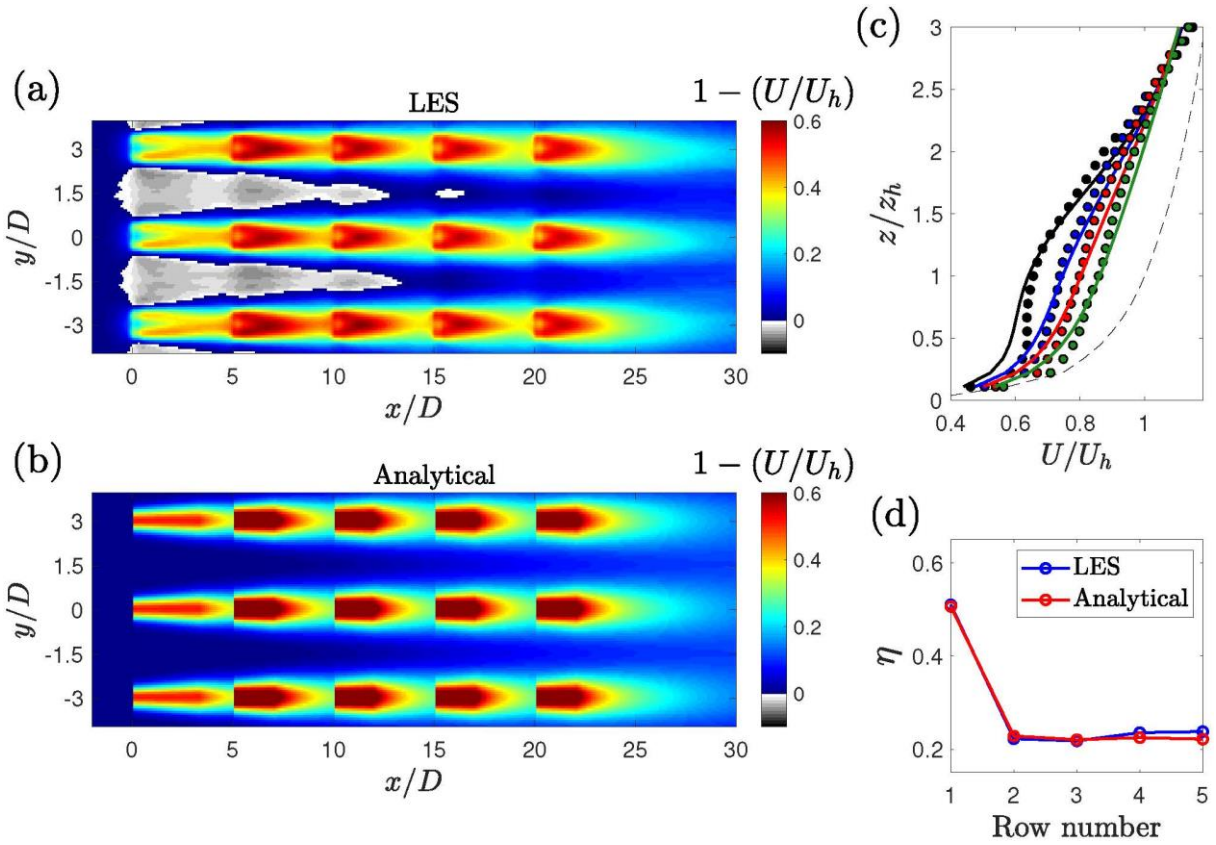


Figure 1: Contours of normalised velocity deficit based on (a) LES and (b) analytical model. (c) Vertical profiles of the normalised streamwise velocity based on the LES (circles), and the analytical model (solid lines) downwind of the middle turbine in the fifth row: 4D (black), 6D (blue), 8D (red), and 12D (green). (d) Efficiency of turbines in the middle column.

Model predictions in comparison with the LES data are shown in figure 1 for an aligned wind farm. According to this new model, the wake velocity deficit associated with each turbine depends on a coefficient, which is a function of turbine configuration as well as inflow conditions. This coefficient, obtained analytically, functions similarly to empirical models (e.g., the `mosaic-tile' approach) that aim to quantify the net contribution of overlapping wakes.

The validity of the common single turbine wake (STW) superposition models is also analysed in this study. It is shown that common superposition models can be derived by making approximations to the analytical wind farm flow solution presented in this work. Detailed discussion on the model derivation and comparison of results with the LES data can be found in Bastankhah et al. (2021).

References:

Bastankhah, M., Welch, B.L., Martínez-Tossas, L.A., King, J. and Fleming, P., 2021. Analytical solution for the cumulative wake of wind turbines in wind farms. Journal of Fluid Mechanics (in press).

Porté-Agel, F., Bastankhah, M. and Shamsoddin, S., 2020. Wind-turbine and wind-farm flows: a review. Boundary-Layer Meteorology, 174(1), pp.1-59.

Stevens, R.J. and Meneveau, C., 2017. Flow structure and turbulence in wind farms. Annual review of fluid mechanics, 49.

Understanding the wake of floating wind turbines with high-fidelity wind tunnel experiments

Alessandro Fontanella*, Alberto Zasso, and Marco Belloli
Politecnico di Milano
*Presenting author

Keywords: Wake | Wind tunnel experiments | PIV | Floating offshore wind

Introduction

The first floating farms are starting to produce power, and many others are under development. With a growing interest in floating farms, understanding and modeling the wake interaction is of utmost importance [1].

The large-scale low-frequency motion of the wind turbine rotor, allowed by the floating foundation, has significant effects on the wind turbine wake, and hence on the wake-interaction for the downstream units.

The main objective of this work is to use high-fidelity wind tunnel experiments to get a deeper understanding of the effect the fore-aft motion of the rotor associated with the rigid-body motion of the floating platform has on the wind turbine wake.

Then, this knowledge can be leveraged to develop an engineering model of the wake of a floating wind turbine.

Methodology

Wind tunnel experiments were performed in the EU H2020 LIFES50+ [2] and EU-EERA/IRPWIND UNAFLOW [3] projects.

The experiments utilized a 1/75 scale model of the DTU 10MW reference wind turbine [4]. The rotor was designed based on the performance-scaling approach [5, 6] to have a realistic thrust force coefficient.

The wave-induced rigid-body motion of the floating platform was simulated imposing a monoharmonic surge translation to the wind turbine model. Amplitude and frequencies were selected to represent the response of the platform modes.

The experiments considered three wind turbine operating conditions, and a steady-uniform wind field.

The wind turbine near-wake (2.3D) was scanned with hot-wire anemometers to measure the three component velocity at hub-height, along the cross-wind direction.

In addition, a PIV system was utilized to investigate the tip-vortex, scanning the region of the wake closer to the rotor.

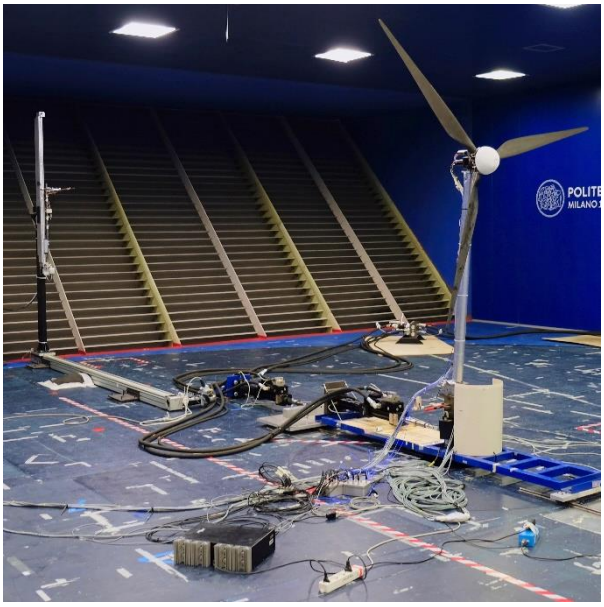


Figure 1: Test setup for hot-wire measurements

Results

Hot-wire measurements give an insight of the wake shape, and the mean wake deficit does not show any significant alteration because of the surge motion. Despite off the different experimental setup, that utilized a porous disk, this agrees with [7].

The spectral analysis of the velocity measurements, shown in Fig. 2, shows the presence of a pronounced harmonic component at the surge-motion frequency. The spectrum with motion is similar to the spectrum of the corresponding case with no motion (steady), except for a peak at the surge frequency, that demonstrates some energy of the surge motion is transferred in the wake.

The surge motion also amplifies the 1P harmonic and the amplification depends on the operating condition.

The focus of PIV measurements is the blade-tip vortex, since it holds most of the wake energy. The position of the tip-vortices is modified by the presence of the surge motion, and it varies periodically with the motion frequency.

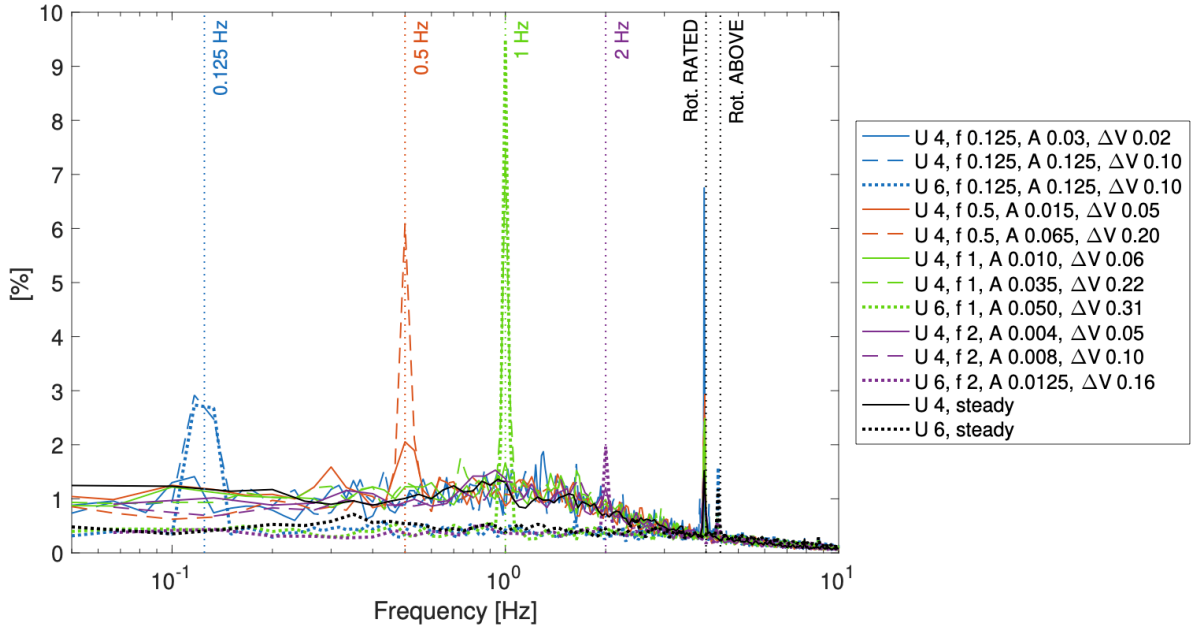


Figure 2: Spectra of the hub-height axial velocity component in the wind turbine wake at 2.3D downstream. The vertical lines show the frequency of surge motion and the rotor frequency. In the legend: U is the mean wind speed, f the surge frequency, A the surge amplitude, DeltaV the maximum surge velocity.

When the rotor moves with a downwind velocity the tip vortices are released with a lower velocity than in the stationary case, and travel a lower distance in the wake. The opposite is true when the rotor moves with an upwind velocity. This mechanism explains the increase of the surge-frequency energy content of the wake seen in hot-wire measurements.

Conclusion

Advanced wind tunnel measurements show that the surge motion has a weak influence on the average shape of the wake, but it effects in a significant way the blade-tip vortex shedding mechanism, increasing the energy of the wake at the frequency of motion.

This effect should be considered in any engineering wake model for floating wind turbines, as well as for the design of floating farm control strategies.

References:

[1] Adam S. Wise and Erin E. Bachynski. Wake meandering effects on floating wind turbines. Wind Energy, 23(5):1266–1285, 2020.

[2] I. Bayati, M. Belloli, L. Bernini, and A. Zasso. Wind tunnel validation of aerodyn within lifes50+ project: Imposed surge and pitch tests. volume 753, 2016.

[3] I. Bayati, M. Belloli, L. Bernini, D.M. Boldrin, K. Boorsma, M. Caboni, M. Cormier, R. Mikkelsen, T. Lutz, and A. Zasso. Unaflow project: Unsteady aerodynamics of floating wind turbines. volume 1037, 2018.

[4] C. Bak, F. Zahle, R. Bitsche, K. Taeseong, A. Yde, L. C. Henriksen, M. H. Hansen, J. P. A. A. Jose, M. Gaunaa, and A. Natarajan. The DTU 10-MW Reference Wind Turbine. DTU Wind Energy Report, 2013.

[5] H. R. Martin, R. W. Kimball, A. M. Viselli, and A. J. Goupee. Methodology for Wind/Wave Basin Testing of Floating Offshore Wind Turbines. Journal of Offshore Mechanics and Arctic Engineering, 136(2), 2014.
[6] Ilmas Bayati, Marco Belloli, Luca Bernini, and Alberto Zasso. Aerodynamic design methodol- ogy for wind tunnel tests of wind turbine rotors. Journal of Wind Engineering and Industrial Aerodynamics, 167:217 – 227, 2017.
[7] Benyamin Schliffke, Sandrine Aubrun, and Boris Conan. Wind tunnel study of a "floating" 3 [%] 0.125 Hz 0.5 Hz Rot. RATED Rot. ABOVE 1 Hz 2 Hz wind turbine's wake in an atmospheric boundary layer with imposed characteristic surge motion. Journal of Physics: Conference Series, 1618:062015, sep 2020.

A global blockage model for wind farm development

Jesper Grønnegaard Pedersen*, and Nicolai Gayle Nygaard
Ørsted
*Presenting author

Keywords: Global blockage | Model validation | Engineering model | Wind farm induction

In recent years, wind farm induction, also known as global blockage, has received increased attention; mainly as a possible source of error in wind farm energy yield assessment. There is a growing consensus that failing to account for global blockage will lead to an overestimation of the annual energy production (AEP). Here, we define global blockage as the wind speed reduction upstream of a wind farm and possible speed-up effects within and on the sides of the wind farm caused by the wind farm itself.
Global blockage effects are typically small compared to other flow effects such as wakes from neighbouring wind farms, coastal wind speed gradients, and other naturally occurring variations in the freestream wind. However, recent studies based on measurements (Bleeg et al, 2018; Schneemann et al, 2020) show compelling evidence that an operating wind farm will indeed cause a significant upstream reduction in wind speed, particularly under stable atmospheric stratification and when the turbines are operating near the maximum of their thrust curve. Similar conclusions can be drawn from computational fluid dynamics (CFD) studies of wind farm flows (Bleeg et al, 2018; Forsting et al, 2017) which also show evidence of speed-up effects.
Wind farm development requires fast AEP calculations including losses due to turbine interaction effects. At present, CFD simulations are still too computationally expensive to be used for e.g. day-today layout optimization, and accurate engineering-type flow models are needed. Wake modelling has historically received a great deal of attention, but only in recent years have we seen a similar focus on modelling of global blockage (Branlard et al, 2020; Nygaard et al, 2020). While the induction of a single turbine is relatively well understood and models describing the phenomenon can be found in the literature (e.g. Medici et al, 2011), the combined induction of multiple turbines (i.e. global blockage) needs further investigation and the existing models need validation against measurements.
In this presentation, we introduce a newly developed global blockage model and show how model results compare to SCADA data from operating wind farms. The new model is an extension of work done by Gribben and Hawkes of Frazer-Nash Consultancy as part of the Offshore Wind Accelerator programme. It is based on the potential flow around a Rankine half-body and 1-D momentum theory.

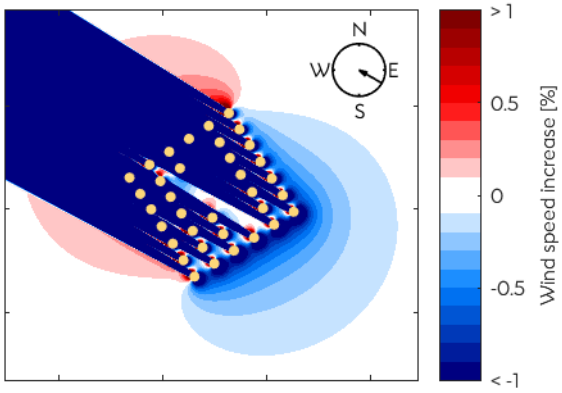


Figure 1: An example of the output from the newly developed global blockage model coupled with our standard wake model. It shows the predicted change in wind speed at the Westermost Rough wind farm relative to the freestream wind speed of 8 m/s. Each yellow circle represents a turbine position and the wind is from 120 degrees.

An example of the output from the model is shown in Figure 1. A key issue with validation of any global blockage model using SCADA data, is that the freestream wind speed, on which the induction depends, is

typically unknown. We avoid this problem by focusing on the relative variation in wind speed and power generation across front-row turbines. The model is found to predict such variations quite well, but in many cases the flow is dominated by horizontal gradients caused by other phenomena than global blockage. Examples are presented and discussed. Finally, we also describe the coupling between the new global blockage model and existing wake models, and we discuss the possibility of including the height of the atmospheric boundary layer as input to the models.

References:

Bleeg, J., Purcell, M., Ruisi, R., & Traiger, E. (2018). Wind farm blockage and the consequences of neglecting its impact on energy production. Energies, 11(6), 1609.

Branlard, E., Quon, E., Forsting, A. R. M., King, J., & Moriarty, P. (2020). Wind farm blockage effects: comparison of different engineering models. Journal of Physics: Conference Series, 1618(6), 062036.

Forsting, A. R. M., Troldborg, N., & Gaunaa, M. (2017). The flow upstream of a row of aligned wind turbine rotors and its effect on power production. Wind Energy, 20(1), 63-77.

Medici, D., Ivanell, S., Dahlberg, J.-Å., & Alfredsson, P. H. (2011). The upstream flow of a wind turbine: blockage effect. Wind Energy, 14(5), 691-697.

Nygaard, N. G., Steen, S. T., Poulsen, L., & Pedersen, J. G. (2020). Modelling cluster wakes and wind farm blockage. Journal of Physics: Conference Series, 1618(6), 062072.

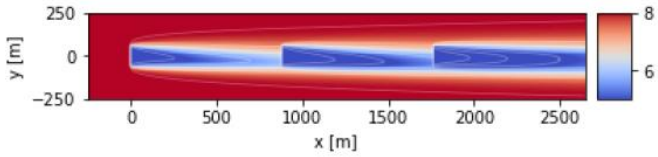
Schneemann, J., Theuer, F., Rott, A., Dörenkämper, M., and Kühn, M. (2020). Offshore wind farm global blockage measured with scanning lidar. Wind Energy Science Discussions, in review.

Vortex displacement in the curled wake model: Implementation and impact evaluation

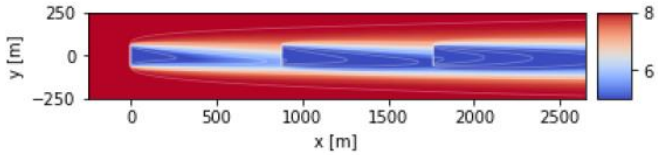
António Narciso[1], and Ricardo Balbino Dos Santos Pereira[2]
[1]Instituto Superior Tecnico
[2]Delft University of Technology

Keywords: Wind Farm Control | Wake Deflection Models | Curled Wake Model | Vortices' Displacement

The continuous development of wind farm control presents itself as an excellent opportunity to increase efficiency and economic viability of wind power plants.
One of the most popular approaches for wind farm control is related with the minimization of turbine's wake losses. This approach can be implemented by changing the direction of the wake using the intentional misalignment of the rotor with respect to the incoming flow, through the manipulation of the yaw angle. By diverting the wake away of the downstream turbines, the wake steering approach promotes the presence of a higher energy content in the incoming flow of those downstream wind turbines, improving their energy output and, ultimately, contributing to a higher energy yield of the entire wind farm.
The success of this strategy is intrinsically related to the ability of the analytical wake models used by the controllers to accurately predict the velocity deficit and the deflection of the wake under each operating condition. Several models, aiming at representing both the wake velocity deficit and the wake deflection, have been developed in the past few years. Some of these models have been used in FLORIS (FLOw Redirection and Induction in Steady-state), which is a software framework consisting in a wind farm analysis and optimization tool, thanks to its ability to predict the steady-state wake locations and flow velocities at each turbine.
This paper seeks to introduce improvements in terms of the wake deflection models present in FLORIS, namely in the curled wake model. The original formulation of this model assumes the existence of a distribution of vortices shed through the wake, which is responsible for influencing both its shape and deflection. The newly proposed model includes an important characteristic of the wake, which is implemented and studied in this work: the possibility of the vortices to move in the direction perpendicular to the incoming flow. The implementation of this new wake feature ensures that the velocity field in the spanwise direction is taken into account, influencing the position of the vortices and, consequently, the behaviour of the wake as a whole.



(a) Curl Model



(b) New Model

Figure 7: Comparison between the curl model and the new model simulations, with the yaw angles $\gamma_{T1} = 25°$, $\gamma_{T2} = 15°$ and $\gamma_{T3} = 0$

Figure 1: Comparison between the Curled Wake Model and the New Model. The New Model predicts lower deflection of the wake under the same yaw conditions, which has an impact in the energy output predictions of the wind farm.

In terms of wake predictions, qualitative effects of the displacement of the wake vortices include a more circular shape of the wake, lower yaw-induced wake deflections and a spanwise velocity field closer to SOWFA predictions, with these characteristics being compared with relevant data and simulations from literature. In addition, the new feature of the wake model has a significant impact in terms of the downstream turbines' power output. A detailed performance study of sets of 3 and 7 turbines disposed in a linear array showed the new model to predict a decrease in the energy output ranging from 2,8% to 16,4%, depending on the specified operating conditions.

References:
C. J. Bay, J. King, P. Fleming, and L. A. Martínez-Tossas. 'Unlocking the Full Potentialof Wake Steering: Implementation and Assessment of a Controls-Oriented Model'. Wind Energy Science Discussions, 2019.
L. A. Martínez-Tossas, J. Annoni, P. Fleming, and M. J. Churchfield. 'The aerodynamics of the curled wake: a simplified model in view of flow control'. Wind Energy Science, 4(1):127–138, 2019

Comparison of analytical wake model predictions with experimental data for a non-uniform porous disc for uniform and non-uniform inflow conditions

Anas Abdulrahim*, Tugrul Akpolat, Mustafa Perçi, and Oguz Uzol
Middle East Technical University
*Presenting author

Keywords: wind turbine wake | porous disc | wake model

Analytical wake models are widely used in the industry due to their reasonably accurate prediction capability at low computational cost. In wind tunnel studies, wind turbine wakes are frequently modeled using porous discs that have uniform or non-uniform radial porosity (e.g. Camp and Cal [2016]). Amiri et al. [2019] compared wake model predictions to measurements for uniform and nonuniform porous discs. They showed that some model predictions agree well with measured wakes.
Recently, we investigated the impact of inflow wind shear on the wake of a 0.12 m diameter nonuniform porous disc by successively immersing it into a boundary layer (Abdulrahim et al [2021]).
Two-Dimensional Particle Image Velocimetry (PIV) measurements were performed on vertical (i.e. along the inflow shear direction) planes downstream of the disc at the disc center plane. It was shown that the wakes get strained and become asymmetric as expected due to the non-uniform inflow. Furthermore, a wake scaling methodology proposed by Chow et al [2005] was implemented to scale these non-uniform asymmetric wakes and it was shown that all data can be collapsed on to a single distribution. This scaling methodology is based on a scaling parameter β, which is the ratio of local shear strain to average shear strain within the wake. This parameter is used to obtain a velocity scale ($U\beta$-U0) and a length scale ($\delta\beta$) for either side of an asymmetric wake (for a uniform inflow the wakes are symmetric and both sides of the wake produce a single streamwise distribution for $U\beta$ and $\delta\beta$).
In this study, we investigate how these wake scaling parameters, $U\beta$ and $\delta\beta$, evolve within the disc wake and compare the experimental results with those obtained from Bastankhah and Porte-Agel [2014] wake model. The comparisons are made first for the flow outside the boundary layer, i.e. uniform inflow. For the cases when the disc is within the boundary layer, we first calculated the downstream wake profiles from the analytical model on horizontal planes with different inflow velocity values matching the local inflow velocity level calculated from the inflow shear. Then, combining the predicted minimum wake velocities on horizontal planes at the disc center, vertical profiles are generated to be compared to the PIV data. These distributions are in turn used to calculate the streamwise variations of $U\beta$ and $\delta\beta$, and results are compared to the ones obtained from porous disc experiments.

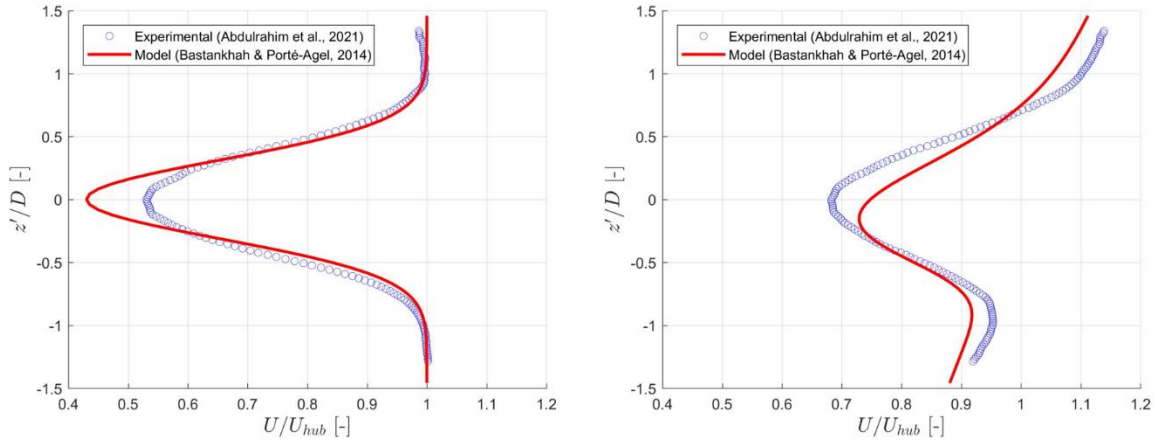


Figure 1: Comparison of predicted and experimental wake velocity profiles four diameters downstream of the disc outside the boundary layer at z/δ=1.17 (left) and within the boundary layer at z/δ=0.32 (right).

Figure 1 shows the comparison of predicted and experimental wake velocity profiles four diameters downstream of the disc outside the boundary layer at z/δ=1.17 (left) and within the boundary layer at z/δ=0.32 (right). The model coefficients are used as suggested in Bastankhah and Porte-Agel [2014] and Niayifar and Porte-Agel [2016]. The profiles are reasonably well predicted and the impact of inflow shear is evident.

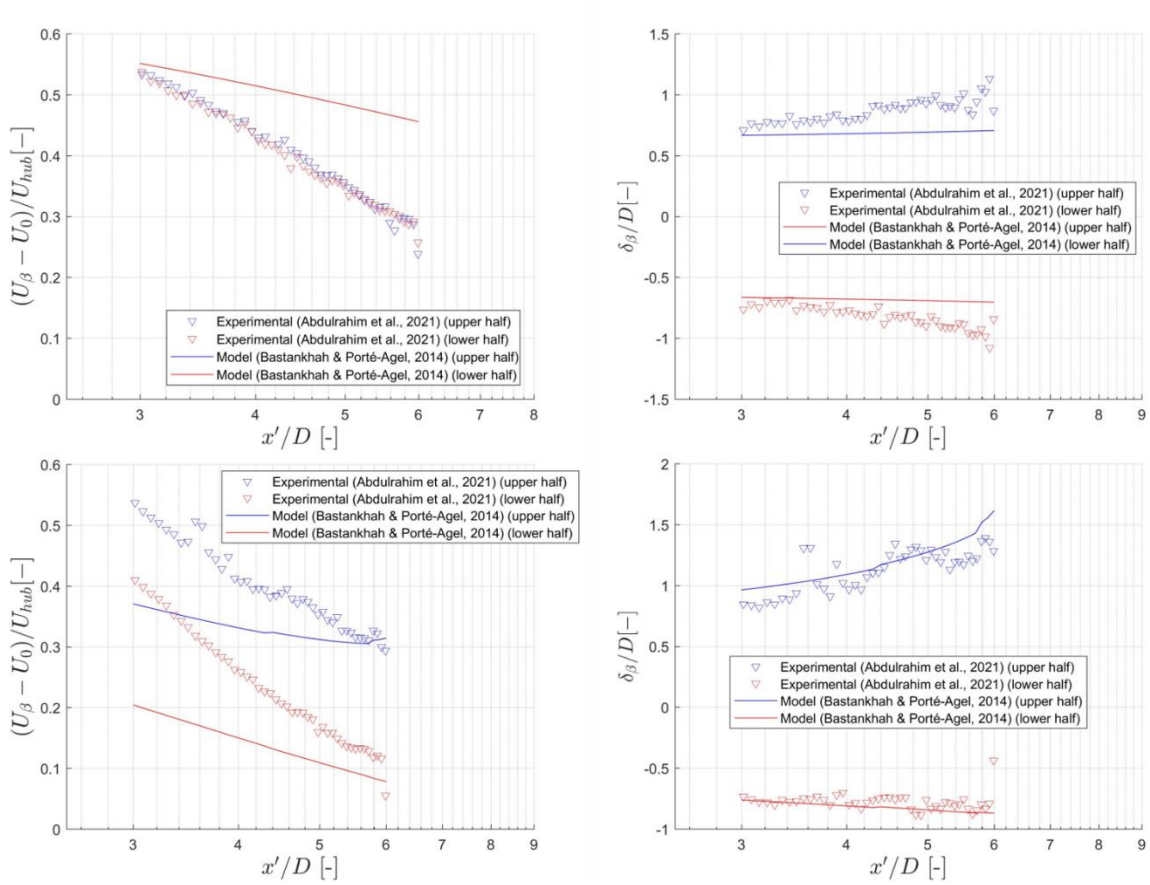


Figure 2: Comparisons of streamwise variations of Uβ and δβ at z/δ=1.17 (top row) and within the boundary layer at z/δ=0.32 (bottom row).

Figure 2 top and bottom rows show the comparisons of streamwise variations of Uβ and δβ at z/δ=1.17 (where the wake is symmetric) and within the boundary layer at z/δ=0.32 (where the wake is asymmetric on the vertical plane as explained before), respectively. As can be seen there are differences between the analytical model and the PIV data for the porous disc especially for Uβ variations both for the uniform and non-uniform inflow cases. More results will be presented in the final presentation and solutions to overcome the observed differences will be proposed.

References:

Camp, E. H., Cal, R. B. "Mean kinetic energy transport and event classification in a model wind turbine array versus an array of porous disks: Energy budget and octant analysis." Phys. Rev. Fluids 1 (2016).

Amiri Hazaveh, H., Bay, A., Aysan, M.S., Yanık, T., Yazdanpanah, M., Yığılı, I., Yağmur, A. S., Perçin, M., Uzol, O., 2019, "Comparison of Wake Models with Porous Disc Wake Profile Measurements", Wind Energy Science Conference (WESC), University College Cork (UCC), Ireland, 17 – 20 June 2019.

Abdulrahim, A., Akpolat, T., Percin, M., Uzol, O., 2021, "Effects of inflow wind-shear on the wake of a radially non-uniform porous disc", Journal of Renewable and Sustainable Energy Special Issue: Wind Tunnel Research, Dynamics, and Scaling for Wind Energy (submitted).

Chow, Y-C., Uzol, O., Katz, J., Meneveau, C., 2005, "Decomposition of the spatially filtered and ensemble averaged kinetic energy, the associated fluxes and scaling trends in a rotor wake." Physics of Fluids 17, 085102.

Bastankhah, M., Porte-Agel, F., 2014, "A new analytical model for wind turbine wakes" Renewable Energy, http://dx.doi.org/10.1016/j.renene.2014.01.002.

Amin Niayifar and Fernando Porté-Agel. Analytical modeling of wind farms: A new approach for power prediction. Energies, 9(9):741, 2016.

A Dynamic Wind Farm Wake Model Implemented in OpenFAST

Ali Raza Ashgar*, Antonio Cioffi, Paolo Schito, and Alberto Zasso
Politecnico di Milano
*Presenting author

Keywords: Wind Farm | Dynamic Wake Model | Wind Model | Wind Tunnel | Wake Model Validation

A very important research topic in the field of wind energy is the optimization of wind farms, in terms of layout and control system, in order to maximize the electrical power produced. In this field, models are needed in order to predict how upstream turbines influence the flow impacting downstream machines and how loads and power production are affected by this phenomenon. At present, the most accurate models used to evaluate flow characteristics in a wind farm are the ones coupling computational fluid dynamics (CFD) with an actuator line model (ALM). Despite being the approach that most closely reproduces reality, it cannot be used for control purposes on real machines as it requires extensive computational power. This is the reason why control-oriented algorithms, that make use of simplified analytical models efficient enough to run in real-time, are used to estimate the generated power and loads acting on the blades with sufficient accuracy.



Figure 1: G1 Turbine in Polimi Wind Tunnel (GVPM)

Among these models, there is the steady flow Gaussian Wake Model (GWM) proposed by Bastankhah and Portè-Agel (2014; 2016). It can be considered a state-of-the-art analytical model since it is able to capture the wake characteristics for a wide range of operating conditions as shown in the work performed by Campagnolo et al. (2019). For a long period of time, the most used tool to develop and analyze control algorithms has been NREL's FLORIS which uses pre- tabulated values of Ct – TSR in order to predict the velocity deficit and orientation of the wake. In Cioffi et al. (2020) the authors proposed a modified version of the GWM; the wake model has been coupled with the aeroservo-elastic wind turbine simulator OpenFAST.

This leads to higher accuracy because the dynamics of the wind turbine is taken into account. The purpose of the present work is to further investigate and improve this GWM model. In the first part of the work an OpenFAST model of a scaled wind turbine will be validated. Within the CL-Windcon project, a large amount of experimental data on a scaled wind turbine (the image below pictures it in GVPM), tested at the Galleria del vento Polimi (GVPM), has been gathered. Experiments have been conducted for both the single turbine case and two turbines in a row configuration. At first, the focus will be on replicating the experimental setup in OpenFAST and compare the results obtained by simulation against the experimental data. The validation will be firstly done on a single turbine working in smooth flow conditions which will be tested for different yaw angles (results of the simulations will be compared with averaged figures extracted from experimental data). Finally turbulence and more than one wind turbines will also be considered. Then, the focus will be shifted on tuning the GWM parameters implemented in OpenFAST by comparing the velocity deficit predicted by the numerical simulation with measurements of the velocity taken with hot-wire measurements downstream of G1 turbines.
Finally, the GWM implemented in OpenFAST will be changed in order to take into account the dynamics of the flow as proposed by Becker (2020). The goal is to obtain a model that is able to take into account spatially and time-wise heterogeneous field conditions, leading to a computationally cheap model that includes the dynamic effects of both the turbine and the flow.

References:

M. Bastankhah and F. Porté-Agel. A new analytical model for wind-turbine wakes. Renewable Energy, 70:116 – 123, 2014. Special issue on aerodynamics of offshore wind energy systems and wakes.
M. Bastankhah and F. Porté-Agel. Experimental and theoretical study of wind tur- bine wakes in yawed conditions. Journal of Fluid Mechanics, 806:506–541, 2016.
M. Becker. Maturing FLORIS towards a dynamics wind farm model. 11 2020. DELFT University of technology.
F. Campagnolo, A. Molder, J. Schreiber, and C. L. Bottasso. Comparison of analytical wake models with wind tunnel data. Journal of Physics: Conference Series, 1256:012006, jul 2019.
A. Cioffi, C. Muscari, P. Schito, and A. Zasso. A Steady-State Wind Farm Wake Model Implemented in OpenFAST. Energies, 13(23):1–1, November 2020.

Regular Session: High-Fidelity Wake Modeling

A model for wind-farm power prediction in presence of meso-scale background gradients

Luca Lanzilao*, and Johan Meyers
Katholieke Universiteit Leuven
*Presenting author

Keywords: Analytical wake model | Wake-merging method | Wakes | Coastal gradient

The different surface roughness and temperature found over land and sea and the flow obstructions caused by orographic obstacles induce heterogeneity in the flow field (Barthelmie et al., 2007). As a consequence, wind farms operate in velocity fields which are rarely uniform. However, a single value of wind speed and turbulence intensity measured several hundreds of meters upstream of the farm are usually the only flow characteristics used by existing wake-merging methods in engineering windfarm wake models. Moreover, the choice of these values impacts the estimation of both wind-farm power and loads. To relax these assumptions, we derive a new wake-merging method capable of superimposing the waked flow on a heterogeneous background velocity field. To compute the waked flow through the farm, we use a recursive formula based on self-similarity in the wake of the turbines for both uni- and multi-directional flow. Moreover, we assume that the axial velocity deficit is transported along the streamlines of the background flow, with no velocity changes in the direction parallel to the turbine rotor. The model's inputs are the background velocity field and the turbulence intensity.
Four different single-wake models, i.e. the Gaussian (Bastankhah and Porté-Agel, 2014), super- Gaussian (Blondel and Cathelain, 2020), double-Gaussian (Schreiber et al, 2020) and Ishihara (Ishihara and Qian, 2018) model, are coupled with two wake-merging methods, i.e. the one proposed by the authors and linear superposition of velocity deficits (Niayifar and Porté-Agel, 2016). Moreover, the standard Jensen model (Jensen, 1983) with quadratic superposition is also included in the analysis. Large-eddy simulations (LES) data, dual-Doppler radar measurements and supervisory control and data acquisition (SCADA) data from the Horns Rev, London Array, and Westermost Rough farm are used to test the nine analytical wind-farm flow models' performance. The data collected at the Horns Rev and London Array farms refer to a single velocity value which is assumed to be constant in and around the farm. In such homogeneous conditions (i.e., the background velocity is not space-dependent), the wind-farm power predictions obtained with the new wake-mergingmethod ar e similar to the ones computed with linear superposition of velocity deficits. On the other hand, the velocity field reconstructed from dual-Doppler radar measurements at the Westermost farm location (Nygaard and Newcombe, 2018) allows us to test the performance of the new model in heterogeneous conditions. The figure attached shows the freestream and waked velocity fields at hub height of this case study, highlighting the different features of the two wake-merging methods.

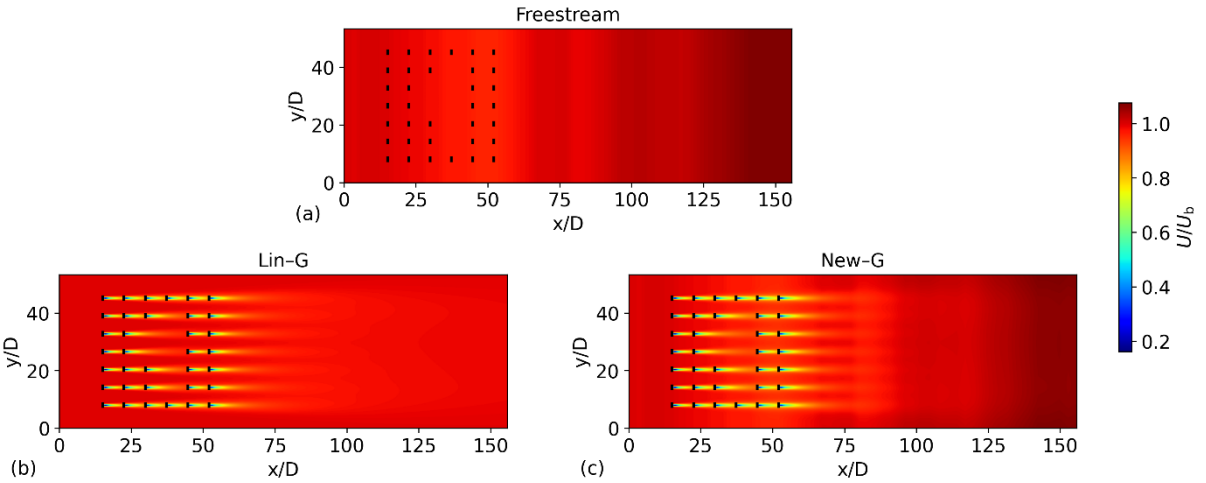


Figure 1: (a) Freestream wind speed and (b,c) velocity field predicted with the linear superposition and the new wakemerging method coupled with the Gaussian wake model, respectively. The black lines denote the wind-turbine rotor locations.

In such conditions, the new superposition method outperforms linear superposition, providing more accurate estimates of wind-farm power extraction. Overall, the most accurate power predictions are obtained when the wake-merging methods are coupled with the double-Gaussian and Gaussian single-wake model. The Ishihara model also shows good agreements with observations. In contrast to this, the Jensen and super-Gaussian wake model underestimate the farm power output for all wind speeds, wind directions and wind farms considered in our analysis.

References:
Barthelmie RJ, Badger J, Pryor SC, Hasager CB, Christiansen MB, Jørgensen BH. (2007). Offshore Coastal Wind Speed Gradients: issues for the design and development of large offshore windfarms. Wind Engng, 31 (6): 369-382.
Bastankhah M, Porté-Agel F. (2014). A new analytical model for wind-turbine wakes. Renew. Energy, 70: 116-123.
Blondel F, Cathelain M. (2020). An alternative form of the super-Gaussian wind turbine wake model. Wind Energy Science.
Schreiber J, Balbaa A, Bottasso CL. (2020). Brief communication: A double-Gaussian wake model. Wind Energy Science, 5: 237-244.
Ishihara T, Qian GW. (2018). A new Gaussian-based analytical wake model for wind turbines considering ambient turbulence intensities and thrust coefficient effects. J. Wind Eng. Ind. Aerod., 177: 275-292.
Niayifar A, Porté-Agel F. Analytical modeling of wind farms: A new approach for power prediction. Energies 2016; 9: 741.
Jensen N. (1983). A Note on Wind Generator Interaction. Technical report Ris-M-2411, Risø National Laboratory: Roskilde, Denmark.
Nygaard NG, Newcombe AC. (2018). Wake behind an offshore wind farm observed with dual-Doppler radars. J. Phys.: Conf. Ser, 1037: 072008.

Large eddy simulations of wind farm cluster wakes

Anja Stieren*, and Richard Stevens
University of Twente
*Presenting author

Keywords: wind farm cluster | wake recovery | wind farm efficiency

Large Eddy Simulations (LES) are frequently used to study the wakes of individual turbines or the interaction of wakes within a wind farm. The benefit of LES is that it provides a realistic representation of spatial and temporal flow structures in the atmospheric boundary layer. Accurately capturing these flow structures is crucial to understand the wake recovery not only behind individual turbines, but also far downstream of a wind farm. Here, we use LES to study the wake recovery behind a large scale wind farm and its influence on a downstream-positioned wind farm.
Understanding the physics in the far wind farm wake and the interaction of wind farms is of significant concern for the successful planning of future wind farm clusters (Canadillas et al. (2020)).
We study the wake of a wind farm consisting of 72 turbines and its influence on an identical wind farm positioned downstream. The layout of the farms is horizontally staggered, and one aligned case is considered to study the effect of the wind farm layout on the cluster wake. Similar to existing farms in the North Sea (Schneemann et al. (2020)), the distance between the farms is varied between 5, 10 and 15 km (see figure 1a). The simulations are performed for neutral atmospheric boundary layer conditions driven by a geostrophic wind. The subgrid-scale turbulent stress is parametrized using the anisotropic minimum dissipation model (Abkar et al. (2016)), while turbine-induced forces are modeled using the actuator-disk approach (Calaf et al. (2010)).

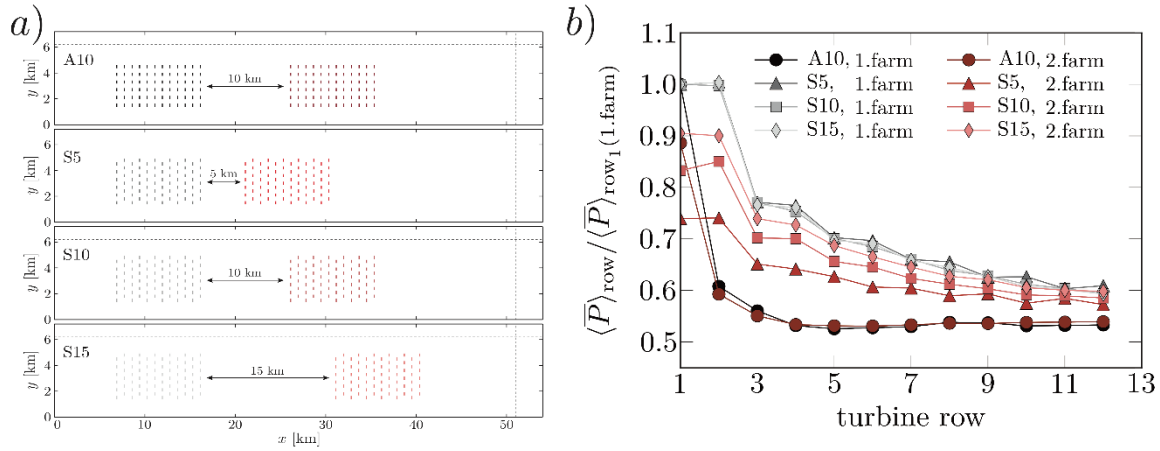


Figure 1: a) Schematic of the four cases under consideration, including the colors used in b. The dashed lines represent the start of the fringe regions, where the inflow conditions are obtained by the concurrent precursor method (Stevens et al. (2014)). b) Wind farm power output, normalized by the power output of the first row in the first farm.

Figure 1b shows the wind farm power output of each row in the first and the second wind farm, normalized by the power output of the first row in the first farm. For an aligned layout, the first row of the second farm produces 89% of the power produced by the first row of the farm 10 km upstream. Further downstream, starting from the third row, the first and second farm perform the same. As a consequence, the total power output of the second farm is only reduced by 2% compared to the upstream farm. For the staggered layout, the wake recovery is weaker compared to the aligned case, such that the difference in power output between the farms is larger. The second farm produces 86%, 92%, and 96% of the power produced by the first farm when positioned 5, 10, and 15 km downstream. Interestingly, the power output in the downstream wind farm with a staggered layout is not only reduced in the first row, where the power is reduced by 74% (5 km), 83% (10 km), and 91% (15 km), but also in the rows further downstream. For the smallest inter-farm spacing (5

km), even the last row of the second farm is affected by the presence of the upstream farm. Its power output is 6% lower than the power output of the last row of the first farm.

References:
Abkar, M., Bae, H. and Moin, P. [2016], 'Minimum-dissipation scalar transport model for large-eddy simulation of turbulent flows', Phys. Rev. Fluids 1(4), 041701.
Calaf, M., Meneveau, C. and Meyers, J. [2010], 'Large eddy simulations of fully developed wind-turbine array boundary layers', Phys. Fluids 22, 015110.
Canadillas, B., Foreman, R., Barth, V., Siedersleben, S., Lampert, A., Platis, A., Djath, B., Schulz-Stellenfleth, J., Bange, J., Emeis, S. and Neumann, T. [2020], 'Offshore wind farm wake recovery: Airborne measurements and its representation in engineering models', Wind Energy 23(5), 1249-1265.
Schneemann, J., Rott, A., Dörenkämper, M., Steinfeld, G. and Kühn, M. [2020], 'Cluster wakes impact on a far-distant offshore wind farm's power', Wind Energy Science 5(1), 29-49.
Stevens, R. J. A. M., Graham, J. and Meneveau, C. [2014], 'A concurrent precursor inflow method for large eddy simulations and applications to finite length wind farms', Renewable Energy 68, 46-50.

On the free stream velocity sampling in ActuatorLine Models: review and assessment with respect to wake description

Claudia Muscari[1,2,*], Alberto Zasso[1], Jan-Willem van Wingerden[2], Paolo Schito[1], and Axelle Viré[2]
[1]Politecnico di Milano
[2]Delft University of Technology
[*]Presenting author

Keywords: Wind Farm Control | Actuator Line Model | LES Wake modelling | Free stream velocity sampling

Wake interaction is the most critical phenomenon to be considered when dealing with wind farm control: a turbine placed in the wake of another will produce less power because of the wake deficit and experience more severe loads because of the increased turbulence. The role of high fidelity modeling of wind turbines in this scenario is to give results that are reliable enough to be used for the tuning of wake models and for the assessment of the performance of wind farm control strategies, in particular for the new ones involving active wake manipulation. A known limit of the actuator line is the difficulty in the simultaneous prediction of power and thrust (and wake deficit as a consequence). This is mostly due to two issues that could already be identified as the method made its appearance in Sorensen and Shen, 2022: the ambiguity in the definition of the free stream velocity and the tunability of the kernel amplitude. The sampled free stream velocity should contain the deceleration caused by the rotor induction but not the blade-local flow effects. The simplest way to
do that Is to sample directly in the cell center closest to the considered actuator line point, where, for flow potential theory the bound vorticity should be null (MartínezTossas, Churchfield, and Leonardi, 2015). The regularization kernel, on the other hand is the smearing function used to distribute the force in multiple cells. It has been shown that the predicted loads are very sensitive to its width, which in turn, should be set taking into account both the grid resolution and geometrical parameters such as the chord (MartínezTossas, Churchfield, and Meneveau, 2017).

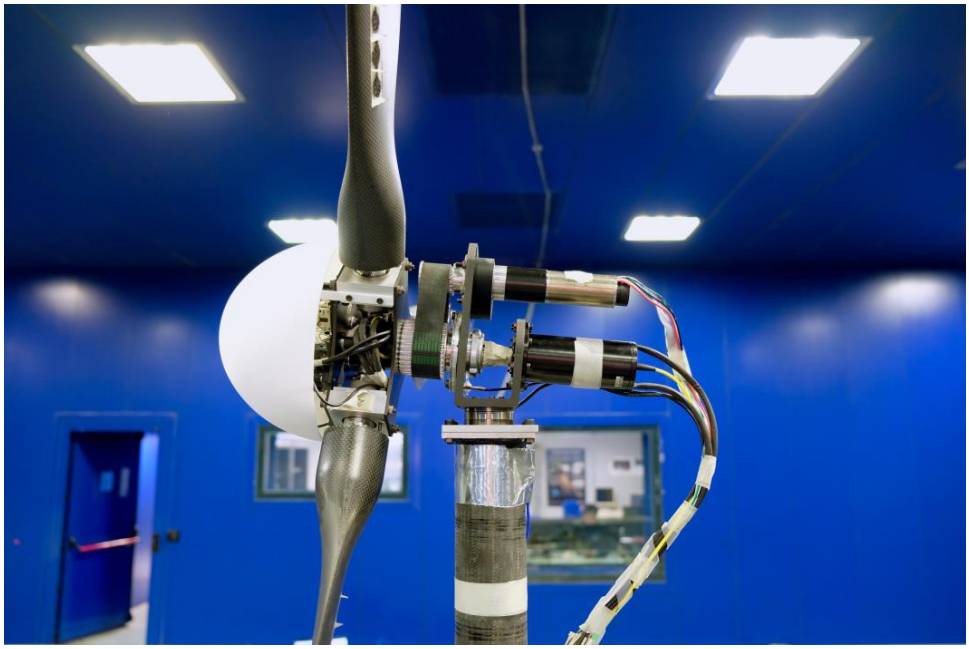


Figure 1: On-board control and measurement system of the DTU 10MW 1_75 wind turbine scale model (Courtesy of GVPM Polimi)

We conduct a LES study on the scaled DTU 10 MW turbine using SOWFA coupled with FAST, comparing the available velocity sampling methods (linear, integral) and the Effective Velocity Method (Schito, Zasso, 2014) in terms of accuracy, computational cost, robustness, to experimental data and BEM results. Similar

parametric studies have been performed before (Merabet and Laurendau, 2019) but only in a 2D framework so that the added complexities of 3D effects and the possible interaction of neighboring Actuator Line elements and tip vortices were neglected.

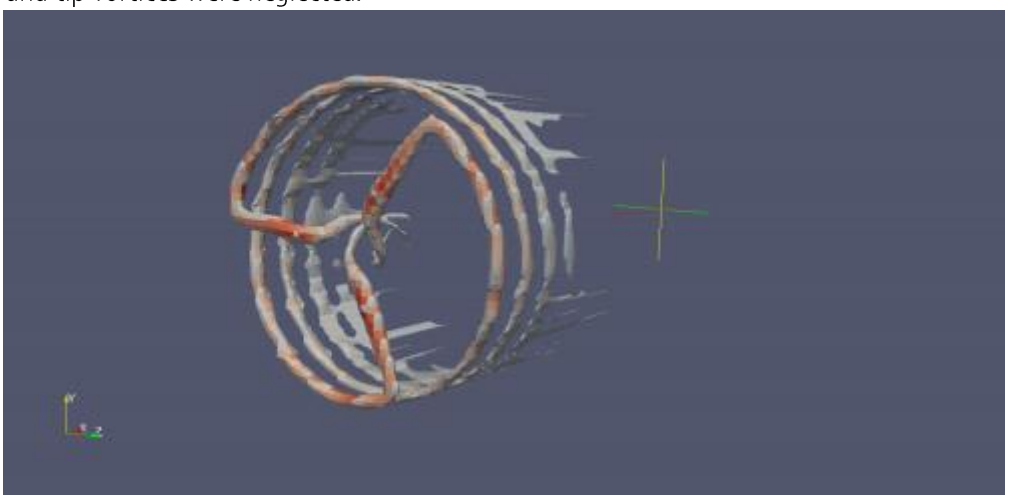


Figure 2: IsoVorticity visualization of a wind turbine wake in a LES

The considered data comes from the experiments on the scaled model of the DTU 10 MW turbine performed in the Politecnico di Milano Wind Tunnel during the CL-Windcon project.

We discuss the presence of spurious high-frequency content in the methods relying on interpolation. We also test the capability of a subfilter-scale velocity model, proposed in Martínez-Tossas, and Meneveau, 2019 as a correction of the velocity along the blade when using kernel sizes larger than the optimal one to perform well in different operating conditions and with and without flexibility of the blades.

References:

Sorensen, J.N. and Shen, W.Z., 2002. Numerical modeling of wind turbine wakes. J. Fluids Eng., 124(2), pp.393-399.

Merabet, R. and Laurendeau, E., 2019. Parametric study on the velocity sampling techniques for the actuator line method in 2d. In AIAA Scitech 2019 Forum (p. 1797).

Churchfield, M.J., Schreck, S.J., Martinez, L.A., Meneveau, C. and Spalart, P.R., 2017. An advanced actuator line method for wind energy applications and beyond. In 35th Wind Energy Symposium (p. 1998).

Schito, P. and Zasso, A., 2014, June. Actuator forces in CFD: RANS and LES modeling in OpenFOAM. In J. Phys. Conf. Ser (Vol. 524, No. 1).

Martínez-Tossas, L.A. and Meneveau, C., 2019. Filtered lifting line theory and application to the actuator line model. Journal of Fluid Mechanics, 863(NREL/JA-5000-72646).

Martínez-Tossas, L.A., Churchfield, M.J. and Leonardi, S., 2015. Large eddy simulations of the flow past wind turbines: actuator line and disk modeling. Wind Energy, 18(6), pp.1047-1060.

Martínez-Tossas, L.A., Churchfield, M.J. and Meneveau, C., 2017. Optimal smoothing length scale for actuator line models of wind turbine blades based on Gaussian body force distribution. Wind Energy, 20(6), pp.1083-1096.

Model-form uncertainty quantification in RANS simulations of wind turbine wakes

Simon D. Hornshøj-Møller[1], Peter D. Nielsen[1], Ali Eidi[1,2], Pourya Forooghi[1], and Mahdi Abkar[1,*]
[1]Aarhus University, Denmark
[2]University of Tehran, Iran
*Presenting author

Keywords: Wind turbine wakes | Power deficit | CFD RANS | Turbulence modelling | Uncertainty quantification

Reynolds-averaged Navier Stokes (RANS) based modeling is considered the mainstream computational fluid dynamics (CFD) approach for wind energy applications. Considering the inherent shortcomings associated with RANS models, quantification of uncertainties is of obvious importance if these models are to be used for the design and optimization of wind farms. In the present work, model-form uncertainties of RANS closure are quantified for simulations of wake flow behind a stand-alone wind turbine. The uncertainty is modeled by introducing perturbations to the Reynolds stress tensor. We specifically focus on perturbations in the eigenvalues of the tensor. The twoequation k-ω SST RANS model and large-eddy simulation (LES) data are used as the baseline RANS model and reference data, respectively. Initially we compare the unperturbed RANS simulation against LES data, and show that the two-equation RANS model generally tends to predict higher levels of isotropy, especially in the turbine-induced shear layer. A comparison between LES data and differently perturbed RANS simulations is made for the evolution of velocity deficit and turbulence intensity behind the turbine. A satisfactory coverage of LES profiles is observed when the amount of introduced perturbation is adjusted based on a priori comparison of the baseline RANS and LES results with the exception of the turbulent intensity immediately behind the turbine. The framework is also extended to the simulation of turbine wakes and power losses in wind farms.
Figure 1 shows the evolution of the averaged velocity deficit and turbulence intensity behind a standalone wind turbine for $\delta_B=0.5$, where δ_B is the amount of perturbations toward different limiting states of turbulence . $\delta_B=0.5$ is the perturbation coefficient based on the maximum deviation observed a priori between the LES and the baseline RANS results. In this figure, the band between the one and three component results is highlighted. Results indicate that the band between the one and three component curves covers the LES results well. Generally speaking, the velocity deficit results confirm that mixing and the resulting wake recovery becomes faster when approaching the three component state. The opposite is the case for the one component state.

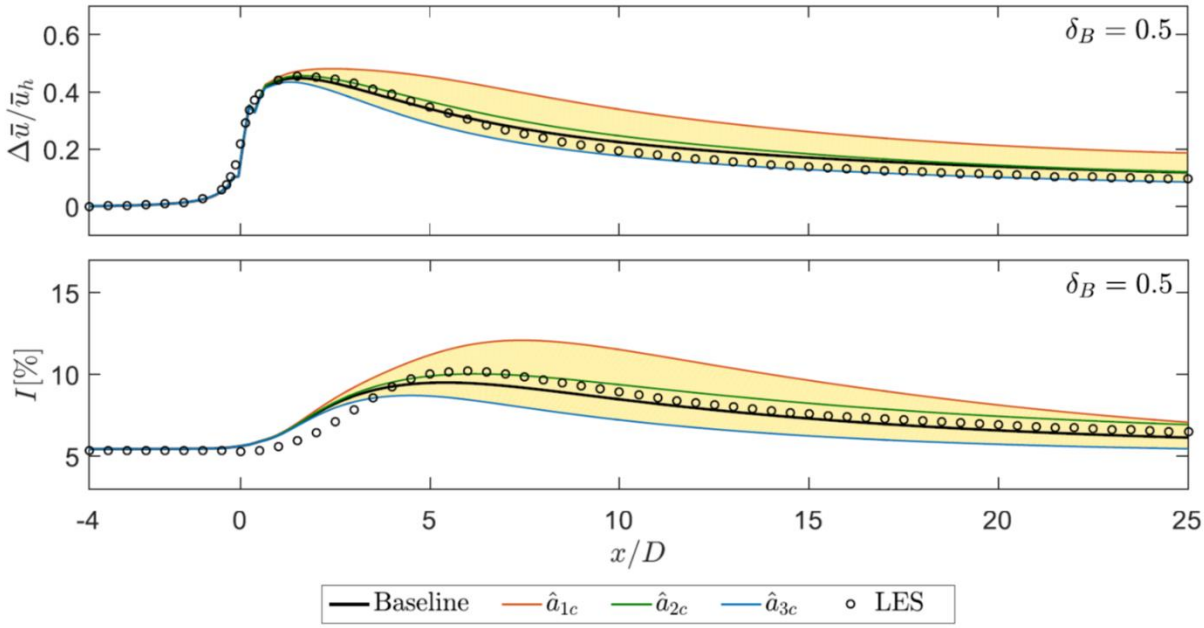


Figure 1: Normalized velocity deficit (top) and turbulence intensity (bottom), averaged over the rotor area, with downstream distance for the baseline RANS, LES and perturbed RANS simulations. The band between the one and three component results is highlighted. a_1c, a_2c, and a_3c represent one-component, two-component and three-component (isotropic) turbulence, respectively.

Evolution of averaged turbulence intensity is studied in this figure as well, where the perturbation bounds capture the LES data well, except in the vicinity of the turbine and in the near wake region up to about $x/D=4$, where the LES-predicted increase in TKE lags behind those of RANS. The near wake deviation indicates that variations in the eigenvalue of anisotropy tensor most likely are inadequate for matching the high-fidelity data in the region immediately downstream of the turbine. This can be related to the inadequacy of the baseline model in capturing the magnitude of TKE. In the downstream region, however, the baseline model seems to be able to match the turbulence intensity magnitude relatively well [1].

References:

[1] Hornshøj-Møller, S.D., Nielsen, P.D., Forooghi, P. and Abkar, M., 2021. Quantifying structural uncertainties in Reynoldsaveraged Navier–Stokes simulations of wind turbine wakes. Renewable Energy, 164, pp.1550-1558.

Comparison of wake flow, power and load measurements from three mid-fidelity wake models based on the DWM approach

Øyvind Waage Hanssen-Bauer[1,*], Jacobus Bernardus De Vaal[2,1], Murat Tutkun[1], Roy Stenbro[1], Paula Doubrawa[3], Jason Jonkman[3], Helge Aagaard Madsen[4], Gunner Chr. Larsen[4], Henrik Asmuth[5], and Stefan Ivanell[5]

[1]Institute for Energy Technology
[2]Norwegian University of Science and Technology
[3]National Renewable Energy Laboratory
[4]Technical University of Denmark
[5]Uppsala University
[*]Presenting author

Keywords: DWM | turbine wakes | wind farm | wake merging | turbine loads

In this study we compare the performance of three mid-fidelity wake models based on the Dynamic Wake Meandering (DWM) model. The original DWM model (Larsen et al., 2008) developed at DTU has shown to be a promising approach for estimating both power and, when coupled to an aeroelastic solver, loads in a wind farm. It is now a well-established model in the wind energy community and has recently been included in the new edition of the IEC code as a recommended practice. The DWM model is based on the assumption that the quasi-steady wake deficit, obtained from a thin shear-layer approximation of the Navier-Stokes equations, meanders as a passive tracer by the large-scale structures in the incoming wind. Another core element of the DWM model is the wake added turbulence; an increase of the turbulence level in the turbine wake relative to the ambient, caused by the breakdown of tip vortices and from the shear of the velocity deficit.

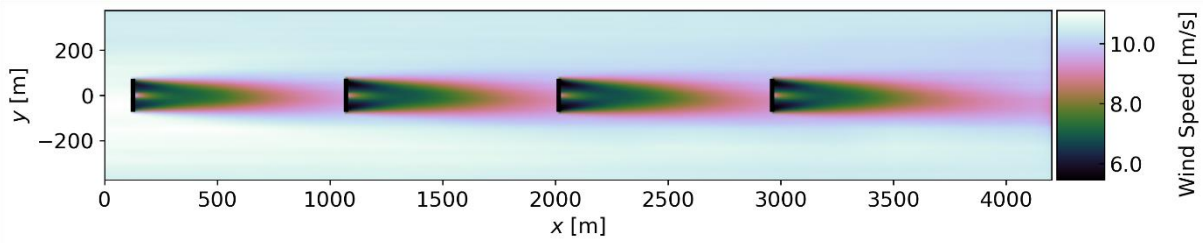


Figure 1: Preliminary results of the flow field through a farm with turbines in fully waked conditions

Since the introduction of the DWM model, several improvements have been suggested and other wake models based on the main DWM ideas have been developed. FAST.Farm (Jonkman et al., 2017) developed at NREL, and WIFET Farm Simulator developed at IFE (Hanssen-Bauer et al., 2020) are two such wake models, and are compared against the original DWM model in this study. The comparison is carried out by testing the three models on different farm configurations. Figure 1 and 2 shows preliminary results of the flow field through two such farm configurations. In figure 1, four NREL 5MW reference turbines are aligned with 7.5D spacing resulting in fully waked conditions. In figure 2, the inflow angle has changed and the turbines experience partially waked conditions. A third example of a farm setup, two turbines side-by-side, is investigated to compare how the DWM models handle the merging of these turbine wakes. To focus on the wake modelling, the difference in inflow models is eliminated by feeding all the DWM models with the same Large Eddy Simulation (LES) precursor-generated inflow for the comparison. As a reference to the three DWM models, LES with turbines modeled as actuator lines were performed for some of the inflow and farm configurations simulated by the DWM models.

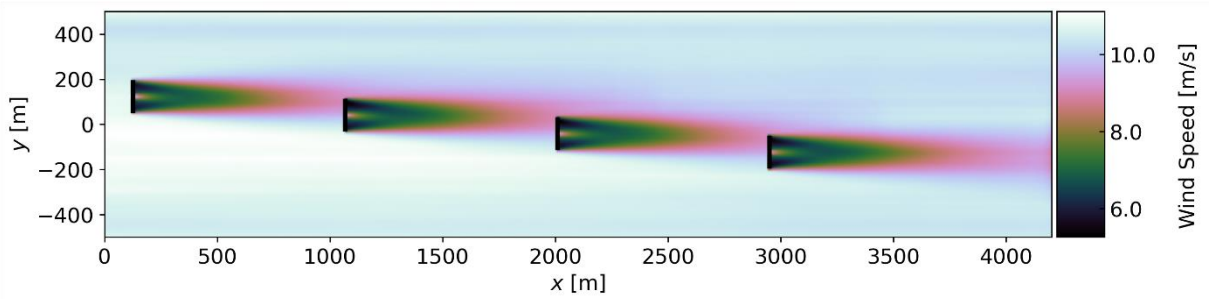


Figure 2: Preliminary results of the flow field through a farm with turbines in partially waked conditions

Despite the similarities between the wake models, this comparison shows differences in simulated wake flow, and turbine power and loads. Variations in model implementation when it comes to treating e.g. wake added turbulence, wake summation and merging, eddy viscosity closure and wake transport velocity are addressed, and their impact on the results are discussed. The results of this comparison will help quantify simulation uncertainty as it pertains to model implementation. In addition, we identify strengths and weaknesses of current mid-fidelity wake modeling strategies.

From these results, we suggest priorities for future model developments so that robust and low-uncertainty model implementations can be used in wind farm design.

References:

Larsen, G. C., Madsen, H. Aa., Thomsen, K., and Larsen, T. J. (2008). Wake meandering: A pragmatic approach. Wind Energy: An International Journal for Progress and Applications in Wind Power Conversion Technology, 11(4):377–395.

Jonkman, J. M., Annoni, J., Hayman, G., Jonkman, B., and Purkayastha, A. (2017). Development of FAST. Farm: A new Multiphysics engineering tool for wind-farm design and analysis. In 35th Wind Energy Symposium, page 0454.

Hanssen-Bauer, Ø. W., De Vaal, J. B., Tutkun, M., Asmuth, H., Ivanell, S., and Stenbro, R. (2020). Dependence of wind turbine loads on inlet flow field. In Journal of Physics: Conference Series, volume 1618, page 062065. IOP Publishing.

Validation of different multiple wake models for wind turbines in combination with the DWM model

Inga Reinwardt[1,*], Levin Schilling[1], Peter Dalhoff[1], Dirk Steudel[2], and Michael Breuer[3]
[1]HAW Hamburg
[2]Nordex Energy GmbH
[3]Helmut-Schmidt University Hamburg
*Presenting author

Keywords: Multiple wakes | DWM model | Lidar | Fatigue loads

Light detection and ranging (lidar) systems are nowadays often used measurement devices for analysing wind turbine wakes. The aim of the present measurement campaign is to analyse double wake situations in a compact onshore wind farm and to compare them with multiple wake models.
The lidar measurements are used to assess the wake meandering in a double wake situation and in a further step to validate the wind speed deficit of the merged wake in the meandering frame of reference (MFR) and the fixed frame of reference (FFR). Moreover, turbine load measurements are used to compare measured and simulated fatigue loads in double wake situations taking the analysed multiple wake models into account.
At the investigated onshore wind farm two turbine nacelles are equipped with pulsed scanning lidar systems (Galion G4000). Additionally, three turbines are equipped with load measurement devices providing loads of double wake situations. The wind farm is located in the southeast of Hamburg (Germany) and consists of five Nordex turbines (1 x N117 3 MW and 4x N117 2.4 MW) with small turbine distances. A met mast is placed two rotor diameters in front of the wind farm in main wind direction to capture the ambient conditions. The lidar systems perform a horizontal line scan, so that only the horizontal meandering can be captured. Pulsed lidar systems are capable of measuring simultaneously at different distances. Hence the wind speed deficit in the MFR and FFR in front and behind of the wake affecting turbines can be investigated in detail.

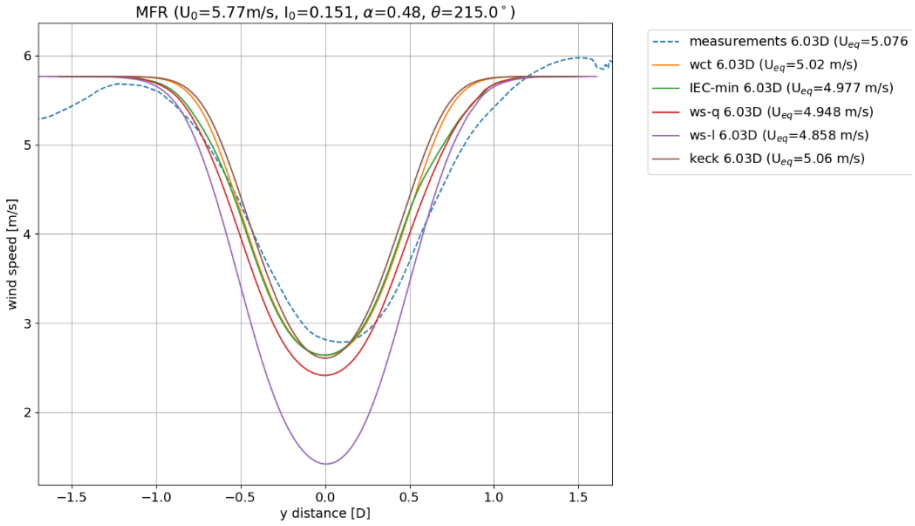


Figure 1: Measured and simulated wind speed deficit in the MFR in a double wake situation over the distance from the nacelle in rotor diameters D. The measurements are collected at a downstream distance of 6.03D from the first turbine in the row. The ambient conditions are given in the title. The lidar measurements are compared to different multiple wake models in combination with the DWM model.

An example of the measured mean wind speed in the MFR of a double wake situation is illustrated in the attached figure. The ambient conditions (ambient wind speed, turbulence intensity, wind shear, and wind

direction) determined by the met mast are given in the title of the figure. The figure depicts the wind speed deficit as a function of the distance from the nacelle provided in rotor diameters D.
The measurements are collected at a downstream distance of 6.03D from the first turbine in the row.
The distance between the two turbines is 3.46D. The measured deficits are compared to the simulated wind speed deficit from the wake of the closest turbine (wct), the minimum wind speed at each point of interest of all upstream turbines (IEC-min (Larsen, 2013, IEC, 2019)), the quadratic (wsq (Katic´, 1987)) and the linear (ws-l (IEC, 2019)) summation of all upstream wakes as well as an approach, which considers the inflow at each upstream turbine successively, so that the inflow conditions change at each turbine in the row and the wake effects of all upstream turbines are included implicitly (Keck (Keck, 2015)). The linear summation overpredicts the double wake, whereas all other models agree considerably better with the measurements. The IEC-min method coincides very well with the measurements towards the transition zone to the ambient wind speed. Similar results as the one presented in attached figure have been collected for various ambient conditions and compared to simulations to confirm the model accuracy.

References:
Larsen, T. J., Madsen, H. A., Larsen, G. C., and Hansen, K. S. (2013) 'Validation of the dynamic wake meander model for loads and power production in the Egmond aan Zee wind farm', Wind Energy, 16(4),p 605–624.
IEC (2019) 'IEC 61400-1 Ed. 4 Wind energy generation systems - Part 1: Design requirements', Guideline, International Electrotechnical Commission (IEC).
Katic´, I., Højstrup, J., and Jensen, N. O. (1987) 'A Simple Model for Cluster Efficiency', In Proceedings of the European wind energy association conference and exhibition, pp. 407–410. Rome, Italy.
Keck, R.-E. (2015) 'Validation of the standalone implementation of the dynamic wake meandering model for power production', Wind Energy, 18(9), p1579–1591.

Regular Session: Wake Models and Data

Application of bluff-body wake models to wind turbine wakes

Ingrid Neunaber[1,*], Joachim Peinke[2], and Martin Obligado[3]
[1]Centrale Nantes
[2]ForWind - University of Oldenburg
[3]Université Grenoble Alpes, Grenoble-INP
[*]Presenting author

Keywords: Wind turbine Wake | Wind tunnel experiments | Wake modelling | Turbulence

Wind turbines are normally clustered in wind farms. As a consequence, downstream turbines will operate in the full or partial wakes of upstream turbines. In this situation, the downstream turbines produce less energy due to the velocity deficit behind the upstream turbine. At the same time, they experience higher loads due to the enhanced turbulence in the wake [1]. To optimize the wind farm layout with respect to annual power production and maintenance time, and to refine control algorithms, a good knowledge of the evolution of the wind turbine wake is thus important. Wind turbine wakes have therefore been object of many studies but they are still not fully understood.
To improve the knowledge, one can look into the modeling of wakes generated by bluff bodies that have been studied intensively over the past decades. A. Townsend and W. George derived the formulas for the scaling of the mean centerline velocity deficit downstream of a bluff body, using a set of hypotheses that include energy scalings consistent with the Richardson-Kolmogorov phenomenology [2][3]. Subsequent studies have adapted this theory to address non-equilibrium energy scalings [4]. Therefore, two different sets of scalings can been obtained that allow to differentiate between equilibrium and non-equilibrium turbulence in the wake, i.e. whether the energy dissipation follows or not the standard Richardson-Kolmogorov scalings.

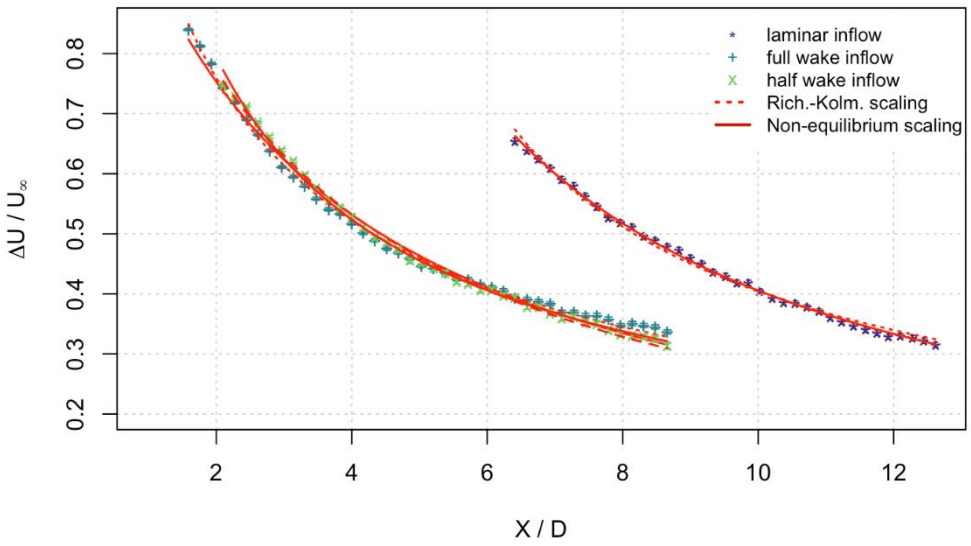


Figure 1: Mean normalized velocity deficit for the three scenarios laminar inflow (*) full wake inflow (+) and half-wake inflow (x), and the Richardson-Kolmogorov (- -) and the non-equilibrium (-) scalings from the Townsend-George theory.

In this work, we will present the application of the Townsend-George theory to three wind turbine wake scenarios measured in the wind tunnel using a hot-wire array. For the three scenarios, the wind turbine was exposed to laminar inflow, to the central wake of an upstream turbine, and to half of the wake of an upstream turbine [5]. First, we discuss and check all the requirements the wakes have to fulfill for the Townsend-George theory to apply. This includes a region with fully developed, decaying turbulence where the velocity profiles



are self-similar and axisymmetric and the integral length scale is related to the wake width. In the next step, the dissipation is investigated to determine whether Richardson-Kolmogorov or non-equilibrium turbulence is present, and finally, the scalings for the mean velocity deficit are applied and compared to the Jensen wake model and the Bastankhah-Porté-Agel model (both summarized in [6]). We find that the bluff body wake models fit well (cf. Fig. 1) and also outperform the wind turbine wake models for the three cases that are investigated. This result is of interest as the assumptions underlying the bluff body wake models are purely physical. All information from the inflow and the turbine operation state is included in a few fit parameters that need to be derived. In addition, the investigation of the dissipation gives important information on how to simulate the turbulence within the wake which has an influence on the wake evolution.

References:
[1] Vermeer, L.J. ; Sørensen, J. N.; Crespo A. (2003) Wind turbine wake aerodynamics. Prog Aerosp Sci, 39, 467–510
[2] Townsend, A. (1976) The structure of turbulent shear flow, Cambridge university press
[3] George, W. (1989) The self-preservation of turbulent flows and its relation to initial conditions and coherent structures. Advances in Turbulence, edited by George, W. and Arndt, R., Springer
[4] Vassilicos, J. (2015) Dissipation in Turbulent Flows, Annual Review of Fluid Mechanics, 47, 95–114
[5] Neunaber, I.; Hölling, M.; Stevens, R.; Schepers, G.; Peinke, J. (2020) Distinct Turbulent Regions in the Wake of a Wind Turbine and Their Inflow-Dependent Locations: The Creation of a Wake Map. Energies, 13
[6] Porté-Agel, F.; Bastankhah, M.; Shamsoddin S. (2020) Wind-Turbine and Wind-Farm Flows: A Review. Boundary Layer Meteorol, 174, 1–59

Power production of five aligned wind turbines

Alessandro Sebastiani*, Alfredo Peña, Niels Troldborg, and Alexander Meyer Forsting
DTU Wind Energy
*Presenting author

Keywords: Power production | Blockage | Lidar | CFD

Global blockage has recently started to draw attention among the wind energy community. It might be defined as the induction due to the presence of a cluster of wind turbines, which is added to the induction of the single turbines. The production of the upstream turbines is thus different from that of an isolated turbine. McTavish et al. (2015) and Meyer Forsting et al. (2017) evaluated the blockage effect for the case of a single row of turbines perpendicular to the wind direction, and showed a clear difference with the power output of an isolated turbine. This raises the question on whether power curve testing is affected by global blockage, as it is often conducted at a test site on a row of aligned wind turbines rather than on an isolated turbine. This work extends the analysis of Meyer Forsting et al. (2017) by evaluating the difference between the row of turbines with the isolated case as function of the wind speed and the inter-turbine spacing. Additionally, the power output is related to the inflow velocity in order to further investigate whether the power curve measured on a row of aligned wind turbines differs from that of an isolated wind turbine.

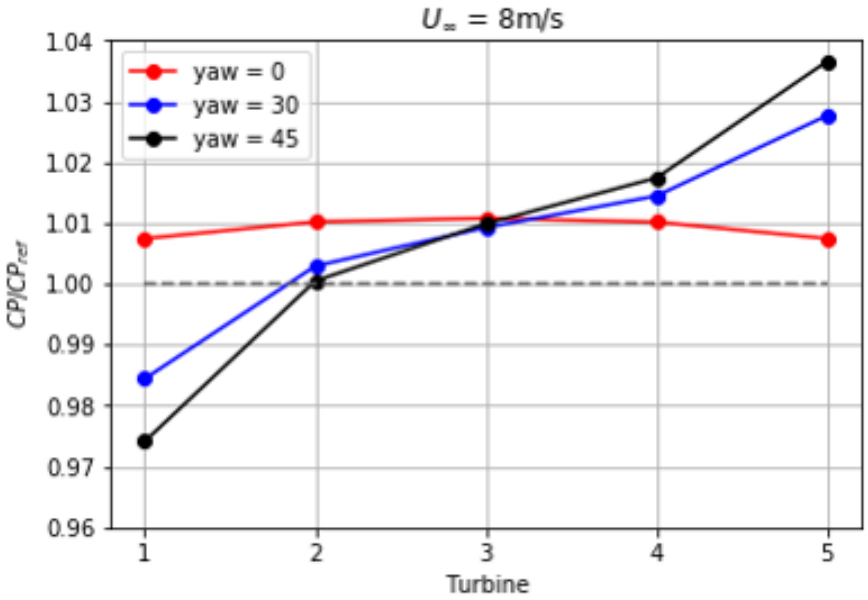


Figure 1: Power output of 5 turbines in a row normalized by the output of an isolated turbine under the same conditions (RANS simulations) with a wind speed of 8 m/s and three different wind directions: orthogonally to the row of turbines (yaw = 0^0) and along lines forming angles of 30^0 and 45^0 with the orthogonal one. Turbine 1 is the upstream one in the yawed cases. The inter-space is equal to 2 D.

The flow over the turbine site is simulated with Reynolds averaged Navier-Stokes and the turbines are modelled as actuator disks. Details about the numerical setup can be found in Meyer Forsting et al. (2017). Different cases are tested by varying the inflow wind speed, direction and turbine spacing. Specifically, the wind speed range covers the entire power curve and the wind direction varies up to 45o with respect to the orthogonal line to the turbines row. The turbine spacing varies from 1.8 to 3 rotor diameters (D). In order to correlate the power output and the incoming wind speed, values for the velocity are extracted in front of the rotors by virtual met masts and nacelle lidars.

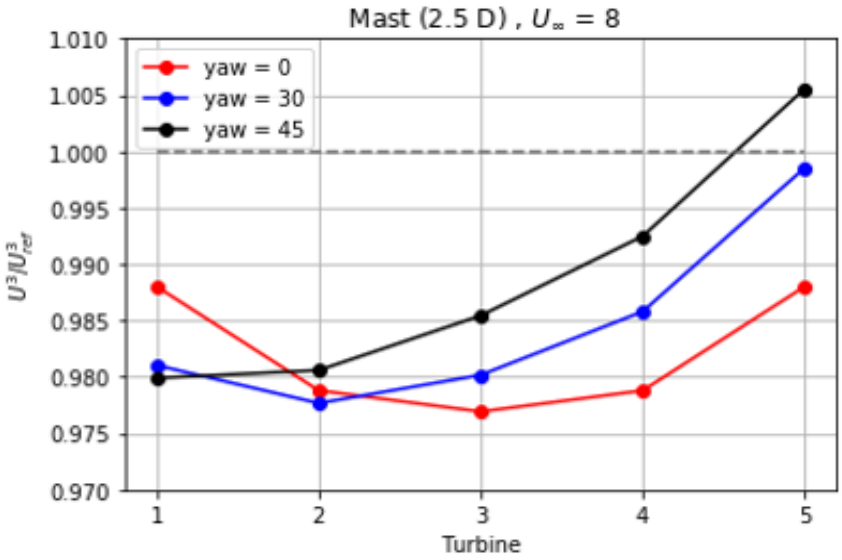


Figure 2: Wind speed at hub height and 2.5 D in front of each turbine normalized by the same wind speed extracted in the isolated case. The free-stream velocity is 8 m/s with three different wind directions: orthogonally to the row of turbines (yaw = 0^0) and along lines forming angles of 30^0 and 45^0 with the orthogonal one. Turbine 1 is the upstream one in the yawed cases. The inter-space is equal to 2 D.

Results show that there is a significant difference between the power output of each of the turbines in the row and that of an isolated turbine. Additionally, this difference varies with the wind direction and the position of the turbine in the row, with either a gain or a loss with respect to the isolated case. This is shown in the first image for a wind speed of 8 m/s and a turbine spacing of 2 D.

However, the power output over the whole row increases compared to the output of the isolated turbine multiplied by 5. As shown in the second image, the opposite trend is found for the velocity measured upstream of the rotors. Since the induction due to the 5 turbines as a whole is combined to that of the single turbines, the wind speed measured in front of the row is lower than that measured in the isolated case. This suggests a different effect on power output and incoming wind speed compared to the isolated case, with a possible bias of power curve measurements.

Furthermore, it is found that the difference with the isolated case in terms of both gains and losses is increased when decreasing the inter-turbine spacing or the inflow wind speed.

References:

McTavish, S., Rodrigue, S., Feszty, D., Nitzsche, F. 36855865400;56417871300;14053852300;7003905404; An investigation of in-field blockage effects in closely spaced lateral wind farm configurations (2015) Wind Energy, 18 (11), pp. 1989-2011

Meyer Forsting, A.R., Troldborg, N., Gaunaa, M. 57189499245;8668052100;9241548100; The flow upstream of a row of aligned wind turbine rotors and its effect on power production (2017) Wind Energy, 20 (1), pp. 63-77

Investigating the evolution of wake turbulence with nacelle-based lidar measurements

David Bastine*, and Martin Kühn
ForWind - University of Oldenburg
*Presenting author

Keywords: turbulence | wake | lidar

Since lidars measure only a volume-averaged line-of-sight velocity, they have rarely been used to investigate turbulence characteristics of wake flows. Despite their inherent limitations, however, they can still offer qualitative insight into wake turbulence, as indicated e.g. by Garcia et al. (2019), Bastine et al., (2015); Iungo et al. (2013). In this study, we use nacelle-based lidar measurements to investigate the evolution of turbulence along the centerline of the wake. This extends our work in Bastine et al. (2015), where only one distance to the turbine was investigated.

Our measurements are performed within the scope of the German project CompactWind II in cooperation with eno energy systems. The measurement campaign is located in a small array of wind turbines in Northwest Germany, as partially presented in Figure 1. The inflow and state of the atmosphere is measured via a nearby met mast using cup anemometers and eddy covariance stations. On top of the nacelle of a 3.5 MW wind turbine (WT3), a pulsed long range lidar (lidar 1) is placed to measure the wake of the turbine. In one of our measurement scenarios, this lidar operates in a staring mode with a fixed direction of the laser beam. The line-of-sight velocity is measured at several range gates with a temporal resolution of 10 Hz facilitating the investigation of dynamics on relatively short time scales. While the nacelle-based lidar operates in a staring mode, additional plane position indicator (PPI) scans of a second ground based long range lidar (lidar2) are used to gain insight into the instationary trajectory the wake flow, as shown in Figure 1. Despite the relatively high elevation angle, such scans can still be helpful to visualize important regions of the wake.

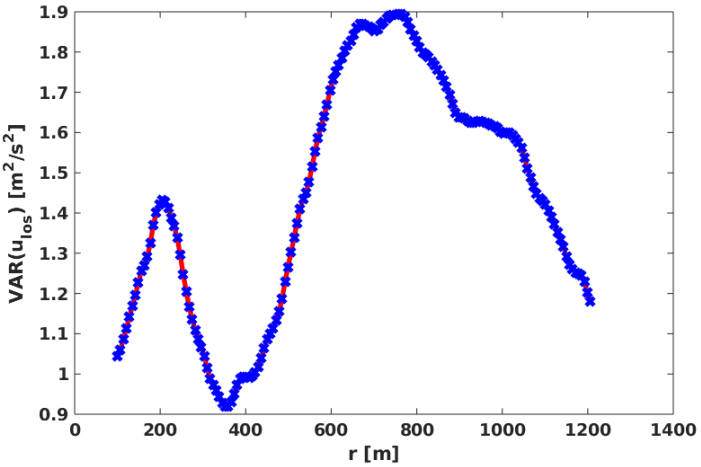


Figure 1: Variance of the line-of-velocity versus the range gate of the fixed laser beam (red line in Figure 1). The variance is estimated for an example time series of 30 minutes.

In order to study the evolution of the wake flow at the measurement locations along the fixed laser beam, several turbulence characteristics are calculated for all range gates, such as variance, turbulence intensity, power spectral density, increment statistics and turbulent length scales. As an example, the variance of the line-of-sight velocity along the laser beam is shown in Figure 2. High variance indicates a high turbulent kinetic energy. As also found e.g. in Neunaber (2019), the turbulence builds up in the near wake before a decrease is found indicating decaying turbulence in the transition region. In Figure 2, another increase can be seen with a second peak of the variance.

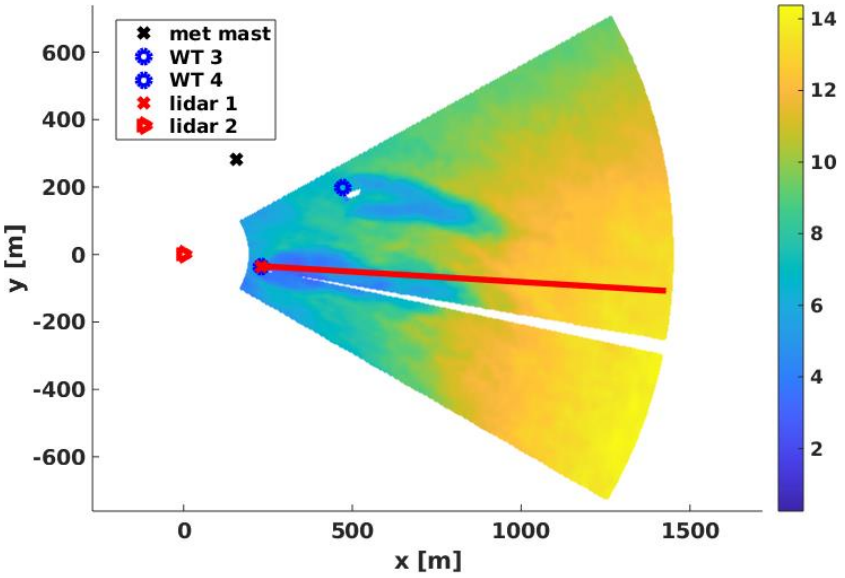


Figure 2: Overview of our Measurement Scenario: Colors denote the 30-minute-average of the line-of-sight velocity obtained from a PPI Scan of the ground-based lidar (lidar 2). Please note that due to an elevation angle of approximately 13 degrees, only parts of the wake can be observed with the scan. The red line represents the lidar beam of the nacelle-based lidar on wind turbine 3 (WT 3) at a hub height of 117 m.

This peak is likely caused by the beam leaving the central wake region due to an imperfect alignment with the wind direction (yaw error) and probably also by the meandering motion of the wake.

The different statistical characteristics of the wake flow are compared to the inflow characteristics in order to describe the modulation of the incoming turbulence by the turbine. Studies, such as Neunaber (2019), Bastine et al. (2015) and Singh et al. (2014) suggest that despite the complex anisotropic inflow of the atmosphere, some characteristics of homogeneous isotropic turbulence can be found in the central region of the far wake. We will reassess this hypothesis in our field study.

Additionally, the effect of the lidar measurement volume on the analyzed turbulence measures will be discussed. This effect is particularly complex, since the averaging takes place in the strongly nonhomogeneous wake flow.

References:

Bastine, D. et al. (2015) "Characterizing wake turbulence with staring lidar measurements", Journal of Physics: Conference Series, 625, p. 012006.

Garcia, E. T. et al. (2019) "Statistical characteristics of interacting wind turbine wakes from a 7-month LiDAR measurement campaign", Renewable Energy, 130, pp. 1-11.

Neunaber, I. (2019) "Stochastic investigation of the evolution of small-scale turbulence in the wake of a wind turbine exposed to different inflow conditions". PhD thesis. Carl von Ossietzky Universität Oldenburg.

Iungo, G. V. et al. (2013) "Field Measurements of Wind Turbine Wakes with Lidars", Journal of atmospheric and oceanic technology, 30, pp.274-287.

Singh, A. et al. (2014) "On the homogenization of turbulent flow structures in the wake of a model wind turbine", Physics of Fluids, 26 (2), p. 025103.

Experimental assessment of the velocity field in a wind farm induction zone

Magnus K. Vinnes[1], Antonio Segalini[2], Nicholas A. Worth[1], and R. Jason Hearst[1]
[1]Norwegian University of Science and Technology
[2]KTH Royal Institute of Technology

Keywords: Induction | Wind farm blockage | PIV | Flow field

Wind turbines are often located in clusters, referred to as wind farms, where they are affected by the presence of other nearby turbines. Many turbines in wind farms operate in the wake of other turbines, where they experience reduced wind velocity and increased turbulence intensity. In the literature from the last 40 years, numerous studies which investigated this effect are found.
However, it has been recently observed that the turbines located farthest upstream in the farm experience incoming wind velocities lower than the actual wind speed, contrary to the general "wake only" idea. This is due to the wind farm induction, a cumulative effect of the induction of each single turbine in the farm. Typically, energy production assessments do not take this effect into account, as many wake models assume that each turbine influences only the flow around downstream turbines.
However, Ebenhoch et al. (2016) showed, during a series of wind tunnel tests, that the global blockage effect reduces the flow velocity as far as 30 diameters upstream of the leading row of turbines. Bleeg et al. (2018) showed that this effect is not limited to idealized experiments and found that the wind farm induction zone exists also upstream of real wind farms. They compared meteorological mast wind measurements with Reynolds-averaged Navier-Stokes (RANS) simulations, and for three different onshore wind farms, both measurements and simulations showed reduced velocity upstream of the farm compared to the freestream wind velocity. Segalini and Dahlberg (2019) performed wind tunnel experiments, changing the distance between the first row of turbines and the rest of the farm for different farm layouts. The results show that the size of the farm, and the distance to downstream turbines, changes the operation of the leading turbines, with velocity decreases up to 2.5%.

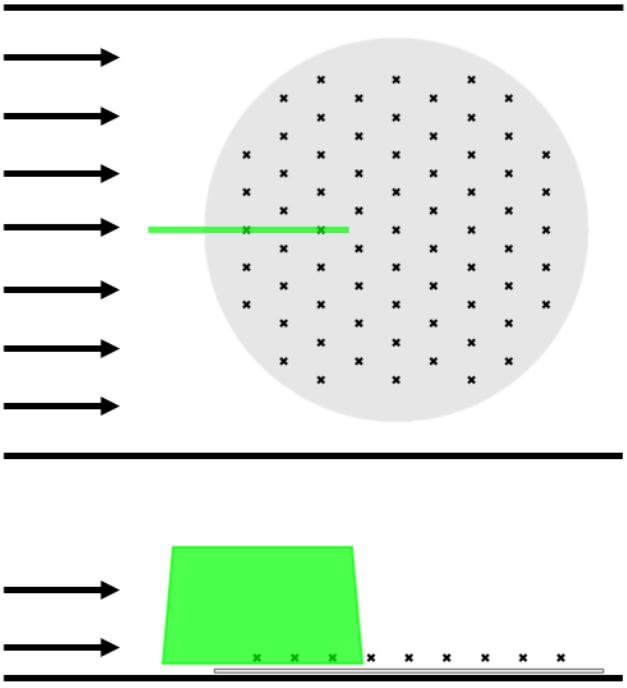


Figure 1: Schematics showing the staggered wind farm layout.

The wind farm induction zone, or the global wind farm blockage, influences the operating condition of even the first row of turbines. However, the phenomenon is not yet well described for different farm operating

conditions, including wind direction and farm layout. To that end, a series of wind tunnel experiments has been conducted. A wind farm, consisting of 69 freely rotating wind turbine models, was examined in the large closed-loop wind tunnel at NTNU. Particle image velocimetry measurements were performed around one turbine in the leading row of the farm, covering a region of more than 10 diameters upstream and 6 diameters downstream of the turbine. Both aligned and staggered layouts were evaluated, and two different incoming boundary layer profiles were used.

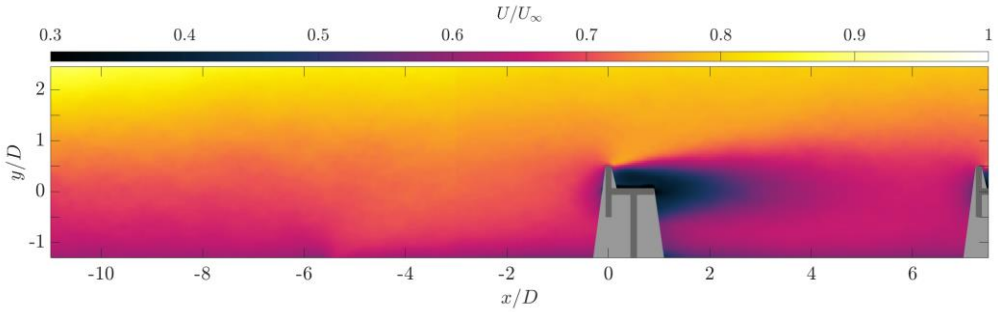


Figure 2: Example flow field. The velocity is normalized by the freestream velocity, measured by a pitot tube.

The staggered layout is shown in Figure 1. For all cases, the farm was rotated to investigate different incoming wind directions, namely 0°, 15°, and 30° compared to Figure 1. The present work will focus on how the different wind directions, boundary layers, and layouts affect the mean flow fields (one example is shown in Figure 2), the turbulence statistics, and the vorticity fields in the wind farm induction zone.

References:

Bleeg, J., Purcell, M., Ruisi, R. and Traiger, E. (2018). Wind farm blockage and the consequences of neglecting its impact on energy production. Energies, 11(6), p. 1609.

Ebenhoch, R., Muro, B., Dahlberg, J.Å., Hägglund, P.B. and Segalini, A (2017). A linearized model of wind-farm flows. Wind Energy, 20, pp. 859-875.

Segalini, A. and Dahlberg, J.Å. (2020). Blockage effects in wind farms. Wind Energy, 23, pp. 120-128.

Data-driven offshore cluster wake effects for wind energy hub design

Juan Pablo Murcia Leon[1], and Matti J. Koivisto[2]
[1]DTU Wind Energy
[2]Technical University of Denmark

Keywords: offshore cluster wake effects | offshore wind energy hub | large energy system

The share of offshore wind energy production to the European energy system is expected to grow in the next 20 years. Offshore energy hub is a cluster of offshore wind power plants with a central connection point from which the energy can be collected and transported to other regions. The design of energy hubs in the North and Baltic Sea requires a large scale energy system optimization that has as an objective to find the best cost-effective installed capacity per hub, interconnection network (layout and capacity). This large energy system optimization tries to balance the energy demand at each time with the energy produced from each source (onshore wind, offshore wind, solar, etc.) plus the energy transported from other regions.
The wind energy production time-series in an offshore energy hub depends on two aspects: (1) wind time-series, (2) cluster wake losses. Previous large-scale wake studies using a wake parametrization of wake losses in mesoscale models considered fixed installed capacity and installation density scenarios [Volker et al, Agora-Energiewende]. This requires a separate meteorological simulation, which can be computationally heavy, for each scenario.

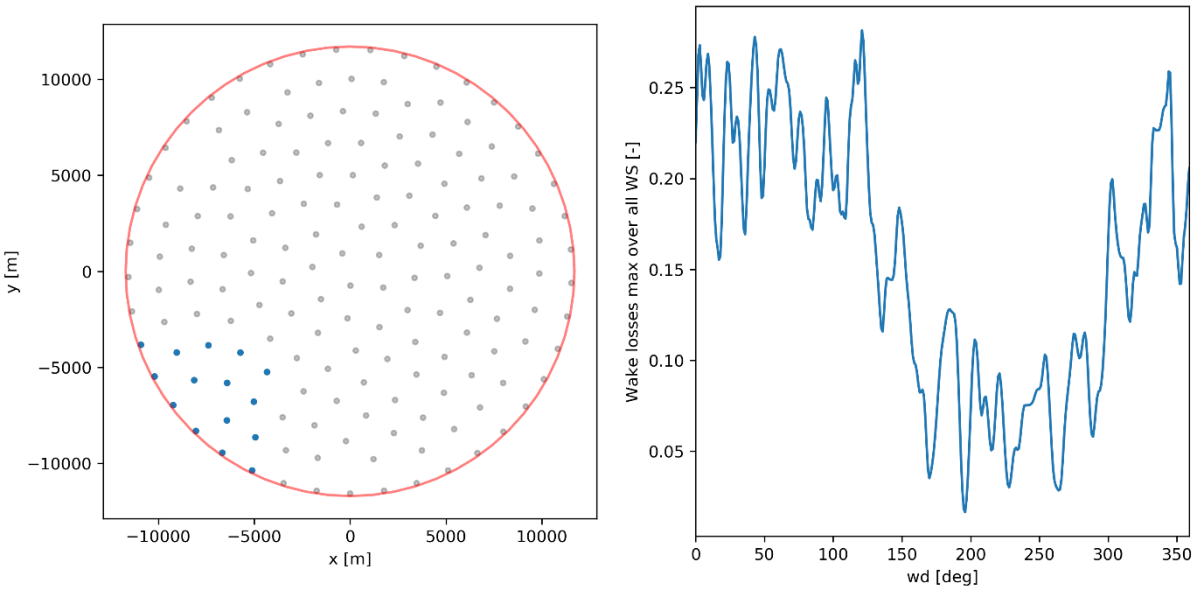


Figure 1: Wake losses from a farm (turbines in blue, on the left) within a large 3GW energy hub.

This work introduces a machine learning surrogate model that generalizes the large-scale wake losses and can be easily integrated into energy system optimization. This helps to build a robust strategy to achieve cost-efficient exploitation of offshore wind resources by balancing the added costs of electric infrastructure and the need for larger installation areas to mitigate wake losses.
A deep neural network (DNN) regression model is trained to predict the farm to farm wake losses using a databse of model simulations as training. The farm to farm interaction is defined as a wind speed reduction factor (s_WL) and it has the following analytical dependencies:
s_WL = f (WSi, WSj, WDi, WDj, dij, Ai, Aj, Ni, Nj, 1/L)
where WS, WD are the averaged representative wind speed and wind direction in each of both farms, dij is the distance between the farms (in averaged rotor diameters), Ai and Aj are the areas of each farm, Ni and Nj are their number of turbines, and 1/L is the inverse of the Monin-Obukovh length.

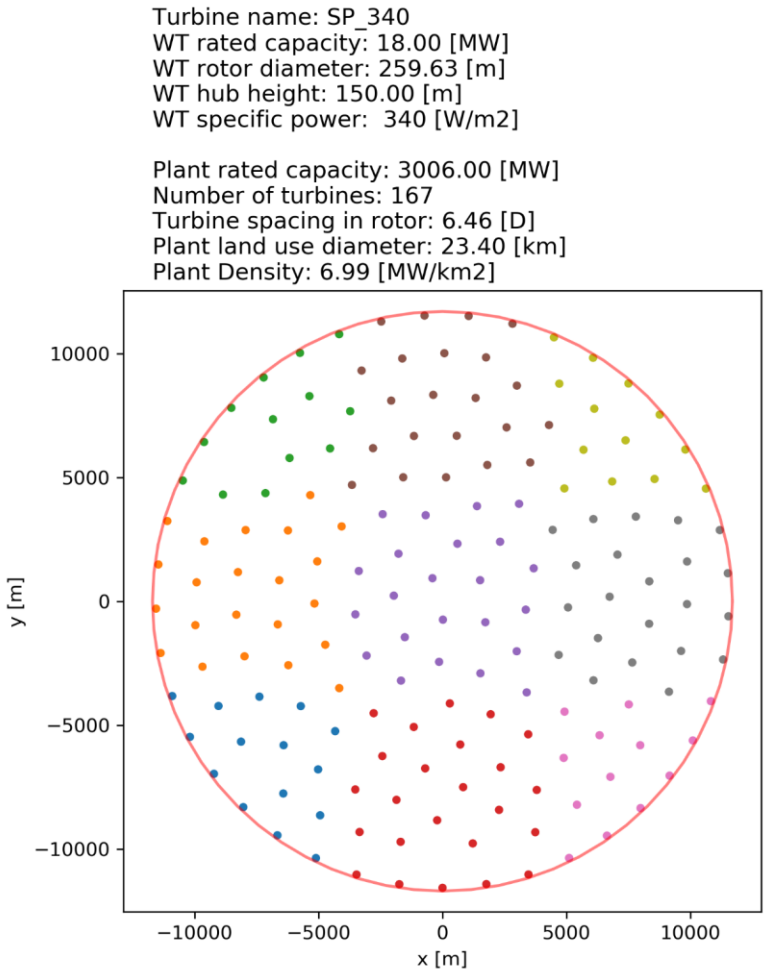


Figure 2: Layout of a large 3GW energy hub.

The s_WL factor predicts how much wind speed reduction will be experience in the downstream farm for a given flow case. This model is evaluated over 30yr of mesoscale reanalysis time-series given in ERA5, and using a multi-dimensional plant power curve for each farm in the energy hub can simulate the energy generation time-series for varying energy hub designs without computational effort.

In this study the surrogate is compared against several cases: (1) Nysted and Rødsand farm to farm interaction, and (2) the existing simulation of WRF with parameterized wind farm wakes over Denmark [Imberger et al].

References:

Volker, P. J. H., Badger, J., Hahmann, A. N., and Ott, S., 2015, The Explicit Wake Parametrisation V1.0: a wind farm parametrisation in the mesoscale model WRF, Geoscientific Model Development, 8, 3715–3731, https://doi.org/10.5194/gmd-8-3715-2015

Agora-Energiewende, 2020. Making the most of offshore wind: Re-evaluating the potential of offshore wind in the German North Sea. Agora Energiewende, pp.1-81.

Imberger, M., Larsén, X.G. and Davis, N., 2019, January. Offshore wind farm wakes in global circulation model MPAS compared with WRF and measurements. In Geophysical Research Abstracts (Vol. 21).

Irregular versus regular: a quantitative assessment of offshore wind park layout performance

Maaike Sickler[1,*], Bart Ummels[1,2], Michiel Zaaijer[2], Roland Schmehl[2], and Katherine Dykes[3]
[1]Ventolines B.V.
[2]Delft University of Technology
[3]DTU Wind Energy
*Presenting author

Keywords: Wind Park Layout | Wind Park Performance | Irregular Layout

To increase the energy yield in offshore wind farms, a general trend from regular to irregular wind farm layouts is observed over time. The wind turbine generator (WTG) locations in the wind farm drive the wake losses, fatigue loads, inter-array cable length and many more factors which influence the profitability of the project. Yield optimizing algorithms mostly result in irregular wind farm layouts. However, this does not mean the business case of the wind energy project has been optimized from a levelized cost of energy or net present value perspective. In this presentation a comparative case study is presented to quantify the effect of the farm layout on the overall performance of offshore wind projects [1]. The performance of both regular and irregular wind farm layouts is assessed for the Borssele site on the basis of selected performance indicator groups relating to power performance and wake-induced fatigue.
The power performance is evaluated using WindPRO [2]. It is found that the irregular wind farm layout has a higher annual energy and a higher persistence to wind direction changes than regular layouts. A higher persistence to wind direction means that the power output is less sensitive to fluctuations in wind direction. With a regular layout, modest changes in wind direction may have a significant impact on power production. This characteristic increases the predictability of the output, which may increase the market value of offshore wind power and/or decrease the imbalance costs on the electricity market.
The Frandsen model [3] is implemented to calculate the effective turbulence levels on individual turbines, which is translated to wake-induced tower fatigue and an increase in tower-wall thickness.
In industry, offshore WTG OEMs typically design a single tower per project based on the worst-case fatigue location, which means the irregular wind farm layout results in an increase in steel consumption for the tower design. Irregular wind farm layouts typically include a limited number of wind turbine locations very close to each other (around three rotor diameters). It is found that for those locations, wake-induced fatigue may be around 24% higher than in regular wind farm layouts.

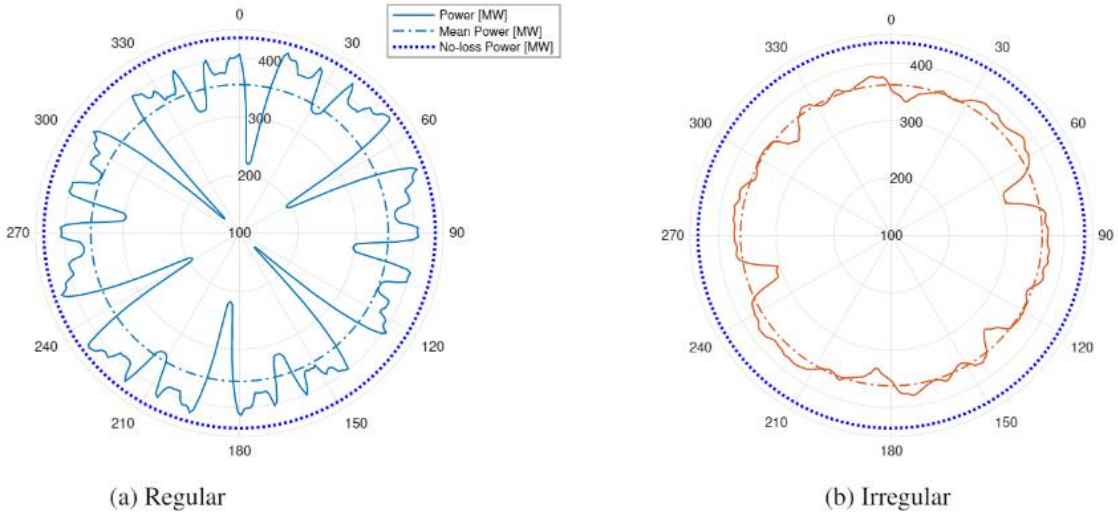


Figure 1: Power output of the regular and irregular wind farm subjected to a mean wind speed of 9.5 m/s in steps of 1°

For fatigue-driven wind turbine tower designs, this can be related to an increase in the tower wall thickness. Therefore, this presentation investigates the application of a lower limit on inter-turbine spacing to ameliorate the negative effect of wakes on fatigue. Changes in a few turbine positions with high fatigue levels within an already 'optimized' irregular layout can potentially lead to a decrease of 20% of tower material use. As the optimization also appears to slightly improve yield, the overall business case of the project is improved.
A sensitivity analysis is performed confirming that the results for wakes, tower steel and persistence to wind direction apply generally, as is shown for multiple regular and irregular wind farm cases.

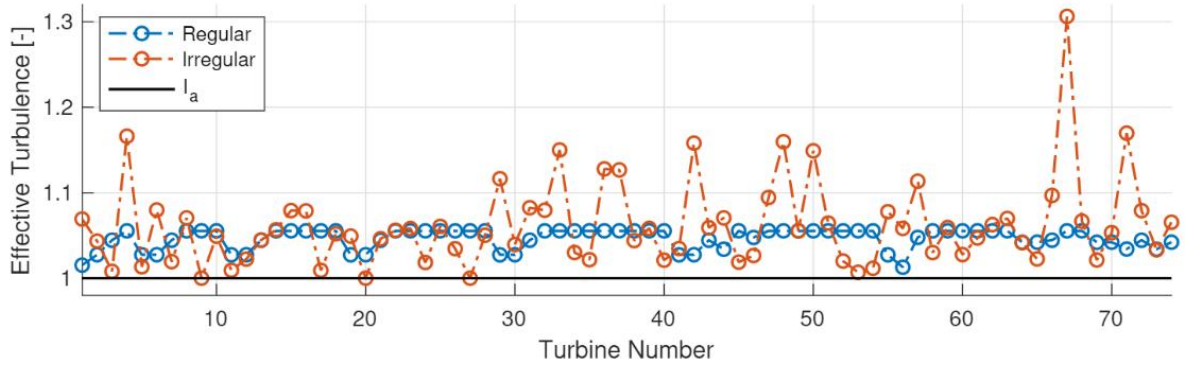


Figure 2: Fraction of effective turbulence divided by the ambient turbulence Ia for each turbine in the regular (blue) and irregular (red) wind farm layout due to wake added turbulence using Frandsen [3].

The presentation concludes that while irregular layouts do tend to produce higher energy production, they can also result in higher fatigue on support structures and larger ramps in power production with changing wind directions. Future work will further investigate the ability to impose constraints on irregular layout designs (such as minimum turbine spacing) in order to mitigate these effects and improve overall plant performance and lower overall plant costs.

References:
[1] M. Sickler: Offshore Wind Farm Optimisation: A Comparison of Performance between Regular and Irregular Wind Turbine Layouts. MSc Thesis, Delft University of Technology, 2020. http://resolver.tudelft.nl/uuid:c7d52141-1218-4754-bf16-8cbb1a46fee0
[2] EMD International A/S: WindPRO user manual, 2019.
[3] S.T. Frandsen: Turbulence and turbulence- generated structural loading in wind turbine clusters, Technical Report Risoe-R, No. 1188(EN), 2007.

Regular Session: Mesoscale Modeling and Forecasting (I)

Short Term Power Forecasts for Distributed Wind Turbines Using Support Vector Regression

Ghali Yakoub*, Sathyajith Mathew, and Joao Leal
University of Agder
*Presenting author

Keywords: wind power forecasting | distributed wind energy | support vector regression

The global installed capacity of the distributed wind energy systems (DWES) is steadily increasing (Orrell et al., 2020). These systems, ranging from few kilowatts to megawatts in size, are increasingly integrated with the microgrids in the recent years (Foster et al., 2020). For the efficient management of such microgrids, variations in energy contributed by DWES in different time scales due to the stochastic nature of wind, have to be quantified. Accurate wind power forecasts are required to understand these power fluctuations and manage the resulting uncertainties. However, wind power forecasting systems available today are mostly tailored for large wind farms. In this paper, we propose a point power forecasting scheme, specifically for distributed wind energy systems.

The forecasting horizons considered are hour-ahead (t + 1) and day-ahead (t + 36), which align with the Nord pool`s energy market requirements. The forecasting system integrates two sub-models based on Support Vector Regression: (i) A downscaling model proposed by the authors (Ghali et.al., 2020), which downscales the coarser wind forecasts from Numerical Weather Predictions (NWP) to finer resolutions, corresponding to the coordinates of the wind turbine hub. (ii) A turbine performance model, which predicts the power generated at these wind velocities 'felt' by the turbine. Instead of the conventional power curves, SVR based site-specific performance models are used to accurately define the power response of the turbines.

The proposed point wind power forecasting system has been implemented to a 5-kW wind turbine in Smøla, Norway. The relevant weather parameters from the METCoOp Ensemble Prediction System (MEPS) (spatial resolution of 2.5 km) and the corresponding on-site wind measurements from a meteorological mast adjacent to the turbine were used to develop the downscaling model. With Normalized Root Mean Square Errors (NRMSEs) of 0.054 and 0.098 respectively for the hour-ahead and day-ahead wind forecasts, the model could perform well in enhancing the resolution of NWP.

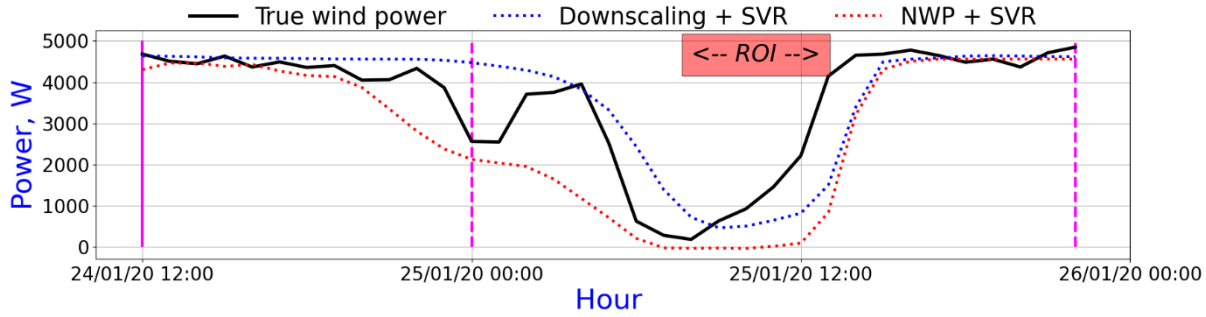


Figure 1a): Day ahead wind power forecasts compared with real observations

The turbine performance model was developed using the one year generation data collected from the site. The wind velocity measured at the hub height of the turbine and the corresponding power were used to develop this SVR based turbine performance model 'power curve'. As evident from the high R2 of 0.985, the model could accurately capture the velocity-power characteristics of the turbine.

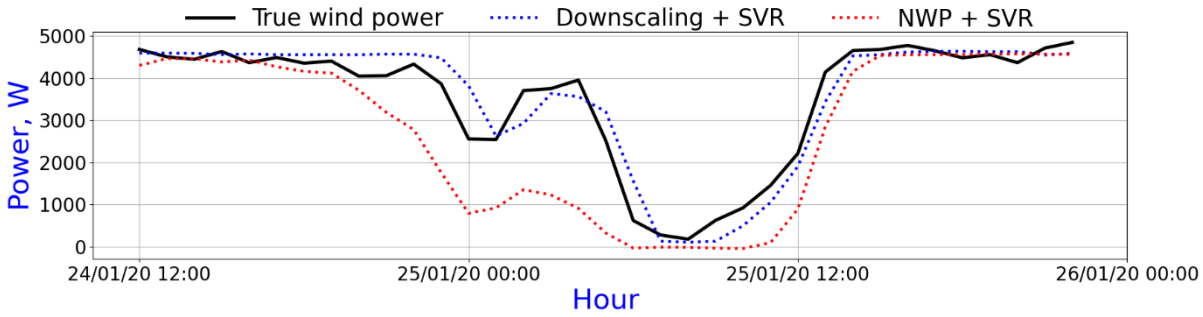


Figure 1b): Hour-ahead wind power forecasts compared with real observations

Both the above sub-models i.e. power curve and wind speed downscaling, were integrated for developing the end-to-end point forecasting system. Performances of this system in hour-ahead and day-ahead wind power forecasts are shown in Fig. 1 (a) and (b) respectively. The NRMSEs for the hour-ahead and day-ahead power forecasts are 0.121 and 0.240, respectively. In both cases, the proposed approach with the 'downscaled wind profile' improved the accuracy of wind power forecasting significantly, compared to the option with the NWP wind predictions.

References:

[1] Orrell et al. (2020) 'Distributed Wind Data Summary', Pacific Northwest National Laboratory, Report No. PNNL-30168.
[2] Yakoub, Mathew and Leal. (2020) 'Downscaling and improving the wind forecasts from NWP for wind energy applications using support vector regression', Journal of Physics: Conference Series, 1618: 1-11.
[3] Foster et al. (2020) 'The "perfect storm" for distributed wind markets', Renewable Energy, 145: 1033-1039.

Correlations in NEWA time series: evaluation and model sensitivity

Graziela Luzia*, Andrea N. Hahmann, and Matti Juhani Koivisto
Technical University of Denmark
*Presenting author

Keywords: time series | NEWA | correlations | wind speed | mesoscale modelling

As wind energy increases its share of total energy generation, the importance of meteorological data representing variability in wind becomes crucial. In power systems, wind variability impacts, e.g., optimal energy system planning (Gea-Bermúdez et al., 2020), power system ramp rates and vulnerability to storm shutdowns (Murcia Leon et al., 2020), and available voltage stability support (Souxes, Granitsas and Vournas, 2019). Wind output from various weather prediction models perform differently in different applications and, therefore, distinct evaluations are required. For example, for a wind resource atlas, accurate wind speed distributions are necessary; for wind power forecasting, accurate timing is necessary. Power system modelling applications, on the other hand, require an accurate representation of wind's temporal dependencies (at least on hourly, or even higher temporal resolution) and correlations between different locations.

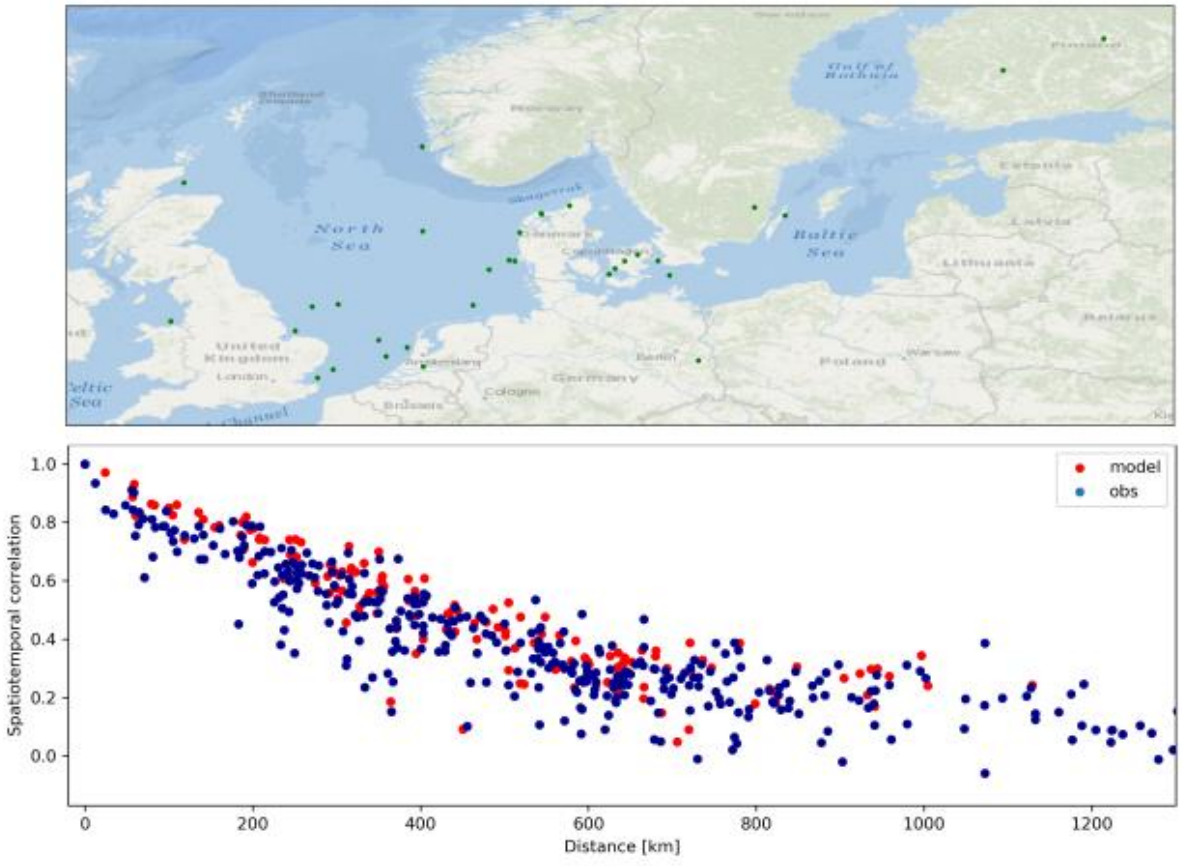


Figure 1: (lower) Example of comparison between measurement (obs) and NEWA (model) wind speed spatiotemporal correlation versus distance for each pair of sites (upper).

In this work we evaluate the New European Wind Atlas (NEWA, Hahmann et al., 2020; Dörenkämper et al., 2020) and perform model sensitivity analysis, focusing on the time series characteristics of the data. First, we compare extracted time series from some of the NEWA ensemble members presented in Hahmann et al. (2020) with wind speed observational data provided by different sources, at height closest to 100 m. As the atlas is based on the open-source model Weather and Forecast Research (WRF, Skamarock et al., 2008) and all codes and tables are freely available, additional tests in the model setup and physics parametrizations are carried

out. We compare all the different NEWA/WRF simulations in their accuracy in representing correlations 1) between measured and simulated data; and 2) on modelling the spatiotemporal correlations observed in measured data (e.g., Figure 1). For 2), we assess temporal correlations (autocorrelations) and spatial correlations (correlations between locations). Validation metrics for time series properties are applied for comparing the wind speed simulations on multiple locations over Northern Europe. These comparisons add to the previous work on validating NEWA in modelling the distributional properties of wind speeds in Europe (Dörenkämper et al., 2020).

References:

Dörenkämper, M., Olsen, B., Witha, B., Hahmann, A. et al., 2020. The Making of the New European Wind Atlas – Part 2: Production and evaluation. Geoscientific Model Development, 13(10), pp. 5079-5102, doi: https://doi.org/10.5194/gmd-13-5079-2020

Gea-Bermúdez, J., Pade, L., Koivisto, M. and Ravn, H., 2020. Optimal generation and transmission development of the North Sea region: Impact of grid architecture and planning horizon. Energy, 191, 116512, doi: https://doi.org/10.1016/j.energy.2019.116512

Hahmann, A., Sīle, T., Witha, B., Davis, N., Dörenkämper, M. et al., 2020. The making of the New European Wind Atlas – Part 1: Model sensitivity. Geoscientific Model Development, 13(10), pp. 5053-5078, doi: https://doi.org/10.5194/gmd-13-5053-2020

Murcia Leon, J., Koivisto, M., Sørensen, P. and Magnant, P., 2020. Power fluctuations in high installation density offshore wind fleets. Wind Energy Science, Preprint, doi: https://doi.org/10.5194/wes-2020-95

Skamarock, W., Klemp, J., Dudhia, J., Gill, D. et al., 2008. A Description of the Advanced Research WRF Version 3, Tech. Rep. NCAR/TN–475+STR, National Center for Atmospheric Research, doi: http://dx.doi.org/10.5065/D68S4MVH

Souxes, T., Granitsas, I. and Vournas, C., 2019. Effect of stochasticity on voltage stability support provided by wind farms: Application to the Hellenic interconnected system. Electric Power Systems Research, 170, pp.48-56, doi: https://doi.org/10.1016/j.epsr.2019.01.007

Impact study of WFIP2 results on an operational wind energy forecasting system

Gorka Pérez-Landa[1,*], Sergio De María Casado[1], Begoña Luaces[1], Markel García Diez[2], Antonio Pérez[2], and Luís Prieto Godino[1]
[1]IBERDROLA RENEWABLES
[2]Predictia
[*]Presenting author

Keywords: operational wind power forecast | numerical weather prediction | machine learning | complex terrain | mesoscale

MeteoFlow is the renewable energy forecasting system which provides operational predictions for the IBERDROLA 372 wind farms (20GW of installed capacity worldwide). Few of them, 12 wind farms with 1.4 GW of installed capacity, are located in the Columbia River Gorge in eastern Oregon-Washington (USA) as Figure 1 shows, where the 2nd Wind Forecast Improvement Project (WFIP2) took place between 2015 and 2017. The availability of an operational forecasting system in the region is an excellent opportunity to test the benefits of the modelling improvements identified in WFIP2 against an operational system of the wind industry like MeteoFlow.
Our forecast system integrates atmospheric forecast from operational models available in the area with real time wind production by means of machine learning techniques. One of these models is the version 3.3.1 of WRF (1), which run four times per day in our computer resources forced by GFS and will be considered as the benchmark of this study.
WFIP2 is a project sponsored by the USA Department of Energy and NOAA, with the objective of the improvement of weather prediction modelling in complex terrain (2). An intensive field campaign took place (3) and important efforts were made to characterize complex terrain atmospheric processes in the area (4) and validating (5) and improving (6, 7) weather prediction models.
During WFIP2, a daily brief synopsis of the weather was written, assessing the significance of the key phenomena and their impact on wind power generation (3). The availability of this event log allowed us to select 50 days representatives of the main processes relevant for wind energy in the area. Thus, a sensitivity test was performed simulating these 50 days with three different parameterizations and with grid lengths going to 1.5 or 0.75 km, allowing to identify an optimal configuration. Results were evaluated against wind speed of each wind farm (an average of the nacelle wind measurements).

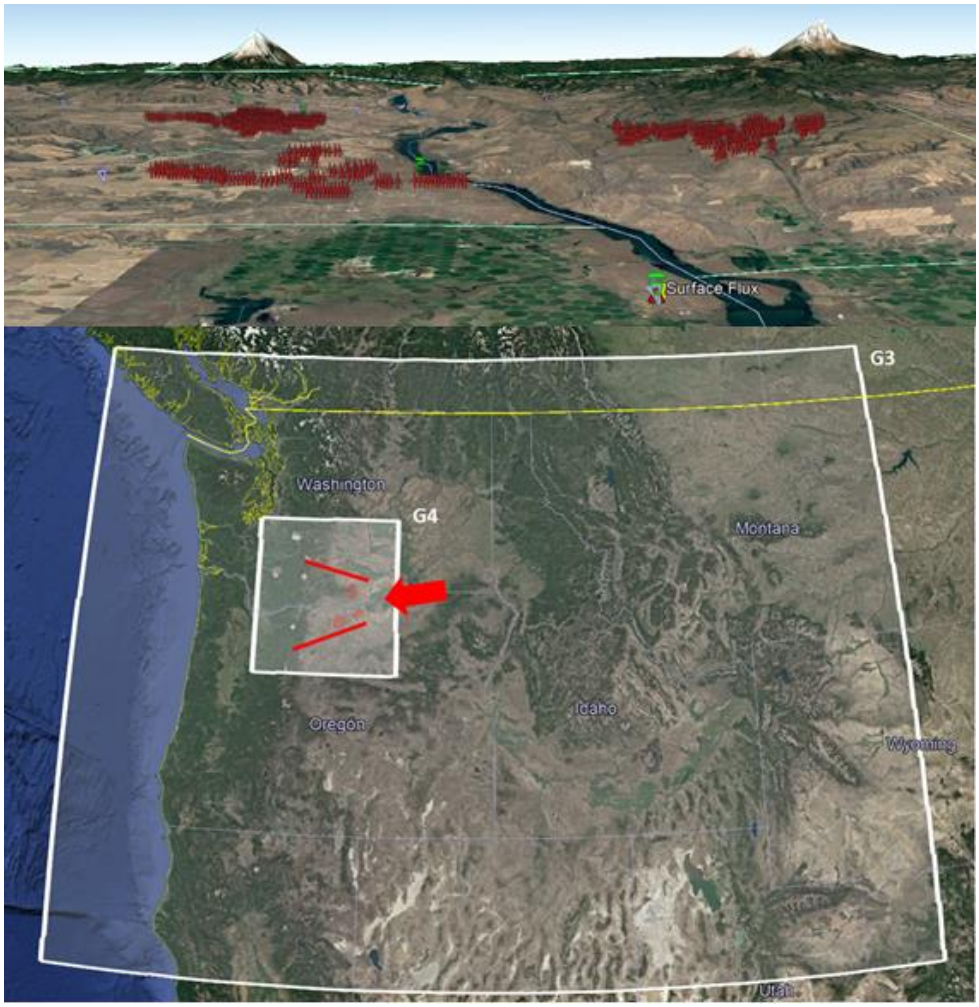


Figure 1: Bottom: white lines are G4 (4km) and G3 (1.33km) domains, red shaded areas show the 3 main clusters of wind farms and the red arrow and lines show de perspective of the view showed on the top. Top: 3D view of Columbia Gorge with the turbines of the 12 wind farms (red), main wind profiler sensors of WFIP2 (lidars in green, sodars in purple and radars in red) and mountains Hood and Adams.

Then a WFIP2 EXP configuration (see Table 2 in 7) was selected as the best option, but changing RUC land surface model by Noah-MP LSM (1) and without wind farm drag parameterization. It was found that the results for the 0.75 km domain were very similar to the larger grid length. Therefore, four telescopic domains using grid cells of 36, 12, 4 and 1.33 km were setup (Figure 1), with domain sizes compatible with an affordable operational approach. This configuration was employed to simulate 12 hours ahead forecast for one year period, using GFS- forecast data as input.

The results showed an improvement against the benchmark (our operational WRF 3.3.1) of a 28% in the hourly wind speed NMAE for 1.33km and 16% for 4km grid, which was more evident during winter (Figure 2).

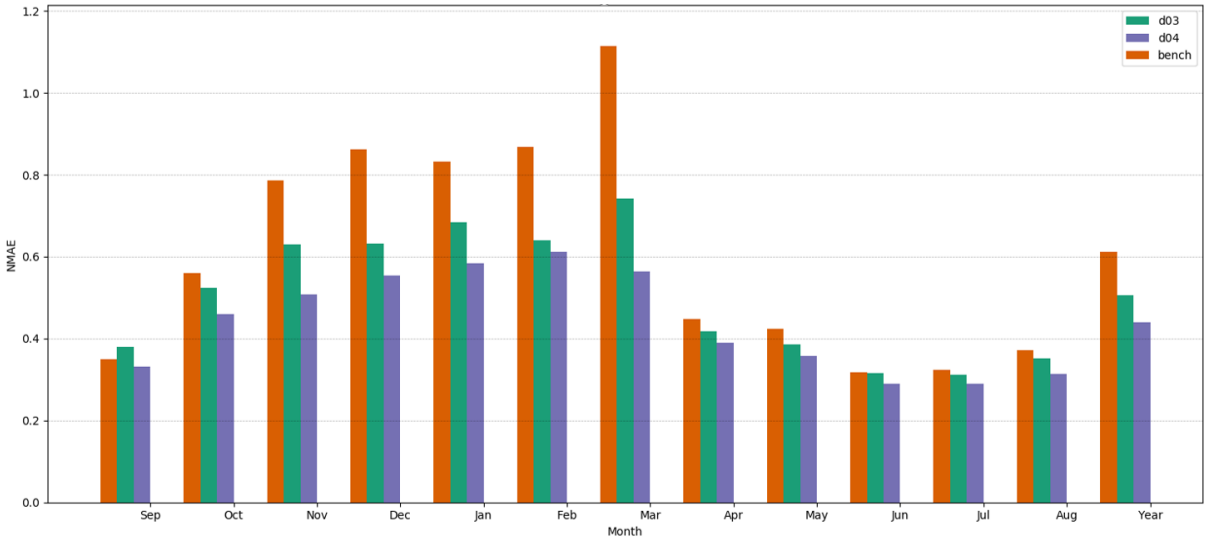


Figure 2: Hourly NMAE by month and during the whole year 2018-Sep to 2019-Aug for benchmark (WRF 3.3.1), d03 (WRF 4.2.1 domain with 4km grid length) and d04 (1.33km grig length).

Finally, the new improved configuration is run for three years in a 4 days ahead approach to be used in the machine learning training employed in MeteoFlow. Two trainings will be done: one with our current WRF3.3.1 operational version and the second with the improved configuration and both will be evaluated against wind energy measurements.

Thus, the presentation will show the results of the evaluation of WRF improvements forecasting wind, but also wind energy after applying machine learning techniques and real time in an operational context, which is expected to be interesting for both, the scientific and wind industry communities.

References:

(1) Jordan G. Powers and Coauthors, 2017: The Weather Research and Forecasting Model: Overview, System Efforts, and Future Directions. Bull. Amer. Meteor. Soc., 98 (8): 1717–1737.

(2) Shaw, W. J., and Coauthors 2019: The Second Wind Forecast Improvement Project (WFIP2): General overview. Bull. Amer. Meteor. Soc., 100, 1687–1699.

(3) Wilczak, J., and Coauthors, 2019b: The Second Wind Forecast Improvement Project (WFIP2): Observational field campaign. Bull. Amer. Meteor. Soc., 100, 1701–1723.

(4) McCaffrey, Katherine L and Coauthors,2019: Identification and Characterization of Persistent Cold Pool Events from Temperature and Wind Profilers in the Columbia River Basin. J. Appl. Meteor. Climatol. 58 (12): 2533–2551.

(5) Y. L. Pichugina and Coauthors, 2019: Spatial Variability of Winds and HRRR–NCEP Model Error Statistics at Three Doppler-Lidar Sites in the Wind-Energy Generation Region of the Columbia River Basin, J. Appl. Meteor. Climatol. 58 (8): 1633–1656.

(6) Y. L. Pichugina and Coauthors, 2019: Evaluating the WFIP2 Updates to the HRRR Model Using Scanning Doppler Lidar Measurements in the Complex Terrain of the Columbia River Basin, J. Renew. Sust. Energy, 12(4), 043301.

(7) Olson, and Coauthors, 2019: "Improving wind energy forecasting through numerical weather prediction model development," Bull. Am. Meteorol. Soc. 100, 2201–2220.

Multiscale stochastic refinement and stochastic interpolation of sparse time signals and fields

Jan Friedrich, Michael Sinhuber, and Joachim Peinke
ForWind - Centre for Wind Energy Research

Keywords: Intermittency | Synthetic Turbulence | Synthetic Wind fields | Stochastic Interpolation

In earth sciences, astrophysics or turbulent environments such as wind parks, many relevant physical quantities fluctuate in a non-Gaussian fashion. This oftentimes imposes major challenges for the acquisition of finely-resolved measurements which would be necessary for a detailed analysis or modeling of the underlying physical processes or as a foundation for machine learning training. E.g., comprehensive assessments of operational performance and maintenance levels (and ultimately cost efficiency) of wind parks, are in strong need of an accurate determination of wind speeds with a temporal resolution of approximately 0.1 seconds. As of today, however, industrial standards record solely the statistics of ten-minute-means of wind speed and turbulence intensity. It is therefore, of the utmost importance to develop methods that allow for an accurate reconstructions of wind fields from sparse wind data.
In this talk, we present paths to generate synthetic signals from sparsely sampled data points, based on stochastic properties of the original field as well as elementary scaling properties. For the case that the underlying field obeys Markov properties in scale, stochastic refinement approaches prove fruitful to generate synthetic data. A more general approach relies on a generalization of fractional Brownian bridges and provides an optimization method for determining the scaling exponent of the underlying fluctuating process. We test both approaches on experimental measurements of high-Reynolds number flows and - for the case of fractional Brownian bridges - uncover limitations regarding the occurrence of extreme events in the signal which can be related to fluctuations of the optimal Hurst exponent. Correctly reproducing these fluctuation imposes mathematical and computational challenges which might improve our current understanding of non-Gaussian stochastic processes considerably. Furthermore, the proposed methods can directly be applied in order to generate finely resolved wind fields.

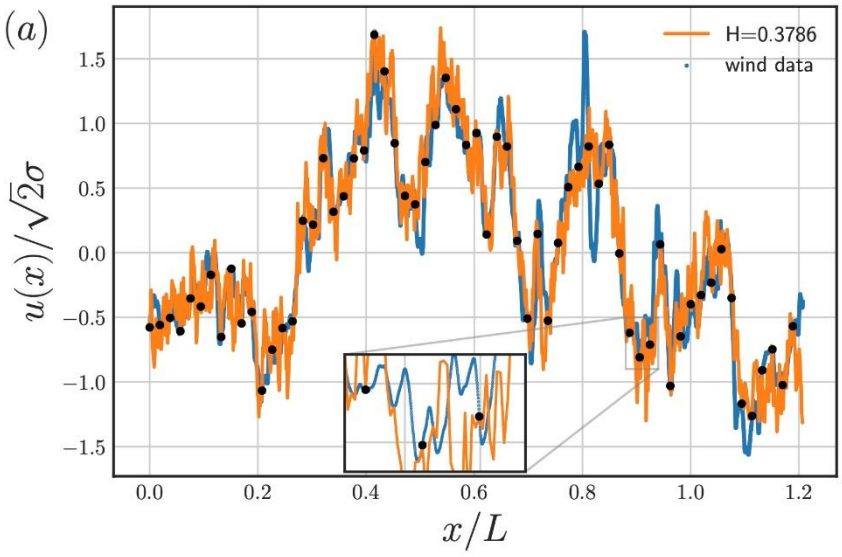


Figure 1: Turbulent velocity field measurements (blue) in a von Karman experiment using normal Helium and interpolated signal using a multipoint fractional Brownian bridge (orange).

Potential applications of the proposed method range from better statistical estimates for power output and fatigue loads on individual wind turbines to mesoscale models of meteorologic turbulence simulations. E.g.,

the stochastic interpolation might be used to resolve small time scales of individual wind turbine measurements, for instance from cup anemometers. This may ultimately lead to a more genuine assessment of past (for instance, for the past 5 years) extreme fatigue loads on rotor and blades which may help preventing unscheduled maintenance. Furthermore, spatiotemporal wind fields of entire wind plants might be reconstructed on the basis of simultaneous wind speed measurements at multiple space points, for example by laser doppler anemometry (LIDAR).
We also discuss the reconstruction of Eulerian velocity fields (in a fixed frame of reference) from a couple of Lagrangian trajectories by means of spatiotemporal fractional Brownian bridge processes.

References:
J. Friedrich, S. Gallon, A. Pumir, R. Grauer, Phys. Rev. Lett. 125 (17), 170602

How do mesoscale weather systems interact with off-shore wind farms: A study for the Kattegat (Denmark, Sweden) with the mesoscale model COSMO-CLM and satellite scatterometer data

Jérôme Neirynck[2,*], Jonas Van de Walle[2], Ad Stoffelen[1], Johan Meyers[2], and Nicole van Lipzig[2]
[1]KNMI
[2]Katholieke Universiteit Leuven
[*]Presenting author

Keywords: Mesoscale weather effects | Intereaction | Resource assessment

Accurately determining the wind speed distribution is indispensable for a thorough wind resource assessment of a wind farm. Mesoscale weather systems are the main cause of variability in wind speed, and consequently wind farm energy production in the Kattegat region, the sea straight located between Denmark and Sweden. In particular, this sea strait has an irregularly shaped coastline, thereby exhibiting strong coastal effects on the wind fields. One of the main wind farms in the region is the Anholt wind farm, located just 21 km away from the Danish coast, providing the opportunity to study mesoscale weather systems and their interactions with wind farms.
Since these mesoscale weather systems are not sufficiently resolved in global reanalysis data such as ERA5, regional climate modelling can support the quantification of the variability in wind speed.
Previous studies have already shown that convective cells, gravity waves and sea/land breeze systems have a major impact on the surface wind speed variability, but how these weather effects interact with wind farms is lacking in these studies. In this study we use a high resolution (horizontal grid resolution of 1.5 km) mesoscale atmospheric model (COSMO-CLM) to better understand how variability in wind speed is related to mesoscale weather systems in the Kattegat region. Moreover we aim at studying how wind farms interact with these mesoscale weather systems.

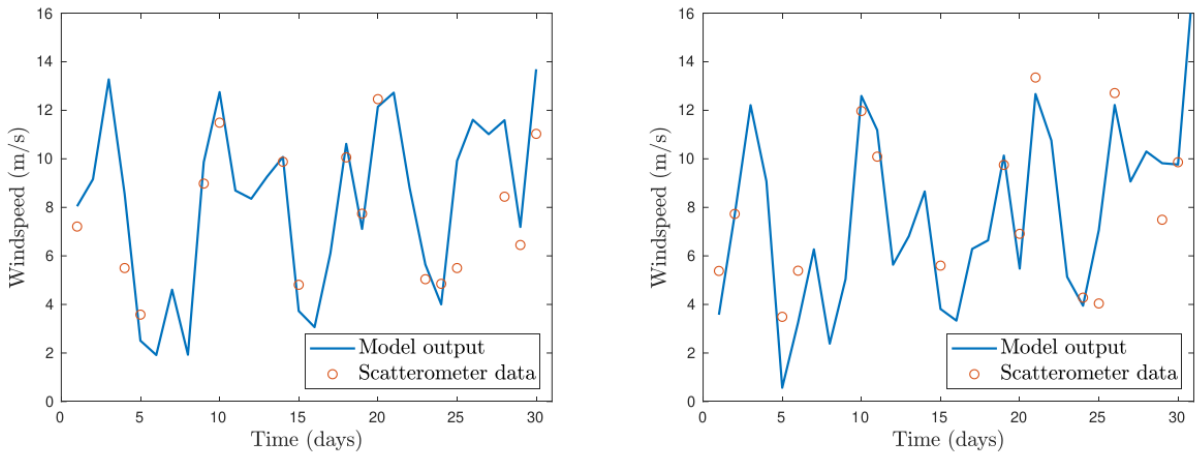
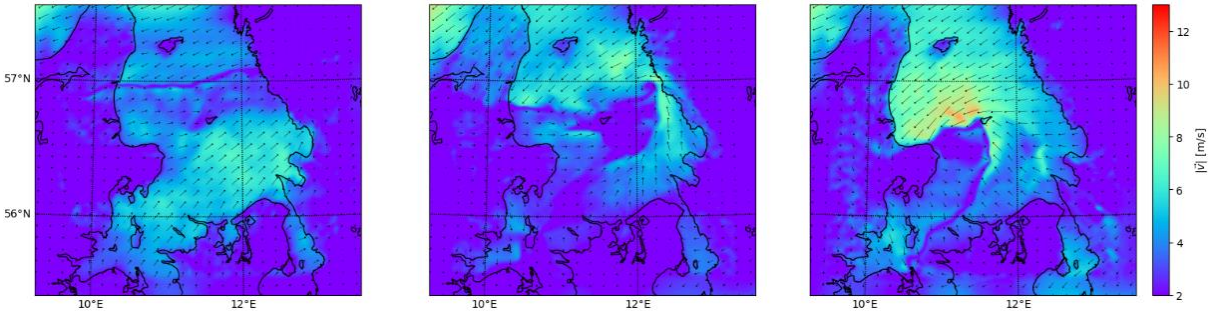


Figure 1: Model output of a surface wind speed compared with the scatterometer data at the point N56.4375°, E11.9375°.

In order to validate our simulation we have compared the model output with scatterometer data from the Metop-A weather satellite. A time series of the surface wind speed at the point indicated in figure 1 of the model is plotted against scatterometer data. Since the simulation has a higher resolution than the scatterometer data, the spatial average of the model output is taken over all the points corresponding to the single scatterometer data pixel. Because the Metop-A satellite doesn't cover the Kattegat every day, there are some days missing from the scatterometer data. The model data satisfactorily clearly represents the wind evolution measured by the scatterometer satellite.



(a) 16h 15/01/2013 (b) 10h 16/01/2013 (c) 20h 16/01/2013

Figure 2: Model output of the surface wind speed of a storm over the Kattegat. (a) shows the front. As the system evolves further, a region with faster wind speeds develops to the North West of the isle of Anholt, as can be seen in (c).

Output of our simulations show substantial temporal and spatial variability, mainly related to frontal systems travelling across the Kattegat, as can be seen in figure 2. In the presentation we will examine the effect of spectral nudging on the surface wind speed variability, investigate downscaling strategies and study the interactions of mesoscale weather systems with the Anholt wind farm. The simulation period will be extended to a full year in order to chart the seasonal trends in wind speed variability. As more and more wind farms are being constructed it becomes important to study the two way interactions between wind farms and mesoscale weather systems for a more accurate resource assessment concerning future wind farms and this is a first step towards this overarching goal.

The influence of free-atmosphere wave reflection on wind-farm gravity-wave interaction

Koen Devesse*, and Johan Meyers
Katholieke Universiteit Leuven
*Presenting author

Keywords: Gravity waves | Atmospheric Boundary Layer | Mesoscale effects

Recent research suggests that wind farms can trigger atmospheric gravity waves, which reduce the upstream flow velocity and the power output of a wind farm. Allaerts and Meyers (2019) proposed a simplified Atmospheric Perturbation Model (APM) focused on the interaction between wind turbines and gravity waves. While the model is not as accurate and flexible in use as eg. Large-Eddy Simulations (LES) or Reynolds-Averaged Navier-Stokes (RANS) methods, it is far less computationally demanding. As in earlier work by Smith (2010), the model explicitly simulates the flow in the Atmospheric Boundary Layer (ABL). The free atmosphere is represented by a boundary condition at the top of the ABL, which links variations in ABL height to the pressure gradients induced by the corresponding gravity waves.
Currently, the APM can only describe uniformly stratified free atmospheres, which strongly restricts the atmospheric conditions that can be represented. This work applies the APM to flow profiles that vary with altitude, and studies how this height-dependence changes the interaction between the ABL flow and gravity waves. This extension is validated with relevant mountain wave studies.

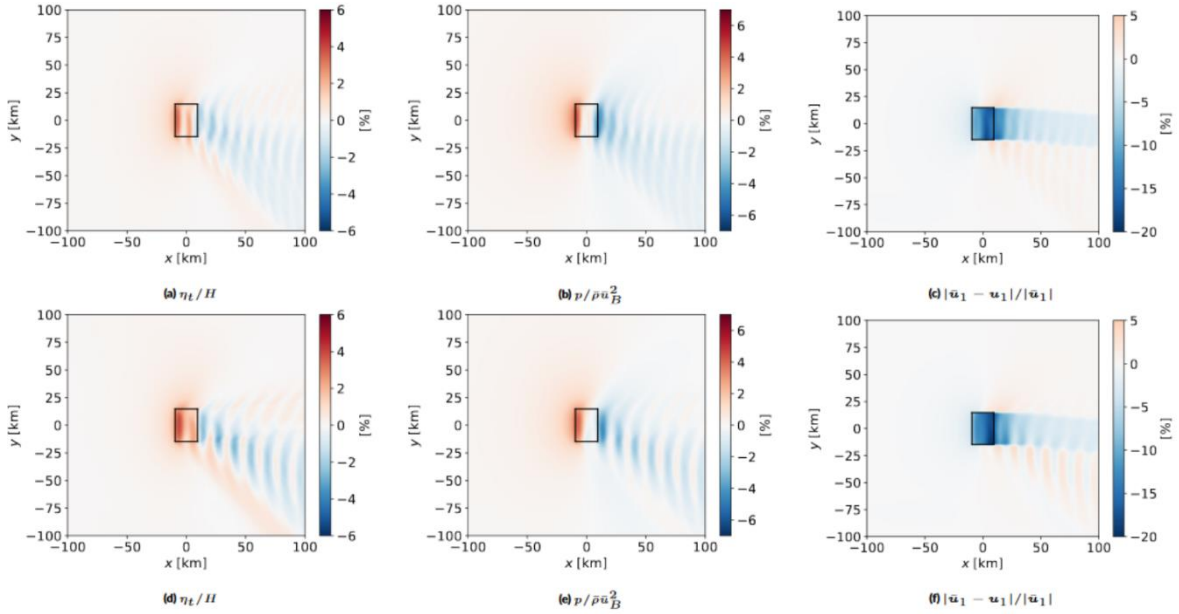


Figure 1: Resonant lee waves in the ABL.

We find that the appearance of gravity wave resonance plays an important role in the interaction between the ABL and the free atmosphere. The variations in the atmospheric properties can cause wave reflection, which leads to constructive and destructive interference in the wave patterns. When resonance appears, the pressure feedback in the ABL increases drastically, and as a result, the resonant wavenumbers are strongly dampened in the ABL flow. In contrast, destructive interference in the upper atmosphere causes the pressure feedback associated with perturbations at these wavenumbers to become minimal. The flow in the ABL can then more easily go into resonance itself, since there is no more damping, as illustrated in Figure 1.

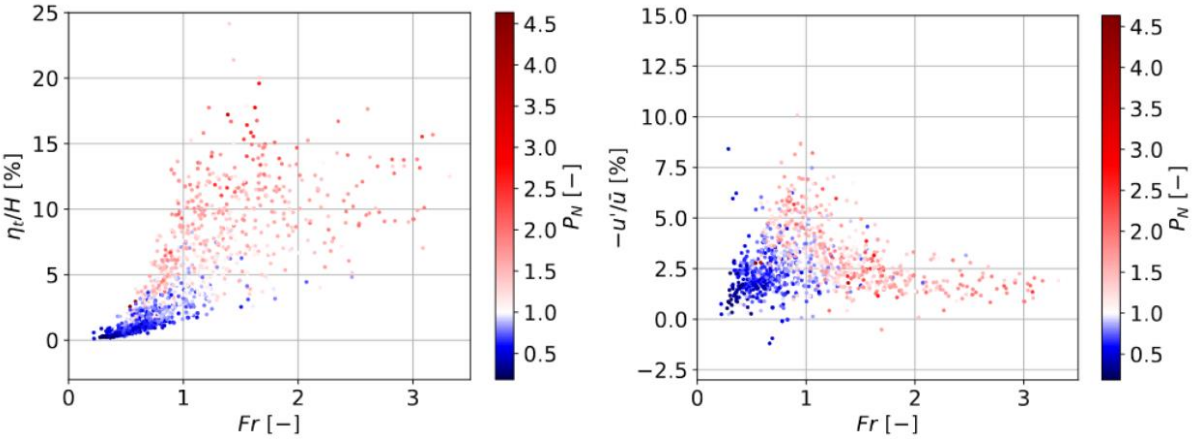


Figure 2: The governing parameters Fr and P_N still describe the general behaviour of the flow

To determine the overall impact of the free atmosphere's height-dependence on wind farm operation, the extended model is used to simulate one year of operation of the Belgian-Dutch windfarm cluster. When only variations in the first 5 km of the upper atmosphere are taken into account, we find that the impact of height-dependence on individual flow cases is often of the same order of magnitude as the total flow perturbation. In roughly 10% of the analysed flows, the difference in upstream velocity reduction between uniform and height-dependent free atmospheres is more than 50%. However, the average impact of height-dependence over all flow cases is small. The parameters that govern the model behaviour when the upper atmosphere is uniform, still predict the general trends in power output fairly accurately, as seen in Figure 2. This might change if variations in stratification strength and wind speed are taken into account up to the tropopause. The strong increase in the stratification strength in the stratosphere may facilitate gravity wave resonance.

References:

Allaerts, D. and Meyers, J.: Sensitivity and feedback of wind-farm induced gravity waves., Journal of fluid mechanics, 862, 990–1028, 2019.

Smith, R. B.: Gravity wave effects on wind farm efficiency, Wind Energy, 13, 449–458, 2010

Regular Session: Mesoscale Modeling and Forecasting (II)

Satellite-based estimation of roughness lengths and displacement heights for wind resource modelling

Rogier Floors[1], Merete Badger[1], Finn-Hendrik Permien[2], and Kenneth Grogan[3]
[1]Technical University of Denmark
[2]Siemens Gamesa
[3]DHI GRAS

Keywords: Forest | Roughness length | Land cover | Wind resource | Displacement length

Low levelized cost of energy in onshore wind demonstrates that renewable is competitive with fossil fuel generation. 90 percent of the global added wind energy capacity in 2019 is installed on land (Global Wind Energy Council 2019). That amounts to 95% of the installed global wind energy capacity (International Renewable Energy Agency 2019). In the temperate climates of northern Europe, a vast amount of the land surface is covered by forest. The exploitation of wind power within forests has become widespread and 2GW was installed in Sweden and Finland in 2019 (Enevoldsen, 2016, WindEurope 2019). At the same time, new airborne and satellite borne sensors offer an opportunity to map forest properties at an unprecedented level of detail.

Wind resource assessment for forested, non-complex sites is typically performed with linear flow models implemented in site assessment tools (e.g. WAsP or WindPRO), which contains several submodels to predict the flow based on an input wind histogram and topography maps (Troen and Petersen 1989). We made modifications to the WAsP model to allow input of maps of land cover, tree height (h) and leaf-area index (LAI) from the novel Sentinel and ICESAT satellites. New roughness analysis algorithms were developed that can compute roughness length and displacement height from h and LAI by applying a pre-processing step. Three methods were implemented and evaluated: an approach where z_0 and d are estimated as a fraction of h, a simple model suggested by Raupach (1994) and a simplified 1D k–ω model modified from Sogachev and Panferov (2006). Internally in the WAsP model, an option to use sectorwise displacement heights in the generalization and downscaling of wind climates was added. Finally, the displacement heights were added to the terrain height grid that is used for the computation of orographic speedups.

The new maps based on Sentinel data were compared with frequently used landcover databases in wind resource modelling, i.e. Corine Land Cover 2018, GlobeCover, GLCC and MODIS land cover data.

10 sites with at least one meteorological mast were used to perform cross-predictions and compare the land cover maps. The sites were characterized by both open and forested landscapes and by gentle and steep-sloped terrain. An example of the four land cover databases (a–d) and the new sentinel based maps (e) after assigning z_0 is shown in Fig. 1. In panel (e) h and LAI have been used to compute z_0, which results in varying roughness values in different parts of the map.

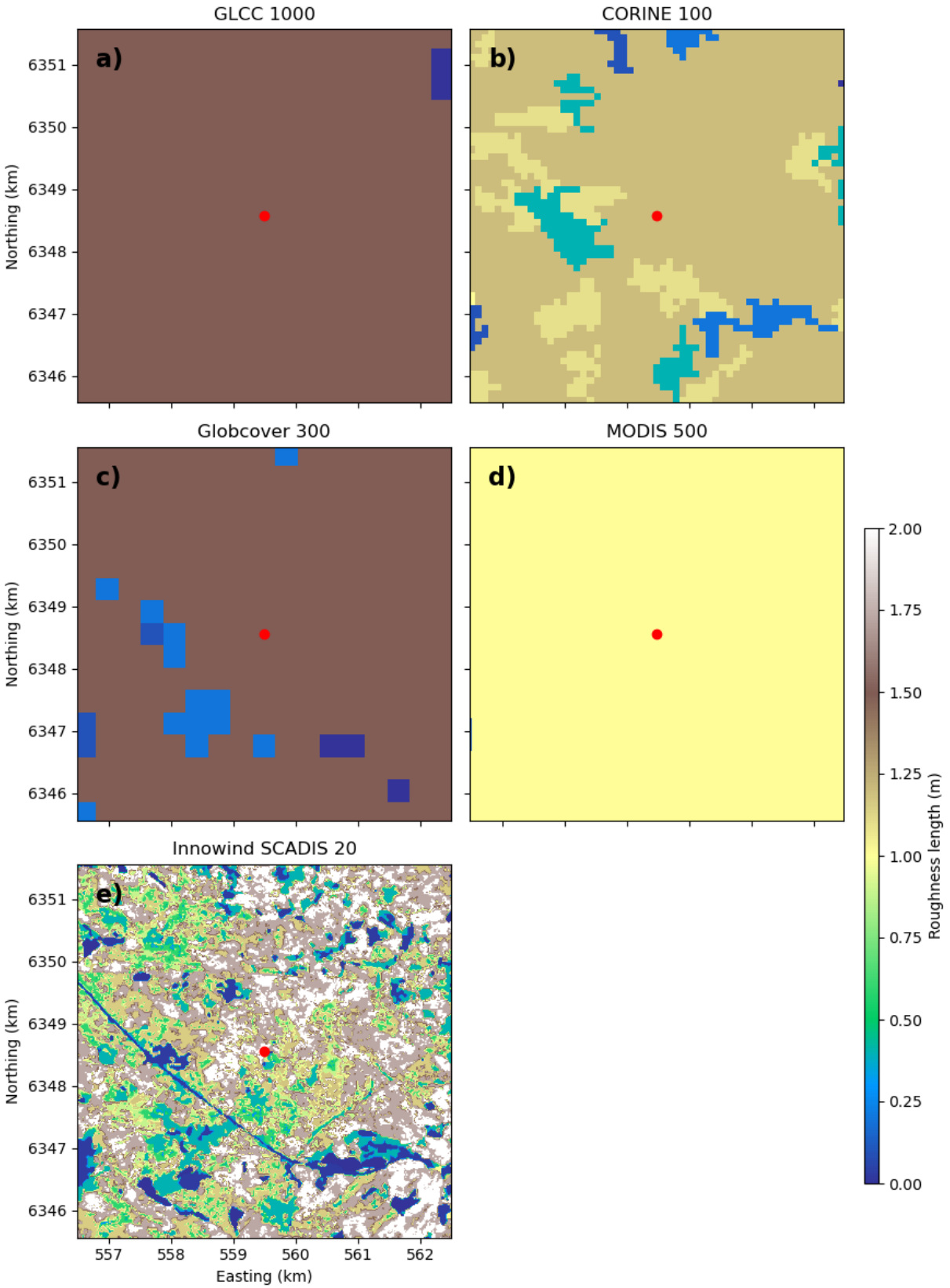


Figure 1: Land cover obtained from a 3×3 km square around the Rynignsnäs site (red point) from GLCC 1000 (a), CORINE 100 (b), Globcover 300 (c), MODIS 500 (d) and Sentinel SCADIS 20 (e). The approach to obtain z_0 from a landcover class is described in the text.

All Sentinel based maps on average gave lower errors in cross-predictions of power density than any of the landcover databases, but the sensitivity to the three models used for converting h and LAI to z_0 and d was found to be small. The root-mean-square errors in power density decreased with 3-8% compared to cross-predictions using the land cover databases at non-complex sites. Large errors were observed at complex sites, in accordance with previous studies (Bowen and Mortensen 1996).
The largest error reductions were found at forested sites, but the large-scale roughness length was found to be too low there.
Acknowledgement: This work was funded by Innovation Fund Denmark through the InnoWind project (6172-00004A).

References:
Bowen, Anthony J, and Niels G Mortensen. 1996. "Exploring the limits of WAsP the wind atlas analysis and application program." In Eur. Union Wind Energy Conf. Proc., edited by P. Helm A. Zervos, H. Ehmann, 584–87. Bedford: H.S. Stephens; Associates. https://orbit.dtu.dk/en/publications/exploring-the-limits-of-wasp-the-wind-atlas-analysis-and-applicat
Enevoldsen, Peter. 2016. "Onshore wind energy in Northern European forests: Reviewing the risks." Elsevier Ltd. https://doi.org/10.1016/j.rser.2016.02.027.
Global Wind Energy Council. 2019. "Global Wind Report 2019." Brussels, Belgium: Global Wind Energy Council. www.gwec.net.
International Renewable Energy Agency. 2019. "Wind Energy." https://irena.org/wind.
Raupach, M. R. 1994. "Simplified expressions for vegetation roughness length and zero-plane displacement as functions of canopy height and area index." Boundary-Layer Meteorol. 71 (1-2): 211–16. https://doi.org/10.1007/BF00709229.
Sogachev, Andrey, and Oleg Panferov. 2006. "Modification of two-equation models to account for plant drag." Boundary-Layer Meteorol. 121 (2): 229–66. https://doi.org/10.1007/s10546-006-9073-5.
Troen, Ib, and Erik Lundtang Petersen. 1989. European Wind Atlas. Roskilde, Denmark: Risø National Laboratory.
WindEurope. 2019. "Wind energy in Europe in 2019 - Trends and statistics." https://windeurope.org/data-andanalysis/product/wind-energy-in-europe-in-2019-trends-and-statistics/.

The role of sea surface temperature forcing in offshore wind energy forecasting

Stephanie Redfern*, and Mike Optis
National Renewable Energy Laboratory
*Presenting author

Keywords: Offshore wind resource assessment | Air-sea interactions | Sensitivity analysis

As offshore wind farm development expands, accurate wind resource forecasting over the ocean is needed. One important yet relatively unexplored aspect of offshore wind resource assessment is the role of sea surface temperature (SST). Models are generally forced with reanalysis datasets, which employ daily SST products. Compared with observations, significant variations in SSTs that occur on finer time scales are often not captured (Optis et al., 2019). Additionally, during periods of cold pool activity in the North Atlantic, quality control measures applied to these products may mistakenly assume cold ocean pixels correspond to cloud presence and remove the data. This can result in a bias towards warmer coastal waters in reanalysis datasets (Murphy et al., 2020). Consequently, events such as sea breezes and stratification-derived wind phenomena, which are driven by and influenced by SSTs (Debnath et al., 2020), may not be correctly represented in model results. The use of hourly, corrected SST products may improve the forecasting of these events.
In this study, we examine the sensitivity of model output to different input parameters, with the main focus being the influence of SST forcing. We run an ensemble of simulations with the Weather Research and Forecasting model (WRF) Version 4.1.2 for a year-long time period between 2019-2020, using different reanalysis datasets (atmospheric forcing), SST products, land surface schemes, and turbulence schemes. In total, we produce 24 sets of results. Sixteen of our ensemble members employ daily, satellite-derived SST products (OSTIA and MUR), while eight are forced with gap-filled GOES-16 hourly data. In addition to the model output, we consider observational data taken from the Atlantic Shores, Mayflower, and NYSERDA floating lidars, as well as the Atlantic Shores buoy and Rutgers Coastal Metocean Monitoring Station. We compare SST and wind speed model output with observations to develop a better understanding of the role SSTs play in offshore wind forecasting.

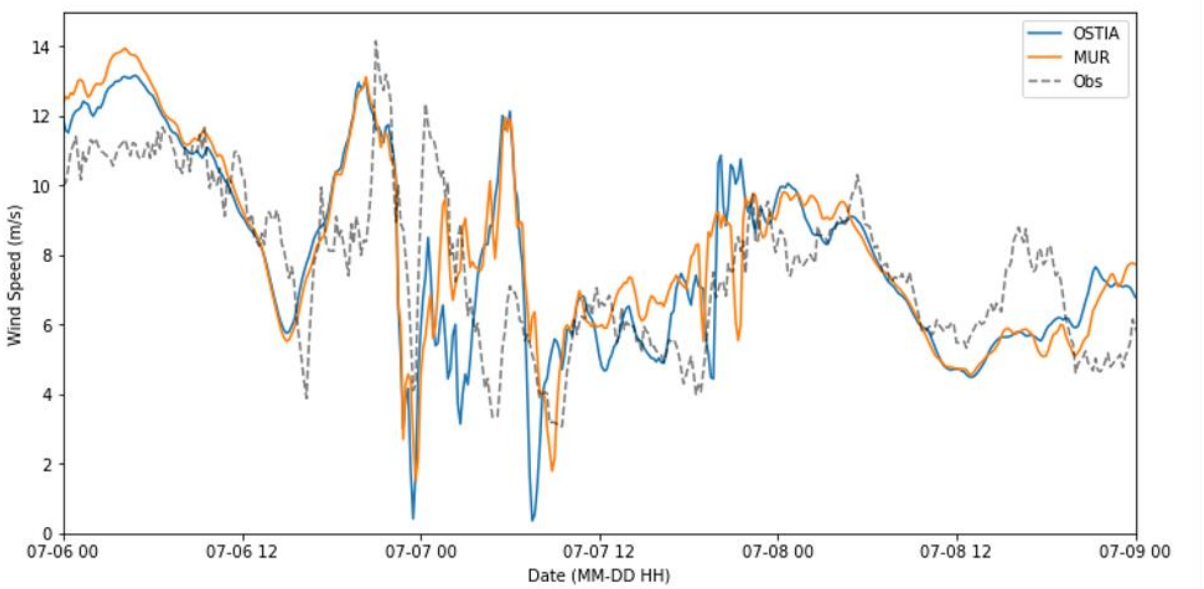


Figure 1: Time series of 140-m wind speeds at the Atlantic Shores lidar location. Results are from simulations using OSTIA SST data (blue) and MUR SST data (orange), as well as observations taken at the Atlantic Shores lidar (gray, dashed). Sizable differences between the model results can be seen in the early morning and afternoon of 07/07/2020.

Our analysis focuses specifically on a multi-week case study in the United States Mid-Atlantic region during the 2019-2020 simulation period. Preliminary results comparing the simulations forced by daily SST products

(otherwise with identical configurations) with each other and with observational data taken with the Atlantic Shores floating lidar show, at times, significant differences in wind speeds. These differences can reach, for example, well over several meters per second in the period shown in Figure 1, where model output using OSTIA and MUR SST data is compared with observations from the Atlantic Shores lidar. Neither model demonstrates a robust ability to capture actual wind speeds during this time period.

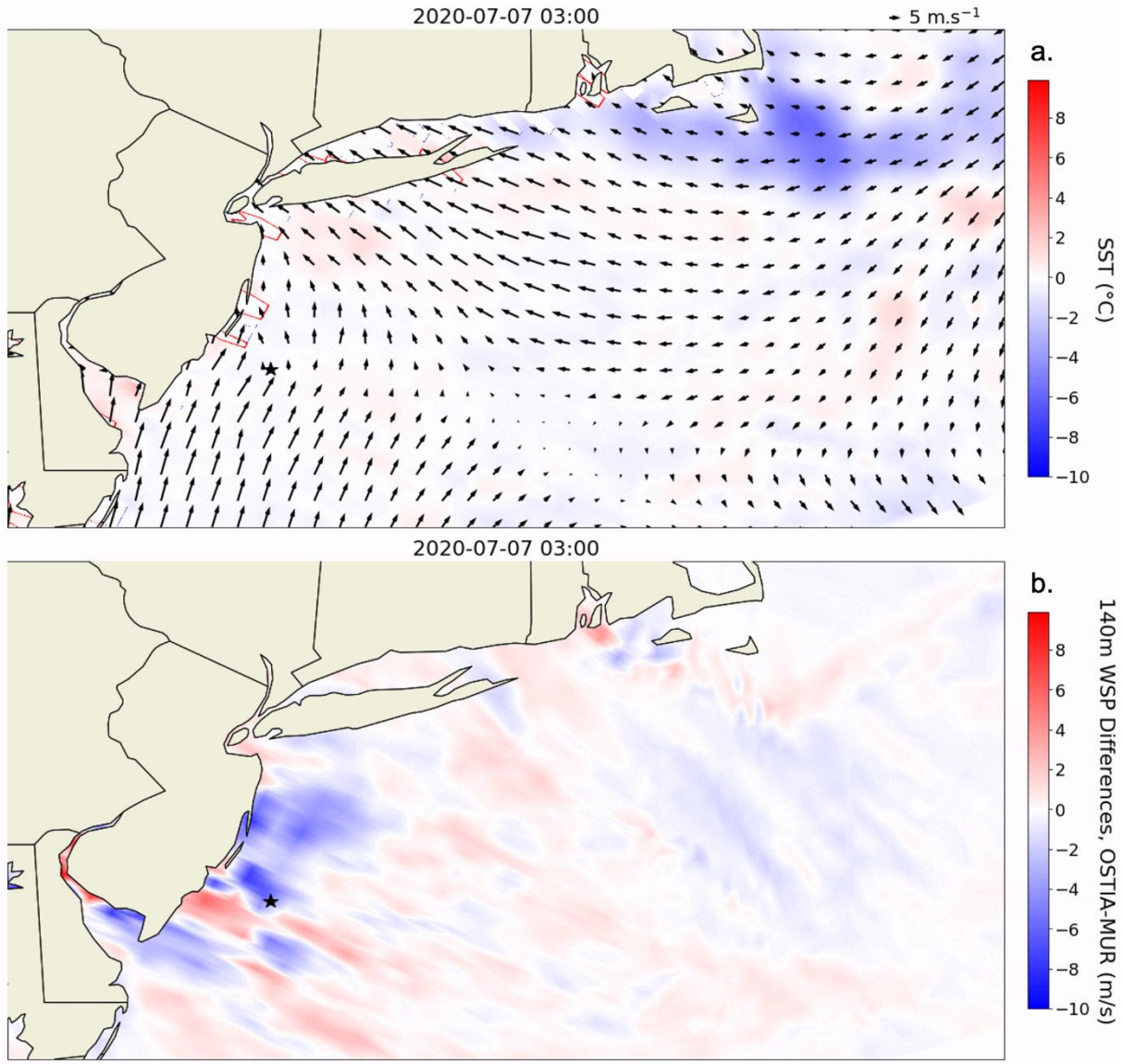


Figure 2: Sea surface temperature differences (OSTIA-MUR), overlaid by modeled 140-m OSTIA winds, at 3UTC on 07-07-2020 (a). Wind speed differences (OSTIA-MUR) at 140-m, at 3UTC on 07-07-2020 (b). The Atlantic Shores lidar location is marked by the star icon.

We also compare model results on a spatial scale and find differences between the simulations forced by different SST products. For example, in the snapshot from 3UTC on 07-07-2020 shown in Figure 2, we see that SSTs north of the Atlantic Shores lidar location in the OSTIA simulation are higher than those in the MUR simulation. This corresponds with slower southwesterly winds at the lidar location in the OSTIA simulation and indicates that there is a weaker sea breeze event, driven by SSTs, in the OSTIA model run, which contributes to the weaker wind speeds to the south.

References:
Debnath, M., Doubrawa, P., Optis, M., Hawbecker, P. and Bodini, N., 2020. Extreme Wind Shear Events in US Offshore Wind Energy Areas and the Role of Induced Stratification. Wind Energy Science Discussions, pp.1-22.
Murphy, S. et al., 2020, 'Persistent Upwelling in the Mid-Atlantic detected using Gap-Filled, High-Resolution Satellite SST', Master's thesis, Rutgers University, New Jersey, USA.
Optis, M., Optis, M., Kumler, A., Scott, G.N., Debnath, M.C. and Moriarty, P.J., 2020. Validation of RU-WRF, the Custom Atmospheric Mesoscale Model of the Rutgers Center for Ocean Observing Leadership (No. NREL/TP-5000-75209). National Renewable Energy Lab.(NREL), Golden, CO (United States).

Time series based approach for wind flow prediction

Jamal Adib*, Hamza Musaddiq, and Marcus Letzel
ENERCON
*Presenting author

Keywords: wind resource assessment | calibration | time series | CFD

The numerical wind resource assessment has become an essential tool for siting engineers where nonlinear models, such as CFD, are used on daily basis. ENERCON has developed its own highly automatized CFD tool chain "E-Wind" (Alletto, et al. 2018), which is used in the current study.
To increase the tool accuracy, a calibration process is required due to the uncertainty associated with the measurements and the topographical data. The siting engineer typically has to calibrate the model input parameters in order to match the measured conditions. The surface roughness and thermal stability parameters are the two main model input parameters that accumulate a significant impact on the flow field and a high uncertainty and therefore require a correction process. Until now, ENERCON had only applied wind direction dependent corrections, here named as "statistical approach", to extrapolate measured wind conditions from mast location to planned turbine locations. The main reasons were the limited computational resources and the required time resources to perform the manual calibration process. Recently, a new high performance cluster at ENERCON has significantly increased the available computational resources (11500 cores and 500
TFLOPS) and a fully automatized calibration process was implemented in E-Wind (Adib, et al. 2019).
These two upgrades have made possible the development of a time dependent correction strategy, here named as "time series approach".
As mentioned earlier, the calibration process intends to correct two model input parameters. Each parameter requires a specific time binning with the time series approach. The surface roughness correction uses a 2-month time bin to capture seasonal effects whereas the thermal stability correction uses a 1-hour time bin to capture diurnal effects. The calibration process uses an optimization algorithm to bring iteratively the error differences, between the measured and the simulated situations, below a certain threshold.

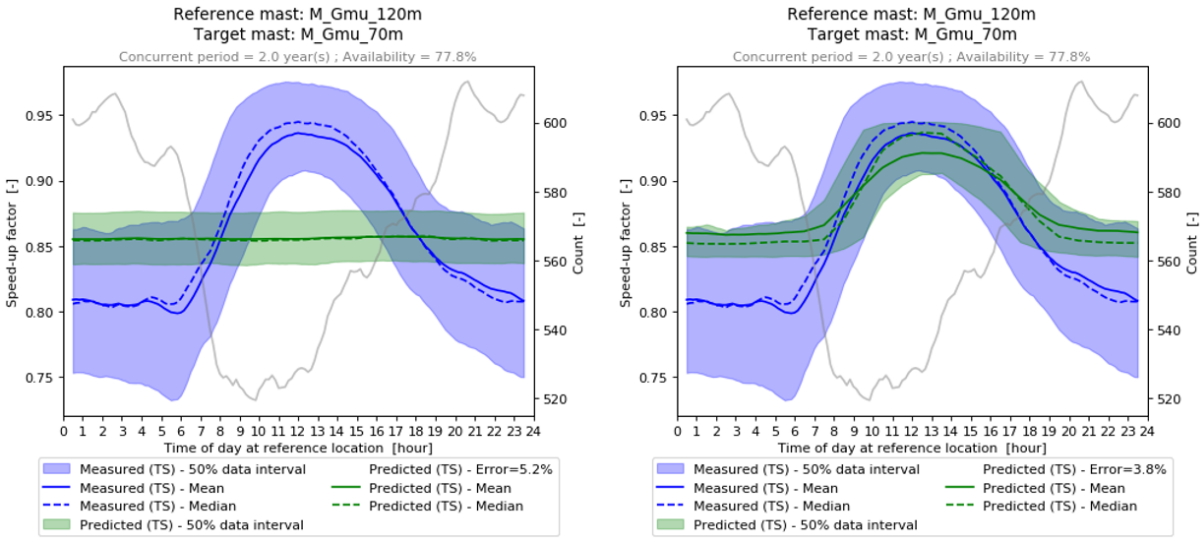


Figure 1: Time of day binning of the measured (in blue) and the simulated (in green) speed-up factor for the statistical approach (left) and the time series approach (right).

The preliminary tests of the time series approach are performed on a site with simple terrain for which the statistical approach is performing well in regards to the yearly averaged wind speed and theoretical power errors. Figure 1 shows the clear diurnal cycle in the measured data that the statistical approach is completely missing, as it does not involve any time-dependent parameter in the prediction process. On the contrary, the

time series approach is capturing the shape of the diurnal cycle with a good match during the day with the unstable atmospheric conditions but fails at night where the atmospheric conditions are very stable.
These preliminary results have shown both the potential and the limits of the time series approach.
As expected, the predicted time series now show time of day and wind speed dependency. However, the wind speed and theoretical power errors are not improved. A possible reason seems to be error cancellation that benefits the statistical approach (day vs night or low vs high wind speed errors).
Furthermore, the time series approach is strongly limited by the current shear range the CFD solver can produce. The authors will continue their work to further test the time series approach on multiple sites with various terrain complexity as well as enhance the solver capabilities to simulate larger wind shear range, which currently only covers the near neutral atmospheric conditions.

References:
Alletto, Michael, Alexander Radi, Jamal Adib, Judith Langner, Carlos Peralta, Andree Altmikus, and Marcus Letzel. 2018. "EWind: Steady state CFD approach for stratified flows used for site assessment at Enercon." J. Phys. Conf. Ser. 1037 (7): 072020.
Adib, Jamal. (2019, September). 1.28_ADIB: Comparison of two automatic calibration methods for a CFD based wind resource assessment tool. Presented at the Wind Energy Science Conference (WESC), Cork, Ireland: Zenodo. http://doi.org/10.5281/zenodo

Forecastability of a wind site based on meteorological time series structure

Jaume Manero[1,2], Javier Béjar[1], and Ulises Cortés[1]
[1]Technical University Catalonia
[2]Barcelona SuperComputing Center

Keywords: wind prediction | forecastability | time series | wind resource | wind resource evaluation

Wind will be a relevant component in the future energy generation mix (Jacobson 2017), (Walsh 2019)
The accuracy of the wind energy algorithms depends on many local features of a geographical site.
An algorithm that obtains good results in a location may have a low ability to predict in other places. To understand the implications of predictability and site location, first, we analyze the forecasts in many different sites, trying to understand the correlation of prediction approach and site. The high correlation between different prediction methods allows us to define a site property, which we call forecastability, defined as the ease of prediction for that place. This work defines this property for a site by analyzing the meteorological time series's internal structure. Properties like non-linearity or stationarity contribute to the complexity of the site prediction. Assessing a site's forecastability has economic value by better understanding the prediction's limits, the best prediction approach, or the future investment cost to obtain good forecasts (Girard 2013, Frias 2017, Rodrigo 2013).
Forecastability characterization can be based on several time series measures, that we can call primary, obtained with techniques like time series decomposition, internal aggregations of values or spectral analysis. Some primary measures show high correlation with site accuracy (Feng 2017, Feng 2019). Combining primary measures, we obtain secondary ones, which show higher correlation with the accuracy prediction for a site.
In this work we define novel primary and secondary measures and we explore how they fit real predictions that have been calculated using deep learning.
The experimental work has been performed using the National Renewable Laboratory (NREL) dataset with (192,296 sites), including a broad spectrum of wind sites from all different climate regions in the US. In this way, the validation of results is highly relevant and unbiased (Draxl 2015).

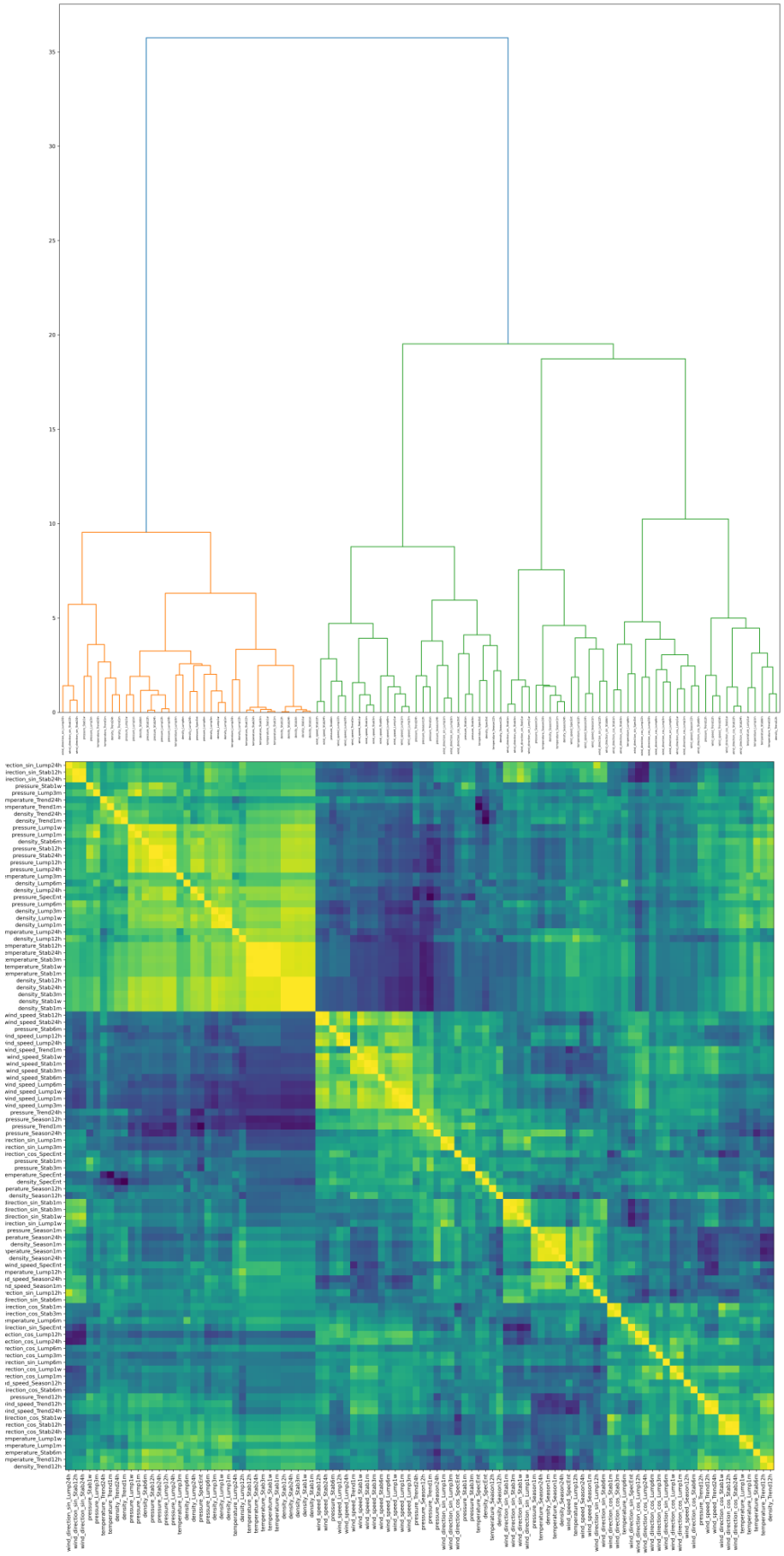


Figure 1: Correlations between over 100 forecastability measures using wind speed, wind direction, temperature, humidity.

We perform multiple regressions with all the possible measures (as it is illustrated in Figure 1) , and then we use several statistical tools to analyze the primary measure's contribution. By using this information we obtain an optimal combination of them, generating a forecastability predictor that rates how easy a prediction will be for a specific location, based on the basic time series features (Manero 2019).
The best primary predictors are based on the correct description of seasonality and trend of a site, while spectral analysis offers some descriptive measures with high potential (Wang 2017). Identifying seasonality on a site is a complex task due to the high variability of wind patterns across different sites. Further exploration on how to identify seasonality and thus define the best measure needs to be performed to obtain even more accurate forecastability ratings. The regression fit to the predictions can be seen in Figure 2.

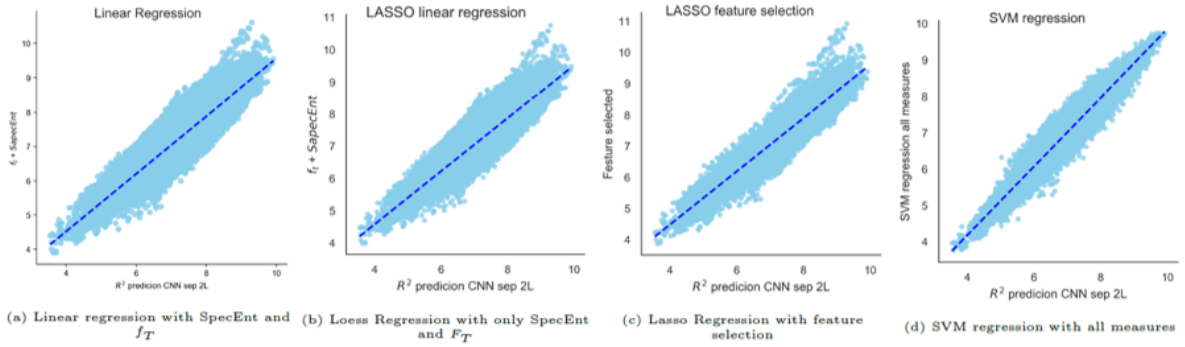


Figure 2: Scatterplots between multiple forecastability measures and prediction. With an R^2 = 0.95 SVM obtains the best fit with the prediction.

Wind resource is usually described based on the intensity and variance of winds in a location across time. Direction changes and amount of wind over the productive margins are important to evaluate the quality of a site. We strongly believe that including forecastability measures into the wind resource evaluation contributes to the site qualification as rating the ease of forecast of a location will help to understand better how difficult is to transform the original wind resource into a commercially feasible electricity energy.

References:

(Jacobson 2017) Jacobson, M. Z. et al. (2017) '100% Clean and Renewable Wind, Water, and Sunlight All-Sector Energy Roadmaps for 139 Countries of the World', Joule, 1(1), pp. 108–121. doi: 10.1016/j.joule.2017.07.005.
(Walsh 2019) C. Walsh, I. Pineda, Wind energy in europe in 2018 trends and statistics, published by Windeurope.org (February 2019).
(Frias 2017), The role of pre-dictability in the investment phase of wind farms, in: Renewable Energy Forecasting: From Models to Applications, Woodhead Publishing Series in Energy, Elsevier - Woodhead Publishing,2017, pp. Chapter 14 –pages 341–357. doi:10.1016/B978-0-08-100504-0.00014-7.
(Girard 2013) R. Girard, K. Laquaine, G. Kariniotakis, Assessment of windpower predictability as a decision factor in the investment phase of wind farms, Applied Energy 101 (2013) 609 – 617, sustain-able Development of Energy, Water and Environment Systems.doi: https://doi.org/10.1016/j.apenergy.2012.06.064.
(Rodrigo 2013) J. Rodrigo, L. Paredes, N. Stoffels, L. Bremen, Wind power predictability assessment from large to local scale, European Wind Energy Conference and Exhibition, EWEC 2013 1 (2013) 625-634.
(Feng 2017) C. Feng, E. K. Chartan, B.-M. Hodge, J. Zhang, Characterizing time series data diversity for wind forecasting, in: Proceedings of the Fourth IEEE/ACM International Conference on Big Data Computing, Applications and Technologies, BDCAT '17, Association for Computing Machinery, New York, NY, USA, 2017, p. 113{119. doi:10.1145/3148055.3148065.
(Feng 2019) C. Feng, M. Sun, M. Cui, E. K. Chartan, B.-M. Hodge, J. Zhang, Characterizing forecastability of wind sites in the United States, Renewable Energy 133 (2019) 1352-1365. doi: https://doi.org/10.1016/j.renene.2018.08.085.
(Manero 2019) J. Manero, J. Bejar, U. Cortes, "Dust in the wind...", deep learning application to wind energy time series forecasting, Energies 12 (12) (2019) 2385. doi:10.3390/en12122385.
(Draxl 2015) C. Draxl, A. Clifton, B.-M. Hodge, J. McCaa, The wind integration national dataset (wind) toolkit, Applied Energy 151 (2015) 355-366.
(Wang 2006) X. Wang, K. Smith, R. Hyndman, Characteristic-based clustering for time series data, Data Mining and Knowledge Discovery 13 (3) (2006) 335{364. doi:10.1007/s10618-005-0039-x.

Wind velocity spectra at Vindeby Offshore Wind Farm

Rieska Mawarni Putri[1,*], Etienne Cheynet[2], Charlotte Obhrai[1], and Jasna Jakobsen[1]
[1]University of Stavanger
[2]University of Bergen
*Presenting author

Keywords: Vindeby | wind measurement | wind spectra | atmospheric stability

Located about 1.5 to 3 km from the northwestern coast of Lolland Island, Vindeby Wind Farm is one of the first offshore wind farms which operated in Denmark, from 1991 to 2016 (Barthelmie et al., 1994). In this study, the wind measurement data from one of the two offshore meteorological masts at the Vindeby Wind Farm, recorded from April 1994 to July 1995, is analysed. The mast is equipped with three 3D sonic anemometers, at 6, 18, and 45 m above the mean sea level (MSL), sampling at a rate of 20 Hz. The averaging period selected for the study is 30 minutes. Although the dataset was briefly studied in the 1990s (Barthelmie et al., 1994; Barthelmie et al., 1996; Barthelmie, 1999), it has not yet been explored in detail in terms of the spectral wind characteristics. This information is valuable for the assessment of offshore wind turbine design. Non-neutral atmospheric stability has a significant effect on the wind spectral characteristics (Barthelmie, 1999; Sathe et al., 2012; Chougule et al., 2018; Cheynet, Jakobsen, and Reuder, 2018). The loads and motions on both fixed and floating offshore wind turbines may be influenced by nonneutral atmospheric stability conditions (Chougule et al., 2018; Putri et al., 2020). Therefore, it is important to carefully assess the offshore wind resources in terms of atmospheric stability, whenever possible. The present work aims to quantify the variability of the turbulence characteristics at Vindeby with the atmospheric stability. Also, the presence of measurements close to the sea surface gives a unique occasion to investigate the applicability of surface layer scaling in the wave sublayer as well as the dependency of turbulence on the sea state.

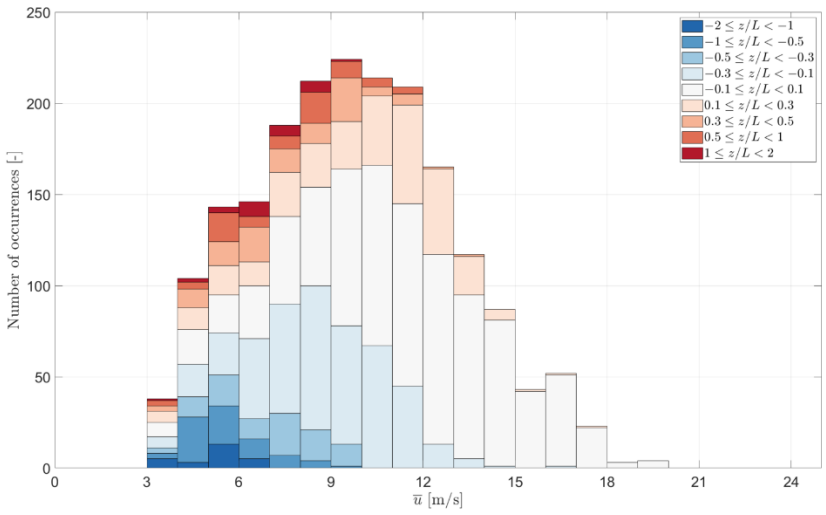


Figure 1: Atmospheric stability distribution for each mean wind speed observed from April 1994 to July 1995.

Figure 1 shows the distribution of the atmospheric stability as a function of mean wind speed from April 1994 to July 1995, using the non-dimensional Obukhov length. The atmospheric stability is presented as the non-dimensional parameter z/L, where z is the height above MSL, and L is the Obukhov length, which is computed using the sonic anemometer data at z = 18 m. The atmospheric stability for the mean wind speeds 4-12 m/s includes a considerable portion of non-neutral conditions, from 10 to 95% of occurrences, depending on the mean wind speed, in a similar fashion as (Barthelmie, 1999).

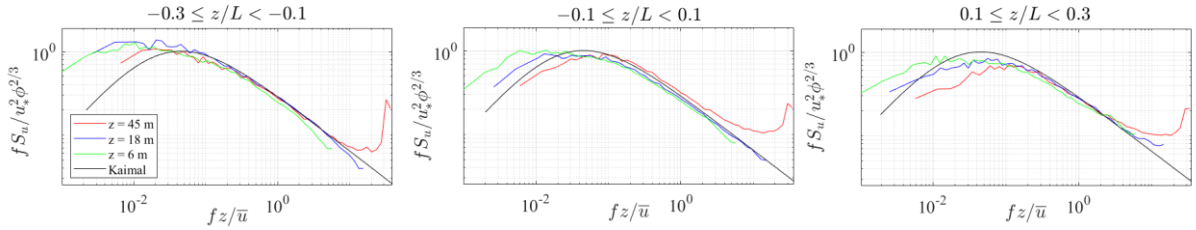


Figure 2: One-point spectra of the along wind component for different atmospheric stability conditions at the three observation heights.

Figure 2 presents the one-point spectra of the along wind component for different atmospheric conditions at the three heights. The normalised spectra are presented as the median values of the 30-min time series for mean wind speeds 10 m/s and above. As atmospheric stability conditions change from unstable to neutral to stable, the spectral peaks shift towards higher frequency, which agrees with observations from the Kansas experiment (Kaimal and Finnigan, 1994). The full-length article will provide further details on the in-depth quality assessment of the dataset, including the application of surface layer scaling in the vicinity of the wave sublayer.

References:

Barthelmie, R. J., Courtney, M., Højstrup, J. and Sanderhoff, P., 1994. The Vindeby project: A description. Risø National Laboratory. Denmark. Forskningscenter Risoe. Risoe-R, No. 741.

Barthelmie, R., Courtney, M., Højstrup, J. and Larsen, S., 1996. Meteorological aspects of offshore wind energy: Observations from the Vindeby wind farm. Journal of Wind Engineering and Industrial Aerodynamics, 62(2-3), pp.191-211.

Barthelmie, R., 1999. The effects of atmospheric stability on coastal wind climates. Meteorological Applications: A journal of forecasting, practical applications, training techniques and modelling, 6(1), pp.39-47.

Sathe, A., Mann, J., Barlas, T., Bierbooms, W. and van Bussel, G., 2012. Influence of atmospheric stability on wind turbine loads. Wind Energy, 16(7), pp.1013-1032.

Chougule, A., Mann, J., Kelly, M. and Larsen, G., 2018. Simplification and Validation of a Spectral-Tensor Model for Turbulence Including Atmospheric Stability. Boundary-Layer Meteorology, 167(3), pp.371-397.

Cheynet, E., Jakobsen, J. and Reuder, J., 2018. Velocity Spectra and Coherence Estimates in the Marine Atmospheric Boundary Layer. Boundary-Layer Meteorology, 169(3), pp.429-460.

Putri, R., Obhrai, C., Jakobsen, J. and Ong, M., 2020. Numerical Analysis of the Effect of Offshore Turbulent Wind Inflow on the Response of a Spar Wind Turbine. Energies, 13(10), pp.2506.

Kaimal, J. C. and Finnigan, J. J., 1994. Atmospheric boundary layer flows: their structure and measurement. Oxford university press.

Seasonal Effects in the Long-Term Correction of Short-Term Wind Measurements

Alexander Basse[1,2,*], Doron Callies[2,1], Anselm Grötzner[3], and Lukas Pauscher[2]
[1]University of Kassel
[2]Fraunhofer Institute for Energy Economics and Energy System Technology (IEE)
[3]Ramboll Deutschland GmbH
[*]Presenting author

Keywords: Measure-Correlate-Predict | Reanalysis Data | Long-Term Assessment | Correlation

Wind measurement campaigns in resource assessments usually do not reflect the long-term wind conditions on site. Therefore, one essential step of wind resource assessment is the long-term correction of the measured wind data. In this context, often Measure-Correlate-Predict (MCP) approaches are applied, which correlate the measured data with reference wind data. Nowadays mostly reanalysis data are used.
In order to save time and reduce costs, it is an appealing option to keep measurement time short.
The uncertainty of the long-term correction, however, can rise significantly if measurement periods shorter than one year are used. Our work investigates systematic errors (seasonal biases) in MCPbased long-term corrections which occur if the measurement on site does not cover a whole year but only a few months.
Two common linear MCP methods are tested and compared, namely Variance Ratio (Rogers et al., 2005) and Linear Regression with Residuals (Weekes and Tomlin, 2014). Two global reanalysis data sets (Merra-2, ERA-5) as well as four mesoscale data sets (distributed by anemos GmbH and EMD international) serve as long-term reference data. MCP calculations based on different 3-months measurement periods are performed and the results are compared with respect to the performance of both the MCP methods and reanalysis data sets. Wind data from 18 sites in Germany with different terrain complexity are used in the analysis. The measurement heights are in the range of 100 and 140 m, representing typical hub heights of modern wind turbines.
The results show that, in general, summer and winter measurements lead to strongly biased estimates of mean wind speed and energy production. This can be traced to biases in the reference wind data; all reanalysis data sets investigated in this study showed an "over-pronounced" seasonal course, i.e., too small wind speeds in summer and too strong winds in winter. Hence, measurements in transitional seasons yielded much better results. Furthermore, it is shown that the pattern of these biases not only depends on the selected reference data. Additionally, a strong dependence on the MCP method exists. Remarkable differences were observed for the two MCP approaches applied in this study: The Variance Ratio method yields overestimations in summer, while underestimations were observed when the measurement was conducted in winter periods. For the linear regression approach, mostly contrary characteristics were obtained (s. Fig. 01).

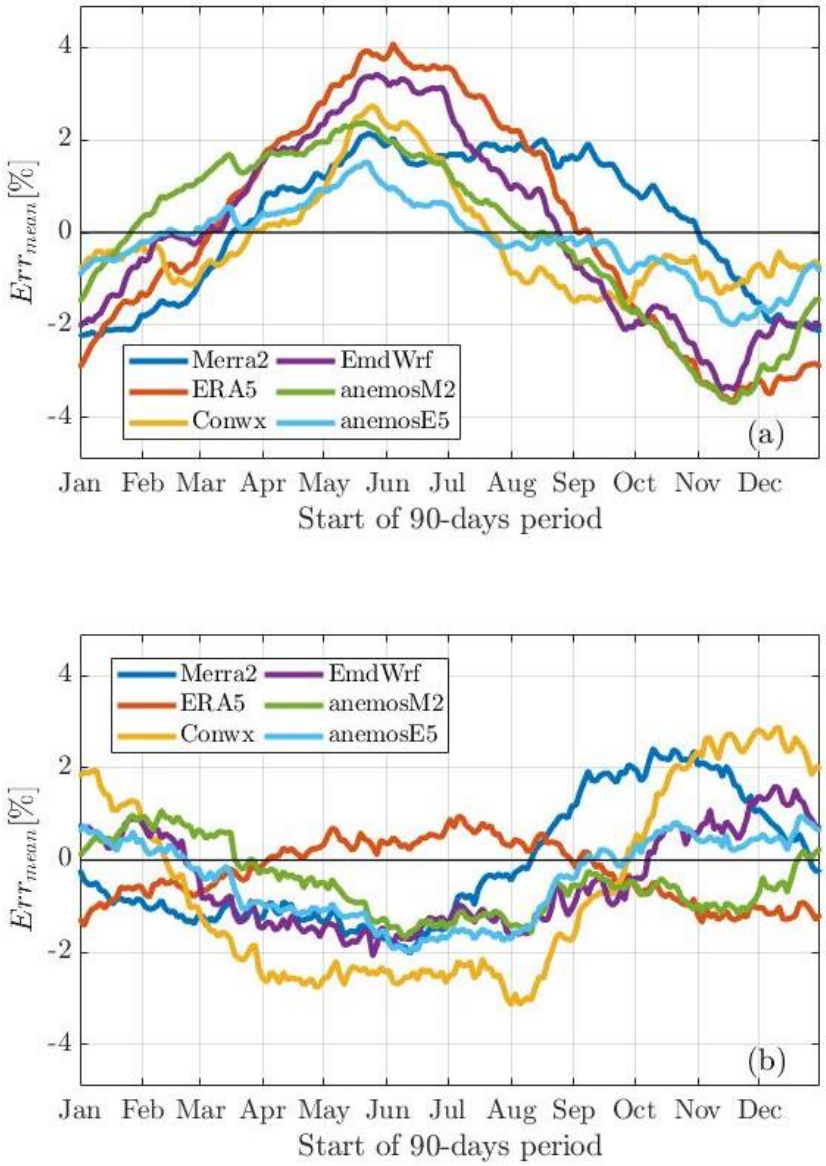


Figure 1: Bias in mean wind speed for MCP calculations based on 90 days of measurement data using (a) Variance Ratio, (b) Linear Regression with Residuals. Each line represents the (time-dependent) bias which is obtained using one of the six reanalysis data sets.

In addition to the experimental investigations, theoretical analysis is presented which provides the mathematical background for understanding the observations. The seasonal biases are traced to properties of the reference data as well as to the mechanics of the MCP methods. This allows a universal explanation for the seasonal biases which can be transferred to different measurement durations, other reference data and other regions of the world as well.

Based on the results, recommendations for the wind industry can be derived on 1.) the time of the measurement within the year and the biases to be expected, 2.) the choice of the reanalysis data, 3.) the choice of the MCP method.

References:

Weekes, S. M. and Tomlin, A. S.: Data efficient measure-correlate-predict approaches to wind resource assessment for small-scale wind energy, Renewable Energy, 63, 162–171, 85 https://doi.org/10.1016/j.renene.2013.08.033, 2014

Rogers, A. L., Rogers, J. W., and Manwell, J. F.: Comparison of the performance of four measure–correlate–predict algorithms, Journal of Wind Engineering and Industrial Aerodynamics, 93, 243–264, https://doi.org/10.1016/j.jweia.2004.12.002, 2005

Regular Session: Minute-Scale Forecasting and Power Fluctuations

Analysing correlations of power output fluctuations of offshore wind turbines based on high resolution SCADA data

Janna Kristina Seifert*, Martin Kraft, Martin Kühn, and Laura J. Lukassen
ForWind - University of Oldenburg
*Presenting author

Keywords: power fluctuations | SCADA data | correlations

Nowadays, offshore wind farms are continuously increasing in size. In this context, the determination of the influence of power output fluctuations of single wind turbines on the wind farm power output delivers a crucial information for the wind farm operation. Temporal correlations of power output fluctuations of single wind turbines or wind turbine pairs give insights on flow conditions within a wind farm and wind turbine interactions. This plays an important role for wind farm control and minute-scale power forecasting.
Bossuyt et al (2017) and Lukassen et al (2018) presented investigations of power and wind speed space-time correlations in wind tunnel experiments and LES simulations. In contrast to experimental conditions and numerical simulations, the flow conditions in a free-field wind farm, are highly dynamic. This is caused by the individually operating wind turbines, the wind farm layout and environmental effects like wind direction or wind speed changes which create varying correlation curves, here named correlation states. Thus, to analyse the correlations of power output fluctuations of wind turbines with their SCADA data, these correlation states must be identified and considered individually.
Here, we present our recent work on the analysis of space-time correlations of power output fluctuations of wind turbine pairs and the temporal correlation of single wind turbines with 1 Hz SCADA data. The results are based on 8 months of SCADA data measurements of 80 wind turbines in the offshore wind farm "Global Tech I". For the space-time correlations, we focus on power output fluctuations of stream-wise aligned wind turbine pairs for time intervals of 600 s. The duration of the time intervals and the stream-wise alignment of the wind turbine pairs is chosen to capture flow effects like small-scale turbulence evolving throughout the wind farm passing the two considered wind turbines. We find that the standard deviation of the power output fluctuations of the wind turbines together with the normalised power difference of the wind turbines in a pair are suitable parameters to distinguish correlation states. Finally, we show that these parameters, combined with the data-driven clustering approach k-means (Lloyd, 1982) allow to separate the data according to the underlying correlation states (Seifert et al., 2020).
Following up (Seifert et al.,2020), we investigate the temporal autocorrelations of power output fluctuations. We analyse the influence of power output fluctuations of single wind turbines in different sectors of the wind farm on the dynamics of power output fluctuations of a whole wind farm. This especially finds its application in the context of the ongoing wind-to-hydrogen research.
Figure 1 indicates the average temporal autocorrelation of single wind turbines per wind farm row. It shows the influence of the positions of the wind turbines within the wind farm. The temporal autocorrelation decreases for wind turbines towards the downstream end of the wind farm.

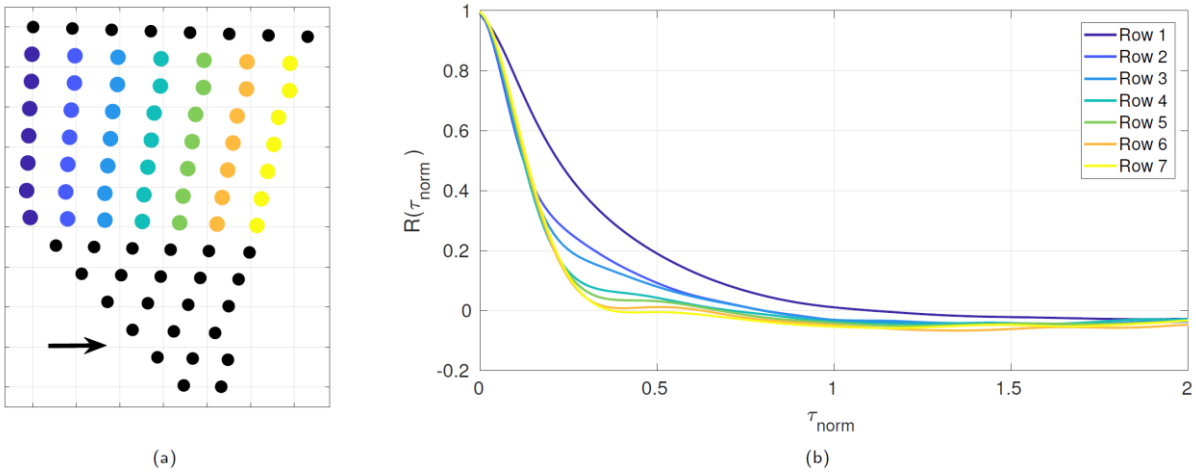


Figure 1: (a) Wind farm layout of Global Tech I. The colors indicate the considered wind turbines for a westerly wind direction interval of 20° indicated by the arrow. (b): Average temporal autocorrelation of single wind turbines per wind farm row. The lag of the correlations is normalised for the average wind speed and a characteristic spatial distance per correlation interval and here noted as τ_{norm}.

References:
Bossuyt, J., Howland, M. F., Meneveau, C., Meyers, J. (2017) 'Measurement of unsteady loading and power output variability in a micro wind farm model in a wind tunnel', Exp Fluids., 58(1), https://doi.org/10.1007/s00348-016-2278-6
Lloyd, S. P. (1982) 'Least squares quantization in PCM', IEEE Transactions on Information Theory, 28(2), pp. 129–137, https://doi.org/10.1109/TIT.1982.1056489
Lukassen, L. J., Stevens, R. J. A. M., Meneveau, C., Wilczek, M. (2018) 'Modeling space-time correlations of velocity fluctuations in wind farms', Wind Energy, 21, pp. 474- 487, https://doi.org/10.1002/we.2172
Seifert, J. K., Kraft, M., Kühn, M., Lukassen, L. J. (2020) ' Correlations of power output fluctuations in an offshore wind farm using high-resolution SCADA data', Wind Energ. Sci. Discuss. [preprint], https://doi.org/10.5194/wes-2020-96, in review

Minute-Scale Forecasting of Wind Power at the Wind Farm Scale Using Long-range Doppler Lidar

Mathieu Pichault*, Claire Vicent, Grant Skidmore, and Jason Monty
University of Melbourne
*Presenting author

Keywords: Short-term Forecasting | Doppler Lidar | Wind Power Ramp | Probabilistic Forecasting

Worldwide energy markets are undergoing a rapid shift towards low carbon technologies and renewable energy sources. With ever-increasing wind energy penetration levels, accurate short-term predictions of wind power generation are becoming essential to optimise the integration of wind farms into electricity networks. Motivated by the latest technological advancements in optoelectronics, remote sensing instruments probing the incoming wind field, such as scanning-head Doppler lidars, have great potential for short-term wind power forecasting. However, few studies are tackling the problem at the wind farm scale, generally focusing on wind speed or power generation from a limited number of turbines under ideal conditions. As a result, it is still unclear to what extent remote sensing instruments can effectively improve the accuracy of short-term wind power forecasts.
This research seeks to address this question through the development and testing of two novel forecasting methodologies, based on measurements from a state-of-the-art long-range scanning Doppler lidar (Leosphere WindCube400S). The lidar is set up to continuously sample the incoming wind field through 80° low-elevation sector scans. An example of the reconstructed two-dimensional wind field based on lidar data is shown in Figure 1.

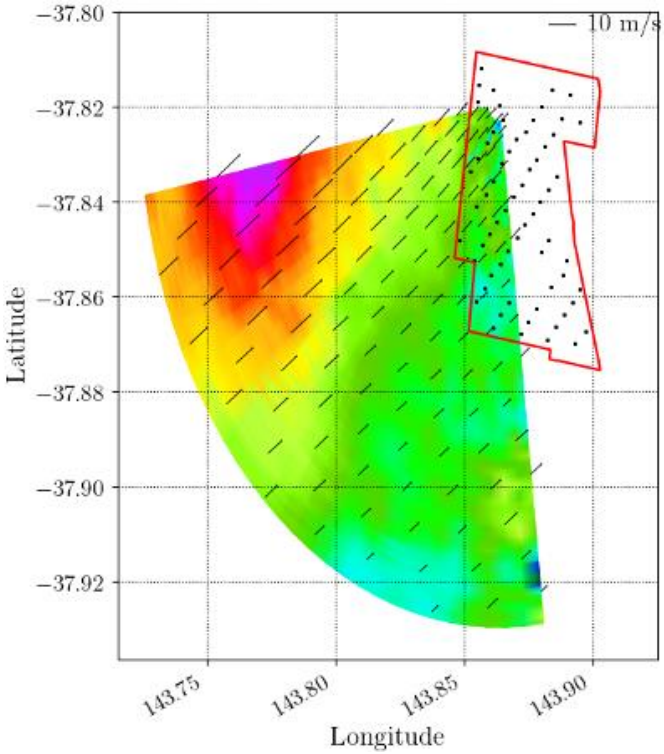


Figure 1: Reconstructed wind field based on lidar data on 01-Nov-2019 at 22:38:40 [UTC+10] during a cold air outbreak. The red lines and black dots depict the site boundaries and the wind turbines locations, respectively.

Both approaches aim to predict the total power generated at the wind farm scale with a lead time of five minutes. The first approach is physically based and is an adaptation of the solar short-term forecasting approach referred to as 'smart-persistence'. The proposed methodology includes a hubheight wind speed extrapolation module, a wind field reconstruction module, a propagation model and a direction-dependent

probabilistic power curve model. The second approach tackles the same short-term forecasting challenge using deep learning methods, in particular Convolutional Neural Networks. The flowchart for both methodologies is presented in Figure 2, in which the top and bottom arrows represent the physical and deep learning approaches, respectively.

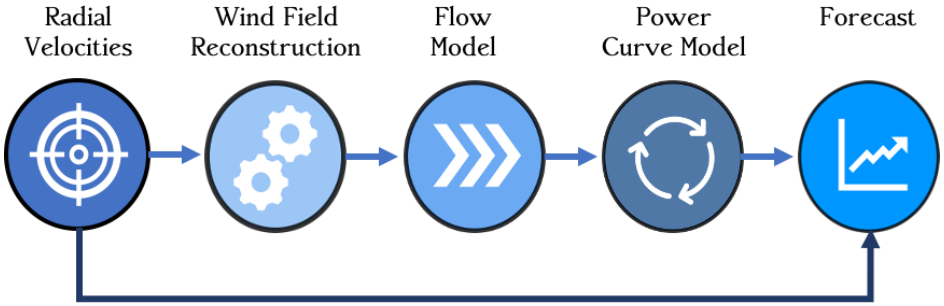


Figure 2: Flow diagram for lidar-based short-term forecasting. The top and bottom arrows represent the physical and deep learning approaches, respectively.

The methods are tested over an uninterrupted six month assessment period at a large wind farm site in Victoria (southeast Australia), which comprises 64 wind turbines distributed over an area of 2650 ha. The forecasting errors are compared against the persistence benchmark in terms of mean absolute error, root-mean-square error and continuous ranked probability score. Forecast performances during ramp events and under various stability conditions are further discussed and several wind power ramp case studies are presented. Finally, the different opportunities and challenges of remote sensing instruments for short-term wind power forecasting applications are discussed.

This research is undertaken in close collaboration with Meridian Energy Australia as part of the 5- minute self-forecasting project (5MSFP); an initiative of the Australian Renewable Energy Agency (ARENA) aiming at assessing potential gains from using semi-scheduled generator self-forecasts to optimise the operation of power systems. Overall, this research is part of a broader initiative aiming at mitigating greenhouse gas emissions by making wind energy a more controllable resource.

Doppler LiDAR observations of wake meandering at a utility scale wind turbine

Peter Brugger[1,*], Corey Markfort[2], and Fernando Porté-Agel[1]
[1]École Polytechnique Fédérale de Lausanne
[2]University of Iowa
*Presenting author

Keywords: wake meandering | Doppler LiDAR | field measurements

Wake meandering is a low-frequency oscillation of the entire wind turbine wake with respect to the time-averaged centerline. These oscillations of the instantaneous wake position contribute to the turbulence received by a downstream turbine in a wind farm leading to power and load fluctuations.
One hypothesis on the origin of wake meandering assumes that large scale turbulent eddies in the atmospheric boundary layer cause a lateral and vertical displacement of the wake as it is transported downstream (Larsen et al., 2008). For modelling purposes, a common assumption is that the wake behaves like a passive scalar during this advection process. Here, we investigate (i) the downstream propagation velocity of the wake meandering, (ii) the quality of a linear relationship between large scale turbulence and the instantaneous wake center position, and (iii) the errors of a passive advection based prediction of the instantaneous wake center position.
Field measurements of wake meandering from two Doppler LiDARs mounted on the nacelle of a utility scale wind turbine (79 m hub height, 96 m rotor diameter) are used for the investigation. One Doppler LiDAR was scanning the longitudinal velocity field of the wake at hub height, from which the instantaneous wake center position was estimated. The other Doppler LiDAR used a stare setup to provide the lateral inflow velocity component. The dataset covers a wide range of wind speeds (5 – 11 m s-1) and turbulence intensities (1% - 9%).

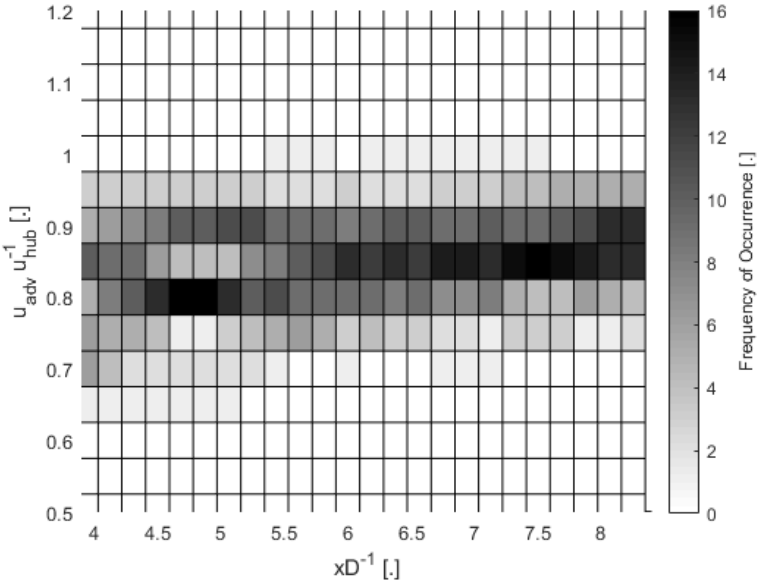


Figure 1: Ratio of the downstream propagation velocity of the wake meandering (u_adv) to the inflow wind speed at hub height (u_hub) as a function of downstream distance. Colors are showing the frequency of occurrence.

First, the wake measurements were used to investigate the downstream propagation velocity of wake meandering. The downstream propagation was estimated with a cross-correlation approach between the instantaneous wake center positions at downstream distances separated by three rotor diameters. The results yielded downstream propagation velocities between 0.7uhub and 0.9uhub (with uhub being the inflow wind speed measured at the nacelle) and that it increased slightly with downstream distance (Fig. 1). The found

downstream propagation velocities were lower than the wind speed outside of the wake, but higher than the velocity at the wake center.

Second, we investigated the relationship between the lateral velocity and instantaneous wake center position. In agreement with wind tunnel studies (e.g. Bastankhah and Porté-Agel, 2017), we found that the wake meandering strength (or amplitude) increases with the lateral turbulence intensity and with downstream distance. Further, we found that the correlation between the lateral velocity and the instantaneous wake center position shows a dependency to the ratio of the integral time scale of the lateral velocity to the time delay due to downstream advection (Fig. 2). This finding could imply that wake meandering predictions based on a passive advection might exhibit increasing errors for large downstream distances or fast evolving turbulent velocity fields.

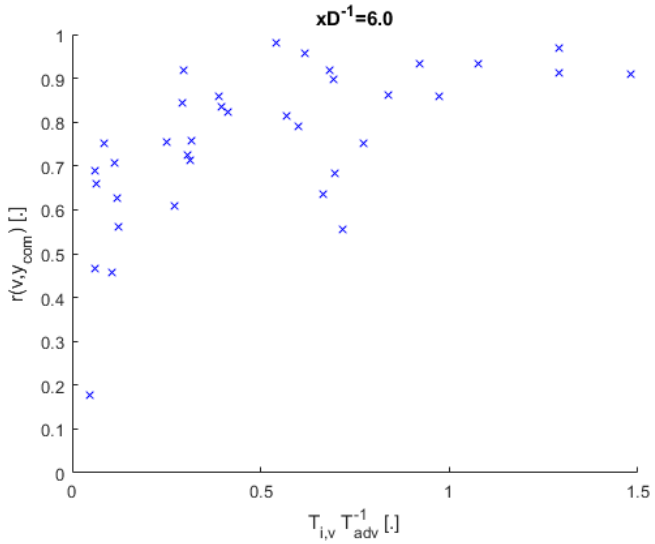


Figure 2: The correlation coefficient between lateral velocity (v) and instantaneous wake center position (y_com) as a function of the ratio of the integral time scale of the lateral velocity (T_i,v) to time delay due to downstream advection (T_adv) at a downstream distance of six rotor diameters. Both time series were low-pass filtered

Lastly, we made predictions of the instantaneous wake center position using the lateral velocity and the downstream propagation velocity. Preliminary results show that these predictions underestimate the strength of wake meandering compared to the measurements, and that the root-mean-square error between predictions and measurements increases with the aforementioned ratio of integral time scale to downstream propagation time.

References:

Larsen, G.C., Madsen, H.A., Thomsen, K. and Larsen, T.J., 2008. Wake meandering: a pragmatic approach. Wind Energy, 11(4), pp.377-395.

Bastankhah, M. and Porté-Agel, F., 2017. A new miniature wind turbine for wind tunnel experiments. Part II: Wake structure and flow dynamics. Energies, 10(7), p.923.

Minute-scale forecasting using a long-range lidar: lessons learned from onshore and offshore campaigns

Ines Würth*, and Po Wen Cheng
Stuttgart University
*Presenting author

Keywords: Minute-scale forecasting | Scanning-lidar | Complex terrain | Offshore measurements | alpha ventus

With the increasing amount of renewable energy sources installed in the grid, the demand for minute-scale forecasts increases simultaneously, as grid operators need information of the power fluctuation in order to take measures to balance the grid. Minute-scale forecasts of up to one hour are usually implemented using the persistence method [1]. For this method it is assumed that there will be no changes in wind speed within the next designated time period, meaning the upcoming wind speed is equal to the present one. However, persistence can be problematic for locations in which wind conditions frequently change and therefore are not accurately predicted using historic information of the wind or power conditions.
We propose a novel approach for minute-scale forecasting of the wind power, which is based on wind speed measurements upwind of the wind turbines. Within the national funded WindForS research projects VORKAST and ParkCast, the use of a long-range wind lidar for wind power forecasting for time horizons up to 30 minutes was - and still is - investigated. In VORKAST, a longrange lidar was installed on a fixed platform next to a wind turbine on a complex terrain site in the south of Germany and probabilistic power forecasts were derived from measurements up to 10 km upwind of the turbine. In ParkCast the same lidar was then installed on top of the nacelle of a wind turbine behind the rotor in the offshore wind farm alpha ventus, measuring upwind and yawing along with the turbine. Again, power forecasts were derived from the lidar measurements for the turbine the lidar was mounted on. Additionally, probabilistic benchmark persistence forecasts were calculated from SCADA power data of the wind turbine at both sites. An evaluation of the continuous ranked probability score (CRPS) of both methods at both sites shows that lidar forecasts are less accurate than persistence at the onshore site (see Figure 1). At the offshore site, lidar forecasts are more accurate compared to persistence, but only for certain conditions. Results of the offshore site cannot be shown in this abstract due to confidentiality reasons, but will be available for the presentation.

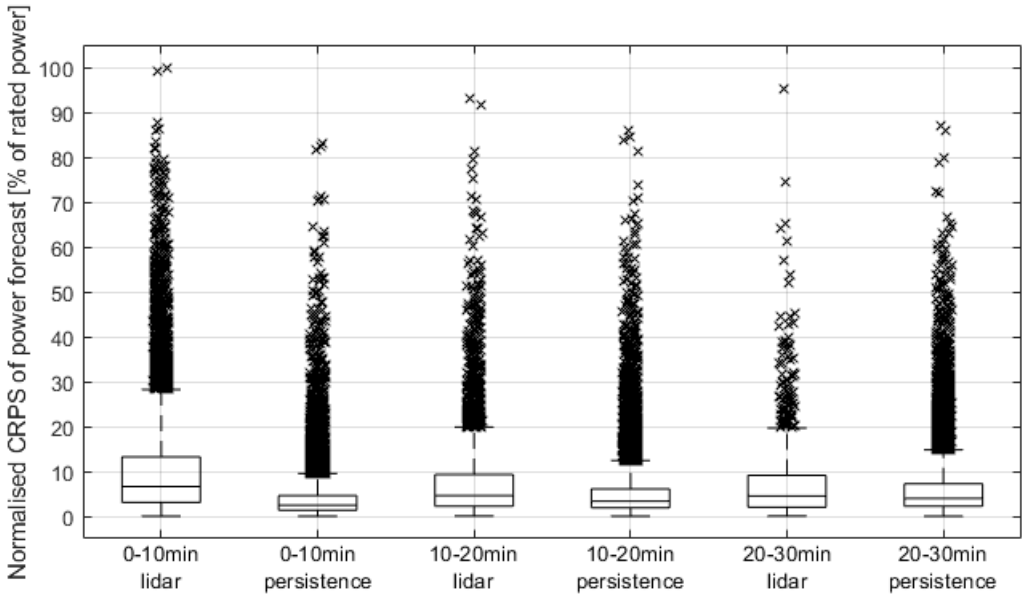


Figure 1: Boxplot of normalised CRPS of the power forecast of the onshore site for different forecasting horizons, comparing lidar forecasts and persistence.

In general, lidar measurements seem to be a valuable input for forecast models, as also recent investigations from colleagues have shown [2, 3]. However, they only add value under certain conditions. Onshore, the biggest obstacle seems to be the terrain type. The challenge when wanting to use upstream data for forecasting is that the data needs to be propagated in time and space. We used Taylor's frozen turbulence hypothesis, which claims that turbulent structures are propagated with the mean wind speed and are not changed but remain frozen. This might be valid offshore or for flat terrain and stable or neutral conditions, however in complex terrain, the atmospheric conditions are more complex. This contribution will discuss the results from both campaigns and share the lessons learned on the conditions under which long-range lidars can add value to minute-scale forecasting.

References:
[1] Würth, I 2019 Minute-Scale Forecasting of Wind Power—Results from the Collaborative Workshop of IEA Wind Task 32 and 36 Energies 2019, 12(4), 712; https://doi.org/10.3390/en12040712
[2] Valldecabres, L 2018 Very short-term forecast of near-coastal flow using scanning lidars, Wind Energ. Sci. 2018, 3, 313-327, https://doi.org/10.5194/wes-3-313-2018
[3] Theuer, F 2020 Minute-scale power forecast of offshore wind turbines using long-range single-Doppler lidar measurements, Wind Energ. Sci. 2020, 5, 1449–1468, https://doi.org/10.5194/wes-5-1449-2020

Lidar-based minute-scale wind speed and power forecast of free-stream and wake-influenced offshore wind turbines

Frauke Theuer[1,*], Marijn Floris van Dooren[1], Lueder von Bremen[2], and Martin Kühn[1]
[1]ForWind - University of Oldenburg
[2]DLR Institute of Networked Energy Systems
*Presenting author

Keywords: minute-scale forecast | remote sensing | scanning lidar | offshore

The increasing share of renewable energies in our energy system causes a rising demand for minutescale wind speed and power forecasts. These forecasts are able to support both the physical and economical balancing of power and can thus significantly contribute to grid stability and the reduction of curtailment (Würth et al.,2019). In this context, especially probabilistic forecasts are considered valuable for decision-making processes (Dowell and Pinson, 2016). Recently, the high potential of remote sensing measurements for the purpose of minute-scale forecasting was proven (Valldecabres et al.,2018,2020; Theuer et al.,2020).
Aim of this work is to further develop a recently developed lidar-based forecasting methodology (Theuer et al., 2020a) in order to increase its accuracy and make it applicable not only to free-stream but also wake-influenced wind turbines.

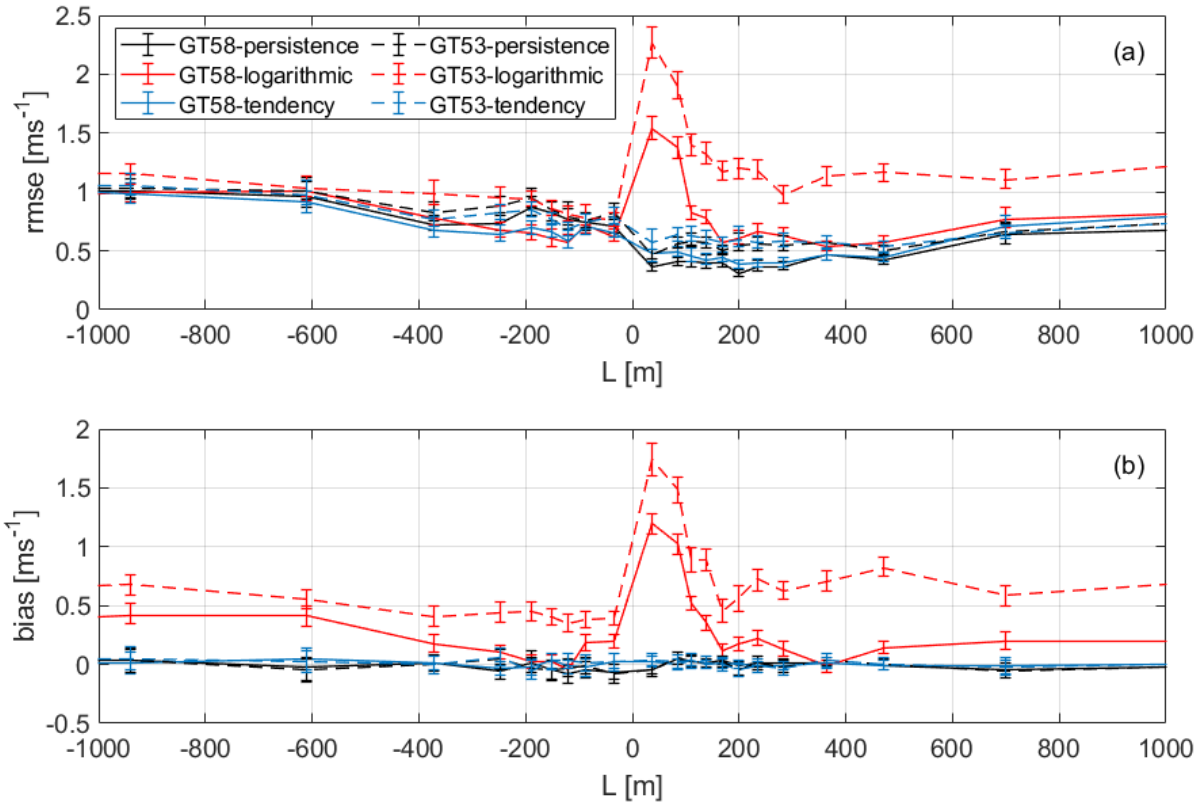


Figure 1: (a) rmse and (b) bias of 5-minute ahead wind speed forecasts at a free-stream turbine (GT58, solid lines) and a wake-influenced turbine (GT53, dashed lines) at GTI dependent on Obukhov length L. Persistence is shown in black, the lidar-based forecast using a logarithmic extrapolation in red and the lidar-based tendency forecast in blue.

We utilised long-range horizontal plan position indicator (PPI) lidar scans performed at the 400 MW offshore wind farm Global Tech I (GTI) in the German North Sea (Figure 1) to construct 5-minuteahead probabilistic wind speed forecasts of individual wind turbines in GTI. The scans span an azimuth of 150° with a resolution of 2°, have an averaging time of 2 s per measurement and cover range gates between 0.5 km and 8 km with 35 m spacing. The forecasting methodology is based on the recent work of Theuer et al. (2020a), where wind

vectors are derived from lidar scans and propagated by means of a Lagrangian advection technique. All vectors falling into a predefined temporal and spatial window were further selected to contribute to the forecast. The model's main source of error was found to be the extrapolation of wind speed from measuring height (24.6 m) to hub height (92 m) by means of a stability-corrected logarithmic profile, especially during very stable atmospheric conditions (Theuer et al. 2020a,2020b). We thus introduce an alternative model, that additionally utilises high-frequency SCADA (supervisory control and data acquisition) data and avoids the extrapolation across large height differences. Here, two consecutive lidar-based forecasts at measuring height and at times t and t+k, with lead time k, are used to determine a tendency of wind speed from time t to t+k. The estimated tendency is then applied to current SCADA data at time t to determine the wind speed at hub height at forecasting time t+k. In a final step, a probabilistic power curve is applied to translate wind speed distributions into power distributions (Theuer et al. 2020a).

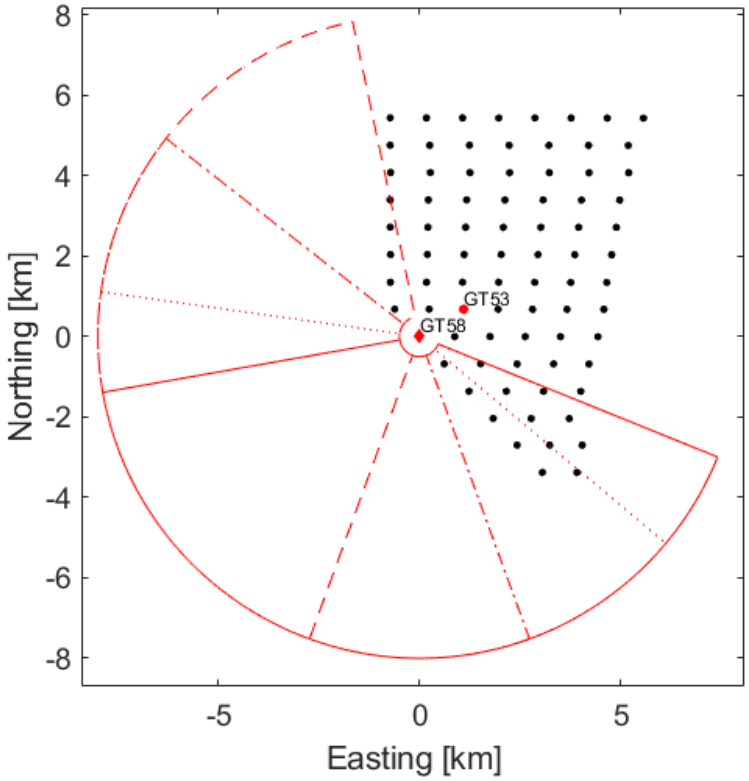


Figure 2: Layout of offshore wind farm Global Tech I (red) in the North Sea with the position of the lidar at GT58 marked as red diamond. Scan trajectories varying for different wind directions are shown in red.

Forecasts are evaluated by means of deterministic as well as probabilistic scores and compared against the benchmark persistence (Würth et al., 2019). Initial results show the lidar-based wind speed forecast's ability to outperform persistence during unstable and neutral atmospheric conditions for free-stream as well as wake-influenced wind turbines in terms of the rmse. In stable conditions results can be significantly improved as compared to lidar-based forecasts using a logarithmic extrapolation, however, were not yet able to outperform persistence. Generally, forecasts of waked turbines were found to be less accurate than those of free-stream turbines. In Figure 2 the rmse and bias of persistence, the lidar-based forecast using a logarithmic extrapolation and the lidar-based tendency forecast are depicted for two exemplarily turbines, i.e. the free-stream turbine GT58 and the waked turbine GT53, and dependent on Obukhov length L. Further analysis will include the evaluation of probabilistic scores and power forecasts.

References:
Dowell, J. and Pinson, P.: Very-Short-Term Probabilistic and Wind Power Forecasts by Sparse Vector Autoregression, IEEE Transactions on Smart Grid, 7, 763–770, https://doi.org/10.1109/TSG.2015.2424078, 2016.
Theuer, F., van Dooren, M. F., von Bremen, L., and Kühn, M.: Minute-scale power forecast of offshore wind turbines using long-range single-Doppler lidar measurements, Wind Energy Science, 5, 1449–1468, https://doi.org/10.5194/wes-5-1449-2020, 2020a.
Theuer, F., van Dooren, M. F., von Bremen, L., and Küuhn, M.: On the accuracy of a logarithmic extrapolation of the wind speed measured by horizontal lidar scans, Journal of Physics: Conference Series, 1618, 032 043, https://doi.org/10.1088/1742-6596/1618/3/032043, 2020b.
Valldecabres, L.; Nygaard, N.G.; Vera-Tudela, L.; Von Bremen, L.; Kühn, M.: On the Use of Dual-Doppler Radar Measurements for Very Short-Term Wind Power Forecasts. Remote Sens., 10, 1701, 2018.
Valldecabres, L., von Bremen, L.,Kühn, M.: Minute-scale detection and probabilistic prediction of offshore wind turbine power ramps using dual-Doppler radar, Wind Energy, 23, 2202-2224, https://doi.org/10.1002/we.2553, 2020.
Würth, I.; Valldecabres, L.; Simon, E.; Möhrlen, C.; Uzunoğlu, B.; Gilbert, C.; Giebel, G.; Schlipf, D.; Kaifel, A.: Minute-Scale Forecasting of Wind Power—Results from the Collaborative Workshop of IEA Wind Task 32 and 36. Energies, 12, 712, 2019.

Regular Session: Wind Farm Design and Optimization

Wind-turbine wake expansion in the atmospheric boundary layer; A physics-based analytical model

Dara Vahidi*, and Fernando Porté-Agel
Wind Engineering and Renewable Energy Laboratory (WiRE), École Polytechnique Fédérale de Lausanne
*Presenting author

Keywords: Wake growth rate | Analytical model | Near wake length | Ambient turbulence

In the wind energy community, analytical wake models provide the advantage of predicting the wind turbine wake flow and power production with a low computational cost compared to high-fidelity numerical simulations. With the recent developments of the wake superposition techniques (Zong and Porté-Agel 2020; Lanzilao and Meyers 2020), the power production of wind farms can be accurately estimated with a proper choice of the wake growth rate parameter. However, within the framework of existing analytical wake models (Jensen 1983; Frandsen et al. 2006; Bastankhah and Porté-Agel 2014), the wake growth rate parameter is either a constant or specified based on empirical formulations (Porté-Agel, Bastankhah, and Shamsoddin 2020). Due to the sensitivity of analytical wake model predictions to the estimation of this parameter, an accurate model of the wake growth rate based on the incoming flow characteristics is of great importance to the wind energy community.

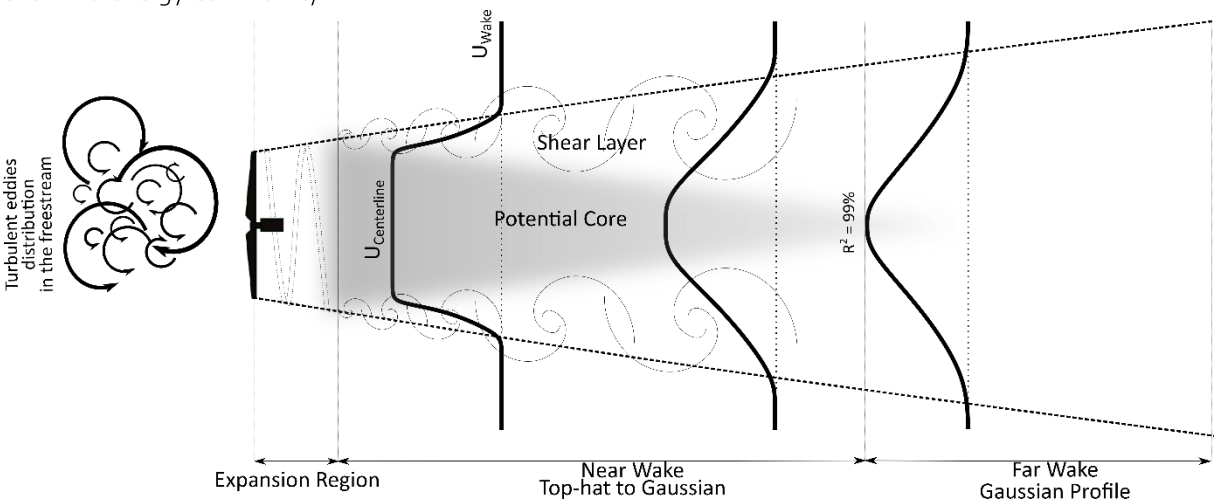


Figure 1: A schematic of the gradual growth of the wake, including the effect of shear layer and the incoming turbulence

In this study, a new physics-based wake model is proposed and validated to predict the wake growth rate downstream of a turbine based on the incoming ambient turbulence and the turbine operating condition. The new model, as a revised version of the one proposed by Cheng and Porté-Agel (2018), is built upon the application of Taylor diffusion theory, the Gaussian wake model, turbulent mixing layer theory, and the analogy between wind turbine wake expansion and scalar dispersion. These building blocks ensure that the model conserves mass and momentum in the far wake and accounts for the effect of both ambient turbulence and turbine-induced turbulence on the wake expansion.

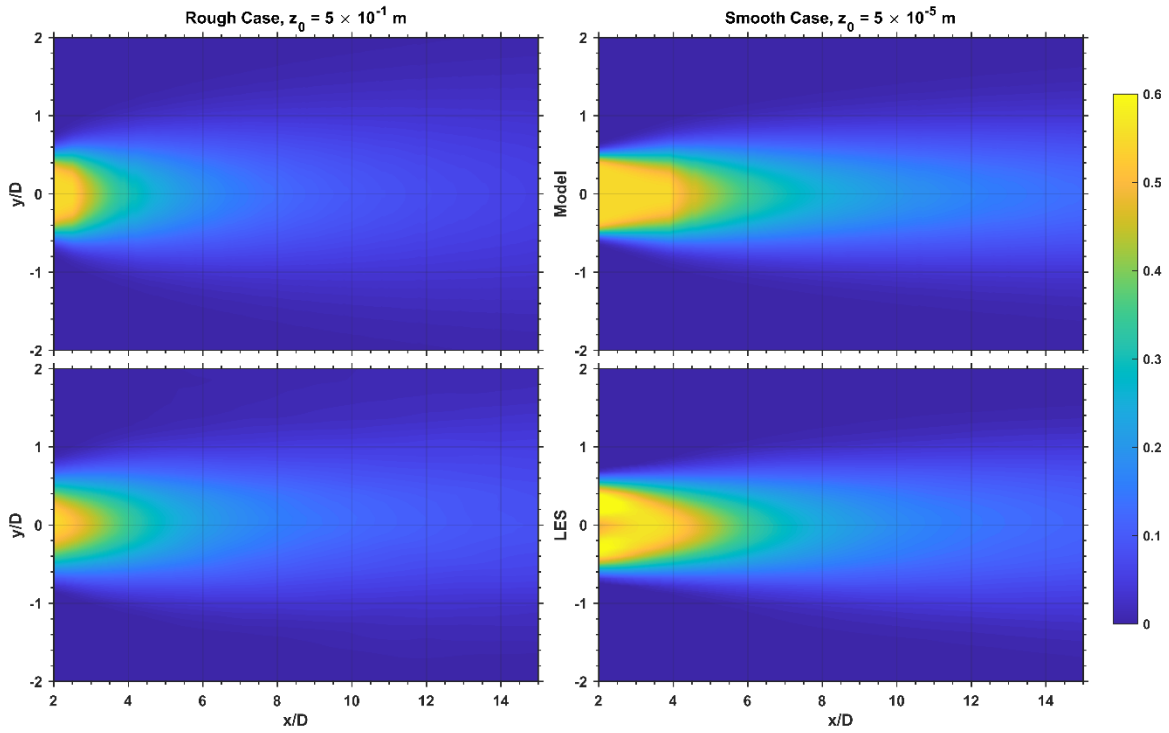


Figure 2: Wake velocity deficit, comparison of the model and LES results for a high turbulence inflow (left) and low turbulence inflow (right)

The latter is particularly important under low ambient turbulence conditions. As an integral part of the model, a new relation for the near wake length is derived as a function of the incoming ambient turbulence and turbine operating condition. It is important to note that all the model parameters are defined based on the existing literature without any parameter tuning. The only input for the wake model is a velocity time-series, which is sampled upstream of the turbine at hub height and represents the incoming atmospheric boundary layer (ABL) turbulence characteristics and distribution of the turbulent eddies. The results of the proposed model are then validated by a series of Large-Eddy Simulations of a utility-scale wind turbine wake under neutral ABL conditions with a wide range of incoming ambient turbulence levels. The results show an acceptable agreement between the model prediction and LES data for the wake growth rate and the near wake length.

Moreover, it is found that in the low ambient turbulence cases, the turbine-induced contribution to the wake expansion is between 30% to 40% of the total wake width. Therefore, including this factor plays a critical role in order to have a reasonable prediction of the wake flow in a wide range of ambient turbulence levels.

References:

Bastankhah, M. and Porté-Agel, F., 2014. A new analytical model for wind-turbine wakes. Renewable Energy, 70, pp.116-123.

Cheng, W.C. and Porté-Agel, F., 2018. A simple physically-based model for wind-turbine wake growth in a turbulent boundary layer. Boundary-Layer Meteorology, 169(1), pp.1-10.

Frandsen, S., Barthelmie, R., Pryor, S., Rathmann, O., Larsen, S., Højstrup, J. and Thøgersen, M., 2006. Analytical modelling of wind speed deficit in large offshore wind farms. Wind Energy: An International Journal for Progress and Applications in Wind Power Conversion Technology, 9(1-2), pp.39-53.

Jensen, N.O., 1983. A note on wind turbine interaction. Riso-M-2411, Risoe National Laboratory, Roskilde, Denmark.

Lanzilao, L. and Meyers, J., 2020. A new wake-merging method for wind-farm power prediction in presence of heterogeneous background velocity fields. arXiv preprint arXiv:2010.03873.

Porté-Agel, F., Bastankhah, M. and Shamsoddin, S., 2020. Wind-turbine and wind-farm flows: a review. Boundary-Layer Meteorology, 174(1), pp.1-59.

Zong, H. and Porté-Agel, F. (2020) "A momentum-conserving wake superposition method for wind farm power prediction," Journal of Fluid Mechanics. Cambridge University Press, 889, p. A8. doi: 10.1017/jfm.2020.77.

Computational Investigation of Wind Turbine Tilt Steering

Samuel Roach*, Hannah Johlas, Matthew Lackner, and Nuo Li
University of Massachusetts Amherst
*Presenting author

Keywords: tilt steering | wake deflection | yaw steering | potential flow

Wind farms experience power losses due to wakes of upwind turbines acting upon downwind turbines (Archer et al, 2018). Wake losses reduce energy production and have caused wind farm operators to announce reduced estimates of power production in large wind farms (Orsted, 2019).

Yaw steering is a method for reducing wake losses in which the wake of the upstream turbine is deflected by yawing the turbine slightly out of the wind, reducing the power production of the upstream turbine but resulting in net power gain of the combined turbines. Yaw steering has been tested at full scale, increasing power capture of a commercial farm (Fleming et al, 2017).

Preliminary research shows the potential of tilting (rather than yawing) the upstream rotor to deflect wakes below the rotor plane of downstream turbines (Annoni et al, 2017), (Fleming et al 2014), (Fleming et al 2015), (Miao et al 2016). Tilting may be effective because it entrains higher momentum wind from above the array downwards into the array, re-energizing the flow faster than yawing (Annoni et al, 2017).

In this study, tilt steering is evaluated using two models, an in-house free-wake vortex ring (FWVR) code and large eddy simulations (LES) using the Simulator fOr Wind Farm Applications (SOWFA).

Baldacchino and van Bussel (2014) and Vaal, Hansen, and Moan (2014) show a wind turbine wake can be approximated as a series of vortex rings. A FWVR code is implemented in this research to calculate steady-state wake strength and wake trajectories.

Each time step, a ring releases behind the rotor plane. Ring strength is determined by thrust, rotational speed, rotor relative wind speed, and free-stream wind velocity. An analytical solution for the velocity induced by a vortex ring at any point is used to calculate the induced velocity of points on the perimeter of each ring due to the influence of all other rings. The trajectory of each ring perimeter point is determined and the rings are reconstructed each step, allowing for wake expansion and skew. As in Vaal, Hansen, and Moan, (2014), the final vortex ring is eliminated as a new ring sheds from the rotor. The loop runs until the induced velocity at the rotor reaches a value within 1% of the previous time step. Figure1 shows the FWVR.

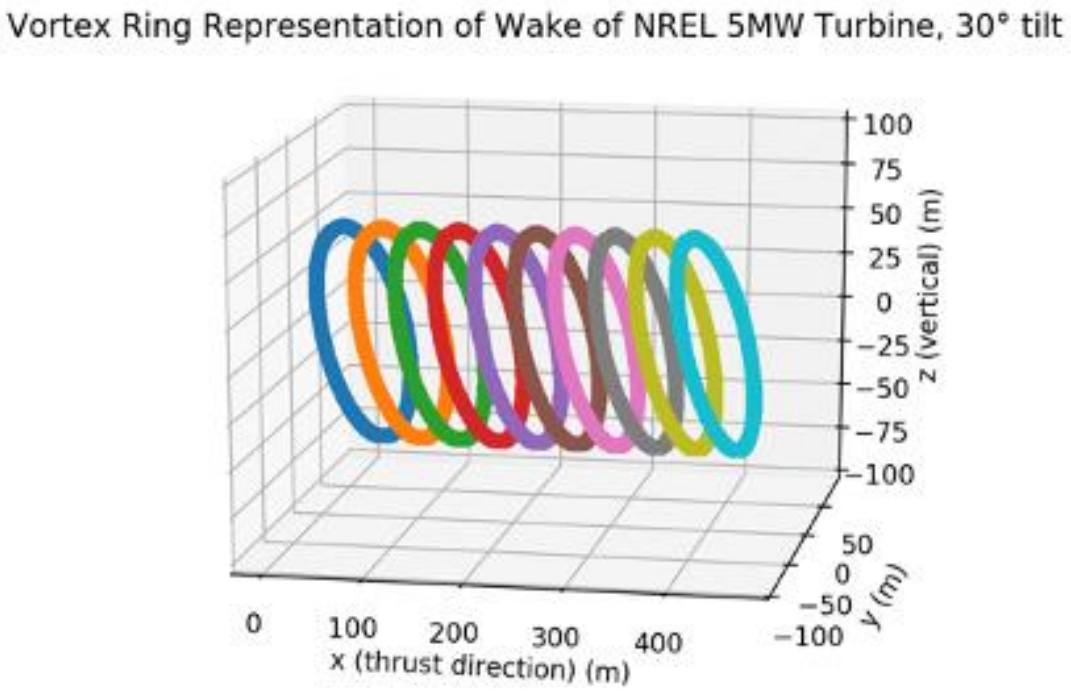


Figure 1: Visualization of steady state wake behind NREL 5MW turbine using vortex rings

Tilting results in the ground altering the wake. Because the ground acts as a "no-entry" boundary condition, the wake cannot pass through the ground and is pushed upwards. The method of images accounts for the ground effect in the FWVR, as recommended by Storm (2018). This simulates the ground effect by mirroring the rings of the wake over the ground plane and calculating the effect of their induced velocity upon wake rings.

Parametric studies using FWVR are used to assess turbine configurations and wake trajectories. The results elucidate the ground effect, quantifying the air entrainment rate from above the array.

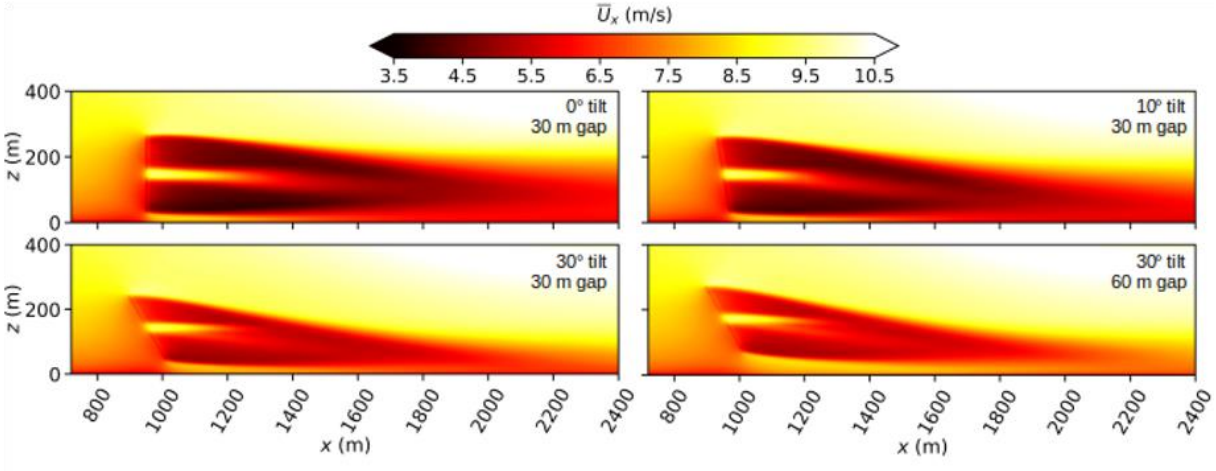


Figure 2: Preliminary LES wake velocity fields (side view) for different turbine configurations

LES analysis is used to validate the potential flow analysis performed. LES of the tilted-rotor wake from the IEA 15MW reference turbine (Gaertner 2020) is performed in SOWFA, using an actuator disc model for the tilted rotor. These simulations of a single turbine examine several rotor tilt angles up to 30 degrees as well as multiple hub heights, to address the wake interaction with the surface for different rotor-ground gaps. Figure2 shows LES results.

References:

Archer C., Vasel-Be-Hagh A., Yan C., Wu S., Pan Y., Brodie J., Maguire A., "Review and Evaluation of Wake Loss Models for Wind Energy Applications" Applied Energy, Vol. 226, 2018, pp 1187-1207

Orsted, "Orsted present update on it long-term financial target", 2019. URL: https://orsted.com/en/companyannouncement-list/2019/10/1937002

Fleming, P., Annoni, J., Shah, J.J., Wang, L., Ananthan, S., Zhang, Z., Hutchings, K., Wang, P., Chen, W., Chen, L. (2017). Field Test of Wake Steering at An Offshore Wind Farm. Wind Energy Science. Vol 2, 2017, 229-239.

Annoni, J. Scholbrock, A., Churchfield, M., Fleming, P. "Evaluating Tilt for Wind Plants," American Control Conference, Seattle, 2017.

Fleming P., Gebraad P., Lee S., van Wingerden, J.W., Johnson, K., Churchfield, M., Michalakes, J., Spalart, P., and Moriarty, P., "Evaluating Techniques for Redirecting Turbine Wakes Using SOWFA." Renewable Energy, Vol. 70, 2014, pp. 211-218.

Fleming P., Gebraad P., Lee S., van Wingerden, J.W., Johnson, K., Churchfield, M., Michalakes, J., Spalart, P., and Moriarty, P., "Simulation Comparison of Wake Mitigation Control Strategies for a Two-Turbine Case," Wind Energy, Vol. 18, 2015, pp. 2135-2143

Miao, W., Li, C., Yang, J., Xie, X. "Numerical Investigation of the yawed wake and its effects on the downstream wind turbine" Journal of Renewable and Sustainable Energy, Vol 8, 2016 https://doi.org/10.1063/1.4953791

Baldacchino,D., van Bussel, G.J.W., "Wind turbine wake stability investigations using a vortex ring modelling approach" Journal of Physics: Conference Series. 555, 012111, 2014

Vaal, J.B., Hansen, M.O.L, Moan, T. "Validation of a vortex ring wake model suited for aeroelastic simulations of floating wind turbines". Journal of Physics: Conference Series. Vol 555, 2014. 12-25

Storm, R.M.. "Wake Control Using Rotor Tilting". Master's thesis. Delft University of Technology (TU Delft), 2018

Gaertner, E., Rinker, J. Sethuraman, F.Z., et al. "Definition of the IEA 15-Megawatt Offshore Reference Wind Turbine. NREL Technical Report NREL/TP-5000-75698. National Renewable Energy Laboratory, 2020

A low computational cost framework for the testing of wind farm control strategies through wake steering

Felipe Novais[1], David Schlipf[2], and Steffen Raach[3]
[1]Politecnico di Milano
[2]Flensburg University of Applied Sciences
[3]sowento GmbH

Keywords: Wake steering | Wind farm control | Wind farm optimization

As the global installed capacity of wind energy expands, the interest towards improving the efficiency of wind farms also grows. The idea of wind turbines acting greedily aiming to maximize its own power production has given place to coordinate control strategies, in which each turbine of the wind farm acts collectively to achieve a common objective [1]. The concept of wind farm control lies on the assumption that neglecting the dynamic interactions between turbines might lead to a sub-optimal state. Wind farm control could be achieved through different techniques, however this work will be limited to wake steering, which consists in applying an intentional yaw misalignment to the upfront turbine in order to divert the disturbed flow to minimize its impact over the downstream turbine, increasing the power production of the wind farm as whole whilst decreasing structural loads over waked turbines [2].
In order to achieve the optimal wake steering setting, it is necessary that each turbine has the correct set of demanded yaw misalignment assigned. The standard approach utilized in recent field tests is to estimate the flow with low-fidelity surrogate wake models and obtain the optimal set of yaw misalignment [3][4]. The main issue consists in the idea that if the model is inherently unable, due to the simplification of the physics involved, to satisfactorily approximate the wind flow, then the wake steering effectiveness might be impaired. Therefore, different means to obtain the optimal yaw misalignment are worth investigating.
This work presents the development of a closed-loop modular framework, which allows to test with ease and low-computational cost different strategies to reach the optimal wind farm control wake steering settings. The framework utilizes surrogate models and a Gaussian distributed deviation from the demanded yaw misalignment to emulate wind farm data and applies for each optimization process an algorithm to optimize the control settings.

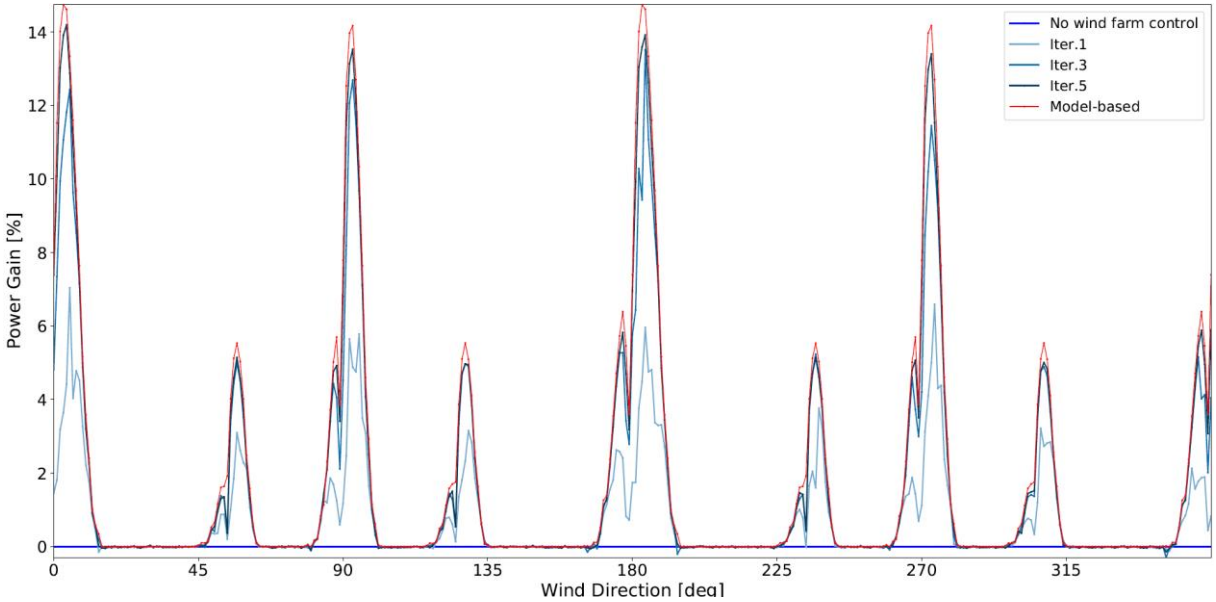


Figure 1: Maximum Power Point Tracking (MPPT) algorithm iterative optimization process for a 2x2 wind farm considering a fixed turbulence, wind speed and a normally distributed wind direction.

Further, three algorithms are presented and investigated for different level of complexities, including varying inflow conditions and number of turbines, in order to explore its efficacy. Firstly, a model fitting approach which consists in estimating the tuning parameters out of the wake surrogate lowfidelity models. Secondly a purely data-driven strategy which aims to track the set of yaw misalignment observed which returns the highest generated wind farm power. Thirdly, an approach based on fitting a surrogate machine learning model to a set of data in order to predict under a defined optimization boundary what is the optimal setting.
Overall, it was observed that data-driven approaches relies heavily on data quality and quantity and requires data processing steps in order to make different data points comparable in varying inflow conditions. Furthermore, they might need several iterations to reach the optimal. Whereas, model fitting algorithms based on the low-fidelity models are capable of extrapolating optimal control inputs to unseen flow conditions and reach the optimal demanded yaw misalignment on the first iteration, yet their reliability and capability to approximate the flow in real conditions is still limited.

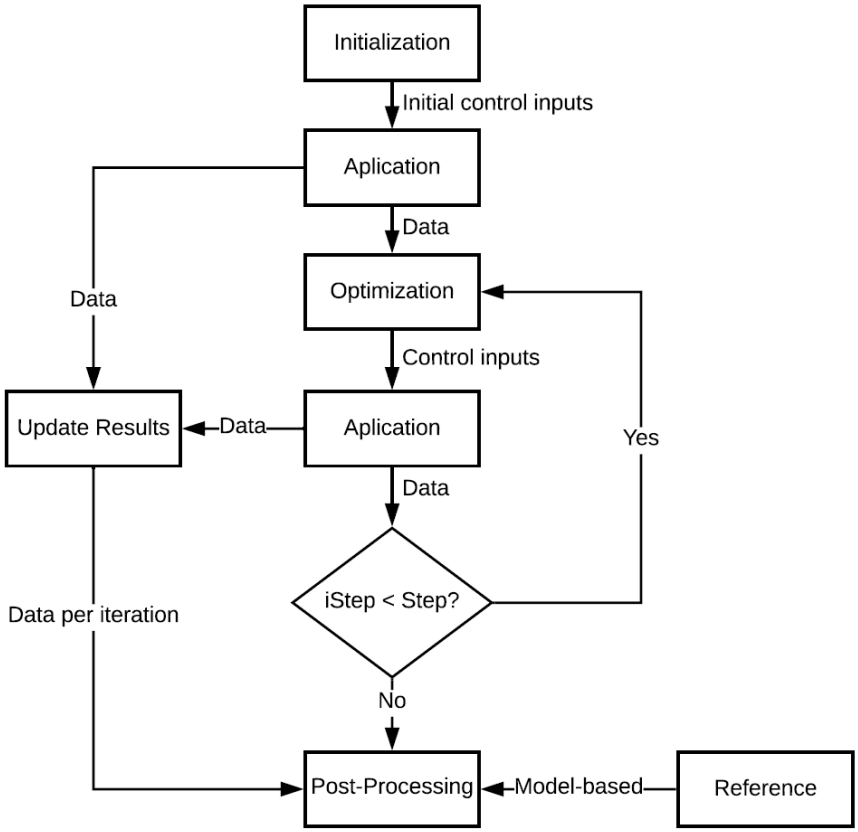


Figure 2: Implementation of the low computational cost closed-loop control framework with FLOw Redirection and Induction in Steady-state (FLORIS) [5].

The framework demonstrated to be a valuable tool due to its low computational effort required to simulate potential gains of different algorithms over a year or even the lifetime of a wind farm. Such tool could be utilized as a first step, for tuning and verification, of algorithms which could then be later validated with high-fidelity simulations.

References:
[1] M. Steinbuch, W. Boer, de, O. Bosgra, S. Peeters, and J. Ploeg (1998). Optimal control of wind power plants. Journal of Wind Engineering and Industrial Aerodynamics, 27(1-3):237–246.
[2] J-W. van Wingerden, P. A. Fleming, T. Göçmen, I. Eguinoa, B. M. Doekemeijer, K. Dykes, M. Lawson, E. Simley, J. King, D. Astrain, and et al. (2020). Expert elicitation on wind farm control Journal of Physics: Conference Series, 1618:022025, Sep 2020.
[3] B. M. Doekemeijer, S. Kern, S. Maturu, S. Kanev, B. Salbert, J. Schreiber,F. Campagnolo, C. L. Bottasso, S. Schuler, F. Wilts, T. Neumann,G. Potenza, F. Calabretta, F. Fioretti, and J.-W. van Wingerden (2021). Fieldexperiment for openloop yaw-based wake steering at a commercial onshorewind farm in italy. Wind Energy Science, 6(1):159–176.



[4] P. Fleming, J. King, E. Simley, J. Roadman, A. Scholbrock, P. Murphy,J. K. Lundquist, P. Moriarty, K. Fleming, J. van Dam, C. Bay, R. Mudafort,D. Jager, J. Skopek, M. Scott, B. Ryan, C. Guernsey, and D. Brake. Continued results from a field campaign of wake steering applied at a commercial wind farm part 2 (2020).Wind Energy Science, 5(3):945–958.
[5]: NREL (2020). FLORIS Version 2.2.3. Available at: https://github.com/NREL/floris

Wind Farm Optimization in PyWake/TOPFARM Using Gradients and Smart-Start Algorithms

Rafael Valotta Rodrigues[1,*], Pierre-Elouan Réthoré[2], Mads Mølgaard Pedersen[1], and Katherine Dykes[2]
[1]Technical University of Denmark
[2]DTU Wind Energy
[*]Presenting author

Keywords: TOPFARM | PyWake | Wind farm Layout optimization | Wind turbine wakes | wind farm arrays

Abstract: The development of more cost-efficient wind farms depends on improvements in wind farm layout optimization techniques. In this context, TOPFARM is a computational tool that enables fast wind farm models evaluation [1]. TOPFARM uses OpenMDAO for optimization and PyWake for Annual Energy Production (AEP) computation with different wake models. OpenMDAO is a High-Performance Computing (HPC) tool for multidisciplinary analysis and optimization especially suited for performing gradient-based optimization [2]. Different gradient evaluation methods have been implemented for AEP optimization with respect to the wind turbine positions in TOPFARM/PyWake, including: automatic differentiation, Complex-Step (CS), and Finite Differences (FD). Automatic differentiation is performed using Autograd, a python package that computes exact derivatives (Jacobian matrix) of an objective function. The CS approach uses complex numbers to calculate directional derivatives. FD essentially perturbs the design variables to calculate all the partial derivatives, while the CS carries the perturbations on the imaginary part of the design variables.
Autograd only requires one function evaluation to obtain all the gradients, while FD and CS require two times the number of design variables function evaluation. In this work, we compare these gradient estimation methods to run wind farm optimization through different wind farm scales. The simulations were performed using a smart-start algorithm to identify an initial layout that potentially maximizes AEP by selecting turbine positions that are less affected by wake effects. The same cases were also simulated not using the smart-start option aiming to compare the two strategies.

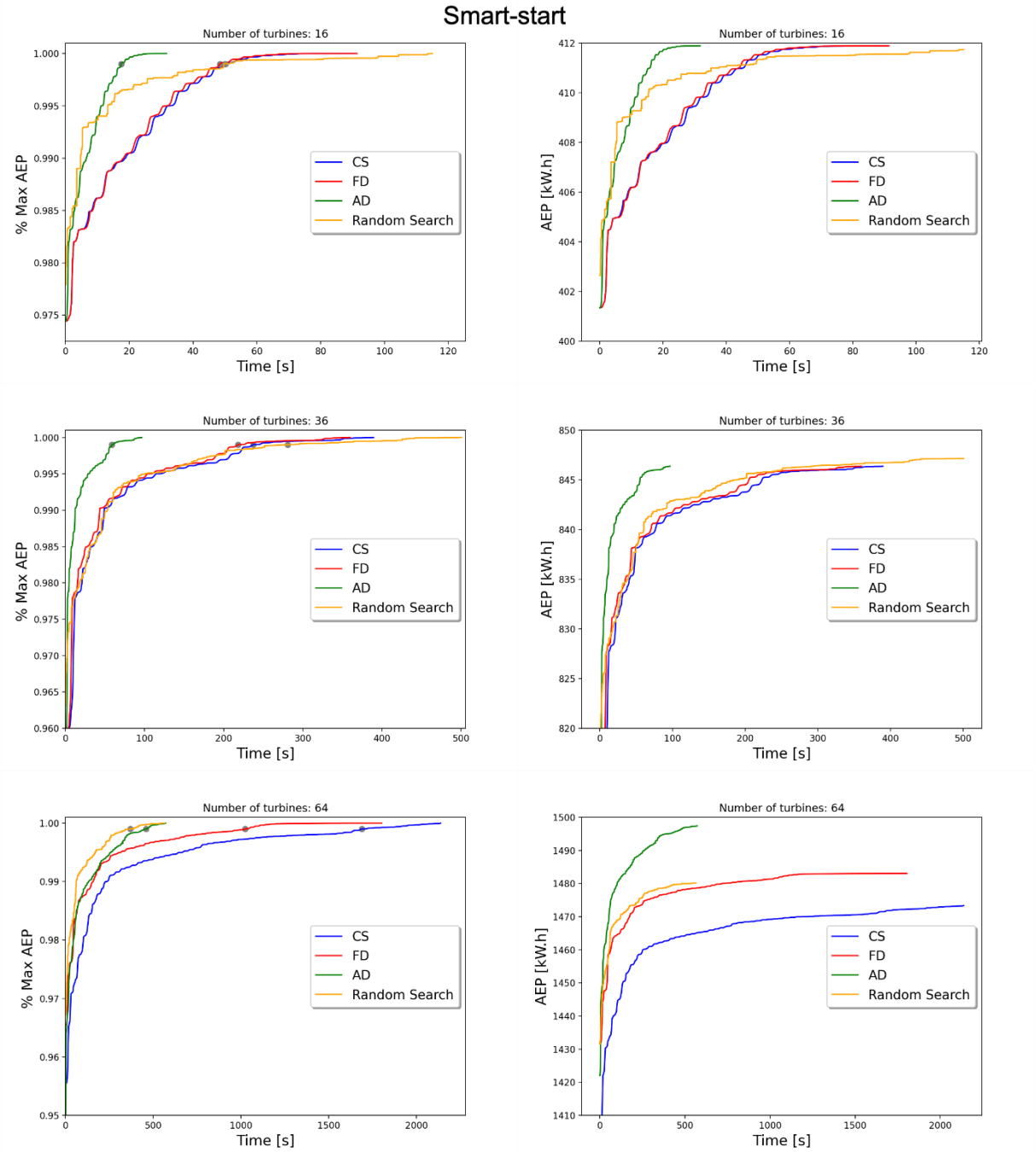


Figure 1: Smart-start AEP optimization using autograd, complex-step, finite-differences, and random search.

Additionally, we compare these methods with other gradient-free optimization algorithms such as random search. A TOPFARM problem was defined with the position of the turbines as the design variables and spacing between turbines and boundaries as constraints. The site was defined as described in the IEA Wind task 37 case study 1 [3] site with the wind direction discretized into 16 bins, a constant wind speed of 9.8m/s, and a fixed CT curve. The turbines were placed considering a circular boundary constraint surrounding the farm, and different numbers of turbines were analyzed.

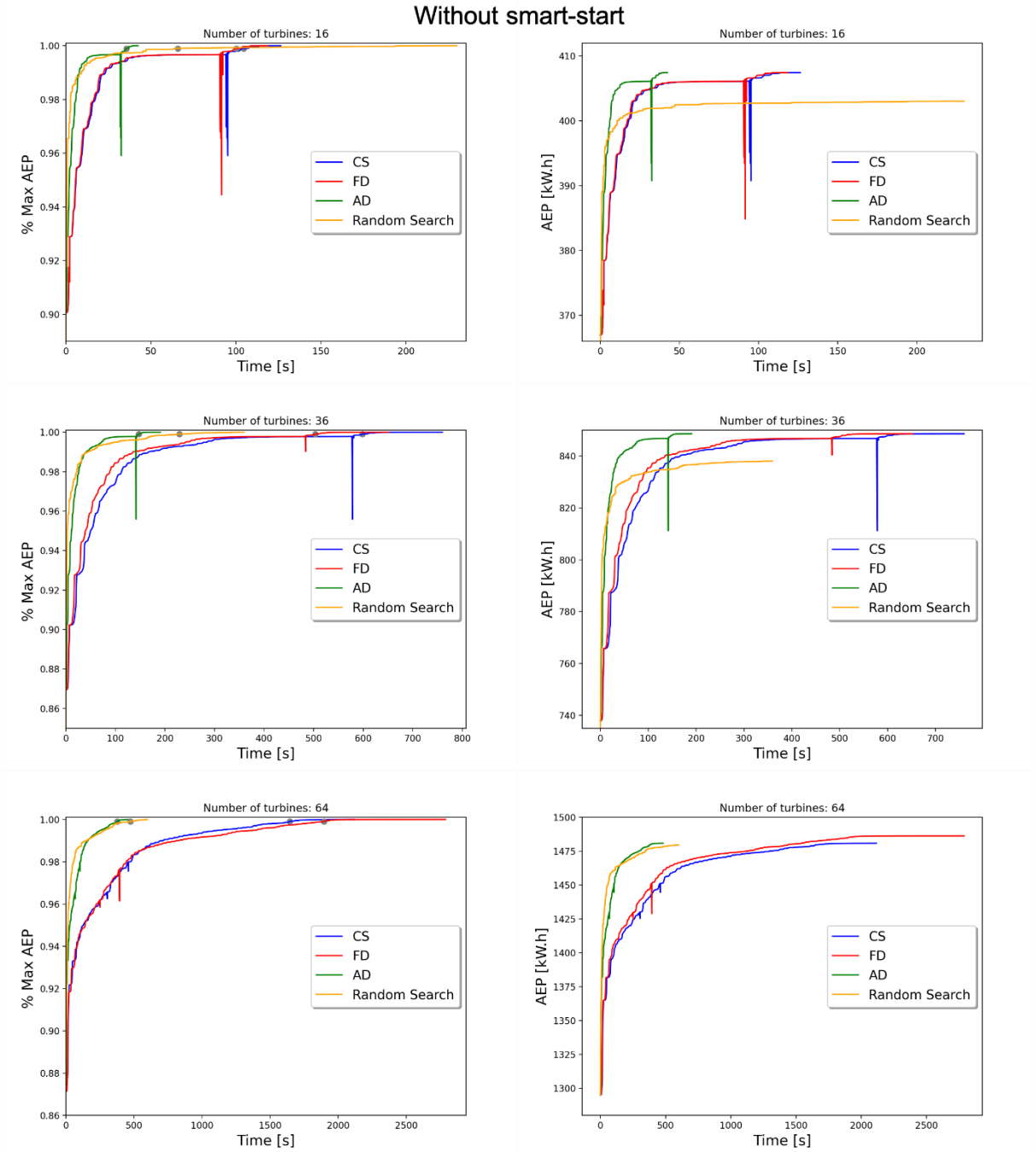


Figure 2: AEP optimization without using the smart-start, considering autograd, complex-step, finitedifferences, and random search.

For the analysis mentioned above, the ratio between the area of the circular boundary constraint and the rotors area was kept constant for the different number of turbines. Figures 1 and 2 show the results for the simulations across scales with and without the smart-start, respectively. In terms of AEP, the level of improvement consistently agrees with previous results from the existing literature [3]. The autograd achieved optimized results faster through all the scales, whereas the randomsearch performed similarly to the complex-step and the finite-differences for the 16 and 36 turbines case. For the 64 turbines case, the random-search converged faster than the complex-step and the finite-differences. Additionally, the autograd with smart-start converged to a higher AEP value compared to all the other options for the 64-turbines case. Moreover, the use of the smart-start allowed a faster convergence to optimized layouts. Further analysis will consider multiple smart-start simulations (with multiple attempts of initial layout) to assess its impact on AEP and processing time.



References:
[1] Réthoré, PE, Fuglsang, P, Larsen, GC, Buhl, T, Larsen, TJ, & Madsen, HA 2014. 'TOPFARM: Multi-fidelity optimization of wind farms', Wind Energy, vol 17, no. 12, pp. 1797-1816.
[2] Gray, JS, Hwang, JT, Martins, JRRA, Moore, KT, and Naylor, BA 2019, 'OpenMDAO: An Open-Source Framework for Multidisciplinary Design, Analysis, and Optimization', Structural and Multidisciplinary Optimization.
3] Baker, NF, Stanley, AP, Thomas, JJ, Ning, A, and Dykes, K 2019, 'Best practices for wake model and optimization algorithm selection in wind farm layout optimization', In AIAA Scitech 2019 Forum, pp. 0540-0544.

Progress on optimizing wind farms and rotor designs using adjoints

Jeffery Allen*, John Jasa, Ethan Young, Ryan King, and Garrett Barter
National Renewable Energy Laboratory
*Presenting author

Keywords: Optimization | adjoints | farm layout | roter design | wake deflection

Modern wind plants are increasingly tasked with multiple performance objectives. In addition to designing plants that maximize power output and minimize the levelized cost of energy (LCOE), the design and operation of wind plants is increasingly influenced by challenges regarding grid integration of variable generation renewables. This places a growing emphasis on making wind plants more controllable and predictable. WindSE is a Reynolds-averaged Navier-Stokes (RANS) model designed around analytical gradient and adjoint methods, with the ability to capture terrain-induced effects, as shown in Figure 1. The recent addition of an unsteady solver with an actuator line method (ALM) and ongoing work to enable massively parallel optimizations gives it a unique niche to explore coupled plant-level controls and design problems. This code is an open source python package built on the FEniCS framework that utilizes fast, parallel PETSc solvers to model fluid flow throughout wind-farm scale domains.

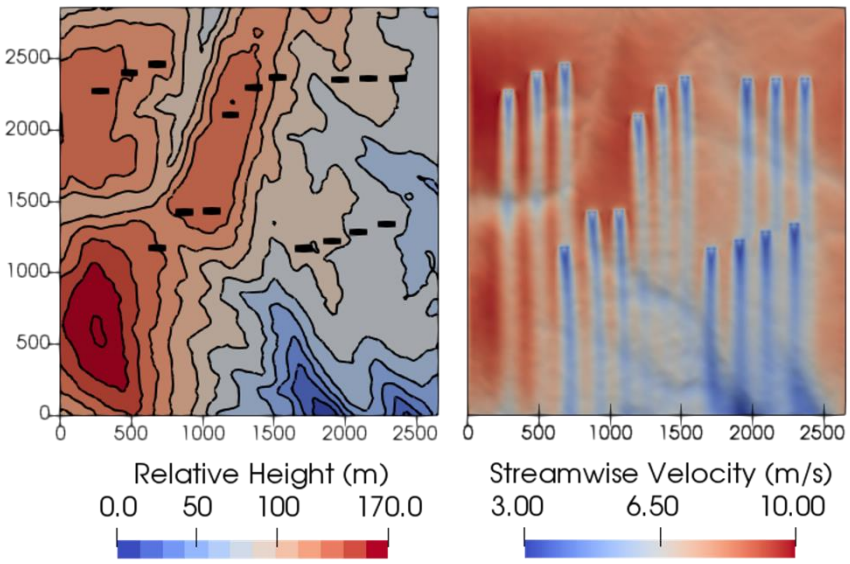


Figure 1: The effect of terrain on the path and downstream interactions of turbine wakes.

Two recent studies performed using WindSE demonstrate the capability to optimize under a wide variety of flow conditions and objective functions. In the first, we present an optimization focused on modifying the layout of a wind farm with a fixed number of turbines for maximum total power output [1]. This study highlights the ability to quickly perform simulations using the steady Navier-Stokes solver combined with rotors represented as actuator disks while also stressing the importance of capturing terrain-induced effects. Gradient-based optimization using the RANS equations is viable due to the inclusion of efficiently computed adjoint derivatives. We interpret the physical results of the optimal layout and also discuss the computational cost of scaling to larger problems.

In the second study, we present the capabilities of the unsteady Navier-Stokes solver, where rotorblade profiles represented by actuator lines are optimized to enhance wake steering effects and overall power production [2]. We quantify the wind plant performance gains obtained from this type of simultaneous control co-design optimization as compared to optimizing the blade design and yaw independently. Figure 2 shows the differences between a baseline two-turbine system and an optimized system where we fine-tune

the blade chord profile. Results and challenges from each study are quickly summarized and used to motivate the current development efforts within WindSE.

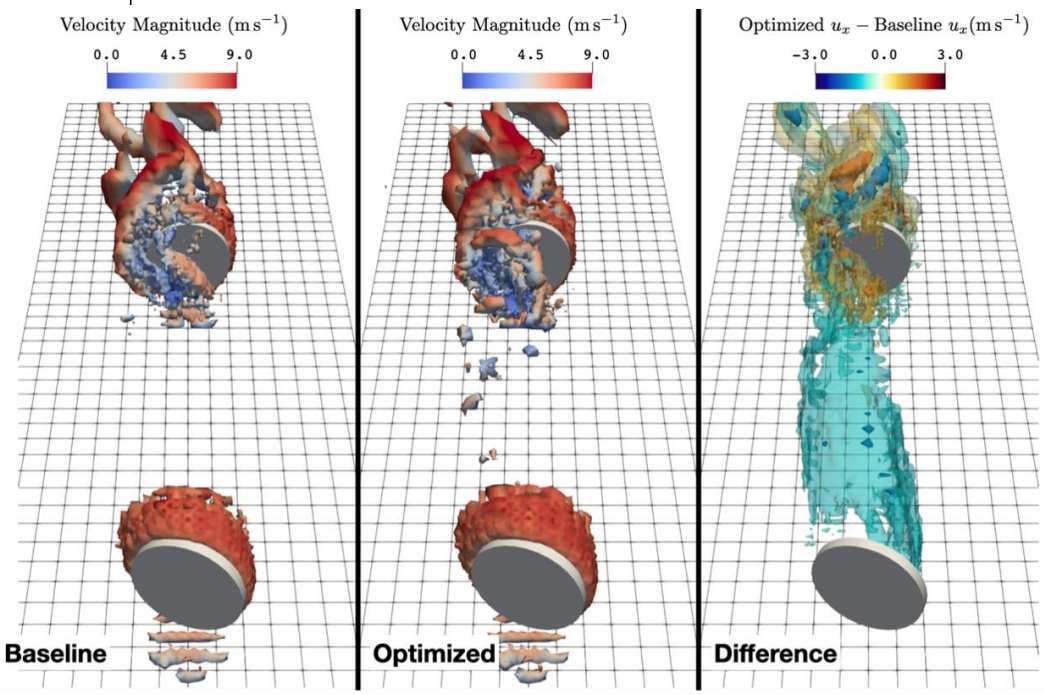


Figure 2: A two-turbine system where the upstream turbine uses the baseline chord profile versus a chord profile optimized for total power of the system.

Current and future work is focused on enabling higher-resolution studies with more degrees of freedom through parallelization of both the simulation and optimization algorithms. We present benchmarking results to show that WindSE performs well in both weak- and strong-scaling tests and further demonstrate that the optimizer obtains the same convergence rates in both shared- and distributed-memory environments. Using larger wind farms, we can study deep-array effects within an optimization context, allowing the use of objective functions that have been previously unstudied.
As an example, we present ongoing work on a blockage metric which characterizes the loss of available kinetic energy due to wake effects from multiple upstream turbines.

References:
J. Allen, R. King, and G. Barter, "Wind Farm Simulation and Layout Optimization in Complex Terrain", Journal of Physics: Conference Series, 2020
J. Allen, E. Young, P. Bortolotti, R. King, and G. Barter, "Blade Design Optimization to Enhance Wind Plant Flow Control", submitted to Wind Energy

Airflow modelling over hybrid solar/wind farm

Andrey Sogachev*
DTU Wind Energy
*Presenting author

Keywords: Hybrid farm | CFD approach | turbulent flow | roughness

Combining solar photovoltaics (PV) panels and wind turbines at the same location is a new trend in renewable energy. Co-located different energy sources allow to stabilize energy production and to reduce the operational cost. The combination can yield up to twice the amount of electricity as having either system working alone. Yet the solar-wind co-located hybrid power plants face some technical and operational challenges. One of them is the interaction of airflow and PV panels. Many CFD simulations and wind tunnel tests were conducted to investigate the effects of different spacing parameters on the wind loading of both the ground and roof-mounted PV-panels arrays. The number of studies dealing with the impact of solar panels on wind patterns is significantly lower. There is a lack of data on wind energy availability above the arrays, where a wind energy developer may find an opportunity to install a wind farm. In the absence of experimental data, the CFD approach is a useful tool capable of providing spatial patterns of wind and turbulence over a solar plant and developing optimal installation strategies.

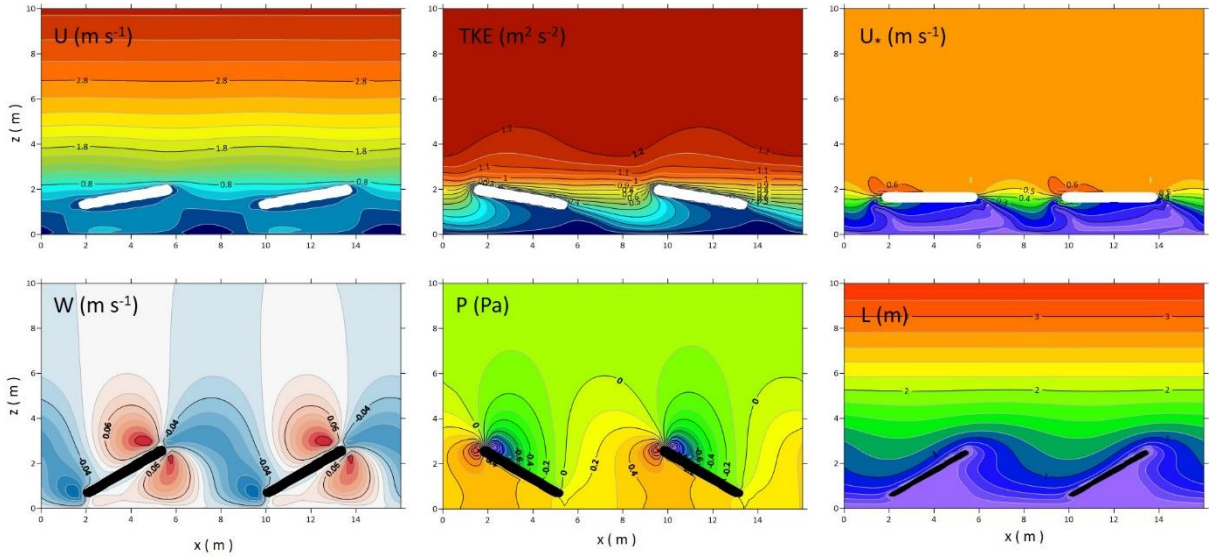


Figure 1: Examples of airflow parameters (streamwise wind speed, U; turbulent kinetic energy, TKE; local friction velocity, U; vertical velocity, W; kinematic pressure, P and turbulence scale, L) simulated by SCADIS model for different PV layouts.*

The atmospheric boundary layer model SCADIS was used in this study. First, the model adapted for simulation of airflow over the periodic array of PV panels was used to investigate the effect of different solar panels layouts (height over the ground, inclination angle) on the underlying surface's aerodynamic properties. In this computationally more expensive mode with a high spatial resolution description of each panel, the model demonstrated a good qualitative agreement with flow patterns obtained in wind tunnel tests (see Fig. 1). Numerical experiments with ground-mounted arrays showed that the effective roughness (roughness that satisfies the geostrophic drag law) of a horizontally infinite solar plant depends on panels inclination angle to incoming airflow. For example, for PV array rows of 4 m wide with a gap between the rows of 4 m, the roughness values for the inclinations of 0 and 30 degrees would be about 0.6 m and about 2.9 m respectively. Secondly, determining relations between solar panels layouts and surface roughness allows replacement in the model spatially distributed PV panels drag by one parameter. The model in this computationally less expensive mode was used to estimate solar panels effect on wind inside the boundary layer where wind turbines operate. For example, numerical experiments showed that a solar farm with a longitudinal extent of

300 m could have a remarkable effect on flow statistics inside the 100 m surface boundary layer. Airflow is affected up to 1 km distance downwind of the solar farm: a decrease of wind speed (5-10%) and an increase of turbulence intensity (at the farm's near-wake zone till 2-3 times)(see Fig. 2). Modified flow properties can create large amounts of stress on the turbines, causing difficulties in their operation and fatigue issues over time.

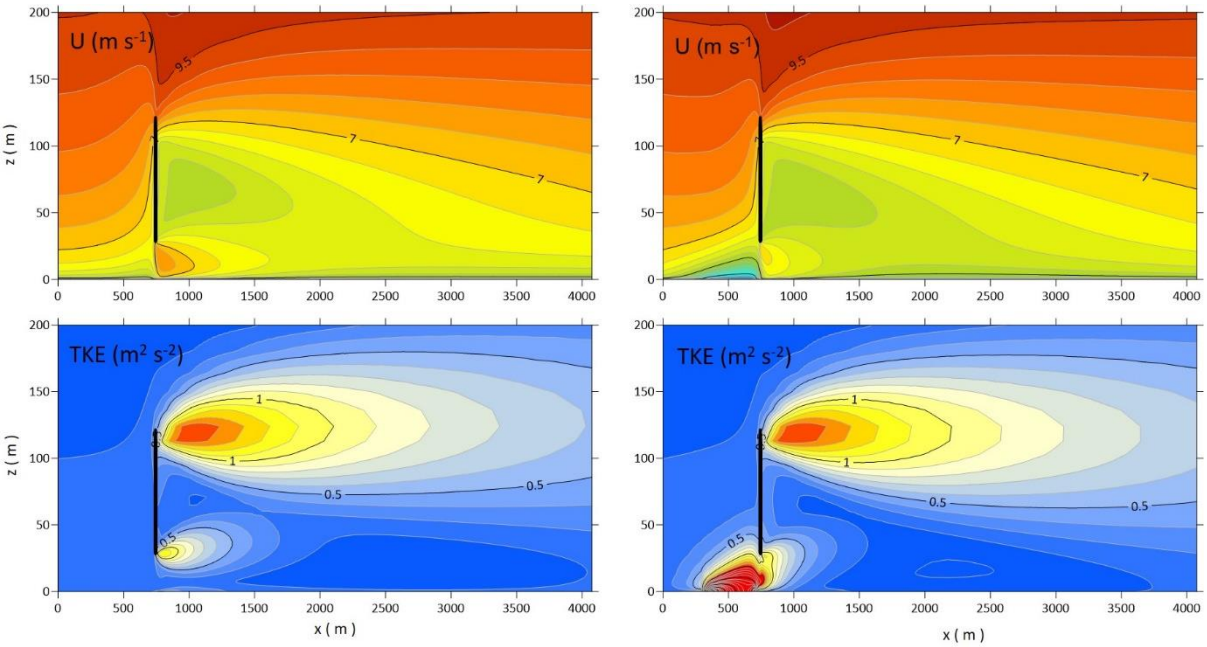


Figure 2: Airflow parameters (streamwise wind speed, U and turbulent kinetic energy, TKE) around a single wind turbine simulated by SCADIS model in the absence (left panels) and the presence (right panels) a solar farm upwind.

The work provides the first step in developing a methodology to estimate turbulent flows affected by solar panels. The improved method (stability, topography) can benefit site assessment and development (e.g. Global Wind Atlas) for high insolation zones. The model will have to be coupled to an aeroelastic model to predict the consequences of upwind PV panels for power production and dynamic loads on wind turbines quantitatively.

Regular Session: Meteorology and Microscale Modelling (I)

Multiscale wind turbine wake modeling within a wind farm using the WRF-LES model: An application to the Lillgrund offshore wind farm

Baris KALE[1,2,*], Sophia Buckingham[1], Jeroen van Beeck[1], and Alvaro Cuerva-Tejero[2]
[1]von Karman Institute for Fluid Dynamics
[2]Universidad Politécnica de Madrid
[*]Presenting author

Keywords: wind turbine wakes | blade-element momentum theory | large-eddy simulation | generalized actuator disk Model | Weather Research and Forecasting model

The increasing demand for wind power in recent years has led to an increase in the usage of numerical simulations in wind energy applications such as optimizing the design and efficiency of real-world wind farms. Accurate modeling of the atmospheric boundary layer (ABL) flows and their interactions with clustered wind turbines within a wind farm, depends on the proper representation of atmospheric conditions and the correct parameterization of wind turbine dynamics. Mesoscale models used to predict the average state of the atmospheric boundary layer and simulate large turbulent structures occurring in atmospheric events are not capable enough to capture turbineinduced wakes in a utility-scale wind farm, due to their limited spatial and temporal resolutions.
Unlike wind farm parameterizations utilized in mesoscale applications, microscale modelling combined with an adequate wind turbine model can provide both, a more precise prediction of the turbulent flow, and therefore, a more accurate estimation of the characteristics of wind turbine wakes and wind farm performance. Recent studies on wind energy applications have demonstrated the advantages of large-eddy simulation (LES) that permits the accurate reproduction of temporal and spatial turbulence scales that characterize wind farm flows in the ABL when performing microscale simulations.
In this research, we evaluate the performance of a generalized actuator disk (GAD) wind turbine parameterization, which is based on blade-element momentum (BEM) theory[1], and is designed to be used in large-eddy simulation applications in the Weather Research and Forecasting (WRF) framework[2]. This GAD model combined with BEM theory reproduces the turbine-induced flow rotation in the near-wake region as well as the non-uniform force distribution, and therefore, has the ability to model lift and drag forces along the blades, based on local flow information and blade characteristics[3].
Prior to the application to a real wind farm, an idealized WRF-LES simulation with the GAD model is employed to test the model performance in flow-wind turbine interaction for a stand-alone wind turbine under different atmospheric stability conditions. This work is then extended to a real test site, the Lillgrund Offshore Wind Farm, located about 10 km off the southern coast of Sweden. These results are compared with in-situ observations over a certain period of time. The WRF's dynamic downscaling feature is used to force mesoscale features and ABL turbulence from tens of kilometers (~ 20 km) to several meters (~ 10 m) in the horizontal direction in order to provide realistic timevarying lateral boundary conditions to the LES domain(s).

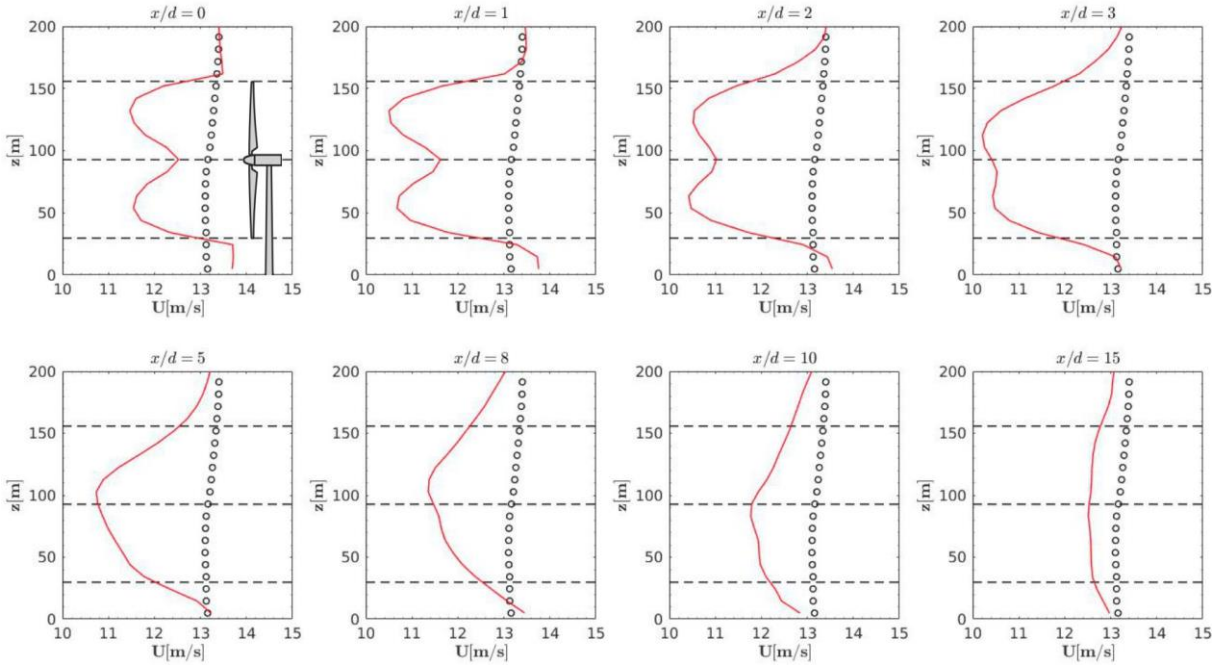


Figure 1: Representation of vertical profiles of the 2h-averaged streamwise velocity, U [m/s], in idealized WRF-LES/GAD simulation: 1D upstream of the wind turbine (open black circles), different downstream locations (red solid lines). The upper and lower horizontal dashed lines indicate vertical levels cut by the turbine blades and the middle one shows the hub height. D = 126m is rotor diameter.

The main conclusion of this work is that the WRF-LES with the GAD model has a high potential for multiscale modeling of wind turbine wake structures within a wind farm operating in real atmospheric conditions, even considering wind turbine yaw dynamics[4]. In figure 1, results of vertical profiles of the 2hours-averaged streamwise velocity, U, for the idealized WRF-LES/GAD simulation inside a moderately convective ABL over a flat terrain are presented for 1D upstream of the wind turbine rotor and different downstream locations without any pre-cursor simulation to speed up turbulence mixing and ground effects. The wind turbine data is taken from the publicly available National Renewable Energy Laboratory (NREL) 5-MW reference turbine[5].

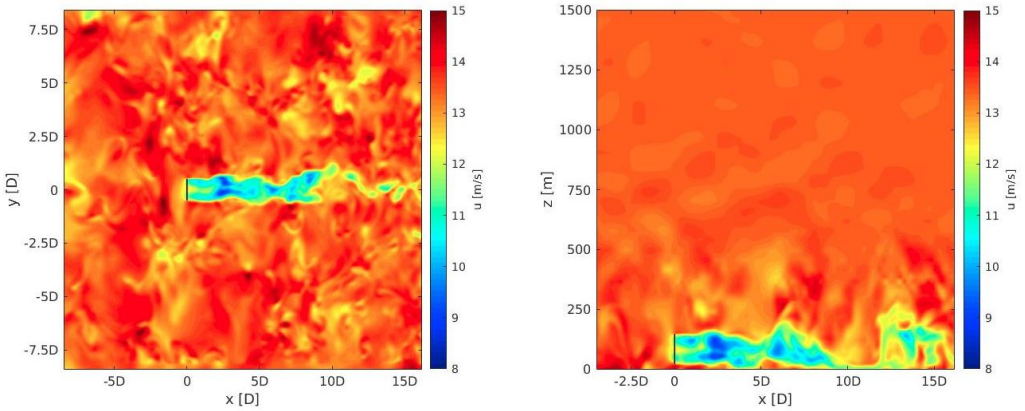


Figure 2: Instantaneous u [m/s] values at x = 0 at 1h from the moderately convective WRF-LES simulation, x-y domain (left), x-z domain (right). The solid black line shows the position of the GAD at x = y = 0.

In figure 2, the instantaneous values of the longitudinal component of the wind velocity, u, values at x = 0 at 1h from the moderately convective WRF-LES simulation for the 5-MW wind turbine.

References:

[1] Glauert, H., 1935. Airplane propellers. In Aerodynamic theory (pp. 169-360). Springer, Berlin, Heidelberg.

[2] Skamarock, W.C. and Klemp, J.B., 2008. A time-split nonhydrostatic atmospheric model for weather research and forecasting applications. Journal of computational physics, 227(7), pp.3465-3485.

[3] Mirocha, J.D., Kosovic, B., Aitken, M.L. and Lundquist, J.K., 2014. Implementation of a generalized actuator disk wind turbine model into the weather research and forecasting model for large-eddy simulation applications. Journal of Renewable and Sustainable Energy, 6(1), p.013104.
[4] Arthur, R.S., Mirocha, J.D., Marjanovic, N., Hirth, B.D., Schroeder, J.L., Wharton, S. and Chow, F.K., 2020. Multi-scale simulation of wind farm performance during a frontal passage. Atmosphere, 11(3), p.245.
[5] Jonkman, J., Butterfield, S., Musial, W. and Scott, G., 2009. Definition of a 5-MW reference wind turbine for offshore system development. Technical report NREL/TP-500-38060, National Renewable Energy Laboratory, Colorado.

Wake properties and power output of very large wind farms for different meteorological conditions and turbine spacings: A large-eddy simulation case study for the German Bight

Oliver Maas*, and Siegfried Raasch
Institut für Meteorologie und Klimatologie
*Presenting author

Keywords: very large wind farm | wake | large-eddy simulation | power output | meteorological conditions

Large portions of the Exclusive Economic Zone in the German Bight will be covered with wind farms in the future. Since these wind farms will be at least one order of magnitude larger than existing wind farms, their power output and wake structure may not be accurately predicted by simple, empirical wake models that are tuned with data of existing, smaller wind farms. More accurate results can be achieved by numerical models that consider the relevant physical processes, such as large-eddy simulation models.
In this work the large-eddy simulation model PALM is used to investigate the power output and wake properties of potential wind farms in the German Bight. The wind farms consist of the IEA 15 MW reference wind turbine with a rotor diameter of 240 m that is represented by an advanced actuator disc model including wake rotation. In order to determine the influence of different turbine spacings, boundary layer heights and atmospheric stabilities, five simulations were carried out.
Wind speed and direction at hub height are tuned to 10 m/s and 225°, respectively, which represents a very common situation in the German Bight. The largest setup contains more than 2000 wind turbines in a model domain of 200 km x 160 km x 3 km. With a grid spacing of 20 m and more than 7 billion grid points the simulation took about 50 h of computing time on 5120 cores.
Results valid for all five simulations are the following: The wind speed deficit induced by the wind turbines spreads vertically up to the boundary layer top due to turbulent vertical mixing. The reduced mean wind speed forces the boundary layer to grow in order to keep the mass flow inside the boundary layer constant. Since there is no turbulent momentum transport from the free atmosphere into the boundary layer, the wind speed recovery in the wake is only driven by the relatively weak pressure gradient force. Consequently, the wake (in terms of speed deficit) is very long (> 100 km). In terms of turbulence intensity, the wake is much shorter. The wake flow is deflected counterclockwise which is a direct consequence of the reduced Coriolis force inside the wake (Figure 1).

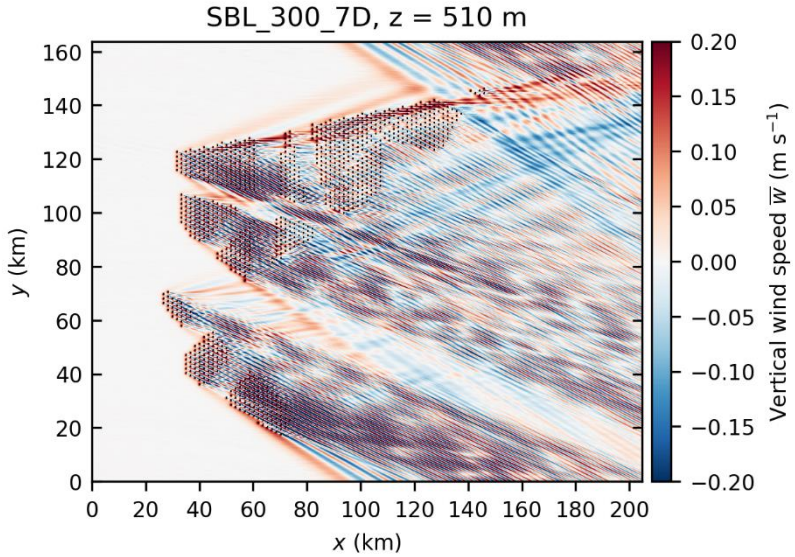


Figure 1: Mean vertical wind speed at 510 m height (above the stable boundary layer): Wind turbines excite gravity waves.

Reducing the turbine spacing from 7D to 5D leads to a wind farm power increase of only 40 %. Doubling the boundary layer height from 700 m to 1400 m in the convective case results in a wind farm power increase of nearly 20 %, suggesting that the boundary layer height should be considered as an important parameter in site assessments for very large wind farms. The wind speed deficit is less pronounced for the 1400 m – boundary layer, since it can distribute over a thicker column of air.

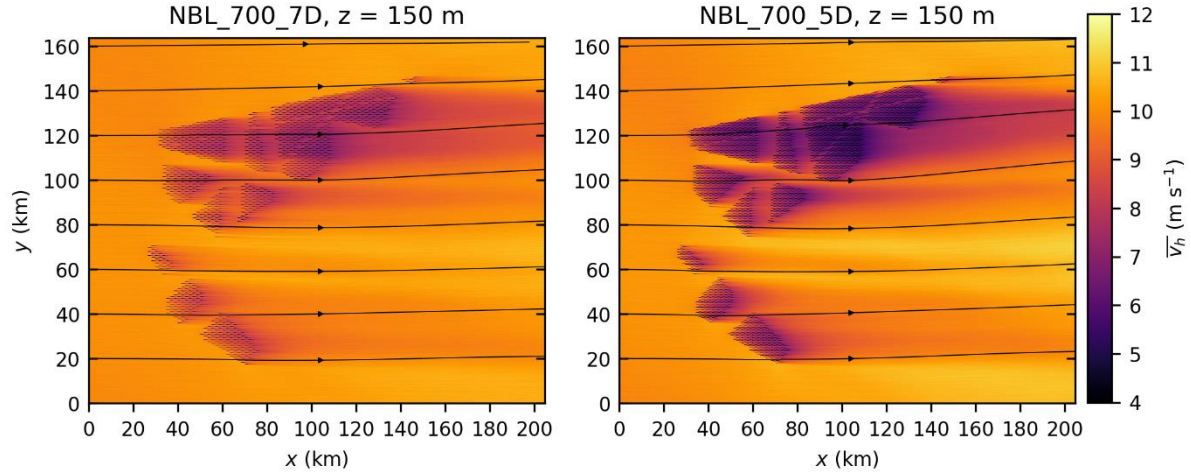


Figure 2: Mean horizontal wind speed at hub height for a turbine spacing of 7D (left) and 5D (right). Streamlines show counterclockwise wake deflection. Inflow from the left. Neutral boundary layer with a height of 700 m.

The wind turbine induced turbulence leads to entrainment of warm air into the stable boundary layer and therefore results in significant boundary layer growth. The wind turbine rotor tops at 270 m nearly reach the boundary layer top at 300 m and thus are able to excite gravity waves in the free atmosphere (Figure 2).

Large eddy simulations of interaction between low-level jet and wind farm

Srinidhi N. Gadde*, and Richard Stevens
University of Twente
*Presenting author

Keywords: Low-level jet | Wind farm | Large eddy simulations | Stable boundary layers

Low-level jets (LLJs) are the wind maxima found in the lowest heights of the atmosphere (Smedman et al., 1996). LLJs have high wind potential and most often form at the top of surface inversion and have both positive and negative shear regions in the velocity profile due to the presence of maximum. The positive shear regions in an LLJ is turbulent, while the negative shear region is a region of high stability and mostly non-turbulent.

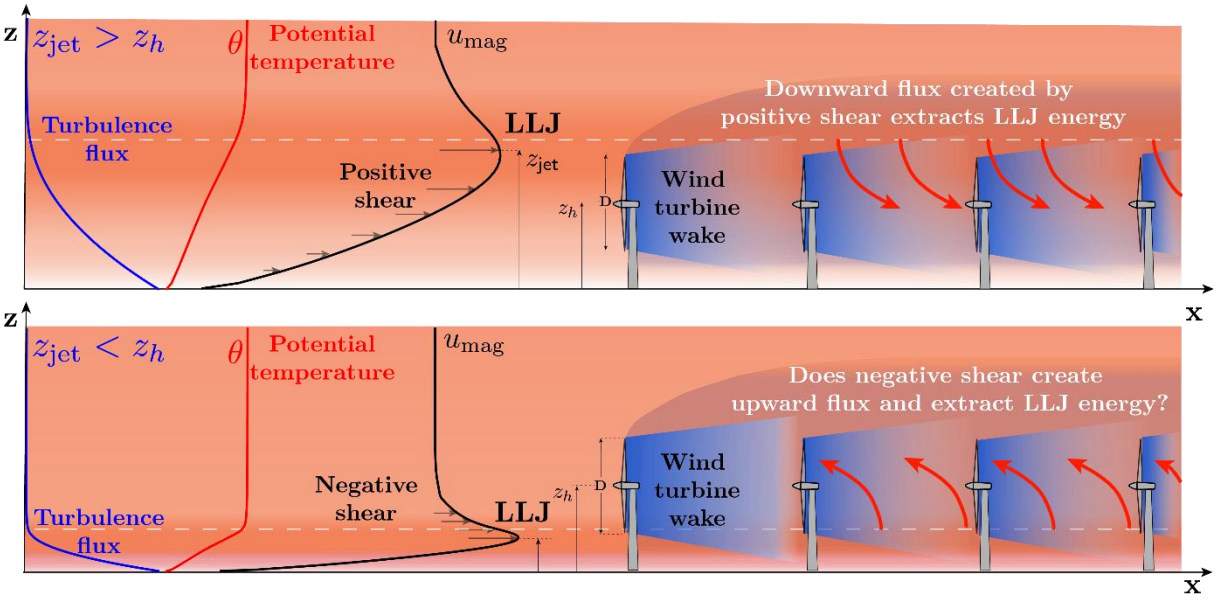


Figure 1: Problem definition. The top figure shows turbines operating in positive shear when the LLJ is above the turbine rotor swept area. The bottom figure shows turbines operating in negative shear when the LLJ is below the turbine rotor swept area.

In this study, we present large-eddy simulations (LES) of interaction between LLJs and a wind farm when the LLJ is above, below, or in the middle of the turbine rotor swept area, see Fig. 1. We employ actuator disk theory to model the turbines, the wall stress is modeled using the Monin-Obukhov similarity theory with stability correction functions. See Gadde and Stevens (2021) for governing equations and numerical methods. The boundary layer is stably stratified with a cooling rate of 0.5 K/hour. We consider a wind farm with 10 x 4 turbines and the jet height is approximately 120 m. We find that when the turbines are below the LLJs, the wakes recover faster due to the downward vertical entrainment of the LLJ energy and the turbulent nature of this region. However, when the LLJ is in the middle or below the turbine swept area the wake recovery is adversely affected due to high stability in this region. The energy budget analysis reveals that downward entrainment flux which aids wake recovery is maximum when the LLJ is above, but minimum when the LLJ is in the middle of the turbine rotor, swept area. For continuous production of turbulence, the production term in the mean energy budget should be negative. When the turbines are in the positive shear region, this couples with negative turbulent flux from above resulting in negative entrainment flux aiding power production.

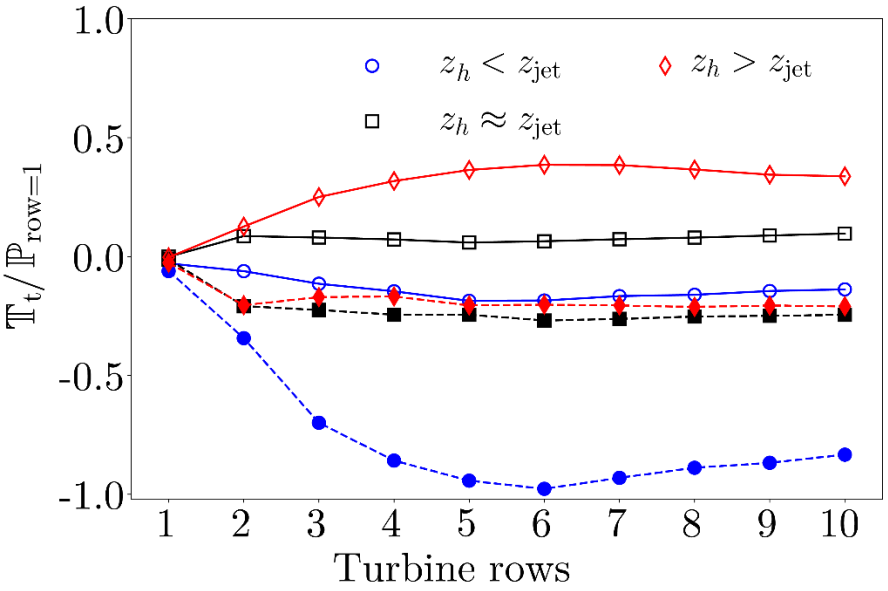


Figure 2: Integrated entrainment flux over top and bottom planes of the control volume. Dashed lines with filled symbols and solid lines with open symbols represent on the top and bottom plane, respectively.

However, in the presence of negative shear, for sustaining turbulence the momentum flux has to be positive. Figure 2 shows that the integrated entrainment flux over the top and bottom planes of the control volume covering the wind farm. We found that when the LLJ is below the turbine swept area, i.e. when turbines operate in the negative shear region, there is a significant upward entrainment flux from below. In this case, the entrainment from below is dominant than the entrainment from above in contrast to what is normally observed in a wind farm. The relative power production normalized with the first-row power is maximum when an LLJ is above turbines, minimum when the LLJ is in the middle of the turbine rotor swept area. However, when the LLJ is below the turbine swept area, power production recovers owing to the positive/upward entrainment flux from below due to the negative shear.

References:

Smedman, A.S., Högström, U. and Bergström, H., 1996. Low level jets–a decisive factor for off-shore wind energy siting in the Baltic Sea. Wind Engineering, pp.137-147.

Gadde, S.N. and Stevens, R.J.A.M. (2021). Interaction between low-level jets and wind farms in a stable atmospheric boundary layer. Physical Review Fluids, 6(1)

Measurement-Driven Large-Eddy Simulation of a Wind Turbine Array during a Wake Steering Field Campaign

Eliot Quon*, Paula Doubrawa, and Matthew Churchfield
National Renewable Energy Laboratory
*Presenting author

Keywords: large-eddy simulation | mesoscale-to-microscale coupling | wake steering | experimental observations

Wake steering has continued to gain traction as an effective wind farm control strategy, but the effectiveness of that strategy requires an understanding of dynamic wind-direction variations. A recent study has demonstrated significant improvements in the efficiency of an array of turbines, achieving up to 6.6% reduction in wake losses; however, this is only approximately half of the static optimal result (Fleming et al., 2020). In this work, we apply high-fidelity modeling with mesoscale-tomicroscale coupling (MMC) to evaluate the performance of the turbine array in Fleming et al. (2020) under turbulent, dynamic inflow conditions.
We have selected a day during the field campaign for detailed evaluation, during which conditions were amenable to wake steering, and high-quality flow and turbine measurements were collected. A challenge encountered in simulations with MMC is to establish temporally and spatially varying inflow conditions within the simulated microscale, or wind-farm scale, region. While the background mesoscale conditions may be simulated with a model such as the well-established Weather Research and Forecasting (WRF) model, there are model sensitivities to boundary and initial conditions, physics parameterization choices, and grid resolution. Preliminary WRF simulations were unable to reproduce the evolution of hub-height mean-flow quantities, likely due to a combination of local terrain and weather effects during our case study. Therefore, we have had to reconstruct the inflow conditions based on available lidar and met-mast measurements.

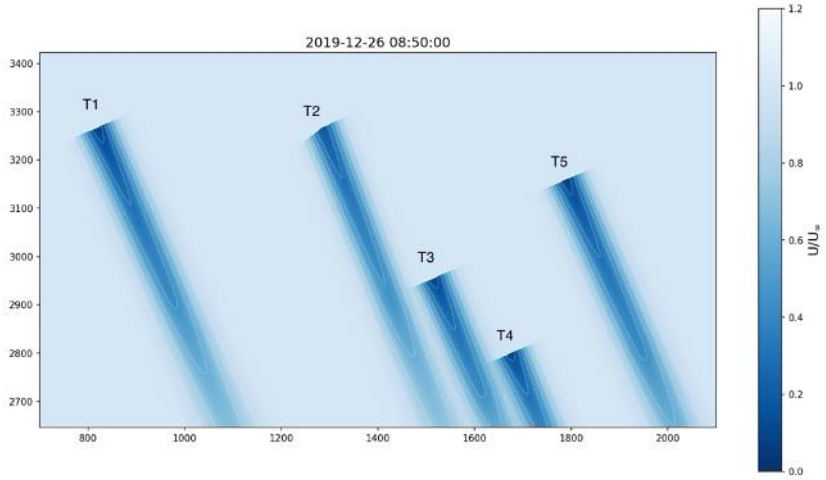


Figure 1: Steady state wake model of turbine array, with 15° of yaw offset at T2

With the inflow reconstruction, we perform a large-eddy simulation (LES) of wind turbines operating under the observed conditions. We first applied a recently developed coupling technique (Allaerts et al., 2020) to assimilate mean wind time–height histories and mean virtual potential temperature time histories from measurements into a precursor LES of the atmospheric boundary layer (ABL). The ABL simulation was started in the morning prior to sunrise and continued for 24 hours with the study period occurring after midnight. Starting under convective daytime conditions allows for realistic spin-up of turbulence and validation of our coupling technique under a range of atmospheric conditions. We observed that the addition of temperature assimilation allowed the LES to reproduce a realistic ABL in the afternoon, despite not explicitly modeling the change in moisture that appeared in our observations. Resolved turbulent flow from the precursor ABL was then applied as inflow to an LES with turbines modeled as actuator disks. The latter simulation captured

turbine response to an evolving nocturnal boundary layer over 4.5 hours, during periods both without wake steering and with yaw offset up to 15°.

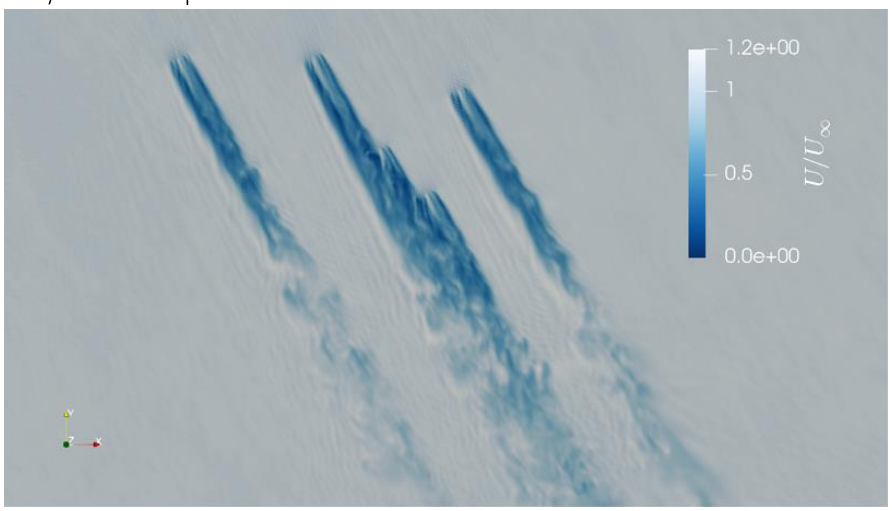


Figure 2: Measurement-driven large-eddy simulation of turbine array, during the same conditions as shown in Figure 1

We will present our coupling strategy and turbine LES, comparing turbine performance from a steady state wake model (Figure 1) and time-accurate results from the measurement-driven LES (preliminary results in Figure 2) with field campaign data. In particular, we will highlight differences between the predicted mean and fluctuating power under nonstationary conditions.

References:
Allaerts, D. J. N. et al. (2020) 'Development of a Time–Height Profile Assimilation Technique for Large-Eddy Simulation', Boundary-Layer Meteorology, 176(3). doi: 10.1007/s10546-020-00538-5.
Fleming, P. et al. (2020) 'Continued results from a field campaign of wake steering applied at a commercial wind farm – Part 2', Wind Energy Science, 5(3), pp. 945–958. doi: https://doi.org/10.5194/wes-5-945-2020.

Mesocale-to-microscale coupled simulations of low-level jets along US North Atlantic Coastline

Eliot Quon[1,*], Jing Li[2], Shashank Yellapantula[2], Matthew Churchfield[1], Shreyas Ananthan[1], and Mike Optis[1]
[1]National Renewable Energy Laboratory
[2]GE Research
[*]Presenting author

Keywords: large-eddy simulation | mesoscale-to-microscale coupling | low-level jets | lidar | offshore wind

Offshore wind farms near the US North Atlantic East Coast encounter specific atmospheric phenomena which can have a significant effect on power production. One such phenomenon is the occurrence of coastal low-level jets (LLJs) within the lower atmosphere. LLJs are characterized by a layer of high-shear, high-velocity wind from the ocean surface up to a peak velocity altitude, and a layer of negative shear above it. In an offshore environment, an LLJ can persist longer than onshore and occur during the daytime; the mechanism behind generation of these LLJs and their impact on wind farms in the Atlantic East Coast have not been fully investigated. In this study, mesoscale to microscale coupled (MMC) Large Eddy Simulations (LES) of the atmospheric boundary layer (ABL) will be used to study LLJs. Weather Research and Forecasting (WRF) simulation is used as the mesoscale model to force the microscale LES of ABLs.

The MMC simulations presented in this study will be focused on metocean buoys deployed in the New York Bight [1]. In addition to floating lidar-measured wind speed and direction at 10 levels from 20 to 200 m above mean sea level (MSL), these buoys also provide near-surface (2 m MSL) meteorological and sea-state measurements. A WRF model centered around the buoys was developed and used to simulate the mesoscale atmospheric condition. Values of model parameters were selected based on an extensive sensitivity study where the best-performing model configuration was chosen out of 16 model set-ups that vary in input sources, physics parameterizations, and grid and temporal variations [2].

A set of criteria was developed to identify LLJ observations, periods, and events; it was applied to one year of data in September 2019 to August 2020. We found that LLJ cases account for over 2% of the entire set of 10-min observations. A well-predicted event on May 15th, 2020, persisting over approximately 7 hours with LLJ nose near typical wind-turbine hub height, was then selected to perform a mesoscale-forced microscale LES. Details of the forcing methodology along with microscale LES techniques will be discussed in this study—preliminary results showing comparisons between MMC LES and lidar measurements are presented in Figure 1.

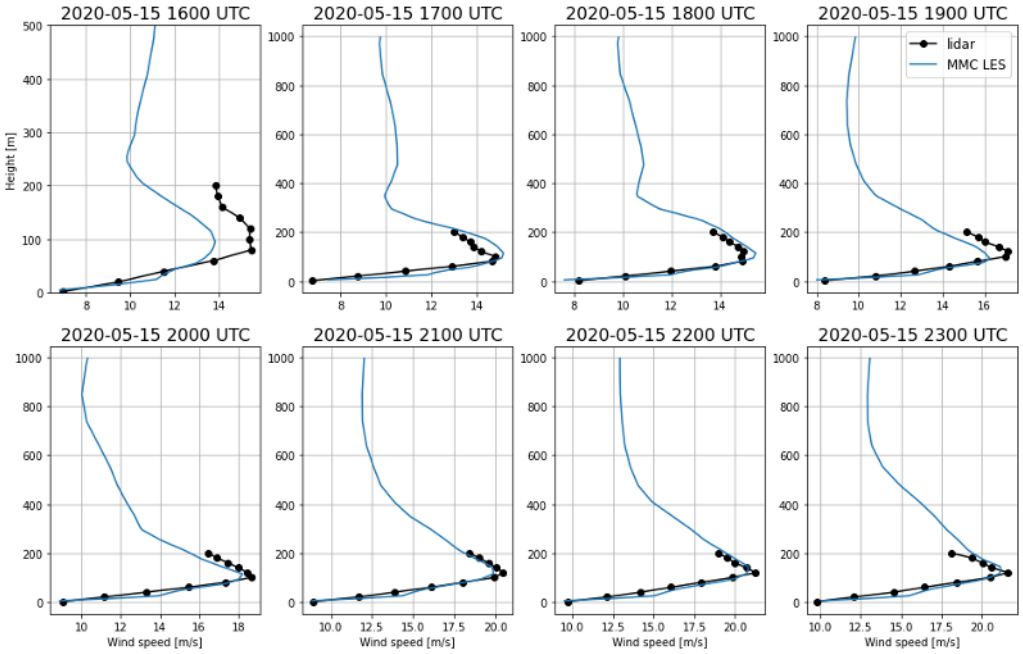


Figure 1: Comparison of wind profiles measured by lidar and simulated by WRF-forced microscale large-eddy simulation

We will present results from the MMC LES and assess the validity of the resolved microscale turbulence, which are essential for characterizing wind turbine wake recovery and fatigue loads. The simulated mean wind field will be compared to the lidar profiles, while the fluctuating wind field will be compared to both the lidar turbulence intensity and near-surface wind speed extrema. In addition, we will identify the dominant coastal processes modeled by WRF, unique to the US Atlantic Coastline, that drive the evolution of the coastal LLJ. Through this study, we will lay the foundation for a future LES-based study of offshore turbines responding to LLJ events.

References:
NYSERDA Floating LiDAR Buoy Data in New York Bight, https://oswbuoysny.resourcepanorama.dnvgl.com/.
Optis, M. et al. (2020) "2020 Offshore Wind Resource Assessment for the California Pacific Outer Continental Shelf," National Renewable Energy Laboratory, Golden, CO, USA, NREL/TP-5000-77642, Oct. 2020. doi: https://doi.org/10.2172/1677466.

A comparison of mesoscale-to-microscale coupling techniques for atmospheric flows over flat terrain

Dries Allaerts[1,*], Colleen M. Kaul[2], Raj K. Rai[2], Eliot W. Quon[3], Patrick Hawbecker[4], and Matthew J. Churchfield[3]

[1]Delft University of Technology
[2]Pacific Northwest National Laboratory
[3]National Renewable Energy Laboratory
[4]National Center for Atmospheric Research
[*]Presenting author

Keywords: Mesoscale-to-microscale coupling | Large-eddy simulation | Diurnal cycle | Atmospheric turbulence

Increasing the realism of numerical simulations of atmospheric flows is an important step forward for the wind energy industry as it is essential for a better understanding of the wind resource. The turbulent wind flow impacting wind turbines and wind farms, and, ultimately, the amount of energy available to harvest, is exposed to a wide range of weather phenomena and meteorological variabilities on many different scales. Coupling the mesoscale (i.e., phenomena that cover length scales ranging from 10 to more than 100 km) to the microscale (flow features with length scales of the order of 1 km or less) circumvents the limited scope of traditional microscale simulations, and it represents a new numerical simulation strategy that is able to cover the full range of atmospheric flow conditions. The ability to couple these scales is particularly important for the study of transient meteorological conditions (such as frontal passages, thunderstorm outflows, baroclinic systems, and low-level jets) or when considering changes of atmospheric stability associated with diurnal cycles.

There are a variety of different mesoscale-to-microscale coupling (MMC) techniques, which may differ in their communication strategy (online versus offline coupling), the type of information transferred (direct quantities such as velocity components versus indirect quantities such as mesoscale momentum transport equation terms), and the location of information transfer (on the microscale domain boundaries versus over the entire microscale volume). In the current study, we compare numerical predictions obtained with several different coupling techniques that were developed as part of the U.S. Department of Energy's (DOE's) Atmosphere to Electrons (A2e) MMC project. We focus on atmospheric flow conditions during a quiescent diurnal cycle that occurred on November 8, 2013 over the Scaled Wind Farm Technology (SWiFT) facility in west Texas. The overall goal of the comparison is not to identify a single superior coupling technique, but rather to uncover the advantages and limitations of each coupling technique in the context of different wind energy applications.

Initial results are presented in Figure 1, showing daytime profiles of mean-flow quantities obtained with three different mesoscale-to-microscale coupling techniques: WRF to SOWFA with internal forcing based on mesoscale budget components (internal-indirect), WRF to SOWFA with internal forcing based on velocity and temperature profiles (internal-direct), and WRF to WRF-LES with boundary forcing (boundary-direct). The simulation results are compared with data from the WRF mesoscale simulation, and with observations from the TTU meteorological tower and from a windprofiling radar. The results indicate that the predictions of mean flow quantities and turbulence levels can differ considerably among the various coupling methods, despite using the same mesoscale setup and microscale domain size and grid resolutions. Further, we will also investigate turbulence frequency spectra, spatial structures of turbulence (by means of 2D cross-sections of the instantaneous flow fields), and various quantities of interest for wind energy applications.

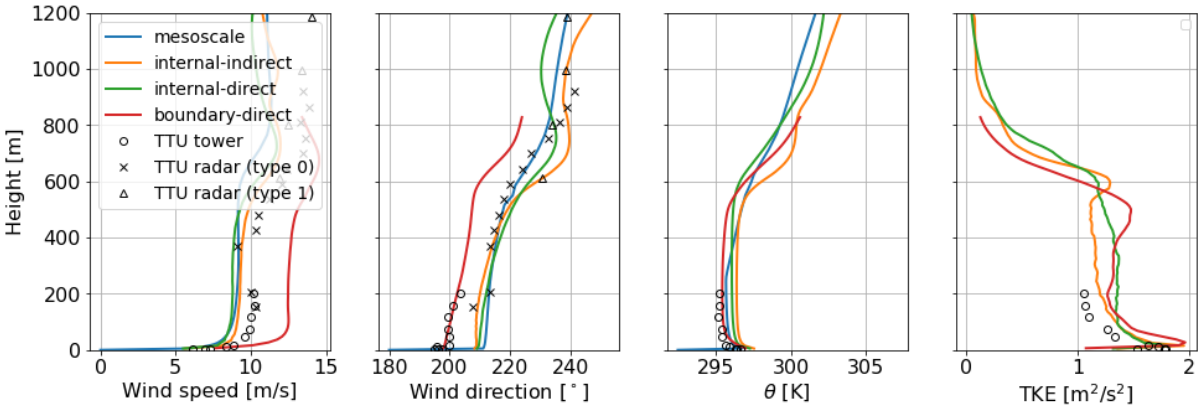


Figure 1: Daytime profiles (12pm local time, 1hr-average) of mean-flow quantities obtained with different mesoscale-to-microscale coupling techniques: internal-indirect (WRF to SOWFA with internal forcing based on mesoscale budget components), internal-direct (WRF to SOWFA with internal forcing based on velocity and temperature profiles) and boundary-direct (WRF to WRF-LES with boundary forcing).

Regular Session: Meteorology and Microscale Modelling (II)

Effects of atmospheric stability on the performance of a wind turbine located behind a three-dimensional hill

Luoqin Liu*, and Richard Stevens
University of Twente
*Presenting author

Keywords: atmospheric boundary layer | atmospheric stability | large eddy simulation | power output | three-dimensional hill

As more and more wind turbines will be installed in complex terrains, it is crucial to study the effect of atmospheric stability on the performance of wind turbines in hilly terrain. This will help wind energy assessment and models that are used to optimize wind farm siting. A significant amount of research has been carried out to investigate the effect of topography on wind turbine performance.
Most of previous studies were performed under neutral stratification conditions. However, only a few studies considered the effect of thermal stratification in complex terrain.
In this study, we investigate the effect of thermal stratification on the performance of the NREL 5MW wind turbine behind a three-dimensional hill. We use large-eddy simulations to solve the spatially filtered Navier-Stokes equations and the potential temperature equation. We employ a recently developed immersed boundary method to model the hill (Liu and Stevens, 2020). We apply the actuator line model (Sørensen and Shen, 2002) to simulate the wind turbine. To ensure that the wind turbine is always behind the hill, we utilize a controller to align the incoming wind with the hill and the wind turbine. We consider a stable, neutral, and convective boundary layer case. For each thermal stability case, we consider the flow around a three-dimensional hill, the flow around a standalone wind turbine, and the case in which the turbine is located behind the hill. The three layouts considered in this study is shown in figure 1, where the hill height and the hub height are the same.

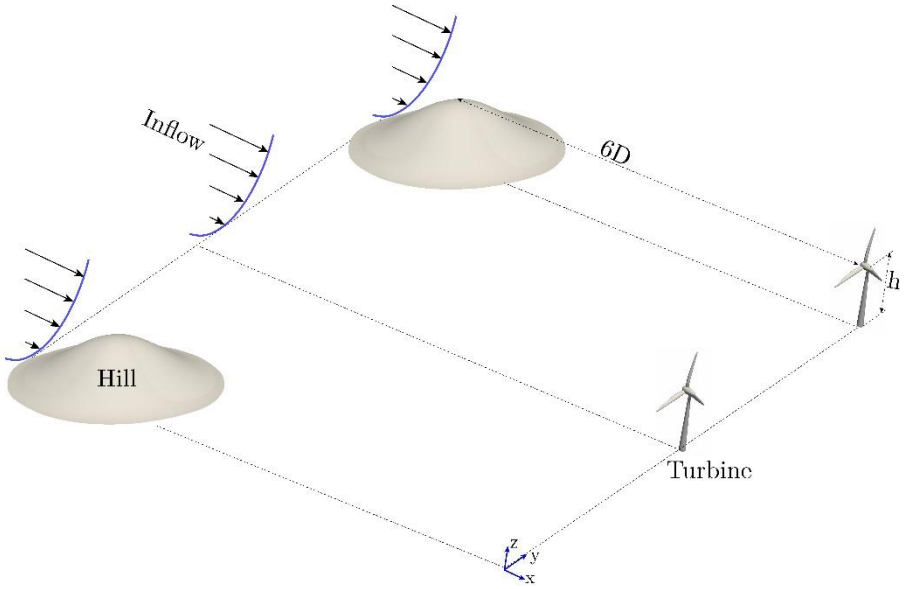


Figure 1: The three layouts considered in the present work. The hill height and the hub height are h, the turbine diameter is D, and the distance between the hill and the turbine is 6D. The inflow is the atmospheric boundary layer under stable, neutral, and convective conditions.

Figure 2 shows the time history of the power output of the stand-alone wind turbine and when the wind turbine is placed behind the hill for the final hour of the simulation when the quasi-equilibrium state has been reached. For the convective case, the mean power production is reduced about 35%.
For the neutral case, the mean power output is nearly not affected. Interestingly we find that for the stable case considered here, the mean power production is increased about 24%. For all cases, the power fluctuations are increased significantly by the upstream hill.

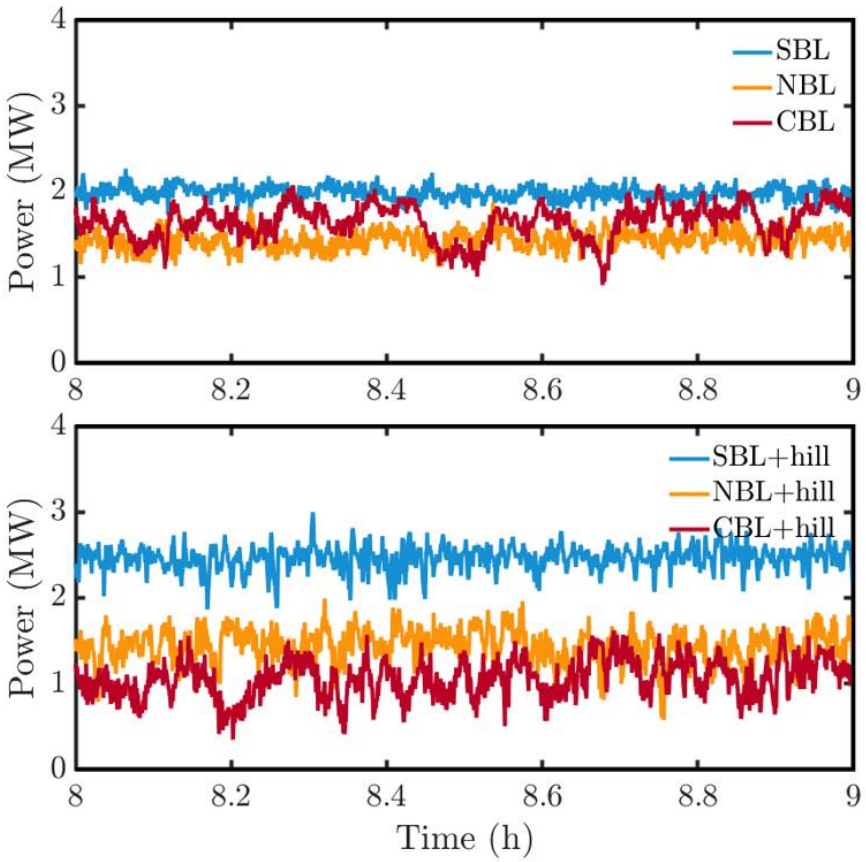


Figure 2: Time history of the power production of the NREL 5MW wind turbine in the stable (SBL), neutral (NBL), and convective boundary layer (CBL) case with and without an upstream three-dimensional hill. Note that the the increase in the mean power production is about 24%, 0%, and -35% for the SBL, NBL, and CBL cases, respectively.

In agreement with the observation that the average power output is not affected by the hill for the neutral case, we find that the aerodynamic lift and drag forces along the blades are nearly the same for the stand-alone turbine and when the turbine is located behind the hill. However, although the mean blade quantities are not affected by the upstream hill due to the deflection of the hill wake, the standard deviations of aerodynamic loads are increased due to the increased turbulence intensity by the hill wake.
For the stable boundary layer, the incoming axial velocity at the blades is increased significantly by the upstream hill since the wind veer turns the hill wake away, and the low-level jet just above the hill is entrained into the hill-shade region. As the angle of attack at the blades is increased, the aerodynamic loads and the resultant power production are increased accordingly. For the convective case, the incoming axial velocity at the blades is decreased since the wind veer is too weak to turn the hill wake away. As a result, the angle of attack, the aerodynamic loads, and the power production are reduced correspondingly.

References:
Liu, L. and Stevens, R.J.A.M. (2020) 'Wall modeled immersed boundary method for high Reynolds number flow over complex terrain', Comput. Fluids, 208, p. 104604
Sørensen, J. N. and Shen, W. Z. (2002) 'Numerical modeling of wind turbine wakes', J. Fluids Eng., 124, pp. 393-399

Dynamic mesh adaptation to capture wind turbine wakes during LES simulations

Ulysse Vigny[1,2,*], Stéphanie Zeoli[1], Patrick Tene Hedje[1], Félix Houtin-Mongrolle[2], Laurent Bricteux[1], and Pierre Benard[2]
[1]Polytechnic Faculty of the University of Mons
[2]CORIA, CNRS UMR6614, Normandie Université, INSA and University of Rouen
*Presenting author

Keywords: dynamic mesh adaptation | wake | LES | turbulence | YALES2

According to the current energetic and environmental challenges, maximizing the electric power generated in wind farms is a societal concern. A better understanding of the flow physics around wind turbines in farms become important to achieve this goal. Since experimental data on actual wind farm scales are not affordable and given the constant growth of computational resources, high order numerical simulations tend to be a promising approach [1]. Nonetheless, simulation predictability and reliability still need to be improved.
Large-eddy simulation (LES) consists in explicitly resolving the large scales of the fluid motion and modeling the influence of the smallest scales. LES can today be used to study realistic wind turbines with complex geometries [2]. To perform valid LES, the mesh has to adequate to capture wake meandering and instabilities. Indeed, such unsteady effects are critical issues in wind farms as this oscillatory motion of the wakes increases fatigue loads on downstream machines and impacts their power production. Thus, a compromise between computational cost and wake accuracy must be found. By following this tenet, dynamic mesh adaptation is applied to adapt the mesh based on flow characteristics. The first image is an illustration of mesh adaptation on NREL 5MW wind turbine flow under dynamic yawing condition.

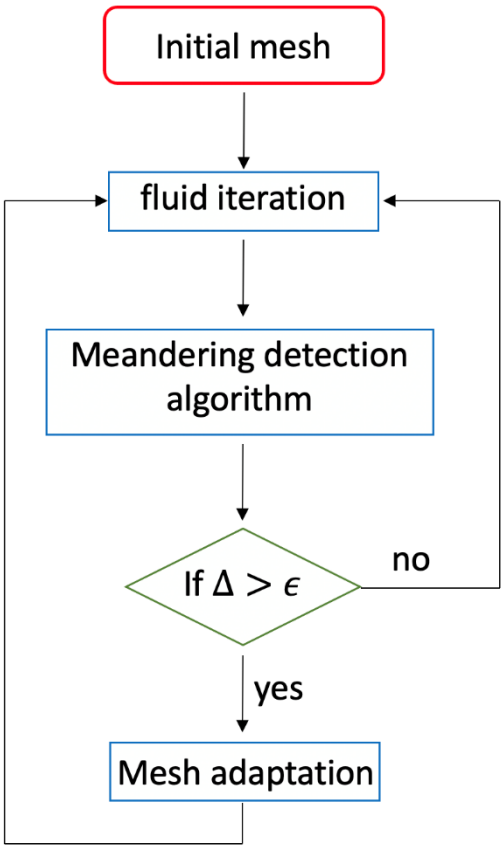


Figure 1: dynamic mesh adaptation algorithm diagram

Dynamic mesh adaptation goal is to generate a mesh that best matches the flow physics at every fluid iteration. Based on large velocity gradients as a refinement criteria, the mesh follows large scales movements and wind turbine wake. With turbulent wind, tracking the wake is not trivial. A wake meandering detection algorithm [3] is therefore used. Gaussian shape circular mask is convoluted on transverse planes with velocity deficit. This algorithm locates the convolution's maximum and thereby the wake centering. The wake envelope is then compared to the one of the previous fluid iteration. If the difference exceeds a given threshold, the dynamic mesh adaptation is triggered; otherwise, the simulation continues. Its robustness enable to correctly capture the wake centerline even with turbulent wind injection or yaw misalignment configurations. The second image shows the dynamic mesh adaptation algorithm diagram for more understanding.

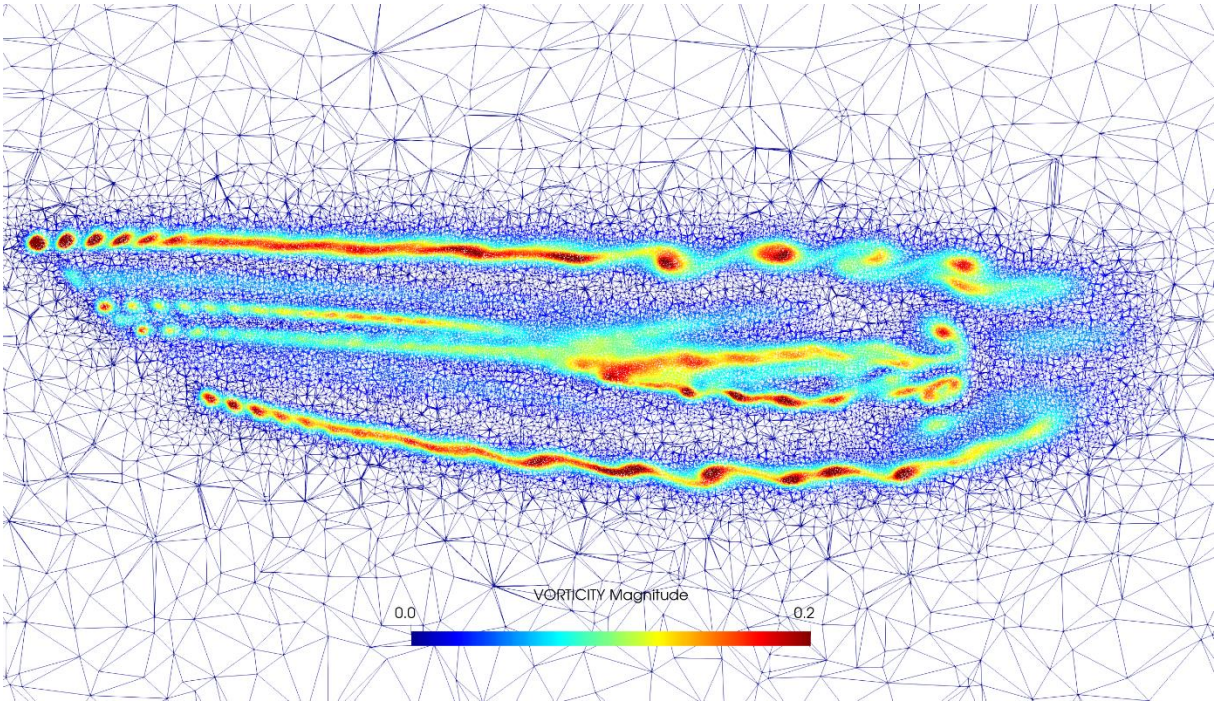


Figure 2: Illustration of mesh adaptation on NREL 5MW wind turbine flow under dynamic yawing condition

The dynamic mesh adaptation methodology will be calibrated on a laminar wind non-yawed DTU10MW wind turbine wake study. Cases where grid adaptation would reveal its potential, i.e. with turbulent wind and yawed wind turbine, will be tested. The rotor modeling is performed using an Actuator LineMethod [4] (ALM), coupled to the low Mach-number massively-parallel finite-volume Large-Eddy Simulation (LES) flow solver on unstructured meshes, called YALES2 [5, 6]. Global quantities will be compared, such as averaged power and thrust coefficient. This will be followed by local characteristics analysis. That will include velocity and turbulent intensity profiles as well as wake scan downstream of the turbine.

References:

S-P Breton et al., Phil.Trans.R.Soc.A 375 (2017)
P. Bénard et al. Mesh adaptation for large-eddy simulations in complex geometries. International Journal for Numerical Methods in Fluids. 81. n/a-n/a. 10.1002/fld.4204. (2015).
S. Zeoli et al. Large eddy simulation of wind turbine wakes using adaptative mesh refinement. Torque (2020)
N. Coudou et al. Development of wake meandering detection algorithms and their application to large eddy simulations of an isolated wind turbine and a wind farm. Journal of Physics: Conference Series. 1037. 072024. 10.1088/1742-6596/1037/7/072024. (2018)
J. Sørensen t al., J. Fluids Eng 124(2), 393 (2002)
P. Benard et al., Comput. Fluids 173, 133 (2018).
V. Moureau et al., C.R. Mec. 339(2/3), 141, (2011).

Nested high-resolution atmospheric boundary layer simulations using WRF-LES for Perdigão

Erkan Yılmaz[1,*], S. Sibel Mentes[1], and Gökhan Kirkil[2]
[1]Istanbul Technical University
[2]Kadir Has University
*Presenting author

Keywords: WRF-LES | Wind Resource | Boundary Layer Meteorology

WRF model provides a potentially powerful framework for coupled simulations of flow covering a wide range of spatial and temporal scales via a successive grid nesting capability. Nesting can be repeated down to turbulence solving large eddy simulation (LES) scales, providing a means for significant improvements of simulation of turbulent atmospheric boundary layers. We performed multi-scale simulations using WRF's different Planetary Boundary Layer (PBL) parameterizations as well as Large Eddy Simulation (LES) and compared the results with the detailed field measurements.

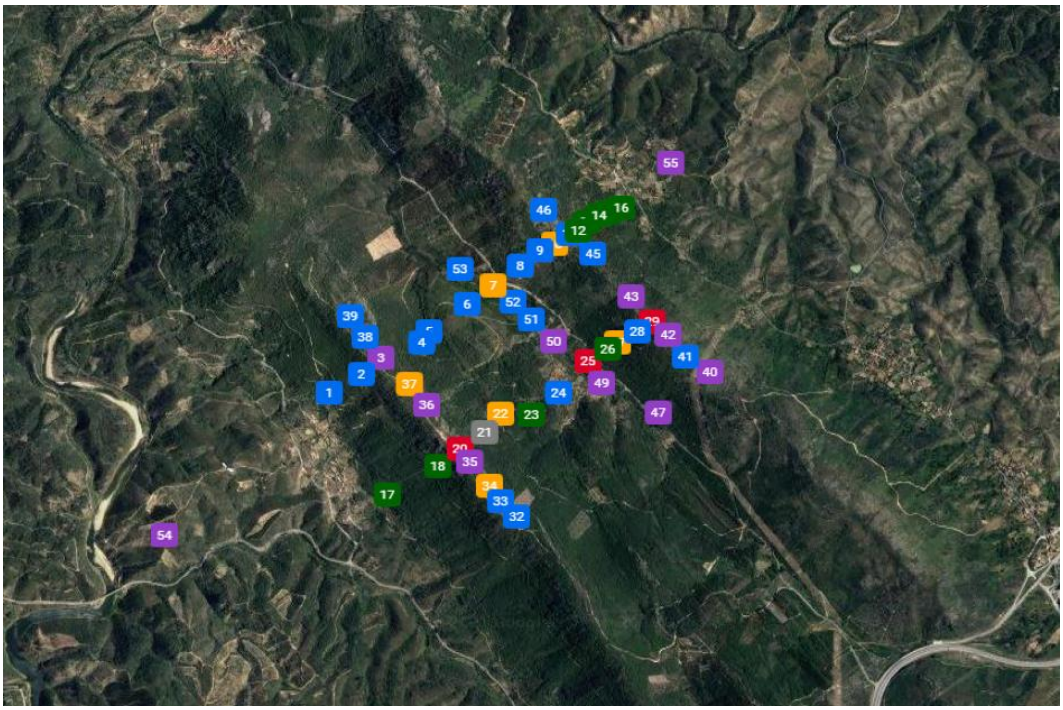


Figure 1: Perdigao Measurement Points

Large-eddy simulation (LES) application technically solves the 3-dimensional energy generation of atmospheric turbulence, while removing the smaller-scale motion in the turbulence spectrum from the flow by using an areal filter. While the turbulence kinetic energy (TKE) production and transport of this turbulence in the flow is resolved, the dissipative part of the turbulence with the filter used is cascaded in the turbulence spectrum. The process of cascading the components dissolved in the stream with this filter is called the subfilter-scale (SFS) model. Subfilter-scale stress model plays a different role in large eddy simulation technique than under Planetary Boundary Layer parameterization in large scale models. While Planetary Boundary Layer plays a role in the simulation of turbulence, momentum transport, heat, and other scalar models in large scale motion models, large eddy simulation enables these parameters to be analyzed directly with subfilter-scale.

Perdigao is a settlement with a complex land structure close to the Portuguese-Spanish border. Within the scope of the project, short and long-term measurements were made at different points and different heights with more than 100 measuring instruments. ERA-5 reanalysis data were used to determine the initial and

boundary conditions. In the study, 3 domains with the nested structures were used. These areas, named d01, d02, and d03, have resolutions of 5000 m x 5000 m, 1000 m x 1000 m, and 200 m x 200 m, respectively. While the first 2 domains of these domains were run with mesoscale parameters, only the d03 domain was run with large-eddy simulation parameterization. In order to test the performance of the model within the scope of the project, a comparison was made with the observation data by selecting 2 days for 2017, 04, and 05 May. The run study for 36 hours in the time interval selected for the study was started from 04 October noon, and the first 12 hours was considered the run spin-up time. SRTM, high resolution 90m orographic data, was used in the D3 domain area of the study. The roughness values of the field were used in the Corine data set. WRFLES model improved the mean flow field as well as second-order flow statistics. Mean fluctuations and turbulent kinetic energy fields are investigated in several cross-sections around the hill.

Modelling biases in the simulation of wind farms over forest canopies

Antonio Segalini[1,*], Johan Arnqvist[2], and Ebba Dellwik[3]
[1]KTH Royal Institute of Technology
[2]Uppsala University
[3]Technical University of Denmark
[*]Presenting author

Keywords: Canopy flows | Roughness models | Linearised RANS

Modern tall wind turbines are nowadays often placed in forested areas. These are however characterised by a significant footprint of the trees that generate drag and influence the atmosphere within a region thick enough to affect the operating conditions of the installed turbines. In general, from the lower to the upper tip of the rotor, these turbines are exposed to a large gradient in both turbulence and mean wind speed, experiencing higher fatigue loads. On the other hand, the higher turbulent environment should facilitate the wake recovery, potentially decreasing the wake losses.
Several models have been used in order to assess the energy yield of a farm placed over a forest. This can be done either by a high value of the surface roughness, z0, or by introducing a drag force that realistically simulates the porous nature of the forest. The latter approach has been implemented in some numerical models, which however lead to long simulation times. The use of an enhanced z0 value implies a boundary condition change rather than a force directly imposed to the incoming flow and therefore it is more appealing from the computational cost point of view. However this boundary condition will not enable to see the inflectional point in the velocity profile near the canopy top and therefore it should be applied very well above the region directly influenced by the trees. The alternative method requires the introduction of a drag force in the momentum-conservation equations related to the tree drag and the leaf-area density: this has the added benefit of also including the displacement height in the analysis and to modify the roughness height consistently at large distances above the canopy. Despite the better physical modelling, this method is rarely adopted in the wind industry due to the lack of knowledge of the forest details and the fact that many fast tools are still only using the roughness approximation.

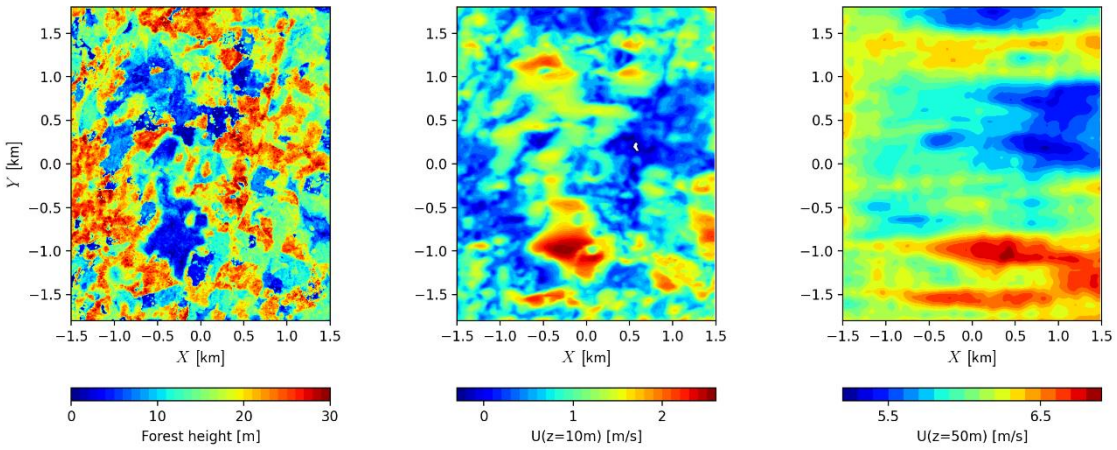


Figure 1: Velocity magnitude simulated over Hornamossen (the forest height is reported on the left side) without terrain elevation at z=10m (Middle) and z=50m (Right).

The linearised code ORFEUS has been developed to account for forestry with both the roughness and force models, providing the possibility to rapidly assess forested sites with both approaches. The figure shows results of simulations over Hornamossen at z=10 m (slightly below the canopy top) and z=50m (two-three times the canopy height) without terrain height (to single out the effect of just the forest canopy), showing significant footprints due to the canopy still visible far above the surface; the computational cost was of

about a couple of minutes with 5 millions grid points. The code has been recently extended to account for turbulence evolution by means of a parabolised k-epsilon model and to include for non-linearities in the calculations by means of a pseudo-spectral method.
How to account for the large gradients generated by a forest in simulations remains a challenge in the wind industry sector and here, we investigate the capability of the ORFEUS model to accurately reproduce the spatially-varying gradients in the height range relevant for the lower part of turbine rotors.
Atmospheric measurements over several forested sites, where some turbines have been installed, provide a good testbench to assess errors in the farm production due to forest modelling in ORFEUS.
In this work a comparison of simulations and observations from mast and remote-sensing anemometers will be presented under different forest-modelling assumptions and about how these influence the wake recovery.

Simulation of wind field with three back to back actuator discs using parallel numerical algorithms

Sudipta Lal Basu*, Kirk Soodhalter, Breiffni Fitzgerald, and Biswajit Basu
Trinity College Dublin, Ireland
*Presenting author

Keywords: Wind Farms | Parallel numerical algorithms | Irrotational Flow

Most of the studies related to wind energy till date have been confined to investigations on single wind turbine and very little has been explored in the context of wind farms as a whole. This is in particular because of the extensive computation time and memory requirement in analysing the entire wind field. It is a well known fact that the wake structure behind one turbine influences the performance and operation of the wind turbines located further downstream. This is where parallel numerical algorithms can offer advantages by providing computational time and memory efficiency in handling large domains. In the recent past, researchers have started focussing on developing numerical codes to analyse wind farms (Chand et al. 2010) (Ivanellet al. 2008). For example, the work of Department of Mechanical Engineering, Danmarks Tekniske Universitet, Denmark and The Department of Wind Energy at Risø National Laboratory in developing Ellipsys2D/3D deserves a mention (Sørensen 2015).
In our current work, we have implemented Finite Difference Equations and Message Passing Interface coupled with parallel numerical algorithms to simulate the wind field in the presence of three back to back actuator discs.The wind flow is assumed to be 2D, steady and irrotational. In the context of our analysis and application, the use of conventional steady state potential flow equation poses some problem. This has been circumvented by a new formulation inspired by a recent work of (Basu 2016).
Consider the domain as shown in Fig.1.

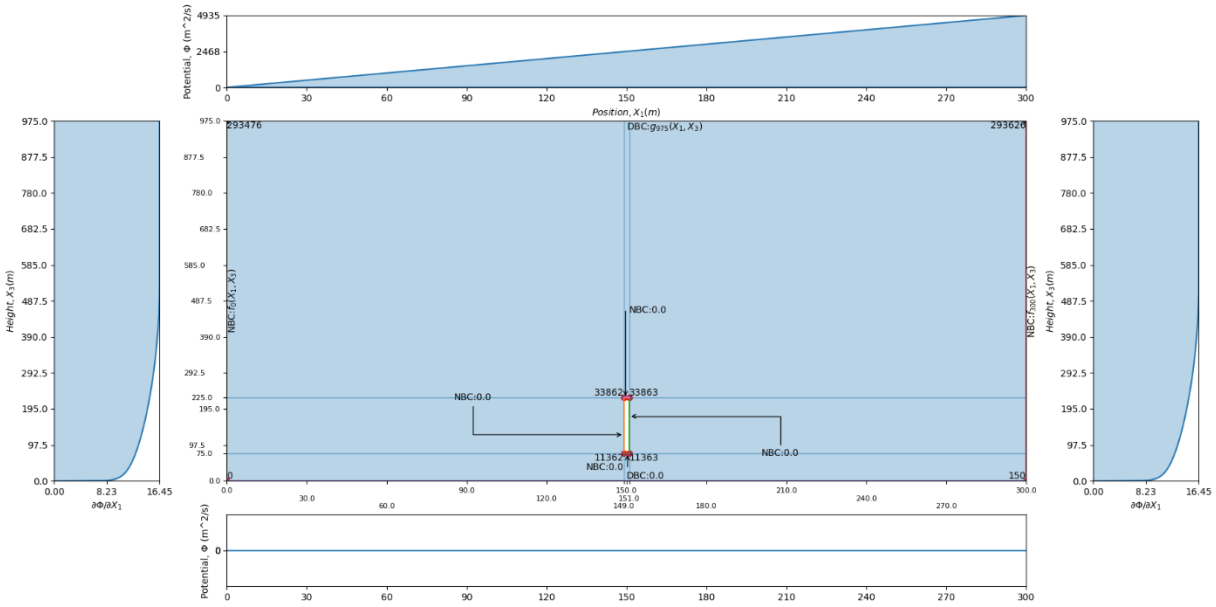


Figure 1: Domain with potential, φ as primary variable and actuator modelled as an opening

1. Geometrical model of actuator disc: The actuator disc can be modelled either as an interior opening in the domain with height equal to the diameter of the disc and the thickness equal to the average blade thickness, or as a solid disc of zero thickness. However, the solution explodes in this case because the presence of the actuators introduce discontinuity in the model.

2. Boundary conditions: From an initial assessment, it seems that the obvious boundary conditions (BCs) are to assign Dirichlet BC (DBC) =k, say 0 at bottom and Neumann BC (NBC) = 0 at top, and Neumann BC =V1(X3)(mean horizontal velocity as a function of height, X3) on left and right boundaries. However, the effect of the velocity components tangential to the domain boundary have no effect on the solution of the velocity field if potential,$\phi$is considered for modelling the field.

3. Compatibility at corner nodes: With only one parameter, ϕ governing the values of both V1 and V3 (mean vertical velocity), another challenge faced is the compatibility at the corner nodes of the domain. The values of ϕ assumed at boundary nodes should be such that the value we want for V1 w.r.t. both boundaries forming the corner should also satisfy the requirement of V3. This is difficult to achieve.

Hence to avoid the difficulties, we have reformulated the problem such that instead of the potential, the velocity fields become the primary variables. We then simulate the wind field with this new reformulation.

References:

Basu, B (2016). "Irrotational two-dimensional free-surface steady water flowsover a flat bed with underlying currents". In:Nonlinear Analysis: Theory,Methods & Applications147, pp. 110–124

Chand, K et al. (2010). "CgWind: A high-order accurate simulation tool forwind turbines and wind farms". In: The Fifth International Symposiumon Computational Wind Engineering. North Carolina, USA.

Ivanell, S et al. (2008). "Three dimensional actuator disc modelling of windfarm wake interaction". In: European Wind Energy Conference and Ex-hibition. European Wind Energy Association. Brussels, Belgium, pp. 1–10.

Sørensen, N N (2015).EllipSys2D/3D.url: http://www.the-numerical-wind-tunnel.dtu.dk/ellipsys.

Regular Session: Wakes and Farms

Effect of atmospheric thermal stratification on wind farm blockage

Jessica Strickland*, Srinidhi Gadde, and Richard Stevens
University of Twente
*Presenting author

Keywords: wind farm | blockage | large eddy simulation | thermal stratification

Wind farms are being constructed at an unprecedented rate. In order to optimize their productivity, we require accurate wind farm modelling. The performance of a wind farm is affected by a large variety of factors and a great deal of research has been focusing on improving our understanding of wind farm physics. Models typically include downstream development such as wake propagation, but many engineering wind farm models do not account for flow induction or blockage effects. Blockage is a phenomenon in which incoming airflow is influenced by an upcoming obstacle such as a wind farm. Therefore, blockage may impact the kinetic energy available for extraction and assuming that the first row of a wind farm receives undisturbed flow is not valid.

The blockage effect is recently being given attention. Low-fidelity models, wind tunnel experiments, and field measurements claim that there is a significant influence on turbine performance due to blockage. However, more research is required with higher fidelity models, such as large eddy simulations, to study the influence of various turbulent atmospheric conditions for multiple largescale wind farm configurations. Therefore, we use large eddy simulations to investigate blockage at the entrance of a wind farm, where the effects are most clearly observed. We compare the performance of the first row of a wind farm to that of a solitary infinite row and a free-standing turbine (see figure 1).

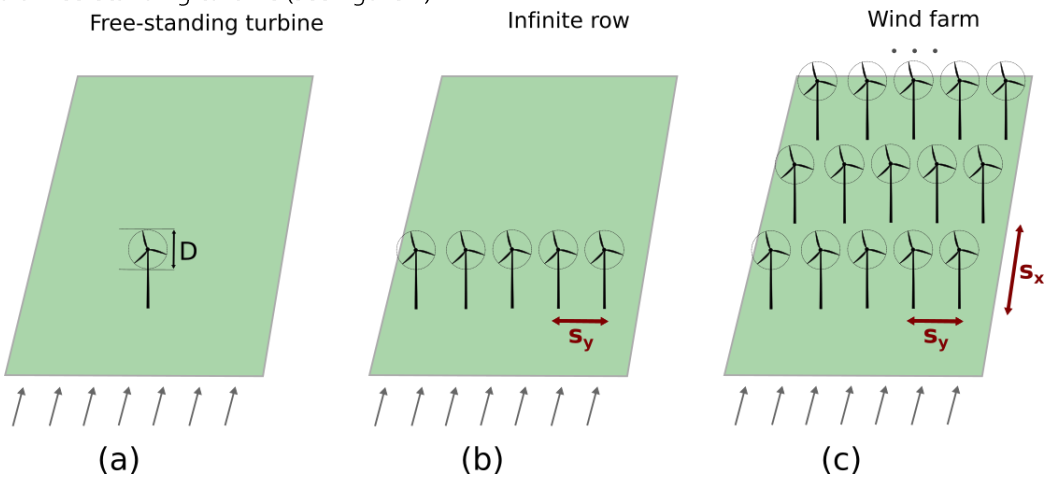


Figure 1: Schematic depicting the three main cases considered in this study: (a) a free-standing turbine (b) an infinite row, and (c) a wind farm. The streamwise (Sx) and spanwise spacing (Sy) are also shown.

First, we consider a neutral atmospheric boundary layer. Overall, we find that the impact of close neighbouring turbines depends primarily on the relative position of the turbines. Turbines placed downstream have a negative impact on the performance of the first row of a wind farm when compared to a solitary row of turbines. However, when compared to a free-standing turbine, the impact of the downstream turbines may be compensated or overcome by spanwise blockage. For instance, within a solitary infinite row, close lateral neighbours ($S_y < 3.93D$) appear to benefit from each other and are more productive than if they were stand-alone turbines. Ultimately, blockage becomes increasingly significant as the turbines are placed closer together.

Next, we consider a stable boundary layer, as limited research has addressed blockage in a thermally stratified boundary layer. Large eddy simulations which incorporate thermal stratification have shown that air flow is inclined to pass over the wind farm in a stable boundary layer. Such movement is expected to increase the blockage effect and the performance of the first row of turbines is expected to decrease accordingly. Therefore, we investigate this by comparing the performance at the entrance of a wind farm to a solitary infinite row for three different stratification levels. We compare the results for a neutral boundary layer to that of a boundary layer with a surface cooling rate of 0.5K/hr and 1.0K/hr.

The impact of the rotational direction of a wind turbine on its wake

Antonia Englberger[1,*], Julie K. Lundquist[2,3], and Andreas Dörnbrack[1]
[1]German Aerospace Center
[2]University of Colorado - Boulder
[3]National Renewable Energy Laboratory
[*]Presenting author

Keywords: wind-turbine wake | LES | stable boundary layer | rotational direction | Ekman spiral

Stably stratified atmospheric boundary layers are often characterized by a veering wind profile, in which the wind direction changes clockwise (counterclockwise) with height in the Northern Hemisphere (Southern Hemisphere). Wind-turbine wakes respond to this veer in the incoming wind by stretching from a circular shape into an ellipsoid. Englberger, Dörnbrack and Lundquist (2020) investigate the relationship between this stretching and the direction of the turbine rotation by means of large-eddy simulations. Clockwise rotating and counterclockwise rotating actuator disc turbines are embedded in wind fields of a precursor simulation with no wind veer and in wind fields with a Northern Hemispheric Ekman spiral, resulting in four combinations of rotor rotation and inflow wind condition.
The wake strength, extension, width and deflection depend on the interaction of the meridional component of the Ekman spiral with the rotational direction of the actuator disc, whereas the direction of the disc rotation only marginally modifies the wake if no veer is present. In more detail, a veering wind in combination with a counterclockwise rotating actuator results in a larger streamwise velocity output, a larger spanwise wake width, and a larger wake deflection angle at the same downwind distance in comparison to a clockwise rotating turbine (Fig. 1).

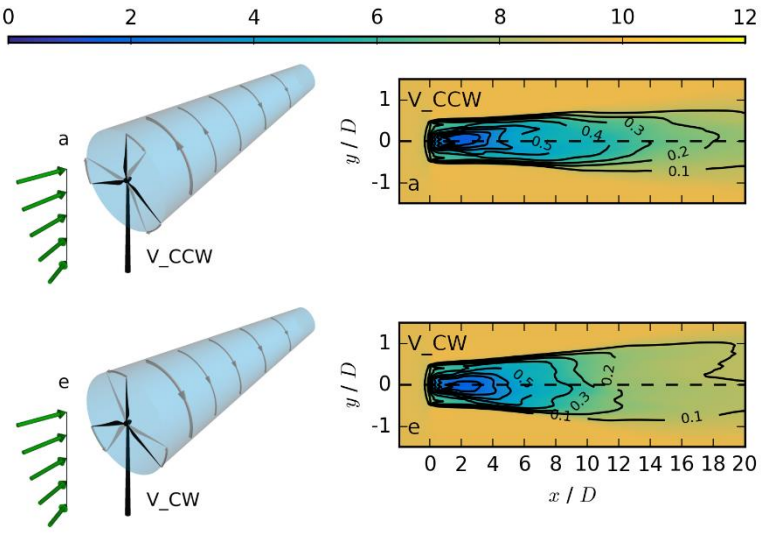


Figure 1: Schematic illustration of the rotational direction of the wake under veering inflow in case of a clockwise (top) and a counterclockwise (bottom) rotational direction of the rotor with the corresponding colored contours of the streamwise velocity and black contours representing the velocity deficit at hub height.

The differences result from the amplification or weakening/reversion of the spanwise and the vertical wind components due to the superposed disc rotation. They are also present in the streamwise wind component of the wake and in the total turbulence intensity. In the case of a counterclockwise rotating actuator, the spanwise and vertical wind components increase directly behind the rotor resulting in the same rotational direction in the whole wake while its strength decreases downwind.
In the case of a clockwise rotating actuator, however, the spanwise and vertical wind components of the near wake are weakened or even reversed in comparison to the inflow. This weakening/reversion results in a downwind increase of the strength of the flow rotation in the wake or even a different rotational direction in

the near wake in comparison to the far wake. The physical mechanism responsible for this difference can be explained by a simple linear superposition of a veering inflow with a Rankine vortex.
In idealized large-eddy simulations, Englberger, Lundquist and Dörnbrack (2020) investigate the rotational direction impact on the respective wakes for veering and backing winds in both hemispheres. The differences in the strength, extension, width and deflection of the wake between a clockwise and a counterclockwise rotating actuator occur in both hemispheres, however, the wake characteristics of a counterclockwise rotating actuator interacting with veering wind in the Northern Hemisphere are the same as if a turbine rotates clockwise in the Southern Hemisphere and vice versa. This results from the hemispheric dependency of the rotational direction of the wind vector with height in the Ekman spiral.
Further, a parameter study investigates the impact of the magnitude of the geostrophic wind, the directional shear, and the rotational frequency of the rotor on the wake characteristic differences between clockwise and counterclockwise rotating actuators in case of a veering inflow in the Northern Hemisphere. An increase of the directional shear or the rotational frequency of the rotor increases the difference in the spanwise wake width and the wake deflection angle between clockwise and counterclockwise rotating actuators, whereas the wind speed lacks a significant impact.

References:
Englberger, Dörnbrack and Lundquist, 2020, Does the rotational direction of a wind turbine impact the wake in a stably stratified atmospheric boundary layer? Wind Energ. Sci. 5, 1359-1374.
Englberger, Lundquist and Dörnbrack, 2020, Changing the rotational direction of a wind turbine under veering inflow: a parameter study. Wind Energ. Sci. 5, 1623-1644.

Effect of wind veer on the counter-rotating vortex pair behind yawed wind turbines

Ghanesh Narasimhan*, Dennice Gayme, and Charles Meneveau
Johns Hopkins University
*Presenting author

Keywords: Yawed wind turbines | Turbulent boundary layer | Vortex Dynamics | wakes/jets

Yawing wind turbines deflects the turbine wake away from the downstream turbines thereby increasing their power output potential. Yawing can therefore provide an efficient method to increase the overall wind farm production. Yawing a turbine produces a counter-rotating vortex pair (CVP) downstream of the turbine (Bastankhah & Porté-Agel 2016). In neutral atmospheric conditions the induced velocity in the spanwise direction from the CVP leads to the formation of a curled wake (Howland et al. 2016), however this phenomenon is not well studied when the farm is subject to wind veer. Wind veer arises in large wind farms which are influenced by Earth's rotation through the Coriolis effect. Near the Earth's surface, the Ekman spiral (Ekman 1905) arising from the balance between the Coriolis and frictional forces introduces a crosswind component to the mean flow that causes the wind veer.

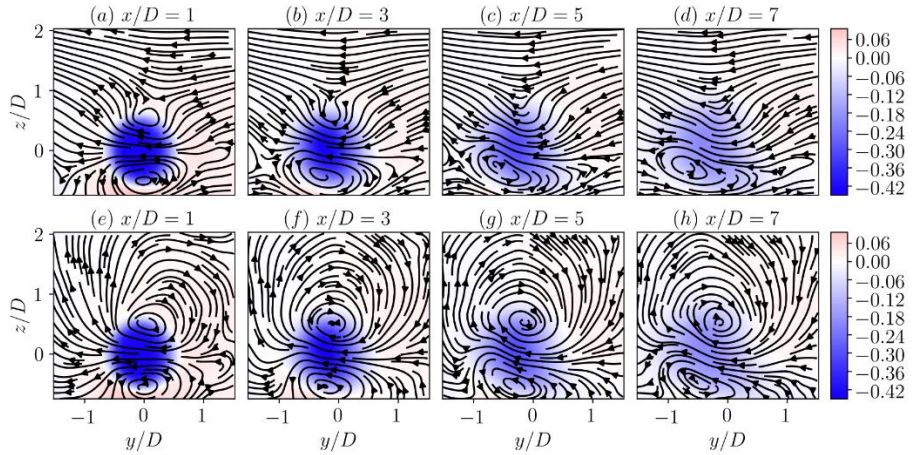


Figure 1: Contours of streamwise velocity deficit $(u - U_\infty)$ with streamlines of transverse flow (y-z plane) at downstream locations $x/D = 1, 3, 5, 7$ behind the wind turbine of diameter $D = 100$ m. The streamlines in (a)-(d) and (e)-(h) are with and without wind veer respectively.

In this work we investigate the effect of wind veer on the wake evolution and properties of the CVP. We perform Large Eddy Simulations (LES) of a single yawed wind turbine in a neutrally stratified atmospheric boundary layer (ABL) with geostrophic forcing. The scale-dependent Lagrangian dynamic sub-grid scale model (Bou-Zeid et al. 2005) is used in this study. The geostrophic wind direction is controlled to have a streamwise aligned mean flow at the hub height using the algorithm implemented in Sescu and Meneveau (2014). For such a flow configuration, the wind veer velocity profile is antisymmetric about the hub height such that the veer decreases the streamwise vorticity of the mean flow and the circulation of the top vortex while increasing the mean vorticity and circulation of the bottom vortex as shown in figure 1 (a)-(d). The transverse velocity streamlines show that the wind veer reduces the top vortex induced velocity while it accelerates the bottom vortex causing an asymmetry in the circulation strengths of the CVP. These effects change the shape of the CVP in the turbine wake. Our main observation is that when the wind veer component of the mean flow is subtracted from the spanwise velocity field, the CVP with similar circulation strength for the top and bottom vortex is retrieved as shown in figure 1 (e)-(h). The circulation strength of the CVP decays downstream due to turbulent diffusion. The decay of the maximum vorticity at the core of the vortices agrees well with the analytical model for the turbulent decay of the CVP's maximum vorticity and circulation strength proposed in Shapiro et al. (2020), but only if the wind veer vorticity is subtracted as shown in figure 2 (a) & (b).

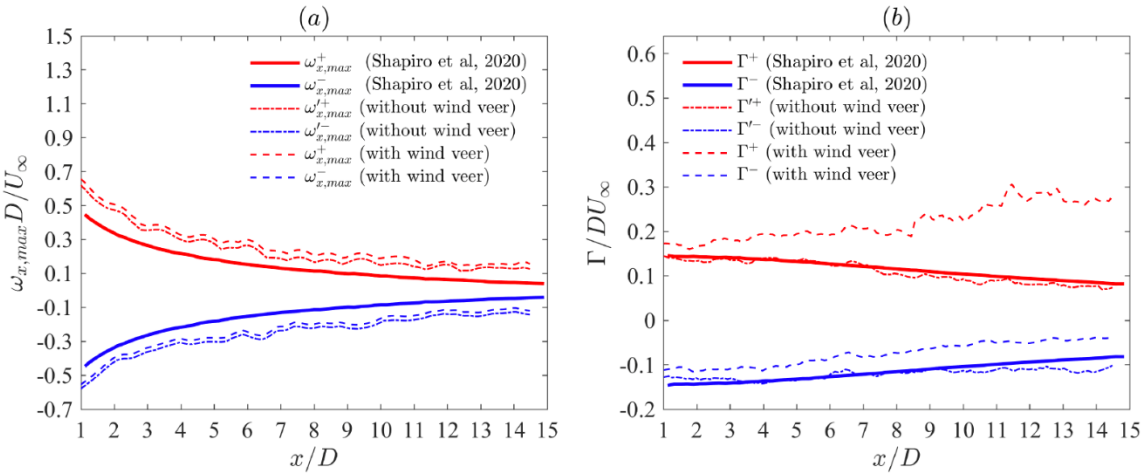


Figure 2: Decay of (a) maximum streamwise vorticity ($\omega_{x,max}$) and (b) circulation (Γ) of the CVP behind the wind turbine compared with analytical estimates from Shapiro et al. (2020).

Our results demonstrate that Coriolis-induced wind veer plays an important role in determining the vortex dynamics and wake shape evolution behind the yawed turbines. Any modeling attempt of the CVP should include the effect of wind veer for improved predictions of the wake properties.

Acknowledgment: Funding for this research was provided by NSF (CBET- 1949778).

References:

1. Bastankhah, M. & Porté-Agel, F. (2016) Experimental and theoretical study of wind turbine wakes in yawed conditions. J. Fluid Mech. 806, 506-541.

2. Howland, M. F., Bossuyt, J., Martinez-Tossas, L. A., Meyers, J. & Meneveau, C. (2016) Wake structure in actuator disk models of wind turbines in yaw under uniform inflow conditions. J. Renew. Sust. Energy 8 (4), 043301.

3. Ekman, V. W. (1905) On the influence of the Earth's rotation on ocean-currents, Archive for Mathematics. Astronomical Physics 2, 1.

4. Bou-Zeid, E., Meneveau, C., Parlange, M. B. (2005) A scale-dependent Lagrangian dynamic model for large eddy simulation of complex turbulent flows. Phys. of Fluids 17, 025105.

5. Sescu, A. & Meneveau, C. (2014) A control algorithm for statistically stationary large-eddy simulations of thermally stratified boundary layers. Q. J. R. Meteorol. Soc. 140 (683), 2017-2022.

6. Shapiro, C., Gayme, D., & Meneveau, C. (2020). Generation and decay of counter-rotating vortices downstream of yawed wind turbines in the atmospheric boundary layer. J. of Fluid Mech., 903, R2.

Dependence of the evolution of wind turbine wakes on the atmospheric turbulence: A LiDAR field study

Ingrid Neunaber, and Sandrine Aubrun
Centrale Nantes

Keywords: Wind turbine wake | LiDAR | Field experiments | Wake evolution

Wind turbines operate in the naturally turbulent atmospheric wind, and they are often clustered in wind farms. As a consequence, downstream turbines will often operate in the full or partial wakes of the upstream wind turbines. On the one side, the downstream turbines will produce less energy due to the reduced velocity it the wake. On the other side, downstream turbines will experience higher load fluctuations due to the enhanced turbulence in the wake [1]. To optimize the wind farm layout, maintenance time and control algorithms, it is therefore important to know how wakes are evolving.
Therefore, over the past decades, a lot of effort has been put into the analysis and description of wakes [2]. However, the accurate modeling of wakes is complicated by the variation of the atmospheric conditions (e.g. the wind speed, wind direction and stability) and by the variation of the turbine's operation mode as a response to it. For example, it has been shown that wind turbine wakes recover faster in higher ambient turbulence due to the enhanced mixing and thus faster entrainment of energy [3]. As a consequence of this variety of wake recoveries, a downstream turbine may be exposed to different regions in the wake of an upstream turbine which will have an influence on the turbulence degree the downstream turbine is exposed to [4].

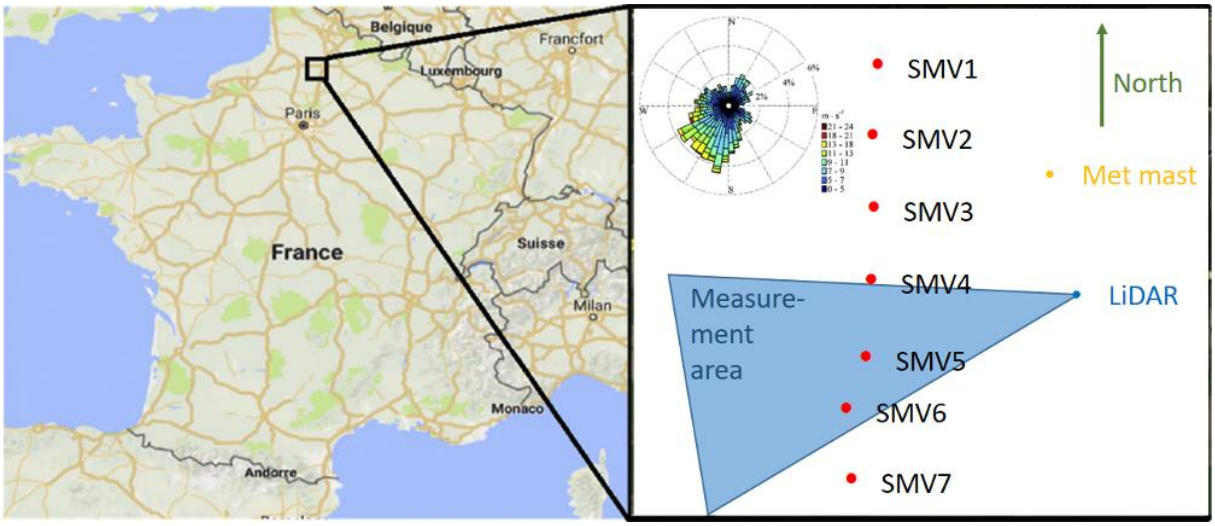


Figure 1: Measurement site – left: location of the wind farm in France; right: location of wind turbines, the met mast and the LiDAR with the scanned area. In addition, a wind rose indicates the wind distribution.

To gain knowledge on the dependence of the evolution of the wind turbine wake on the atmospheric conditions, it is possible to perform field studies, for example with Light Detection and Ranging (LiDAR) systems. In this study, we present results from a LiDAR measurement campaign that has been carried out over the duration of 7 months (11/2015-5/2016) in a small wind farm in the north of France [4], cf. Fig. 1. PPI scans were made at three elevation angles. The wakes of two wind turbines have been scanned for different levels of wake interactions, which depend on the wind direction. The analysis will focus on the evaluation of the data with respect to different atmospheric conditions, i.e. the atmospheric stability (and thus turbulence) and the wind speed. This will expand the results presented in [4] for an inflow velocity of 13 m/s and a neutral atmosphere. Different wind directions can in addition be used to investigate the wake interaction of the two wind turbines SMV5 and SMV6 (cf. fig. 1). To identify the different atmospheric inflow conditions, we will

follow the strategy presented in [4] where the atmospheric stability and wind direction are determined from the Modern-Era Retroperspective analysis for Research and Applications, version 2, data.
In summary, this study will give new insight into the dependence of the evolution of the wind turbine wake on the atmospheric conditions.

References:
[1] Vermeer, L.J. ; Sørensen, J. N.; Crespo A. (2003) Wind turbine wake aerodynamics. Prog Aerosp Sci, 39, 467–510
[2] Porté-Agel, F.; Bastankhah, M.; Shamsoddin S. (2020) Wind-Turbine and Wind-Farm Flows: A Review. Boundary Layer Meteorol, 174, 1–59
[3] Wu, Y.-T.; Porté-Agel, F. (2012) Atmospheric Turbulence Effects on Wind-Turbine Wakes: An LES Study. Energies, 5, 5340-5362
[4] Torres Garcia, E.; Aubrun, S., Coupiac, O.; Girard, N.; Boquet, M. (2019) Statistical characteristics of interacting wind turbine wakes from a 7-month LiDAR measurement campaign. Renew Energ 130, 1-11
[5] Neunaber, I.; Hölling, M.; Stevens, R.; Schepers, G.; Peinke, J. (2020) Distinct Turbulent Regions in the Wake of a Wind Turbine and Their Inflow-Dependent Locations: The Creation of a Wake Map. Energies, 13

Actuator line model development using simplified methods for forces calculation

Gonzalo Pablo Navarro Diaz[1,*], Alejandro Daniel Otero[2,3], Henrik Asmuth[1], Jens Nørkær Sørensen[4], Karl Nilsson[1], and Stefan Ivanell[1]

[1]Uppsala University
[2]Facultad de Ingeniería, Universidad de Buenos Aires
[3]Centro de Simulación Computacional para Aplicaciones Tecnológicas
[4]Technical University of Denmark
*Presenting author

Keywords: Actuator line model | Actuator disc model | wake | LES

In this work, the capability to simulate transient wind turbine (WT) wake interaction problems is extended to the use of limited basic manufacturer WT information. For this purpose, two new variants of the actuator line model (ALM) are proposed, which forces are now locally computed using only standard WT data, i.e. any combination of the thrust and power coefficient and the tip speed ratio. These implementations come as an extension of the actuator disc model (ADM) in which the local adaptation is obtained by means of a numerical (Navarro Diaz et al., 2019) or analytical (Sørensen et al., 2020) procedure.
In this study, the new ALMs with analytical and numerical adaptations are compared with the ADM, built from the same data, and also with the classical ALM based on blade element theory (Sørensen and Shen, 2002), which provides more detailed force distributions by using airfoil data. In order to evaluate the local force calculation, the analysis of a partial wake interaction case between two WTs is carried out, first for an uniform and then for a turbulent neutral atmospheric boundary layer inflow. Large Eddy Simulation is used, choosing the OpenFOAM project SOWFA (Churchfield et al., 2012) and the reference NREL 5MW wind turbine as a test case.

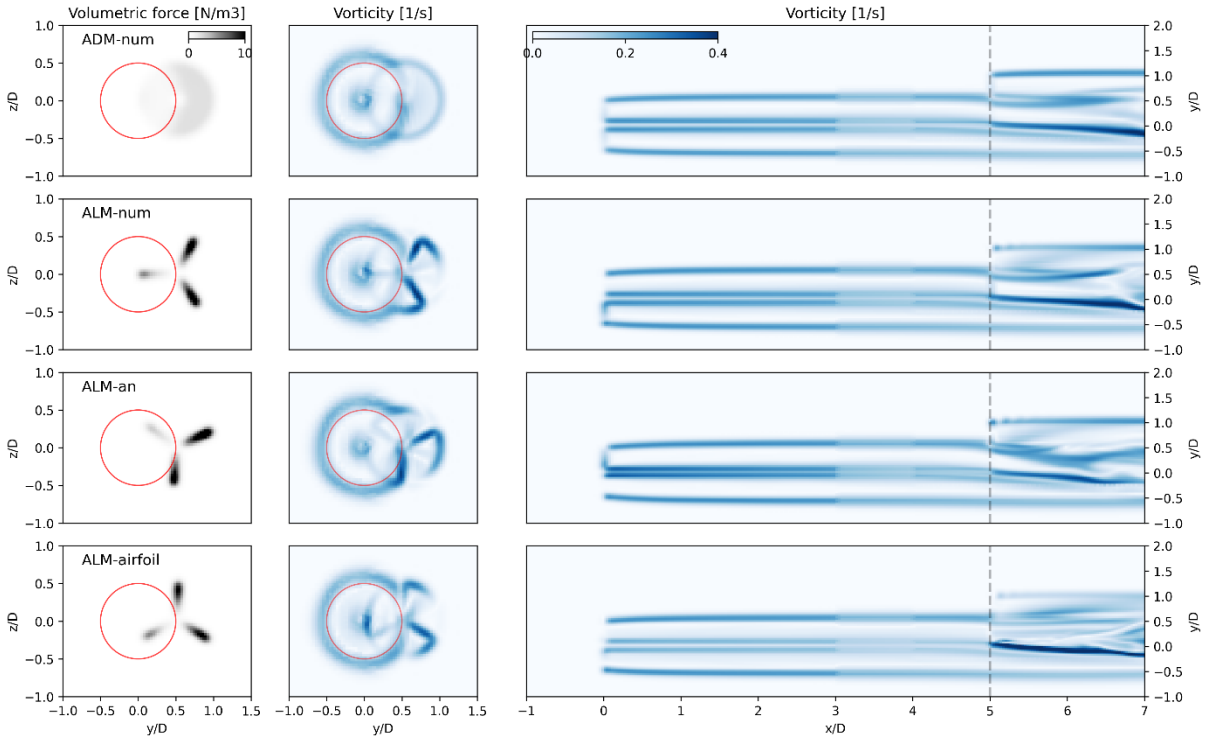


Figure 1: Uniform inflow case for a below rated velocity: (left and middle) instantaneous volumetric blade force and vorticity, respectively, on vertical planes at the position of the impacted WT, and (right) instantaneous vorticity on horizontal planes at hub height. All the results correspond to the same runtime.

For the uniform inflow case a below and above rated velocities are tested. In Figure 1 it can be seen the results for the below rated velocity, showing the instantaneous volumetric blade force and vorticity on vertical planes at the position of the impacted WT, and instantaneous vorticity on horizontal planes at hub height. Four models are compared; the ADM with numerical local adaptation approach (ADM-num), two ALMs with numerical and analytical local adaptation (ALMnum and ALM-an, respectively) and the classical ALM build from airfoil data (ALM-airfoil). In this figure it can be noticed that all ALMs show the advantage of a better transient WT-airflow interaction and near wake description by applying the forces along each blade, as was also achieved by Martinez et al. (2012) and Marjanovic et al. (2017).

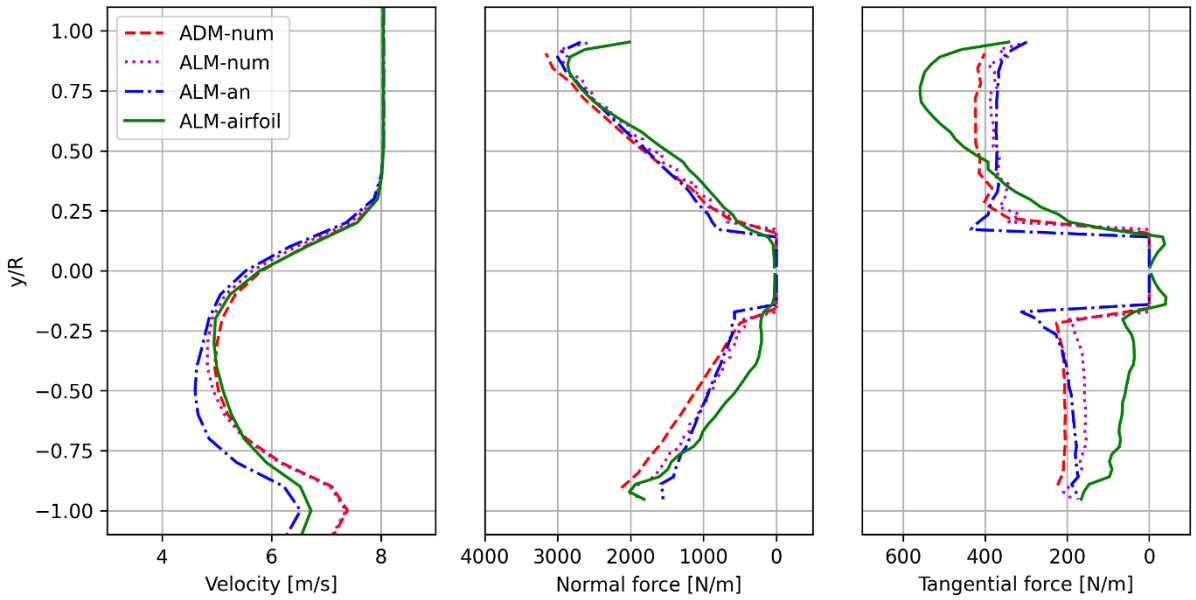


Figure 2: Uniform inflow case for a below rated velocity: (left) time averaged velocity on a horizontal line at hub height and 2 diameter upstream the impacted WT; (center and middle) time averaged normal and tangential forces distribution when blades are at 90° and 270° azimuth angles (blades in horizontal position).

Analyzing the same case, in Figure 2 it can be seen the time averaged velocity on a horizontal line at hub height and 2 diameter upstream the impacted WT. On this WT, also the time averaged normal and tangential forces distribution when blades are in horizontal position is shown. From this figure, it can be noticed that the new ALMs give similar results in the forces calculation at each side of the rotor. These results show that both ALMs and the ADM manage to capture the trend in the normal force distribution obtained with airfoil data. Bigger differences are found in the tangential force comparison. These new developments increase the possibilities on the simulation of transient WT interaction problems in wind farms using easily found manufacturer WT information.

References:

Churchfield, M.J., Lee, S., Michalakes, J. and Moriarty, P.J., 2012. A numerical study of the effects of atmospheric and wake turbulence on wind turbine dynamics. Journal of turbulence, (13), p.N14.

Marjanovic, N., Mirocha, J.D., Kosović, B., Lundquist, J.K. and Chow, F.K., 2017. Implementation of a generalized actuator line model for wind turbine parameterization in the Weather Research and Forecasting model. Journal of Renewable and Sustainable Energy, 9(6), p.063308.

Martinez, L., Leonardi, S., Churchfield, M. and Moriarty, P., 2012, January. A comparison of actuator disk and actuator line wind turbine models and best practices for their use. In 50th AIAA Aerospace Sciences Meeting including the New Horizons Forum and Aerospace Exposition (p. 900).

Navarro Diaz, G.P., Saulo, A.C. and Otero, A.D., 2019. Wind farm interference and terrain interaction simulation by means of an adaptive actuator disc. Journal of Wind Engineering and Industrial Aerodynamics, 186, pp.58-67.

Sørensen, J.N. and Shen, W.Z., 2002. Numerical modeling of wind turbine wakes. J. Fluids Eng., 124(2), pp.393-399.

Sørensen, J.N., Nilsson, K., Ivanell, S., Asmuth, H. and Mikkelsen, R.F., 2020. Analytical body forces in numerical actuator disc model of wind turbines. Renewable energy, 147, pp.2259-2271.